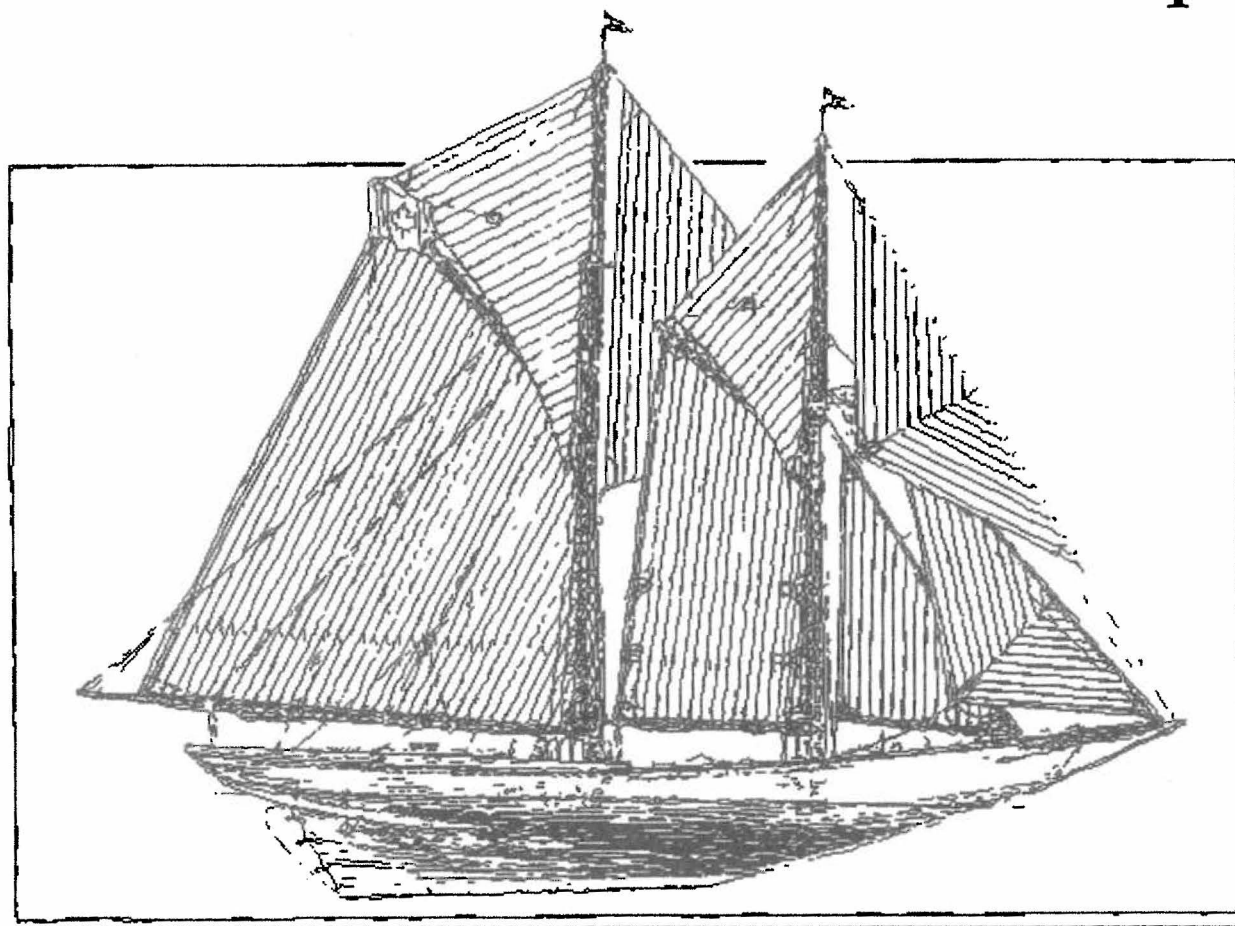# 13th
Biennial Conference

Canadian Society for Biomechanics
Société Canadienne de Biomécanique

August 4th – 7th, 2004
Halifax, Nova Scotia, Canada

Message from the Chair of the XIIIth Biennial Conference of the Canadian Society for Biomechanics/ Société Canadienne de Biomécanique

On behalf of the CSB2004 Organizing Committee I would like to welcome you to Halifax and Dalhousie University. This is the first time in the 31-year history of the CSB that the meeting has been held in Atlantic Canada, and it is the first CSB only meeting since 1996. We are very excited about the scientific content of the program including two keynotes, four symposia/workshops on: i) Arthritis, ii) Mobility Disabilities, iii) Sport Biomechanics and iv) Occupational Biomechanics/Ergonomics, as well as, 92 podium and 98 poster presentations. We have over 200 delegates registered, from all over the world including, New Zealand, Czech Republic, Germany, the United States and Canada, from Newfoundland to British Columbia. Therefore, it should provide an opportunity for excellent networking and both intellectual and cultural exchanges. We hope you enjoy your stay and are able to visit the many historic sites, great restaurants and of course the many social establishments that Halifax has to offer.

Best wishes for a great conference experience!

Cheryl Kozey

Message de la Maître de cérémonie de la XIII^{ieme} Conférence Biannuelle de la Société Canadienne de Biomécanique

Au nom du comité organisateur de la SCB 2004, je vous souhaite la bienvenue à Halifax et à l'Université de Dalhousie. C'est la première fois dans l'histoire des 31 ans de la SCB que la réunion est tenue dans les provinces maritimes, et c'est la première fois depuis 1996 que la conférence est organisée uniquement par SCB. Nous sommes très excités du contenu scientifique du programme comprenant deux conférenciers invités et quatre colloques sur: 1) l'Arthrite, 2) Mobilité, 3) Biomécanique du sport et 4) Biomécanique occupationnelle/Ergonomique. Notre programme compte aussi 92 présentations orales et 98 présentations d'affiches. Nous avons plus de 200 délégués inscrits, de partout dans le monde comprenant, entre autre, la Nouvelle-Zélande, République Tchèque, l'Allemagne, les États-Unis et finalement de toutes les provinces canadiennes de Terre Neuve à la Colombie-Britannique. Donc, nous présentons une excellente gestion du réseau d'échanges intellectuel et culturel au Canada. Nous espérons que vous apprécierez votre séjour et pourrez visiter les nombreux sites historiques, restaurants et naturellement les nombreux établissements sociaux que Halifax vous offrent.

Meilleurs vœux pour une expérience supérieure à la conférence 2004 de la SCB.

Cheryl Kozey

Message from the President of Dalhousie University

On behalf of the Dalhousie community, I am delighted to welcome you to the XIIIth Biennial Conference of the Canadian Society for Biomechanics/ Société Canadienne de Biomécanique (CSB2004) **"Expanding Biomechanical Solutions"**

This is the first time in the 22-year history of the CSB that the meeting has been held in Atlantic Canada, and we are pleased to offer you an outstanding program with distinguished speakers, over 200 scientific presentations and the famous hospitality for which the East Coast is known. I guarantee that the CSB 2004 will provide you many opportunitiesto attend events that will appeal to both your intellectual and social tastes.

Dalhousie University was founded in 1818 by Lord Dalhousie, and is now a comprehensive university that offers the greatest range of undergraduate, graduate, and professional degree programs of any institution in Atlantic Canada. Dalhousie is spread over 79 acres comprising of the three campuses, and I invite you to visit as much of the University as possible during your stay.

I also hope that you will find time during the CSB 2004 to explore Halifax and its surrounds, where you will find a mix of rich history and contemporary charm. Enjoy your stay in Halifax, Nova Scotia, and you visit to Dalhousie University. In extend my best wishes for an enjoyable and highly successful event.

Tom Traves

Contents

Meeting Information

Speaker Ready Room

Location: Bedford Room
Please bring your presentation to the speaker ready room to load your file(s) for presentation. Bring the file(s) to the room at least 4 hours before your presentation time. If you have an early morning presentation, please prepare the file(s) the day before.

Podium presentations are scheduled for 15 minutes each (12 presentation and 3 minutes questions). Please prepare your presentation on an IBM compatible computer using MS PowerPoint and bring a copy (on CD or USB memory stick) of the presentation to the conference to load on the conference computers. These computers will be running MS PowerPoint version 2003 on Windows XP and should (within the limitations of MicroSoft™) be backwards compatible with previous versions of MS PowerPoint.

Annual General Meeting

Friday August 6th from 5:30 – 6:30 pm in the Atlantic Ballroom
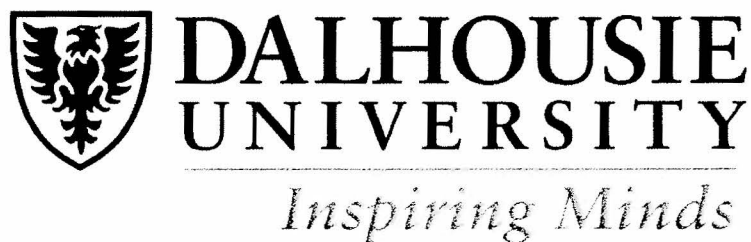
Cover

The picture on the cover is of the Bluenose II Schooner. The Bluenose II is a Canadian icon and is recognized as the symbol of Nova Scotia around the world. The image was provided by the Bluenose II Preservation Trust (http://www.bluenose2.ns.ca/). This is a volunteer organization established to preserve and operate Bluenose II for the people of Nova Scotia.

Sponsors

NOVA SCOTIA Health Research FOUNDATION

CIHR IRSC
Canadian Institutes of Health Research
Instituts de recherche en santé du Canada

Institute of Institut de
Musculoskeletal l'appareil locomoteur
Health and Arthritis et de l'arthrite

DALHOUSIE UNIVERSITY
Inspiring Minds

Dalhousie University Support
- Faculty of Graduate Studies
- Faculty of Health Professions
- Research Services
- Office of Vice President Academic and Provost
- School of Physiotherapy

Exhibitors

1. **Motion Lab Systems Inc.**
   15045 Old Hammond
   Baton Rouge, LA 70816
   225-272-7364
   www.motion-labs.com

2. **Measurand Inc.**
   2111 Hanwell Road
   Fredericton, NB E3C 1M7
   506-462-9119
   www.measurand.com

3. **Tekscan**
   307 West First St.
   Boston, MA 02127
   617-464-4500
   www.tekscan.com

4. **Human Kinetics Inc.**
   475 Devonshire Rd., Suite
   100
   Windsor, ON N8Y 2L8
   www.humankinetics.com

5. **FMA Lab Inc.**
   226 Boland Cr.
   Campbellville, ON L0P 1B0
   905-854-1450
   www.fmalab.com

6. **NexGen Ergonomics Inc.**
   6600 Trans Canada Highway,
   Suite 750
   Pointe-Claire (Monteal), QC
   H9R 4S2
   514-685-8593
   www.nexgenergo.com

7. **HMA Technology Inc.**
   165 Warren Rd.
   King City, ON L7B 1H1
   www.hma-tech.com

8. **Peak Performance
   Technologies Inc.**
   7388 South Revere
   Parkway Suite 901
   Centennial, CO 80112
   303-799-8686
   www.**peakperform.com**

9. **Advanced Mechanical
   Technology Inc.**
   176 Waltham St.
   Watertown, MA 02472-4800
   617-926-6700
   www.amtiweb.com

10. **Zflo Motion Inc.**
    67 Federal Avenue
    Quincy, MA 02169
    617-890-1041
    www.**zflo**motion.com

Corporate Sponsors

1. Nike, Inc.
   One Bowerman Drive
   Beaverton, OR 97005
   1-800-344-6453
   www.nike.com

2. Noraxon USA Inc.
   13430 N. Scottsdale Road,
   Suite 104
   Scottsdale, Arizona 85254
   480-443-3413
   www.noraxon.com

Conference Organizing Committee

Conference Chairperson
Cheryl Kozey, Ph.D., Dalhousie University

Scientific Co-Chairs
Kevin Deluzio, Ph.D., Dalhousie University
John Kozey, Ph.D., Dalhousie University

Committee Members
Wayne Albert, Ph.D., University of New Brunswick
Heather Butler, MSc., Dalhousie University
Katherine Harman, Ph.D., Dalhousie University
Lee Kirby, M.D., Dalhousie University
Lori Livingston, Ph.D., Dalhousie University
Don MacLeod, MSc., Nova Scotia Rehabilitation Centre
William Stanish, MD, FRCS(C) FACS, Dalhousie University

Conference Coordinator
Candace Fawcett

Conference Secretary
Shirley Wheaton
Assistant
Kate Paige

Volunteers

Jenn McNutt	Janie Astephen
Scott Landry	Elise Laende
Adam Henderson	Robyn Newell
Joni Snair	Stephen Sheridan
Andrew Horne	Laura Diamond
Kelly MacKean	Sherma Dewey

Scientific Program Committee

Wayne Albert, University of New Brunswick
Dave Andrews, University of Windsor
Graham Caldwell, University of Massachusetts
Pat Costigan, Queen's University
Kevin Deluzio, Dalhousie University
Lee Kirby, Dalhousie University
Cheryl Kozey, Dalhousie University
John Kozey, Dalhousie University
Lori Livingston, Dalhousie University

New Investigators Award Committee

Stephen Prentice, University of Waterloo, Chair
David Andrews, University of Windsor
Benno Nigg, University of Calgary
Francois Prince, University of Montreal

CSB Executive Committee

President
Ron Zernicke, University of Calgary

Secretary – Treasurer
Stephen Prentice, University of Waterloo

Member Affairs and Secretariat
Darren J. Stefanyshyn, University of Calgary

Conference Chairperson
Cheryl Kozey, Dalhousie University

Communications and Webpage
Gordon Robertson, University of Ottawa

Members-at-Large
Janet Ronsky, University of Calgary
Joe Hamill, University of Massachusetts

Past President
Francois Prince, University of Montreal

Student Representatives
Heather Butler, Dalhousie University
Jennifer Durkin, University of Waterloo

CSB 2004 Timetable

Time	Wed. Aug 4th	Thurs. Aug 5th		Fri. Aug 6th		Sat. Aug 7th	
7:00		Registration					
8:00		Keynote Address		Career Award			
9:00						Session 11a	Session 11b
9:15		Session 1a Locomotion 1	Session 1b Muscle 1	Session 6a Spine 1	Session 6b Muscle 2	Osteoarthrits 1	Muscle 3
						Break 10:15-10:30	
10:15		Break 10:15-10:30		Break 10:15-10:30		Session 12a	Session 12b
10:30		Session 2a Symposium 1 Locomotion	Session 2b Tissue	Session 7a Symposium 3 Occupational Biomechanics	Session 7b Rehab	Symposium 4 Osteoarthritis	Ergonomics 3
12:00		Lunch (1.5 hours) *Grant writing workshop*		Box Lunch (2.0 hours) *Lab Tours &*		Lunch (1.0 hours)	
1:00				*Wheelchair Workshop*		Session 13a	Session 13b
1:30		Session 3a	Session 3b			Locomotion 3	Spine 2
2:00		Clinical Biom.	Sport 1	Session 8a	Session 8b		
2:30				Locomotion 2	Ergonomics 1	Session 14	
3:00		Session 4 Posters & Refreshment break		Session 9 Posters & Refreshment break		Posters & Refreshment break	
3:30						Session 15a	Session 15b
4:00	Registration	Session 5a Symposium 2	Session 5b	Session 10a New	Session 10b	Osteoarthritis 2	Sport 2
4:30		Sport Biomechanics	Posture	Investigator Awards	Ergonomics 2		
5:30		Student Mentor Session 5:30		Annual General Meeting 5:30-6:30			
6:00		Student Social 6 - ?...				Banquet & Awards at Pier 21 & 22	
6:30						6:00 - 10:00	
7:00	Reception 7 - 9 PM						

9:15am – 10:15am
Parallel Sessions 1a & 1b

	Session 1a - Locomotion 1	Session 1b - Muscle 1
	Location: Atlantic Ballroom **Session Chairs:** **Pat Costigan, Francois Prince**	**Location: Commonwealth B** **Session Chairs:** **Graham Caldwell, John Kozey**
9:15 – 9:30	*Monika Zihlmann*; Gerber, H.; Burckhardt, K.; Stacoff, A.; Stuessi, E. Eidgenössische Technische Hochschule Zürich "THREE DIMENSIONAL IN VIVO KINEMATICS OF ARTIFICIAL KNEE JOINTS DURING LEVEL WALKING USING A MOVING VIDEO-FLUOROSCOPE"	*Dilson Rassier*; Herzog, W. University of Calgary "RELAXATION TIME INCREASES AFTER ACTIVE STRETCH OF SKELELTAL MUSCLE"
9:30 – 9:45	*Sebastien Chapdelaine*; McFadyen, B.J.; Nadeau, S.; St-Vincent, G.; Langelier, E. Centre interdisciplinaire de recherché en réadaptation et intégration sociale "AN INSTRUMENTED STAIRCASE FOR KINETIC ANALYSES OF UPPER AND LOWER LIMB FUNCTION DURING STAIR GAIT"	*Janice Flynn*; Holmes, J.D.; Andrews, D.M. University of Waterloo "LOCALIZED LEG MUSCLE FATIGUE RESULTS IN REDUCED TIBIAL IMPACT ACCELERATION"
9:45 – 10:00	*Jeannette Byrne*; Ishac, M.; Patla, A.E.; Prentice, S.D. University of Waterloo "3D KNEE JOINT MOMENTS DURING LEVEL WALKING AND WHEN STEPPING TO A NEW LEVEL"	*Marco Vaz*; Scheeren, E.M.; Rassier, D.E.; Herzog, W.; MacIntosh, B.R. University of Calgary "MEASURES OF FATIGUE: ARE THEY CONSISTENT?"
10:00 – 10:15	*Janie Astephen*; Deluzio, K.J. Dalhousie University "CONTINUOUS CURVE REGISTRATION IN THE ANALYSIS OF GAIT DATA"	*Allan Wrigley*; Albert, W.J.; Sleivert, G.G.; McLean, R.B. University of New Brunswick "INDUCED LOCALIZED MUSCULAR FATIGUE: METHODOLOGICAL ASPECTS AND GENDER DIFFERENCES IN THE RATE OF FATIGUE AND RECOVERY."

10:15am – 10:30pm
Refreshment Break & Exhibitor Viewing (Commonwealth A)

Wednesday August 4, 2004

4:00 pm – 9:00 pm
Registration
Location: Mezzanine

7:00 pm – 9:00pm

Opening Reception & Book Launch

Co-sponsored by Human Kinetics

Location: Atlantic Ballroom

Thursday August 5, 2004

8:00am – 9:10am
Keynote Address
Location: Atlantic Ballroom

8:00 – 8:10   ***Benno Nigg, Professor***
University of Calgary
KEYNOTE ADDRESS INTRODUCTION

8:10 – 9:10   ***Walter Herzog, Ph.D.***
University of Calgary
"CONSIDERATIONS ON THE HISTORY DEPENDENCE OF MUSCLE
CONTRACTION"

9:15am – 10:15am
Parallel Sessions 1a & 1b

	Session 1a - Locomotion 1	Session 1b - Muscle 1
	Location: Atlantic Ballroom **Session Chairs:** **Pat Costigan, Francois Prince**	**Location: Commonwealth B** **Session Chairs:** **Graham Caldwell, John Kozey**
9:15 – 9:30	*Monika Zihlmann*; Gerber, H.; Burckhardt, K.; Stacoff, A.; Stuessi, E. Eidgenössische Technische Hochschule Zürich "THREE DIMENSIONAL IN VIVO KINEMATICS OF ARTIFICIAL KNEE JOINTS DURING LEVEL WALKING USING A MOVING VIDEO-FLUOROSCOPE"	*Dilson Rassier*; Herzog, W. University of Calgary "RELAXATION TIME INCREASES AFTER ACTIVE STRETCH OF SKELELTAL MUSCLE"
9:30 – 9:45	*Sebastien Chapdelaine*; McFadyen, B.J.; Nadeau, S.; St-Vincent, G.; Langelier, E. Centre interdisciplinaire de recherché en réadaptation et intégration sociale "AN INSTRUMENTED STAIRCASE FOR KINETIC ANALYSES OF UPPER AND LOWER LIMB FUNCTION DURING STAIR GAIT"	*Janice Flynn*; Holmes, J.D.; Andrews, D.M. University of Waterloo "LOCALIZED LEG MUSCLE FATIGUE RESULTS IN REDUCED TIBIAL IMPACT ACCELERATION"
9:45 – 10:00	*Jeannette Byrne*; Ishac, M.; Patla, A.E.; Prentice, S.D. University of Waterloo "3D KNEE JOINT MOMENTS DURING LEVEL WALKING AND WHEN STEPPING TO A NEW LEVEL"	*Marco Vaz*; Scheeren, E.M.; Rassier, D.E.; Herzog, W.; MacIntosh, B.R. University of Calgary "MEASURES OF FATIGUE: ARE THEY CONSISTENT?"
10:00 – 10:15	*Janie Astephen*; Deluzio, K.J. Dalhousie University "CONTINUOUS CURVE REGISTRATION IN THE ANALYSIS OF GAIT DATA"	*Allan Wrigley*; Albert, W.J.; Sleivert, G.G.; McLean, R.B. University of New Brunswick "INDUCED LOCALIZED MUSCULAR FATIGUE: METHODOLOGICAL ASPECTS AND GENDER DIFFERENCES IN THE RATE OF FATIGUE AND RECOVERY."

10:15am – 10:30pm
Refreshment Break & Exhibitor Viewing (Commonwealth A)

Session 2a - Locomotion Symposium *Sponsored by the Institute of Musculoskeletal Health and Arthritis* **Location: Atlantic Ballroom**	Session 2b – Tissue **Location: Commonwealth B** **Session Chairs:** **Edwin Demont, Janet Ronsky**

Session 2a - Locomotion Symposium

Sponsored by the Institute of Musculoskeletal Health and Arthritis

Location: Atlantic Ballroom

Opening Remarks:
Dr. A. Patla, University of Waterloo

Mandar Jog, M.D.
London Health Sciences Centre
"THE EFFECTS OF BASAL GANGLIA DISORDERS ON MOBILITY"

Brad MacFadyen, Ph.D.
Laval University
"THE EFFECT OF TRAUMATIC BRAIN INJURY ON MOBILITY"

Stephen Perry, Ph.D.
Wilfrid Laurier University
"THE EFFICACY OF ASSISTIVE DEVICE TO IMPROVE BALANCE AND MOBILITY IN THE ELDERLY"

Aftab Patla, Ph.D.
University of Waterloo
"THE EFFICACY OF DIFFERENT EXERCISE INTERVENTION PROGRAMS FOR IMPROVING MOBILITY IN THE ELDERLY"

Session 2b – Tissue

Location: Commonwealth B
Session Chairs:
Edwin Demont, Janet Ronsky

10:30 – 10:45   *Sang Kuy Han*; Federico, S.F.; Herzog, W.H.
University of Calgary
"ARTICULAR CARTILAGE STRESS STATE IN MISALIGNED JOINTS"

10:45 – 11:00   *Farzan Ghalichi*; Behnia, S.; Sadigh Rad, E.; Bonabi, A.
Sahand University of Technology
"ULTRASOUND INDUCED HYPERTHERMIA TEMPERATURE TRACKING OF CERVIX TUMORS INCLUDING VASCULAR NETWORK EFFECTS"

11:00 – 11:15   *Adrian Ranga*; Mongrain R.; Biadillah, Y.; Cartier, R.
McGill University
"A COMPLIANT DYNAMIC FEA MODEL OF THE AORTIC VALVE WITH HYPERELASTIC MATERIAL PROPERTIES"

11:15 – 11:30   Nguyen, T.T.; *Rosaire Mongrain*; Prakash, S.; Tardif, J.C.
McGill University
"DEVELOPMENT OF A BLOOD ANALOG MICROPARTICLE SUSPENSION FOR HEMOLYTIC POTENTIAL ASSESSMENT OF CARDIOVASCULAR DEVICES"

11:30 – 11:45   *Pablo Vasquez*; Nuño, N.; de Guise, J.
Université du Québec
"EFFECT OF RESIDUAL STRESSES DUE TO CEMENT CURING IN THE LOAD TRANSFER OF A PERSONALIZED CEMENTED HIP IMPLANT"

12:00pm – 1:30pm
Lunch (Commonwealth A)
12:30pm – 1:30pm
Grant Writing Workshop (Commonwealth B)

	Session 3a - Clinical Biomechanics	**Session 3b - Sport 1**
	Location: Atlantic Ballroom **Session Chairs:** **Sylvie Nadeau, Gordon Robertson**	**Location: Commonwealth B** **Session Chairs:** **Irene McClay Davis, Pierre Gervais**
1:30 – 1:45	*Karen Siegel*; Kepple, T.M.; Stanhope, S.J. National Institutes of Health "GAIT COMPENSATIONS FOR HIP MUSCLE WEAKNESS IN IDIOPATHIC INFLAMMATORY MYOPATHY"	*Jeremy Determan*; Swanson, S.; McDermott, W.; Hamill, J. University of Massachusetts "GROUND REACTION FORCES IN TREADMILL VS. OVERGROUND RUNNING"
1:45 – 2:00	*Guylaine Roy*; Nadeau, S.; Gravel, D.; Malouin, F.; McFadyen, B.; Lecours, J.; Piotte, F. Université de Montréal "FOOT POSITIONS AND ASYMMETRY OF VERTICAL REACTION FORCES DURING RISING FROM A CHAIR IN PERSONS WITH HEMIPARESIS"	*Sharon Bullimore*; Burn, J.F. University of Bristol "MODELLING THE EFFECTS OF POINT OF FORCE TRANSLATION IN RUNNING GAITS"
2:00 – 2:15	*Flora Stephenson*; Spaulding, S.J. The University of Western Ontario "GAIT ADAPTATION IN INDIVIDUALS WITH PARKINSON'S DISEASE"	*Luke Savage*; Butterwick, D.J.; Loitz-Ramage, B.; Ronsky, J. University of Calgary "ESTIMATION OF GROUND REACTION FORCES IN BUCKING RODEO BULLS"
2:15 – 2:30	*Daina Sturnieks*; Besier, T.F.; Lloyd, D.G. University of Western Australia "GAIT PATTERNS AND KNEE FUNCTION FOLLOWING ATHRTOSCOPIC PARTIAL MENISCECTOMY"	*Jay Worobets*; Stefanyshyn, D.J. University of Calgary "CORRELATIONS BETWEEN GROUND REACTION FORCE COMPONENTS AND BODY MASS IN HEEL-TOE RUNNING
2:30 – 2:45	*Ben Orlik*; Dunbar, M.J.; Amirault, D.J.; Hennigar, A.W.; Leahey, J.L. Dalhousie University "VALIDITY AND RELIABILITY OF ACCELEROMETRIC GAIT ANALYSIS IN THE ASSESSMENT OF OSTEOARTHRITIS OF THE KNEE"	*Jeremy Determan*; Frederick, E.C.; Cox, J. Sole Technology Institute "IMPACT FORCES DURING SKATEBOARDING LANDINGS"
2:45 – 3:00	*T. Ward*; Pandit, H.; Hollinghurst, D.; Moolgavkar, P.; Zavatsky, A.B.; Gill, H.S. University of Oxford "DEVELOPMENT AND IN VITRO VALIDATION OF A MODEL TO PREDICT THE PATELLOFEMORAL CONTACT FORCES OF TKRs"	*Uwe Kersting* University of Auckland "THE EFFECT OF CHANGES IN BINDING ALIGNMENT DURING A SIMULATED SNOWBOARDING LANDING TASK"

3:00pm – 4:00pm
Session 4 – Posters and Refreshment Break

Location: Commonwealth A

1. Goncalves, C.; Moraes, R.; *Aftab E. Patla*
University of Waterloo
"AMENDING FOOT PLACEMENT DURING A STEP TO SUDDEN CHANGE IN OBSTACLE LOCATION AND ORIENTATION"

2. Moraes, R.; *Aftab E. Patla*
University of Waterloo
"STABILITY CONSTRAINT ON ALTERNATE FOOT PLACEMENT DURING HUMAN LOCOMOTION"

3. *Pierre Desjardins*; Nadeau, S.; Gravel, D.; Roy, G.
Centre de Recherche Interdisciplinaire en Réadaptation du Montréal métropolitain
"A CHAIR WITH A PLATFORM SETUP TO MEASURE THE FORCES UNDER EACH THIGH WHEN SEATED; RISING FROM A CHAIR AND SITTING DOWN"

4. *Pierre Desjardins*; Delisle, A.; Plamondon, A.; Salazar, E.; Gagnon, D.
Centre de Recherche Interdisciplinaire en Réadaptation du Montréal métropolitain
"FEASIBILITY OF A 3D RECONSTRUCTION TECHNIQUE USING A SINGLE VIDEO CAMERA"

5. *François Beaulieu*; Pelland, L.; Robertson, D.G.E.
University Of Ottawa
"COMPARISON OF ANKLE; KNEE AND HIP MOMENT POWERS DURING STAIR DESCENT VERSUS LEVEL WALKING"

6. *Xuezhen Liu*; Disheng, X.
Beijing Sport University
"SHOCK ATTENUATION AND KINEMATICS ANALYSIS IN NORMAL WALKING OF THE OLD SOCIAL DANCING EXERCISERS"

7. *Joan Scannell*; Aultman, C.D.; McGill, S.M.
University of Waterloo
"THE DIRECTION OF DISC PROLAPSE IS PREDICTABLE KNOWING THE REPEATED BENDING MOTION CAUSING THE PROLAPSE"

8. *Jessica Preston*; Rees-Milton, K.J.; Anastassiades, T.P.; Wild, P.M.; Wyss, U.P.
Queen's University
"DESIGN OF A MECHANICAL STIMULATION DEVICE FOR CHONDROCYTE SEEDED ALGINATE PUCKS"

9. *Gholamreza Rouhi*; Epstein, M.; Herzog, W.; Sudak, L.
University of Calgary
"GOVERNING EQUATIONS FOR THE PROCESS OF BONE REMODELING USING A MIXTURE THEORY APPROACH: THEORETICAL PREDICTIONS"

10. *Gholamreza Rouhi*; Epstein, M.; Herzog, W.
University of Calgary
"THE ROLE OF GEOMETRIC FEEDBACK AND MICROCRACKS IN BONE REMODELING: THEORETICAL PREDICTIONS"

11. *Julie Nantel*; Brochu, M.B.; Prince, F.P.
University of Montreal
"KINEMATIC AND KINETIC COMPARISON OF OBESE AND NON OBESE CHILDREN DURING SELF-PACED WALKING"

12. *Robyn Wharf*; Robertson, D.G.E.
University of Ottawa
"ACCURACY OF THE CRITICALLY DAMPED AND BUTTERWORTH FILTERS USING THE ACCELERATION OF A FALLING OBJECT"

13. *Christopher MacLean*; van Emmerik, R.; Hamill, J.
University of Massachusetts
"INFLUENCE OF A CUSTOM FOOT ORTHOTIC INTERVENTION ON LOWER EXTREMITY INTRA-LIMB COORDINATION VARIABILITY DURING RUNNING"

14. *Marco Vaz*; Fracao, V.B.; Penz, T.; Da Silveira, E.; Herzog, W.
University of Calgary
"PLANTARFOEXOR TORQUE-ANGLE RELATIONSHIP OF SWIMMERS AND VOLLEYBALL PLAYERS"

15. *Jeffrey Chu*; McKeown, K.A.; Caldwell, G.E.; Hamill, J.
University of Massachusetts
"PRINCIPAL COMPONENT ANALYSIS REVEALS LOWER EXTREMITY CHANGES DURING A 10 KM RUN"

16. *Mike MacLellan*; Pratt, D.; Patla, A.
University of Waterloo
"THE EFFECTS OF A LATERAL PERTURBATION DURING BACKWARDS WALKING"

17. *Ge Wu*; Hitt, J.; Millon, D.
University of Vermont
"LOWER EXTREMITY KINEMATIC
CHARACTERISTICS OF TAI CHI GAIT"

18. *Ge Wu*; Hitt, J.; Millon, D.
University of Vermont
"CHARACTERISTICS OF MUSCLE ACTIVITIES IN
THE LOWER EXTREMITY DURING TAI CHI GAIT"

19. Fortin, C.; *Sylvie Nadeau*; Labelle, H.
Université de Montréal
"INTER-TRIAL AND TEST-RETEST RELIABILITY
OF KINEMATIC AND KINETIC GAIT PARAMETERS
AMONG SUBJECTS WITH ADOLESCENT
IDIOPATHIC SCOLIOSIS"

20. *Cynthia Dunning*; Gordon, K.D.; King, G.J.W.; Johnson,
J.A.
University of Western Ontario
"A MOTION-CONTROLLED DEVICE FOR
ACHIEVING SIMULATED ACTIVE IN-VITRO
ELBOW MOTION"

21. *Nathaly Gaudreault*; Gravel, D.; Nadeau, S.; Houde, S.;
Desjardins, P.
Université de Montréal
"A BIOMECANICAL METHOD TO ASSESS THE
CONTRIBUTION OF PASSIVE MOMENT AT THE
HIP DURING GAIT OF DUCHENNE MUSCULAR
DYSTROPHY CHILDREN"

22. *Mathieu Charbonneau*; Prince, F.
Centre de réadaptation Marie Enfant
"TRUNK CONTROL DURING GAIT WITH ARMS
CROSSED ON THE CHEST IN ADOLESCENT
IDIOPATHIC SCOLIOSIS"

23. *Steven McFaull*; Robertson, G.E.; Post, A.
Health Canada
"MEASUREMENT OF IMPACT FORCES IN A
SIMULATED BICYCLE HANDLEBAR INJURY
CRASH: THE EFFECT OF MASS; IMPACT
VELOCITY AND THE PROPERTIES OF THE
HANDLEBAR ENDS"

24. *Martin Simoneau*; Corbeil, P.
Université Laval
"THE EFFECT OF TIME TO PEAK ANKLE TORQUE
ON BALANCE STABILITY BOUNDARY:
EXPERIMENTAL VALIDATION OF A
MATHEMATICAL MODEL"

25. *Jana Rosenkrancova*; Ruzicka, P.; Sedlacek, R.; Zak, J.
Czech Technical University
"STUDY CONCERNING THE EFFECT OF
CALCITONIN ADMINISTRATION ON THE BONE
STRENGTH OF OVARIECTOMIZED RATS"

26. *James Potvin*; Brown, S.H.M.
University of Windsor
"ENERGY VS MOMENT APPROACH FOR
CALCULATING INDIVIDUAL MUSCLE
CONTRIBUTIONS TO JOINT STABILITY"

27. *Karyn Weiss-Bundy*; Thornton-Trump, A.B.; Chan,
C.Y.A.
University of Calgary
"THREE-DIMENSIONAL VECTOR MODELLING OF
INDIVIDUAL MUSCLE FORCES AT THE ELBOW"

28. *Shirley Rietdyk*
Purdue University
"ANTICIPATORY LOCOMOTOR ADJUSTMENTS OF
THE TRAIL LIMB DURING SURFACE
ACCOMDATION"

29. *Sohrab Behnia*; Ghalichi, F.; Sadigh Rad, E.; Bonabi, A.
IAU
"HYPERTHERMIA TREATMENT OF BREAST
TUMORS APPLYING ULTRASONIC WAVES"

30. *Sebastien Delorme*; Laroche, D.; Holzapfel, G.; Stadler,
M.; Buithieu, J.; DiRaddo, R.
National Research Council Canada - Industrial Material
Institute
"FINITE ELEMENT SIMULATION OF STENT
IMPLANTATION IN A MULTI-LAYER ARTERY
MODEL"

31. *Isam Faik*; Mongrain, R.; Bertrand, O.F.
McGill University
"3D CHARACTERIZATION OF THE WALL SHEAR
STRESS IN A STENTED ARTERY USING MICROPIV
AND CFD"

32. *Chantal Gauvin*; Yousefi, A. M.; DiRaddo, R.;
Fernandes, J.
National Research Council Canada - Industrial Material
Institute
"PERFORMANCE OF POLYMER-TISSUE
CONSTRUCTS IN FUNCTIONAL TISSUE
ENGINEERING"

4:00pm – 5:30pm
Sessions 5a & 5b

Session 5a - Sport Biomechanics Symposium

Location: Atlantic Ballroom

Opening Remarks:
Dr. J. Hamill, Univ. of Massachusetts
Dr. G. Robertson, University of Ottawa

Irene McClay Davis, Ph.D.
University of Delaware
"THE USE OF REAL TIME TIME FEEDBACK TO TRAIN RUNNERS"

Darren Stefanyshyn, Ph.D; Lee, J.-S.; Park, S.-K.; Savage, L.
University of Calgary
"THE INFLUENCE OF SOCCER CLEAT DESIGN ON KNEE MOMENTS"

Graham Caldwell, Ph.D.
University of Massachusetts
"CYCLING BIOMECHANICS – WHERE DO WE GO FROM HERE?"

Gordon Robertson, Ph.D.
University of Ottawa.
"FUTURE DIRECTIONS IN SPORT BIOMECHANICS"

Session 5b - Posture

Location: Commonwealth B
Session Chairs: Aftab Patla, Genevieve Dumas

4:00 – 4:15	*Ewald Hennig*; Beierle, T.; Sterzing, T. University Duisburg – Essen "TOUCH SENSITIVITY THRESHOLDS ACROSS THE DORSAL AND PLANTAR SURFACES OF HUMAN FEET"
4:15 – 4:30	*Charles Cejka*; Patla, A.E. University of Waterloo "GALVANIC VESTIBULAR STIMULATION AFFECTS WHOLE-BODY CENTER OF MASS AND VISUAL-VESTIBULAR SIGNAL INTEGRATION DURING PERTURBED LOCOMOTION"
4:30 – 4:45	*Prism Schneider*; Wakeling, J.M.; Zernicke, R.F. University of Calgary "EFFECT OF DYNAMIC ANKLE JOINT STIFFNESS ON POSTURAL STABILITY"
4:45 – 5:00	*Fabiola Goncalves*; Cheng, P.L.; Leger, A.; Dumas, G.A. Queen's University "POSTURE OF WOMEN STANDING ON AN INCLINE"
5:00 – 5:15	Centomo H.; *Serge Savoie*; Lafond, D.; Prince, F. University of Montreal "POSTURAL RESPONSE FOLLOWING SELF-INITIATED PERTURBATION IN TYPE 2 DIABETIC PATIENTS AND HEALTHY ELDERLY"
5:15 – 5:30	**Michal Kuczynski**; Paluszak, A. Academy of Physical Education, Poland "ADDITIONAL VISUAL CUE ATTENUATES POSTURAL SWAY: IMPLICATIONS FOR PREVENTING FALLS"

5:30pm – 7:30pm
Student Mentoring Session & Mixer
All students are welcome for post-session refreshments and snacks.

Location: Atlantic Ballroom

Friday August 6, 2004

8:00am – 9:10am
Career Award
Location: Atlantic Ballroom

8:00 – 8:10 *Ronald Zernicke, President of the Canadian Society of Biomechanics*
University of Calgary
CAREER AWARD INTRODUCTION

8:10 – 9:10 *Stuart McGill, Ph.D.*
University of Waterloo
"BUILDING THE ULTIMATE BACK: A JOURNEY IN PROGRESS"

9:15am – 10:15am
Parallel Sessions 6a & 6b

	Session 6a – Spine Location: Atlantic Ballroom Session Chairs: Jack Callaghan, Tim Bryant	Session 6b - Muscle 2 Location: Commonwealth B Session Chairs: Linda Maclean, Jennifer Durkin
9:15 – 9:30	*Gordon Alderink* Grand Valley State University "COUPLING OF SIDEBENDING AND AXIAL ROTATION IN THE THORACIC SPINE"	*Cintia Freitas*; Brentano, M.A.; Herzog, W.; Vaz, M.A. University of Calgary "MECHANOMYOGRAPHIC SIGNALS OF THE FIRST DORSAL INTEROSSEOUS AND VASTUS LATERALIS MUSCLES DURING ISOMETRIC CONTRACTIONS"
9:30 – 9:45	*Robert Parkinson*; Durkin, J.L.; Callaghan, J.P. University of Waterloo "PREDICTING THE FAILURE STRENGTH OF PORCINE CERVICAL SPINAL UNITS USING BONE MINERAL CONTENT AND ENDPLATE AREA"	*Usha Kuruganti*; Rickards, J. University of New Brunswick "A COMPARISON OF BILATERAL LIMB DEFICIT IN YOUNGER AND OLDER ADULTS DURING DYNAMIC KNEE EXTENSIONS"
9:45 – 10:00	*Natasa Kavcic*; Grenier, S.; McGill, S. University of Waterloo "QUANTIFYING TISSUE LOADS AND SPINE STABILITY WHILE PERFORMING COMMONLY PRESCRIBED LOW BACK STABILIZATION EXERCISES"	*Michael Agnew*; McLean, L. Queen's University "INVESTIGATING THE MORPHOLOGY AND FIRING CHARACTERISTICS OF EXTENSOR CARPI RADIALIS (ECR) MOTOR UNITS DURING LOW-LEVEL CONTRACTIONS IN HEALTHY SUBJECTS"
10:00 – 10:15	*Einas Al-Eisa*; Egan, D.A.; Deluzio, K.; Wassersug, R. Dalhousie University PELVIC SKELETAL ASYMMETRY AND ASYMMETRY IN SELECTED TRUNK MOVEMENTS: THREE-DIMENSIONAL ANALYSIS IN HEALTHY INDIVIDUALS AND PATIENTS WITH MECHANICAL LOW BACK PAIN."	*Ait-Haddou Rachid*; Herzog, W. University of Calgary "ON THE COLLECTIVE BEHAVIOR OF THE MYOSIN II MOTOR AND MUSCLE CONTRACTION"

10:15am – 10:30pm
Refreshment Break & Exhibitor Viewing (Commonwealth A)

10:30am – 12:00pm
Sessions 7a & 7b

Session 7a - Occupational Biomechanics Symposium	**Session 7b - Rehabilitation**
Location: Atlantic Ballroom	**Location: Commonwealth B** **Session Chairs: Sylvie Nadeau, Lee Kirby**

<table>
<tr>
<td valign="top" width="45%">

Opening Remarks:
Dr. J. Kozey, Dalhousie University,
Dr. W. Albert, University of New Brunswick

Sue Pettit, MSc, CCPE.
Ergonomist
"NOVA SCOTIA ENVIRONMENT AND LABOUR PROVIDE A USERS PERSPECTIVE ON BIOMECHANICALLY DERIVED STANDARDS"

Jack Callaghan, Ph.D.
University of Waterloo
"WHAT ACCURANCY IS REQUIRED IN BIOMECHANICAL MEASURES TO PREVENT INJURIES?"

Joan Stevenson, Ph.D.
Queen's University
"LINKING SEGMENTS: MODELS FOR SUCCESS"

Anne Moore, Ph.D.
York University
"WHY DO WE DO THIS? LINKING OCCUPATIONAL BIOMECHANICAL RESEARCH WITH THE REAL WORLD FOR THE OCUPATIONAL BIOMECHANICS"

</td>
<td valign="top" width="55%">

10:30 – 10:45   *Anabèle Brière*; Nadeau, S.; Gravel, D.
Université de Montréal
"HIP PASSIVE STIFFNESS MEASURES IN HEALTHY SUBJECTS: A RELIABILITY STUDY"

10:45 – 11:00   *Lee Kirby*; Smith, C.; Best, K.L.; Corkum, C.G.; MacLeod, D.A.
Dalhousie University
"WHEELCHAIR SKILLS TESTING AND TRAINING: PROTOCOLS FOR CLINICAL AND RESEARCH PURPOSES"

11:00 – 11:15   *Mary Beshai*; Bryant, J.T.; Gabourie, R.
Queen's University
"GENERALIZED METHOD FOR SIZING TRANSTIBIAL PROSTHETIC SOCKETS IN HOMOGENEOUS POPULATIONS"

11:15 – 11:30   *Colleen Higgs*; Bryant, J.T.; Gabourie, R.; Mechefske, C.K.
Queen's University & Human Mobility Research Centre (Kingston General Hospital)
"A PLANAR KINEMATIC MODEL OF SWING PHASE FOR TRANSFMORAL PROSTHETIC SYSTEMS"

11:30 – 11:45   *Jon Doan*; Whishaw, I.Q.; Pellis, S.M.; Suchowersky, O.; Brown, L.A.
University of Lethbridge
"REACH MOVEMENT IN PARKINSON'S DISEASE: EFFECTS OF DEMAND, MEDICATION, AND PLANNING"

11:45 – 12:00   *Hugo Centomo*; Prince, F.
University of Montreal
"POSTURAL CONTROL IN TRANS-TIBIAL AMPUTEES"

</td>
</tr>
</table>

12:00pm – 2:00pm
Box Lunch (Commonwealth A)
Lab Tours & Wheelchair Workshop

2:00pm – 3:00pm
Parallel Sessions 8a & 8b

	Session 8a - Locomotion 2	Session 8b - Ergonomics 1
	Location: Atlantic Ballroom **Session Chairs:** **Stephen Perry, Brad McFadyen**	**Location: Commonwealth B** **Session Chairs:** **Joan Stevenson, Andre Plamondon**
2:00 – 2:15	Jeffrey Holmes, J.; Flynn, J.M.; *David M. Andrews* University of Western Ontario "THE MASSES OF RIGID AND WOBBLING LEG TISSUES CONTRIBUTE LITTLE TO TIBIAL RESPONSE PARAMETERS FOLLOWING HEEL IMPACT"	*Heather Brackley*; Stevenson, J.M. Queen's University "THE EFFECT OF LOAD PLACEMENT AND FATIGUE ON SPINAL CURVATURE AND POSTURE IN PREPUBESCENT CHILDREN"
2:15 – 2:30	Rao, G.; *David Amarantini*; Berton, E.; Favier, D. Université de la Méditerranée "INFLUENCE OF ANTHROPOMETRIC PREDICTION MODELS ON INVERSE DYNAMICS SOLUTIONS"	*Greg Northey*; Oliver, M. University of Guelph THE EFFECTS OF STIFFNESS AND SPEED ON UPPER LIMB ELECTROMYOGRAPHY DURING JOYSTICK USE"
2:30 – 2:45	*Katherine Boyer*; Nigg, B.M. University of Calgary "MOVEMENT WITHIN THE SOFT TISSUE PACKAGE DURING IMPACT PHASE OF RUNNING"	*James Potvin*; Cort, J.A.; Calder, I.C.; Agnew, M.J. University of Windsor "TOLERANCE LIMIT VALUES FOR MANUAL ELECTRICAL CONNECTOR TASKS"
2:45 – 3:00	*Jeremy Noble*; Prentice, S.D. University of Waterloo "ADAPTATION TO UNILATERAL CHANGES IN LOWER LIMB MECHANICAL PROPERTIES DURING TREADMILL WALKING"	*Gillian Del Monte*; Moore, A.E. York University "THE EFFECT OF WORK PAUSES AND TYPING RATE ON THE BIOMECHANICAL DUTY CYCLE"

3:00pm – 4:00pm
Session 9 – Posters and Refreshment Break
Location: Commonwealth A

1. *Samuel Howarth*; McGill, S.M.
   University of Waterloo
   "SHEAR INSTABILITY OF THE L4-L5 JOINT: EXAMINATION OF SPINAL MUSCULATURE REINFORCEMENT POTENTIAL"

2. *Stephen Brown*; Potvin, J.R.
   University of Waterloo
   "ANTAGONIST MUSCLE FORCES PREDICTED BY AN OPTIMIZATION MODEL OF THE SPINE USING STABILITY AS A CONSTRAINT FACTOR"

3. *Allan Wrigley*; Albert, W.J.; Deluzio, K.J.; Stevenson, J.M.
   University of New Brunswick
   "DIFFERENTIATING LIFTING TECHNIQUE BETWEEN THOSE WHO DEVELOP LOW BACK PAIN AND THOSE WHO DO NOT"

4. *Karyn Weiss-Bundy*; Thornton-Trump, A.B.
   University of Calgary
   "THE SCALING OF THE ANATOMY OF THE BONES OF THE HUMAN ARM"

5. *Angela Tate*; Molgaard, J.
   Memorial University of Newfoundland
   "MEASURING BIOMECHANICAL EXPOSURES DURING SNOW CRAB BUTCHERING"

6. *Steven McFaull*
   Health Canada
   "INJURIES AMONG YOUNG GIRLS (5-14 YEARS) ENGAGED IN COMPETITIVE GYMNASTICS: DATA FROM THE CANADIAN HOSPITALS INJURY REPORTING AND PREVENTION PROGRAM (CHIRPP); 1998-2002"

7. *Scott MacKinnon*; Vaughan, C.L.
   Memorial University of Newfoundland
   "THORACO-LUMBAR KINEMATICS DURING SINGLE LIMB PULLING EXERTIONS"

8. *Brad Monteleone*; Ronsky, J.L.; Meeuwisse, W.H.; Zernicke, R.F.
   University of Calgary
   "EFFECTS OF FUNCTIONALANKLE INSTABILITY ON LANDING KINETICS DURING A LATERAL HOP MOVEMENT"

9. *Alison Godwin*; Eger, T.; Salmoni, A.
   Laurentian University
   "COMPUTER-AIDED DESIGN TO INVESTIGATE LINE-OF-SIGHT AND POSTURAL DEMANDS ON MINING EQUIPMENT"

10. *Julie Cote*; Therrien, M.; Lacoste, M.; Prince, F.
    McGill University
    "DEVELOPMENT OF A CLINICAL MEASURE OF CENTER OF PRESSURE IN SITTING"

11. *Sang Kyoon Park*; Stefanyshyn, D.J.
    University of Calgary
    "INFLUENCE OF Q-ANGLE ON LOWER EXTREMITY MOMENTS DURING RUNNING"

12. *Evelyn Morin*; Stevenson, J.M.; Reid, S.A.; Hare, C.; Bryant, J.T.
    Queen's University
    "THE EFFECT OF ACCELEROMETER PLACEMENT ON ENERGY COST ESTIMATES FOR TREADMILL WALKING AT DIFFERENT SPEEDS AND INCLINES"

13. *Anita Lee*; Bouchard, D.E.; Morin, E.L.
    Royal Military College of Canada
    "ASSESSMENT OF RELATIVE MOTION BETWEEN A BACKPACK AND TORSO FOR DIFFERENT LOADS"

14. *Hongfa Wu*; Poncet, P.; Harder, J.; Chariet, F.; Labelle, H.; Zernicke, R.F.; Ronsky, J.L.
    University of Calgary
    "A QUANTITATIVE CLASSIFICATION TO DETERMINE EXTENT OF SPINAL ARTHRODESIS FOR ADOLESCENT IDIOPATHIC SCOLIOSIS"

15. *Kim McLaughlin*; Dhar, P.; Baker, N.; Ronsky, J.
    University of Calgary
    "IN VIVO ASSESSMENT OF CONGRUENCE IN THE PATELLOFEMORAL JOINT OF HEALTHY SUBJECTS"

16. *Bryan Donnelly*; Ronsky, J.; Gill, R.
    University of Calgary
    "TWO NOVEL TECHNIQUES FOR ERROR REDUCTION IN RSA"

17. *Gye-Rae Tack*; Cole, G.; Nigg, B.
    University of Calgary
    "NARMAX AND ARMAX REPRESENTATION OF DYNAMICS OF ROBOT FOR SHOE TESTING"

18. *Jonathan Singer*; Robertson, D.G.E.
    University of Ottawa
    "DEVELOPMENT OF A NEW METHOD TO DETERMINE KNEE VARUS/VALGUS"

19. *Daniela Robu*; Poncet, P; Cheriet, F; Zernicke,R.; Ronsky, J.
University of Calgary
"OPTICAL IMAGING TECHNIQUES AND STEREO-RADIOGRAPHY APPLIED IN 3D RECONSTRUCTION OF SCOLIOTIC HUMAN TORSO"

20. Lockwood, K.; *Gail Frost*; Brown, A.
Brock University
"HABITUATION OF 10-YEAR-OLD HOCKEY PLAYERS TO TREADMILL SKATING"

21. Moreau, M.; *Pierre Gervais*
University of Alberta
"A KINETMATIC ANALYSIS OF AN ULTRA-MARATHON RUN"

22. *Pierre Gervais*; Wu, T.; LeBlanc, J.S.
University of Alberta
"A COMPARISON OF THREE BACK HANDSPRING PROGRESSIONS"

23. *Carol Murphy*; Brackley, H.; Abdoli, M.; Stevenson, J.
Queen's University
"CHILDREN'S WORKSTATIONS: POSTURAL CHANGES DURING COMPUTER GAMES"

24. *John S. LeBlanc*; Gervais, P.L.
University of Alberta
"ANGULAR KINEMATICS IN ASSISTED AND RESISTED SPRINTING AS COMPARED TO FREE SPRINTING"

25. *Philippe Poncet*; Robu, D.; Jaremko, J.; Harder, J.; Cheriet, F.; Zernicke, R.F.; Ronsky, J.L.
University of Calgary
"COMPARISON OF CHANGES IN TORSO SHAPE ASYMMETRY AND SPINAL DEFORMITY OF SCOLIOTIC SUBJECTS BEFORE AND AFTER SURGERY"

26. *Robert Jack*; Eger, T.; Reed, L.; Whissell, C.
Laurentian University
"THE EFFECTS OF DIFFERENT POSTURES AND ADIPOSE CONTENT ON THE BIODYNAMIC RESPONSE OF THE HUMAN SPINE TO WHOLE-BODY VIBRATION"

27. *Heather Butler*; Kozey, J.; Hubley-Kozey, C; Aquirre, J.
Dalhousie University
"CHANGES IN PELVIC AND LUMBAR ANGLES WHILE PERFORMING THE POSTERIOR PELVIC TILT AND ABDOMINAL HOLLOWING MANEUVER DURING NORMAL AND MAXIMUM REACH LIFTS"

28. Kenny-Scherber, C.; *Mike Greig*; Patla, A.
University of Waterloo
"EVALUATING THE PENALTY FUNCTION IN A ROBOTIC STEP ADJUSTMENT ALGORITHM"

4:00pm – 5:30pm
Parallel Sessions 10a & 10b

	Session 10a New Investigators Award Location: Atlantic Ballroom Session Chairs: Stephen Prentice, Benno Nigg	Session 10b Ergonomics 2 Location: Commonwealth B Session Chairs: Jim Potvin, Anne Moore
4:00 – 4:15	*Tim Leonard*; Herzog, W. University of Calgary "DOES FORCE DEPRESSION IN SKELETAL MUSCLE DEPEND ON THE SPEED OF SHORTENING?"	*Sabrina Sarno*; Potvin, J. University of Windsor "A BIOMECHANICAL EVAULATION OF CHILD SAFETY SEAT INSTALLATION: REAR AND FORWARD FACING"
4:15 – 4:30	*Nicolas Hamilton*; Coombe, D.; Tran, D.; Zernicke, R.F. University of Calgary "LOAD INDUCED FLUID FLOW SIMULATION IN CORTICAL BONE"	*J. Timothy Bryant*; Reid, S.A.; Stevenson, J.M.; Abdoli, M. Queen's University "3D DYNAMIC MODEL OF BIOMECHANICAL FACTORS IN LOAD CARRIAGE"
4:30 – 4:45	*Tyson Beach*; Parkinson, R.J.; Stothart, J.P.; Callaghan, J.P. University of Waterloo "PASSIVE LUMBAR FLEXION STIFFNESS IS ALTERED WITH EXPOSURE TO PROLONGED SITTING"	*Steven Carcone*; Keir, P.J. York University "EFFECTS OF BACKREST DESIGN ON COMFORT AND BIOMECHANICS OF SEATING."
4:45 – 5:00	*Danny Peterson*; Kaya, M.; Herzog, W. University of Calgary "BIOMECHANICAL PROPERTIES WHICH INFLUENCE JUMPING PERFORMANCE IN THE FROG: RANA PIPIENS"	*Donald Russell*; Kendler, O.; Bass, J. Carleton University "DESIGN SPECIFICATIONS FOR AN ACTIVE COMPLIANT SURFACE FOR USE AS AN ABDOMINAL SIGN SIMULATOR"
5:00 – 5:15	*Scott Landry*; McKean, K.A.; Hubley-Kozey, C.L.; Stanish, W.D.; Deluzio, K.J. Dalhousie University "EFFECT OF WALKING SPEED ON KNEE BIOMECHANICS IN A MODERATE KNEE OSTEOARTHRITIC AND ASYMPTOMATIC POPULATION"	*Joan Stevenson*; Morin, E.L.; Johnston, C.L.; Janssen, I.M.; Bryant, J.T.; Reid, S.A. Queen's University "THE EFFECT OF LOAD; SPEED AND INCLINE ON OXYGEN CONSUMPTION DURING LOAD CARRIAGE"
5:15 – 5:30	*Jeremy Mogk*; Keir, P.J. York University "A COMPUTER-GENERATED MODEL OF CARPAL TUNNEL MECHANICS"	

5:30pm – 6:30pm
Annual General Meeting
Location: Atlantic Ballroom

Saturday August 7, 2004

9:00am – 10:00am
Parallel Sessions 11a & 11b

	Session 11a - Osteoarthritis 1	Session 11b - Muscle 3
	Location: Atlantic Ballroom **Session Chairs:** **William Stanish, Ronald Zernicke**	**Location: Commonwealth B** **Session Chairs:** **Jack Callaghan, Walter Herzog**
9:00 – 9:15	*Monica Maly*; Costigan, P.A.; Olney, S.J. Queen's University "KNEE KINEMATICS; KNEE KINETICS AND HIP KINETICS IN MEDIAL COMPARTMENT KNEE OA."	*Timothy Butterfield*; Herzog, W. University of Calgary "THE EFFECT OF MUSCLE ACTIVATION TIMING ON FIBER STRAIN DURING ECCENTRIC CONTRACTIONS"
9:15 – 9:30	*Cheryl Hubley-Kozey*; Deluzio, K.; Landry, S; McNutt, J.; Agarabi, M.; Stanish, W. Dalhousie University "MEDIAL AND LATERAL MUSCLE ACTIVATION DIFFERENCES BETWEEN HEALTHY CONTROLS AND MODERATE KNEE OSTEOARTHRITIC GAIT"	*Mir Ali Eteraf Oskouei*; Rousanoglou, E.N.; Herzog, W. University of Calgary "HISTORY DEPENDENT FORCE PRODUCTION IN SUB-MAXIMAL HUMAN VOLUNTARY CONTRACTIONS"
9:30 – 9:45	*Kevin Deluzio*; Landry, C.S.N.; Astephen, J.A.; Hubley-Kozey, C.L.; Stanish, W.D.; Dunbar, M.J. Dalhousie University "KNEE BIOMECHANICS OF MODERATE AND SEVERE KNEE OSTEOARTHRITIS PATIENTS"	*Jennifer Durkin*; Callaghan, J.P. University of Waterloo "EFFECTS OF OVERSAMPLING AND SIGNAL RECONSTRUCTION ON SURFACE ELECTROMYOGRAPHIC SIGNALS"
9:45 – 10:00	*LePing Li*; Herzog, W. University of Calgary "ELECTROMECHANICAL RESPONSE OF ARTICULAR CARTILAGE IN CONTACT WITH AN ARTHROSCOPIC PROBE"	*David Amarantini*; Martin, L.; Cahouët, V. Université de la Méditerranée "OPTIMIZATION-BASED PROCEDURES FOR THE PREDICTION OF JOINT MUSCULAR EFFORTS"

10:00am – 10:15pm
Refreshment Break & Exhibitor Viewing (Commonwealth A)

Session 12a **Osteoarthritis Symposium** *Sponsored by the Institute of* *Musculoskeletal Health and Arthritis* **Location: Atlantic Ballroom**	**Session 12b** **Ergonomics 3** **Location: Commonwealth B** **Session Chairs: Wayne Albert, David Andrews**
Opening Remarks: **Dr. K. Deluzio, Dalhousie University,** **Dr. J. Ronsky, University of Calgary** *W.D. Stanish, MD* Dalhousie University INTRODUCTION TO THE PROBLEM *H.S. Gill, Ph.D.* Oxford University "PATHOMECHANICS OF KNEE OSTEOARTHRITIS – CAN GAIT EXPLAIN IT?" *K. Deluzio, Ph.D.* Dalhousie University "MECHANICAL FACTORS OF KNEE OSTEOARTHRITIS DETECTED THROUGH GAIT ANALYSIS" *J. Ronsky, Ph.D.* University of Calgary "NEW INSIGHTS INTO OSTEOARTHRITIS USING NOVEL IMAGING MODALITIES, AND ROBOTICS" *W.D. Stanish, MD* Dalhousie University "THE CLINICAL PERSPECTIVE ON THE ROLE OF NON-INVASIVE TREATMENTS"	10:15 – 10:30 *Mei Wang*; Leger, A.L.; Dumas, G.A.D. Queen's University "PREDICTION OF BACK STRENGTH USING ANTHROPOMETRIC AND STRENGTH MEASUREMENTS IN HEALTHY FEMALES" 10:30 – 10:45 *Andre Plamondon*; Delisle, A.; Trimble, K.; Desjardins, P. Institut de reherche Robert-Sauvé en santé et en sécurité du travail "THE EFFECT OF ROD HEIGHTS AND FEET POSITIONS WHEN LIFTING ITH RODS" 10:45 – 11:00 *Diane Gregory*; Kavcic, N.; Dunk, N.; McGill, S.; Callaghan, J. University of Waterloo "THE LUMBAR RESPONSES OF SITING ON A STABILITY BALL AND IN AN OFFICE CHAIR" 11:00 – 11:15 *Diane Grondin*; Potvin, J.R. University of Windsor "EFFECTS OF TRUNK MUSCLE FATIGUE AND LOAD TIMING ON SPINE MECHANICS DURING SUDDEN HAND LOADING" 11:15 – 11:30 *Mohammad Abdoli E.*; Kamalzadeh, A.; Stevenson, J.; Agnew, M. Queen's University "PROOF OF PRINICPLE FOR A PERSONAL LIFTING ASSIST DEVICE" 11:30 – 11:45 *Scott MacKinnon*; Holmes, M.; Behm, D. Memorial University of Newfoundland "EFFECTS OF PLATFORM MOTION ON THORACO-LUMBAR KINEMATICS DURING LIFTING EXERTIONS"

12:00pm – 1:00pm
Lunch (Commonwealth A)

1:00pm –2:30pm
Parallel Sessions 13a & 13b

	Session 13a - Locomotion 3	Session 13b - Spine 2
	Location: Atlantic Ballroom **Session Chairs:** **H.S. Gill, Darren Stefanyshyn**	**Location: Commonwealth B** **Session Chairs:** **Stuart McGill, Cheryl Kozey**
1:00 – 1:15	*François Beaulieu*; Pelland, L.; Robertson, D.G.E. University Of Ottawa "COMPARISON OF MOMENT POWERS PRODUCED DURING FORWARD AND BACKWARD STAIR DESCENT"	*Jeremy LaMothe*; Reimer, R.; Zernicke, R. University of Calgary "GENETIC-RELATED OBESITY DOES NOT ADVERSELY AFFECT BONE MECHANICAL AND MORPHOMETRICAL PROPERTIES"
1:15 – 1:30	*Andrea Hemmerich*; Brown, H.; Knutson, A.; Marthandam; S.S.K.; Wyss; U Queen's University "THREE-DIMENSIONAL KINEMATIC AND KINETIC ANALYSIS OF ACTIVITIES OF DAILY LIVING IN INDIA"	*Simon Wang*; Hentschel, E.P.; McGill, S.M. University of Waterloo "LINKING VENTILATION MECHANICS WITH SPINE STABILITY: NORMAL AND PATIENTS"
1:30 – 1:45	*T. Claire Davies*; Patla, A.E. University of Waterloo "OBSTACLE AVOIDANCE STRATEGIES USING A SONIC PATHFINDER"	*Nadine Dunk*; Brown, S.H.M.; Callaghan, J.P. University of Waterloo "DISTRIBUTION OF TISSUE LOADS SUPPORTING THE LOW BACK DURING THE FLEXION RELAXATION PHENOMENON IN SITTING AND STANDING POSTURES"
1:45 – 2:00	*Erika Hasler*; Carney-Kilian, B.F.D.; Prentice, S.D. University of Waterloo "LOCOMOTOR ADAPTATIONS TO TRUNK LOADING DURING VOLUNTARY GAIT MODIFICATIONS"	*Einas Al-Eisa*; Egan, D.A.; Deluzio, K.; Wassersug, R. Dalhousie University "OBJECTIVE MEASUREMENT OF TRUNK MOTION PATTERNS IN HEALTHY INDIVIDUALS AND PATIENTS WITH MECHANICAL LOW BACK PAIN."
2:00 – 2:15	*Stephen Perry*; Radtke, A.; Goodwin, C. Wilfrid Laurier University "UNEVEN TERRAIN AS A PERTURBATION TO THE CENTRE OF MASS MOTION DURING LOCOMOTION."	*Janessa Drake;* Aultman, C.D.; McGill, S.M.; Callaghan, J.P. University of Waterloo "THE ROLE OF TORSION IN INTERVERTEBRAL JOINT FAILURE MECHANICS"
2:15 – 2:30	*Victoria Chester*; Biden, E.; Tingley, M. University of New Brunswick "THE IDENTIFICATION OF CLINICALLY RELEVANT GAIT VARIABLES IN CHILDREN WITH HYPOTONIA"	*Christina Godin*; Andrews, D.; Callaghan, J.P. University of Windsor "3D TRUNK POSTURES AND CUMULATIVE LOW BACK LOADS DURING NON-OCCUPATIONAL TASKS"

2:30pm – 3:30pm
Session 14 – Posters and Refreshment Break

1. *Thorsten Sterzing*; Uttendorfer, M.; Hennig, E.M.
University of Duisburg – Essen
"FOOT MAPPING OF VIBRATION SENSITIVITY THRESHOLDS"

2. *David Corr*; Herzog, W.
University of Calgary
"A CROSS-BRIDGE-BASED MODEL OF FORCE DEPRESSION: INSIGHTS INTO THE UNDERLYING MECHANISMS"

3. M. Gregor; *Uwe Schomburg*
Helmut-Schmidt-Universität
"BIOMECHANICAL BEHAVIOR OF MUSCLES IN THE ABDOMINAL WALL REINFORCED BY A POLYMER MESH"

4. *Mehrdad Anbarian*; Allard, P.; Hinse, S.; Farahpour, N.; Fall Diagne, A.; Tanaka, C.
University of Montreal
"FOOT TYPE CLASSIFICATION USING DISCRIMINANT FUNCTION ANALYSIS"

5. *Andrew Betik*; Herzog, W.
University of Calgary
"FORCE-LENGTH RELATIONSHIP OF MOUSE SOLEUS AND OPTIMAL STIMULATION PARAMETERS FOR FORCE ENHANCEMENT PROTOCOLS"

6. *Nicolas Termoz*; François, P.
University of Montreal
"DETERMINATION OF CRITICAL TRANSITORY PERIODS IN POSTURAL CONTROL OVER THE ENTIRE LIFE"

7. *Christopher Hasson*; Merrell, R.E.; van Emmerik, R.E.A.; Caldwell, G.E.
University of Massachusetts
"CHANGES IN MONO- AND BIARTICULAR MUSCLE ACTIVATION PATTERNS WHILE LEARNING TO DIRECT PEDAL FORCES"

8. *Beate Praetorius*; Milani, T.L.
University of Duisburg-Essen
"SENSITIVITY OF THE PLANTAR FOOT IN DIFFERENT AGE GROUPS"

9. *Nandini Deshpande*; Patla, A.E.
University of Waterloo
"POSTURAL RESPONSES IN FRONTAL PLANE TO STEPWISE MONOPOLAR ANODAL GVS"

10. *Radek Sedlacek*; Rosenkrancova, J.
Czech Technical University
"EXPERIMENTAL ANALYSIS OF TRIBOLOGICAL PROPERTIES OF BIOMATERIALS USED FOR ORTHOPEDIC IMPLANTS"

11. *Félix Berrigan*; Simoneau, M.
Université Laval
"ADAPTABILITY OF THE POSTURAL CONTROL MECHANISMS TO DELAYED TEMPORAL RELATIONSHIP BETWEEN THE MOTOR ACTION AND ITS CONSEQUENCES"

12. *Jordan Thornley*; Robertson, D.G.E.
University of Ottawa
"COMPARISON OF LOADED AND UNLOADED RAMP DESCENT"

13. *John Gray*; Skaggs, C.D.; McGill, S.M.
University of Waterloo
"DIGASTRIC MUSCLE ACTIVITY: EVIDENCE FOR A ROLE IN NECK FLEXION?"

14. *Dany Gagnon*; Nadeau, S.; Gravel, D.; Noreau, L.
University of Montreal
"EFFECTS OF HAND PLACEMENT STRATEGIES ON MOVEMENT PATTERNS AND MUSCULAR DEMANDS DURING A POSTERIOR TRANSFER IN INDIVIDUALS WITH SPINAL CORD INJURY"

15. *Christopher Goodwin*; Pierrynowski, M.R.
McMaster University
"A BIOMECHANICAL MEASURE TO ASSESS GAIT ECONOMY AND TREATMENT OUTCOME IN RHEUMATOID ARTHRITIS PATIENTS"

16. Haddad, J.; *Joseph Seay*; van Emmerik, R.E.A.; Hamill, J.
University of Massachusetts
"SYMMETRY IN BETWEEN LIMB COORDINATION DURING GAIT TRANSITIONS"

17. *Joseph Seay*; Haddad, J.M.; van Emmerik, R.E.A.; Hamill, J.
University of Massachusetts
"COORDINATION VARIABILITY IN THE GAIT TRANSITION REGION: EFFECTS OF VARYING SPEED INTERVALS"

18. *Graham Caldwell*; Eck, K.A.; King, M.A.; Yeadon, M.R.
University of Massachusetts
"EFFECTS OF MUSCLE MODEL PO VALUES ON SIMULATED JUMPING PERFORMANCE"

19. *Molly Johnson*; Remelius, J.G.; van Emmerik, R.E.A.; Hamill, J.
University of Massachusetts
"POSTURAL ASYMMETRIES DURING QUIET AND UNCONSTRAINED STANDING"

20. *Michael Greig*; Patla, A.E.; Lewis, A.M.
University of Waterloo
"CHARACTERIZING STEP WIDTH AND STEP LENGTH ADJUSTMENTS FOR THE IMPLEMENTATION IN ROBOTIC LOCOMOTION CONTROL"

21. *Heidi-Lynn Ploeg*; Ploeg, L.; Byrne, N.; Garcia, S.; Kersh, M.; Nair; D.
University of Wisconsin
"HOW ACCURATE ARE SOLIDS MODELS MADE FROM CT SCAN DATA?"

22. *Andrew Post*; Robertson, D.G.E.
University of Ottawa
"COMPARISON OF RAMP AND STAIR DESCENT"

23. *John Zettel*; Peters, A.; Holbeche, A.; Chung, Y.; McIlroy, W.E.; Maki, B.E.
University of Toronto
"ROLE OF VISION AND VISUAL ATTENTION IN THE CONTROL OF RAPID STEPPING REACTIONS TRIGGERED BY POSTURAL PERTURBATION"

24. *Sandra Prentice*; Cinelli, M.; Patla, A.
University of Waterloo
"STRATEGIES TO AVOID COLLISION WITH MOVING DOORS"

25. *David Sanderson*; Martin, P.E.
University of British Columbia
"INTERACTION BETWEEN GASTROCNEMIUS AND SOLEUS DURING STEADY-RATE CYCLING"

26. *Gordon Robertson*; Lynch, J.
University of Ottawa
"COMPARISON OF LOADED AND UNLOADED STAIR DESCENT"

27. Nuño, N.; *Dominic Plamondon*
Université du Québec
"ON THE MEASUREMENT OF RESIDUAL STRESSES DUE TO CEMENT POLYMERIZATION PERTINENT TO CEMENTED HIP IMPLANTS"

28. *Fariba Bahrami*; Hill, S.; Patla, A.
University of Waterloo
"RECOVERY FROM AN UNEXPECTED RIGHTWAY PUSH DURING WALKING ON A LATERALLY CONSTRAINED WALKWAY"

29. *Fariba Bahrami*; Hill, S.; Patla, A.
University of Waterloo
"STABILITY ANALYSIS OF MEDIO-LATERALLY PERTURBED GAIT"

30. *Mina Agarabi*; Hubley-Kozey, C.; Deluzio, K.; Landry, S.; McNutt, J.; Stanish, W.
Dalhousie University
"THE QUANTIZATION OF THE THREE QUADRICEPS MUSCLES BETWEEN TWO WALKING CONDITIONS"

31. *K. Polgar*; Murray, D.W.; O'Connor, J.J.; Gill, H.S.
University of Oxford
"FE MODELLING OF DYNAMICALLY INDUCED MICROMOTION FOR A POLISHED THR STEM"

32. *Xiang Liu*; Kim, W.; Drerup, B.
Nanyang Technological University
"3D CHARACTERIZATION AND LOCALIZATION OF ANATOMICAL LANDMARKS OF THE FOOT"

33. Vickers, J.; *Janet Ronsky*; Ramage, B.; Morton, T.B.; Park, S.
University of Calgary
"GAZE STABILIZATION OF BALANCE WITH AND WITHOUT AN ANKLE FOOT ORTHOSIS: A PILOT STUDY"

34. Park, J.S.; *Sharon Bullimore*; Leonard, T.R.; Herzog, W.
University of Calgary
"CONTRACTILE HISTORY INFLUENCES THE FORCE-VELOCITY RELATIONSHIP OF SKELETAL MUSCLE"

3:30pm – 4:30pm
Parallel Sessions 15a & 15b

	Session 15a - Osteoarthritis 2	Session 15b - Sport 2
	Location: Atlantic Ballroom **Session Chairs: Urs Wyss, Kevin Deluzio**	**Location: Commonwealth B** **Session Chairs: Benno Nigg, Joe Hamill**
3:30 – 3:45	Mohammad Alghamdi; Olney, S; *Costigan, P.A.* King Faisal University "SIT-TO-STAND ANALYSIS IN SUBJECTS WITH KNEE OSTEOARTHRITIS."	*Yukiko Toyoda*; Nigg, B.; Wiley, P.; Humble, N. University of Calgary "THE EFFECTS OF CUSTOM-MADE ORTHOSES FOR RUNNERS DIAGNOSED WITH PATELLOFEMORAL PAIN SYNDROME"
3:45 – 4:00	*Scott Lynn*; Costigan, P.A. Queen's University "THE EFFECT OF GAIT LOADS ON THE PROGRESSION OF RADIOGRAPHIC KNEE OSTEOARTHRITIS: A 5-11 YEAR FOLLOW-UP."	*Koon Kiat Teu*; Kim, W.D.; Fuss, F.K.; Tan, J. Nanyang Technological University "SEGMENTAL CONTRIBUTIONS TO THE FINAL CLUB HEAD SPEED IN A GOLF SWING"
4:15 – 4:30	*Kelly McKean*; Landry, S.; Hubley-Kozey, C.; Dunbar, M.; Stanish, W.; Deluzio, K. Dalhousie University "GENDER DIFFERENCES EXIST IN OSTEOARTHRITIC GAIT"	*Cathie Kessler*; Dionne, J.-P.; Bueley, D.; Makris, A.; *El Maach, I* Med-Eng Systems Inc. "REALISTIC TESTING OF RIOT HELMET PROTECTION AGAINST PROJECTILES"
4:30 – 4:45	*Chris MacKay*; Doschak, M.R.; Wohl, G.R.; Zernicke, R.F. University of Calgary "BIOMECHANICS OF THE BONE-LIGAMENT-COMPLEX IN LATE STAGE OSTEOARTHRITIS FOLLOWING ANTIRESORPTIVE DRUG THERAPY"	*Uwe Kersting* University of Auckland "GOLF SWING MECHANICS AND MUSCLE FUNCTION IN TWO DIFFERENT GOLF SWINGS"

6:00pm – 10:00pm

Awards Banquet
"A Maritime Feast"

Enjoy a traditional lobster dinner in a truly unique setting of a renovated cargo shed with a wall of windows overlooking the Halifax harbour.

Casual Dress

Location:
Assemble in Lobby of Westin Hotel
Pier 21 & Pier 22

CONSIDERATIONS ON THE HISTORY DEPENDENCE OF MUSCLE CONTRACTION

Walter Herzog

Faculty of Kinesiology, University of Calgary, Calgary, Alberta T2N 1N4, walter@kin.ucalgary.ca

INTRODUCTION

The topic of this congress is "expanding biomechanical solutions". Here, I would like to illustrate, how we approached the phenomenon of force enhancement and force depression of skeletal muscle contraction, and how we have attempted to identify the mechanisms underlying these phenomena. In order to do this we analyzed the problem on several structural levels of "muscle preparations" including single myofibrils, single fibres, isolated in situ muscles, and intact human skeletal muscles. The idea of "expanding biomechanical solutions" will be illustrated here by showing how sometimes solutions to a scientific problem might be found by working across a range of structural levels while pursuing a given goal.

When an activated muscle is stretched to a given length, its steady-state, isometric force at that new length is greater than the purely isometric force at that same length. This phenomenon is called force enhancement. Similarly, when an activated muscle is shortened, its steady-state, isometric force at that new length is smaller than the purely isometric force at that same length. This is called force depression. Although force enhancement and force depression have been observed for a long time (e.g., Abbott and Aubert, 1952), the mechanisms underlying these muscle properties remain unclear. For a long time force enhancement and depression have been associated with structural non-uniformities on the sarcomere level, but here we would like to present evidence that this is likely not correct, and that these properties might be associated with a history-dependent effect that is directly associated with the molecular interaction of cross-bridges with actin, and thus, might affect the basic mechanism of muscle contraction.

METHODS

We studied history-dependent phenomena for the past seven years, first on the in situ, isolated cat soleus (e.g., Herzog and Leonard, 1997), then on single fibres of the frog *rana pipiens* (e.g., Rassier *et al.*, 2003b) and human adductor pollicis (e.g., Lee and Herzog, 2003), and most recently, on single myofibrils of rabbit psoas (e.g., Rassier *et al.*, 2003a). For precise methods, the interested reader is referred to the literature cited.

RESULTS AND DISCUSSION

It is well accepted that force depression increases with increasing magnitudes of shortening, decreasing speeds of shortening, and increasing amounts of mechanical work (e.g., Abbott and Aubert, 1952). Furthermore, force depression is associated with a distinct decrease in muscle stiffness (Sugi and Tsuchiya, 1988). Force enhancement increases with increasing magnitudes of stretch, but is independent (or nearly so) of the speed of stretch.

Among the novel result found by our team, the following three deserve special attention as they might have profound implications for the mechanism underlying these phenomena, and for eliminating other candidate theories. First, forces in

the enhanced state (after active muscle stretch) can exceed the maximal isometric forces obtained at optimal muscle length. Since we are considering a steady-state situation, this result immediately eliminates the sarcomere length non-uniformity theory (e.g., Morgan *et al.*, 2000) as the sole source for force enhancement. Furthermore, it suggests that there might be an additional, non-cross bridge related force that is responsible for the force enhancement, and/or that there is an increase in the average force per cross-bridge or an increase in the proportion of attached cross-bridges.

Second, force enhancement is associated with a distinct increase in the passive force following deactivation of the force-enhanced muscle, indicating that an additional force might be coming from an essentially passive component that is "recruited" upon active muscle stretch. There is evidence that this passive force enhancement might originate in the molecular spring titin (Herzog *et al.*, 2003; Labeit *et al.*, 2003).

Third, force enhancement is associated with a decrease in the rate of force relaxation. This indicates a possible decrease in Huxley's (Huxley, 1957) detachment rate, and thus, an associated increase in the proportion of attached cross-bridges following stretch of an active muscle compared to the purely isometric reference contraction at the same length.

SUMMARY

Combined, the results of our studies suggest that force enhancement is caused by an increase in passive force, possibly associated with titin stiffening upon activation, and an increase in the proportion of attached cross-bridges, possibly related to a decrease in the rate of cross-bridge detachment. This conclusion could only be reached by working across a range of structural levels. Furthermore, by pursuing a specific research question (history dependence) at different structural levels, we discovered results that might have profound implications for the solution of other questions (mechanisms of contraction) which were not directly targeted. Thus, by working across a range of vastly different structural levels, one might "expand biomechanical solutions" into unknown and exciting territory.

REFERENCES

Abbott,B.C. and Aubert,X.M. (1952). *J Physiol* **117,** 77-86; Herzog,W. and Leonard,T.R. (1997). *J Biomech* **30(9),** 865-872;Herzog,W., et al. (2003). *J Exp Biol* **206,** 3634-3643; Huxley,A.F. (1957). *Prog.Biophys.Biophys.Chem.* **7,** 255-318; Labeit,D., et al. (2003). *Proc Natl Acad Sci U S A* **100,** 13716-13721;Lee,H.D. and Herzog,W. (2003). *J Physiol* **551,** 993-1003;Morgan,D.L., et al. (2000). *J Physiol* **522.3,** 503-513. Rassier,D.E., Herzog,W., and Pollack,G.H. (2003a). *Proc of the Roy Soc Lond B* **270,** 1735-1740;Rassier,D.E., et al. (2003b). *J Biomech* **36,** 1309-1316;Sugi,H. and Tsuchiya,T. (1988). *J Physiol* **407,** 215-229.

THREE DIMENSIONAL IN VIVO KINEMATICS OF ARTIFICIAL KNEE JOINTS DURING LEVEL WALKING USING A MOVING VIDEO-FLUOROSCOPE

Monika Silvia Zihlmann[1], Hans Gerber[1], Kathrin Burckhardt[2], Alex Stacoff[1], Edgar Stuessi[1]

[1]Laboratory for Biomechanics, Department of Materials, ETH Zürich, Wagistrasse 4, 8952 Schlieren, Switzerland
[2]Computer Vision Laboratory, Department of Information Technology and Electrical Engineering, ETH Zürich, 8092 Zürich, Switzerland
Correspondence to Monika S. Zihlmann: zihlmann@biomech.mat.ethz.ch

INTRODUCTION

Accurate in vivo measurements of total knee arthroplasties (TKA) kinematics are fundamental to investigate the biomechanics of the artificial knee joint. This knowledge is crucial to improve implant design and surgical strategies to reach a better clinical outcome. Video-fluoroscopy is a well established method to get kinematic information of artificial joints directly by a three-dimensional numeric reconstruction of the single plane projection view in fluoroscopic images (Banks and Hodge, 1996). Fluoroscopy enables to measure the kinematics of implant parts very accurately, however, within the limited field of view of the fluoroscopic screen only. To measure a full gait cycle, some studies were carried out using a treadmill to analyse kinematic behaviour of the TKA during gait. But, it is known, that gait patterns on a treadmill are not identical to those during level walking (Alton et al., 1998). Enabling a tracking of the joint movement by the fluoroscopic unit allows assessing the accurate kinematic information during overground walking. The goal of the present study was to capture knee component kinematics of a full gait cycle of level walking using a moving video-fluoroscope.

METHODS
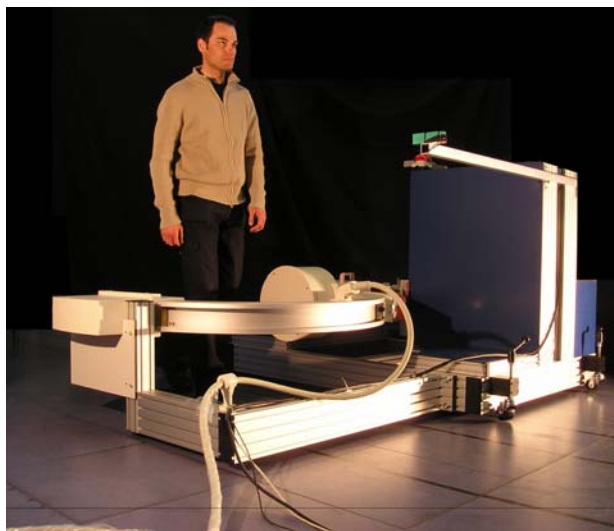
Figure 1: Fluoroscopic Unit Mover with C-Bow (BV Pulsera, Philips Medical Systems)

In this preliminary study two subjects with a TKA (six months after surgery) performed 5 cycles of level walking in our gait laboratory. The knee joint is tracked by a sensor, which controls the movement of the fluoroscopic unit mover. The moved fluoroscope (BV Pulsera, Philips Medical Systems, 12" image intensifier, 25images/sec, 8ms shutter time) is able to follow the knee joint on a walkway of 8 meters to track several gait cycles. The video sequence with the fluoroscopic images is stored on a hard disk. A distortion correction of the fluoroscopic images is performed.

The six DOF of the implant parts are calculated using the single plane projection view in the fluoroscopic images and the CAD model of the implant parts (Mathys AG, Bettlach, Switzerland). The Analysis-by-Synthesis using an intensity based registration algorithm proposed by Burckhardt (Burckhardt, 2002) is applied for finding the position and orientation of each implant component individually. In vitro tests were performed to calculate the error of the application of this reconstruction algorithm to these implant parts.

RESULTS AND DISCUSSION

With the in house developed moving fluoroscopic unit, we are able to: (a) allow the subjects to walk normally - unrestricted from constraints such as a set treadmill walking speed, (b) continuously track the knee joint during several gait cycles; improving previous techniques which had the problem of the fluoroscope's limited field of view, (c) collect kinematic data of artificial knee joints of the stance as well as the swing phase.

To our knowledge this is the first moving video-fluoroscope which tracks a knee joint motion during several gait cycles enabling the subjects to walk naturally, even varying their gait velocity and their gait pattern

Furthermore, the new system makes it possible to gather kinematic information of artificial knee joints also from other daily activities. This allows the differentiation between malfunctions of artificial knee joints and normal artificial knee joint movements.

REFERENCES

Banks, S.A. and Hodge W.A., IEEE Trans Biomed. Eng, **43**, 638-649, (1996).
Alton, F. et al., Clinical Biomechanics, **13**, 434-440 (1998).
Burckhardt, K.V. PhD thesis, Diss ETH No. 14262, ETH Zurich, Switzerland, (2002)

ACKNOWLEDGEMENTS

AN INSTRUMENTED STAIRCASE FOR KINETIC ANALYSES OF
UPPER AND LOWER LIMB FUNCTION DURING STAIR GAIT

Sébastien Chapdelaine[1], Bradford J. McFadyen[1,2], Sylvie Nadeau[3,4], Guy St-Vincent[1], Eve Langelier

[1]Centre for Interdisciplinary Research in Rehabilitation and Social Integration
[2]Department of Rehabilitation, Laval University, brad.mcfadyen@rea.ulaval.ca
[3]Centre for Interdisciplinary Research in Rehabilitation of greater Montreal, Montreal Rehabilitation Institute
[4]School of Rehabilitation, University of Montreal

INTRODUCTION

Stair gait is a common daily activity important for functional autonomy, and forms an integral part of rehabilitation programs. In order to measure stair gait performance in the laboratory, the majority of studies have involved the design of a rigid staircase concentrating on reaction forces under the feet. The purpose of the present paper was to describe a new instrumented, self-contained, adjustable and mobile staircase that provides kinetic analyses of both the lower and upper limbs. Data for ascent are presented.

DESIGN AND METHODOLOGY

The total staircase consists of 5 steps each 18 cm high with the possibility of embedding force platforms (AMTI) in the first three steps and fixing the tread lengths from 25.4 to 35.5 cm (providing slopes from approximately 35 to 27 degrees respectively). A removable 243 cm long wooden platform makes up the highest (fifth) step. Two instrumented handrails range in height from 80.0 to 96.5 cm can be placed at 28 to 54 cm from the staircase centre. The handrails can be of any material and are mounted on two aluminum "proving rings/deflecting beams" assemblies instrumented with 12 strain gauges and supported by steal posts 3.2 cm in diameter. The transducers and assembled railing were calibrated using a mass and pulley system.

Noise in the force transducer signals was expected to be complex due, in particular, to vibration of the staircase unit. Impulse tests were, therefore, performed by dropping a hard ball from a set height onto each step and onto the railing. Power spectral density (PSD) analyses were performed on the impulse data to characterize the frequency responses, and the results were used to create a filtering protocol.

RESULTS AND DISCUSSION

The two handrail transducers were found to be linear. Each transducer has a maximum loading force of 450 N in the vertical directions and 220 N in the horizontal directions.

For the ground reaction forces, PSD analyses showed that the major frequency components related to vibration were above 38 Hz. It was found, however, that the beginning and end of the horizontal ground reaction force signals were not well represented by a simple finite impulse response (FIR) filtering technique using least square minimization. Therefore, a 50 Hz low-pass Butterworth filter was used for the beginning and end

of the signal, and a 32 Hz low pass FIR was used for the remainder of the signal (Figures 1 A to C). For the handrail, PSD analyses showed a simple natural frequency of 15 Hz. It was found that a 12 Hz low-pass, zero-lag, Butterworth filter was sufficient to represent the reaction forces (Figures 1 D to F). In the trial presented, the subject pulls on the handrail.
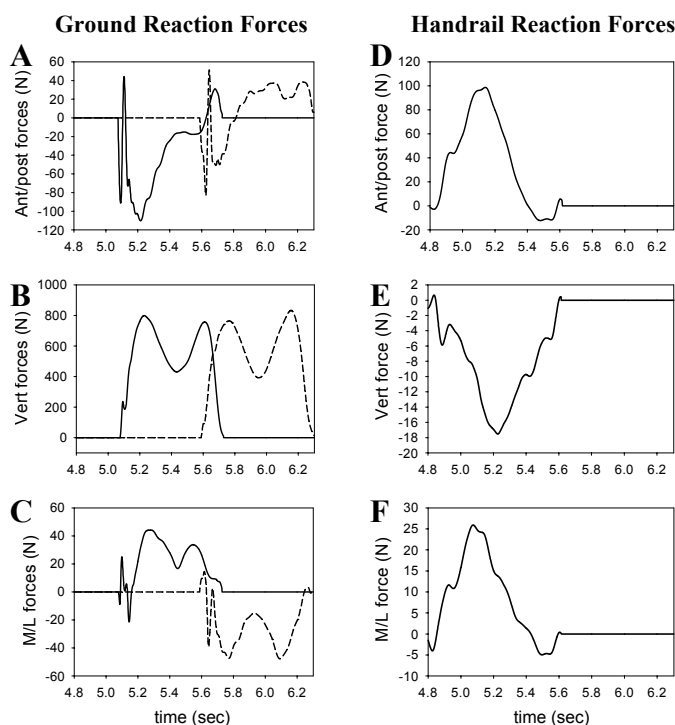
Figure 1: Filtered data for the ground reaction forces (A to C) of the second (solid lines) and third (dashed lines) steps and the right handrail (D to F) for a healthy male subject ascending the staircase. Positive forces correspond to the forward (A, D), upward (B, E) and rightward (C, F) directions.

SUMMARY

This paper presents a new staircase design. The system is easy to move, even during experimentation. In addition, the new system includes an instrumented handrail that will, for the first time, provide data on the role of upper limb function during ascent and descent for different populations.

3D KNEE JOINT MOMENTS DURING LEVEL WALKING AND WHEN STEPPING TO A NEW LEVEL

Jeannette M. Byrne, Milad Ishac, Aftab E. Patla, Stephen D. Prentice
Gait and Posture Laboratory, University of Waterloo, Waterloo, Canada
jmbyrne@ahsmail.uwaterloo.ca

INTRODUCTION

Stepping onto a raised surface, such as a curb, places increased demands on the lower limb. In order to elevate the mass of the body to the new height, extensor moments at both the knee and hip must increase (Byrne et al 2002). While sagital plane moments have been well documented, demands in the frontal and transverse planes have received little attention. The aim of the current research was to quantify the 3D knee moments during a step-up task. In addition to providing insight into the demands of this task, the protocols developed during this study will be applied to a knee replacement population as we endeavor to gain insight into function post joint replacement.

METHODS

Three healthy, female subjects (average age 22 years) performed 15 level walking and 15 step-up trials. During the step-up trials subjects stood with both feet on a lower force plate and then stepped onto an upper plate (20cm). Four IREDS placed on each of the pelvic, thigh and shank segments and 3 on the foot were used to track segment motion. To minimize error due to skin movement singular value decomposition (Challis 1995) was used to reconstruct segment kinematics. An additional 12 anatomical landmarks were digitized and used in conjunction with this tracking data to determine kinematics of the principle axes of each segment. An x-y-z Euler sequence of rotations was used when determining segment kinematics. Kinematic data and segment inertial properties were then input into a customized software package (Mishac Kinetics) to calculate 3D ankle, knee and hip moments. For the current abstract only knee moments were examined. These moments were expressed with respect to the principle axis of the thigh segment. Data for the level walking trials were ensemble averaged across all subjects and compared to the ensemble averaged step-up moments for each subject. Only stance phase data was examined.

RESULTS AND DISCUSSION

Stance phase knee moments during level walking and when stepping onto a 20cm step differ markedly (Fig 1). As expected the largest increases were in the sagittal plane, as the knee extensors must act to elevate the body to the new height. Large increases were also observed in the transverse plane, where a knee external rotation moment dominated through-out stance. The concurrent increase in both the external rotation and extension moment is of interest as it suggests competing action by the hamstrings which must act as the prime mover during rotation and the antagonist during knee extension. Less dramatic differences were observed in the frontal plane. In early stance knee abduction moments were less than those observed during level walking, while mid to late stance phase moments were comparable in magnitude to walking values. Caution must be used when applying these results to clinical populations, however, as the axis system used do not necessarily correspond to standard clinical axes. The next step in data analysis will be to express joint angles and moments with respect to the more clinical relevant joint coordinate system proposed by Grood and Suntay (1983)
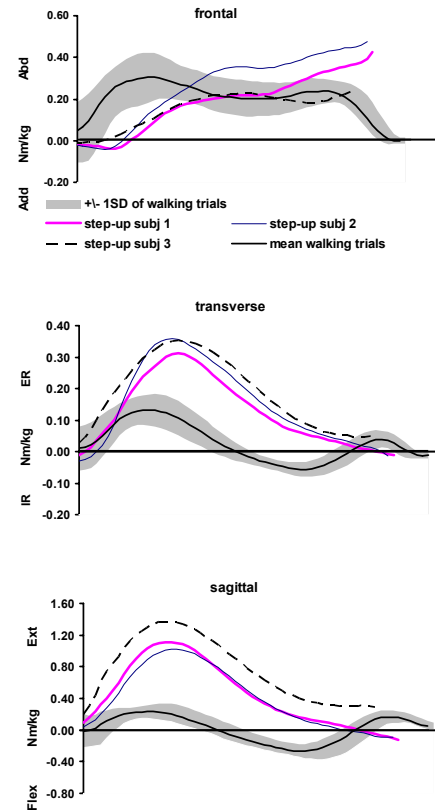
Fig 1: Knee joint moments during level walking (ensemble averaged across 3 subjects) and stepping onto a 20cm step (ensemble averaged with-in subjects). Moments reported for stance phase (walking: RHC to RTO; step-up RHC to LHC)

SUMMARY

Preliminary results confirm the demands placed on the knee joint when stepping to a new height are not limited to the sagittal plane. Increases in transverse plane knee moments and altered frontal plane moments also occur. Further work is required to more clearly define these frontal and transverse plane demands with respect to anatomically relevant axes. This is particularly important if this protocol is to be used to investigate function in a clinical population.

REFERENCES

Byrne JM, et al (2002) *Clinical Biomech,* **17**,580-585.
Challis J (1995) *J Biomech,* **28**(6),733-737
Grood ES, Suntay WJ (1983) *J Biomech Eng*. **105**(2):136-44

ACKNOWLEDGEMENTS

Continuous Curve Registration in the Analysis of Gait Data

J.L. Astephen[1] and K.J. Deluzio[1]

[1]School of Biomedical Engineering, Dalhousie University, Halifax, Canada, jlasteph@dal.ca

Introduction

Variation in gait waveforms can be in amplitude or phase. The common normalization of gait waveforms to the length of the gait cycle can impose artificial data variation in the form of phase shifts between subject curves. In analysing gait waveforms with either parameter extraction or multivariate techniques such as principal component analysis (PCA), phase variation can be difficult to localize and to interpret. Continuous curve registration, a functional data analysis technique, allows separation of amplitude from phase variation, which can allow for more interpretable results (Ramsay and Silverman, 1997).

Dynamic knee moments have been shown to be important to knee osteoarthritis (Kaufman et al., 2001; Hurwitz et al., 2002). Both adduction moment and internal rotation moment waveforms exhibit phase variation. Curve registration applied to these waveforms before the analysis may produce more interpretable results.

Methods

Three-dimensional gait analysis was performed on a group of 43 normal subjects and 40 with moderate osteoarthritis (OA) of the knee. Three components of knee joint moments were calculated. Because we have found differences in the internal rotation moment with moderate knee OA, and this moment exhibits phase variation, a registration by regression technique, introduced by Kneip et al in 2000 was applied to the internal rotation moment waveform data. For each subject, separate regression analyses were used to define time warping functions, using the nonlinear regression model:

$$g_j(t) = e^{\gamma_j}(t + \delta_j)$$

Principal component analyses (PCA) was used to analyse both the registered and unregistered internal rotation moment waveforms. PCA was applied to the 101 time variables that define each gait waveform (Deluzio et al., 1997). PCA is a statistical analysis technique that exploits the correlation in the data in extracting important features (PCs) that explain a maximal amount of the variability in the data.

Results and Discussion

Continuous curve registration removed much of the phase variation in the internal rotation moment waveforms (Figure 1). In the unregistered PCA, three PC's (explaining 88% of the variation) were appropriate for describing the data; in the registered PCA, only two PC's (explaining 81% of the variation) were appropriate. The loading vector of the third

principal component of the unregistered internal rotation moment involves some phase shift between curves, but is difficult to interpret (Figure 2). Subjects with higher PC3 scores have peaks that are shifted to the right. When the curves are registered, much of the phase shift is removed from the data, and the third principal component is no longer important.
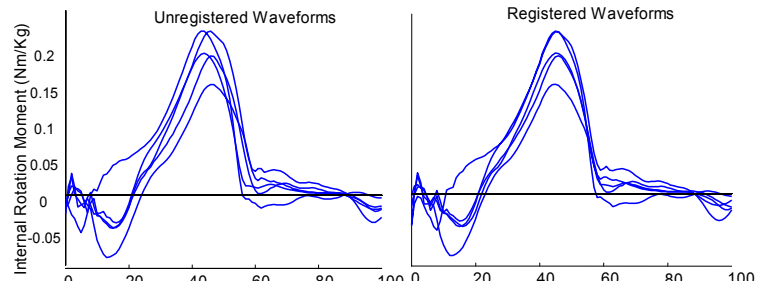
Figure 1: Original and registered knee internal rotation moment waveforms for five example subjects.
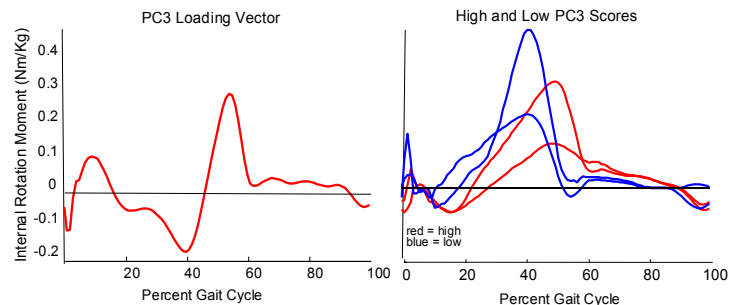
Figure 2: PC3 loading vector for unregistered curves; subjects with high and low PC3 scores.

Summary

Analysing unregistered gait data may produce misleading results because the timing of important features can vary from subject to subject, affecting the mean and other statistical properties of the curves. As well, the rigid metric of physical time may not be directly relevant to the internal dynamics of many real-life systems (Ramsay and Silverman, 1997). When we normalize gait data, the resulting phase shift may distort the results of subsequent analyses. A less arbitrary, more appropriate time normalization may aid in the analysis and interpretation of gait data.

References

Deluzio, K.J. et al. (1997). *J. Hum. Mov. Sc*. **16**:201.
Hurwitz, D.E. et al. (2002). *J. Orthop. Res*. **20**:101.
Kaufman, K.R. et al. (2001). *Jbiomech*, **34**, 907-915.
Kneip, A. et al. (2000). *The Can. J. of Stat*. **28**,1:19-29.
Ramsay, J.O.,B.W. Silverman. (1997) *Functional Data Analysis*. Springer Series in Statistics, NY.

RELAXATION TIME INCREASES AFTER ACTIVE STRETCH OF SKELETAL MUSCLE

Dilson E. Rassier and Walter Herzog

Human Performance Laboratory, University of Calgary, Calgary, AB, Canada
*email: walter@kin.ucalgary.ca

INTRODUCTION

When skeletal muscle is stretched while activated, the force produced is higher than that observed during isometric contractions at the corresponding length. Such phenomenon is referred to as force enhancement. The mechanisms behind force enhancement are not understood, but there is evidence it may be associated with cross-bridge kinetics (Rassier and Herzog, 2004). Although difficult to measure, cross-bridge kinetics may by evaluated by the relaxation rate following deactivation - a longer relaxation rate indicating a decrease in the cross-bridge detachment rate. We investigated if relaxation rate was increased after active stretch of muscle fibers, with and without the cross-bridge inhibitor 2,3-Butanodione monoxime (BDM).

METHODS

Single fibers isolated from the lumbrical muscle of frog were transferred to an experimental chamber (pH = 7.5; temperature: ~9°C). After setting the voltage and frequency of stimulation, an active force-length relationship was defined. Fibers were placed at a length ~20% above the plateau of the force-length relationship (L_o). Active stretches were performed with amplitudes of 5% and 10% L_o, at a velocity of 40% fiber length/s. Isometric contractions at the corresponding initial and final lengths were performed for comparisons. Experiments were done in Ringer solution, and with the addition of 2 mM, 5 mM and 10 mM of BDM, a cross-bridge inhibitor (Horiuti *et al.*, 1988). Force enhancement was calculated as the difference in force after stretch and during isometric contractions at the corresponding length, and half-relaxation time ($50\%R_t$) was the time from deactivation to the point in which force had decreased to 50% of its maximal value.

RESULTS AND DISCUSSION

When active muscle fibers were stretched, force enhancement was observed in all conditions (Fig. 1) and was accompanied by an increased $50\%R_t$ (Fig. 2). BDM significantly decreased tetanic force, as previously shown (Regnier *et al.*, 1995; Horiuti *et al.*, 1988; Sun *et al.*, 2001), but increased the magnitude of force enhancement (Fig. 1). This effect may be explained if we assume that BDM places a large proportion of cross-bridges in a weakly-bound state (Regnier *et al.*, 1995), decreasing isometric force, but increasing the total (weakly + strongly bound) cross-bridges contributing to force during and after stretch. Force enhancement was accompanied by an increased $50\%R_t$ after stretch, and both were enhanced by BDM (Fig. 2).

Altogether, our results suggest that force enhancement is associated with an increased number of cross-bridges (weakly + strongly bound). That may be accomplished by a decreased rate of detachment, which would decrease the speed of relaxation.
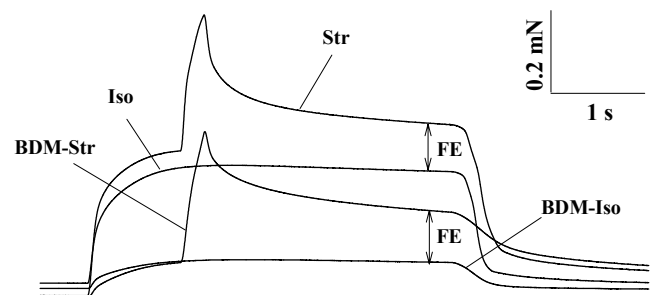
Figure 1: Isometric contractions (Iso), and stretches (Str) of 10% fiber length at 40 fiber length/s performed in Ringer solution without and with 10 mM BDM. FE: Force enhancement.
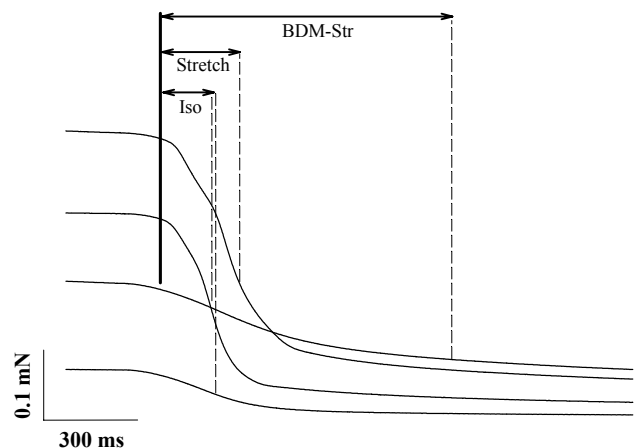

Figure 2: Relaxation phase of the same contractions as shown in Fig 1. Isometric contractions show similar $50\%R_t$ times before and after BDM.

REFERENCES

Horiuti,K. et al (1988). *J.Muscle Res.Cell Motil.* **9**, 156-164.
Rassier,D.E., Herzog,W.(2004). *J.Appl.Physiol* **96**, 419-427.
Regnier,M. et al (1995). *Am.J.Physiol* **269**, C1532-C1539.
Sun,Y.B. et al (2001). *Acta Physiol Scand.* **172**, 53-61.

LOCALIZED LEG MUSCLE FATIGUE RESULTS IN REDUCED TIBIAL IMPACT ACCELERATION

Janice M. Flynn[1], Jeffrey D. Holmes[2], David M. Andrews[3]

[1] Department of Kinesiology, University of Waterloo, Waterloo, Ontario, Canada, jflynn@ahsmail.uwaterloo.ca
[2] Department of Rehabilitation Science, University of Western Ontario, London, Ontario, Canada
[3] Department of Kinesiology, University of Windsor, Windsor, Ontario, Canada

INTRODUCTION

Tibial impact acceleration is known to increase with general body fatigue (Voloshin et al., 1998). The purpose of this study was to determine if localized muscle fatigue of the plantarflexors or dorsiflexors would also cause an increase in peak tibial acceleration. Young women (20 – 25 yrs) were compared to those between 50 and 60 years of age.

METHODS

A human pendulum system similar to Lafortune et al. (1995) was used to control impact velocity and joint angle. Twenty-four women participated in this study: 12 in each age group. Each lay supine on the pendulum, and their unshod dominant heel was impacted into a vertical force plate with a velocity between 1 – 1.15 m/s, and a force approximating 1.8 – 2.8 X body weight. A skin mounted uni-axial accelerometer was pre-loaded to the tibia allowing for measurement of peak tibial acceleration (PTA), time to peak (TTP), and the rate of increase of the acceleration curve (RTAmax), measured between 30 and 70% of the rise. EMG activity of the tibialis anterior (TA) and gastrocnemius (G) was used to define and monitor muscle fatigue. The dorsiflexors and plantarflexors were fatigued on separate days, at least a week apart. Fatigue was accomplished by maintaining an isometric muscle contraction against resistance, until the mean power frequency of the signal had decreased by approximately 15%.

RESULTS AND DISCUSSION

There was a significant decrease in PTA following fatigue (p=0.008)(Figure 1) as well as a significant decrease in RTAmax (p = 0.033)(Table 1). There were no significant main effects or interactions for age group or muscle group. There was a significant increase in %MVC of TA post-fatigue (p=0.003) and a significant fatigue*muscle group interaction (p=0.016), with a greater increase in TA activity when the dorsiflexors were fatigued.

Muscle fatigue results in a decrease in muscle tension (Winter, 1991), causing a decrease in overall shank segment stiffness. As demonstrated, this results in an increase in attenuation properties of the shank.
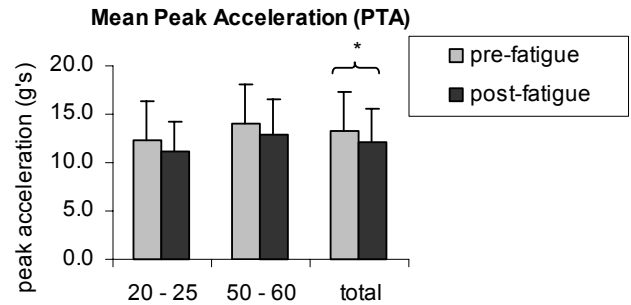
Figure 1. Mean (SD) peak tibial acceleration (PTA), pre- and post-fatigue for both muscle groups combined. A significant main effect for fatigue state was found (* p=0.008).

SUMMARY

The effect of localized fatigue of the dorsiflexors and plantarflexors on tibial impact acceleration was analyzed. Localized leg muscle fatigue resulted in a significant increase in the attenuation properties of the shank, which is opposite to what has been shown in previous studies on full body fatigue (Voloshin et al., 1998). This effect was not age-dependant, nor was there any significant difference in the dependant variables when dorsiflexor fatigue was compared to plantarflexor fatigue.

REFERENCES

Lafortune, M.A., & Lake, M.J. (1995). *Journal of Biomechanics,* **28(9)**. 1111-1114.
Voloshin, A.S. et al (1998). *Clinical Biomechanics,* **13**, 515-520.
Winter, D.A.(1991). *Biomechanics and Motor Control of Human Movement, 2nd ed.* New York, Wiley.

ACKNOWLEDGEMENTS

Table 1: Mean (SD) peak tibial acceleration (PTA), acceleration slope (RTAmax), and time to peak tibial acceleration (TTP) for the pre- and post-fatigue conditions for Tibialis Anterior (TA) and Gastrocnemius (G).

Dependant Variable	Pre-fatigue Session 1 (TA)	Post-fatigue Session 1 (TA)	Pre-fatigue, Session 2 (G)	Post-fatigue Session 2 (G)
PTA (g's)	13.28 (3.7)	12.09 (3.1)	13.21 (4.5)	11.95 (3.5)
RTAmax (g/s)	3067 (1488)	2416 (1363)	2843 (1883)	2589 (1759)
TTP (ms)	10.1 (5.0)	10.9 (6.0)	9.7 (2.0)	10.2 (4.0)

MEASURES OF FATIGUE: ARE THEY CONSISTENT?

Marco A. Vaz[1,2], Eduardo M. Scheeren[1], Dilson E. Rassier[2], Walter Herzog[2], Brian R. MacIntosh[2]
1- Exercise Research Laboratory, Federal University of Rio Grande do Sul, Porto Alegre, RS, Brazil
2- Human Performance Laboratory, Faculty of Kinesiology, University of Calgary, Calgary, AB, Canada
*email: marco@kin.ucalgary.ca

INTRODUCTION

Fatigue is defined as a response that is "less than the expected or anticipated contractile response, for a given stimulation" (MacIntosh and Rassier, 2002). Anticipated force depends on the method of eliciting contractions: i.e., maximal voluntary contractions and electrical stimulation at different frequencies might be expected to elicit different responses. An advantage of electrical stimulation for evaluation of fatigue is that the "stimulation" is known, and can be kept perfectly constant. The purpose of this study was to compare three different methods for assessing fatigue: force response during maximal voluntary contraction (Tmax), force response elicited by 20 Hz (T20) or by 100 Hz (T100) electrical stimulation. This corresponds to relatively low and high frequencies of stimulation, respectively. These methods of assessing fatigue, were used after exercise with either maximal concentric or eccentric contractions.

METHODS

Ten healthy male subjects performed 60 maximal voluntary knee extensor contractions (angular velocity = 60°/s) on a Cybex (NORM) isokinetic dynamometer. Contractions were concentric (MAXCON) or eccentric (MAXECC), with 1 week interval between protocols. Maximal isometric voluntary contractions (MIVCs) and electrically elicited isometric contractions (transcutaneous electrical stimulation of the femoral nerve; 1 ms pulses; at 20 Hz and 100 Hz for 2 s) were performed before (pre-exercise), immediately following (after-exercise), and 60 minutes after the exercise protocol (after-recovery). A two-way ANOVA (contraction type; time of fatigue assessment) for repeated measures was used to determine statistical differences with $\alpha = 0.05$.

RESULTS

The various measures of fatigue did not give the same indications of fatigue and recovery (Figure 1 and Table1). Tmax decreased 25% after MAXCON and returned to pre-exercise levels after-recovery. For the MAXECC condition, Tmax decreased by 12% and did not return to pre-exercise values after the recovery period. T100 decreased by 36% for the two protocols after-exercise, and there was a partial recovery of the torque to within 20% of the pre-exercise value. T20 decreased by 47% following MAXCON and 35% following MAXECC protocols. T20 did not return to pre-exercise levels in the recovery period, but remained at about 54% of the pre-exercise values for both fatigue protocols.

DISCUSSION

The patterns of fatigue and recovery that are observed following either concentric or eccentric contractions depend on the method for measuring fatigue and recovery. Voluntary torque after concentric and eccentric exercises gave different results than electrically elicited contraction. With electrically elicited contractions, the measurements after concentric contractions were similar to those following
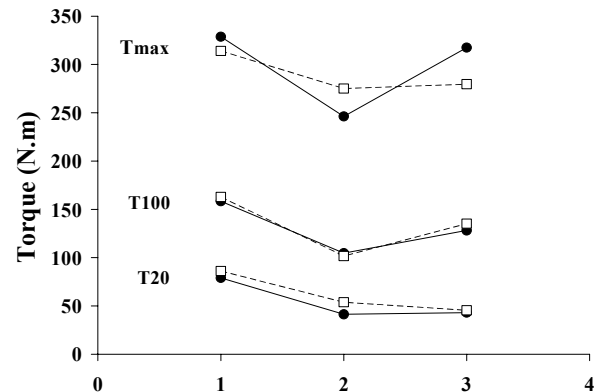

Figure 1: Mean values for Tmax, T100 and T20 at pre-exercise (1), after-exercise (2) and after-recovery (3) periods for the two exercise protocols (●=MAXCON;□=MAXECC).

Table 1: Mean values for the % decrease of Tmax, T100 and T20 from pre-exercise to after-exercise (AE) and after-recovery (AR) periods for the two exercise protocols.

TORQUE	% DECREASE FROM PF	
	AE	AR
TMAX CON	25	3
TMAX EXC	12	12
T100 CON	34	19
T100 EXC	38	17
T20 CON	47	43
T20 EXC	35	44

eccentric contractions. However, recovery depended greatly on the method of measurement. It should be kept in mind that 100 Hz stimulation should have maximally activated a portion of the motor units of the quadriceps muscles. This same motor unit pool should have been activated by the 20 Hz stimulation protocol. The lack of recovery in Tmax following MAXECC in spite of the partial recovery in T100, indicates either an inability to recruit motor units to the same extent, or changes in contractile properties of motor units that were not activated by the 100 Hz stimulation. If we assume that stimulation activates the same motor unit pool with T20 and T100, then the persistent depression of T20 in spite of recovery of T100 indicates the presence of low-frequency fatigue. This is apparently not evident from observation with high frequency stimulation, or with maximal voluntary activation.

REFERENCES

Macintosh, B.R. and Rassier, D.E. (2002) *Can. J. Appl. Physiol.* **27(1)**, 42-55.

INDUCED LOCALIZED MUSCULAR FATIGUE: METHODOLOGICAL ASPECTS AND GENDER DIFFERENCES IN THE RATE OF FATIGUE AND RECOVERY

Allan Wrigley[1], Wayne J. Albert[1], Gordon G. Sleivert[2], and Robert B. McLean[1]

[1]Faculty of Kinesiology, Human Performance Lab, University of New Brunswick, Fredericton, Canada
[2]PacificSport, Canadian Sport Centre, Victoria

INTRODUCTION

Many factors influence the motion performed during lifting including muscular strength and conditioning (Trafimow *et al.*, 1993). Often, participants are required to complete a repetitive or cyclic lifting task where fatigue is assessed continuously, at specific time intervals, or after the testing has been completed. Any findings of localized muscular fatigue are then inferred to have affected the lifting motion (Bonato *et al.*, 2003). Our research goal is to link observed biomechanical changes in lifting technique to specific fatigued muscle groups. Therefore, the purposes of this study were to 1) develop an induced localized muscular fatigue protocol, and 2) quantify gender differences in fatigue accumulation and recovery rate of lower and upper body musculature after repeated bouts of sustained isometric contractions.

METHODS

Twenty-seven healthy males (n=12) and females (n=15) underwent bilateral localized fatigue of either the knee extensors (male: n=8; female: n=8), elbow flexors (male: n=8; female: n=10), or both muscle groups. All participants provided written informed consent in accordance with guidelines set by the university Ethics Review Board. The fatigue protocol consisted of ten 30-second sub-maximal isometric contractions. Changes in maximum voluntary contraction ($MVC_\%$), central activation (CA_Δ), and electrically evoked forces ($EEF_\%$) were assessed from pre- to post-fatigue, and $EEF_\%$ changes and the control of the sustained contractions (CON) during the fatigue protocol were analyzed using mixed three-factor repeated measures ANOVA (gender x side x time) designs.

RESULTS

Statistical significance was accepted at $P < 0.05$. There was only one significant main effect for side ($MVC_\%$ > left leg), however there were time main effects for all leg measures and all arm measures except CON. Pairwise comparisons of main effects revealed significant loss of force, CA_Δ, and $EEF_\%$ from pre- to post-fatigue in both arms and legs. However, pairwise comparisons of EEF% and CON revealed that fatigue accumulated faster and to a greater extent in the legs than in the arms. $MVC_\%$, $EEF_\%$ during the fatiguing contractions, and CON had significant time and gender interactions. Pairwise comparisons revealed males had greater relative loss of isometric force, a higher rate of fatigue accumulation, and were less able to maintain the fatiguing contractions in the legs. Gender differences are illustrated in Figure 1.
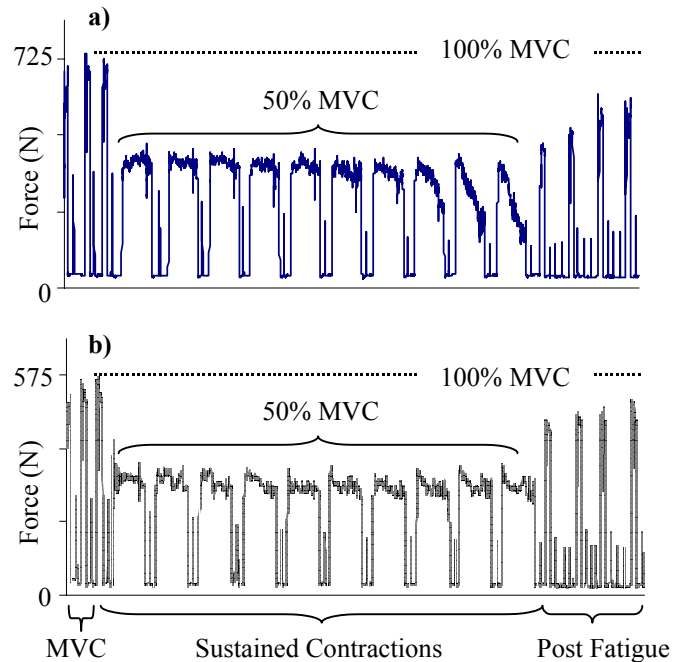
Figure 1: Typical right leg force output for males (a) versus females (b). Males were less capable of maintaining 50% of their MVC during the sustained contractions, and had a significantly greater reduction in post fatigue MVC.

SUMMARY

The fatigue protocol employed resulted in a significant loss of force in both the arms and legs, with the arms being more fatigue resistant. The nature of the induced fatigue was a combination of central and peripheral fatigue that did not fully recover over a 45-minute period. Changes in electrically evoked forces and the control of the sustained isometric contractions during the fatigue protocol proved to be effective indicators of fatigue accumulation**.** When faced with maintaining the same relative load, females have an advantage in terms of resistance to muscular fatigue in the legs only. The slower rate of fatigue accumulation resulted in a lower amount of relative force loss in the legs for females. The results appear to reflect gender differences that are peripheral, and support the muscle mass hypothesis for explaining differences in muscular fatigue.

REFERENCES

Bonato,P. et al. (2003) *Spine* **28,** 1810-1820.
Trafimow,J.H. et al. (1993) *Spine* **18,** 364-367.

CSB LOCOMOTOR SYMPOSIUM: EFFECTS OF TRAUMATIC BRAIN INJURY ON MOBILITY
Bradford J. McFadyen[1,2]

[1]Centre for Interdisciplinary Research in Rehabilitation and Social Integration
[2]Department of Rehabilitation, Laval University, brad.mcfadyen@rea.ulaval.ca

INTRODUCTION

The creation of a handicap situation involves the interaction between one's motor disabilities and the physical and social obstacles of the environment. Both the personal and environmental factors, therefore, combine to create barriers to mobility affecting quality of life.

A traumatic brain injury (TBI) causes neurological sequelae that often include both cognitive and motor problems. Although much is known about cognitive deficits following a TBI and the related social obstacles, very little is known about the motor, particularly locomotor, deficits and the adaptations for physical obstacles. As part of the CSB Locomotion Symposium on Mobility, this talk will focus on locomotor capacity and its adaptation for the physical environment following a TBI. This written abstract provides basic information to complement the talk.

BRIEFLY UNDERSTANDING A TBI

A traumatic brain injury results from an insult to the head. The etiology can be related to a blunt impact that can also cause a skull fracture (e.g., from a fall), acceleration and deceleration of the brain mass (e.g., during motor vehicle accident) or from foreign object penetration (e.g., gunshot). A non-penetrating trauma can result in focal damage at the site of impact as well as from the coup/counter-coup phenomenon (most frequent sites being the frontal and temporal lobes and the brain stem). In addition, more diffuse axonal damage occurs from the acceleration and deceleration of the brain in the cranial vault and pressure gradients projecting to deep structures. The results are impairments to many centres associated with control and function of cognitive and physical abilities.

A TBI can be classified as severe, moderate or mild. Classification involves considering the level of consciousness at the time of trauma (using the Glasgow Coma Scale), the amount of amnesia post-trauma, and the results of brain scanning.

LOCOMOTOR MOBILITY and TBI

Even five years following the appeal for gait-related studies by Esquenazi (1999), there is still very little information on locomotor capacity following a TBI.

What is known is that locomotor ability recovers fairly quickly in general following a TBI (e.g., Wade et al. 1997). Persons with TBI show slower gait overall and shorter stride lengths (Ochi et al., 1999) but maintained rhymicity when capable of speeds greater than 1 m/s (McFadyen et al., 2003). Dynamic stability has been shown to be affected following a TBI in relation to the centre of mass movements that are smaller in the sagittal plane, but greater in the frontal plane (Basford et al. 2003).

In our first study of locomotor capacity in a highly functional TBI group (McFadyen et al., 2003), we showed that residual effects in spatio-temporal variables remained, but may be due to a heightened level of cautiousness, perhaps related to a decreased confidence in dynamic balance ability. Measures of injury severity did not have any relation to locomotor behaviour. Finally, a simple clinical test of one-legged stance with eyes closed appeared to correlate to adapted locomotor capacity.

Preliminary results from more recent projects will also be presented in this talk. These observations are showing further effects of a TBI on obstacle circumvention behaviour, frontal plane movement during level walking that is exaggerated in amplitude, but simplified in frequency, and deficits in locomotor capacity related to increases in the physical and simultaneous cognitive demands of the environment.

REFERENCES
Basford JR, Chou, L-S, Kaufman, KR, Brey RH, Walder A, Malec JF, Moessner AM, Brown AW. An assessment of gait and balance deficits after traumatic brain injury. *Arch Phys Med Rehabil*. 2003;84:343-9.
Esquenazi A. Preface. *J Head Trauma Rehabil.*. 1999;14(2):v.
McFadyen, BJ, Swaine, B, Dumas, D, Durand, A. (2003) The residual effects of a traumatic brain injury on locomotor capacity: A first study of spatio-temporal patterns during unobstructed and obstructed walking. *J. Head Trauma Rehab*. 18:512-525.
Ochi F, Esquenazi A, Hirai B, Talaty M. Temporal-spatial feature of gait after traumatic brain injury. *J Head Trauma Rehabil*. 1999;14:105-115.
Wade LD, Canning CG, Fowler V, Felmingham KL, Baguley IJ. Changes in postural sway and performance of functional tasks during rehabilitation after traumatic brain injury. *Arch Phys Med Rehabil*. 1997;78(10):1107-1111.

ACKNOWLEDGMENTS

THE EFFICACY OF AN ASSISTIVE DEVICE TO IMPROVE BALANCE AND MOBILITY IN THE ELDERLY.

Stephen D. Perry, PhD

Department of Kinesiology & Physical Education, Wilfrid Laurier University, Waterloo, ON, Canada

INTRODUCTION

One of the most pervasive effects of aging is a loss of cutaneous touch and pressure sensation. The loss of cutaneous sensation in the plantar surface (sole) of the feet has been correlated with impaired postural control (poor balance) and an increased risk of falling [1, 2]. Numerous studies support the important contribution of cutaneous sensation from the plantar foot surface, in the control of postural balance. This cutaneous sensation acts, within the central nervous system, to trigger and/or modulate the automatic postural reflexes and reactions that act to prevent loss of balance [3-6]. Age-related loss of plantar pressure sensation, which is very common, can lead to impaired control of these reactions. However, we have shown that it is possible to compensate for balance impairments resulting from this loss of sensation by using mechanical facilitation of the sensation from the perimeter of the foot sole. To date, we have demonstrated the feasibility of this approach in laboratory studies, and we have obtained a U.S. patent for the design concept [7]. However, it remains to be determined whether the benefits of the footwear persist during dynamic balance during gait. Also, we need to determine whether there are any practical problems associated with wearing such footwear, e.g. due to discomfort or irritation of the skin.

METHODS

Fifty-one subjects were recruited from local community centers, adult education classes and through advertisement in the local paper. The targeted population was individuals who had moderately insensitivity of the soles of their feet (unrelated to peripheral neuropathy or other abnormal conditions).

Forty-six (23 males, 23 females) of the initial 51 were recruited to participate in the study (the 5 excluded subjects had much higher sensory thresholds). Of the 46 subjects, 40 subjects (21 men, 19 women; mean age 69; mean weight 74.4kg; mean height 1.7m) completed all components of the study. Prior to participation, each subject provided written informed consent in compliance with ethics approval granted by the Institutional Review Board at Wilfrid Laurier University.

Each subject was fitted with identical walking shoes and two sets of insoles, one with the facilitatory indentors and one without. For the initial testing, each subject performed both gait protocols (gait termination and gait over uneven terrain) once with the test insoles and once with the control insoles. During a three month wearing period participants sent in postcards weekly with information pertaining to insole comfort, hours of wear and falls. At the completion of the 3-month period, the subjects returned to the lab where they repeated both gait protocols with both sets of insoles (the test insole and the control insole).

Testing of balance control involved recording biomechanical responses during two perturbation protocols: gait termination and gait over uneven terrain. Kinematic data was collected using two OptoTrak 3020 (Northern Digital, Waterloo, ON) camera banks. A 13 link-segment model was used to calculate the total body COM using known anthropometric data. Horizontal and vertical ground reaction forces were measured at each foot using 3 force platforms (Advanced Mechanical Technologies, Inc., Watertown, MA).

The primary outcome measures involved the centre of mass/base of support (COM-BOS) relationship, centre of pressure movement, and force production during loading and unloading of the plates. The COM-BOS relationship was evaluated throughout the gait termination and gait over uneven terrain trials as the relative distance of COM from BOS (one or both feet in contact with the ground). Centre of pressure (COP) displacement and velocity was recorded throughout contact with the force platforms and specific values were extracted at important time points during the movement. Force loading and unloading were calculated when the foot contacts and the foot lifts off the force platforms respectively.

A repeated-measures analysis of variance (ANOVA) was used to determine within-subject and between-subject effects on the response measures.

RESULTS

Over the 12-week period of wearing the insoles, we found that 45% of individuals who did not wear the facilitatory insoles fell, while only 30% of the individuals who wore the facilitatory insoles fell. During both gait termination and gait over uneven terrain, multiple COM-BOS and COM-COP relationships, force patterns and step parameters were affected by the facilitatory insole.

DISCUSSION

This work has provided evidence that using a simple mechanical stimulus (via an insole) to the perimeter of the plantar-surface of the foot can influence the control of dynamic balance during gait. Additionally, within the limitations of the short-term falls tracking data, the use of the facilitatory insoles has demonstrated a reduction in fall occurrence.

REFERENCES

1. Lord, SR et al. JAGS. 42. pgs. 1110-1117. 1994.
2. Perry, SD et al. Third NACOB. Waterloo, Canada. pgs. 285-286. 1998.
3. Inglis, JT et al. Adv Exp Med Biol. 508 pgs. 111-7. 2002.
4. Do, MC et al. Exp Brain Res. 79 pgs. 319-324. 1990.
5. Perry, SD et al. Brain Res. 913 (1): pgs. 27-34. 2001.
6. Perry, SD et al. Brain Res. 877 (2): pgs. 401-6. 2000.
7. Maki, BE et al. J Gerontol A Biol Sci Med Sci. 54 (6): pgs. M281-7. 1999.

ACKNOWLEDGEMENTS

Efficacy of different exercise intervention programs for improving mobility in the elderly

Aftab E. Patla , James S. Frank, Lawrence R. Brawley & Nandini Deshpande

Gait and Posture Laboratory, Department of Kinesiology, University of Waterloo, Waterloo, Canada, patla@healthy.uwaterloo.ca

SYMPOSIUM INTRODUCTION

"Mobility is the ability to move independently from one location to another. Since mobility is such an integral component of most activities of daily living, any adverse impact on mobility can lead to disability. Impaired mobility leads to increased risk (3 to 5 times) for dependency in activities of daily living. Mobility disability is in itself therefore worthy of and is the subject of independent study. Incidence of mobility disability increases dramatically as we age from 1% in the general population to over 35% in individuals over 80 years old. There are very few diseases, chronic or acute, that do not adversely impact on mobility: individuals with diseases ranging from arthritis to Parkinson's are eight times more likely to have mobility disability. It is no wonder that we cherish our ability to move independently: we celebrate its natural onset at infancy, try and sustain it throughout our life span and put a premium on recovery of mobility when it is impaired (Patla, 2001)." It is for this reason that the focus of the symposium is on Mobility Disability: identifying and assessing it and trying to improve and/or maintain it at a level that allows the individual to live independently in the community.

EVALUATING EFFICACY OF INTERVENTION PROGRAMS FOR IMPROVING MOBILITY

"It is clear that straight uncluttered level path is the exception rather than being the norm when we move from one place to another. There are relatively few studies that have provided data to support what we intrinsically know from our own experience. The only way to obtain such data is to observe mobility component of instrumental activities of daily living: cataloguing environmental features independent of the individual will miss the choices people make since rarely there is just one path to the end goal. Some challenges (such as adverse weather or some traffic crossings) can be avoided; others (such as uneven surfaces) have to be accommodated in our travel path. These studies show that environments that we routinely encounter at home and within our community are complex. These environments include travel surfaces of different geometrical and physical properties and obstacles both static and moving that have to be avoided (Patla, 2001)." Patla & Shumway-Cook (1999) proposed a conceptual model for identifying the dimensions of mobility for community living elderly (DOMA). Later Shumway-Cook et al. (2002) assessed these dimensions for healthy individuals living in small city, rural environment (Kitchener-Waterloo) and a large city environment (Seattle) during two summer and winter seasons. They also proposed and developed a new test for assessing dynamic mobility in laboratory environment that includes components that measure the effects of the

dimensions of mobility proposed (DYME). This conceptual framework and assessment tool was recently used in a study that evaluated the efficacy of different types of intervention programs on mobility in the elderly.

"The following guidelines based on research into what makes successful adaptable locomotion possible guided our design of special exercise programs . Some examples of tasks included are:
1. Individuals should be trained to make step-by-step modifications to step on specific landing targets and/or avoid obstacles, both located on ground and above ground.
2. Tasks should provide conflict between self-motion detected by vision and environmental motion.
3. Tasks should challenge the predictive balance control system by exaggerating upper body movements.
4. Locomotion should be performed while carrying loads, and also while being distracted by a secondary task (Frank & Patla, 2003)."

The efficacy of specialized exercise programs (Balance Challenged Exercise) were contrasted against standard aerobic exercise programs. DYME Score which measures mobility performance is shown below at three different times during the study, showing improvement following intervention. These and other results will be discussed.
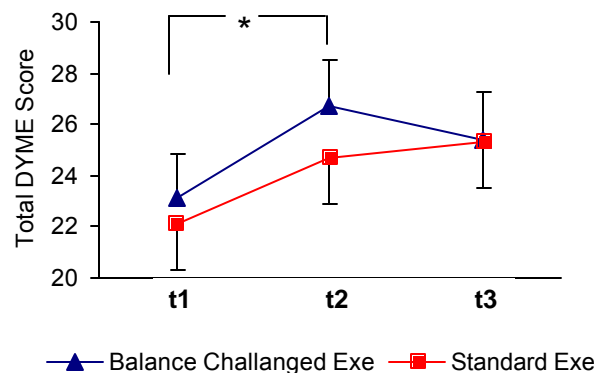
REFERENCES
Patla, A.E. Neurology Report, 25(3): 82-90, 2001.
Frank, J.S., Patla, A.E. Am J. Preventative Medicine, 3 (Suppl. 2): 157-63, 2003.
Patla, A.E. and Shumway-Cook, A. Journal of Aging and Physical Activity, 7(1): 7-10, 1999.
Shumway-Cook, A., Patla, A.E., Stewart, A., Ferrucci, L., Ciol, M.A., Guralnik, J. Physical therapy, 16: 15-19, 2002.

ACKNOWLEDGEMENTS

ARTICUALR CARTILAGE STRESS STATE IN MISALIGNED JOINTS

Sang Kuy Han[1,2], Salvatore Federico[1,3], Marcelo Epstein[2], Walter Herzog[1,2]

[1]Human Performance Laboratory, Faculty of Kinesiology, University of Calgary, Alberta, Canada, shan@ucalgary.ca
[2]Department of Mechanical and Manufacturing Engineering, University of Calgary, Alberta, Canada
[3]Department of Industrial and Mechanical Engineering, University of Catania, Italy

INTRODUCTION

Abnormal or excessive stresses acting on, or within, a joint are speculated to be one of the causes for patellofemoral joint degeneration. Support for this idea comes from experiments in which cartilage degeneration has been initiated in animals by excessive loading. Studies performed on cartilage explants cannot explain the stress-strain states of articular cartilage subjected to loads in the intact joint, because of the artificial boundary conditions required for in vitro testing. Therefore, the purpose of this study was to model cartilage mechanics theoretically, while cartilage surfaces were loaded in their native joint. In order to achieve this goal, an accurate surface geometry of the cat patellofemoral joint was obtained through laser digitization, and the resulting contact problem was solved using a three-dimensional, biphasic, homogeneous, isotropic model of articular cartilage. The contact area, contact pressure, maximum shear stress and tensile stress were calculated for different alignment conditions of the patella relative to femur.

METHODS

In order to represent cartilage *in vivo*, accurate ($< 20mm$) surface geometries of the cat patellofemoral joint were obtained using laser scanning (MicroScan Laser Profilometer, LMI Technologies, Southfield, MI, USA) (Couillard, 2002). Then, a three-dimensional finite element mesh model was created using the commercial software, TrueGRID. Cartilage thickness on the femoral groove and retropatellar surface was approximated to be 0.3 *mm* and 0.5 *mm* respectively (Herzog et al., 1998). The articular cartilage was modeled as being attached to cortical bone of 2.5 *mm* thickness. The patellofemoral joint was modeled for a 70 degree knee angle, which occurs naturally during cat locomotion. A large displacement contact analysis was used with ABAQUS 6.3. Articular cartilage was assumed to be biphasic: the solid phase was assumed linearly elastic and incompressible; and the fluid phase was taken as incompressible, inviscid, and with a deformation-dependent permeability (Holmes and Mow, 1990). The deformation-dependent permeability was described as a function of the void ratio e (ratio of the fluid over the solid fraction) in accordance with Wu and Herzog (2000). The articular cartilage surface was assumed perfectly permeable. In order to compare different joint alignment conditions, the patella was shifted laterally by 0.5 *mm* and 1.0 *mm*, and the reference alignment position was assumed to be a 70 degree knee angle position. A 0 to 3, 100, 150 and 500 *N* ramp load was applied over 2 *s* to the patella.

RESULTS AND DISCUSSION

As the patella was shifted laterally, the contact area decreased, and the peak contact pressure increased. As shown in Fig. 1, the maximum tensile stress (which occurred in the superficial zone) did not show substantial changes. In contrast, a 1 mm misalignment increased the maximum shear stress (in the deep zone) by about 50%.
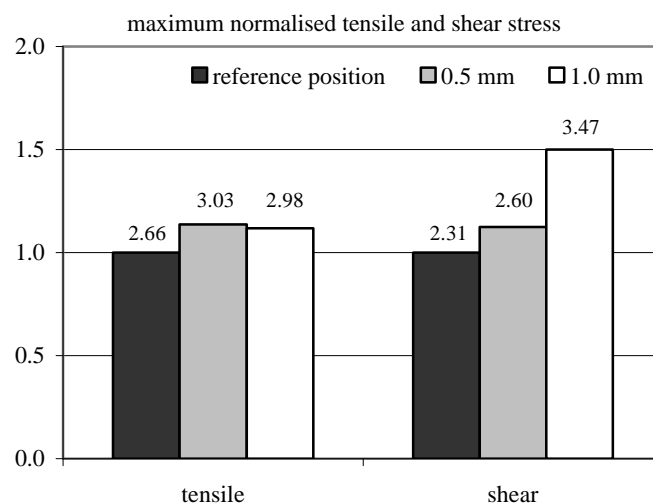

Fig 1. Shear and tensile stress for different alignment conditions for a 150 *N* applied load (absolute values in *MPa*)

Here, we demonstrate that a small change in patellar displacement for a given external load causes relatively large changes in contact area, peak pressures and shear stress, and causes some contact regions to be overloaded. This result might explain the clinical observation that abnormal patellar tracking is associated with knee pain, and possibly, degenerative processes of the knee leading to osteoarthritis.

REFERENCES

Couillard, S (2002) MSc, Thesis, University of Calgary
Herzog, W. et al (1998) *J. Biomech.*, **31**, 1137-45
Holmes, M.H., Mow, V.C. (1990) *J. Biomech* **23**, 1145-56
Wu, J.Z., Herzog, W. (2000) *J. Biomech. Eng*, **28**, 318-330

ACKNOWLEDGEMENTS

Ultrasound Induced Hyperthermia Temperature Tracking of Cervix Tumors Including Vascular Network Effects

F. Ghalichi[1], S. Behnia[2,3], E. Sadigh Rad[3], and A. Bonabi[3]

[1]Department of Biomechanical Engineering, Sahand University of Technology, Tabriz-Iran.
[2]Institute for Studies in Theoretical Physics and Mathematics, Teheran 19395-1795, Iran.
[3]Department of Physics, IAU, Ourmia-Iran, s_behnia@iaushab.ac.ir & sohrab_behnia@yahoo.com .

INTODUCTION

The design of ultrasonic transducer for high power applications, e.g. in medical therapy asks for effects. The response of the living tissue to the effects of strong heating can cause the blood flow rate to vary by an order of magnitude. A mathematical model for the heating of living cancerous tissue is formulated which takes into account the non-local temperature dependence of the blood flow rate when the temperature distribution in the tissue is substantially non-uniform, as in hyperthermia. In the present paper the temperature distribution in the cancerous tissues' of cervix and the results out of simulations by taking into account of the blood flow rate have been mentioned.

MTHODS

Mathematical analysis and estimation of temperature distribution in biological tissue during the process of hyperthermia has been used in the study and optimization of thermal therapies. Within the framework of many different approaches the obtained bio-heat transfer equation is:

$$\rho c \frac{\partial T}{\partial t} = \nabla . K \nabla T - W_b C_b (T - T_a) + Q$$

A more accurate description of the heat transfer process in living tissue is obtained if one takes into account the fact that living tissue form an active, highly heterogeneous medium. In particular, the phase transitions in living tissue dose not occur at a single temperature, but over a temperature range. The influence of this effect has been investigated in [1]. The response of living tissue to the effects of strong cooling or heating can cause the blood flow rate to vary by an order of magnitude [2]. In general, if the temperature distribution in the tissue is substantially non-uniform, then the temperature dependence of the blood flow rate is non-local and the blood flow rate at a given point depends on certain characteristics of the temperature distribution rate, other than the tissue temperature at the point only.

RESULTS AND DISCUSSION

Figure 1 shows 2D temperature distribution in the cancerous cervix. Due to figure 1 we notice that the temperature fluctuates between 37.1 ºC and 52.7 ºC in the focal region, which is enough to destroy the cancerous tissue. Also it should be mentioned that the intervening tissues are safe and undamaged. Fig 2 is the diagram of temperature changes with distance, from the center to the inner septum of cervix. The effect of vascular network and consequently blood flow rate in hyperthermia

treatment indicates that the increase of the radiation duration causes the decrease of temperature increase rate.
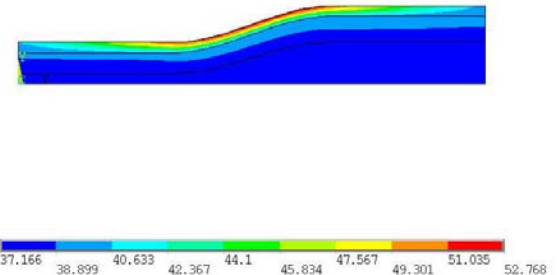
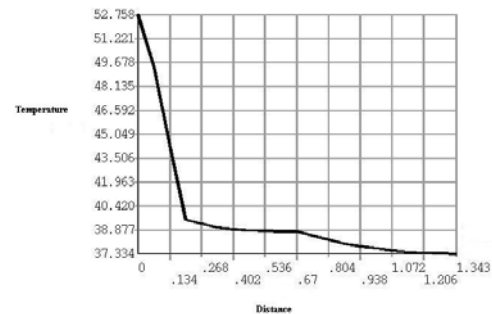Figure 1: 2D temperature distribution in radiated cervix

Figure 2: Temperature distribution due to distance.

SUMMARY

In this paper a phenomenological model for the thermal response in cervix cancerous tissues during the hyperthermia treatment process is formulated that will include the effects of the aforementioned factors. It should be pointed out that the main equations to be formulated is obtained by analysis of the microscopic relations governing the heat transfer process in living tissue and the response of the vascular network, which has been indicated in the temperature distributions diagrams.

REFERENCES

1. R. I. Andrushkiw. Mathematical Modeling of Freezing Front Propagation in Biological Tissue. Math. Comp. Modeling V.B. N.10, 1-9, (1990).
2. G. I. Mchedlishvili. Microcirculation of Blood General Principals of Control and Disturbances. Nayka, Leningrad (1989).

A COMPLIANT DYNAMIC FEA MODEL OF THE AORTIC VALVE
WITH HYPERELASTIC MATERIAL PROPERTIES

Adrian Ranga[1] , Rosaire Mongrain[1,2], Youssef Biadillah[1,] Raymond Cartier[2]

(1) Department of Mechanical Engineering, McGill University, Montreal CANADA
(2) Montreal Heart Institute, Montreal, Quebec, CANADA

1. INTRODUCTION

The aortic valve is a compliant biological structure experiencing dynamic cyclic loading (1). A number of studies have attempted to simulate various aspects of its behavior using finite element analysis techniques (2, 3, 4). Most have used implicit codes to simulate the static loading on the valve at discrete points in the cardiac cycle, and previous work on structural analysis involving dynamic loading did not take into account the physiologically important compliance of the aortic root and the non-linear hyperelastic material properties of the tissues. The present study's aim was to integrate three key physiologically important features into a realistic structural simulation of the aortic valve: compliance of the aortic root wall, non-linear material properties of the tissues, and dynamic loading.

2. METHODS

A geometrically accurate 3D model corresponding to the open valve configuration was created in Pro/Engineer CAD software (Fig. 1). The model was then transferred to the LS-DYNA explicit solver software package, where physiologically realistic thicknesses and boundary conditions were assigned to the shell elements of the valve (4,5, 6). An hyperelastic model (five parameter mooney-rivlin) fitted to experimental data (5) was used to study stress distribution in aortic root.
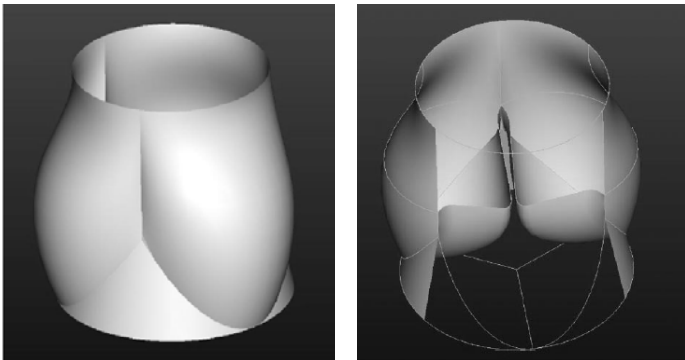
Figure 1. Outer surface of the valve.(left) and Cut-away view of closed valve (right)

3. RESULTS

The aortic root wall was gradually loaded to systolic pressure, and a dynamic loading pattern corresponding to the cardiac pressure cycle was then applied to the wall and leaflets. Results of these simulations demonstrated a number of features previously unreported in previous numerical studies. Hyperelastic material properties (based on experimental stress-strain curves) clearly had an important effect in altering stress patterns. Hyperelasticity dramatically modifies the stress distribution in the aortic root as compared to an elastic model of the same geometry (Fig. 2). More specifically, it is shown that the stress distribution is significantly more homogeneous with an hyperelastic model than with an elastic model.
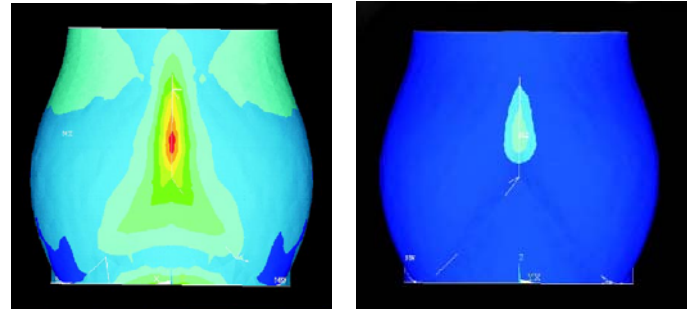
Figure 2 Stress distribution in diastole for a linear elastic model (left) and stress distribution in diastole for nonlinear model (five parameter mooney-rivlin model fitted to experimental data)

4. CONCLUSION & DISCUSSION

As shown the distribution of stresses in linear versus nonlinear models show a significantly more homogeneous distribution in the nonlinear case. This may be indicative of the natural adaptation of the tissue to distribute and bear load in an optimal manner under the physiological conditions (due to the collagen fibre structure). This observation would also have an important impact for grafts design where nonlinear properties would be a mean to better distribute stresses and possibly reduce failure under fatigue loading.

REFERENCES

1. Brewer R. J., Deck, J. D., Capati, B. and Nolan S. P., 1976, The dynamic aortic root – its role in aortic valve function. Journal of Thoracic Cardiovascular Surgery, 72, 413.
2. Grande J., Cochran, R. P., Reinhall, P. G. and Kunzelman K. S., 2000, Mechanisms of aortic valve incompetence: finite element modeling of aortic root dilation. Annals of Thoracic Surgery, 69, 1851 – 1857.
3. Ramakhrisna G., Ramarathnam, K. K. and Kommarkshi R. B., 2002, Dynamic analysis of the aortic valve using a finite element model. Annals of Thoracic Surgery, 73, 1122 – 1129.
4. Beck, A., Thubrikar M. and Robicsek F., 2001, Stress analysis of the aortic valve with and without the sinuses of valsalva. The Journal of Heart Valve Disease, 10, 1 – 11.
5. Okamato R. J., Wagenseil J. E., Delong W. R., Peterson S. J., Kouchoukos, N. T. and Sundt III, T. M., 2002,Mechanical Properties of dilated human ascending aorta.Annals of Biomedical Engineering, 30, 624 – 635.
6. Swanson W. M. and Clark R. E., 1974, Dimensions andGeometric relationships of the human aortic valves as a function of pressure. Circulation Research, 35, 871.

DEVELOPMENT OF A BLOOD ANALOG MICROPARTICLE SUSPENSION FOR HEMOLYTIC POTENTIAL ASSESSMENT OF CARDIOVASCULAR DEVICES

T.T. Nguyen[1], R. Mongrain[1, 3], S. Prakash[2], and J. -C. Tardif[3]

[1]Department of Mechanical Engineering, McGill University, Montréal, Canada, rosaire.mongrain@mcgill.ca
[2]Department of Biomedical Engineering, McGill University, Montréal, Canada
[3]Montreal Heart Institute, Montréal, Canada

INTRODUCTION

Experimental reproduction of the hemolytic potential of blood (i.e. the destruction of red blood cells (RBC)) *in vitro* is very important in the evaluation of cardiovascular prostheses design (aortic valves, left ventricular assist devices (LVAD)). Currently, biological blood from various species is still used for direct evaluation of hemolysis created by cardiovascular prostheses. However, the use of blood often requires special manipulations (filtration, addition of antibiotics and anticoagulants, sterilization). Furthermore, blood samples from various species have different RBC morphology and mechanical properties and thus, may yield different hemolytic potentials. From these different factors, using blood gives incomparable and irreproducible results. Therefore, we have developed a blood analog which is a suspension of microns-sized natural polymeric gel particles, each encapsulating a dye agent. These particles are designed to release the dye agent through shear-induced diffusion and by fragmentation at high, non-physiological shear rates.

MATERIALS AND METHODS

The polymeric particles were made from a chemical interaction between calcium ions and alginic acid (Sigma-Aldrich, St-Louis, MO) that forms a soft and elastic gel material. The production of these particles was done using a high-pressure air-atomization nozzle (Turbotak, Toronto, ON) (Kwok et al. (1991)). The shape of these particles was spherical and their average size was about 17 microns in diameter. These characteristics were not exactly identical to the actual human RBC. However, in this work, we were interested in reproducing the bulk properties of blood (dynamic viscosity and hemolytic behavior). The viscosity dependence (μ) of the blood analog at ~40% hematocrit (volumetric concentration) was measured as a function of shear rate ($d\gamma/dt$) using a double-gap viscometer (Bohlin 120 HR, East Brunswick, NJ) in the physiological range (0.1-300 s^{-1}). The hemolytic behavior of the blood analog was studied within a controlled shear stress range of 60-260 Pa and time exposures to shear stress in the range of 156-1297 milliseconds using an apparatus designed for this purpose as described in Pohl et al (2000).

RESULTS AND DISCUSSION

The average viscosity curve obtained by different authors for human blood was compared to the one obtained from the blood analog suspension (Figure 1). It was observed that the blood analog agrees very well with real blood within physiological shear rates. Furthermore, the diffusive properties of the particles were found to have a similar behavior to that of human blood when compared with literature results (Wurzinger et al (1986)) (Figure 2).
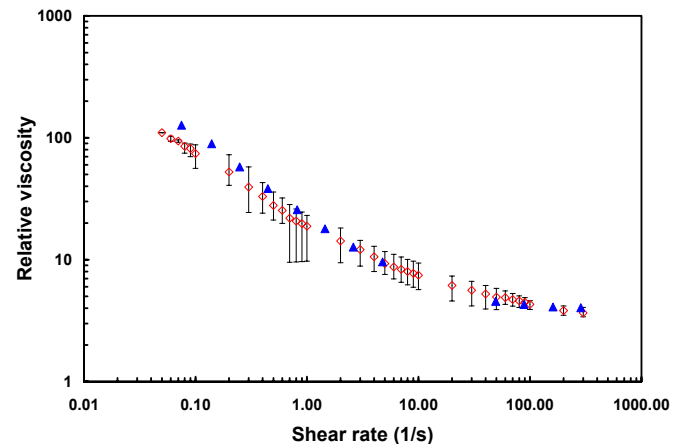

Figure 1. The average viscosity behaviour of the microparticle suspension (triangles) within the applied shear rate range compared to that of whole blood (circles).
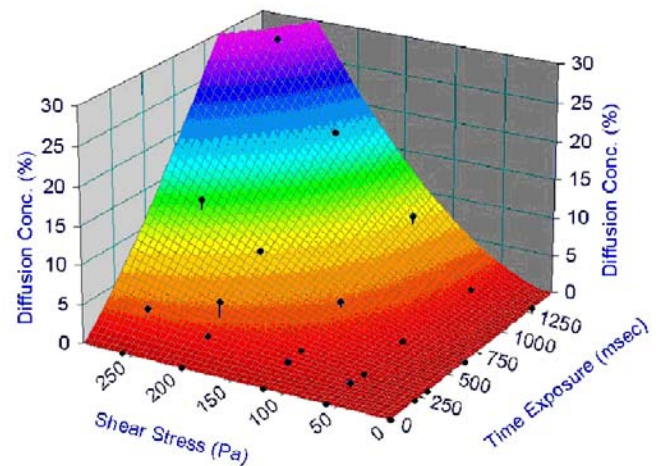

Figure 2. Graph of the experimental diffusion results (dots) correlated and surface fitted with hemolysis data from literature (Wurzinger et al. (1986)).

REFERENCES

Kwok KK et al. (1991), *Pharm. Res.*, **8(3)**, pp. 341-344
Pohl M et al. (2000), *Biorheology*, **37**, pp. 313-324
Wurzinger LJ et al. (1986), *Angéiologie*, **38(3)**, pp. 81-97

EFFECT OF RESIDUAL STRESSES DUE TO CEMENT CURING IN THE LOAD TRANSFER OF A PERSONALIZED CEMENTED HIP IMPLANT

Pablo Vasquez[1], Natalia Nuño[2] and Jacques A. de Guise[2]
[1]Département de génie mécanique, [2]Département de génie de la production automatisée,
Laboratoire de recherche en imagerie et orthopédie
ÉTS, Université du Québec, Montréal, Canada, pablo_vasquez@hotmail.com

INTRODUCTION

In a total hip arthroplasty (THA) using bone cement for fixation of the implant to the bone, residual stresses are generated in the cement mantle due to cement expansion during polymerization. Nuño et al. (2002) have demonstrated that these residual stresses need to be taken into account in numerical models analysing the load transfer of cemented hip implants. Their study was limited to an idealized cement hip implant surrounded by cement and bone mantles. The objective of this study is to investigate the effect of including the residual stresses due to cement polymerization in the load transfer of a personalized THA. The first specific objective is to reconstruct a proximal femur derived from medical images. The second objective is to develop a finite element model of the THA in order to analyze the load transfer from the implant to the bone cement, in order to understand better the aseptic loosening of the stem-cement interface of cemented hip implants, possibly leading to failure of the arthroplasty.

METHODS

Images, as shown in Figure 1, were taken by an helical CT-scanner (resolution 0.8 mm x 0.8 mm) and were used to build a personalized 3D VRML model of the proximal part of the femur. Figure 2 shows the VRML and solid models. The mechanical properties for the cortical and cancellous bones were determined from the CT-scan images. The mean effective density of the bone was derived from the CT images: cortical bone: ρ=2 g/cm^3, cancellous bone: ρ=0.4 g/cm^3. The proximal femur was reconstructed from the medical images, and a Müller Curved stem, made of Co-Cr, was placed inside the femur (Figure 2). The range of the cement mantle thickness surrounding the implant was between 1-6 mm, and the cancellous and cortical bones were modeled based on a previous work of Stolk et al. (2002). Finally, a 3D finite element (FE) model was developed.

The FE model shown in Figure 3 was meshed and solved using the commercial software Ansys 8.0. The model has more than 30 000 elements. The stem, cement and cancellous bone are assumed to be linearly isotropic and homogeneous, whereas the cortical bone is assumed to be anisotropic with the following material properties: E_x= E_y=7.0 GPa; E_z=11.5 GPa; G_{yz}= G_{zx}=3.5 GPa; G_{xy}=2.6 GPa. The stem-cement interface is modeled with surface-to-surface contact elements allowing a debonded interface to be simulated, while the cement-bone interface is assumed to be completely bonded. The magnitude of the hip and abductors forces applied to this numerical model are taken from Stolk et al. (2002).

RESULTS AND DISCUSSION

Different load cases are investigated. In the first load case, the mechanical properties and boundary conditions of Stolk et al. (2002) are used. The stem-cement interface is considered completely bonded to validate the model by comparing the trends of the principal strain distribution in the bone and the cement with the results of Stolk et al. (2002). Then, the stem-cement interface is considered completely debonded and include a coefficient of friction (Nuño et al., 2002) and the residual stresses due to cement curing are simulated by a thermal expansion. The magnitude of the residual stresses are taken from an on-going experiment devised to measure the residual stresses generated in the bone cement during polymerization of the cement.

REFERENCES

Nuño, N., et al. (2002). *J. Biomech, 35*(6), 849-852.
Nuño, N., et al. (2002). *J. Biomed. Mater. Res*, 118, 399-404.
Stolk, J., et al. (2002). *J. Biomech, 35*(4), 499-510.

ACKNOWLEDGEMENTS
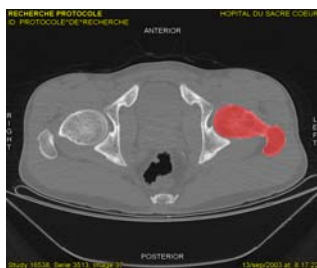
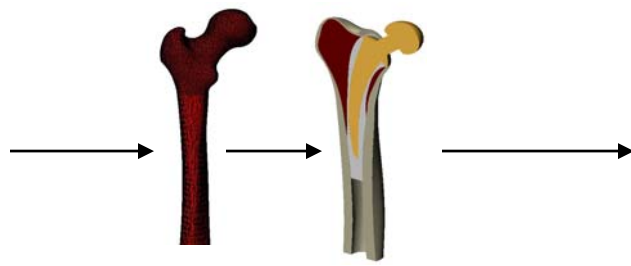**Figure 1**
2D segmentation from CT-scan images

Figure 2
Transfer fromVRML to IGES format.

Figure 3
3D finite element model

GAIT COMPENSATIONS FOR HIP MUSCLE WEAKNESS IN IDIOPATHIC INFLAMMATORY MYOPATHY

Karen Lohmann Siegel, Thomas M. Kepple, and Steven J. Stanhope
Physical Disabilities Branch, National Institutes of Health,
Department of Health and Human Services, Bethesda, MD, USA contact: karen_siegel@nih.gov

INTRODUCTION

Idiopathic inflammatory myopathies (IIM) are disorders of chronic skeletal muscle inflammation that result in symmetrical muscle weakness affecting axial muscles and proximal arm and leg muscles (Amato et al., 1997). Despite moderate to severe weakness, some individuals with IIM continue to ambulate independently, while others do not. The purpose of this report is to present a case series of three patients diagnosed with IIM and hip muscle weakness who each used a different strategy to compensate in gait.

METHODS

Data were reviewed from patients with hip muscle weakness who had been referred for gait analyses as part of their participation in research studies for which they had provided informed consent. From this group, 3 subjects who each used a different compensatory strategy during gait were selected for presentation. Subject 1 (S1), 43 years old, and Subject 3 (S3), 38 years old, were diagnosed with polymyositis, and Subject 2 (S2), 12 years old, was diagnosed with juvenile dermato-myositis. All subjects were female and had less than antigravity strength in their hip muscles. Other lower extremity muscles were able to move against gravity with moderate resistance, except S3 also presented with some ankle plantar flexor weakness.

Analysis was performed on the side of the weaker hip and compared to a normal subject (NL). Subjects walked without assistive devices at a self-selected speed (NL=1.33, S1=0.80, S2=0.76, S3=0.71 m/s). A 6-camera video-based motion capture system (Vicon Motion Systems, Lake Forest, CA), 2 force platforms (AMTI, Watertown, MA), and analysis software (C-Motion, Rockville, MD) were used to obtain bilateral lower extremity joint angles and moments during gait. An induced acceleration analysis was performed during late single limb support using a 7-segment musculoskeletal model (Kepple et al., 1997). It calculated the relative contribution of each joint moment and gravity to producing either hip joint acceleration or the ground reaction force. The ground reaction force vertical component represented upright support and the anterior component indicated propulsion.

RESULTS AND DISCUSSION

In the late single limb support phase of normal gait, the ankle plantar flexor moment generated an upward (not shown) and forward acceleration on the body center of mass, while simultaneously accelerating the hip into extension (Fig). The hip flexors worked eccentrically to control the rate of hip extension during this interval of gait.

Like the normal subject, all 3 impaired subjects used the ankle plantar flexor moment to provide upright support, which simultaneously produced a hip extension acceleration. S1 also used the plantar flexor moment to generate forward propulsion (Fig). However, S1 increased her knee flexion angle, which decreased the relative effect of the ankle plantar flexor moment on producing hip extension acceleration. S1 appeared to generate a hip flexor moment passively by positioning the joint at end range of extension. The other two subjects also altered joint positions and generated propulsion with either the knee flexor moment (S2) or gravity (S3), which had the advantage of accelerating the hip into flexion (Fig). This decreased the demand on the weak hip flexors to oppose the hip extension acceleration produced by the ankle plantar flexor moment (which provided upright support).
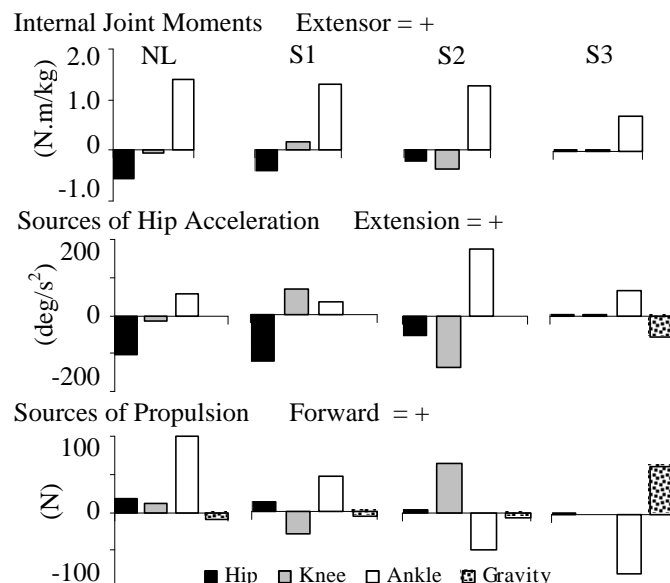

Figure: Data from late single limb support phase for normal gait and the three impaired subjects showing net internal joint moments (top row) at the hip (black), knee (gray), and ankle (white) and the relative contributions of those moments and gravity (dotted fill) to producing hip joint acceleration (middle row) and the anterior ground reaction force (bottom row).

SUMMARY

After midstance, the ankle plantar flexor moment normally provides upright support and forward propulsion while accelerating the hip into extension. The hip flexors of the impaired subjects were too weak to control this hip extension. Subjects altered lower extremity joint positions and moments in gait and produced forward propulsion while minimizing hip extension acceleration. These compensatory strategies permitted independent ambulation, although at a reduced speed as compared to normal gait. Knowledge of these successful strategies can assist the rehabilitation of patients with hip muscle weakness who are unable to ambulate.

REFERENCES

Amato AA, et al. (1997). *Neurol Clin,* **15**, 615-48.
Kepple TM, et al. (1997). *Gait & Posture,* **6**, 1-8.

FOOT POSITIONS AND ASYMMETRY OF VERTICAL REACTION FORCES DURING RISING FROM A CHAIR IN PERSONS WITH HEMIPARESIS

Guylaine Roy[1-2], Sylvie Nadeau[1-2], Denis Gravel[1-2], Francine Malouin[3], Brad McFadyen[3], Julie Lecours[1], France Piotte[1-2]

[1]Centre de recherche interdisciplinaire en réadaptation , site Institut de réadaptation de Montréal,
[2]École de Réadaptation, Université de Montréal, (Québec), Canada, H3S 3J4 sylvie.nadeau@Umontreal.ca
[3] Centre interdisciplinaire de recherche en réadaptation et intégration sociale, IRDPQ et Université Laval, (Québec), Canada

INTRODUCTION

Persons with hemiparesis, in addition to take more time to execute the task, use an asymmetrical limb-loading strategy when rising-up from a chair (Engardt and Olsson, 1992). This unequal limb-loading can be modified by foot placement (Brunt et al., 2002). However, it is not known if the foot placement also affect the limb-loading before seat off i.e. when the subjects still have the thighs in contact with the seat of the chair. This study examined the effect of foot placements on the asymmetry of limb-loading during the rising-up from a chair by measuring the vertical reaction forces (VRF) under the thighs and feet. The results of persons with hemiparesis are compared to those from a control group.

METHODS

Twelve persons with a chronic hemiparesis (49.7 ±9.0 years) and eight healthy subjects (61.6 ±10.6 years) participated. The persons with hemiparesis had scores on the Chedoke McMaster Sroke Assessment Scale ranging from 2 to 6 and 3 to 6 for the foot and the leg, respectively. All were able to stand-up without using their hands and had walking speeds from 0.27 to 1.28 m/sec. The participants were required to rise at natural speed from an instrumented chair adjusted to individual's knee height. The seat of the chair was equipped with a force platform set-up that measured the forces under each thigh. Forces under each foot were also measured by two force plates embedded in the floor. Different foot conditions were assessed: spontaneous (SP), symmetric (S), asymmetric with the affected (AS-A), or dominant foot for the healthy subjects (AS-D) placed behind the non-dominant foot, and asymmetric with un-affected foot placed behind the affected foot (AS-UA). Four distinct events were identified during rising: onset (EV-O), the transition phase that corresponded to almost similar VRFs under the feet and thighs (EV-T), seat-off (EV-SO) and end of task (EV-E). The main dependant variable was an index of asymmetry (IA^{VRF}) of the VRFs between sides, expressed in percent, as follows: $IA^{VRF} = [VRF$ (foot and thigh combined) on the unaffected $– VRF$ of perfect symmetry]/ VRF of perfect symmetry. Where perfect symmetry corresponded to equal forces on the right and left sides (total of VRF /2). Data (mean of two trials) of healthy subjects and patients were compared at EV-T and EV-SO using statistical analyses (ANOVA and t-test) with a p-value adjusted for the number of comparisons.

RESULTS AND DISCUSSION

Healthy subjects showed almost equal VRFs on both feet and thighs in the SP and S conditions at all events with a mean IA^{VRF} less than 5% (Fig.1A). This agreed with results reported in previous studies (e.g. Engardt et Olsson., 1992). The AS-D foot placement increased the asymmetry significantly between sides at events EV-T and EV-SO to reach a mean level around 10%-15%. Persons with hemiparesis presented a high

difference in loading between the affected and unaffected limbs in the SP, S and AS-UA conditions. This difference was lowered in the AS-A condition (affected foot behind) resulting in significantly less asymmetry between sides in comparison to the three others foot placements at EV-T and EV-SO (p<0.003; Fig.1B). It should be emphasised that the asymmetry observed at EV-T originated, in a similar proportion, from unequal VRFs at both the thighs and feet. This indicates that persons with hemiparesis already adopted an asymmetrical pattern before seat-off when forces are exerted by the thighs and feet. At EV-T, the patients were more asymmetrical than the controls for the SP and S conditions. No differences were observed between AS-D and AS-A and between AS-D and AS-UA. At EV-SO, the IAs^{VRF} were different between groups for each condition except between AS-D and AS-A. No difference was obtained in the asymmetry between events EV-T and EV-SO for either group.
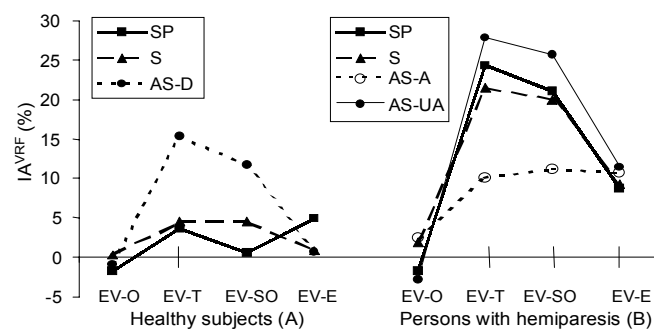

Fig.1: Index of asymmetry of the VRF (IA^{VRF})

SUMMARY

Overall, persons with hemiparesis had a marked deviation from the perfect symmetry when they rose-up from a chair spontaneously. At transition phase (EV-T), the asymmetry was not different from that of seat-off (EV-SO). However, at transition, the asymmetry was due to unequal loading on both the thighs and feet. The results also showed that foot placement corresponding to the affected foot behind the unaffected foot can reduce the asymmetry at the transition (EV-T) and seat-off (EV-SO) events. In rehabilitation, clinicians encourage their patients to rise from a chair with the affected foot behind the good foot to increase loading on the affected lower limb. This clinical practice is well supported by the results of the present study and it contributes to better symmetry of the VRFs exerted by both thighs and foot.

REFERENCES

Engardt M, Olsson E. (1992). Scand J. Rehab Med., 24, 67-74.
Brunt D et al. (2002). Arch Phys Med Rehabil., 83: 924-929.

ACKNOLEDGEMENTS

GAIT ADAPTATION IN INDIVIDUALS WITH PARKINSON'S DISEASE

Flora F. Stephenson[1] and Sandi J. Spaulding[2]
[1]Masters candidate, School of Kinesiology, The University of Western Ontario, London, Canada, fstephe@uwo.ca
[2]School of Occupational Therapy, The University of Western Ontario, London, Canada

INTRODUCTION

Parkinson's disease (PD) affects approximately 100,000 Canadians (Parkinson Society Canada, 2004) and gait disturbances are often a result of the disease. Individuals with PD often walk with smaller step lengths and lower cadences, resulting in decreased velocity and the appearance of "shuffling gait" (Vieregee et al., 1997; Morris et al., 1996). Peak vertical and propulsive ground reaction forces are lower in individuals with PD when walking on level ground (Gantchev et al., 1996; Koozekanani et al., 1987).

Individuals with PD identified walking on level ground and the transition from level ground to up ramp walking as difficult tasks to perform. However, these individuals noticed that transition to up step walking is not a difficult task (Personal communications, September to December 2002). This study examined the ground reaction forces as individuals with PD prepare for the transition from level ground walking to three conditions: continue with level ground walking, change to up ramp or up step walking. The transition is defined as the last step prior to change in walking conditions.

METHODS

Eight individuals with PD (mean age 60.38) and eight without PD (mean age 66.13) participated in the study. Five infrared markers were placed on the right legs of the participants at the hip, knee, ankle, heel and base of 5th metatarsal after informed consents were obtained. The markers were tracked using Optotrak. The participants walked along a walkway with an embedded force plate at their normal pace in each of the three conditions. Each condition was repeated until four successful trials were obtained. Maximal vertical and propulsive ground reaction forces from each condition were averaged and normalised for statistical analysis using SPSS.

RESULTS AND DISCUSSION

Individuals with PD walk with lower maximal vertical and propulsive forces compared to individuals without PD when walking on level ground (Figures 1 and 2), which is consistent with previous research (Ganchev et al., 1996; Koozekanani et al, 1987). Decreased maximal ground reaction forces are recorded in individuals with PD as they are preparing to walk up ramp. However, the differences disappear when the individuals prepare to walk up step.

The decreased magnitude in maximal ground reaction forces results in perceived difficulty in completing level ground and transition to up ramp walking tasks in individuals with PD. Close to normal maximal forces were generated when individuals with PD prepare to walk up step, which suggests that up step walking is an easier way for individuals with PD to traverse vertical distances. Steps should be encouraged in homes of individuals with PD for travelling vertical distances.
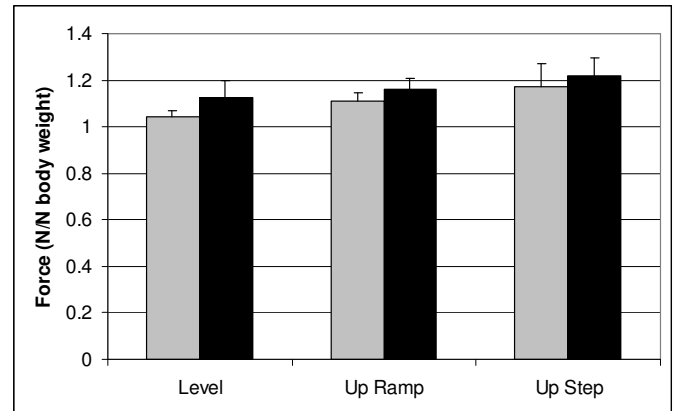

Figure 1: Maximal vertical ground reaction forces in the two groups. Grey bars represent participants with PD and black bars represent participants without PD.
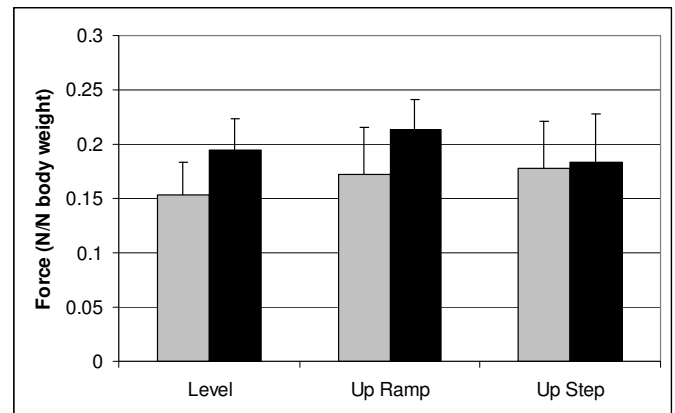

Figure 2: Maximal propulsive ground reaction forces in the two groups. Grey bars represent participants with PD and black bars represent participants without PD.

SUMMARY

Individuals with PD generate lower maximal vertical and propulsive ground reaction forces compared to individuals without PD when they are walking on level ground or preparing to walk up ramp. Close to normal maximal ground reaction forces are generated as individuals with PD prepare to walk up step. The use of steps should be encouraged in homes of individuals with PD for travelling vertical distances.

REFERENCES

Gantchev, N. et al (1996). *Electroencephalogr Clin Neurophysiol*, **101**, 110-120.
Koozekanani, S.H. et al (1987). *Arch Phys Med Rehabil*, **68**, 28-30.
Morris, M.E. et al (1996). *Brain*, **119**, 551-568.
Parkinson Society Canada (2003). http://www.parkinson.ca.
Vieregge, P. et al (1997). *J. Neural Transm*, **104**, 237-248.

GAIT PATTERNS AND KNEE FUNCTION FOLLOWING ARTHROSCOPIC PARTIAL MENISCECTOMY

Daina L Sturnieks, Thor F Besier, David G Lloyd

School of Human Movement and Exercise Science, The University of Western Australia

dlloyd@cyllene.uwa.edu.au

INTRODUCTION

Arthroscopic partial meniscectomy (APM) patients have increased risk of developing knee osteoarthritis (OA), yet the disease pathway remains unclear. Mechanical loading is believed to play a role in the development of knee OA. For example, larger-than-normal knee adduction moments during the stance phase of gait generate large loads on the medial articular surfaces of the tibiofemoral joint and may contribute to degenerative joint changes (Prodromos *et al.*, 1985; Schipplein & Andriacchi, 1991). Limited information currently exists regarding gait patterns and knee function in people following APM. Analysis of lower limb kinetics may provide important information regarding the long-term joint condition in APM patients.

METHODS

Three-dimensional gait analysis, with a 50 Hz VICON motion analysis system, was performed on 106 pain-free APM patients (average 11 weeks post-surgery) and 49 healthy controls, walking at natural, self-selected speed. Peak knee flexion and extension angles, normalised peak knee flexion and extension moments, normalised peak knee adduction moments and trough, and normalised sagittal and frontal plane angular impulses were analysed during stance phase.

Knee pain and function was assessed using the self-administered Knee Osteoarthritis Outcome Survey (KOOS), a superset of the widely used and validated WOMAC questionnaire. The KOOS includes subscales of: 1) Pain; 2) Symptoms; 3) Activities of Daily Living; 4) Sport and Recreation; and 5) Quality of Life.

RESULTS AND DISCUSSION

The APM population was comparable to the controls in spatiotemporal parameters. The APM subject's operated limb demonstrated a reduced range of knee motion (ROM) between heel strike and peak knee flexion at midstance and significantly reduced knee flexion moments, compared to controls ($p<0.02$). The APM group also showed larger than normal knee adduction moments on both operated and non-operated limbs (Figure 1).

Total KOOS score for the APM group (mean=70.6, SD=15.5) was significantly less than that for the CON group (mean=98.4, SD=3.5) ($p<0.01$). The largest differences were in the Sport & Recreation and Quality of Life scales, which were almost half that of the control group. Stride length
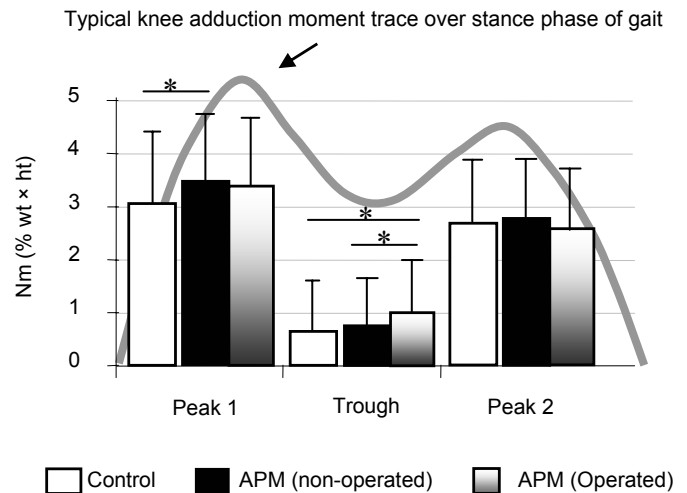

Typical knee adduction moment trace over stance phase of gait

Figure 1: Knee adduction moments during stance in Control and APM groups. *$p<0.05$

showed a weak, yet significant positive correlation with all KOOS subscale scores (r=0.240-0.398, $p<0.05$). Knee ROM showed a weak, yet significant positive correlation with Symptoms (r=0.247, $p<0.05$), while the knee adduction moment trough was correlated with the Pain (r=0.296, $p<0.05$).

SUMMARY

At three months post-surgery, APM demonstrate pathological gait patterns that are weakly related to knee pain and function. The larger than normal knee adduction moments displayed by the APM group likely increases articular loads on the medial compartment of the tibiofemoral joint and may contribute to the high risk of knee OA following arthroscopic meniscal surgery.

REFERENCES

1. Prodromos, C.C. *et al.* (1985). *J Bone Joint Surg*; 67: 1188-94.
2. Schipplein, O.D. and T.P. Andriacchi (1991). *J Orthop Research*; 9: 113-9.

ACKNOWLEDGEMENTS

VALIDITY AND RELIABILITY OF ACCELEROMETRIC GAIT ANALYSIS IN THE ASSESSMENT OF OSTEOARTHRITIS OF THE KNEE

Ben Orlik, Michael J. Dunbar, David J. Amirault, Allan W. Hennigar and Lorne Leahey
Orthopaedic Surgery, Dalhousie University, Halifax, Nova Scotia, Canada
Borlik@dal.ca

INTRODUCTION
The Walkabout Portable Gait Monitor™ (gaitbelt) is a novel instrument worn around the waist that records accelerometric gait data. The purpose of this study was to define objective, quantifiable measures of pathological gait, to determine the reliability (intra-subject and inter-rater) of these measures in a population with knee Osteoarthritis (OA), and to investigate the relationship between gait and the previously validated questionnaires (WOMAC, SF-36) and radiographic evidence of OA.

METHODS
This was a prospective, dual-trial, multi-cycle, convenience survey of 66 patients referred to an orthopaedic surgeon and diagnosed with knee OA in an orthopaedic department of a tertiary care hospital. Outcome measures were WOMAC, SF-36, radiographic feature analysis, and 3-dimensional, accelerometric gait analysis.

RESULTS
The gait measures had very good to excellent intra-subject (ICC=0.81–0.92) and inter-rater (ICC=0.85–0.99) reliability, as well as high internal consistency (Cronbach's Alpha = 0.74). There were significant correlations between gait and the SF-36, WOMAC and radiographic features of OA ($p < 0.05$, $p < 0.01$).

CONCLUSIONS
The proven reliability and validity of the gaitbelt establishes it as a valuable tool for assessing osteoarthritis of the knee joint. It is able to detect asymmetries and inefficiencies in pathological gait, which are related to outcome questionnaires and radiographic evidence of OA. The gaitbelt is easily and economically applicable to a clinical setting. The gaitbelt can be utilized as a surrogate to formal gait analysis for further gait research in OA of the knee. Future research shall include the responsiveness of the gait measures in the context of an applied treatment of OA.

Development and *In Vitro* Validation of a Model to Predict the Patellofemoral Contact Forces of TKRs

T. Ward[1], H. Pandit[2], D. Hollinghurst[2], P. Moolgavkar[3], A.B. Zavatsky[1], H.S. Gill[2]
[1]University of Oxford, Department of Engineering Science, Oxford, UK
[2]OOEC/NDOS, University of Oxford, Oxford, UK
[3]North Hampshire Hospital, Basingstoke, UK
richie.gill@orthopaedic-surgery.oxford.ac.uk

INTRODUCTION

Patellofemoral pain is a significant problem for patients with Total Knee Replacements (TKRs) (Murray *et al*, 1998). It is hypothesized that pain is related to abnormally high patellofemoral forces (PFF) (Singerman *et al*, 1995). The aim of this study is to validate a model to estimate PFF after TKR, using a combination of non-invasive measurement and theoretical modeling.

METHODS

Experiments were performed on four post-mortem knee specimens to compare the PFF and the quadriceps force (QF) estimated by a 2D sagittal plane model (Gill, 1996), with those measured using force transducers. A sagittal model was chosen because the largest component of PFF is in the sagittal plane, and other studies have shown that different designs produce different PFFs in the sagittal plane (Miller *et al*, 1998). Each knee was tested in its initial state and after implantation of three Scorpio designs (Stryker, UK): Cruciate Retaining (CR), Posterior Stabilised (PS), and the Posterior Stabilised Mobile Bearing (PS Plus). The experiments were performed in the Oxford Gait Laboratory which had a twelve camera Vicon612 motion analysis system (Vicon Motion Systems, Oxford, UK). Each knee was extended/flexed between 130° of flexion and full extension under a simulated quadriceps load with 3 kg hung from the distal tibia. Reflective markers were rigidly attached to the femur, patella and tibia to measure the relative movement of the bones. A 6DOF force transducer (Singerman, 1995), was used to measure patellofemoral forces and a uni-axial transducer was used to measure quadriceps forces. A fluoroscope simultaneously captured images of the leg extension activity. Parameters measured from the images were used as inputs to the model to estimate the joint forces.

RESULTS

The measured and estimated PFF and QF of the TKRs match closely between 20° and 80° of knee flexion, after which the model overestimated the PFF by a maximum of 23 N (7.6 % of max) for the PFF and by 31 N for the QF (10.3 % of max) (Fig 1). The estimated and measured Patellar Flexion Angles (PFA) were within 3.5° throughout the flexion range (Fig 2).

DISCUSSION and CONCLUSION

The model accurately predicts sagittal plane patellar kinematics and kinetics, using only fluoroscopy and externally measured forces as inputs.
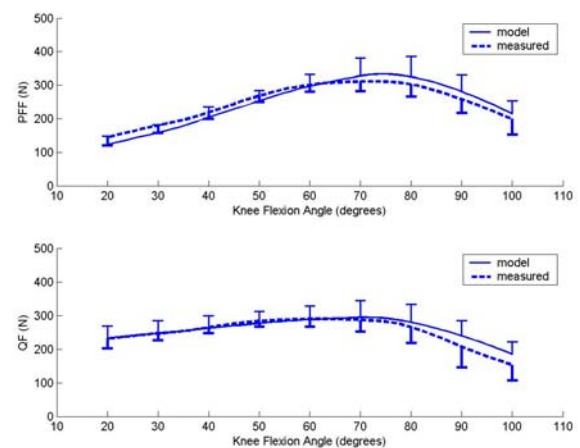

Figure 1: Measured (-1SD) and Estimated (+1SD) PF (top) and QF (bottom).
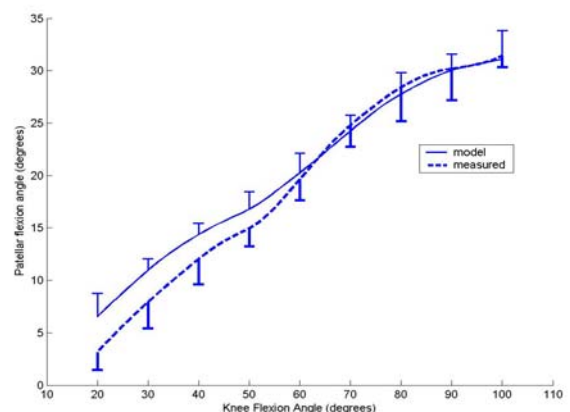

Figure 2: Measured (-1SD) and Estimated (+1SD) Patellar Flexion Angle.

However, the model has a limitation in assuming that the extending moment is only due to the quadriceps.

REFERENCES
Gill H.S. (1996). *Clinical Biomechanics*, **2**, 81-89.
Miller R., Goodfellow J., Murray D., O'Connor (1998). *Journal of Bone and Joint Surgery*,80-b (5), 900-906.
Murray, D., Frost, S. (1998). *Journal of Bone and Joint Surgery (B)*, **80(3)**, 426-431.
Singerman R., Berilla J., Davy D. (1995) *Transactions of the ASME,* **117**, 8-14.

GROUND REACTION FORCES IN TREADMILL VS. OVERGROUND RUNNING

J. Determan, S. Swanson, W. McDermott, and J Hamill
Department of Exercise Science, University of Massachusetts, Jeremy.Determan@soletechnology.com

INTRODUCTION

Previously published studies using ground reaction force (GRF) treadmills either focused on the physical properties of the treadmill or presented limited data on one or two components of the GRF, typically the vertical and anterior-posterior GRF (Kram and Powell, 1989, Kram et al., 1998, Dutto and Smith, 1999, Chang and Kram, 1999). Very few published studies have examined the differences in the GRF between overground and treadmill running. The purpose of this study was to examine the three-dimensional GRF patterns of subjects as they ran overground and on a custom built force treadmill.

METHODS

Three-dimensional GRF data was collected on 15 healthy male heel-toe trained runners as they ran over a force platform (AMTI) and on a custom built force treadmill (Frappier Acceleration). The treadmill consisted of a rigid aluminum frame sitting atop four force transducers (AMTI). The signals originating out of the force transducers were summed together according to their orientation. A variety of static and dynamic tests were performed to evaluate the reliability of the force treadmill. Non-linearity of the vertical force output was less than 1.2%. Point of force application varied by less than 0.3%. The natural frequency of the treadmill system was found to be 164 Hz, 141 Hz, and 36 Hz in the vertical (V), anterior-posterior (AP), and medial-lateral (ML) directions respectively. Vibration noise was found to be ± 80 N, ± 20 N, and ± 15 N in the V, AP, and ML directions. Similar tests were also conducted on the force platform to observe the differences in the measurement properties of the two systems. During the experiment, subjects ran on the treadmill at 3.5 m/s ($\pm 1\%$) while GRF data was collected for 10 seconds, which allowed for the analysis of 10 consecutive right foot falls. Subjects also ran across the force plate at 3.5 m/s ($\pm 2.5\%$) and 10 successful right foot falls were also collected. Running speed for the overground trials was monitored via a radar gun (Stalker ATS) and the order of conditions was randomized. A low pass Butterworth filter was applied to both the overground and treadmill data with cutoff frequencies of 35 Hz, 30 Hz, and 25 Hz corresponding to the V, AP, and ML signals respectively. Seven GRF parameters were selected for examination. A repeated measures one-way ANOVA was then conducted on the 15 mean values of each GRF parameter.

RESULTS

The results from this experiment are summarized below in Table 1. Stance time (defined as the period of time when V exceeded 20 N) was found to be similar in both the overground and treadmill running conditions and the number of subjects who either slightly increased or decreased their stance time when going from one gait environment to the other was equivalent. Although the impact peaks tended to be slightly greater in overground running, no significant difference ($p > 0.05$) was found. The active peak was virtually identical between the two conditions. There was no significant difference ($p > 0.05$) in the propulsive impulse between the two running conditions, although there was a significant difference ($p < 0.05$) in the braking impulse. Examining the differences in the braking and propulsive impulse within each condition we found that the subjects maintained constant velocity while running on the treadmill, but slowed down slightly when running overground. Examining ML, the peak medial force was significantly greater during overground running ($p < 0.05$) and the peak lateral force was significantly greater during treadmill running ($p < 0.05$).

DISCUSSION AND CONCLUSION

In this study, there appears to be a difference in the GRF's during treadmill and overground running. This suggests that the two gait environments are different, at least on a kinetic level. Caution should therefore be used in extrapolating results from one gait environment to the other. It should be noted that there are some confounding factors that could have resulted in a difference between these two conditions. These factors include the differences in support surface stiffness between the treadmill and force plate, lower constraints on constant running speed while running over the force plate, fundamental differences in the task itself, differences in the placement of the foot on the force plate during the overground conditions, and slight differences in the air resistance and friction between the two gait environments. Further investigation on how each of these factors affected the results in this study is needed.

REFERENCES

Kram and Powell (1989). *J. Applied Phys*, **67**, 1692-1698.
Kram et al (1998). *J. Applied Phys*, **85**, 764-769.
Dutto and Smith (1999). *Abstract in 23rd Annual Meeting of the ASB (Ed.)* 239-240.
Chang and Kram (1999) *J. Applied Phys*, **86**, 1657-1662.

Table 1 GRF Parameters for Overground vs. Treadmill Running. Force-N; Time-ms; Impulse-Ns. Mean (SD)

Condition	Stance Time	Impact Peak	Active Peak	Braking Impulse	Propulsive Impulse	Medial Peak	Lateral Peak
Overground	262 (18.9)	1312 (179)	1811 (218)	-19.2 (3.8)	15.5 (2.5)	77.6 (28.2)	-39.9 (21.2)
Treadmill	264 (18.1)	1234 (181)	1797 (195)	-15.2 (3.6)	14.5 (3.1)	57.5 (24.0)	-87.0 (42.2)
P-value	0.94	0.45	0.96	0.01	0.61	0.04	0.01

MODELLING THE EFFECTS OF POINT OF FORCE TRANSLATION IN RUNNING GAITS

Sharon Bullimore[1,2] and Jeremy Burn[1]
[1]Department of Anatomy, University of Bristol, UK.
[2]Human Performance Laboratory, University of Calgary, Alberta. sbullimore@kin.ucalgary.ca

INTRODUCTION

The planar spring-mass model (Blickhan, 1989; McMahon & Cheng, 1990) is a simple and widely-applicable model of running, trotting and hopping in which the animal is represented by a mass bouncing on a spring. The model assumes that the point of application of the ground reaction force (GRF) does not move during the stance phase. However, in running humans, the point of GRF application moves forwards during the stance phase by a distance equal to approximately 18 % of leg length (Lee & Farley, 1998). We investigated the consequences of the absence of point of force translation (POFT) in the spring-mass model for its ability to accurately represent locomotion.

METHODS

The study was divided into three parts. Firstly, to determine the magnitude of the errors which arise from ignoring POFT in the spring-mass model, POFT was incorporated into numerical simulations of the model by assuming that the system was moving in a reference frame with constant forward velocity. Forty-eight such simulations were conducted for a range of input parameter values typical of animals. These simulations were then modelled by traditional spring-mass simulations, with spring stiffness calculated by the method of McMahon & Cheng (1990), and the percentage errors in the contact times, step lengths, peak vertical GRFs and peak horizontal GRFs predicted by the traditional model were calculated.

Secondly, the influence of POFT on the leg stiffness required for running was determined by adapting the equation of McMahon & Cheng (1990), for calculating the spring stiffness in the model, to take POFT into account.

Thirdly, the hypothesis that forward translation of the point of force application during stance phase can occur in quadrupeds was tested by trotting a dog (mass: 11 kg; hip height: 0.3 m) over a force plate (Kistler 9281CA; 600 mm x 400 mm) and recording GRF in three orthogonal directions at 1000 Hz. Only trials in which high-speed video showed that both the fore and hind foot of a diagonal limb pair were on the force plate during stance were used. POFT was calculated for the period over which vertical GRF exceeded 10 % of its maximum value.

RESULTS

The traditional spring-mass model predicted contact time, step length and peak vertical GRF to within 3 % of the values that occurred in the simulations which included POFT, but it overestimated peak horizontal GRF by between 14 % and 75 %.

Incorporating POFT into the equation for spring stiffness showed that POFT increases the leg stiffness required for running (as previously observed by Donelan & Kram, 2000) and that this effect increases with running speed. Therefore, for a constant distance of POFT, leg stiffness would have to increase with running speed in order to maintain a constant spring stiffness in the model (Figure 1).

The point of force application in the trotting dog moved by a minimum of 0.09 m in the craniocaudal direction during the stance phase. However, the pattern of POFT was variable, with the point of force application at the end of stance being between 0.10 m caudal and 0.25 m cranial to its position at the start of the stance phase.
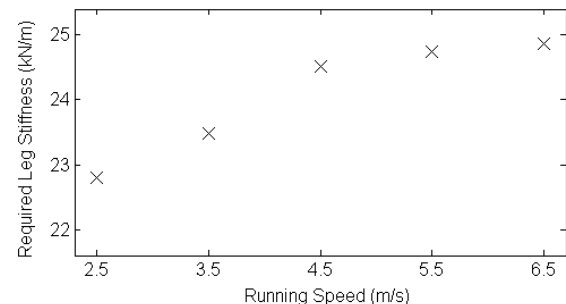

Figure 1: The leg stiffness required to maintain a spring stiffness of 18 kN/m, when point of force translation is 0.18m, increases with running speed.
Parameter values estimated from Arampatzis et al. (1999).

CONCLUSIONS

These results have important implications for the way in which the spring-mass model is used. They show that the absence of POFT in the model does not prevent it from accurately predicting basic running dynamics, although it consistently overestimates horizontal GRF. However, they also show that the spring stiffness calculated by the method of McMahon & Cheng (1990) is not a good measure of changes in the properties of the musculoskeletal system in response to different running conditions because, when POFT occurs, leg stiffness can alter without changes in spring stiffness and vice versa. Because POFT can occur in trotting quadrupeds, these conclusions may also be relevant to species other than humans.

REFERENCES

Arampatzis et al. (1999) *J. Biomech.* **32**, 1349-1353.
Blickhan, R. (1989) *J. Biomech.* **22**, 1217-1227.
Donelan, J. M. & Kram, R. (2000) *J. Exp. Biol.* **203**, 2405-2415.
Lee, C. R. & Farley, C. T. (1998) *J. Exp. Biol.* **201**, 2935-2944.
McMahon, T. A. & Cheng, G. C. (1990) *J. Biomech.* **23**, 65-78.

ESTIMATION OF GROUND REACTION FORCES IN BUCKING RODEO BULLS

Luke Savage[1], Dale Butterwick[1], Barbara Loitz-Ramage[2], Janet Ronsky[1,2,3]
[1]Faculty of Kinesiology, University of Calgary, Calgary, Canada, lcsavage@alumni.ucalgary.ca
[2]McCaig Center for Joint Injury and Arthritis Research, University of Calgary, Calgary, Canada
[3]Mechanical and Manufacturing Engineering, University of Calgary, Calgary, Canada

INTRODUCTION

Serious injury often occurs in bull riding (Butterwick et al., 2002). Flak-jacket type vests worn by riders are made from various combinations of leather, plastic and foam, but offer inadequate protection against compressive forces produced by bull stomping. Protective orthotics for the chest and abdomen have been recommended to reduce morbidity and mortality in bull riding (Ketai et al., 2000), yet no studies have addressed the forces such a vest would have to withstand.

Thus the purpose of this study was to estimate the ground reaction forces (GRFs) produced at the fore and hind hooves in small-, average-, and large-sized bulls while bucking.

METHODS

An 8-segment rigid body model of a bull was developed from digitized position data of a bucking bull in competition. Mass moments of inertia were calculated from measurements of 10 rodeo bulls and published mass values. These values were scaled into three bull models: a small bull of 500 kg; an average sized bull of 732 kg; and a large bull of 885 kg. GRFs were then calculated using computer simulations for the fore and hind hooves during one bucking cycle that occurred orthogonal to the cameras.

RESULTS

Average and maximum GRFs for the fore and hind hooves are shown in Table 1. Average forehoof GRFs were 2.9–4.0 times body weight (BW), up to 31 kN, while maximum forehoof GRFs were 10.0–14.2 BW, reaching 112 kN. In the hind hooves, average GRFs were 9.4–13.0 BW (46.0–106.3 kN) while maximum GRFs were 17.6–25.2 BW (86.5–198.5 kN) depending on the bull size.

Ground contact time for the front hooves was 400ms, with maximum GRF production occurring 267ms after initial ground contact. The maximum GRF for the hind hooves occurred two thirds into the 300ms contact time, at 200ms.

DISCUSSION

Little work has been done examining bulls in a rodeo setting. Evidence from equine studies indicate GRFs of two times bodyweight when jumping small fences, but suggest sharp increases in GRF magnitudes when jumping higher fences (Schamhardt et al., 1993). Equine running velocity was also found to significantly correlate with force production (McLaughlin et al., 1996). Considering the high velocities and erratic movements of a bucking bull, the large GRFs estimated here seem reasonable.

CONCLUSIONS

Data suggest that protective equipment will need to withstand forces of substantial magnitude to effectively protect the bull rider from severe injury.

SIGNIFICANCE

Knowledge of the magnitude of rodeo bull GRFs would assist in the design of protective devices able to withstand such forces, thus reducing injury mortality and morbidity in bull riding and rodeo events.

REFERENCES

Butterwick, D.J. et al. (2002). *Am. J. Sports Med*. **30**: 193-198.
Ketai, L.H. et al. (2000). *Injury*. **31**: 757-759
Schamhardt, H.C. et al. (1993). *Am. J. Vet. Res*. **54**: 675-680.
McLaughlin, R.M. et al. (1996). *Am. J. Vet. Res*. **57**: 7-11.

ACKNOWLEDGEMENTS

Table 1: Average and maximum GRFs for small-, average- and large-sized bull models

Model	Mass (kg)	Weight (kN)	Average Force (kN)	Average Force Relative to Body Weight	Maximum Force (kN)	Maximum Force Relative to Body Weight
Fore Hooves Ground Reaction Forces						
Small Bull	500	4.9	14.3	2.9	49.7	10.1
Average Bull	732	7.0	27.9	4.0	100.0	14.2
Large Bull	885	8.7	31.5	3.6	112.2	12.9
Hind Hooves Ground Reaction Forces						
Small Bull	500	4.9	46.0	9.4	86.5	17.6
Average Bull	732	7.0	91.4	13.0	177.1	25.2
Large Bull	885	8.7	106.3	12.2	198.5	22.9

CORRELATIONS BETWEEN GROUND REACTION FORCE COMPONENTS
AND BODY MASS IN HEEL-TOE RUNNING

Jay T. Worobets and Darren J. Stefanyshyn

Human Performance Laboratory, Faculty of Kinesiology,
University of Calgary, Calgary, Canada, worobets@kin.ucalgary.ca

INTRODUCTION

The sport of running enjoys tremendous popularity from not only the athletic population, but from the biomechanics community as well. The overwhelming number of papers published on the sport alone is testament to the fact that running has been a favorite topic among biomechanists over the past two decades. Despite this attention, however, there still remain fundamental principles of running mechanics which have not been adequately described. For example, does a linear relationship exist between body mass and the magnitudes of the components of the ground reaction force (GRF)? One would be inclined to believe that they are related in such a way, as it is common for authors to normalize these forces to body weight. Evidence supporting or refuting such a relationship, however, is lacking, as the results found by Frederick & Hagy (1986), indicating that body mass was a significant effector of peak vertical GRFs (n=9), were not entirely replicated by Kinoshita et al. (1990), who reported a light body weight group with higher peak vertical impact forces than a medium body weight group (n=17). The purpose of this study, therefore, was to further explore any correlations between GRFs and body mass in running.

METHODS

83 recreational runners (42 male, 41 female) were recruited for the study. The body mass of the subjects ranged from 44.6 to 93.2kg, with an average of 69.1kg and standard deviation of 9.6kg. Data were collected on the left foot of each subject while heel-toe running at 4m/s (± 0.2m/s) in a standard adidas control shoe. The ground reaction forces were measured with a Kistler force plate sampling at 2400Hz.

A fourth-order low-pass Butterworth filter (cutoff frequency of 100Hz) was used to smooth the data before analysis was conducted using Kintrak software. The analyzed variables were: peak vertical impact force (F_{VI}), peak vertical active force (F_{VA}), peak anterior braking force (F_{AB}), and peak posterior propulsive force (F_{PP}). Average values for each subject were calculated from five trials, then each variable was plotted against body mass and linear regressions were calculated.

RESULTS AND DISCUSSION

R-squared values were as follows: 0.00004 for F_{VI}, 0.033 for F_{VA}, 0.1915 for F_{AB}, and 0.3034 for F_{PP}. A plot of the peak vertical impact force versus body mass is depicted in Figure 1.
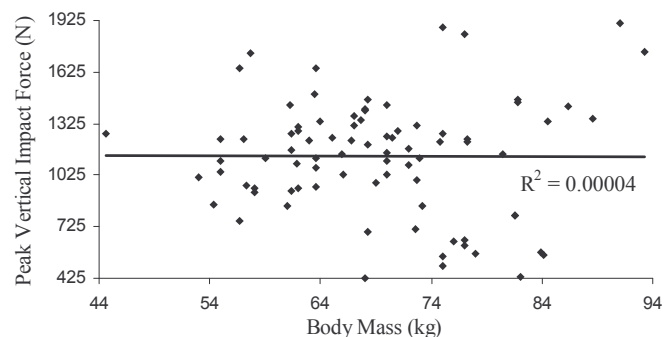

Figure 1: No correlation (R^2=0.00004) was found between peak vertical impact force and body mass.

While the peak magnitudes of the anterior/posterior GRF component were somewhat affected by weight (R^2=0.1915 & 0.3034), body mass was found to have no influence on the peak magnitudes of the vertical GRF component (R^2=0.00004 & 0.033). Although Frederick & Hagy (1986) tested approximately the same range of subject body mass (45.5-90.0kg) as in this paper, the small sample size (n=9) may have affected the outcome of their study.

SUMMARY

Contrary to previous findings, the magnitudes of the impact and active peaks of the vertical GRF component during heel-toe running were found to have no correlation with the body mass of the runner. This finding has an important implication to the method by which GRFs are currently analyzed. Since they are not correlated, normalizing the vertical ground reaction force to body weight, a popular trend among authors, not only fails to scale the variable appropriately, but actually introduces error into the data. It is therefore recommended that the analysis of ground reaction force data be conducted using absolute values (Newtons), rather than in units of body weight.

REFERENCES

Frederick EC & Hagy JL (1986) *Int. J. Sport Biomechanics*, **2**, 41-49.
Kinoshita H, et al (1990) *J. Human Movement Studies*, **19**, 151-170.

ACKNOWLEDGEMENTS

IMPACT FORCES DURING SKATEBOARDING LANDINGS

J. Determan[1], E. C. Frederick[2], and J. Cox[1]

[1]Sole Technology Institute, Lake Forest, CA, USA, Jeremy.Determan@soletechnology.com

[2]Exeter Research, Inc., Brentwood, NH, USA

INTRODUCTION

Skateboarding has several million regular participants in the US alone and a relatively high incidence of injury (Kyle *et al*., 2002). Many of these injuries are the result of un-controlled landings. One of the most popular maneuvers practiced by skateboarders is the *rail slide*, i.e., sliding down a sloping handrail on a skateboard and then landing on a flat surface. When performing rail slides skateboarders land on their skateboards or become separated from their boards in midair and land on their feet. We were curious about how high the vertical ground reaction forces (VGRF) are when landing on the skateboard versus on the feet. Our results indicate that the sprung elements of the skateboard provide significant shock attenuation and offer the skateboarder some protection from the inevitable effects of gravity.

METHODS

VGRF data were collected on 10 healthy top-amateur and professional male skateboarders (BM = 69 ± 9 kg) landing on a large force plate (AMTI model BP12001200). Subjects slid down a sloping handrail on their skateboards, eventually leaving the rail and landing on the force plate at the base of the rail. We recorded data on all cases of landing whether a *land (L)*, i.e., a successful landing on the skateboard, or, a *bail-out (BO)*, i.e., separating from the skateboard in mid-air and landing on their feet. During the L trials, subjects landed with all four wheels completely hitting the force plate. During the BO trials, the subjects landed feet first and fully on the force plate. Each subject performed only 3 trials for the BO and L conditions due to the violent nature of these landings. VGRF data were collected for 8 seconds at 1000 Hz for each condition. A low pass Butterworth filter was applied to the data in both conditions with a cutoff frequency of 100 Hz. All subjects wore the same model of skate shoes. However, each subject used his own skateboard for reasons of safety.

RESULTS

Figure 1 shows typical VGRF curves for L and BO for a single subject. These data show early, rapidly rising impact forces when the subjects first make contact with the force plate and at least one later peak in VGRF. This second peak corresponded with reaching full compliance of the body and equipment system. When BO, 3 of the 10 subjects consistently landed with both feet simultaneously (BO-Spike), while 5 consistently landed one foot before the other (BO-Step).

Two of the subjects, exhibited both types of BO landings. The mean VGRF results for the *L* versus the *BO* conditions for all ten subjects are compared in Table 1. The mean peak VGRF during the impact phase was significantly lower ($p < 0.05$) when our subjects landed on the skateboard. The mean peak VGRF was significantly lower ($p < 0.05$) when our subjects exhibited BO-Step landings.
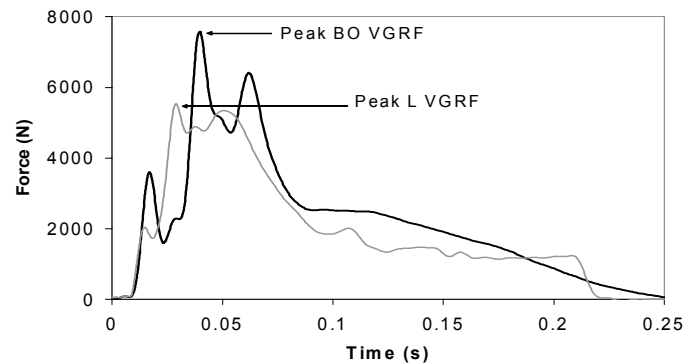

Figure 1: Representative VGRF curves for BO-Step (black) and L (grey).

DISCUSSION AND CONCLUSION

The magnitudes of the landing forces in skateboarding are among the highest reported for sports and other activities. (Nigg, 1985). This supports clinical observations of a relatively high incidence of acute injury among the skateboarding population. The skateboard is a sprung element in the system of skateboarder and skateboard. The board itself flexes and the trucks that support the wheels as well as the wheels themselves are compliant. The skateboard appears to provide significant shock attenuation lessening the peak impact forces experienced by the skateboarder when landing a rail slide. When a bail-out is required and subjects land on their feet, significantly higher forces are experienced. Landing technique and the shock attenuation properties of their footwear become critically important in these circumstances. Further investigations on the shock attenuation properties of skateboarding-specific footwear and landing techniques are needed.

REFERENCES

Nigg, BM. (1985). *Biomechanics IX-B*, Champaign, IL Human Kinetics. 91-96.

Kyle, S B, et al. (2002). *J. Trauma*, **53,** 686-690.

Table 1 Peak VGRF's for L, BO, BO-Step, and BO-Spike Impacts. Force = Newtons; n = Trials. Mean (SD).

L	BO	BO-Step	BO-Spike
n = 30	n = 30	n = 19	n = 11
5347 (800)	8282 (1913)	7724 (1063)	9246 (2639)

THE EFFECT OF CHANGES IN BINDING ALIGNMENT DURING A SIMULATED SNOWBOARDING LANDING TASK

Uwe G. Kersting and Paul R. McAlpine

Department of Sport and Exercise Science, University of Auckland
Auckland, New Zealand, http://www2.auckland.ac.nz/tmk/ses/

INTRODUCTION

A high proportion of fractures to the lateral process of the talus (LPT) has been reported in snowboarding, which accounted for 34% of all ankle fractures (Kirkpatrick et al., 1998). A fracture to the LPT is an injury unique to snowboarders and is often misdiagnosed by physicians as an anterolateral ankle sprain. LPT fractures often involve the articular surface of the subtalar joint and it has been shown that misdiagnosis may lead to severe degeneration of the ankle joint and long term morbidity (Boon et al., 1999). The mechanism of this injury has been studied intensively. LPT fractures are high impact injuries, landing after aerial manoeuvres is thought to be the major cause of LPT fractures (Boon et al., 1999). In a cadaver study no fractures to the LPT were recorded under purely dorsiflexed conditions but in six of the eight specimens fractures occurred with the addition of 20° external rotation. An axial load of 2200 – 8900 N was required to produce a fracture (LPT) in this position. It was proposed by Boon and colleagues that the subsequent 'opening' of the ankle joint seen with heel inversion and external rotation of the talus results in the lateral process shifting upwards on the posterior articular process of the calcaneus.

The purpose of this study was to simulate a snowboard landing in the laboratory with using an inverse dynamics approach to calculate effective joint loading for different binding alignments. It was hypothesised that the 'stance' chosen will affect loading and that an optimum foot alignment will help to minimise joint load.

METHOD

Ten experienced snowboarders participated in this study. Subjects were required to complete a simulated landing on a snowboard mounted upon two BERTEC force plates. Loading was provided by a weighted backpack worn by the subject and the movement task was designed to mimic landing an aerial manoeuvre as closely as possible. Three conditions were used in this experimental design. The conditions were defined by foot position on the snowboard, foot angles and the amount of forward lean set on the achilles support located on the back of the binding. Five trials were collected for each condition.

'Standard'–used by many beginners/rental companies (1).
'Duck'–a wide stance with externally rotated feet (2).
'Duck' Stance with forward lean–as 'duck' with 'forward lean' set at binding (3).

3D kinematic data was recorded using an EVA highres system (Motion Analysis). Twenty six reflective markers were affixed to bony landmarks on the lower extremities to define the foot, shank and thigh segments. A standard snowboard was cut into two pieces and bolted to the force plates to allow correct simulation and freedom of adjustment of the bindings. Force

data was recorded under each foot to allow the calculation of individual ankle joint forces and torques. All inverse dynamic calculations were carried out using the Kintrak (Version 6.0, Motion Analysis). The instant of maximum compression was determined from the resultant joint contact forces (figure 1). At this point in time shear forces and inversion-eversion as well as varus-valgus torques were calculated.
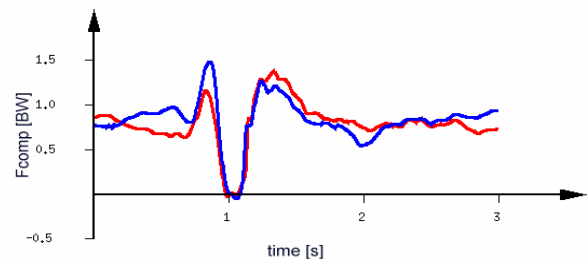

Figure 1: Example of joint contact force at the ankle joints. Red: left ankle, blue: right ankle.

RESULTS AND DISCUSSION

Kinematics and compressive forces did not vary to a great extent with variations in 'stance'. Greatest differences were demonstrated for the internal rotational torque of the tibia (figure 2). These results might indicate that the stance used by beginners has a greater potential for ankle injuries.
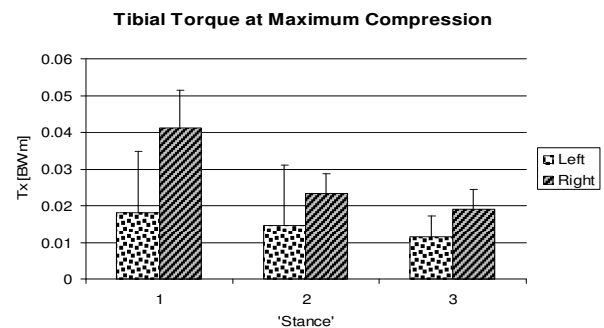

Figure 2: Tibial inversion torques at the time of maximum compression along the longitudinal axis of the leg.

It can be assumed that actual landing forces in snowboarding are much higher and occur under variable conditions such as landing on a slope, on undergrounds of different hardness etc.. Therefore, a direct transfer of these results into practice has to be preceded by further investigation.

REFERENCES

Kirkpatrick DP, Hunter RE, Janes PC, Mastrangelo J, Nicholas RA. Am J Sports Med. 19 (2): 271 – 277, 1998.
Boon AJ, Smith J, Laskowski ER. Phys Sports Med. 27 (4): 94, 1999.

AMENDING FOOT PLACEMENT DURING A STEP TO SUDDEN CHANGE IN OBSTACLE LOCATION AND ORIENTATION

Cândida Taís Gonçalves, Renato Moraes and Aftab E. Patla

Gait and Posture Laboratory, Department of Kinesiology, University of Waterloo, Waterloo, Canada, c2goncal@ahsmail.uwaterloo.ca

INTRODUCTION

Patla et al (1999) have proposed an algorithm that guides the alternate foot placement when faced with a challenge in the environment, with the primary objective being to minimise the displacement of the foot from its normal landing spot. Unexpected changes in obstacle position or orientation would allow us to determine whether the minimal displacement is still used to define the new landing position.

METHODS

Six healthy adults (aged 24.8 years ±2.3) participate in this study. They were invited to walk at their preferred speed, in a 7.3-metres-long walkway with one force plate and a LCD screen (35x27cm) embedded in it. The start position was found for each one of the participants to ensure that they would step on the force plate with their right foot and on the center of the screen with their left foot in some of the trials. When the participants stepped on the force plate, on selected trials a white rectangular obstacle appeared on the screen. They were instructed to avoid stepping on that obstacle. Two conditions (static and dynamic) and 6 obstacles were tested in this experiment. The static conditions consisted in 3 rectangular white obstacles of 12x27 cm that could appear medially (P1), in the centre (P2) or laterally (P3) and 3 obstacles of 9x35 cm on the bottom (P4), middle (P5) or top of the screen (P6). Same obstacles were used in the dynamic conditions in which 100 ms after the first obstacle had appeared in the screen, the obstacle changed to one of the other five. The probability of obstacle appearance was set at 0.3 to avoid any anticipation during the experiment.

RESULTS AND DISCUSSION

Alternate foot placements were classified into one of six categories: long-lateral (LL) long (L), long-medial (LM), short-medial (SM), short (S), and short-lateral (SL). Chi-square analyses identified differences between the dominant foot placement choices for the static and dynamic conditions for obstacle P1, P2, P3, and P4 ($p < 0.05$) (Fig 1). In the dynamic condition the choices are more spread out among all possible modifications even though they did not satisfy the minimum displacement objective. Onset of deviations in the ankle trajectory in the dynamic condition was analyzed for the AP and ML directions using a one-way ANOVA with direction change (e.g. P1 to P2) and orientation change (e.g. P1 to P4). While there was no significant effect in the AP direction, the onset of first deviation in the ML direction was affected ($F_{1,5} = 13.52$; $p = 0.01$). Changes were initiated faster when the obstacle changed direction and slower when the orientation changed. Paulignan et al. (1991) has shown that after an object location perturbation the reorganization of movements in reach-to-grasp is rapidly reorganized. They identified two sub-movements, the first one was directed at the location of the initial target, and second one at location of the new target. Similar results are seen in this study.
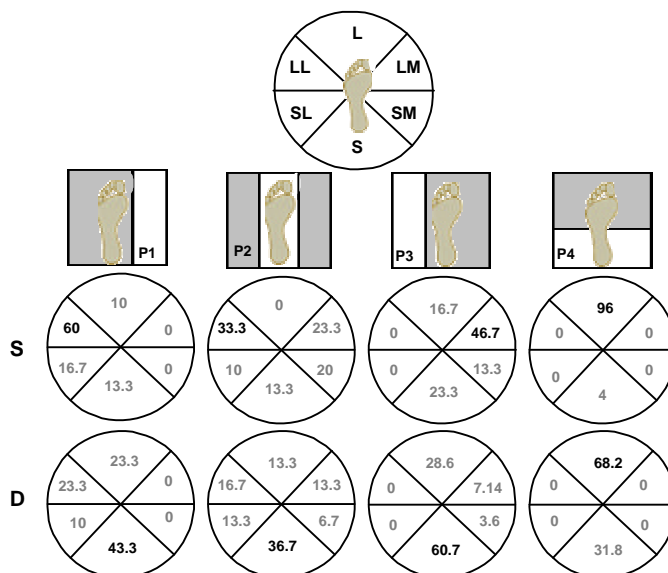

Figure 1: Percentage of modification choices made by the participants during static (S) and dynamic (D) conditions.

A Chi-square analyses comparing position of obstacle and modification chose, for dynamic condition, on P1, P2, P3 and P4, was carried out to identify the possible contributions of the first obstacle appearance to the modification selected. It was interesting to see that for all of the four obstacles when the obstacle P5 and P6 was the first one to appear the percentage of short modification was bigger. Probably the participants decided to do a short modification when they first saw the obstacles P5 and P6. Facing the second obstacle they kept their first choice even if it was not the minimal displacement they needed to do to avoid stepping on the second obstacle. With these results we can assume that changes in obstacle position or orientation can affect the choices made and the minimal displacement is not a primary factor used to define the new landing position in these specific cases.

REFERENCES

Patla, A.E. et al. (1999). *Exp. Brain Res.*, 128, 441-450.
Paulignan, Y. et al. (1991). *Exp. Brain Res.*, 83, 502-512.

ACKNOWLEDGEMENTS

STABILITY CONSTRAINT ON ALTERNATE FOOT PLACEMENT DURING HUMAN LOCOMOTION

Renato Moraes and Aftab E. Patla

Gait and Posture Laboratory, Department of Kinesiology, University of Waterloo, Waterloo, Canada, rmoraes@ahsmail.uwaterloo.ca

INTRODUCTION

It has been proposed that alternate foot placement is achieved by combining three determinants during the planning process of the motor response: stability, economy and response speed, and forward progression (Patla et al., 1999). It is suggested that long and medial choices minimize center of mass (COM) disturbances and, therefore, are preferred. There is still a need for validating these determinants. This study is the first attempt at validating the stability determinant.

METHODS

Four participants were invited to take part of this study (24.5 years ±3.6, 64.7 Kg ±14.8, 167.3 cm ±11.1). They walked at their normal pace on a walkway which contained an LCD monitor embedded in it. The starting position was adjusted for each participant in order to ensure that the left foot landed on the force plate and the right foot at the center of the screen. Their task was to avoid stepping on a rectangular obstacle projected in the screen. Obstacles with different sizes and positions were used. For each obstacle size and position, three conditions were tested: free choice (FC), right forced (RF), and left forced (LF). In the forced trials, an arrow was projected over the obstacle and indicated the direction of the adjustment (left/medial and right/lateral). For two of the participants a probability of 0.5 of obstacle appearance was used (P50), whereas for the other two participants a probability of 0.2 of obstacle appearance was used (P20).

Force plate data under the support foot (left) were collected. Braking and propulsive impulses (BI and PI, respectively) were calculated for all force components. The transition between braking and propulsive impulse was defined based on the zero-crossing instant in the anterior-posterior (AP) force component. Video analyses were used to identify the choices made in the free condition.

RESULTS AND DISCUSSION

The probability of obstacle appearance affected the dominant choice in the free condition. For the obstacle position which results in similar displacement in both ways, the dominant choice was medial/left (66.7 %) for the P50, whereas the dominant choice was lateral/right (62.5 %) for the P20.

One-way repeated measure ANOVAs (condition) indicated main effects for all BIs and PIs. BI was increased in the AP and vertical (VER) directions for the forced conditions in comparison to walk through condition (Figure 1). Therefore, in the forced conditions, participants are slowing down in order to have more time to implement the appropriate response. PI was smaller for the LF condition in both AP and VER directions in comparison to RF, indicating a safer adjustment

mechanism. In the LF condition, the right foot is moving more medially and, consequently, the base of support (BOS) will be reduced at right heel contact. In this case, if the COM acceleration is high, it may cause a fall in the case of a trip of the swing limb. For the medial-lateral (ML) direction, the BI and PI reduces from RF to LF conditions. Less brake indicates less reduction in velocity to the left side during the acceptance phase which in combination to PI to the left facilitates left/medial foot placement and vice-versa to right/lateral foot placement. This again increases the COM acceleration for the RF condition. The analysis of the FC condition indicated the same kind of behavior.
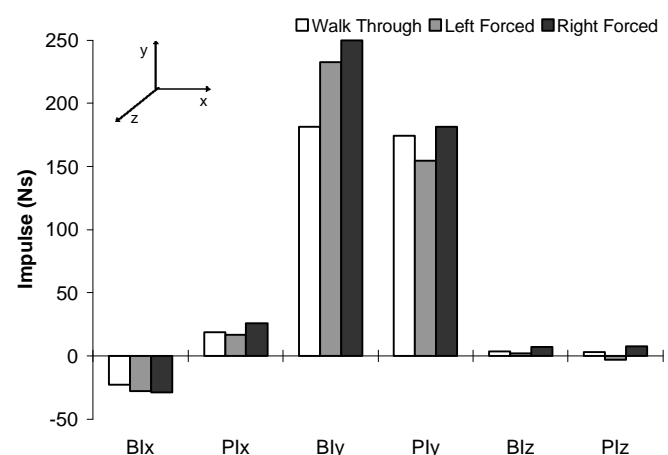

Figure 1: Impulse values for the forced and walk through conditions. (BI = braking impulse; PI = propulsive impulse).

SUMMARY

All of this data together indicates that lateral/right choices may be potentially more destabilizing because of the increase in COM acceleration, whereas medial/left choices are more conservative since it decreases COM acceleration. It could be argued that medial choices minimizes COM acceleration and therefore are safer to implement and would be dominant. Curiously, P50 and P20 presented different dominant choices and, therefore, it is not possible yet to conclude in favor of the previous claim. This study also shows that probability of obstacle appearance may affect the response of the individuals.

REFERENCES

Patla, A.E. et al. (1999). *Exp. Brain Res.*, 128, 441-450.

ACKNOWLEDGEMENTS

A CHAIR WITH A PLATFORM SETUP TO MEASURE THE FORCES UNDER EACH THIGH WHEN SEATED, RISING FROM A CHAIR AND SITTING DOWN

Pierre Desjardins,[1] Sylvie Nadeau,[1,2] Denis Gravel,[1,2] Guylaine Roy[1,2]

[1]Centre de recherche interdisciplinaire en réadaptation du Montréal métropolitain,
site Institut de réadaptation de Montréal, Montréal, Québec, Canada
[2]École de réadaptation, Faculté de médecine, Université de Montréal

Pierre.Desjardins@UMontreal.Ca

INTRODUCTION

While locomotion studies have traditionally concentrated on gait, far fewer studies have examined tasks involving sitting, rising from a chair and sitting down. However, a growing interest in quantifying the biomechanics of rising from a chair and sitting down has recently been observed. These tasks are repeated many times daily (Fleckenstein 1988) and can become a considerable challenge for specific patient groups. The development of a chair designed to measure the kinetics under the thighs might help to better understand the requirements of these tasks and to orient training. The purpose of this paper is to present the characteristics of a newly developed chair equipped with a force platform setup that measures the forces under each thigh.

MATERIAL AND METHODS

An instrumented chair offering a sitting surface of 25.5x51.0cm for each thigh at heights varying from 39 to 77cm. The height can easily be changed by adjusting the scissors-jack (Fig. 1). A lockable structure was integrated to secure and reinforce the chair. This structure was bolted to the concrete floor, which raises the natural frequency and dissipates some vibrations. The platform comprises four AMTI (Advanced Mechanical Technology, Inc., Newton, MA) strain gauge transducers (MC3A-3-250) two for each thigh. These transducers each have a capacity of 1.1kN vertically, 560N horizontally, 14Nm vertically and 28Nm horizontally for measuring the orthogonal force and moment components.

In order to orient and locate the transducers in a common referential system, the position of eight points on each transducer were obtained with an Optotrak system (±0.5mm). Ten infrared LEDs fixed on the chair were used to build a common referential system. Eight 3D vectors (12 force components, 12 moment components) were then transformed into a common referential system using the AMTI calibration matrices provided by the manufacturer and the rotation and translation matrices calculated from the eight points probed on each transducer. From the combination of vectors, the amplitude and direction of the resultant force and the resultant torque were obtained under each thigh. The locations of the 10 LEDs on the chair were then used to correct for any slight motion of the chair and to transform forces and torques into the laboratory reference system. The instrumented chair was used in conjunction with two AMTI (OR6-7-1000) force plate that measure the force and moment components under each foot.

Static Calibration. The static properties of the chair were verified by applying static known forces. For the output corresponding to vertical, dead weights up to 726 N were applied. A total of seven measurements were obtained during the loading process as well as during the unloading process and this test was performed three times. No test was performed for the horizontal shear. The location of the center of pressure was verified by applying a force through a bearing while moving the bearing over the platform surface. An Optotrak system was used to pin-point the location of the center of the bearing (±2mm).
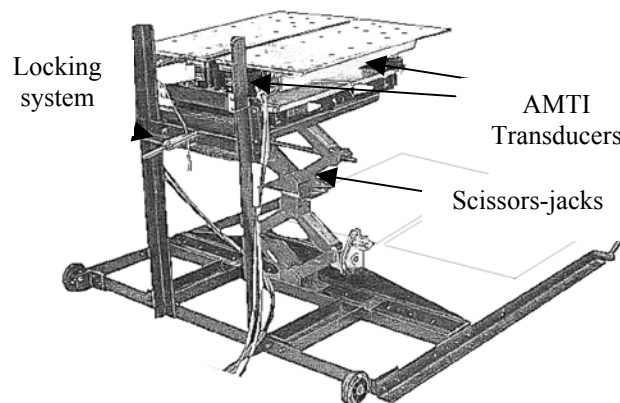

Fig. 1 Diagram of the chair

RESULTS AND DISCUSSION

The maximum deviation from the reference measures was 2% and 1.5% of the full-scale output vertically for the left and right side, respectively. The RMS error of the center of pressure was 5mm with a maximum of 9mm. The natural frequency and damping factor were respectively 14±2Hz and 0.2. This platform was designed for applications with a low-frequency content and is therefore not suitable for tasks such as falling onto the chair. The chair is currently used to assess the biomechanics of rising from a chair and sitting down among healthy and hemiparetic subjects.

REFERENCES

Fleckenstein, S. J. et al. J. of Biomechanics 1988;21:915-918.

ACKNOWLEDGEMENTS

FEASIBILITY OF A 3D RECONSTRUCTION TECHNIQUE USING A SINGLE VIDEO CAMERA

Pierre Desjardins,[1,2] Alain Delisle,[1] André Plamondon,[1] Erik Salazar,[3] Denis Gagnon[3]

[1]Institut de recherche Robert-Sauvé en santé et en sécurité du travail, Montréal, Québec, Canada
[2]Centre de recherche interdisciplinaire en réadaptation du Montréal métropolitain,
site Institut de réadaptation de Montréal, Montréal, Québec, Canada
[3]Laboratoire de biomécanique occupationnelle, Faculté d'éducation physique et sportive,
Université de Sherbrooke, Québec, Canada
Pierre.Desjardins@UMontreal.Ca

INTRODUCTION

The use of a single video camera for 3D reconstruction is attractive for facilitating the biomechanical analysis of workplace exposures. Recovery of the relative orientation and position of an object in a single scene, given the resulting 2D image, is a central problem in computer vision, but relatively new in occupational biomechanics. These techniques make use of known correspondences between model features and their respective images in order to create a set of constraints that can be used to invert the 2D-3D projective transformation performed by the camera (Carceroni 1997). The aim of this study is to use the Direct Linear Transform (DLT; Abdel-Aziz, 1971) to compute successive approximations of a set of points' 3D coordinates from a single camera image.

METHODS

Recording images using a camera is equivalent to mapping object point $\vec{P}_i$ in the object space to image point $\vec{I}_i$ in the film plane. If only one camera is used, the solution of the DLT equations is a line in the object space (fig.1). The line obtained is the trajectory of the ray from the object that intercepts the camera image plane and thus forms a picture of the point.
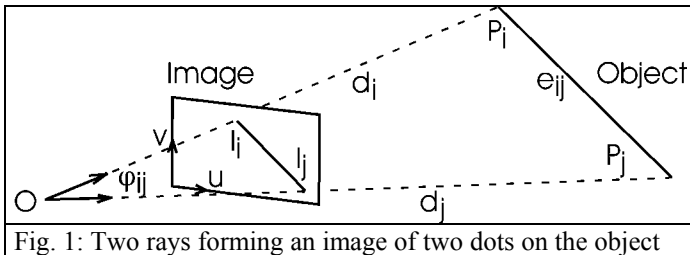

Fig. 1: Two rays forming an image of two dots on the object

Using the ray's equations, the distances between each pair of points on the object were computed. From figure 1, each distance was given by the following equation:

$$d_i^2 + d_j^2 - 2d_i d_j \cos(\varphi_{ij}) = e_{ij}^2 \qquad (1)$$

where e_{ij} is the distance between two points on the object. φ_{ij} is the calculated angle between the two rays. The two unknowns are d_i and d_j, the distances between the camera (nodal point) and each point on the object. A derivative-based numerical optimization technique was used to solve these equations. The key idea for overcoming the non-linearity of equation 1 was to obtain corrective values from successive approximations. From equation 1, the differential equation

with respect to d_i and d_j was obtained:

$$\left(d_i - d_j \cos(\varphi_{ij})\right)\Delta d_i + \left(d_j - d_i \cos(\varphi_{ij})\right)\Delta d_j = \Delta\left(e_{ij}^2\right) \qquad (2)$$

With " N " points on the object, there is N unknowns and $\frac{N(N-1)}{2}$ distinct equations from equation 2. These equations were used to build a linear system to be solved using the Singular Values Decomposition technique. The right side of equation 2 consists of the discrepancy between the actual distance between points on the object and the distance calculated with equation 1, using the previous iteration solution. Providing there are 3 or more points and given an initial approximation, the system formed with equation 2 was solved to find new corrective values $\left(\Delta d_1, \Delta d_2, ..., \Delta d_N\right)$. These corrective values were successively combined with the current approximation for d_i until either this estimate converged to a point that made the right side of equation 2 zero or a maximum of 20 iterations was exceeded.

To test this algorithm, 1725 pictures (640 x 480 pixels) were taken of a volume (78 cm x 78 cm by 60 cm deep) 2.57 m from the camera. A moving cluster composed of six markers (8.5 x 8.5 x 5.5 cm) was digitized (±0.5pixel) and the calculated 3D-coordinates were compared to those obtained from an optoelectronic device (Optotrak 3020: ±0.5mm).

RESULTS AND DISCUSSION

The RMS errors when all six markers were visible were 3 mm in the plane parallel to the image and 25 mm in the optical direction. This could be improved by using higher resolution in the digitizing system. The results indicate that it is usable for biomechanical analysis of workplace exposures.

REFERENCES

Canceroni, R. L. et al. Numerical Methods for Model-Based Pose Recovery, University of Manchester, Computer Science Department, Manchester TR659, 1997.
Abdel-Aziz, Y.I., et al (1971). Proceedings of the Symposium on Close-Range Photogrammetry (pp. 1-18).

COMPARISON OF ANKLE, KNEE AND HIP MOMENT POWERS DURING STAIR DESCENT VERSUS LEVEL WALKING

François D. Beaulieu,[1,3] Pelland, Lucie[1,2,4] and D. Gordon E. Robertson[1,5]

[1]School of Human Kinetics, [2]School of Rehabilitation Sciences, University of Ottawa, Ottawa, Canada
[3]fdbeauli@uottawa.ca, [4]lpelland@uottawa.ca, [5]dger@uottawa.ca

INTRODUCTION

The purpose of this project was to investigate the mechanics of descending stairs to that of level walking. Recognizing that descending stairs was more difficult and dangerous than ascending stairs and that falls from stair descent especially in the elderly can be fatal (Winter 1995), the idea behind this project was to determine how descending stairs differed kinetically from level walking.

METHODS

Ten subjects (4 females, 6 males) between the age of 20 and 35 participated in the study. They first descended stairs at their own pace for five trials then repeated the descent five times at a slower pace. The stairs (20 cm rise, 30 cm tread) were equipped with Kistler force platforms on the last two steps and on the landing. A digital camera filmed one side of the subject at 60 fps while stair forces were collected at 200 Hz. Sagittal planar, inverse dynamics was applied to obtain the forces and moments of force at the ankle, knee and hip joints. Only the data from the second last step will be presented. Moment powers were then computed from the products of the joint angular velocities and the moments of force: $P_j = M_j . \omega_j$. Each subject's moments and powers were body mass normalized and ensemble averaged to create a grand ensemble (GE).

RESULTS AND DISCUSSION

Other than an increase in the stance-to-swing phase ratio, there were no significant differences between normal and slow speed stair descent trials. Only the normal speed trials will be analyzed and compared with "natural cadence" walking reported by Winter (1991).

Figure 1 shows the grand ensemble averages (n=10 subj. × 5 trials) for the ankle moments and powers. The label TO indicates toe-off and the start of swing phase. Three major differences between level walking were apparent. First, no initial dorsiflexor phase was exhibited and instead an eccentric plantar flexor eccentric phase (A0) occurred to permit a controlled lowering of the heel to the step. Second, both plantar flexor bursts A1 and A2 were considerably reduced compared to level walking. In particular, less concentric work (A2) was necessary for stair descent presumably because of the reduction in step distance compared with a walking stride.

Figure 2 shows similar curves for the knee moments and powers. The major significant difference (P<0.001), compared with walking, was the doubling of the eccentric power of the extensors prior to TO (K3). This likely constitutes the most significant difficulty for people with disabilities to overcome because of the heavy loading that must occur to the patellar tendon. Notice that the K2 power reported for level walking did not occur during stair descent. The two other power bursts K1 and K4 were not significantly different from level walking.

The hip moments and powers were relatively smaller then those of the ankle and knee and were highly variable compared to level walking. They appear to not have a major role during the swing phase presumably due to the short step distance (60 cm).
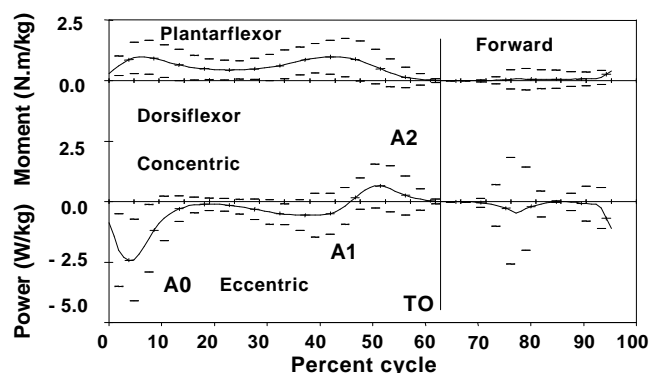

Figure 1. Ensemble averages ±95th% confidence intervals of the ankle moment and powers during forward stair descent.
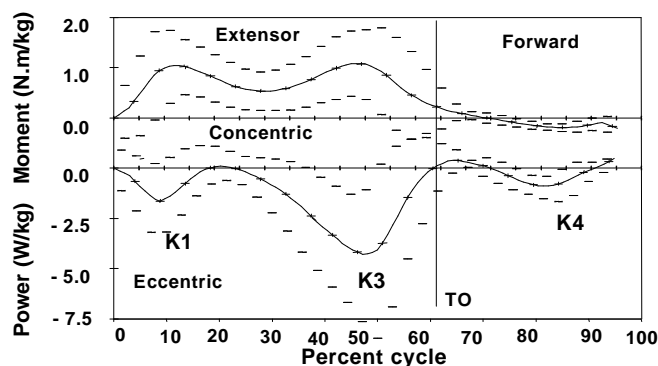

Figure 2. Ensemble averages ±95th% confidence intervals of the knee moment and powers during forward stair descent.

SUMMARY

The major differences between stair descent and level walking was the doubling of the eccentric knee extensor power burst immediately before toe-off and the presence of an additional burst of eccentric power by the ankle plantar flexors immediately after foot contact.

REFERENCES

Winter, D.A. (1991) *The Biomechanics and Motor Control of Human Gait.* 2nd ed. Waterloo: Waterloo Biomechanics.

Winter, D.A. (1995) *A.B.C. of Balance during Standing and Walking*. Waterloo: Waterloo Biomechanics.

ACKNOWLEDGEMENTS

Shock Attenuation and Kinematics Analysis in Normal Walking of the Old Social Dancing Exercisers

Liu Xuezhen   Xu Disheng

(Human sport science department, Beijing Sport University, Beijing, China, 100084)

Introduction

Walking generates shocks transmitted through the body when the foot collides with the ground. Researchers reported that the loads produced by repeated impacts were linked to degenerative joint diseases, cartilage breakdown, osteoarthritis and low back pain. And limiting the shock experienced by the head may be important to limit disturbances of the visual and vestibular sensory organs. Experiments took skin-mounted accelerometers s to detect whether performers with good dancing ways are associated with good attenuation abilities in walking.

Method

Subjects: Fourteen subjects who had obviously different dancing patterns based on the observation of the professional social dance teachers were selected from who had danced more than 3 years. They were divided into: group A (dance with smooth rises and falls, with the proper principle) and group B(dance with abrupt rises and falls, in the improper way)

Instrumentation: BK4393 uni-gain miniature accelerometers (each 2.4grams,) were used and accelerometer signals were amplified and sampled at 1000Hz.

Experimental protocol: Subjects' trials were filmed at the same time to determine the contact phase of each step and to get the kinematics variables. The filming distance was 6.6m.

Data analysis: The natural frequency of the attachment on the tibia was typically between 60 and 90 Hz in preliminary experiments. And it was much greater on the head. So the noise 40Hz- from the accelerometer signal in all trials was removed. The impact shock in each step was quantified by measuring the peak acceleration (PA) that occurred in each stance phase. The attenuation of the impact shock wave between the tibia and head was calculated in the time domain using peak impact accelerations. The formula is: $IA=(1-PA_{head}/PA_{tibia})*100$, Where IA is the impactattenuation, PA_{head} is the peak head acceleration, and PA_{tibia} is the peak tibial acceleration.

Results

1.Kinematic compare

The results of values of MK (maximum knee flexion angle), MA(maximum ankle dorsiflexion angle), $\triangle$ A (total change in ankle dorsiflexion angle) showed significant difference between the two groups. While for all other kinematics variables, there was no significant difference between group A and B.

2.Impact attenuation

During the stance phase, there was no significant difference between the two groups for the mean PA_{tibia} value. And the mean PA_{head} value for group A was less than group B statistical significantly.   .

Using the IA formula mean attenuation values calculated from the peak accelerations at the tibia and head for group A was $67.6\pm7.9\%$, while that for group B was $35.6\pm6.6\%$. The value of this variable for group B was significantly less than that for group A. ($p<0.05$).

Conclusions

The results indicated dancers with good dancing patterns were associated with better shock attenuations. And they had better ankle motion controls, which possibly contributed to their higher values of shock wave absorbing.

THE DIRECTION OF DISC PROLAPSE IS PREDICTABLE KNOWING THE REPEATED BENDING MOTION CAUSING THE PROLAPSE.

Scannell, J.P. [1], Aultman, C.D. [2] and McGill S.M.[3]

[1, 2, 3] Faculty of Applied Health Sciences, University of Waterloo, Ontario, N2L 3G1.
[3] mcgill@healthy.uwaterloo.ca

INTRODUCTION

The purpose of this study was to investigate if the direction of a repeated bending motion influences the direction of tracking of the nucleus within the intervertebral disc (IVD).

Previous in vitro research has shown that particular movements of lumbar spine segments consistently result in disc failure, for example, repeated full flexion of compressed lumbar segments (Callaghan and McGill, 2001). Some clinicians believe that the nucleus tracks in a predictable direction based on the bending motion causing the tracking and thus direct their rehabilitation and prevention in accordance with this belief (McKenzie 1988). The purpose of this study was to repeatedly bend motion segments to create herniations and to change the bending axis to see if this influenced the location of the herniation.

METHODS

Sixteen porcine specimens (C3/4 and C5/6)were obtained from spines that had been bagged and frozen immediately post-mortem. The specimens were stripped of musculature and the C2/3 and C3/4 IVDs were examined for degeneration. All specimens were classified as Grade 1 on Galante's scale of disc degeneration. For the purposes of testing the specimens were held in aluminum cups using gauge steel wires and were surrounded in the cups by a non-exothermic dental stone (Denstone ®, Miles Inc., South Bend, ,IN, USA). The nucleus of the IVD was injected through the anterior aspect of the disc with a 0.55ml mixture of barium sulphate, blue dye and distilled water, which allowed tracking of the nucleus to be recorded on dissection after testing. The specimens were placed in an Instrom jig, compressed (1472N) and bent 6000 times in a plane orientated 30^0 to the left of the sagittal plane.

RESULTS AND DISCUSSION

The direction of tracking of the nucleus was predictable in 15 of the 16 trails. Bending the segments about an axis 30^0 to the left of the sagittal axis produced a right postero-lateral disc prolapse (Figure 1).

The direct clinical benefit of such findings is in the prevention of disc pathology such as prolapse and herniation, particularly in the case of a known previous postero-lateral disc prolapse. These findings increase our understanding of the behavior of the disc and prompt further investigation of the efficiency of physiotherapy treatment techniques.
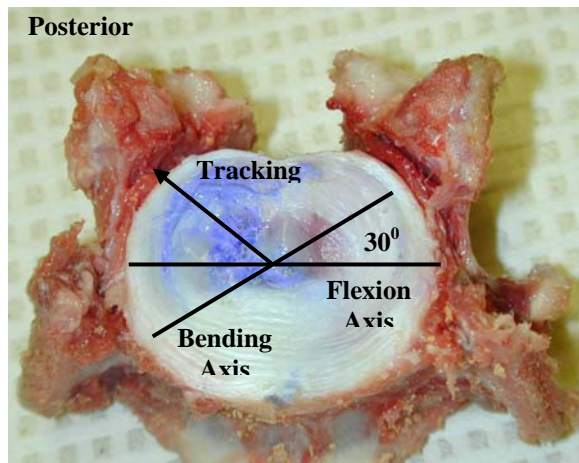

Figure 1: Photograph of the superior aspect of the C3/4 intervertebral disc. Bending the motion segment about an axis 30^0 to the left of the sagittal plane caused a right postero-lateral disc herniation.

SUMMARY

The direction of a repeated bending motion influences the direction of tracking of the nucleus within the intervertebral disc (IVD).

REFERENCES

Callaghan J.P., McGill S.M. (2001) Intervertebral disc herniation : studies on a porcine model exposed to highly repetitive flexion/extension motion with compressive force. *Clinical Biomechanics* **16:** 28-37.

McKenzie R.A. (1981) *The Lumbar Spine - Mechanical Diagnosis and Therapy*. Spinal Publications:

DESIGN OF A MECHANICAL STIMULATION DEVICE FOR CHONDROCYTE SEEDED ALGINATE PUCKS

J.N. Preston[1], K. J. Rees-Milton[3], T.P. Anastassiades[3], P.M. Wild[2], and U.P. Wyss[1]
1. Department of Mechanical and Materials Engineering, Queen's University, Kingston, Canada, preston@me.queensu.ca
2. Department of Mechanical Engineering, University of Victoria, Victoria, Canada
3. Department of Medicine and Rheumatology, Queen's University, Kingston, Canada

INTRODUCTION

Surgical treatment of diseased or damaged articular cartilage is often not possible or suitable, especially for younger patients. Therefore, efforts have shifted to tissue engineering alternatives (Waldman 2003). The current work is part of a project that is developing novel therapies for maintaining healthy cartilage, and repairing damaged tissue. The project's focus is to determine the biosynthetic response of chondrocytes (cartilage cells) as a result of the synergistic effect of biomechanical and biochemical stimuli.

Dynamic mechanical loading plays a crucial role in the development and maintenance of healthy articular cartilage (Frank, 2000). The objective of the current work is to design a device that applies compression and shear loads to chondrocytes seeded in alginate gels. From the data produced by the device, specimen strains can be quantified. Using this information, future research will be able to investigate which environments are conducive to healthy cartilage growth.

METHODS

Bovine chondrocytes are mixed into a 1.5g/100ml alginate concentration. In dialysis tubing, the liquid mixture is placed in a solution of 100mM calcium chloride. After the alginate mixture solidifies, pucks shaped samples, 5mm in diameter by 3mm in height, are extracted.

To maintain sterility, the alginate specimens are contained in an isolated sterile specimen holder. The transparent holder accommodates 6 specimens, as well as a system to circulate and collect nutrient and therapeutic media. The lid of the specimen holder acts as the loading platen, keeping the samples isolated. The holder is slid into the stimulator and locked in place (Figure 1).

The stimulation device (Figure 1), which can be housed inside a standard laboratory incubator, applies shear and compressive loads, either independently or simultaneously, with a Dual Motion Unit that uses stepper motors for both linear and rotary motion. Both motions are displacement controlled using LabView software and microstepping drivers. Torque and compression feedback are collected. The stimulation device is designed to apply 1-3% shear strain, in a steady or reciprocating fashion, and 1-5% dynamic compressive strain, also in a steady or reciprocating fashion. The approximate load ranges required to attain the desired strains in the alginate pucks were determined through static loading tests. Stainless steel pipe is used as the support frame (approximate overall dimensions: 30cm length x 15cm diameter) to accurately position components and keep the device compact.
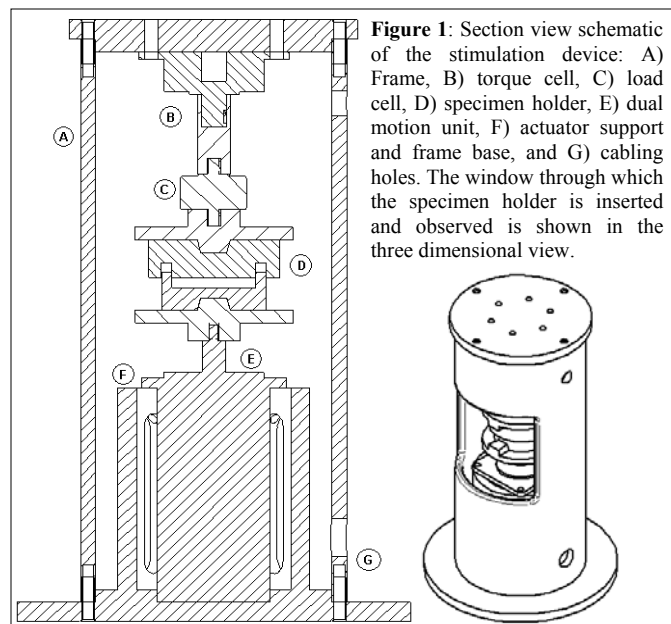

Figure 1: Section view schematic of the stimulation device: A) Frame, B) torque cell, C) load cell, D) specimen holder, E) dual motion unit, F) actuator support and frame base, and G) cabling holes. The window through which the specimen holder is inserted and observed is shown in the three dimensional view.

Validation of the device will be based on the proper functioning of the individual components and the unit as a whole. The limitations and the capabilities of the device, such as load ranges and patterns, and the duration and frequency of load application, will be investigated. Tests to quantify biological activity will be performed separately. However, specimen integrity and cell viability will be verified.

DISCUSSION

There are stimulation devices available for similar applications. However, for this project, modification and/or augmentation would be required. This option was not pursued since it was more desirable to have a small, self-contained and dedicated unit, that could be housed inside an incubator.

SUMMARY

A mechanical device has been designed to apply dynamic compression and shear strains to alginate specimens. Its use as a research tool will aid in the understanding of cellular reaction to biomechanical and biochemical environments, ultimately advancing cartilage treatment therapies.

REFERENCES

Frank, E.H. et al (2000). *J. Biomechanics,* **33**, 1523-1527.
Waldman, S.D. et al (2003). *Journal of Bone and Joint Surgery*, **85 A**, 101-105.

ACKNOWLEDGMENTS

Governing Equations for the Process of Bone Remodeling Using a Mixture Theory Approach: Theoretical Predictions

Gholamreza Rouhi[1]; Marcelo Epstein[2]; Walter Herzog[3]; Les Sudak[4]

[1,2,3,4] Mechanical and Manufacturing Engineering, University of Calgary, AB, Canada

[1,2,3] Human Performance Laboratory, University of Calgary, AB, Canada, walter@kin.ucalgary.ca

INTRODUCTION

Bone is composed of a fluid and a solid phase, and remodeling of bone is caused by the continuous interchange of mass between these two phases. Chemical reactions between the solid and fluid phase cause a mass exchange, which is regulated by bone cells. There are several theories about bone remodeling, but most of these theories are based on single phase continuum mechanics approaches. We have used a mixture theory approach to write the equations that govern bone remodeling. We consider bone as a mixture of a linear elastic solid (bone matrix) and a viscous fluid (the nutrient substratum). The purpose of this study was to model the interaction of solid and fluid phase in bone, and its effect on remodeling of the tissue.

METHODS

Bone is treated as a biphasic mixture of a solid and a fluid, and remodeling as an exchange of mass between these phases. We assume that the solid phase obeys small deformation theory (infinitesimal strains), and is isotropic and linearly elastic. The velocity of the solid phase is assumed to be zero. The fluid phase is assumed to be viscous, and inertial effects are neglected because of the slow fluid velocity. Fluid density is considered to be constant. Using these assumptions, remodeling of bone was derived using the conservation laws (mass, momentum, and energy), as well as entropy inequality, and the appropriate constitutive equations. Conservation equations were written for each constituent, and for the mixture as a whole. Entropy inequality was enforced locally and globally for the whole tissue [1& 2]. All bone resorbtion and apposition was assumed to occur on the free surfaces [3]. In the constitutive equations, the free energy density, the rate of mass supplied to each constituent, enthalpy, and entropy production are assumed to be functions of temperature, deformation gradient, and free surface density (instead of *volume fraction*). Bone remodeling is considered an isothermal, quasi-static process.

RESULTS AND DISCUSSION

From the mass conservation law for each constituent, and the mixture , we can derive:

$$\frac{\partial \rho_s}{\partial t} + \frac{\rho_f V_f}{\rho_s + \rho_f} grad \rho_s = (\rho_f + \rho_s)\{div(\frac{\rho_s V_f}{\rho_s + \rho_f}) + \frac{c_*}{\rho_f}\} \qquad (1)$$

where the density of the solid and fluid phase are denoted by ρ_s and ρ_f, respectively, V_f is the fluid velocity, and c_* represents the rate of mass supplied to the solid phase. c_* can be expressed as:

$$c_* = S_v A_{ij}(E_{ij} - E_{ij*}) \qquad (2)$$

where S_v , A_{ij}, S_{ij} and S_{ij*} are the free surface density, material constants, mechanical stimuli at time t and at the remodeling equilibrium state, respectively. By using the compatibility condition for the first law of thermodynamics, we can derive the following equation:

$$c_* = (\varepsilon_{s*} + \varepsilon_{f*})(\varepsilon_s + \varepsilon_f + \frac{V_f^2}{2})^{-1} \qquad (3)$$

where ε_{s*} and ε_{f*} are energies supplied to the solid and fluid phase, and ε_s and ε_f are the internal energy density of the solid and fluid phase, respectively. From Eq. (2) and (3), the driving force for the bone remodeling process (the difference between mechanical stimuli at time t and at equilibrium) can be found. The driving force is inversely related to the kinetic energy of the fluid phase and the free surface density.

Neglecting the body forces and the linear momentum supply to the fluid phase, and using the compatibility condition, linear momentum equations can be derived:

$$div(2\mu E + \lambda trE) + C_* V_f + div(-pI + 2\mu D) = 0 \qquad (4)$$

where E and D are strain and strain rate tensor, respectively, p is the hydrostatic pressure, and μ and λ are material constants. From the second law of thermodynamics, one can derive the following inequality for a non-rotating fluid flow:

$$\rho_s \frac{\partial \eta_s}{\partial t} + \rho_f(\frac{\partial \eta_f}{\partial t} + grad \eta_f . V_f) \geq \frac{c_*(\eta_f - \eta_s)}{\theta} \qquad (5)$$

where η_s and η_f are entropy production terms for the solid and fluid phase, respectively, and θ is the absolute temperature of the mixture. From inequality (5), another useful inequality for the remodeling equilibrium state can be found. This new inequality shows that, at equilibrium, there is an inverse relation between the solid phase density and the rate of entropy production.

SUMMARY

Bone remodeling was approached here through a mixture theory technique. The equation for the change of solid phase density can be found by using Eq. (1). The rate of mass exchange between the solid and fluid phase is proportional to the sum of the energies supplied to both phases, and has an inverse relation with the sum of the internal energies of the bone constituents and the kinetic energy of the fluid. At equilibrium, entropy production in the solid phase is inversely related to the solid phase density. The net energy supplied to the solid and fluid phase, in the equilibrium state, is zero. Using a mixture theory approach to approximate the remodeling of bone has the advantage that the contribution of individual phases to remodeling can be determined, and that the structural components of bone are represented realistically, thereby providing the possibility for new and unique insight into the mechanisms of bone remodeling, specifically, and bone mechanics and growth in general.

REFERENCES

1.Bowen,R.M.(1976): Theory of mixtures, Continuum Physics III, Edited by Cemal Eringen, Academic Press, New York.
2.Rajagopal, K.R. and Tao, L.(1995): *Mechanics of Mixtures,* world scientific publishing, Singapore.
3.Martin,B.(1984). *CRC, Critical Reviews in Biome. Eng.*, Boca Raton, FL, 179-222.

ACKNOWLEDGMENT

The Role of Geometric Feedback and Microcracks in Bone Remodeling: Theoretical Predictions

Gholamreza Rouhi[1] ; Marcelo Epstein[2] ; Walter Herzog[3]

[1,2,3]Mechanical and Manufacturing Engineering, University of Calgary, AB, Canada

[1,2,3]Human Performance Laboratory, University of Calgary, AB, Canada, walter@kin.ucalgary.ca

INTRODUCTION

Bone is continuously remodeled through a coupled process of bone resorption and bone formation, and this process is called *Bone Remodeling*. Optimal remodeling is responsible for bone health and strength throughout life. Old bone is removed and new bone is created. Bone mass increases until a certain age, reaches its maximum, and then continuously declines for the rest of our lives. An imbalance in bone remodeling may cause diseases, such as osteoporosis or osteopetrosis. Loss of tissue matrix renders bones weak and susceptible to fracture. There are several theories about the mechanisms of bone remodeling, but none of these can predict all features of this process. We have derived a new model of bone remodeling using a continuum mechanics approach for a single phase continuous material and infinitesimal strains. In this model, volume fraction was replaced by the bone surface density in the constitutive laws governing the remodeling process. Also, we used an effective volume fraction that considers microcracks in an explicit manner.

METHODS

Bone is considered a poro-elastic material, and remodeling as an exchange of mass between the solid and fluid phase. We have used conservation equations (mass, momentum and energy), entropy inequality, constitutive equations, and methods of approximation for deriving a new model of bone.

All bone resorbtion and apposition was assumed to occur on the free surfaces [1]. Thus, we defined a free surface density, and used it in the constitutive equations, instead of the traditional use of volume fraction [2]. Also, we used an effective volume fraction with a microcrack factor (d) as proposed by Ramtani & Zidi [3], in the conservation and constitutive equations. By using these constitutive assumptions in the conservation of mass equation, small strain approximation, Taylor series expansion, and two fundamental assumptions, we have found a new and more realistic relation for analyzing the remodeling process of bone than is available to date.

The assumptions underlying the bone model are: (i) when there is no free surface, there will be no bone remodeling; (ii) if mechanical stimuli are in a neutral zone that is insufficient to cause biological responses, *and* if the rate of microcrack production is zero, there will be no remodeling. The second assumption implies that the mechanical stimulus and microdamage production are not equivalent variables, and that loading history is an important factor in the remodeling process [4]. Finally, by using the constitutive equation in the entropy inequality, we found expressions for the stress tensor, rate of microcrack production, and entropy production.

RESULTS AND DISCUSSION

The rate of change in volume fraction is a function of the free surface density (S_v), mechanical stimuli (e.g. strain,

E_{ij}), microcrack factor (d), rate of microcrack production ($\dot{d}$), initial volume fraction, and material properties of the bone (Eq.(1)):

$$\frac{de}{dt} = \frac{S_v}{(1-d)}\{A_{ij}{}^{1}(E_{ij} - E_{ij}{}^{0}) + \dot{d}\} \qquad (1)$$

Furthermore, the rate of microcrack production can be obtained by using the first assumption made in equation (1), which shows that the rate of microcrack production is a function of the material properties, the initial conditions, and the mechanical stimuli in the bone. Therefore, the remodeling equation can be represented in another form as:

$$\frac{de}{dt} = \frac{S \cdot A^{1}{}_{ij}}{(1-d)}\{(A_{ij}{}^{1} - a)E_{ij} - A_{ij}{}^{1}E_{ij}{}^{\circ} + b\} \qquad (2)$$

Equation (2) shows that the rate of remodeling is a function of the material properties, the microcrack factor (d), and the mechanical stimuli (E). Also, by using the entropy inequality and the constitutive equations, the stress tensor can be found as:

$$T_{ij} = (1-d)^{2}\frac{\gamma\zeta}{J}\frac{\partial\psi}{\partial F_{ik}}F_{jk} \qquad (3)$$

Equation (3) shows that the stress tensor is a function of the material properties, the microcrack factor, the partial derivatives of the free energy with respect to the deformation gradient, the volume fraction, and the Jacobian of the deformation. Also, equations for the entropy production and the mechanical stimuli, which produce no net remodeling, can be derived from this model.

SUMMARY

The novelty of our approach to bone remodeling is the idea that microdamage and mechanical stimuli are coupled and influence the behavior of bone adaptation. Bone remodeling should be considered as a life-long continuous process whose rate depends upon the pattern of the mechanical stimuli and the structure of bone, as reflected by its mass distribution (geometry and shape of the bone). Furthermore, numerical and experimental research is needed to evaluate the conceptual framework proposed here on theoretical grounds, so as to quantify the material properties governing bone adaptation.

REFERENCES
1. Martin, B.(1984). *CRC, Critical Reviews in Biomedical Engineering*, Boca Raton, FL, 179-222.
2. Cowin, S.C. et al. (1976). *J. of Elasticity,* **6**, 313-325.
3. Ramtani, S. et al. (2001). *J. Biomechanics, 34*,471-479.
4. Whalen, R.T. et al. (1988). *J. Biomechanics,2,*825-837.

ACKNOWLEDGMENT

KINEMATIC AND KINETIC COMPARISON OF OBESE AND NON OBESE CHILDREN DURING SELF-PACED WALKING

Julie Nantel[1,2], Martin Brochu[3] and François Prince[1,2,3].
[1]Gait and Posture Laboratory, Marie Enfant Rehabilitation Center, Montreal, Canada
[2]Department of Kinesiology, University of Montreal, Montreal, Canada
[3]Department of Surgery, University of Montreal, Montreal, Canada
jcnantel1@hotmail.com

INTRODUCTION

Obesity is now considered as a major health problem in industrialized countries. Only few investigators have documented this pandemic concern in regard to possible modification in gait. Studies on obese adults, reported changes in temporal parameters such as cadence, walking speed and single and double support phases[1,3]. They also reported modifications in joint angular excursion. Comparable temporal results were found in obese children[2]. Nevertheless, further investigations are needed to have a better knowledge of dynamic changes in obese children locomotion. The purpose of this study was to compare temporal, kinematic and kinetic parameters between obese and non obese children during self-paced walking.

MATERIALS AND METHODS

Three-dimensional gait analysis was performed on 10 non obese (weight: 32.5 SD 9.3kg) and 10 obese (weight: 55.7 SD 16.2kg) children aged between 8 to 13 years old. Obese children were selected on the basis of a body weight above the 95e percentile of weight for their age. Subjects were asked to walk at their own pace on a 10m walkway instrumented with 2 AMTI force plates sampled at 960 Hz. Kinematics were captured with 8 VICON optoelectronic cameras recording at 60 Hz. Four trials were kept for analysis and normalized to 100% of the gait cycle (%GC). Mechanical work ($J \cdot kg^{-1}$) was assessed by calculating the time integral of the power curve[4].

RESULTS

Temporal parameters revealed a significant decrease ($p<0.01$) in the single support phase in the obese group (36%GC) compared to non obese (39%GC). No significant difference was found in other temporal parameters. The walking speed, cadence, and stride length were respectively for non obese and obese children: 111.6 vs. 113.2 step·min^{-1}; 0.98 vs. 1.01 m·s^{-1} and 1.06 vs. 1.08m. For the hip moment curve, obese children switch from extensor to flexor moment significantly ($p<0.05$) earlier (15%GC) in the gait cycle compare to the non obese group (27%GC). Results of mechanical work at each joint are reported in Table 1. Total negative work was significantly increased in the obese group. Finally, H2 burst and the H2/H3 ratio were also significantly ($p<0.05$) increased while H1 was significantly decreased ($p<0.01$).

DISCUSSION AND CONCLUSION

The presence of a diminished work during H1 burst demonstrates a lower contribution from the hip extensors in early stance in the obese group. The increase in the H2 burst indicates a larger absorption of energy by the hip flexors. In spite of these results, the H2/H3 ratio shows that non obese children transferred more energy from absorption and generation with the hip flexors.

Table 1: Means and standard deviations of the work ($J \cdot kg^{-1}$).

VARIABLES	NON OBESE		OBESE		P values
	Mean	SD	Mean	SD	
H1	0.04	0.02	0.01	0.01	**0.01**
H2	0.10	0.07	0.18	0.06	**0.01**
H3	0.09	0.03	0.11	0.03	0.22
H2/H3 ratio	1.05	0.54	1.72	0.66	**0.02**
K1	0.03	0.02	0.04	0.04	0.85
K2	0.08	0.05	0.11	0.04	0.19
K3	0.05	0.03	0.08	0.06	0.39
K4	0.07	0.02	0.07	0.02	0.48
A1	0.18	0.05	0.20	0.06	0.80
A2	0.18	0.08	0.19	0.06	0.85
Work -	0.42	0.12	0.56	0.12	**0.02**

These results suggest that obese children use a passive absorption strategy to minimize the energy cost in spite of their excess of total adipose tissue. They might take advantage of passive elastic components (tendon and fascia) to maintain gait efficiency in the absence of a larger power generation from the ankle plantar flexors during push-off. Finally, this modification in the walking pattern could explain why we did not find difference in cadence, walking speed and stride length.

REFERENCES

1- DeVita P., Hortobágyi T. (2003) *J Biomech.* 36:1355-62.
2- Hills AP, Parker AW. (1991) *Arch Phys Med Rehabil.* 72: 403-7.
3- Spyropoulos P. et al. (1991) *Arch Phys Med Rehabil.* 72: 65-70.
4- Winter DA. 1990. *Biomechanics and Motor Control of Human Movement (2nd Edn).* John Wiley, New York.l

ACKNOWLEDGMENTS

ACCURACY OF THE CRITICALLY DAMPED AND BUTTERWORTH FILTERS USING THE ACCELERATION OF A FALLING OBJECT

Robyn Wharf, M.A. candidate[1] and D.G.E. Robertson, Ph.D.[1,2]
[1]School of Human Kinetics, Ottawa, Ontario. [2]dger@uottawa.ca

INTRODUCTION

The Butterworth filter has been the gold standard in filtering motion data since D.A. Winter introduced it in 1974. It was selected for its superior roll-off and its "flatness" in the passband. Unfortunately, it has the undesirable characteristic of being underdamped and therefore will overshoot the data during rapid transitions (Robertson & Dowling, 2003). An alternate filter that solves this problem–it is the critically damped filter (Robertson & Dowling, 2003). This filter has poorer roll-off than the Butterworth but by cascading the data through the filter a similar roll-off can be achieved. The purpose of this study is to compare the effectiveness of the critically damped and Butterworth filter using the known acceleration of a falling body–a golf ball.

METHODS

To validate the filters a golf ball was dropped and filmed while it bounced twice by a digital video camera in SP mode. The image was calibrated by a 1.0 x 2.0 m grid of control points. The plane was calibrated by a fractional linear transform that corrected for any camera misalignment. The motion data were captured and digitized using the APAS and then processed by the Biomech Motion Analysis System. The latter software allowed for filtering the data with 4th, 8th, 12th, 16th and 20th-order Butterworth or the critically damped filters.

RESULTS AND DISCUSSION

Figure 1 demonstrates that using 4th-order critically damped or Butterworth filters (CD-4 & BW-4) do not yield acceptably flat periods of constant acceleration during the flight phase of a ball. Although the average values of the acceleration (–10.00 & –10.05) were close to the correct value of –9.81

m/s^2 their standard deviations were quite high (0.69 & 0.48). Using 20th-order filters (CD-20 & BW-20) achieved better results by reducing the variability (0.23 & 0.34), but only the critically damped filter improved on predicting the correct acceleration (–9.96 vs. –10.11).

Figure 2 show the flight phase results when the data file includes the bounces that occur before and after the fight. In this case the 20th-order Butterworth caused significant distortion of the signal after and then before the two bounces. Some of these distortions were removed by clipping the fight phase so that the results did not exceed the boundaries of the graph. The Butterworth filter caused greater distortion as the order was increased whereas the critically damped filter caused less distortion at the ends of the flight phase.
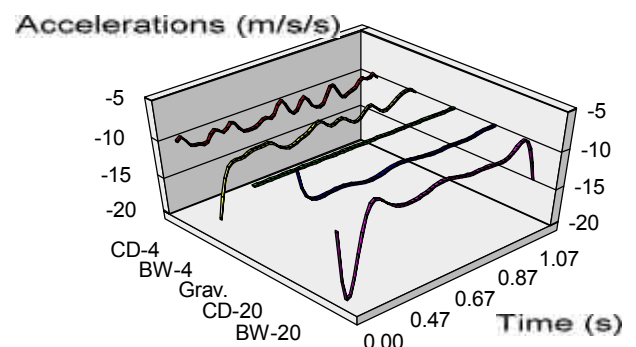

Figure 2. Ball acceleration during flight between bounces after various types of filtering

SUMMARY

The critically damped filter was shown to produce superior acceleration results as compared to the Butterworth filter when as suggested 20th-order was used to filter the motion of a body accelerated due to gravity. Higher order Butterworth filters caused significant distortion in the accelerations of the ball when rapid transitions precede or follow the flight phase. Caution should therefore be used with the Butterworth filter when higher order filtering is required.

REFERENCES

Pezzack, JC. et al. (1977) *J Biomech* 10:377-82.
Robertson DGE, Dowling, JJ (2003). *J Electromyogr Kines* 13: 569-73.
Winter, DA. et al. (1974) *J Biomech* **7:**157-9.

Figure 1. Accelerations of a ball in flight after various types of filtering

INFLUENCE OF A CUSTOM FOOT ORTHOTIC INTERVENTION ON LOWER EXTREMITY INTRA-LIMB COORDINATION VARIABILITY DURING RUNNING

Christopher L. MacLean, Richard van Emmerik and Joseph Hamill

Biomechanics Laboratory, University of Massachusetts-Amherst, Amherst, Massachusetts, USA

E-mail: cmaclean@excsci.umass.edu

INTRODUCTION

The coupling or coordination of segments and joints has long been of interest to movement scientists who study the mechanism of running injuries. Specifically, the interaction between the foot (calcaneus) and leg (tibia) and how this coupling affects the dynamics of the knee. The variability of coordinative patterns has received recent interest in the running injury literature (Hamill et al., 1999; Heiderscheit et al., 2002). To date, only two studies have investigated CFO influence on lower extremity coupling (Bates et al., 1979; Nawoczenski et al., 1995).

The purpose of the current investigation was to analyze the influence of CFO intervention on the variability of lower extremity intra-limb coupling in healthy subjects during overground running.

METHODS

Eight healthy female (age: mean = 23.75 years, mass = 56.46 kg) recreational and competitive runners were selected for participation in the study. Subjects exhibiting a peak ankle eversion angle of ≤10 degrees were included in the study. Each subject performed 5 overground running trials with (CFO) and without (SHO) custom foot orthoses (Paris Orthotics Lab, Vancouver, BC, Canada).

Kinematic data were collected using Qualisys® software (Glastonbury, CT, USA) at 200Hz. Data were reduced using custom MatLab software and processed using Visual 3D® (C-Motion, Inc. Rockville, MD, USA). A vector-coding technique was employed to calculate the coordination patterns and variability for the intra-limb couplings in the frontal (FP) and transverse (TP) planes.

RESULTS AND DISCUSSION

Custom foot orthotic intervention resulted in significant decreases in the mean coordination variability for the Ankle Rotation$_{FP}$/Knee Rotation$_{FP}$ and Calcaneal Rotation$_{FP}$/Tibial Rotation$_{TP}$ couplings ($p<0.05$). Mean coordination variability was significantly lower when analyzed: 1) across the entire stance phase and 2) from heel strike to 50% of the stance phase. There were no significant changes in mean coordination variability for any of the other intra-limb couplings examined.

For the most part, the results of this study reveal that the variability of coordination was unaffected by CFO intervention in healthy subjects who exhibit WNL peak ankle eversion angle. However, the results of this study for the AnkRot$_{FP}$/KneeRot$_{TP}$ and CalRot$_{FP}$/TibRot$_{TP}$ couplings may indicate that the prescription of such devices in subjects of this description may perturb the knee in an unhealthy manner by decreasing the intra-limb coordination variability (Hamill et al., 1999; Heiderscheit et al., 2002)). Further research is required to investigate similar parameters in subjects who have a prior history running injury and who exhibit excessive ankle eversion during running.
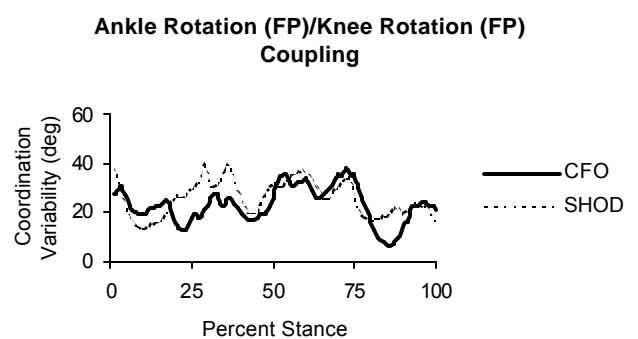

Figure 1: Mean coordination variability for the Ankle Rotation (FP)/Knee Rotation (FP) intra-limb coupling.
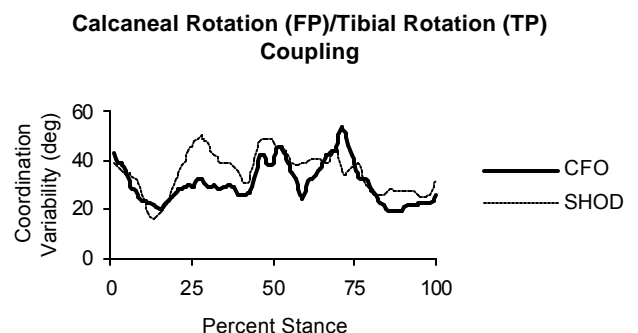

Figure 2: Mean coordination variability for the Calcaneal Rotation (FP)/Tibial Rotation (TP) intra-limb coupling.

REFERENCES

Bates et al., (1979). *Am J Sports Med,* **7(6)**, 338-342.
Hamill et al., (1999). *Clin Biomech,* **14**, 297-308.
Heiderscheit et al., (2002) *Journal of Applied Biomechanics,* **16(2)**, 110-121.
Nawoczenski et al., (1995) *JOSPT,* **21**, 317-327.

PLANTARFLEXOR TORQUE-ANGLE RELATIONSHIP OF SWIMMERS AND VOLLEYBALL PLAYERS

Marco Aurélio Vaz[1,3], Viviane Bortoluzzi Fração[1,2], Tatiana Penz[1], Érico da Silveira[1], Walter Herzog[3]
[1] Exercise Research Laboratory, School of Physical Education, Federal University of Rio Grande do Sul (UFRGS), Brazil
[2] Faculty of Physical Therapy, Pontific Catholic University (PUC), Brazil
[3] Human Performance Laboratory, Faculty of Kinesiology, The University of Calgary (UofC), Canada
marco@kin.ucalgary.ca

INTRODUCTION

The plantar flexor (PF) torque-angle (T-A) relationship of athletes competing in various sports has been shown to be different (Fração and Vaz, 2001). We tried to assess if such differences would also be observed for swimmers and volleyball players, two groups of athletes who use their PF muscles in distinctly different ways. Swimmers use their PF muscles at short lengths to maintain the ankle joint in a PF position, while volleyball players use these muscles at long lengths in a more dorsiflexed position. We hypothesized that swimmers should have a higher force production capacity at short compared to long PF muscle lengths when compared to volleyball players due to the above different functional demands.

METHODS

Peak torque (T_{max}) and surface electromyographic (EMG) signals of the PF (MG=medial gastrocnemius; SOL=soleus) muscles of 18 male subjects (swimmers=11; volleyball players=7) were evaluated during maximal voluntary isometric contractions at ankle angles of -10°, 0°, 10°, 20°, 30°, 40°, and 50° (0°=right angle between the shank and the foot) using a Cybex (NORM) isokinetic dynamometer. Root mean square (RMS) values were calculated from the raw EMG signals. T_{max} and RMS values were normalized relative to the values obtained during maximal voluntary contractions for each subject. A two-way ANOVA (ankle angle and group) for repeated measures was used to evaluate differences between parameters. The level of significance was 0.05 for all tests.

RESULTS

The PF T-A curve of the swimmers was shifted upwards relative to that of the volleyball players (Figure 1). Swimmers had relatively higher torque values at short PF lengths compared to those of the volleyball players. The normalized EMG RMS values of MG and SOL decreased with decreasing muscle length in both groups, with the difference in SOL being significantly different between the two groups (Figure 2).

DISCUSSION

Differences in the T-A relation between two populations of athletes may occur because of differences in muscle properties or differences in activation patterns (Herzog et al., 1991). Here, it appears that swimmers are relatively stronger than volleyball players at short muscle lengths because of their enhanced capacity to activate the PF at short lengths (Figure 2). In a previous study, we also found a shift in the T-A relation for ballet dancers compared to volleyball players. However, in that case activation could not fully explain the leftward shift of the T-A relationship of the ballet dancers,

suggesting that the differences in the T-A relationships were caused by differences in the muscle properties, possibly the force-length relationship. Therefore, it appears that, compared to volleyball players, swimmers are strong at short PF length because of increased activation, and ballet dancers are strong because of changed force-length properties. Although we do not know why adaptations in these two athlete groups might have occurred in distinctly different ways, ballet dancers require high forces at short PF length, while swimmers need great PF flexibility but little force at short length. These functional differences may provide hints about how T-A relationships may be changed for different functional requirements.
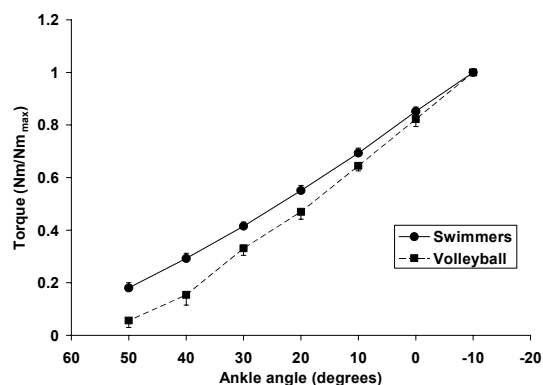

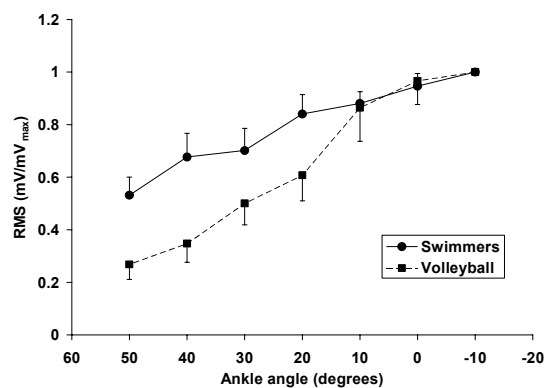**Figure 1.** Normalized PF torque-angle relation (mean ± SE).

Figure 2. Normalized RMS values of SOL EMG as a function of ankle angle (mean ± SE).

REFERENCES

Fração VB; Vaz MA. (2001). *Proceedings of XVIII ISB*, 286.
Herzog W et al. (1991). *Med. Sci. Sports Exerc.*, **23**(1):289-296.

PRINCIPAL COMPONENT ANALYSIS REVEALS LOWER EXTREMITY CHANGES DURING A 10 KM RUN

Jeffrey J. Chu[1,2], Kelly Anne Mckeown[1], Graham E. Caldwell[1] and Joseph Hamill[1]
[1] Department of Exercise Science, University of Massachusetts, Amherst, MA, USA
[2]Simbex, Lebanon, NH, USA

INTRODUCTION

Maintaining stable lower extremity joint patterns may be an important injury prevention mechanism (Bates et al., 1992). Our previous work demonstrated coordination changes over a prolonged run using a modified poincarè section (McKeown et al., 2001), but the analysis was limited by the use of discrete points of the gait cycle. In this study we use principal component analysis (PCA) of a combined 3-joint, 3D kinematic vector for greater insight to lower extremity joint pattern changes throughout the gait cycle during a 10-km run.

METHODS

Four experienced healthy male runners ran 10 km on a treadmill at their self-selected race pace. Lower extremity kinematic data were collected at the end of each km for a period of 20s (approximately 15 strides). Data were smoothed with a 4th order zero lag butterworth filter (Fc: 9). 3D hip, knee and ankle angles were calculated and normalized to percent gait cycle (0 to 100%, 101 points). These 9 variables were concatenated to form a 909-point angle vector and ensemble averaged for each subject at each km. For each subject, the angle vector was mean-centered and normalized by the variance of the average angle vector from all 10 km.

PCA was used to reduce the angle vector waveform to a few principal component scores (PC Scores) and loading vectors, which represent important features of the data (Deluzio et al, 1999). Kinematics at each km were discriminated by the PC Scores. The loading vectors were used to illustrate temporal differences throughout the gait cycle. A fuzzy c-means clustering algorithm separated the PC Scores into 2 distinct groups to highlight kinematic changes as the run progressed.

RESULTS AND DISCUSSION

PCA successfully reduced the number of variables, with the first two principal components accounting for more than 70% of all variance for each subject. Although 3 PC Scores were used in the clustering algorithm to discriminate kinematics at each km, PC Score 1 accounted for more than 50% of the variability and was the primary discriminating feature. All subjects exhibited a systematic change in their joint kinematic patterns throughout the 10 km run (Figure 1), increasing from a negative to positive PC Score 1. Combining the loading vectors with the PC Scores provides insight to these pattern changes. Subjects altered their kinematic patterns in different ways. For example, with increasing running distance S3 exhibited a general increase in lower extremity joint flexion while S4 had greater ankle plantar flexion with decreased knee and hip flexion (Figure 2 top). Moreover, the loading vector accounted for variance at differing periods of the gait cycle (Figure 2 bottom), indicating substantial subject-specific differences in kinematic pattern changes. The reasons (e.g.. fatigue or strategy) for these changes are unknown.
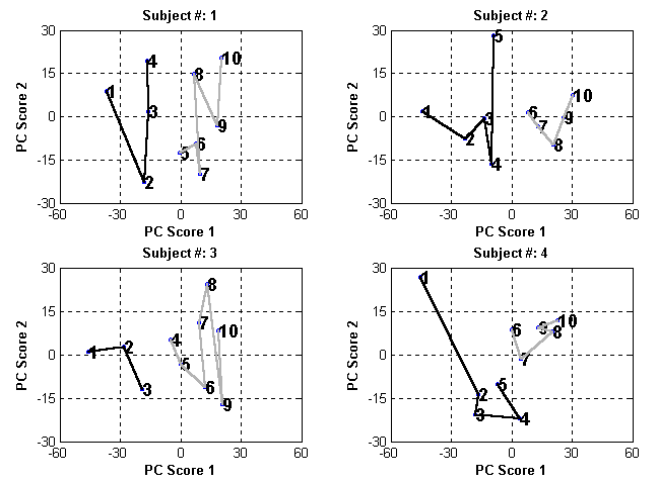

Figure 1: PC Scores for each subject at each km (numbered). The dark and light lines illustrate the 2 distinct data clusters.
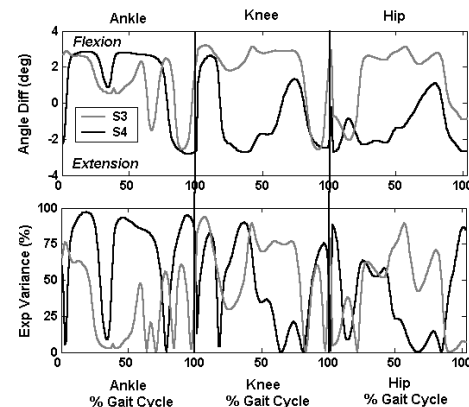

Figure 2: Top: Differences in joint flexion/extension angle between km 1 and 10 for subjects S3 and S4, reconstructed using only the first principal component. Bottom: Explained variance over the gait cycle for loading vector 1.

SUMMARY

PCA was able to differentiate changes in lower extremity joint angles and provided insight to these changes throughout the gait cycle during a 10-km run. The combined angle vector approach was more sensitive to kinematic changes than single-joint measures. Modifications in lower extremity kinematics were subject-specific. However, PCA can only identify the alterations, thus other techniques (e.g. physiological measures, movement simulations) will be needed to explore the reasons behind these kinematic modifications.

REFERENCES

Bates et al., *MSSE*, 24(7), 807-813,1992
McKeown et al., *ISB Zurich* 2001
Deluzio, K.J., et al. *Hum. Move. Sci.*, 18, 701-711, 1999.

THE EFFECTS OF A LATERAL PERTURBATION DURING BACKWARDS WALKING

Mike MacLellan[1], Daniella Pratt[2], and Aftab Patla
Gait and Posture Lab, Department of Kinesiology, University of Waterloo, Waterloo, Canada
[1]email: mikemaclellan@canoemail.com, [2]email: dapratt@ahsmail.uwaterloo.ca

INTRODUCTION

Instability during motion is attributed to a narrow base of support, a constantly moving center of mass and altering gait patterns in response to a perturbation (Feeber et al., 2003). To recover from instability the body will use the vestibular system, visual system and proprioception (Patla, 2002). This work examined strategies used to maintain normal gait patterns following a lateral perturbation with minimal contribution of the visual system.

METHODS

Two male and four female university students were recruited for participation in the study. Three walking conditions (knowledge of perturbation, no perturbation and no knowledge) were used to evaluate center of mass deviations in gait patterns following a lateral perturbation. The probability of a perturbation during a trail was 0.1. Participants walked backwards to minimize the use of vision to guide center of mass recovery from the perturbation. Trunk center of mass was measured using Northern Digital's OptoTrak system with IRED (Infrared Emitting Diodes) placement on the xiphoid process, right and left acromioclavicular joints, right and left anterior superior iliac crests, and right and left lateral malleoli. Center of mass (COM) was sampled at a frequency of 80 Hz. Step characteristics were measured using a 12m GaitRite mat. GaitRite was sampled at a frequency of 80 Hz. Muscle activation latency was measured bilaterally using electromyography on erector spinae, external obliques, gluteus medius, and adductor longus. Electromyography was sampled at a rate of 1200 Hz. Watjerk (University of Waterloo) was used to elicit lateral perturbations during experimental trials. The height of perturbation was adjusted vertically to the level of the participant's right deltoid muscle insertion.

The experimental trial began when the experimenter informed the participant what kind of trial was about to occur (walkthrough, perturbation, or unknown). The participant was then asked to begin walking backwards with their eyes focused on a target on the wall. The participant would continue walking until the experimenter asked them to stop. The protocol consisted of 100 trials for each participant.

RESULTS AND DISCUSSION

Step width was measured 2 steps before perturbation (N-3, N-2) and 4 steps after perturbation (N, N+1, N+2, N+3). The perturbation was elicited at left heel contact of the N-1 step. For each subject, an average walkthrough step width was calculated and subtracted from all perturbation steps so the changes in step width could be observed. The results for step width can be seen in Figure 1. Analysis of variance determined that the first 2 steps after a perturbation were significantly narrower than corresponding steps in a walkthrough trial [$F_{(6,30)} = (25.25)$, $p < 0.0001$]. This would suggest that 2 steps following perturbation onset the COM returned to its original trajectory. There was no statistical difference in step width between known and unknown perturbations [$F_{(6, 30)} = (1.01)$, $p > 0.4356$] which could be attributed to the absence of vision to guide step placement.
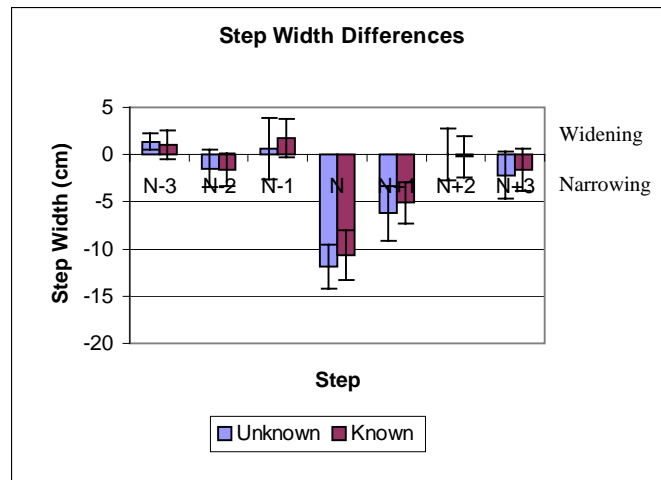

Figure 1: Plot of step differences in known and unknown perturbations. (N-1 = perturbation)

An analysis of electromyography showed a trend that the right adductor longus was activated earlier during a known perturbation when compared to an unknown perturbation. No other trends have been observed within muscle activation.

SUMMARY

Results have shown that during backwards walking, there are no significant differences in step width between knowledge and no knowledge conditions. There may be a trend seen in adductor magnus electromyography latency, which may suggest that knowledge can increase reaction time of muscles to maintain posture.

REFERENCES

Feeber, R. et al (2003). *Gait and Posture*, **16**, 238-248.
Patla, A. (2002). *Kinesiology 422 Course Notes*. Waterloo, University of Waterloo.

ACKNOWLEDGEMENTS

LOWER EXTREMITY KINEMATIC CHARACTERISTICS OF TAI CHI GAIT

Ge Wu[1,2], Juvena Hitt[1], Debra Millon[2]

[1]Department of Physical Therapy, [2]Bioengineering Program, University of Vermont, Burlington, VT, 05401, ge.wu@uvm.edu

INTRODUCTION

Tai Chi Chuan (TCQ), a form of exercise, has been shown to have positive effects for improving balance and for preventing falls in the elderly [1]. In order to understand the mechanism of its effects on balance, we examined the biomechanical characteristics of a basic and primary TCQ movement, the Tai Chi gait (TCG). This paper compared the spatial and temporal characteristics of TCG with normal gait (NG), and between proficient and novice TCQ practitioners.

METHODS

Ten healthy young subjects participated in the study. One subject was a proficient TCQ practitioner, and nine were beginners. All subjects signed an Informed Consent Form.

The temporal features of gait were measured by two biomechanical force plates (AMTI, USA). The spatial features of gait were measured by a Motion Analysis System (BTS, Italy) with three 50Hz cameras. Reflective markers were placed on the left side of the subject at the 5th metatarsal head, the heel, the lateral malleolus, femoral epicondyle, and greater trochanter. Two additional markers were placed at mid-shank, mid-thigh and shoulder, respectively. Three-dimensional joint motion for the ankle, knee and hip was computed based on the Joint Coordinate System convention formed by the markers [2].

Subjects performed NG and TCG, with bare feet, at a self-determined speed, five times each. The data from the cameras and the force plates was simultaneously collected by a personal computer with a sampling frequency of 50Hz. A calibration trial was also collected, during which subjects stood upright with their natural posture.

RESULTS

TCG had significantly longer cycle time (11.9±2.4sec) and single stance time (1.8±0.6sec) than that of the NG (1.3±0.2sec, 0.4±0.05sec, respectively).

There was no significant difference in stride length between the two gaits (1.05±0.11m for TCG, 1.09±0.09m for NG).

Comparing to NG, TCG showed significantly larger and sustained lower extremity joint motion in three dimensions (see Figure), especially in ankle dorsiflexion, knee flexion, hip flexion and abduction.

Comparing to the TCQ proficient subject, the joint motion patterns of the beginners were qualitatively similar (see Figure). However, the TCQ proficient subject had significantly larger knee flexion, ankle internal rotation and hip abduction throughout the TCG gait cycle.

DISCUSSION AND CONCLUSION

This study is one of the first attempts to quantitatively document and examine the biomechanical features of a TCQ movement. The findings in this study suggest that TCG, comparing to NG, is a significantly slower gait with a larger and sustained lower extremity motion in three dimensions.

These unique kinematic features of TCG contribute favorably to the maintenance of joint function and sensory integrity, enhancing postural control and balance.

The mastery of TCQ movements takes time [3]. In this study, all but one subjects are considered beginners. The temporal and spatial kinematic patterns of these beginners are qualitatively similar to, but quantitatively different from those of the proficient subject. While the similarities indicate that TCG may be a relatively easy movement to mimic, the differences suggest that performing TCG at a higher proficiency level may need a longer period of regular practice. The quantitative comparison of joint motions during TCQ movements between proficient and novice TCQ practitioners can facilitate learning and control the quality of the practice.
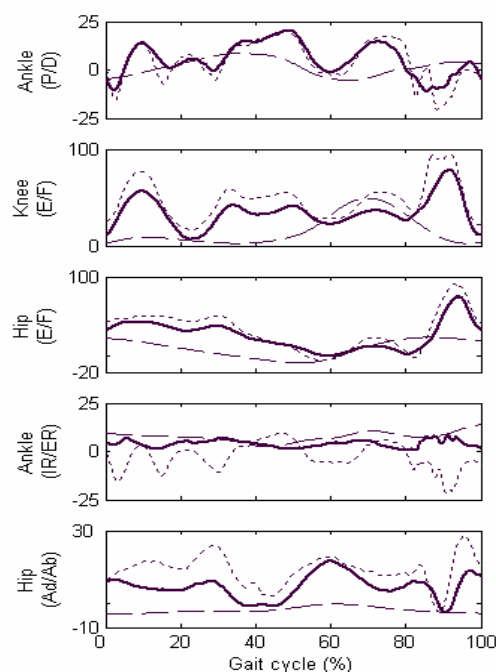

Figure. Ensemble average of angular motion (in degrees) of the ankle, knee and hip joints during TCG (solid line for beginners, dotted line for the proficient practitioner) and NG (dash line). Zero refers to the position at neutral stance. The positive sign is for ankle dorsiflexion, knee and hip flexion, ankle external rotation, and hip abduction, respectively, and vice versa for the negative sign.

REFERENCES

1. Wu G. JAGS, 2002. 50:746
2. Grood ES, Suntay WJ. J Biom Eng, 1983. 105:136
3. Farrell SJ et al. Phy Med Reh Cli North Ame, 1999. 10:617

ACKNOWLEDGEMENT

CHARACTERISTICS OF MUSCLE ACTIVITIES IN THE LOWER EXTREMITY DURING TAI CHI GAIT

Ge Wu[1,2], Juvena Hitt[1], Debra Millon[2]

[1]Department of Physical Therapy, [2]Bioengineering Program, University of Vermont, Burlington, VT, 05401, ge.wu@uvm.edu

INTRODUCTION

Falling and fall-related injuries in the elderly are a major health problem for the nation. The reduced lower extremity strength in the elderly has been considered one of the contributing factors. Tai Chi Quan (TCQ) is a beneficial exercise for improving lower extremity strength, and for reducing the incidence of falls in the elderly. The purpose of this study was to examine muscle activities in the lower extremity during a basic TCQ movement, the Tai Chi gait (TCG), in comparison to those during normal gait (NG) in order to understand the mechanisms of TCQ for strength gains and fall prevention.

METHODS

Ten healthy, young individuals participated in the study. Nine were TCQ beginners and one was a proficient TCQ practitioner. Surface electromyography (EMG, BTS, Italy) was measured from six muscles in the left leg (tibialis anterior (TA), soleus (SO), peronaeus longus (PL), rectus femoris (RF), biceps femoris (ST), and tensor fasciae latae (TFL)). Body movement was recorded by a three-camera motion analysis system (BTS, Italy). Two force plates (AMTI, USA) were embedded in a walkway to record the ground reaction forces. The integrated EMG signals, the ground reaction forces and body movements were collected simultaneously at 50 Hz. During testing, subjects were asked to walk at a normal speed and then to do the TCG, five times each.

RESULTS AND DISCUSSION

It was found that the TA, RF and TFL muscles were active for a significantly longer percentage of a gait cycle, and at a significantly higher level during TCG than during NG (Fig. 1). Also, these muscles had a significantly longer time for isometric and eccentric actions during TCG than during NG (Fig. 2).

Comparing to the proficient TCQ practitioner, the beginners had similar muscle action pattern and action level for all muscles except for the TA and TFL (Fig. 1).

The results in the study suggest that TCG is different from NG in that it involves the use of a special group of muscles such as ankle dorsiflexors, knee extensors and hip abductors. These muscles are found to play important roles in maintaining upright balance. Moreover, these muscle activations during TCG are prolonged isometric and eccentric actions rather than quick ballistic contractions as seen in walking. These types of actions are believed to recruit type II muscle fibers that atrophy more quickly with age. It is possible that with TCQ exercise these muscles are recruited regularly, resulting in increased strength and, thus, improved postural stability.

In conclusion, the results of this study will shed lights on the mechanisms of TCQ for postural control and fall prevention.
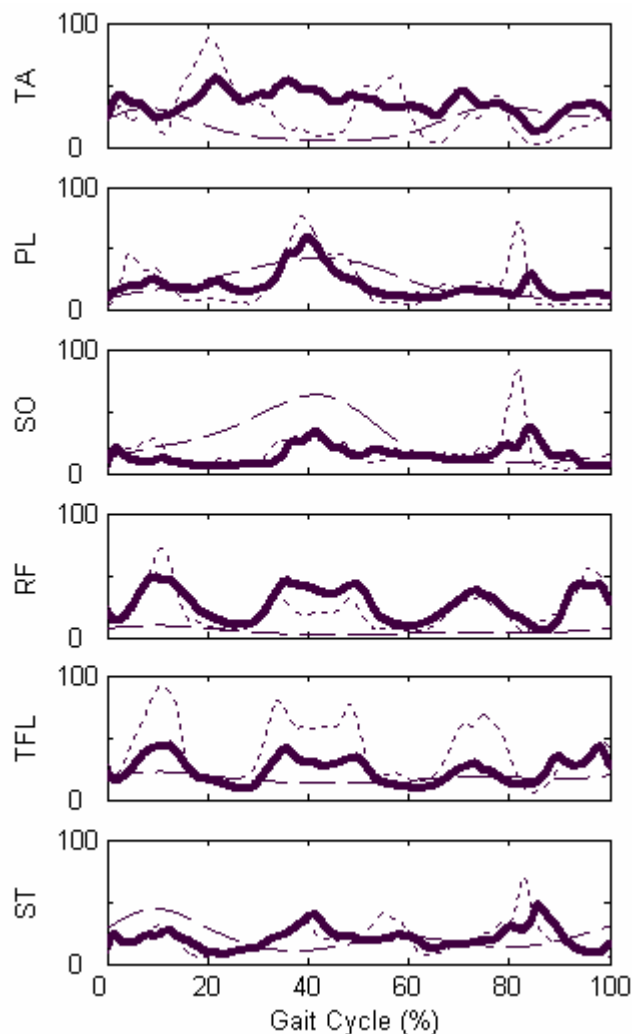
ACKNOWLEDGEMENT

Figure 1. Ensemble EMG of six muscles (% max activation) during TCG (solid line for beginners, dotted line for proficient TCQ practitioner) and NG (dash line).
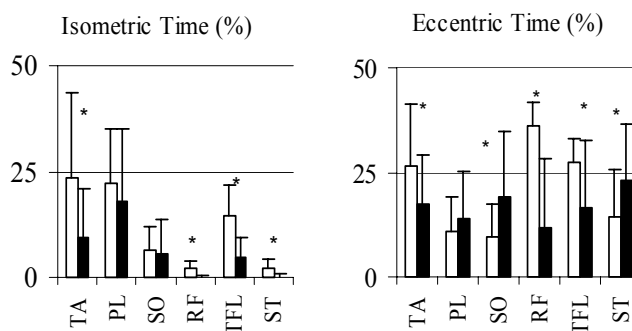

Figure 2. Mean and Std of isometric and eccentric action time of six muscles in TCG (open bar) and NG (filled bar). Symbol * indicates a significant difference ($p < 0.05$) between TCG and NG.

INTER-TRIAL AND TEST-RETEST RELIABILITY OF KINEMATIC AND KINETIC GAIT PARAMETERS AMONG SUBJECTS WITH ADOLESCENT IDIOPATHIC SCOLIOSIS

Carole Fortin, M.Sc. P.T.[1,2] Sylvie Nadeau, Ph.D,[1,2] Hubert Labelle, M.D[3]

[1]Centre de recherche interdisciplinaire en réadaptation , Institut de réadaptation de Montréal, Canada
[2]École de réadaptation, Université de Montréal, Canada, H3S 3J4 sylvie.nadeau@Umontreal.ca
[3]Centre de recherche de l'Hôpital Sainte-Justine, Montréal, Québec, Canada

INTRODUCTION

Previous studies have recognized the relevance of assessing functional activities in subjects with adolescent idiopathic scoliosis (AIS) (Lenke et al., 2001). Since some authors have suggested that walking can be associated with the pathogenesis and evolution of scoliosis (Burwell et al., 1992), better characterization of the gait pattern in subjects with AIS is now essential. It may also be interesting to document changes in the gait pattern after treatment or over the course of development of the scoliosis. However, the latter aspects will require knowing the reliability of the gait parameters before interpreting any of the results. This study has therefore assessed the inter-trial and test-retest reliability of the time-distance, kinematic and kinetic parameters in three and five trials, in subjects with AIS walking at natural and maximal speeds.

METHODS

A convenience sample of 20 teenage girls from 12 to 17 years old with an idiopathic scoliosis of type I, II or III of the King classification and a lateral deformity between 17° and 50° (Cobb angle) participated in the study. Subjects were recruited at Sainte-Justine Hospital (Montreal). The adolescents' gait pattern was assessed by the same physical therapist when they performed the test at their natural and maximal speeds on two occasions, five to ten days apart.

Spatio-temporal parameters were obtained by foot-switches placed under the subject's shoe. A three-dimensional motion analysis system (Optotrak) was used for kinematic data (angular displacement) of the lower limbs. Ground reaction forces (GRFs) were collected by force-plates while an inverse dynamic approach was used to calculate the net moments of force at the ankle, knee and hip joints. Five good trials, each consisting of natural and maximal level walking, were recorded for each participant. The generalizability theory (Shavelson and Webb, 1991) and standard errors of measurement (SEMs) served to assess the reliability of specific maximum and minimum peak values on the kinematic and kinetic curve profiles of the gait parameters for the right lower limb.

RESULTS AND DISCUSSION

Overall, the inter-trial reliability for three trials was good for all time-distance, kinematic and kinetic gait parameters at both speeds. The coefficient of dependability (ϕ) ranged from 0.60 to 0.99 with lower values observed for the medio-lateral GRF component at both speeds but more noticeable at maximal speed. Giakas et al. (1996), who also found lower reliability for this parameter, attributed it to a difficulty controlling the balance of the foot during gait.

As in previous studies, the test-retest reliability was found to be lower than the inter-trial reliability (Steinwender et al., 2000; Kadaba et al., 1989). The test-retest dependability coefficients were higher for the kinetic than for the kinematic parameters (Table 1). The SEMs, in the sagittal plane, ranged from 1.6 Nm to 7.9 Nm and from 1.5° to 3.3° for the moment and angular displacement parameters, respectively. The vertical GRF component showed the highest coefficients of dependability (ϕ: 0.92 to 0.98) with SEMs ranging from 17.8 to 30.4 N. Kadaba et al. (1989) stated that most of the variability for the GRF was attributable to the subject's physiological factors because the source of error of the force-plate measurement system was very small. However, other gait parameters might be more affected by differences in marker positions and other parameters required in their calculation. The level of reliability was comparable for many gait parameters using three or five trials.

Table 1. Dependability coefficients (ϕ) for test-retest reliability of gait parameters (three trials).

Parameters	Natural speed	Maximal speed
Time-distance	ϕ: 0.42 to 0.57	ϕ: 0.71 to 0.90
Angular displacements	ϕ: 0.52 to 0.86	ϕ: 0.46 to 0.83
GRFs	ϕ: 0.66 to 0.98	ϕ: 0.56 to 0.97
Moments	ϕ: 0.51 to 0.96	ϕ: 0.34 to 0.95

SUMMARY

This study is the first to assess the reliability of a large gait data set in adolescents with idiopathic scoliosis walking at natural and maximal speeds. The results showed good inter-trial reliability for most of the gait parameters. The test-retest reliability varies from moderate to good except for some parameters. In conclusion, several gait parameters are reliable among subjects with AIS and can therefore be used to document changes in the gait pattern after treatment or during the course of development of the scoliosis.

REFERENCES

Burwell, et al (1992). *Acta Orthopaedica Belgica*, **58**, suppl.1.
Giakas, G. et al (1996). *Spine*, **21**(19), 2235-2242.
Kadaba, MP. et al (1989). *J. Orthop Research*, **7**(6), 849-860.
Lenke, et al (2001). *Spine*, July 15; **26** (14), E330-E337.
Steinwender, G. et al (2000). *Clin Biomech*., **15**, 134-139.
Shavelson, RJ. and Webb, NM. (1991). *Generalizability Theory* Newbury Park. Sage.

ACKNOWLEDGEMENTS

A MOTION-CONTROLLED DEVICE FOR ACHIEVING SIMULATED ACTIVE IN-VITRO ELBOW MOTION

Cynthia E. Dunning[1,2]; Karen D. Gordon[3]; Graham J.W. King[2]; James A. Johnson[1,2]

[1]Department of Mechanical and Materials Engineering, University of Western Ontario, London, Canada, cdunning@uwo.ca
[2]Bioengineering Research Laboratory, Hand and Upper Limb Centre, St. Joseph's Health Centre, London, Canada
[3]School of Engineering, University of Guelph, Guelph, Canada

INTRODUCTION

Laboratory testing plays an important role in advancing patient care by helping to develop new treatment techniques and improved rehabilitation therapies. By simulating active elbow motion in-vitro, injury mechanisms can be explored and new clinical approaches can be studied prior to implementation in-vivo (Johnson et al, 2000; Dunning et al, 2001; Bottlang et al 1999, 2000; Madey et al, 2000). The purpose of this study was to develop a motion-controlled testing system to study kinematics in the stable and unstable elbow in various orientations, and to evaluate its performance.

METHODS

Figure 1 shows the motion-controlled elbow simulator. Cables are sutured to the tendons of biceps, brachialis, brachioradialis, triceps and pronator teres, and connected to computer-controlled pneumatic actuators. The actuator attached to the brachialis tendon (which is the prime mover for elbow flexion) is operated under velocity control, using custom-written software incorporating a real-time PID controller with position feedback.

Figure 1: Elbow simulator

Load applied to the brachialis is monitored, and used to apportion loads the remaining (load-controlled) actuators according to ratios developed from EMG (Funk et al, 1987) and pCSA (Amis et al, 1979) data.
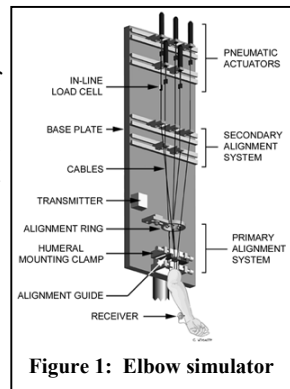
Elbow flexion was produced in eight cadaveric elbows (mean age 67 ± 19 years), before and after sectioning of the lateral collateral ligament (LCL). Testing was conducted with the elbow positioned in the vertical (Figure 1), varus, and valgus orientations, and with the forearm maintained in pronation or supination. Ulnohumeral kinematics were recorded using an electromagnetic tracking device (Flock of Birds, Ascension Technology, Burlington, VT). Each motion trial was repeated 5 times to assess repeatability. Data were analyzed using two-way repeated-measures ANOVAs and post-hoc Student-Newman-Keuls tests (α=0.05).

RESULTS

The simulator produced repeatable flexion angle versus time curves (Figure 2A), with an average velocity of 35.8±5.8°/sec in vertical orientation (i.e. inter-specimen variability = 16%). Repeatability was quantified by determining the maximum standard deviation in flexion angle as a function of time from the five successive trials (Figure 2B). In the vertical orientation, repeatability was not affected by forearm position (p=0.5) or LCL sectioning (p=0.8). Comparably, results were less repeatable in valgus (p=0.008) and varus (p=0.023), but LCL sectioning still had no effect (p_{valgus}=0.6; p_{varus}=0.6).
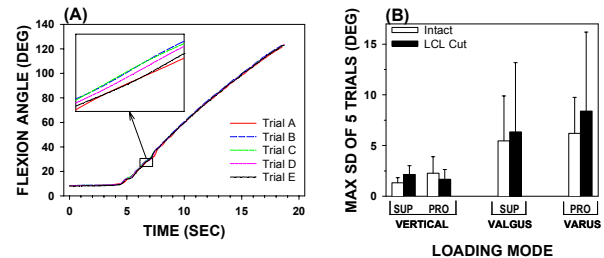

Figure 2: Flexion Angle versus Time
(A) Data for one specimen with the forearm supinated in the vertical orientation; (B) Repeatability (mean ± SD) for n=8.

Repeatable V-V and I-E motion pathways (as a function of flexion angle) were also achieved. The maximum standard deviations in these values over the five successive trials ranged from 0.11 to 0.19 degrees. There was no effect of LCL sectioning (p>0.5) or forearm position (p>0.6) on repeatability of the motion pathways.

DISCUSSION

This study details the development of the first elbow simulator to achieve motion-controlled tendon loading, and to use pneumatic actuators as the motion source. Compared to a previous load-controlled design (Johnson et al, 2000; Dunning et al, 2001), the motion-controlled simulator produces kinematic pathways that are of equal or improved repeatability. The resulting motions are also more consistent, with the current inter-specimen velocity variability of 16% compared to 82% reported in our previous work (Johnson et al, 2000). Unlike the load-controlled device, this simulator is capable of producing simulated active motion in the varus and valgus orientations (although they are somewhat less repeatable). Future studies will address the need to improve repeatability in the varus and valgus orientations, and to expand the types of motion simulation (i.e. new orientations).

SUMMARY

A motion-controlled testing apparatus capable of generating smooth, gentle pathways of in-vitro elbow flexion in vertical, varus, and valgus orientations has been developed. This is an important tool for laboratory studies aimed at increasing our knowledge of elbow mechanics.

REFERENCES

Johnson, J.A. et al, (2000). *J Biomech*, **33**, 635-9; Dunning, C.E. et al, (2001). *J Biomech*, **34**, 1039-48; Bottlang et al (2000). *J Orthop Res*, **18**, 195-202; Bottlang et al (1999). *Trans ORS*, **24**, 367; Madey et al (2000). *J Orthop Trauma*, **14**, 41-7; Funk et al (1987). *J Orthop Res*, **5**, 529-38; Amis et al (1979). *Eng Med*, **8**, 41-8.

A BIOMECHANICAL METHOD TO ASSESS THE CONTRIBUTION OF PASSIVE MOMENT AT THE HIP DURING GAIT OF DUCHENNE MUSCULAR DYSTROPHY CHILDREN

Nathaly Gaudreault [1], Denis Gravel [1,2], Sylvie Nadeau [1,2], Sylvie Houde [3], Pierre Desjardins [1]

[1]*Centre de recherche interdisciplinaire en réadaptation du Montréal métropolitain,*
Institut de réadaptation de Montréal, [2]*École de Réadaptation, Université de Montréal, Qc, Canada*
E-mail : Denis.Gravel@umontreal.ca
[3]*Hôpital Ste-Justine, Centre de réadaptation Marie-Enfant*

INTRODUCTION

After muscle weakness, contractures are the second problem affecting the locomotor system of children with Duchenne muscular dystrophy (DMD). For the lower extremities, they are mainly present in plantar flexors, knee flexors, hip flexors and tensor fascia lata muscles. Their negative influence on gait was demonstrated in previous studies (Brown and Cooke, 1981). However, contractures could also be beneficial during gait since the passive moments they produce could partially compensate for the low moments generated by the weak contraction of muscles. The goal of this paper is to present a biomechanical method that will rigorously quantify the hip flexor contractures and will determine their relative contributions during gait of DMD children.

METHOD

MODEL: Kinematic and kinetic parameters will be estimated and from these data, the net flexion moment generated at the hip will be known for all angles. The following model will then be applied to evaluate the relative contribution of the hip flexor passive moment generated at a specific angle throughout the gait cycle:

$$RCC = (EPMom/Nmom) \times 100$$

where RCC = Relative Contribution of Contracture, Nmom = Net moment for a given angle during gait, EPMom = estimated passive moment for a given angle. Passive moment produce by the hip flexor contractures will be estimated from moment-angle passive curves obtained during an extension movement**.** GAIT PARAMETERS MEASUREMENTS: Kinematic gait parameters will be measured with an Optotrak infrared movement analysis system using 3D co-ordinates obtained from markers placed on the body segments. For the kinetic parameters, AMTI (Advanced Mechanical Technology) force plates embedded in the floor will record the ground reaction force. Hip force and moment components will be obtained using the inverse dynamic method. CONTRACTURE MEASUREMENTS: The subject will be positioned in side- lying, on the non-tested side. The limb being evaluated will be supported by a suspension system that eliminates the effect of gravity and allows the subject to relax his muscles. To evaluate EPMom produced by the hip flexor contractures, the moment-angle curves will be obtained by moving passively the lower extremity in extension with a triaxial dynamometer

(AMTI SGA6-4) placed between the segment and the evaluator's hand. The range of movement to be evaluated will be equivalent to the range covered by that joint during walking. To record all the forces applied on the lower extremity, a force transducer (Inter Technology, 363-D3-200-20P3) in the cable of the suspension system will also be used. Orientation and position of the segment, the dynamometer and the suspension cable will be measured with an Optotrak system. To eliminate unwanted muscle activity, electromyography will be used as a biofeedback device during passive measurement.
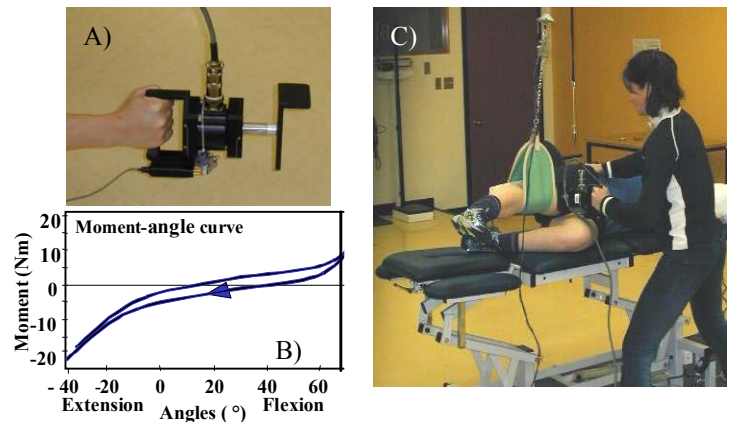

Fig.1 Passive moment measurement at the hip. A) dynamometer B) expected moment-angle curve and C) experimental setup.

DISCUSSION AND CONCLUSION

This is a new approach to evaluate hip muscle stiffness. The expected results will be that the contribution of the hip flexor contracture will be beneficial in the early stages of the disease, more precisely when the muscles will be in a lengthened position. The study is still in progress and data using this method will allow the verification of this hypothesis.

REFERENCES

1.Brown, SH and Cooke JD (1981). *J Physiol* 316: 97-107
2. Riener, R and Edrich, T. (1999). *J Biomech* 32: 539-54

ACKNOWLEDGEMENT:

TRUNK CONTROL DURING GAIT WITH ARMS CROSSED ON THE CHEST IN ADOLESCENT IDIOPATHIC SCOLIOSIS

Mathieu Charbonneau and François Prince

Département de kinésiologie, Université de Montréal, Montréal, Québec, Canada mathieu.charbonneau@etsmtl.ca

Centre de réadaptation Marie Enfant, Hôpital Sainte-Justine, Montréal, Québec, Canada

INTRODUCTION

Adolescent idiopathic scoliosis (AIS) presents osseous deformations of the vertebrae and rib cage as well as modifications of the muscular composition. The pathology has multifactorial etiology (Lowe et al., 2000) and one of the possible causes is an asymmetric neuromuscular command (Wiener-Vacher et Mazda, 1998; Catanzariti et al., 2001).

It is known that young adults control their trunk by a top-down muscular activation beginning at the cervical levels towards the lumbar ones (Prince et al., 1994). To our knowledge, these sequences of activation and the behaviour of the trunk in terms of anteroposterior (A/P) and vertical accelerations during gait among patients with scoliotic deformations were never investigated. The objective of this project is thus to determine the behaviour of the spinal column (A/P and vertical accelerations) and the paraspinal muscles activity during gait in healthy children and AIS patients.

METHODS

A total of nine AIS patients (thoraco-lumbar curve) and 10 control subjects were recruited. The two groups had a mean age of 14 years and were comparable relative to their anthropometry, gait speed and cadence. A total of 30 reflective markers were placed on spinous process of C7, T2, T4, T6, T8, T10, T12, L2, L4 and S1 vertebrae, mandibular articulation, posterior and anterior superior iliac spines, acromion processes and on lower limb (to detect gait events). Markers were tracked at 60 Hz and their 3D coordinates were recorded by a 8-cameras VICON 512™ system (Oxford Metrics, UK) during 10 trials of walking at comfortable speed. Subject's arms were crossed on their chest to avoid paraspinal muscles' signal contamination.

Bilateral EMG was recorded at 960 Hz with a passband of 20-450 Hz. Electrodes were placed at C7, T4, T10 and L2 levels on the paraspinal muscle on each side (2-3cm) of the spine. Cross-correlation was applied to the EMG signals to calculate the shift between onset time of each muscle level compared to lumbar level (L2). Mean values of variables were compared between the two groups using ANOVA and Fisher post-hoc test. The significance level was set at $p < 0.05$.

RESULTS AND DISCUSSION

For the AIS subjects, A/P accelerations near the apex (T10-L2) become similar with those calculated at the pelvis. The vertical accelerations of AIS subjects were about 11% greater than the control group (Fig.1) and no damping was observed regarding that direction for either groups.

The muscles activation shifts were not significantly different between the conditions but suggest a difference between the two groups (Fig.2). AIS patients were showing earlier muscle activation at each levels compared to controls. Also, the integrated EMG signal showed some more muscle activation asymmetry in the AIS group.
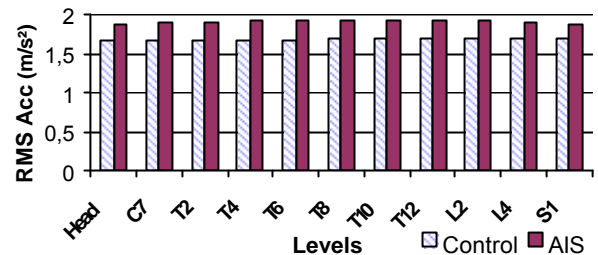

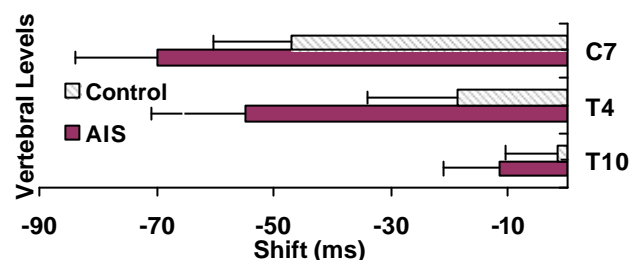Figure 1: Vertical RMS acceleration of vertebral level between the two groups.

Figure 2: Muscle activation shift at each vertebral level with respect to L2 muscular onset.

The results of this study confirm that stiffness is increased around the apex zone in AIS during gait. The increased vertical acceleration and a poorer muscular control in AIS during gait could also be an aggravating factor in scoliosis deformation.

SUMMARY

An increased stiffness near the apex area was detected in AIS during gait. Augmented vertical acceleration calculated, a desynchronized and more asymmetrical muscular activity during gait in AIS children could be an aggravating factor of the deformations.

REFERENCES

Prince et al., (1994). *Gait & Posture*, **2:**19-25.
Lowe et al., (2000). *JBJS*, **82:**1157-68.
Wiener-Vacher and Mazda (1998). *J Ped*, **132:**1028-32.
Catanzariti et al., (2001). *Spine*, **26:**48-52.

ACKNOWLEDGEMENTS

MEASUREMENT OF IMPACT FORCES IN A SIMULATED BICYCLE HANDLEBAR INJURY CRASH: THE EFFECT OF MASS, IMPACT VELOCITY AND THE PROPERTIES OF THE HANDLEBAR ENDS

Steven R. McFaull [1], D. Gordon E. Robertson [2] and Andrew Post [2]

[1] Research Analyst, Injury and Child Maltreatment Section, Health Surveillance and Epidemiology Division, Centre for Healthy Human Development, Population and Public Health Branch, Health Canada
[2] School of Human Kinetics, University of Ottawa

INTRODUCTION

Bicycling is a common activity among children of all ages. For young children there is a "hidden" hazard associated with bicycling. The bicycle handlebar injury (HBI) is an infrequent but potentially lethal injury mechanism that has been well known to clinicians for over 30 years. The child, usually 5-10 years of age, moving at a slow speed, meets a disturbance (pothole, rocks, etc.) which causes a fall onto the handlebar end, often resulting in an internal abdominal injury. Even through changing bicycle designs, the HBI mechanism still persists. Recently, a group of researchers (Winston et al, 1998; Arbogast et al, 2001) have looked at the detailed mechanism of the HBI. They developed a theoretical approach to estimate the impact forces based on actual crash information and compared the results to organ tolerance data. The purpose of the present study was to add to the understanding of the HBI mechanism by measuring actual impact forces in a simulated HBI crash.

METHODS

Two heavy bags approximating the mass of a 3rd and 50th percentile 8-year old boy (19.88 kg and 25.17 kg) were used to represent the falling body. Two experiments were conducted using the handlebars of a suitable children's bicycle. The two experiments represent slightly different scenarios of the HBI mechanism. The first was a simple drop test and the second was a pendulum drop test. Only the results of the simple drop test are presented here. The two bags were dropped from various heights set to represent the magnitudes of speeds and the momentums expected in an HBI crash (Arbogast et al, 2001). Drop heights of 11, 32, 62 and 102 cm were used to create impact velocities of 1.5, 2.5, 3.5 and 4.5 m/s, respectively. The handlebars were secured perpendicularly to the plane of a Kistler force platform (model 9261A) and the bags were dropped so that the centre of gravity of the bag impacted the handlebar. The force data were sampled at 12,500 hertz for 0.16 seconds and stored for later processing. Data after this time were unreliable and did not represent the true impact of the bag with the handlebars. Tests indicated that hitting eccentrically always yielded lower peak forces during the impact. The force data were collected using BioWare software available from Kistler and then processed by our own customized software (BioProc2, University of Ottawa Biomechanics Laboratory). Peak forces and rates of force development were then derived from the raw force data. During the testing, accelerometers (Brüel and Kjær, model 7264C-500) were attached to both ends of the handlebars to directly measure the impact shock transmitted through the handlebars from the ground to the end that impacts with the bag. These measures were recorded simultaneously at 10 kHz with the force platform data using the BioWare software and then processed by the BioProc2 data analysis system. The experiments were repeated for five different types of handlebar end (2 masses × 4 impact velocities × 5 handlebar end types).

RESULTS AND DISCUSSION

Figure 1 shows the averaged impact forces for the 19.88 kg bag drops normalized to the impact duration. There was a linear increase in peak force with increasing impact velocity r=0.983, p=0.017). Curiously, the impact forces of the 25.17 kg bag were not significantly different than the 19.88 kg bag - probably due to the non-rigidity of the bag and the deflection upon impact. In other words, the effective mass of the two bags was the same. This is feasible in an actual crash scenario. There were also differences in the peak force by handlebar end type.
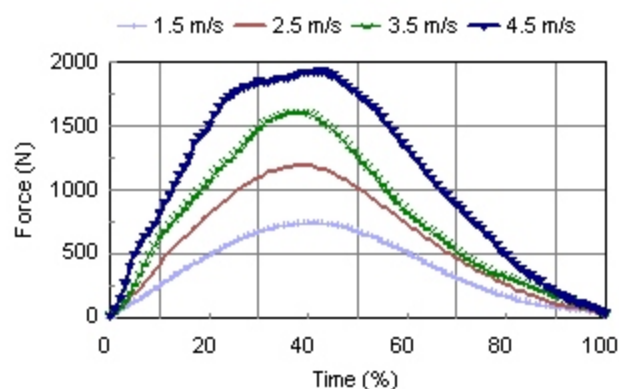

Figure 1. Averaged and time normalized impact curves for the four impact velocities of the 19.88 kg bag.

SUMMARY

Peak impact forces ranged between approximately 750 N and 2,000 N, which exceeds published data on the tolerance of the pediatric spleen (785 N) and approaches that of the liver (2,649 N). The impact velocity, which is dependant on the initial riding speed, heavily influences the peak impact force.

REFERENCES

Winston, F.K. et al (1998). *Pediatrics*, **102**, 596-601.
Arbogast, K.B. et al (2001). *Accident Analysis & Prevention*, **33**, 753-757.

THE EFFECT OF TIME TO PEAK ANKLE TORQUE ON BALANCE STABILITY BOUNDARY: EXPERIMENTAL VALIDATION OF A MATHEMATICAL MODEL

Martin Simoneau[1] and Philippe Corbeil[2]
[1]Faculté de Médecine, Division de Kinésiologie, Université Laval, Québec, Québec, Canada,
E-mail: Martin.Simoneau@kin.msp.ulaval.ca
[2]Centre for Studies in Aging, Sunnybrook & Women's College Health Sciences Centre, Toronto, Canada

INTRODUCTION

Pai and Patton (1997), using a mathematical model, determined a set of feasible center of mass (CM) velocity-position combinations (balance stability boundary) that guarantees upright stability but did not consider time to peak ankle torque. Recent experimental studies demonstrated that the ability to maintain a stable posture depended not only on the magnitude of the restoring torque but also on the time to peak of the restoring torque. The objectives of the present study were: (1) to build a mathematical model that predicts the balance stability boundary which includes time to peak ankle torque, (2) to determine the capability of that model to predict experimental successful and failed balance recovery trials, and (3) to compare the predictive capability of the mathematical model with that of a statistical model (logistic regression).

METHODS

Mathematical model

An inverted pendulum rotating about a base of support was used to model the postural system. Dynamic equation of angular motion and mechanical constraints similar to that of Pai and Patton (1997) were used to predict the forward balance stability boundaries for different time to peak ankle torque. Hence, boundaries were constrained by environmental (ground reaction force), anatomical (foot geometry), and physiological (time to peak ankle torque and torque amplitude) conditions.

Experimental validation

Participants were standing upright barefoot with their feet 10 cm apart. Following an initial auditory signal, they self-initiated a forward destabilization keeping their body straight; they had their arms flexed at the sternum level and they were encouraged not to bend their knee and hip joints or to raise their heels. A second auditory signal indicated that they had to initiate, as fast as possible, a recovery response in order to return to their initial position. The participants were told not to step. The time elapsed between both auditory signals was set to 800 or 1000 ms to ascertain time to peak ankle torque variability, to increase the likelihood of forward unsuccessful balance recovery and to acquire various CM position-velocity profiles.

RESULTS AND DISCUSSION

Mathematical model

When the stability boundaries were computed using time varying ankle torque input, the mathematical model predicted 73.3 % of the experimental failed trials, compared to 5.6 % for constant ankle torque input. On the other hand, the model's capability to predict successful trials was 73.3 % and 100 % for time varying ankle torque and constant ankle torque input, respectively.
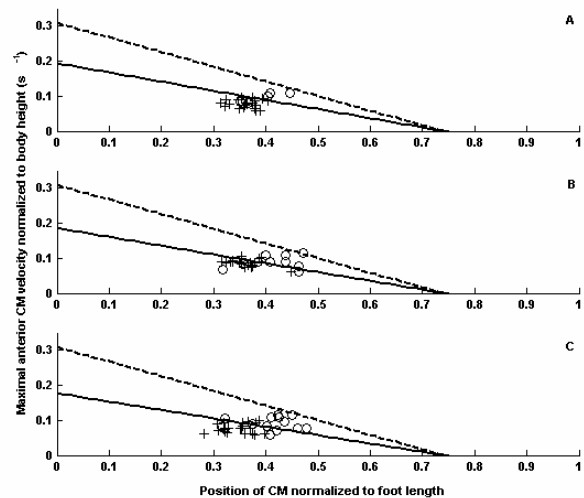

Figure 1: Successful (crossed) and failed (open circle) experimental trials for time to peak ankle torque of 0.7 s, 0.8 s, and 0.9 s (A, B and C respectively). Upper balance stability boundary (dashed line) is for constant ankle torque input, whereas lower balance stability boundary (solid line) is for the time varying ankle torque input.

The experimental successful trials are inside the lower balance stability boundary, whereas the experimental failed trials are outside. In contrast, most of the experimental failed trials are inside the upper balance stability boundary. Some experimental failed trials were outside both balance stability boundaries. Finally, all experimental successful trials were correctly identified by both stability boundaries.

Statistical model

The predictive capability of the statistical model increased as the number of independent variable is considered in the logistic regression. Adding ankle time to peak as predictor improved the percentage of prediction of experimental failed trials from 45.4% to 54.1%.

SUMMARY

The mathematical model predicted 73.3% of the experimental failed trials and 73.3% of the experimental successful trials. The stepwise logistic regression predicted 54.1% of the experimental failed and 91.9% of the successful trials. Hence, the mathematical model showed better predictive capability than the statistical model for identifying unsuccessful balance recovery.

REFERENCES

Pai Y-C & Patton JL. (1997). J Biomech, 30:347-54.

STUDY CONCERNING THE EFFECT OF CALCITONIN ADMINISTRATION ON THE BONE STRENGTH OF OVARIECTOMIZED RATS

J. Rosenkrancova[1], P. Ruzicka[1], R. Sedlacek[1], J. Zak[2]

[1]Laboratory of Human Biomechanics, Czech Technical University in Prague, Prague, Czech Republic, e-mail:
rosenkra@biomed.fsid.cvut.cz
[2]The First Faculty of Medicine, Charles University, Prague, Czech Republic

INTRODUCTION

Osteoporosis is a disease in which the density and quality of bone are reduced, leading to weakness of the skeleton and increased risk of fracture, particularly of the spine, wrist, hip, pelvis and upper arm.

Calcitonin is a polypeptide hormone secreted by the parafollicular cells of the thyroid gland in mammals and by the ultimobranchial gland of birds and fish. Calcitonin (salmon) is a synthetic polypeptide of 32 amino acids in the same linear sequence that is found in calcitonin of salmon origin. Calcitonin is used in human medicine as a drug for osteoporosis. The long administration of Calcitonin prevents bone decomposition and that way inhibits lowering the mechanical resistance and incidence of osteoporotic fractures.

The experimental osteoporotic models are used for testing anti-osteoporotic effects of various drugs. Rat oöphorectomy (OOX) is often used as an osteoporotic model. After oöphorectomy, the estrogen production falls off, increases significantly the osteoclastic activity and develops the osteoporosis. It is possible to administrate the tested agents to this model. If we administrate the Calcitonin to OOX rats, it prevents incidence of osteoporosis (Shen, 1997). Calcitonin belongs to the agents that recover some mechanical properties of osteoporotic bone, e.g. degree of elastic load (Fukushima, 2000).

MATERIALS AND METHODS

The study was performed on two experiments with 60 female rats that were divided into four groups: I – baseline control, II – oöphorectomy (OOX) and placebo application s.c., III – sham operation + Calcitonin IV – Calcitonin + OOX. Calcitonin was administered subcutaneous (s.c.) in 0.2 ml on alternate days 3 days in week. In volume 0.2 ml there is 10 units of Salmon Calcitonin. The intermittent administration of calcitonin has a similar effect as a continuous administration (Li, 1996).

After four weeks of treatment, the animals were killed by decapitation. The left femur was removed and cleaned of tissue and storied in 96% alcohol. During 24 hours before testing the bones were hydrated in the distilled water at room temperature. Biomechanical testing system MTS Mini Bionix 858.02 was used for the three-point bending test. The program controls crosshead speed and measures important quantities such as load, deflection and time. Bending strength σ_{omax} [MPa] was calculated from the force F_{max} and cross-section of bone W_{omin}, $\sigma_{omax} = F_{max}L/4W_{omin}$, where L is distance between two supporting bars.

Methodology of the bone dimensions measuring was affected this way: The fracture area of the broken femur is resurfaced, the bone cross-section is marked by the coloured felt-tip and scanned by means of a tabletop flat scanner and the acquired full colour digital image is saved on a PC hard drive. We use the scanner resolution 1200x1200 dpi. The picture obtained from scanner is put through the process of segmentation. The binary image of the same resolution and size is derived from the original full colour image. This image contains values 0 or 1. Value 1 belongs to the bone cross-section and value 0 does not belong to the bone. The cross-section characteristic values are computed by the algorithm that has been implemented in the computer program written in MATLAB. This method is detailed in the article (Ruzicka, 2002). Output of this program is especially the value of cross-section of bone W_{omin}.

RESULTS AND DISCUSSION

Table 1 shows the bone bending strength values for all four groups of both experiments. The effect of Calcitonin treatment on the bone mechanical properties was not statistic significant. We will use the bending test on the femoral neck for further experiments. From this type of the experiment we will obtain more authoritative values because the fracture of femoral neck is the most frequent condition within osteoporosis.

Table 1

Group	Bending strength [MPa]	
I	$206,4 \pm 9,9$	$230,65 \pm 14,87$
II	$190,9 \pm 10,1$	$229,83 \pm 12,07$
III	$198,5 \pm 12,8$	$237,58 \pm 13,04$
IV	$203,2 \pm 7,7$	$213,99 \pm 13,70$

SUMMARY

The aim of this study is the determination of the effect of Calcitonin administration on the bending strength of rat osteoporotic bones. For experiments, we used the three-point bending test.

REFERENCES

Shen, Y. et al (1997). *Calcif Tissue Int.,* 60(5), 457-461.
Fukushima, T. et al (2000). *J. Pharmacol*, 82(3), 240-246.
Li, M. et al (1996). *Bone*, 18, 375-380.
Ruzicka, P. et al (2002). *Proc. of Workshop*, 6, 910-911.

ACKNOWLEDGEMENTS

ENERGY vs MOMENT APPROACH FOR CALCULATING
INDIVIDUAL MUSCLE CONTRIBUTIONS TO JOINT STABILITY

Jim R. Potvin[1] and Steve H.M. Brown[2]

1Department of Kinesiology, University of Windsor, Windsor, Ontario   jpotvin@uwindsor.ca
2 Department of Kinesiology, University of Waterloo, Waterloo, Ontario

INTRODUCTION

To date, almost all efforts to quantify muscle contributions to joint stability have used the "Energy" approach. However, recently, Stokes and Gardner-Morse (2003) noted that stability can also be calculated as the rate of change of moment for a small rotation. One advantage of a "Moment" approach is that it may presents and easier means of interpreting individual muscle contributions to stability. The purpose of this paper is to compare the Energy and Moment approaches to quantifying joint stability.

METHODS

Figure 1 illustrates a muscle origin and insertion before (B) and after (B2) a small rotation about the z axis of a particular joint. The change in length was calculated using the rotated minus the original muscle length.
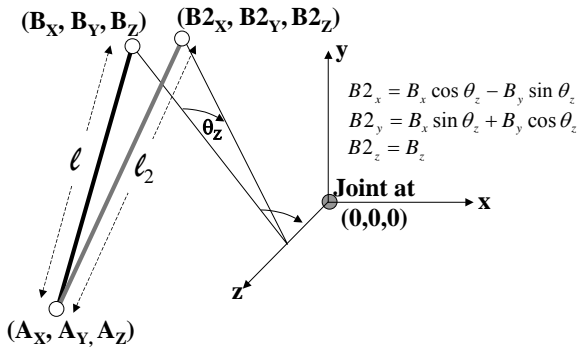

$$B2_x = B_x \cos \theta_z - B_y \sin \theta_z$$
$$B2_y = B_x \sin \theta_z + B_y \cos \theta_z$$
$$B2_z = B_z$$

Figure 1: Origin (A) and insertion initial (B) and final (B2) location after a small rotation about the joint assumed to be at (0,0,0) m. (x axis: lateral, y: axial, z: flexion/extension).

Energy approach: the elastic potential energy stored in the muscle is calculated by:

$$U(m) = F \, \Delta \ell + \frac{1}{2}k \, \Delta \ell^2 \qquad [1]$$

where: U(m) = potential energy stored in the muscle, F = muscle force (N), k = muscle stiffness (N/m), ℓ = muscle length (m). The stability contribution of a muscle about the z axis (Sz), is calculated as the second derivative of U(m) with respect to an small rotation angle. This was determined by substituting the length equations for AB and AB2 into [1], applying a Taylor Series expansion, differentiating twice with respect to θ, and simplifying. A further substitution of k=qF/ℓ, from Bergmark (1989), was made yielding [2]:

$$S_z = F \left[\frac{(A_X B_X + A_Y B_Y)}{\ell} + \frac{(q-1)(B_X A_Y - A_X B_Y)^2}{\ell^3} \right]$$

Moment approach: the change in length with a very small θ_Z (1×10^{-8} rad) was used to calculate the change in passive muscle force due to stiffness. In addition, the change in muscle moment arm was calculated with the small insertion rotation and these two variables were combined to determine the net change in moment. Stability was calculated as the change in moment over the small change in angle.

To compare the two approaches, a large number of muscles were simulated and rotated by the very small angle. Insertions were simulated with all combinations of x, y and z coordinates ranging from 0 to 10, by 1 (n=1331). Origins were simulated with all combinations of x and z coordinates from 0 to 10 and y coordinates from –10 to 10 (n=2541) for a total of 3,382,071 origin/insertion combinations (ie. muscles). Simulated muscles were removed if they either created a negative moment about z (ie: extension) and/or had an origin that was superior to the insertion, leaving 2,189,253 muscles (65% of the total). Each muscle was given a q value of 10, a force of 100 N. The Sz for each muscle was then calculated with both the Energy and Moment approaches and a difference value (error) was calculated in each case.

RESULTS AND DISCUSSION

Of the 2,189,253 muscles tested in the simulation, the average stability value was calculated to be 25.1 Nm/rad/rad. Amongst all these comparisons between the Energy and Moment approaches, the largest error was only 0.00013 Nm/rad/rad and this was only 0.0003% of the mean stability. Thus, the Moment approach appears to provide an accurate and easy method for calculating muscle contributions to joint stability. One advantage of this method, beyond its ease of use in biomechanical models, is that equivalent cocontracting muscle pairs can be studied to better understand the stability contribution associated muscle orientation. The passive muscle stiffness will always provide a stabilizing influence, even if it is not sufficient to overcome the instability caused by the external load. However, in many cases, the effect of the initial force was often found to be destabilizing because, with a small rotation, the shortening (destabilizing) muscle in the pair actually had a smaller decrease in moment than the subsequent increase observed with the opposing lengthening muscle, resulting in a net destabilizing moment.

REFERENCES

Bergmark, A. (1989) *Acta Orthop Scand* 230(suppl):1-54.
Stokes, I.A., Gardner-Morse, M. (2003) *JEK*, 13:397-402.

THREE-DIMENSIONAL VECTOR MODELLING OF INDIVIDUAL MUSCLE FORCES AT THE ELBOW

K.M.A. Weiss-Bundy[1], A.B. Thornton-Trump[2], and C.Y.A. Chan[2]

[1] Human Performance Laboratory, University of Calgary, Calgary, Canada, karyn@kin.ucalgary.ca
[2] Department of Mechanical and Industrial Engineering, University of Manitoba, Winnipeg, Canada

INTRODUCTION

A significant problem in the biomechanics of human motion is the sharing of force within a functional musculoskeletal functional group (Crowninshield and Brand, 1981). The fundamental difficulty is that if several muscles share the force in creating moments about a joint, the problem is statically indeterminate. Since the main determinant of motion about a joint is the net moment created by the muscles crossing it, the muscle forces must be first related to the net joint moment required for a particular acceleration of limb segments. The individual muscle forces would still remain indeterminate until a muscle activation strategy is formulated and applied to the appropriate equations.

This study presents a method of determining the moment arms of muscles in the flexor and extensor groups acting about the elbow joint. A three-dimensional vector model of the elbow joint is presented, muscle moment arms are determined and a simple muscle activation strategy is applied, including antagonistic muscle action. Individual muscle forces are then predicted for a given net joint moment.

METHODS

From dissection information given in the literature (Murray, 1997) the required definition of bone and muscle anatomy was extracted, including the three-dimensional co-ordinates of the muscle origins and insertions. The intersection of the central axis of the humerus with the medial-lateral axis of the proximal ulna and radius were used to locate the elbow joint centre. The muscle lines of action were considered as straight lines and individual muscle moment arms about the elbow joint were calculated using a vector analysis. Assuming each muscle creates a force directly proportional to the cross-sectional area of the muscle belly, the proportional force carried by each muscle is equivalent to the ratio of the individual muscle cross-sectional area to the total cross-sectional area of all the muscles in the functional group. The summation of the individual flexor (biceps brachii, brachialis, brachioradialis, pronator teres, and extensor carpi radialis longus) and extensor (triceps brachii) muscle force terms along with their moment arms is equivalent to the instantaneous net joint moment. This dynamic net joint moment may be determined from a known hand trajectory coupled with accelerations along that trajectory as developed by Chan et al. (2003). Assuming an activation strategy that gives a constant stress over all the muscles of the functional group and knowing the muscle cross-sectional areas and the total muscle force across the joint, the individual muscle forces are thus calculated.

RESULTS AND DISCUSSION

A known hand trajectory for a human subject flexing the forearm in the coronal plane while keeping the upper arm horizontal and stationary is used. A simulated parabolic acceleration profile along that trajectory was assumed to consist of the first half of the trajectory to be acceleration and the latter half being deceleration. The simulation provides the advantage of using a 180 degree flexion/extension cycle. Thus the static moments are known and equal for both flexion and extension, therefore the muscle force changes with cycle time are due to the accelerations of the mass of the forearm and hand only. Figure 1 illustrates these changes with the individual muscle forces required by brachialis for a long task cycle time (quasi-static movement) vs. that for short cycle time (dynamic movement). It can be seen that the increased acceleration effects in the dynamic situation result in an increase in the muscle forces by a magnitude of approximately 400%.
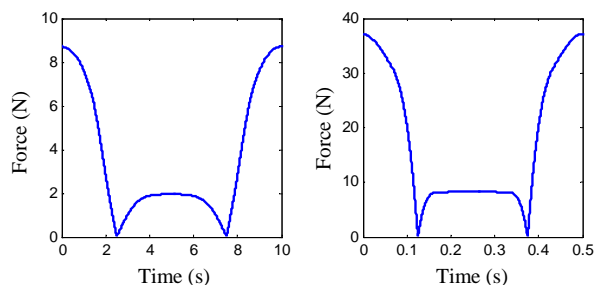

Figure 1. Exemplar Brachialis muscle force at the elbow, 180° flexion/extension cycle in coronal plane with neutral forearm for 10 second (left) and 0.5 second (right) task cycle times.

SUMMARY

It has been shown that a three-dimensional, vector model of the elbow joint and flexor/extensor muscles can be coupled with a muscle activation strategy assumption to yield a prediction of the forces in the individual muscles of the group when joint net moments are available. The predictions are only as accurate as the activation strategy assumption and the dynamic analyses that calculate the net joint moments required for the motion.

REFERENCES

Chan, C.Y.A, et al. (2003). *Computer Methods in Biomechanics and Biomedical Engineering.* Submitted.
Crowninshield, R.D. and Brand, R.A. (1981). *Journal of Biomechanics*, **14**, 793-801.
Murray, W.M. (1997). *Ph.D. Thesis*, Northwestern University.

ANTICIPATORY LOCOMOTOR ADJUSTMENTS OF THE TRAIL LIMB DURING SURFACE ACCOMODATION

Shirley Rietdyk

Department of Health and Kinesiology, Purdue University, West Lafayette, IN

INTRODUCTION

Locomotion is regularly adapted based on the environment and the desired movement goals (Forssberg et al., 1980). When the adaptations are proactive, they are termed "anticipatory locomotor adjustments" (ALAs). Research on gait modifications while avoiding or accommodating the environment has focused on modifications to the swing limb (e.g. McFadyen & Carnahan, 1997), and examination of the trail limb has been limited to the stance phase through joint angle and moment analyses (e.g. Chou & Draganich, 1997). Mechanical power analyses provide insight into the general principles of anticipatory control and coordinative behaviour.

This project extends knowledge regarding the general principles of anticipatory control of the trail limb during stance and swing while stepping up onto a platform.

METHODS

Nine subjects participated, 6 female and 3 male (24.2 ± 2.7 years). All subjects were free from any known neuromuscular disorder. Subjects walked at a self-selected pace down a 10 m walkway, and accommodated a raised surface (0.15 m high, 1 m wide, 3.7 m long) when present. Twenty trials of each condition were observed.

Infra-red emitting diodes placed bilaterally on the toe, heel, ankle, knee, hip and shoulder were recorded at 60 Hz with Optotrak (NDI). Ground reaction forces were recorded at 60 Hz with an AMTI forceplate. Optotrak and force plate data were filtered at 6 Hz and 30 Hz, respectively with a Butterworth dual-pass zero-lag digital filter. Standard 2D joint moment and power analyses were conducted.

RESULTS AND DISCUSSION

The knee energy of the trail limb during toe-off changed from absorption (K3 in Fig. 1) to generation (K5): -0.08 ± 0.03 J/kg vs. 0.06 ± 0.03 J/kg, p < 0.0001. The hip energy at the same time (H3) reduced: 0.07 ± 0.04 J/kg vs. 0.01 ± 0.04 J/kg, p < 0.0001. The changes in energy patterns indicate that stepping up to a new level with the trail foot was accomplished with the reorganized knee flexor strategy, previously identified for obstacle avoidance with the lead limb (McFadyen & Winter, 1991). If the trailing foot was elevated by means of hip flexion, a passive knee extensor torque would result (Bernstein, 1967) and the foot would contact the platform. Therefore, the hip flexor strategy was dampened and the knee was actively flexed to provide clearance.

These results further support the robust nature of the reorganized knee flexor strategy. Although the central nervous system appears to favour increased hip pull-off during platform accomodation with the lead limb, the trail limb demonstrated the reorganized knee strategy.
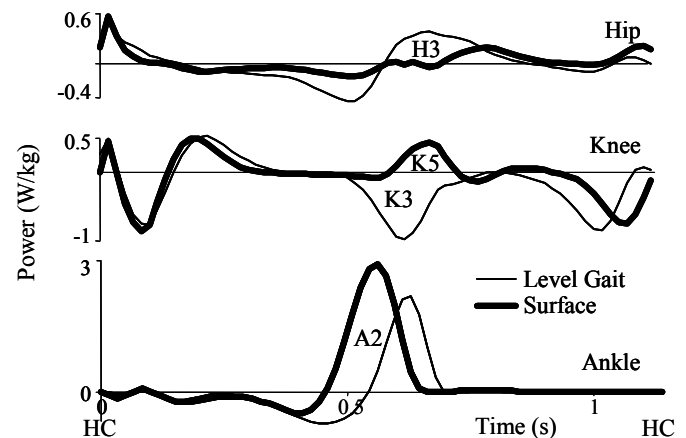

Figure 1: Average power profiles of a single subject. Note that the data was not normalized to stance or swing phases.

The peak ankle plantarflexor moment of the trail limb increased 16% during push-off (p < 0.0001), similar to the 11% increase for the trail limb during obstacle avoidance (Chou & Draganich, 1997). Despite relatively small increases in the ankle moment, the energy generation (A2) increased almost 100%: 0.24 ± 0.04 J/kg vs. 0.43 ± 0.11 J/kg, for level gait and surface accommodation, respectively, p < 0.0001.

The participants doubled the trail limb ankle push-off energy generation in order to step up 15 cm. Ankle energy generation of the lead limb was not altered for obstacle avoidance or surface accommodation (McFadyen & Carnahan, 1997). The large push-off energy of the trail limb would act to raise the head, arms, trunk and lead limb to a new level.

SUMMARY

Previous research has shown that the hip pull-off strategy is augmented to increase toe clearance of the lead limb while stepping up onto a surface (McFadyen & Carnahan, 1997). In the trail limb, the knee muscles act to flex the lower limb to provide adequate clearance. The body was raised to a new level largely through the actions of the ankle muscles of the trail limb after the lead limb had crossed the surface.

REFERENCES

Bernstein (1967) *The coordination and regulation of movements.* Pergamon Press, London.
Chou Draganich (1997) J Biomech 30(4):331-337.
McFadyen Winter (1991) Neurosc Res Comm 9(1):37-44.
McFadyen Carnahan (1997) Exp Brain Res 114:500-506.
Winter (1991) *The Biomechanics and Motor Control of Human Gait: Normal, Elderly and Pathological.* Waterloo Biomechanics.

ACKNOWLEDGEMENTS

Hyperthermia Treatment of Breast Tumors Applying Ultrasonic Waves

S. Behnia[1], F. Ghalichi[3], E. Sadigh Rad[1], and A. Bonabi[1]

[1]Department of Physics, IAU, Ourmia-Iran, s_behnia@iaushab.ac.ir & sohrab_behnia@yahoo.com .
[3]Department of Biomechanical Engineering, Sahand University of Technology, Tabriz-Iran.

INTODUCTION

The heating effect of the ultrasound is used in therapeutical applications such as hyperthermia treatment and ultrasound surgery. The advantages of the ultrasound therapy are that the heating is non-invasive, there are no side effects and ultrasound exposure can be focused [1,2]. Ultrasound hyperthermia involves higher acoustic intensity with shorter application time during which temperatures as high as 45-60 °C are achieved. The size of the lesions is determined by the wavelength, the configuration of the focal spots, and the applied energy of the treatment. Therefore, the ultrasound applicator design is a critical step in the treatment process.

Meanwhile it should be noticed that high power ultrasound phased arrays have potential in several therapeutic applications. These arrays can increase the focal necrosis volume through multiple focus patterns and electronically steer foci to reduce the reliance on mechanical positioning systems. Direct control of heating process is advantageous in reducing the spatial-peak temporal-peak intensity required to produce the desired time-average heating pattern. This might be necessary to avoid certain non-linear phenomena associated with high-intensity ultrasound.

MTHODS

In this study our approach to solving the linear acoustic pressure equation is to use Galerkin finite element method (FEM) in the spatial domain, combined with finite difference approximations of the temporal derivatives. Considering the biological characteristics of breast and boundary conditions of the problem, the most suitable transducer has been designed which focuses the energy in a focal zone in a period less than tissues' vibration period (ms), and enables temperature rising up to 45 °C to destroy cancerous tissue. A thermal model of the tumor and surrounding tissue is obtained by using the FEM to approximate the BHTE, in which the temperature, T, at any location in a volume of interest satisfies the partial differential equation – BHTE-.

RESULTS AND DISCUSSION

The designed transducer is made of piezo-electric cells containing 192 square elements with 7 mm long sides. These elements are mounted on 8 square modules with sides 40 mm long. The modules are mounted on a superstructure, which direct them towards a geometric center 40 mm from the front of the array. The influence of various methods of distribution of the elements of the surface of the spherical array on the distributions of thermal sources and temperatures in breast tissues is investigated. For theoretical modeling of heating process, the problem is divided into two parts. In the first part, the acoustic field and the corresponding field of thermal sources are modeled. For this purpose, a phased array is considered: having the radius of curvature 30 mm, operating frequency ν=410 KHz and the number of elements is 192. In the second part the temperature changes and cancerous tissues' destruction are modeled. For the purpose of temperature rise and high amount of energy absorption, frequency is a dominant point. Using a range of frequency below 1 MHz mostly the frequencies between 410-600 KHz makes the temperature rise up to the desired amount in hyperthermia treatment.
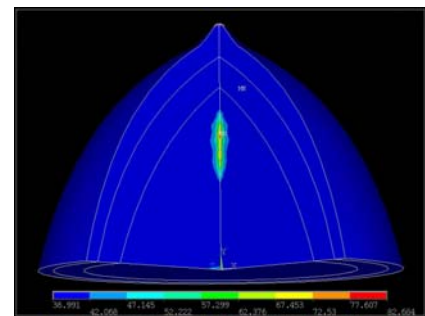
Spatial temperature distribution
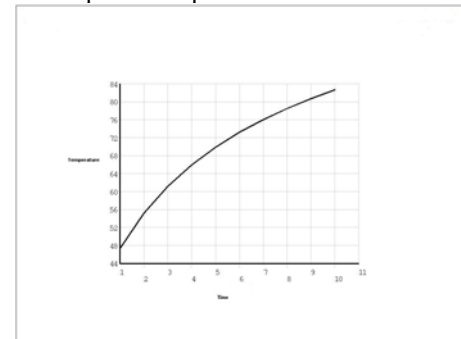
Temperature distribution due to time

SUMMARY

In this paper a brief study of breast physiology and clinical background of breast cancer, ultrasound therapy, mathematical models for ultrasound therapy, and at last results out of simulations have been presented to destroy the tumors of breast a critical cancer prevalent among women. The presented results were tested with numerical simulations in 3D. The mathematical models which are used for ultrasound therapy modeling discusses wave field and thermal therapy modeling. The wave field is modeled using acoustic pressure equation using FEM. Thermal treatment process modeling has been done using Pennes' bioheat transfer equation. Temperature distribution and the process of temperature rise in the focal region in relation with time is presented.

REFERENCES

1. K. Hynynen. *Focused Ultrasound Surgery Guided by MRI*, P.62, (1997), Science & Medicine.
2. G. ter Harr. *Acoustic Surgery,* P.29, (2001), Physics Today.

FINITE ELEMENT SIMULATION OF STENT IMPLANTATION IN A MULTI-LAYER ARTERY MODEL

Sebastien Delorme[1], Denis Laroche[1], Gerhard Holzapfel[2], Michael Stadler[2], Jean Buithieu[3], and Robert DiRaddo[1]

[1]Industrial Materials Institute (IMI), Boucherville, QC, Canada, sebastien.delorme@cnrc-nrc.gc.ca
[2]Graz University of Technology, Graz, Austria
[3]McGill University Health Center, Montreal, QC, Canada

INTRODUCTION

Percutaneous Transluminal Coronary Angioplasty (PTCA) consists of deploying a polymer balloon, with or without a metallic stent, at a controlled pressure until it contacts, deforms and unblocks a stenosed artery. PTCA induce vascular wall fractures or dissections, and achieves apparent luminal enlargement by a combination of plaque compression, plaque redistribution and vascular wall expansion, depending on the original composition of the atherosclerotic lesion.

The numerical prediction of luminal area and vascular wall injury for an angioplasty on specific high-risk patients could help select a balloon size, stent type and balloon inflation pressure that would minimize vascular injury and reduce the risk of clinical complications, such as restenosis. A finite element model has been developed to predict deformation and stresses in an homegeneous artery during balloon angioplasty (Laroche 2003, Delorme 2004). The goal of this study is to demonstrate the feasibility of the approach for stent implantation in a layer-specific artery.

METHODS

A finite element modeling software developed at IMI for the analysis of large deformations of soft materials was improved to solve angioplasty mechanics. One of the most important improvement to the software was the capability to properly model the contact and slip between deformable bodies using a slave-node/master-surface technique.

An artery geometrical model (Holzapfel 2002) was obtained from high-resolution magnetic resonance imaging of a human artery. Seven distinct layers were traced on the scans, correlated with histological analysis, and meshed in 3D with 8-node hexahedrons (Figure 1). A stent similar to a commercial type and shortened to fit the artery was modeled in 3D and meshed with 8-node hexahedrons.
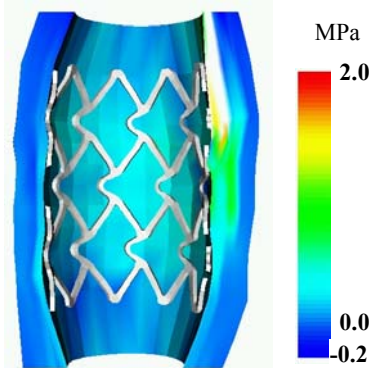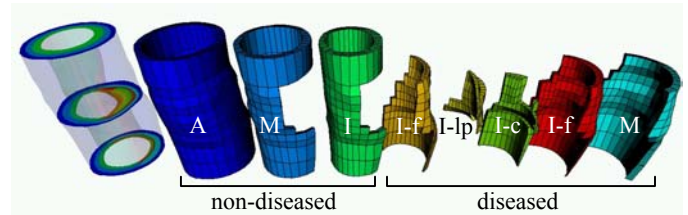

Figure 1: Exploded view of the multi-layer geometrical model of an artery. A: adventita; M: media; I: intima; f: fibrous; lp: lipid pool; c: calcification.

The stent and artery materials were considered incompressible and were modeled as hyperelastic materials with the two-parameter *Mooney-Rivlin* constitutive equation. The Mooney-Rivlin parameter values for the stent, the artery and the plaque components were calculated from published shear moduli (Holzapfel 2002).

A gradually increasing pressure was applied on the inner surface of the stent. The nodes at the bottom and top of the artery were fixed.

RESULTS AND CONCLUSION

The deformed meshes at the end of simulation of stent deployment are represented in Figures 2 and 3. Stretch ratios up to 1.6 and stresses higher than failure limits were predicted in some regions.

The presented finite element approach is capable of predicting artery deformations and stresses during stent implantation. Further work in underway to combine folded balloon, stent and artery in one single simulation.

REFERENCES

Delorme, S. et al (2004) *Annual Technical Conference (ANTEC) of the Society of Plastic Engineers*, Chicago, IL.
Holzapfel, G.A. et al. (2002) *J Biomed Eng,* **30**, 753-767.
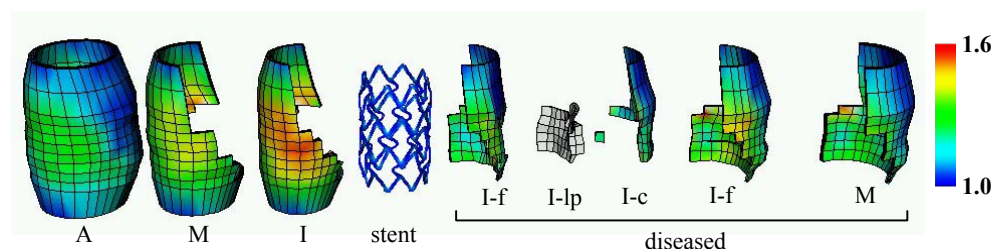Laroche, D. et al (2003) *ASM Materials & Processes for Medical Devices Conference*, Anaheim, CA.

Figure 2: Distribution of principal stresses.

Figure 3: Exploded view of the distribution of stretch ratios (λ) in the principal direction (except for lipid pool).

3D Characterization of the wall Shear Stress in a Stented Artery Using MicroPIV and CFD

Isam Faik[1], Rosaire Mongrain[1,2], Olivier Bertrand[3]

[1]Mechanical Engineering Department, McGill University, Montreal, QC, Canada
[2]Montreal Heart Institute, Montreal, QC, Canada
[3]Quebec Heart Institute, Quebec, QC, Canada

Background: Stenting is becoming the major interventional cardiology procedure worldwide. However restenosis remains a major limitation to the effectiveness of stents. Non- physiological values of wall shear stress (WSS) are considered by some groups as a potential factor in the development of in-stent restenosis. The characterization of WSS and of flow patterns in a stented artery would therefore be necessary for a good understanding of the phenomenon.

Methods: This study uses numerical and in-vitro experimental tools to characterize the wall shear stress in a stented artery and compare the results with available clinical data. We carry out a numerical analysis on the 3D model of an experimental coronary stent using Computational Fluid Dynamics (FIDAP). A coronary flow waveform is used to establish flow pulsatility. We then use microscopic particle image velocimetry (MicroPIV) to obtain the velocity field for a transparent blood analog flowing through a scale up silicone model of the stent ($\times$12.5) and then deduce the shear stress distribution.

Results: 3D simulations of the stent allow us to investigate the global WSS distribution that cannot be obtained by simple 2D analyses. This is especially true for stents with complex shapes and for the description of the circumferential intra-struts WSS distribution (Fig 1).
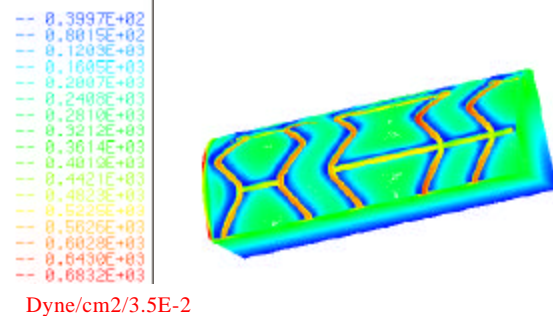

Dyne/cm2/3.5E-2

Figure 1: Wall Shear Stress distribution in a stented artery

We notice relatively high shear stress values at the struts (24.5dyne/cm^2) adjacent to a relatively low shear level in between the struts(1.4 dyne/cm^2). This proximity of alternating shear stress levels could be involved in the pathogenesis.

References:

1- Frank, A. O., P. W. Walsh, et al. (2002). "Computational fluid dynamics and stent design." Artif Organs 26(7): 614-21

2- LaDisa, J. F., L. E. Olson, et al. (2004). "Stent Design Properties and Deployment Ratio Influence Indices of Wall Shear Stress: A 3d Computational Fluid Dynamics Investigation within a Normal Artery." J Appl Physiol

3- Stone, P. H., A. U. Coskun, et al. (2003). "Effect of endothelial shear stress on the progression of coronary artery disease, vascular remodeling, and in-stent restenosis in humans: in vivo 6-month follow-up study." Circulation **108**(4): 438-44

4- Benard, N., D. Coisne, et al. (2003). "Experimental study of laminar blood flow through an artery treated by a stent implantation: characterisation of intra-stent wall shear stress." J Biomech **36**(7): 991-8.

PERFORMANCE OF POLYMER-TISSUE CONSTRUCTS IN FUNCTIONAL TISSUE ENGINEERING

Chantal Gauvin[1], Azizeh M. Yousefi[1], Robert DiRaddo[1], and Julio Fernandes[2]

[1]Industrial Materials Institute (IMI), Boucherville, QC, Canada, chantal.gauvin@cnrc-nrc.gc.ca
[2]Department of Orthopaedics, Sacré-Coeur Hospital, Montreal, Quebec, Canada

INTRODUCTION

Articular cartilage exhibits a very limited capacity to regenerate and to repair under injury or arthritic disease. Tissue engineering approach using porous polymeric scaffolds is a novel alternative to conventional repair techniques. The scaffold provides temporary mechanical support during tissue regeneration while shaping the in-growing tissues. The overall stiffness of the polymer-tissue constructs in bone/cartilage tissue engineering can affect the tissue in-growth by altering the local mechanical environment around the cells (Guilak 2003). A modeling tool is developed to predict the stress distribution under physiological load throughout scaffolds surrounded by native tissues.

METHODS

A biphasic model (Mow 1980) was used to describe the load-bearing characteristics of cartilage. The biphasic model applies as well to scaffolds since they have a porous structure to be filled with a fluid either in a bioreactor or in a physiological environment. The transient deformation curves from mechanical testing are fitted to the biphasic model to estimate the parameters of the constitutive equation.

A finite element modeling software developed at NRC (Laroche 1999) was used to predict the stress distribution under compression for scaffold and cartilage samples. The hyperelastic Mooney-Rivlin model and the linear K-BKZ viscoelastic model were used to capture the flow-independent viscoelasticity of the scaffold and the cartilage.

RESULTS AND DISCUSSION

The stress field in a cartilage under a compressive load at equilibrium is shown in Fig. 1a. The non-homogeneity of the tissue was accounted for by assigning different material properties to different layers of cartilage, as shown in Fig. 1b. The level of deformation for the superficial zone of the cartilage is greater because of its lower Young's modulus compared to the deeper zones. This brings up the issue of designing polymeric scaffolds featuring similar variation in properties through the thickness (Hollister 2002).   Figure 2 presents a comparison between the mechanical response of a normal cartilage and a typical scaffold under a compressive strain. A much lower compressive stress field for the scaffold is because of its lower stiffness value. This implies that once the scaffold is implanted, the mechanical environment around the construct could be highly altered by the presence of scaffold. This has the potential of affecting the level of tissue in-growth.   Figure 3a shows a planar cut of the steady-state pore-fluid pressure through the thickness of the cartilage under the compressive strain. The response of the tissue in 3D is given in Fig. 3b. Since the permeability of polymeric scaffolds strongly depends on their porosity level, the pressure distribution in the implanted scaffold has the potential of perturbing the kinematics of the flow in cartilage.
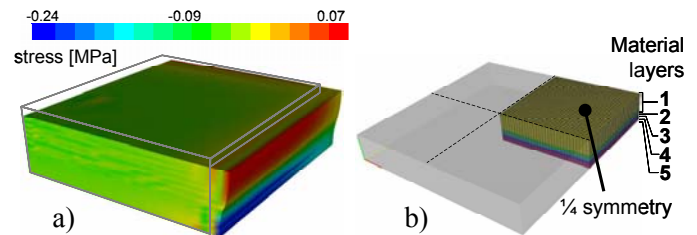

Figure 1: a) Stress distribution at equilibrium under 8% unconfined compressive strain based on Mooney-Rivlin model b) The FE mesh of a multilayer cartilage.
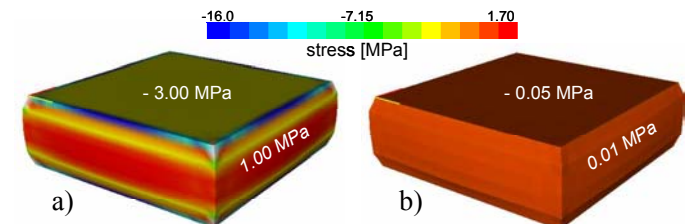

Figure 2: Comparison between the equilibrium stress distribution in a cartilage (a) and a typical scaffold (b) under 10% compressive strain based on linear K-BKZ model.
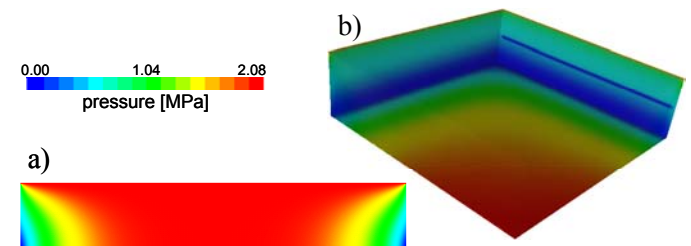

Figure 3. Steady state pore-fluid pressure through the thickness of cartilage; (a) planar cut, (b) 3D representation.

SUMMARY

A modeling tool based on biphasic model is used to predict the perturbation in the local stress environment for polymer-tissue constructs. This information in combination with a topology optimization tool will be used in our future work to improve the design of scaffolds.

REFERENCES

Guilak, F. et al. (2003). *Functional tissue engineering*, Springer, New York.
Mow, V.C. et al. (1980). *J. Biomech. Engng*., **102**, 73-84.
Laroche D. et al. (1999). *Polymer Eng. Sci*., **39**.

THE USE OF REAL-TIME FEEDBACK FOR GAIT RETRAINING IN RUNNERS

Irene McClay Davis

Physical Therapy Department, University of Delaware, Newark, DE, USA
E-mail: mcclay@udel.edu

INTRODUCTION

Running is an important component of many fitness regimens with 15-20 million Americans engaging in the sport. However, overuse injuries among runners are common. Evidence for mechanical causes of these injuries is emerging. In prospective studies, we have demonstrated that increased tibial shock places one at greater risk for tibial stress fractures (Davis et al., 2004). In addition, we have shown that runners who develop patellofemoral pain syndrome demonstrate greater hip internal rotation and adduction than healthy controls (McClay et al., 2003). If these mechanics are not altered, it is likely that the injuries will recur. One method of altering these mechanics is to retrain the runner's gait pattern such that the risk factors are reduced. Two case studies involving gait retraining will be discussed. In addition, data from an ongoing gait retraining study will be presented.

METHODS

Case Study 1

In the first case, a runner with plantar fasciitis presented with a common malalignment of excessive hip adduction and internal rotation and knee abduction (valgus). She was provided verbal feedback and visual feedback (via a mirror) twice a week for 8 weeks to reduce her hip adduction and internal rotation. An instrumented gait analysis was performed initially, at the end of 8 weeks and at 6 months post.

Case Study 2

The second case study involves a runner with anterior knee pain with similar mechanics to the first. However, with the advent of real-time motion analysis, the mirror has now been replaced with a computer monitor. Markers were placed on the segments of her lower extremity, and her hip internal rotation angle was presented on the monitor placed in front of her. She was instructed to reduce her hip internal rotation (without changing her foot position). She underwent this gait retraining twice a week for 8 weeks.

Preliminary Study on Shock Reduction

Four healthy recreational runners (age 25-35 yrs) volunteered for this pilot study. An accelerometer was attached to their right distal tibias in an anteromedial position. Subjects ran on the treadmill at their own comfortable speed (range 6-7 mph) for 5 minutes. A monitor, placed in front of the treadmill, provided a real-time visual display of their shock pattern as the subject ran. Subjects were instructed to reduce the size of the acceleration peaks by "running more softly". They were allowed to practice this new pattern with the continuous visual feedback from the tibial shock curve for a period of 5 minutes, after which a second 5-second trial was again collected.

RESULTS AND DISCUSSION

Case Study 1

After 8 weeks of training, the patient was able to reduce her hip adduction and internal rotation as well as knee abduction. These alterations led to a resolution of her symptoms, which would return if she resumed her original mechanics. In addition, she was able to maintain most of the changes after 6 months of termination of the feedback training.

Case Study 2

Following 8 weeks of training, this runner reduced her hip internal rotation. Two years later, she remains pain free.

Figure 3: Hip and knee joint position curves prior to, and following gait re-training.
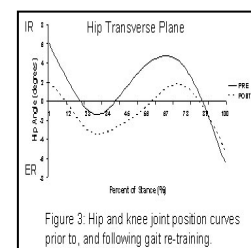
Pre (left) and post (right) training Hip IR – note the reduction following gait retraining.

Preliminary Study on Shock Reduction

These preliminary data demonstrate that runners are able to reduce their tibial shock by an average of 30% with a very brief training session.

Table 1: Baseline and Post-training tibial shock values (* p=0.08).

Subject	Baseline (g)	Post Training (g)	Reduction (%)
1	4.51 ± 0.89	3.92 ± 0.67	13.22
2	3.71 ± 0.73	3.44 ± 0.43	7.19
3	4.77 ± 0.26	2.64 ± 1.67	44.54
4	9.41 ± 0.48	4.05 ± 1.27	57.00
Mean	**5.60 ± 2.58**	**3.51 ± 0.63 ***	**30.49**

CONCLUSIONS

Based on the results of these case studies and preliminary data, it appears that runners are able to alter their mechanics such that they reduce their risk of injury. Current studies are ongoing to further explore the ability of real-time feedback to alter abnormal running mechanics. Prospective studies are needed to determine whether these changes result in a reduction of running-related injuries.

REFERENCES

Davis et al. (2004) Proceedings of ACSM, Indianapolis, IN.
McClay et al. (2003) Proceedings of ASB, Toledo, OH.

THE INFLUENCE OF SOCCER CLEAT DESIGN ON KNEE JOINT MOMENTS

Darren J. Stefanyshyn, Joong-Sook Lee*, Sang-Kyoon Park and Luke Savage

Human Performance Laboratory, Faculty of Kinesiology, University of Calgary, Calgary, Canada, darren@kin.ucalgary.ca
*Division of Physical Education, Silla University, Busan, Korea

INTRODUCTION

A few epidemiological studies have linked lower extremity injuries to high rotational resistance between shoe and surface. Torg et al. (1971, 1974) found that injuries in American football were more common under conditions where there was high rotational traction between the surface and shoe. A more recent prospective study (Lambson et al., 1996) on high school players reaffirmed the findings of Torg et al. They found a significantly higher Anterior Cruciate Ligament (ACL) injury rate with shoes that had higher torsional resistance. These studies suggest that shoe cleat designs with high rotational friction between shoe and surface are associated with knee injuries. However, the actual mechanism of how traction affects knee joint injury remains unknown. We hypothesized that traction of the shoe and surface influences the joint moments and loads at the knee. Therefore, the purpose of this study was to determine how soccer cleats of different designs and traction influence knee joint moments.

METHODS

Twelve recreational soccer players were recruited for this experiment. All subjects performed a running v-cut with four different shoes. The v-cuts were performed by running straight ahead and then cutting at a 45° angle. All trials were performed on a sample of infilled artificial turf and were conducted at 4.0 m/s. The four different footwear conditions tested (Fig. 1) were a standard adidas running shoe and three different soccer cleats.

Fig. 1   Starting at top left and moving clockwise: Adidas Nova running shoe, Adidas Copa Soccer Cleats, Adidas World Cup Soccer Cleats and Adidas Trx Soccer Cleats.

Eight trials per condition were collected with reflective markers place on the right leg of the subjects. Eight high-speed cameras (240 Hz) were used to record kinematic data. Ground reaction forces were collected by a Kistler force plate (2400 Hz). Joint moments were calculated with inverse dynamics. A repeated measures ANOVA was used to compare the conditions with a level of significance set at $\alpha < 0.05$.

RESULTS AND DISCUSSION

There were no significant differences between shoes for the knee extension moments. However, the Copa and World Cup cleats had significantly higher knee abduction and external rotation moments than the Nova running shoes (Fig. 2). The Copa cleats had significantly higher external rotation moments than the Trx Cleats.
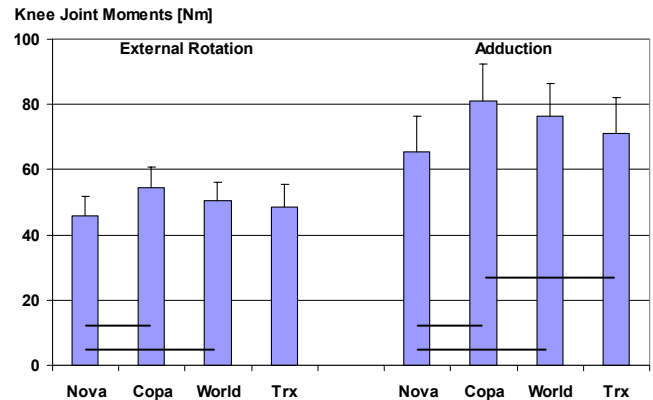

Fig 2.   Knee joint moments for the different shoes (average and standard error). The horizontal lines indicate significant differences between conditions.

Knee joint loading in the transverse and frontal plane have been proposed to be associated with running injuries (Stefanyshyn et al., 1999) such as patellofemoral pain syndrome. Higher knee joint moments with the traditional soccer cleats (Copa and World Cup) may lead to higher local stress and overuse injuries in the knee joint. Also, the higher moments are likely closer to the ultimate limits of structures like the ACL. Thus, there is less room for error from unexpected perturbations during the movement, increasing the potential for acute injuries. The actual characteristics of the footwear (e.g. rotational and translational traction, stability, etc.) that result in these differences at the knee joint are still being investigated.

SUMMARY

Cleat design influences knee joint moments during a v-cut. These influences could affect knee injury rates in soccer and may be due to different friction characteristics of the footwear.

REFERENCES

Torg, J.S et al. (1971) *Research Quarterly*, **42**, 203-211.
Torg, J.S. et al. (1974) *Journal of Sports Medicine*, **2**, 261-269.
Lambson, R.B. et al. (1996) *Am. J. Sports Med*., **24,** 155-159.
Stefanyshyn, D. et al. (1999) *Proc. 4th Foot Biom. Symp.,* 86-87.

CYCLING BIOMECHANICS – WHERE DO WE GO FROM HERE?

Graham E. Caldwell

Department of Exercise Science, University of Massachusetts, Amherst, MA, USA, gc@excsci.umass.edu

INTRODUCTION

To effect forward motion, cyclists must generate propulsive forces at the road / tire interface while overcoming resistance from wind, friction and, when going uphill, gravity. Cyclists use their powerful leg muscles to apply force on the pedals; the chain and freewheel translate the resulting crank torque into wheel motion to generate the propulsive forces. From previous studies, the kinematics of lower extremity motion and associated muscle activity patterns are well known, and instrumented pedals have been used to measure applied pedal forces and crank torque throughout the 360° of crank rotation. The contributions of specific joints have been delineated with joint moments and powers computed through inverse dynamics, while individual muscle forces have been estimated from musculoskeletal models. Despite this wealth of data, there are still many unanswered questions concerning cycling performance, strategy, and training. In this presentation, the importance of interpreting experimental data within the context of mechanical events underlying the cycling performance is emphasized. To that end, an example regarding uphill cycling strategy is presented, followed by a list of issues that should be addressed in future cycling studies.

UPHILL CYCLING – WHY STAND?

Why do cyclists choose to stand when pedaling up a steep grade? In a series of papers we have described the kinematic, kinetic and EMG changes that occur when cyclists alter their posture from seated to standing while climbing a hill (Caldwell et al., 1998, 1999; Li & Caldwell, 1998). Yet it is only when these data are viewed within the context of a *performance goal* that we are able to appreciate how these changes are useful to the cyclist (Caldwell et al., 2000). When climbing a hill, the goal is to apply sufficient positive crank torque to overcome the gravitational load acting to reduce forward velocity. For geometrical and anatomical reasons, crank torque varies considerably as each foot spins through the crank cycle from its highest position (0°) to its lowest (180°) and back to 0° (360°). In seated cycling, the highest crank torque occurs with one foot pushing downward ~90° and the other pulling upward ~270° (Fig. 1). In contrast, with the feet near 0° and 180° less torque is produced, as the rider is in poor position to apply forces in the forward and backward directions necessary for positive crank torque. In this weak position, the rider may not be able to apply the minimum torque needed to maintain forward velocity (Fig. 1) and continue climbing. The minimum required torque increases with steeper uphill grades. Failure to maintain sufficient velocity just prior to the 0°/180° position can result in inadvertent weight bearing on the upper pedal, and therefore zero torque due to the unidirectional freewheel mechanism.

When the cyclist stands, the crank torque profile displays a greater peak but a more exaggerated minimum, both occurring later in the crank cycle (Fig. 1). This altered torque pattern allows greater acceleration between 90° and 180° before the torque falls below the required minimum and slowing begins. The weak point is shifted to *after* the 0°/180° position, when the rider is in a better position to apply propulsive torque. While standing in this position, merely leaning on the front pedal that just passed 0° can generate propulsive torque, while strong flexion of the extended back leg pulls the other pedal upward to augment the positive torque. Although the minimum applied torque is actually less than when seated, standing provides a means of overcoming the weak point that diminishes forward velocity within the crank torque cycle. In addition, joint moments and muscle activity at the ankle and knee are modified when standing, indicating that an intermittent seated/standing strategy might alter muscular loading to offset fatigue while on long climbs.
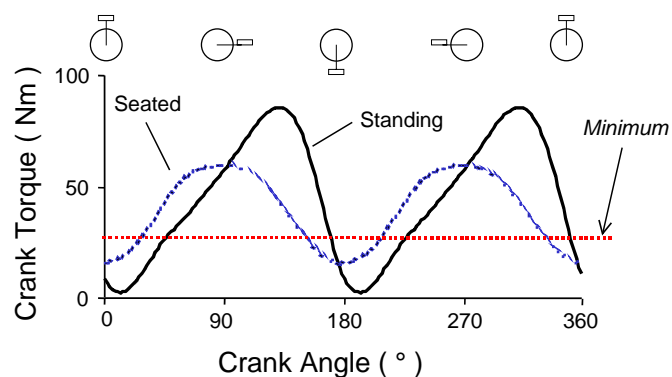

Fig 1. Seated and standing uphill crank torque (both feet). *Minimum* refers to the minimum torque required to counteract resistive forces; this minimum changes with uphill grade.

FUTURE DIRECTIONS

One of the most important future developments in cycling biomechanics will be the measurement of kinematics, kinetics and muscle activities in the field (on road) rather than in the laboratory, permitting verification of existing laboratory data. This will also allow new studies that are impossible within the lab, including investigations of multi-rider pacing strategies, the effect of rider position within a peleton, and influence of course elevation profile on fatigue and endurance. Other areas of interest include the muscular coordination changes that occur as cyclists learn to control the direction of their pedal force vector, the role of 3D kinematics and kinetics in knee injuries, and effects of bilateral asymmetry. Finally, as musculoskeletal simulations of cycling become more prevalent, it is important to assess the effect of individual model parameters on the predicted individual muscle forces.

REFERENCES

Caldwell, G.E. et al. (1998). *J. Appl. Biomech.* **14**, 245-259.
Caldwell, G.E. et al. (1999). *J. Appl. Biomech.* **15**, 166-181.
Caldwell, G.E. et al. (2000). In: *Energetics of Human Activity*, W.A. Sparrow (ed.), Human Kinetics, pp 66-95.
Li, L. & Caldwell, G.E. (1998). *J. Appl. Physiol.* **85**, 927-934.

TOUCH SENSITIVITY THRESHOLDS ACROSS THE DORSAL AND PLANTAR SURFACES OF HUMAN FEET

Ewald M. Hennig, Thorsten Beierle, Thorsten Sterzing

Biomechanics Laboratory, University of Duisburg – Essen, Germany, ewald.hennig@uni-essen.de

INTRODUCTION
Various mechanoreceptors in the skin with slow, medium and fast adaptation speeds are able to detect displacement, velocity and acceleration of the skin surface. The detection of such mechanical stimuli by the foot may be an important factor for balance control during standing and walking for healthy subjects [1] and patients [2]. It has previously been shown that touch threshold sensitivity values increase with age [3] and that women generally show lower threshold values as compared to men [3]. Using "Semmes Weinstein" monofilaments Jeng et al. studied 14 plantar, 3 dorsal, and each 1 lateral and medial heel locations across the foot [4]. The purpose of the present study was to provide a more detailed touch threshold sensitivity map of the feet in healthy women and men.

METHODS
Touch sensitivity thresholds were determined by using "Semmes Weinstein" monofilaments. 24 women and 24 men between 20 and 30 years participated in this study. The order of the anatomical sites was randomised between subjects and an infrared lamp was used to maintain constant foot temperature. Including zero force stimuli, threshold detection was recognized for an anatomical site if four out of five right answers were given [5].

P1	heel	D6	dorsal metatarsal head III
P2	arch medial	D7	dorsal metatarsal head V
P3	arch intermedius	D8	dorsal distal phalanx I
P4	arch lateral	D9	dorsal medial phalanx III
P5	metatarsal head I	D10	dorsal medial phalanx V
P6	metatarsal head III	M1	medial malleolus
P7	metatarsal head V	M2	medial calcaneus
P8	hallux	M3	base of os naviculare
P9	distal phalanx III	M4	medial base of metatarsus I
P10	distal phalanx V	M5	medial aspect of metatarsal head I
D1	articulatio talocruralis	L1	lateral malleolus
D2	dorsal base of metatarsus I	L2	lateral calcaneus
D3	dorsal base of metatarsus III	L3	lateral base of metatarsus V
D4	dorsal base of metatarsus V	L4	lateral aspect of metatarsal head V
D5	dorsal metatarsal head I	A1	achilles tendon

RESULTS AND DISCUSSION
Using a t-test across the measurements of all anatomical sites women showed significantly (p<0.01) lower sensitivity threshold levels as compared to the men. However, the multiple site comparison ANOVA revealed no statistical gender difference. Therefore, figure 1 depicts the different sensitivity thresholds across all 48 subjects for the various anatomical sites. Large threshold differences (p<0.01) are apparent between different locations. The least sensitive sites are located under the heel, above the Achilles tendon, medial and lateral malleoli and above the articulatio talocruralis. The most sensitive skin locations are found under the medial arch and the distal phalanges III and V. The dorsal toes and the medial and lateral calcaneus also demonstrate higher sensitivities. From the plantar surface measurement locations it appears, that those regions, primarily loaded during standing and walking, are the least sensitive for touch detection. However, generally these locations also have an increased callous built-up. Callous formation above the skin will reduce the peak pressure under the filament contact area and may thus reduce mechanical input to the skin receptors.

When dividing the foot anatomically in plantar, dorsal, medial and lateral regions, similar threshold values are apparent. Individual comparisons only show significantly higher threshold values (p<0.05) of the lateral foot against the medial and dorsal foot regions.
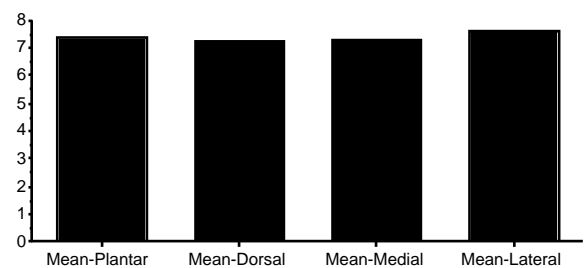

Figure 2: Mean thresholds across foot areas (n=48 subjects)

For balance control the foot as a sensory organ has received increasingly attention in recent years. Therefore, a sensitivity map of the foot, as provided by this research, may be used in manifold applications.

REFERENCES
[1] Perry, S.D. et al (2000). Brain Res. 877, 401-406.
[2] Prätorius, B. et al (2003). Neurosci. Letters 346, 173 -176.
[3] Thornbury, J.M. (1981). J. Gerontology, 36, 34-39.
[4] Jeng, C. et al (2000). Foot & Ankle Int., 6, 501-504.
[5] Mueller, M.J. et al (1996). Physical Therapy, 1, 68-71.

ACKNOWLEDGEMENTS

Figure 1: Mean touch threshold values, as calculated from the recorded filament numbers (1 = least, 20 = max. filament strength)
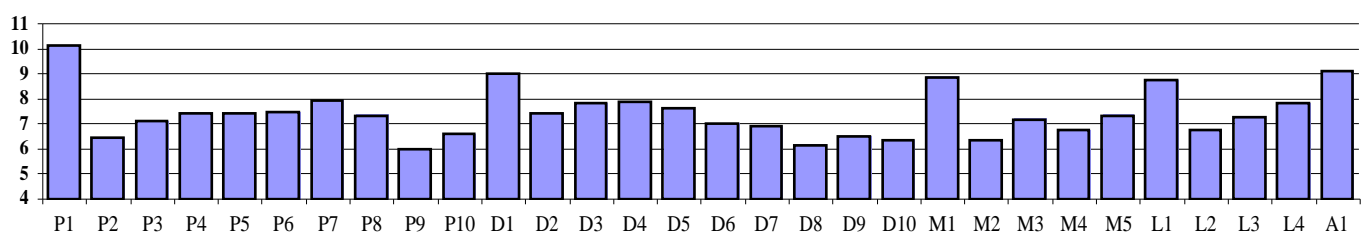
GALVANIC VESTIBULAR STIMULATION AFFECTS WHOLE-BODY CENTER OF MASS AND VISUAL-VESTIBULAR SIGNAL INTEGRATION DURING PERTURBED LOCOMOTION

Charles Cejka and Aftab E. Patla

Department of Kinesiology, University of Waterloo, Waterloo, Canada, ccejka@ahsmail.uwaterloo.ca

INTRODUCTION

While walking, lateral stability is maintained through a visual-vestibular feedback mechanism where closing the eyes induces a destabilizing effect in the lateral direction (Bauby and Kuo, 2000). Galvanic vestibular stimulation (GVS) is an effective method of manipulating vestibular afferent input and evokes a lateral postural lean in the direction of the anodal electrode. Traditionally, vision has been thought to suppress vestibular input and accordingly, most studies in the perturbation literature have used GVS with the eyes closed (Hlavacka et al, 1999; Scinicariello et al, 2001). Another feature of these studies is that they focused on standing posture. One of the purposes of the present study was to examine the visual-vestibular interaction during perturbed locomotion with unobstructed vision.

Moreover, vestibular input has been argued to affect trunk movement but not whole-body center of mass (COM) (Horak and Hlavacka, 2001; Mergner and Rosemeier, 1998). Once again, these studies focused on standing posture. Therefore, a second purpose of this study was to determine whether GVS has any effect on whole-body posture during perturbed locomotion.

METHODS

Six healthy, young subjects walked forward with the eyes open towards a target at a self-selected cadence over a 6-m travel path. In 20% of trials, a 200 N mechanical perturbation (P) was elicited onto the left shoulder of the participant during right single support. GVS (1.0 mA) was administered concurrently with some of these perturbations for 2 seconds with the anode electrode either behind the left (anLt) or right (anRt) mastoid process. In the remaining 80% of trials, no mechanical perturbation was present but some of these trials involved GVS with the anode electrode either behind the left or right mastoid process. All trials were completely randomized to discourage the use of adaptive strategies by the participants. Foot markers were used to monitor foot placement while shoulder and hip markers were used to estimate lateral trunk COM movement.

RESULTS AND DISCUSSION

A significant directional effect of GVS on peak lateral trunk COM displacement was observed during perturbed locomotion but not for unperturbed locomotion. When the anodal current was to the left and opposed the rightward mechanical perturbation, the magnitude of lateral trunk deviation was reduced. In contrast, lateral trunk deviation was increased when the anodal current was to the right and in the same direction as the perturbation. Interestingly, GVS had a similar directional effect on step width (see Figure 1). During perturbed locomotion, the degree of foot crossover was greatest when the GVS-induced postural sway was in the same direction as the perturbation (i.e., anRt) and lowest when GVS and the perturbation were in opposition (i.e., anLt).
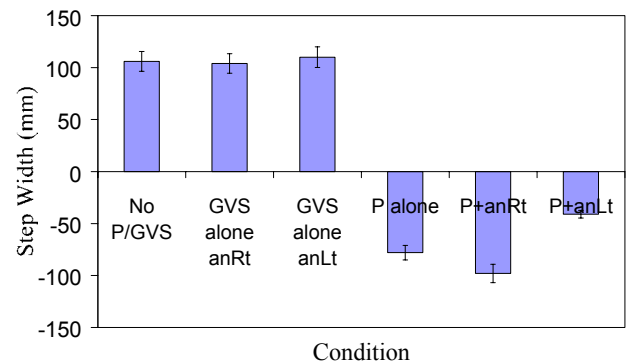

Figure 1: Peak step width (-ve values = foot crossover)

Since GVS affected foot placement in addition to trunk movement, it can be inferred that vestibular input is used to control whole-body COM and not just trunk COM during more dynamic tasks such as walking. Therefore, the role of vestibular input may differ between standing posture and locomotion. Furthermore, sensory input seems to undergo a re-weighting such that vision no longer suppresses vestibular input when stability becomes threatened. When encountering an unexpected perturbation, vestibular signals become important in stabilizing the posture. However, during unperturbed locomotion, where stability is less threatened, vision plays a more dominant role in postural control.

SUMMARY

The role of vestibular input in locomotion differs from its role in static tasks such as stance. While walking, vestibular input is not limited to the control of trunk movement; rather it is involved in more global control of whole-body posture. In addition, signals from vestibular afferents become more influential when the risk of falling is elevated. In novel tasks, vision is clearly the sensory modality of greatest influence.

REFERENCES

Bauby C.E. and Kuo A.D. (2000). *J. Biomech*, **33**, 1433-1440.
Hlavacka F. et al (1999). *Brain Res*, **821**, 8-16.
Horak F.B. and Hlavacka F. (2001). *J. Neurophysiol*, **86**, 575-585.
Mergner T. and Rosemeier T. (1998). *Brain Res. Rev*, **28**, 118-135.
Scinicariello A.P. et al (2001). *Biol. Cybern*, **84**, 475-480.

EFFECT OF DYNAMIC ANKLE JOINT STIFFNESS ON POSTURAL STABILITY

P. S. Schneider[1], J. M.Wakeling[2], R. F. Zernicke[1]

[1]Human Performance Laboratory, University of Calgary, Calgary, Canada, prism@kin.ucalgary.ca
[2] Department of Basic Veterinary Sciences, The Royal Veterinary College, London, United Kingdom

INTRODUCTION

Ankle-foot orthotics (AFO) are externally applied orthopaedic devices that provide support for foot-drop or ankle instability associated with neuromuscular disorders. Currently, AFOs are either articulated (moveable) or rigid (ankle is locked at a specific ankle joint angle).

Dynamic stiffness is a relation between joint position and moment acting about the joint. Dynamic joint stiffness is calculated as the slope of the joint angle vs. moment plot, and stiffness is an important constraint on the motor control system as it affects the generation of voluntary movements and the displacement resulting from an external perturbation (Hunter & Kearney, 1982). Understanding joint stiffness is essential to design of orthoses and the quantitative evaluation of neuromuscular diseases (Davis & DeLuca, 1995). In the past, ankle joint stiffness was varied by external stimuli and applied external moments (Gottlieb & Agarwal, 1978), but joint stiffness has not been examined experimentally or dynamically with the use of AFOs in human static or dynamic balance. The effects of AFO stiffness on joint kinematics, centre of pressure (COP) excursion, muscular co-contraction, and mechanical joint energetics were the focus of this study.

METHODS

Bilateral AFOs were instrumented with hydraulic disc brakes to allow for adjustable AFO stiffness, which allowed for varied external resistance of ankle motion, graded from fixed to freely moving. The study design was prospective, randomized, and consisted of six adult males.

Three-dimensional (3D) kinematics were acquired using bilateral lower-extremity reflective marker placement (3/segment) and an 8-camera, high-speed motion analysis system (Motion Analysis Corp, Santa Rosa, CA; EVA© software). Force plate (Kistler, 9286; 2400 Hz), electromyographic (Biovision, Germany; 2400 Hz), and video (240 Hz) data were collected during 3 successful 30-s standing trials for each AFO stiffness condition: shoes only (Shod), shod with rigid AFOs (Rigid), shod with articulated AFOs (Art), and shod with intermediate AFO stiffness (Inter).

Three dimensional knee and ankle joint kinematics (joint angle and angular velocity) and kinetics (joint moments and centre of pressure) (Kintrak© software, Motion Analysis Corp, Santa Rosa, CA) were calculated. Standing ankle and knee joint stiffnesses were calculated as the slope of joint angle-moment curves. Ankle and knee mechanical powers were calculated as the product of the resultant joint moment and joint angular velocity. Multivariate analysis of variance with a *post-hoc* test ($\alpha = 0.05$) revealed significant differences.

RESULTS AND DISCUSSION

During standing, the articulated AFO induced the COP to move posteriorly in 5 of the 6 subjects ($p \leq 0.05$ with non-parametric Sign Test). Negligible change occurred in the medial-lateral

COP excursion between Shod and AFO conditions. Mean ankle angle (Fig.1) was significantly different between the Rigid and Shod conditions for 5 of 6 subjects. All other AFO conditions were significantly different than the Shod condition for 4 subjects. Significant differences in mean knee angle (Fig.1) were found between the Rigid and Shod conditions and Art and Shod conditions for 5 subjects. There were no statistically significant differences in mean ankle or knee moments or mechanical joint power between AFO and Shod conditions across all subjects.
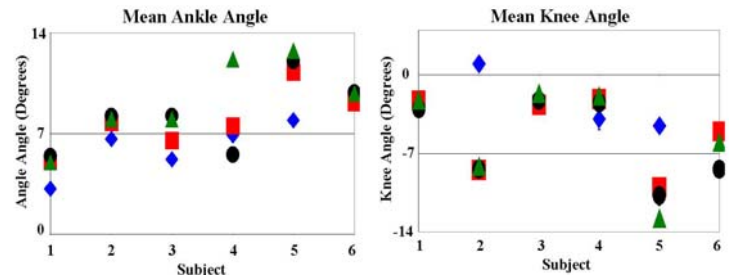

Fig. 1 Mean (±SD) ankle angle (left) and mean knee angle (right) for subjects across shod (♦), articulated AFO (■) intermediate stiffness AFO (●) and rigid AFO (▲) conditions, where positive values indicated dorisflexion angle in excess of 90˚ and knee extension angles in excess of 180˚.

Differences were observed in the mean ankle and knee joint stiffnesses (Fig.2), however, there were no significant differences when the means for all subjects were compared.
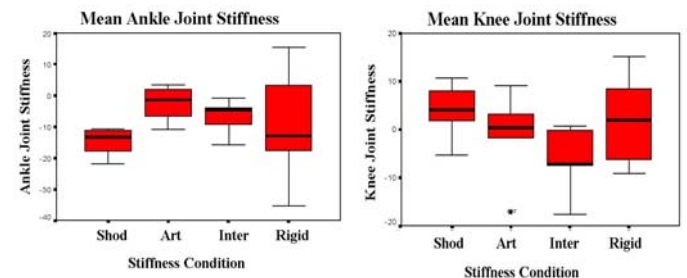

Fig. 2 Mean (±SD) ankle (left) and knee (right) joint stiffness for all subjects across all conditions.

CLINICAL RELEVANCE

Results from this study provide an original contribution to the understanding of how AFO prescription may affect postural control. Dynamic joint stiffness analysis with the use of AFO may provide insight into dynamic motor control mechanisms and joint dynamics that characterize neuromuscular diseases.

REFERENCES

Hunter, I. & Kearney, R. (1982) *J Biomech,* **15**, 747-52.
Davis, R. & DeLuca, P. (1995) *Gait & Posture,* **3**, 79-80.
Gottlieb, G. & Agarwal, G. (1978) *J Biomech,* **11**, 177-81.

ACKNOWLEDGMENTS

POSTURE OF WOMEN STANDING ON AN INCLINE

Fabiola Goncalves[a], Pei Lai Cheng[b], Andy Leger[a], Genevieve A Dumas[b]

[a]School of Rehabilitation Therapy, [b]Department of Mechanical Engineering, Queen's University, Kingston, Ontario, Canada

INTRODUCTION

Standing is the most common posture that affects our daily living. Changes in standing posture could affect the load on the spine and major joints or even cause back pain (Lee et al., 2001) and musculoskeletal injures. Standing on an incline (simulating high heeled shoes) is a typical alternative standing posture commonly seen in women. Previous studies (Bendix et al., 1984; Franklin et al., 1995, Snow & Williams, 1994) focused on the changes of total body mass center position and curves of the lumbar spine, and reported conflicting results on whether there are significant differences between the two standing postures. There is little information available for the change of mass center position of individual body parts and the changes of relative positions and orientations between body segments. The objective of this study was to compare the postures of women standing on an incline and on flat floor, and to investigate how each body part adapted to the posture changes.

METHODS

The standing posture of the subject was recorded by using five sensors of an electromagnetic motion analysis system, MotionStar (Ascension Technologies, Burlington, VT, USA). The sensors were secured on the forehead, C7, T10, L1 and S1 using double-sided tape and elastic bands. The sensors were aligned with anatomical axes of the body segments. The motion analysis system recorded the position and orientation of each sensor relative to a reference coordinate system. Distances in anterior-posterior direction and relative orientation in the sagittal plane of the sensors on the forehead, C7, T10 and L1 with respect to S1 were determined.

Mass center positions of whole body and seventeen body parts (head, neck, upper trunk, lower trunk, upper arms, forearms, hands, thighs, shanks and feet) relative to the ankle joint in anterior-posterior direction were determined using a geometric method (Jensen, 1978). Two photographs (front view and side view) of the subject were taken for each posture simultaneously. Each segment was considered as a series of elliptical cylinders of 2cm height. A total of 25 markers were placed on the relevant anatomical landmarks to identify joint positions and lines between segments. The segment contours and joint positions were digitized from the photographs. The data between standing on a 45 degrees incline and on flat floor were compared using paired-tests.

RESULTS AND DISCUSSION

Nineteen healthy women (24.4±5.4yrs, 164.8±7.2cm, 61.5±9.3kg) without musculoskeletal or neurological problems participated in this study with written informed consent approved by the Ethics Committee of Queen's University.

The total body mass center moved about 0.7cm backward when standing on an incline compared to flat floor standing (Table 1). The change was mostly contributed by the upper body including head, neck, and trunk. Relative tilt angle between head and pelvis was significantly lower for standing on the incline (Table 2). Inclination angle of the pelvis was 3.5˚ lower for standing on the incline compared to flat floor standing, but it was only marginally significant (p=0.076).

Table 1. Mean (StD) anterior-posterior distance (cm) from mass center of body segments to the ankle joint.

	On 45˚ incline	On flat floor
Head*	6.4 (2.9)	7.7 (2.2)
Neck*	3.3 (4.2)	4.8 (2.0)
Upper trunk*	2.1 (2.1)	3.4 (1.9)
Lower trunk*	4.4 (1.5)	5.3 (1.4)
Upper arm*	-0.2 (2.2)	1.0 (2.1)
Forearm	0.4 (2.4)	1.2 (2.9)
Hand	2.0 (3.3)	2.6 (3.6)
Thigh	4.0 (1.5)	4.3 (1.5)
Shank	0.4 (1.3)	0.0 (1.1)
Foot*	2.8 (0.9)	5.0 (1.3)
Whole body*	3.4 (1.3)	4.1 (1.3)

*: significant at $p < 0.05$.

Table 2. Mean (StD) anterior-posterior distances (cm) and tilt angles (degree) between sensors on head and spine and the sensor on S1.

	On 45˚ incline	On flat floor
Head-pelvis angle*	33.4 (8.0)	36.9 (11.4)
C7-pelvis angle	14.4 (6.6)	14.7 (7.6)
T10-pelvis angle	26.6 (8.3)	28.2 (10.1)
L1-pelvis angle	28.4 (7.8)	28.4 (8.3)
Head-pelvis distance*	24.9 (3.1)	25.5 (2.9)
C7-pelvis distance	4.8 (2.5)	5.6 (2.4)
T10-pelvis distance	0.8 (1.9)	1.1 (1.8)
L1-pelvis distance	1.3 (1.3)	1.6 (1.4)

*: significant at $p < 0.05$.

The results indicate that upper body and pelvis tend to lean backward when standing on the incline with a smaller base of support. This adaptation of the upper body allows to maintain balance and to respond to the changes of total body center of mass. How skeletal muscles actively response to the posture changes need to be further investigated.

REFERENCES

Bendix T et al (1984). *Spine*, **9**, 223-227, 1984.
Franklin ME et al (1995). *J. Orthop Sport Phys*, **21**, 94-99.
Jensen RK (1996). *J. Biomech*, **29**, 251-256.
Lee GM et al (2001). *Int J Ind Ergonom*, **28**, 321-326.
Snow & Williams (1994). *Arch Phys Med Rehab*, **75**, 568-576.

POSTURAL RESPONSE FOLLOWING SELF-INITIATED PERTURBATION IN TYPE-2 DIABETIC PATIENTS AND HEALTHY ELDERLY.

Hugo Centomo[1,2], Serge Savoie[1,2], Danik Lafond[1,2] and François Prince[1,2,3]
[1] Department of Kinesiology, University of Montreal, Canada
[2] Gait and Posture Laboratory, Marie Enfant Rehabilitation Center, Montreal, Canada
[3] Department of Surgery, Faculty of Medicine, University of Montreal, Canada, hugo.centomo@umontreal.ca

INTRODUCTION

Impaired postural balance and mobility have been raised as factors that increase the risk of falls, falls-related injuries and functional dependency in elderly population (Tinetti, 1988; O'Loughlin et al., 1993). In recent years, several performance-based tests have been proposed to assess balance and functional mobility of elderly individuals. The clinical test of interest in this study is the Functional Reach (FR) test and it measures the maximal safe standing forward reach representing the clinical approximation of the margin of stability (Duncan et al., 1992). Meanwhile, in posturography, postural control is typically quantified using two main biomechanical variables: the center of pressure (COP) and the center of mass (COM). The purpose of this study is to compare healthy elderly subjects and patients with Type-2 (non-insulino dependent) diabetes mellitus in order to detect any differences in postural parameters of the FR performance.

METHODS

Seven healthy subjects (51 ± 10 years) were compared to nine type-2 diabetic patients (55 ± 9 years; Fasting blood glucose=8.4 ± 1.7mmol/l; HbA1c=0.055 ± 0.003mmol/l). The subjects were requested to stand as still as possible on a force platform and then to achieve a maximal FR. COP velocity (V_{COP}) and COP-COM amplitude were calculated during three specific periods of the FR performance: "Before", "During" and "After". Student t-test was computed on each dependant variable and a Bonferroni adjustment was used.

RESULTS AND DISCUSSION

No significant difference was found for the FR performance between the healthy elders (29.9 ± 4.1 cm) and the diabetic patients (27 ± 4.1 cm). There is no significant difference in the V_{COP} values between the diabetic group and the control group in "Before" and "During" phases of the FR task. Nevertheless, a significant difference ($p < 0.01$) for the V_{COP} "After" the FR task was found. Figure 2 shows no significant difference between the COP-COM amplitude in the "Before" and "During" phases, but the COP-COM amplitude was significantly ($p<0.01$) increased in the diabetic group compared to the control in the "After" phase.

Diabetic patients obtained similar performances in FR test compared to control subjects but they present trends of postural instability when they reach an area close to the limit of the base of support at the end of the FR task. Even with no evidence of peripheral neuropathy, diabetic subjects may increase their risk of falling during a forward reaching movement. The use of a quantitative and noninvasive technique, such as computerized dynamic posturography during a self-initiated perturbation, may help to discriminate early stage of postural instability in type-2 diabetic patients. Although the present results of FR performance and COP

postural steadiness measures are not associated with risks of falls in diabetes patients, the dynamic posturography reveals that they have problems to regain balance after a self-induced postural perturbation.
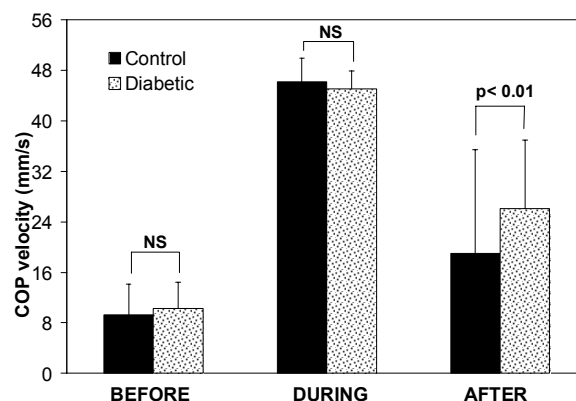

Figure 1. V_{COP} (in mm/s) during the three periods (Before, During and After) of the FR test in diabetic group (dotted) and control group (black). NS = not significant.
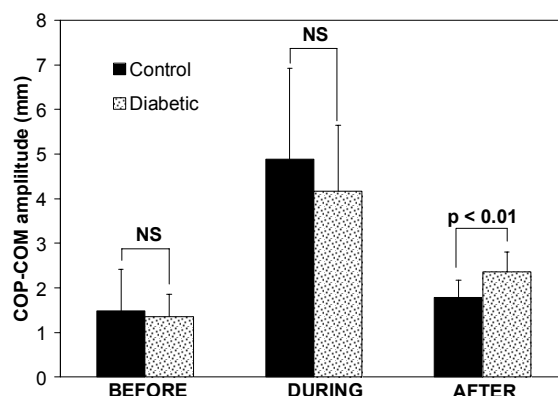

Figure 2. COP-COM (mm) amplitude during the three periods (Before, During and After) of the FR test in diabetic group (dotted) and control group (black). NS = not significant.

REFERENCES

Duncan P.W. et al (1992). *J Gerontol* **47**, M93-M98
Tinetti ME. (1988). *New Engl J Med,* **319**, 1701-1707.
O'Loughlin J.L. et al (1993). *Am J Epidemiol.* **137**, 342-54.

ACKNOWLEDGMENTS

BUILDING THE ULTIMATE BACK: A JOURNEY IN PROGRESS

Stuart M. McGill
Department of Kinesiology, University of Waterloo

INTRODUCTION

I have now recovered from the initial shock of Dr Zernicke informing me of this recognition – and am deeply appreciating the honor of it all. This presentation will tell a story directed more towards the younger folks. My professional life now consists of leading a team of graduate students in research, seeing difficult back patients referred for consult, consulting with corporations and governments on evidence-based foundations for legislation and policy, consulting with professional teams and athletes for performance enhancement, advising lawyers needing strategic guidance or testimony, and teaching (I'm also department chair but that is another topic completely). The story will describe how this happened. Throughout the lecture many hypotheses and issues will be discussed together with experiences in application and consulting. Working with these various groups has helped to direct us towards the next important question – the consultant/scientist/teacher synergy has been critical – many examples will be given.
The journey has taken many interesting twists that could not have been predicted 20 years ago.

BRIEF HISTORY – Mythology or Truth

My grade 2 report card stated that "Stuart continually disrupts the class asking questions…" – my consolation now is that I get paid for it. All sorts of claims continue to be made about how the back functions, how injury should be avoided, or how the back/torso should be trained. I started out with the intention of developing the most comprehensive model of the torso, driven from the motion and motor patterns of live people, in order to assess these many proposals/hypotheses. I realized that understanding function was limited without actually creating and defining the damage in real tissue – hence the development of our spine tissue in vitro lab.

SERENDIPITY

In many instances important discoveries resulted from accident. Perhaps one of the more important events in my career was witnessing an injury in a powerlifters' spine while lifting. Using videoflouroscopy we watched the spine buckle, or experience instability. That single event was the impetus for much of our recent work into spine stability. The lesson: what turned out to be our most creative work resulted from the way that we handled unexpected events. Other advice: go to the anatomy lab; "play" in the lab and stretch your questions – get a little crazy; don't restrict yourself by stating "my area of interest is……" – be interested in everything; be nice to your supervisor and previous students who built the facility you are now able to enjoy.

RECENT WORK

Spine stabilization exercise is currently a popular topic yet so much of current practice is conducted without data based guidelines for exercise choice or progressions. Examples of this work together with some high performance training techniques will be introduced. The training approaches of some of the best athletes, some of it based on quantifying some older Russian research, will be introduced.

ACKNOWLEDGEMENT

REFERENCES

Our work is summarized and synthesized in:

McGill, S.M., (2002) Low Back Disorders: Evidence Based Prevention and Rehabilitation, Human Kinetics Publishers, Champaign, Illinois.

McGill, S.M., (2004) Ultimate Back Fitness and Performance, Wabuno Publishers, Waterloo. Available from: www.backfitpro.com

COUPLING OF SIDEBENDING AND AXIAL ROTATION IN THE THORACIC SPINE

Gordon J. Alderink
Biomechanics and Motor Performance Laboratory
Grand Valley State University, Grand Rapids, MI, USA
aldering@gvsu.edu

INTRODUCTION

Fryette (1918) described the nature of vertebral coupling for sidebending (SB) and axial rotation (AR) in order to provide a foundation for osteopathic manual medicine procedures. In the thoracic spine, Fryette stated that when the spine was neutral, SB and AR coupled opposite, but when the spine was hyperflexed or hyperextended SB/AR coupled to the same side. Since Fryette, many have examined thoracic kinematics, but no one has specifically tested Fryette's hypotheses; nor is there a consensus on vertebral coupling in the thoracic spine. Therefore, the purpose of this research was to examine thoracic vertebral coupling in normal individuals.

METHODS

Fifteen male and 15 female (22.5 ± 3.0 yrs; 70 ± 14 kg; 1.75 ± 0.09 m) volunteers were screened and participated in the testing protocol after written informed consent was obtained. Unique to this study was that participants were considered normal only if they had no back or extremity injuries within the past six months and demonstrated normal gait, posture, and extremity and spine range of motion (Greenman, 2003).

A minimum of three non-collinear markers were placed on the skin overlying spinous processes T3-T6, T12-L3, and bilateral pelvic ASIS and PSIS, so that local coordinate systems could be created (positive *xyz* defined as right, anterior, and upward, respectively). Marker positions were recorded at 30 Hz using six VICON 512™ (Oxford Metrics, LTD., Oxford, England) cameras.

Five repetitions were recorded for each of the following thoracic motions: standing flexion/extension, SB, and AR (neutral spine), sitting SB and AR with neutral, hyperflexed, and hyperextended spine. Raw 3D position data were filtered (0.5 Hz Butterworth) and Cardan angles were determined using custom MATLAB™ (Mathworks, Natick, MA) programs. Three test cycles were time normalized and then ensemble averaged for data analysis. Cycle-to-cycle coefficients of variation (Winter, 1991) averaged 14.6% and 36% for the primary and secondary motions, respectively. The *xyz* convention was used to calculate Cardan angles of the thoracic spine relative to the lumbar spine, since this rotation sequence minimized cross-talk (Crawford et al., 1996). Three-dimensional angle-angle plots and cross-correlation analyses were used to determine vertebral coupling patterns. Coefficients of multiple correlation (CMC) (Growney et al., 1997, for a group of randomly selected subjects (n=10) who attended two test sessions, were determined for test-retest consistency.

RESULTS AND DISCUSSION

CMCs for primary and coupled motions ranged from 0.97 for to 0.78, indicting good to excellent repeatability. Cross-correlation (R^2) for SB and AR tests averaged 0.76 (± 0.21) suggesting that 76% of the total variance of SB or AR could be explained by corresponding coupled motion. Contrary to Fryette and others (Buchalter et al., 1989; Willems et al., 1996), SB and AR were coupled in the same direction 90% of the time during standing and sitting motion tests when the spine was neutral. When the spine was hyperflexed or hyperextended, SB/AR were coupled in the same direction 79% of the time, which is consistent with Fryette's, but not Lovett's (1902), findings (Table 1).

Table 1. Frequency of Coupling Patterns

	StN SB/AR	SitN SB/AR	SitFl SB/AR	SitE SB/AR
Same	45	54	46	52
Opposite	8	3	18	5

StN=stand neutal spine; SitN=sit neutral spine; SitFl=sit hyperflexed; SitE=sit hyperextended.

SUMMARY

The fidelity of 3D motion of a group of vertebrae that mimics intervertebral coupling was established with high test-retest reliability. Data suggest that thoracic coupling of SB/AR occurs in the same direction most of the time. Manual medicine practitioners who base examination, diagnosis, and intervention strategies on Fryette's concepts of vertebral coupling may need to reconsider mechanisms of action.

REFERENCES

Buchalter, D. et al (1989). *J. Spinal Disorders*, **1**, 279-283.
Crawford, N.R. et al (1996). *Hum. Move. Sci.*, **15**, 55-78.
Fryette, H.H. (1918). *J. Am. Osteopathic Assoc*, **18**, 1-2.
Greenman, P.E. (2003). *Principles of Manual Medicine* (3rd ed.). Philadelphia, Lippincott Williams & Wilkins.
Growney, E. et al (1997). *Gait and Posture*, **6**, 147-162.
Lovette, R.W. (1902). *Am. J. Anatomy*, **2**, 457-462.
Willems, J.M. et al (1996). *Clin Biomechanics*, **11**, 311-316.
Winter, D.A. (1991). *The Biomechanics and Motor Control of Human Gait*. (2nd ed.). University of Waterloo Press.

ACKNOWLEDGEMENTS

PREDICTING THE FAILURE STRENGTH OF PORCINE CERVICAL SPINAL UNITS USING BONE MINERAL CONTENT AND ENDPLATE AREA

Robert J. Parkinson, Jennifer L. Durkin and Jack P. Callaghan
Department of Kinesiology, University of Waterloo, Waterloo, Canada, rjparkin@uwaterloo.ca

INTRODUCTION

In order to perform in vitro compressive tests at normalized submaximal loads, it is necessary to have a non-destructive method of predicting the ultimate strength of a test specimen. Dual energy X-ray absorptiometry (DXA) is a non-invasive scanning technique used to measure bone mineral content (BMC). Given the well established relationship between BMC and vertebral strength, this study aimed to develop a regression equation based on non-destructive measures to enable the accurate prediction of the failure strength of porcine cervical spinal units.

METHODS

Ten frozen porcine cervical spines were obtained from an abattoir. A porcine model was chosen to allow control over age, weight, diet and activity. Specimens remained frozen while being scanned with a Hologic Discovery system (Hologic Inc., Bedford, MA, USA). Laser alignment was used to position the longitudinal axis of the cervical spine with the travel path of the scanner. Specimens were placed on their left side for lateral scanning. Hologic software was used to define each vertebrae of interest (figure 1) and determine the BMC.
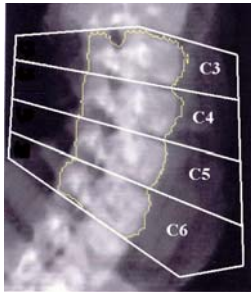

Figure 1: Example of DXA output, showing the isolation of individual vertebrae.

Cervical spines were thawed overnight and dissected to isolate the osteoligamentous C3C4 and C5C6 segments. The exposed intervertebral discs were assessed to ensure the use of only non-degenerated specimens. Prior to fixation, the exposed endplates of each segment were measured and the area calculated using the equation of an ellipse. The average endplate area of the segment was used as a variable in the regression analysis.

The upper and lower endplates were fixed in aluminum cups using dental plaster, with the mid-plane of the disc aligned parallel to cup rims. The superior vertebra was mounted to the actuator of an Instron (8872) materials testing machine. The lower cup was placed on a bearing table to allow unrestricted translation along two axes. A 300N compressive preload was then applied for 15 minutes. Units were compressed to failure at a rate of 3000N/second. Failure was defined as a 3.125% drop in the force level in a 10ms window. Throughout testing the specimen was surrounded by saline soaked paper towel and plastic wrap.

Multiple linear regression (stepwise) was performed to determine the correlation between failure load (dependent measure), BMC and endplate area (independent measures). The results of the regression analysis are listed in table 1.

Table 1: Regression analysis results.

Variable	Partial R^2	Model R^2	p-value
Area	0.5329	0.5329	0.0003
BMC	0.0802	0.6131	0.0777

RESULTS AND DISCUSSION

Average BMC, endplate area, and failure load ±1 standard deviation were 9.61 ±1.66g, 720.66 ± 59.59mm, and 10.46 ±1.11kN respectively. Paired t-tests revealed no significant differences between spinal levels.

The regression analysis identified area as the variable most highly correlated to failure load. This result is surprising given the poor correlation reported in similar studies (Edmonston et al., 1997). This difference may be due to the use of a much older human model in the earlier study. BMC was found to further improve the model correlation by 8%. An increase in correlation with the inclusion of both variables has been observed previously (Yang et al., 1998). The improvement in failure load estimation may justify the inclusion of BMC despite the lack of significance at the p<0.05 level. When the specimen data was input into the 2 variable equation, the average absolute error of the estimate was 0.55kN. Using only area in the model the average absolute error of the estimate was 0.64kN.

This work has shown that the use of a predictive equation is beneficial, even when using a controlled animal model. Employing the equation to predict failure strength resulted in lower variability than assuming a homogenous ultimate strength, with an improvement in root mean square difference of 1kN.

REFERENCES
- Edmonston, S.J. et al. (1997). *Osteoporosis Int* **7**: 142-14.
- Yang, R.S. et al. (1998). *Calcif Tissue Int* **63**: 86-90.

ACKNOWLEDGMENTS

QUANTIFYING TISSUE LOADS AND SPINE STABILITY WHILE PERFORMING COMMONLY PRESCRIBED LOW BACK STABILIZATION EXERCISES

Natasa S. Kavcic, Sylvain Grenier, Stuart M. McGill

Occupational Biomechanics Laboratory, University of Waterloo, Waterloo, Ontario, Canada

Contact: nkavcic@ahsmail.uwaterloo.ca

INTRODUCTION

The notion of spine stability, together with low back stabilization exercise has become a major focus in both rehabilitation efforts and prophylactic care. Spine stability has been identified as the result of a coordinated effort between active, passive and neural control subsystems of the spinal region (Panjabi 1992). Low back pain and injury have been shown to lead to inappropriate muscle activation patterns (Hodges and Richardson 1999) and these perturbed patterns have been linked to unstable events and subsequent reinjury (McGill 2002, Ching et al 1992). Consequently, clinicians use various exercise approaches to train motor patterns for the purpose of improving spine stability. With proper technique and repetition, it is hypothesized that the subsequent motor patterns developed during the exercises will translate to more functional activities (Stevens and Green Hall 1998). Despite the prevalence of stabilization exercises in fitness and rehabilitation programs, to date, very little research has attempted to quantify the stability in the lumbar spine resulting from the muscle activation patterns generated during specific exercises. The purpose of this study was to quantify tissue loading characteristics and estimate spine stability in an attempt to provide clinicians with information to aid exercise design and prescription.

METHODS

The stabilization exercises measured in this study were the abdominal curl, four-point-kneeling with a leg lift, four-point kneeling with contralateral arm and leg lift, back bridging, back bridging with leg lift, side bridging and sitting on a gym ball. Each stabilization exercise was performed statically for a period of 2 seconds. Spine kinematics and 14 channels of torso EMG were recorded. Reaction forces were measured from the upper body segments that were in contact with the ground.

Data was input into a stability model of an in vivo lumbar spine first described by Cholewicki and McGill (1996) with subsequent anatomical improvements, and the average measures of muscle activation, L4-L5 compression and spine stability for the duration of the trail were calculated.

RESULTS AND DISCUSSION

Across the isometric exercises tested, both the side bridge and the abdominal curl produced the highest levels of abdominal muscle activity. The bridging and four-point kneeling exercises created the highest activation levels in the extensor musculature. Sitting on the ball and on the chair produced the lowest levels of activation across all muscles compared to the other exercises tested and differences between them were negligible.

In terms of the calculated levels of spine stability, across all of the tested exercises, the ball and chair tasks produced the lowest levels of stability ($p<0.05$), where the level of stability for the ball was 575 Nm/rad and for the chair 582 Nm/rad. In contrast, the four-point kneeling task with contra-lateral arm and leg lift produced the highest level of spine stability (1386 Nm/rad), which was significantly greater than all the other exercises tested ($p<0.05$). Across the remaining exercises no significant differences existed.

In terms of L4-L5 compression the lowest level existed for the four-point kneeling task with single leg lift (2018 N). The ball, chair and bridge exercises produce the next lowest levels of compression; 2097N, 2128N, 2387N, respectively, and these were followed by the abdominal curl at 2615N. Although calculated differences exist between the compression values for these five exercises, they were not statistically different. The highest levels of compression were calculated for the side bridge, bridge with single leg lift and the four-point kneeling task with contra-lateral arm and leg lift (2726N, 2707N and 2740N, respectively).

SUMMARY

The role of clinicians is to first, assess a patient and determine the most appropriate exercise therapy, and second, to devise the most appropriate exercise progression. Knowledge of resultant muscle activity levels together with spine compression and stability will aid in these decisions.

REFERENCES

Panjabi MM. (1992). *J Spinal Disord*. 5:383-9.

Hodges PW, Richardson CA. (1999). *Arch Phys Med Rehabil.* 1999; 80: 1005-12.

McGill S. (2002). *Low Back Disorders: Evidence-Based Prevention and Rehabilitation*. Champaign, Illinois: Human Kinetics: 143.

Ching RP, Tencer AF, Anderson PA, Harrington RM, Daly CH. (1992). *Trans Orthop Res Soc*. 17:68.

Stevens J, Green Hall K. (1998). *JOSPT*. 1998; 28: 165-167.

PELVIC SKELETAL ASYMMETRY AND ASYMMETRY IN SELECTED TRUNK MOVEMENTS: THREE-DIMENSIONAL ANALYSIS IN HEALTHY INDIVIDUALS AND PATIENTS WITH MECHANICAL LOW BACK PAIN

Einas Al-Eisa[1], David Egan[1], Kevin Deluzio[2], and Richard Wassersug[1]
[1]Department of Anatomy & Neurobiology, Dalhousie University, Halifax, Canada
[2]School of Biomedical Engineering, Dalhousie University, Halifax, Canada

INTRODUCTION

Many individuals move asymmetrically (Gomez, 1994), but factors and constraints that lead to such asymmetries in either normal or patient populations are not well understood. We ask in this paper could asymmetries in trunk motion be associated with a subtle structural abnormality such as pelvic asymmetry, which is commonly linked to low back pain (LBP). Pelvic structural asymmetry is associated with soft tissue changes in the back as well as with compensatory postures (Riegger-Krugh & Keysor, 1996). Hence, if people adapt to pelvic asymmetry over time, interventions to correct the asymmetry may not be necessary. However, if the pelvic asymmetry leads to altered movement pattern which could negatively affect the individual's activities, then there is a need to better understand this association to develop appropriate interventions. To date, the relationship between pelvic asymmetry and altered spinal movement remains unclear in both symptomatic and asymptomatic populations. The purpose of our study was to examine the relationship between anthropometry and function in normal and LBP subjects.

METHODS

A total of 113 male and female subjects were classified into two groups: control group with no history of LBP (n=59; 25 males and 34 females, mean age ± SD = 31.1 ± 6.9), and LBP group with predominantly unilateral symptoms that persisted in the 6 months prior to the study (n=54; 27 males and 27 females, mean age ± SD = 33.4 ± 7.2).

Pelvic asymmetry and trunk motion (lateral flexion and axial rotation) were measured using an anthropometric frame and a Qualisys™ Motion Analysis System respectively. Movement asymmetry was defined as the percentage of the absolute difference between the right and left end range divided by the total range, thus:
Movement asymmetry = 100 [|R-L| / (R+L)]

RESULTS AND DISCUSSION

Table 1: Correlations between pelvic asymmetry and asymmetry in trunk motion

Movement	Control (n = 59)	LBP (n = 54)	Total (n = 113)
Lumbar lateral flexion	.713**	.834**	.798**
Lumbar axial rotation	.437**	.191	.360**
Thoracic lateral flexion	.150	.448**	.338**
Thoracic axial rotation	.164	.054	.052

* indicates correlation significant at the 0.05 level
** indicates correlation significant at the 0.01 level

We believe that asymmetries in movement probably indicate some underlying mechanical abnormality that could be either structural or habitual. Our results suggest that asymmetry in lumbar lateral flexion is highly associated with pelvic asymmetry in both normal and LBP populations. On the other hand, asymmetry in lumbar axial rotation was less correlated with pelvic asymmetry in the normal group, but not so in the LBP group. Pelvic asymmetry was not correlated with asymmetry in thoracic rotation and thoracic lateral flexion.

Asymmetry in axial rotation in the LBP group may be due to protective guarding, increase in apprehension, or asymmetrical pain distribution rather than actual tissue constraints. Low back injuries commonly involve some trunk twisting; thus asymmetric injury to lateral structures (including the lateral part of the disc) could produce asymmetry of movement.

This study demonstrates that subtle anatomical abnormality in the pelvis is associated with altered mechanics in the lumbar spine. This emphasizes the need for correction of structural asymmetry in patients with mechanical LBP to prevent abnormal movement patterns that may cause tissue changes.

REFERENCES

Gomez TT (1994). *JOSPT*, **19**, 42-48.
Riegger-Krugh C, Keysor JJ (1996). *JOSPT*, **23**, 164-170.

MECHANOMYOGRAPHIC SIGNALS OF THE FIRST DORSAL INTEROSSEOUS AND VASTUS LATERALIS MUSCLES DURING ISOMETRIC CONTRACTIONS

Cintia de la Rocha Freitas[1,2], Michel Arias Brentano[1], Walter Herzog[2], Marco Aurélio Vaz[1,2]
1 - Exercise Research Laboratory, Federal University of Rio Grande do Sul, RS, Brazil
2 - Human Performance Laboratory, University of Calgary, Calgary, AB, Canada
*email: croche@kin.ucalgary.ca

INTRODUCTION

The mechanomyogram (MMG) measures the lateral force oscillations of muscles during contraction (3). It has been hypothesized that the MMG might be a powerful tool to determine motor unit recruitment strategies. This notion has gained support by findings that MMG signal magnitude decreases with increasing motor unit stimulation frequencies (4), and increases with increasing number of active motor units (5).During voluntary contractions, force is increased by an increase in the number of activated motor units (increase in MMG) and a simultaneous increase in the motor unit firing rates (decrease in MMG). Therefore, one would expect that the MMG increases for a graded voluntary contraction as long as the recruitment of new motor units dominates the increase in firing frequency (i.e. at low force levels), and that the MMG decreases when the increase in firing frequencies dominates the recruitment of new motor units (i.e. at high force levels). Therefore, voluntary contractions of increasing force should show an increase in the MMG first, followed by a decrease. The peak MMG signal should then be associated with the change in strategy from new motor unit recruitment dominance to firing frequency dominance. The purpose of this study was to determine the MMG signal for two muscles which are known (1) to use new motor recruitment up to about 50-60% of the maximal voluntary force (MVF) (first dorsal interosseus) and up to about 80-100% MVF (vatus lateralis). If our prediction is correct, MMG signals should increase to a greater percentage of MVF in vastus lateralis compared to the first dorsal interosseus.

METHODS

MMG signals from the first dorsal interosseus (n=15) and the vastus lateralis (n=20) were measured using a small accelerometer during voluntary contractions at levels of 10, 20, 30, 40, 50, 60, 70, 80, 90 e 100% MVF. RMS values of the MMG signals were calculated.

RESULTS AND DISCUSSION

MMG signals increased with increasing force in vastus lateralis and reached a peak at 50% of MVC in the first dorsal interosseus (figures 1 and 2, respectively). Therefore, our hypothesis was found to be correct. Although there are a variety of possible explanations for these observations, the most obvious appears to be that MMG signals increase up to the point where new motor units are recruited. In vastus lateralis, new motor units are recruited for forces up to 80-100% of the MVF (3), and in accordance with this strategy, MMG increases throughout the force range. In the first dorsal interosseus, MMG signals increase up to 50%, the precise value up to which one would expect the recruitment of new motor units in this muscle (2). Although the present results are by no means proof that the MMG is a reliable and accurate indicator of motor unit recruitment strategies, the current results warrant further investigation. As for now, we propose that the MMG signal may provide valuable information on the recruitment of motor units that cannot be obtained easily with other methods, such as electromyography or force measurements.
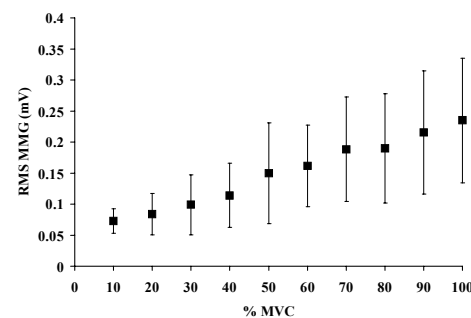

Figure 1. Vastus lateralis MMG RMS values (mean ± SD) during different levels of voluntary effort.
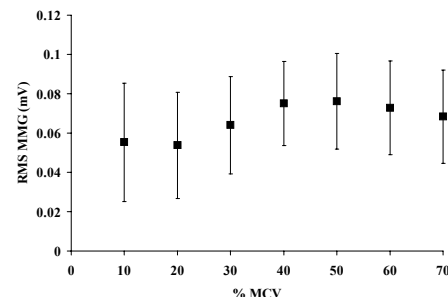
Figure 2. First dorsal interosseus MMG RMS values (mean ± SD) during different levels of voluntary effort.

REFERENCES

1.Basmajian, J.V.; De Luca, C.J. (1985). *Muscles Alive.* Baltimore, Williams & Wilkins.
2.Freitas, C.R. (2002). *Proceedings IV WCB*, Calgary.
3.Stokes, M.J. and Dalton, P.A. (1991). J. Neurol. Sci., **101**:163-167.
4.Vaz et al. (1996). *Muscle & Nerve*, **19**:774 –776.
5.Vaz et al (1997). *J.Electromyogr.Kinesiol.*, **2**:113-121.

A COMPARISON OF BILATERAL LIMB DEFICIT IN YOUNGER AND OLDER ADULTS DURING DYNAMIC KNEE EXTENSIONS

Usha Kuruganti and Jeremy Rickards

Institute of Biomedical Engineering, University of New Brunswick, Fredericton, Canada, ukurugan@unb.ca

INTRODUCTION

The ability to efficiently move our limbs to accomplish normal tasks is a complex process that is yet to be completely understood. One limitation of the neuromuscular system is the 'Bilateral Limb Deficit' (BLD). The BLD is the difference in the maximal or near maximal force generating capacity of muscles when a muscle is contracted alone or in unison with another muscle. While the BLD has been shown to occur in a variety of movements, the source of the BLD remains unknown. It had been suggested that if there is a difference in the amount of BLD present in older adults this could indicate that the deficit might be due to a reduction of one type of muscle fibre as it is known that muscle fibre type composition changes with age. Those studies that have looked at the BLD with respect to age have been limited and contradictory (Hernandez, et. al., 2003, Häkkinen et. al., 1996a, 1996b, 1997, Owings and Grabiner, 1998a, 1998b). In addition, only four studies included a younger group for comparison and, of these three studies, did not detect a BLD in either group. The objectives of this study were to examine the presence of the BLD in younger and older adults during dynamic knee extensions and to determine if there is a difference in the BLD due to age.

METHODS

Thirty-three subjects in two age groups (18 – 35 years and 55 – 75 years) participated in this study. Subjects were required to perform a series of slow (45 deg/sec) isokinetic knee extensions using a Cybex II (Lumex Incorporated, NY) isokinetic dynamometer. Surface electrodes were used to monitor the myoelectric signal (MES) from the quadriceps and hamstrings muscles. During testing sessions subjects were required to produce two maximum voluntary contractions of three conditions, bilateral (BL), unilateral right (ULR) and unilateral left (ULL). The BLD was then quantified using a ratio of bilateral to unilateral strength measurements as defined by Ohtsuki (1983), known as the Bilateral Limb Ratio (BLR). The BLR indicates the amount of deficit present during the contraction. A high BLR indicates a low deficit, while a low BLR indicates a large deficit. The BLR was calculated using both torque data (BLR_{Torque}) and MES data (BLR_{MES}).

RESULTS AND DISCUSSION

The mean BLR_{Torque} and BLR_{MES} for the younger and older groups are shown in Table 1. No statistically significant difference was detected in the mean BLR_{Torque} or the BLR_{MES} that was attributable to age. Although the sample size is small, the data suggested that there are no practically (clinically) significant differences in the BLD between older and younger adults. It is known that aging results in loss of muscle fibres and, especially type II fibres. These results suggest that the BLD is not caused primarily by a reduction of fast twitch motor units. The results from this study agreed with previous findings, which investigated the presence of the bilateral deficit in older adults and found a mean BLR_{Torque} of between 87.34 and 90.65 % in 35 subjects between the ages of 56 and 83 during an isometric knee extension (Owings and Grabiner, 1998b).

Table 1 Mean BLR values for younger and older groups calculated using torque (BLR_{Torque}) and MES data (BLR_{MES}). Data are mean (SD).

	BLR_{Torque} (%)	BLR_{MES} (%)
Younger	83.66 (13.24)	83.86 (13.71)
Older	78.81 (12.30)	78.38 (14.81)
P-value	0.2	0.2

SUMMARY

This study showed that the BLD is present and similar between younger and older adults during dynamic knee extensions. This suggests that the BLD is not primarily due to the loss of particular (i.e. fast twitch) motor units. Previous studies of older adults were limited and either did not detect a BLR (Häkkinen et al., 1996a, 1996b, 1997 and 1998) or found bilateral deficit in older people, comparable with reported results for younger people, without testing a younger group (Owings and Grabiner, 1996, 1998a). This limitation was addressed in this study with the inclusion of a younger group of subjects. The findings from the older adult group presented here are similar to those previous studies (Owings and Grabiner, 1996, 1998a).

REFERENCES

Häkkinen, K. et al (1996a). *Acta Physiol Scand*, **158**, 77-88.

Häkkinen, K.et al (1996b). *J. Geront Biol Sci*, **51A**, B21-B29.

Häkkinen, K. et al (1997). *Electromy & Clin Neurophys*, **37**, 131-142.

Häkkinen, K. et al (1998). *J. App Phys*, **84**, 1341-1349.

Hernandez, et al (2003). *J. of Gerontol Series A*, **58**, M536-M541.

Ohtsuki, T. (1983). *Behaviour Br Res*, **7**, 165-178.

Owings, T. & Grabiner, M. (1998a). *Med Sci Sports Ex*, 1257-1262.

Owings, T. & Grabiner, M. (1998b). *J. Geront*, **53A**, B425-B429.

INVESTIGATING THE MORPHOLOGY AND FIRING CHARACTERISTICS OF EXTENSOR CARPI RADIALIS (ECR) MOTOR UNITS DURING LOW-LEVEL CONTRACTIONS IN HEALTHY SUBJECTS

Michael J. Agnew[1] and Linda McLean[2]

[1]School of Physical and Health Education, Queen's University, Kingston, Ontario, Canada
[2]School of Rehabilitation Therapy, Queen's University, Kingston, Ontario, Canada, mcleanl@post.queensu.ca

INTRODUCTION

Within the last decade, the incidence of repetitive strain injuries (RSIs) within the North American workforce has increased rapidly. Despite widespread acceptance of RSI as a diagnosis, the pathophysiology related to this type of injury is not completely understood. This poses a problem to both ergonomists and clinicians, for without a full understanding of this impairment, proper treatment and effective workplace guidelines cannot be developed. Research has identified that myopathic (Larsson el al., 1988) and neuropathic (Watanabe et al., 2001) changes may occur within motor units exposed to low intensity, repetitive strain. Through conventional clinical electromyography (EMG), myopathic and neuropathic conditions can be identified using quantitative and qualitative observations of individual motor unit parameters. The purpose of this study was to quantitatively characterize the muscle morphology and firing characteristics of the extensor carpi radialis longus (ECR) muscle in healthy male and female subjects. In doing so, this will help enable us to identify myopathic and/or neuropathic changes in this muscle group for subjects with RSI symptomatology.

METHODS

To date, fifteen of 30 healthy subjects (15 m, 15 f) with no previous history of an RSI have participated in the study. Surface EMG (Comperio EMG, Neurosoft Inc, Virginia) was used to measure an evoked compound muscle action potential across a mono-polar electrode configuration (Heart trace, Ag/AgCl). Maximum voluntary contraction (MVC) signal voltage was then determined from a separate contraction using the surface channel. Next, a concentric needle (CN) electrode (Neuroline 74038-45\N) was inserted near the motor point of the ECR. EMG data were sampled and recorded simultaneously from both the surface and indwelling channels, while subjects performed a series (up to 10, 30s each) of low-level isometric contractions (10% MVC +/- 2%). The CN electrode was repositioned following each contraction to detect activity from as many different motor units as possible. Using DQEMG software (Stashuk, 1999), the EMG data were analyzed and decomposed to isolate individual motor unit potentials (MUPs). The ECR muscle was characterized by quantifying "normal" MUP morphology (MUP size and complexity measures) and firing characteristics (mean firing rate and variability). Descriptive statistics were used to characterize normal values and analysis of variance models were used to determine if gender differences exist.

RESULTS AND DISCUSSION

Descriptive statistics of our preliminary findings are presented in Table 1. Interestingly, from our small sample to date, there appears to be a larger number of phases in female MUPs as compared to males (F = 16.12, p = 0.02) as well as a trend towards lower MUP peak to peak voltage (F=4.32, p=0.06). However, these differences were not expected, and their meaning will not be commented on until the entire subject pool has been collected and processed. To validate our measures, a test/retest series of collections is currently underway. At the conference, a complete analysis of the 30-subject sample will be presented, as will the findings of the test/retest series.

Observed MUP Characteristics	Mean	S.D.
Contraction Level (%MVC)	9.92	1.36
# of MUPs	197.90	27.77
MUP Peak to Peak Voltage (µV)	395.46	251.00
MUP Duration (ms)	9.50	4.82
# of MUP Phases	2.56	0.25
# of MUP Turns	3.28	0.89
MUP Amplitude/Area Ratio	1.60	0.30
Firing Rate (Hz)	17.54	1.82

Table 1 Descriptive statistics of MUP size and shape, as well as estimated firing rate for low-level isometric contractions.

SUMMARY

To date, we have characterized the morphological and firing statistics of a small sample of individuals. Ideally, data obtained from this study will be used in consequent studies for comparison with the activation characteristics of patients who have been diagnosed with RSI, non-specific arm pain (NSAP), and/or work related upper limb disorders affecting the extensor muscles of the forearm.

ACKNOWLEDGEMENTS

REFERENCES

Dennet X. et al. (1988). *Lancet*, 1(8591):905-908.
Larsson S.E. et al. (1988). *Acta Ortho Scand*, 61, 394-398.
Watanabe M. et al. (2001). *J of Hand Sur*, 26A:4:663-669.
Stashuk D.W. (1999). *Med Eng and Physics,* 21:389-404.

ON THE COLLECTIVE BEHAVIOR OF THE MYOSIN II MOTOR AND MUSCLE CONTRACTION

Rachid Ait-Haddou and Walter Herzog

Human Performance Laboratory, University of Calgary, Calgary, AB, Canada
*email: walter@kin.ucalgary.ca

INTRODUCTION

In recent years, there has been increasing theoretical and applied research on the Brownian ratchet theory and its possible involvement in explaining the fundamental processes of muscle contraction at the molecular level (Ait-Haddou and Herzog, 2003). Brownian ratchet theory refers to the non-intuitive phenomenon that non-equilibrium fluctuations in an isothermal medium and anisotropic system can induce mechanical force and motion. Among the many theories, the so-called flashing ratchet (Astumian, 1997) seems to be the best to explain muscle contraction. In flashing ratchets, a Brownian particle, namely the myosin II motor, fluctuates between two potentials: the first potential (V_1) refers to the detached state, and the second (anisotropic) potential (V_2) to the attached state of the myosin II motor to actin. Fluctuations between the two potentials are induced by ATP hydrolysis (Figure 1).
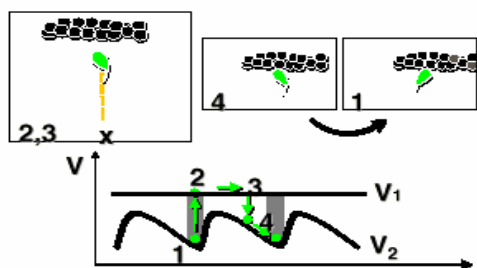

Figure 1: The flashing ratchet mechanism of muscle contraction.

Muscle contraction is the net effect of a large collection of working myosin II motors that are connected to the myosin filament. Because of the stochastic nature of the operating mode of a single myosin II motor, the study of the collective effect becomes a significant theoretical challenge. In this study, we investigated the collective behavior of molecular motors using an analogy by considering a discrete version of the flashing ratchet, the so-called Parrondo game (Harmer and Abbott, 1999).

METHODS

Parrondo's game is a gambling scenario in which a single player switches between two loosing strategies to arrive at a winning strategy. In this study, we created a collective rule between a number of Parrondo's players that mimics the collective rule between myosin II motors in muscle contraction, and we studied the effective potential of the game as well as the steady-state characteristics of the system using a Fokker-Planck description of the model.

RESULTS AND DISCUSSION

Although force generation of a single myosin II motor is stochastic in nature, collectivity leads to a smoothing of the effective potential (Figure 2). Therefore, collectivity of the myosin II motors creates the smoothness in force traces observed experimentally in muscle contraction. We also showed the dramatic increase in the speed of the system from one to two motors, and the stable behaviour of the system with an increasing number of players (Figure 3). These results are observed in experiments with single and large numbers of molecular motors (Inoue et al, 2001). We further discuss, using our formalism, how collectivity leads to well-known experimentally observed phenomena, such as the spontaneous oscillatory contraction at the sarcomere level (SPOC phenomenon; Yasuda et al, 1996), and the break-point at high loads of the force-velocity curve.
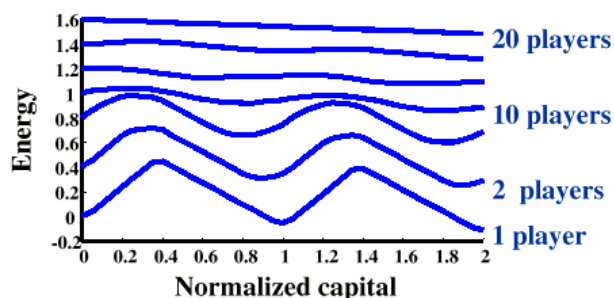

Figure 2: The effective potential with an increase of the number of Parrondo's players

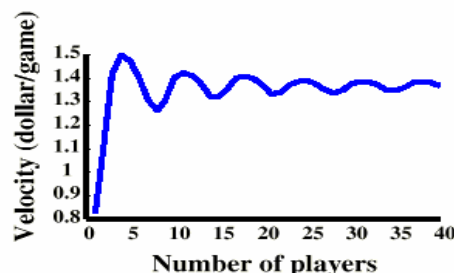

Figure 3: Velocity of the capital versus the number of Parrondo's players.

REFERENCES

Ait-Haddou, R., Herzog, W (2003). *Cell Bioch. Biophys.* **38**, 191-213.
Astumian, D., (1997). Science. **276,**, 917-922.
Harmer, G., P., Abbott, D, (1999). *Nature.* **402**, 846.
Inoue, Y. et al, (2001). *Biophys. J.* **81**, 2838-2850.
Yasuda, K., et al, (1996). *Biophys. J.* **70**, 1823-1829.

BIOMECHANICAL TOOLS AND INFORMATION: DO THEY APPLY TO INDUSTRIAL POPULATIONS?

Suzanne Pettit, M.Sc., CCPE
Ergonomist
Halifax, Canada, pettits@gov.ns.ca

INTRODUCTION

Practitioners working in the field of physical ergonomics use biomechanical principles, assessment methods, and data on a frequent basis. Considering this author's experience, five applications or purposes are identified:

1. *Musculoskeletal disorder (MSD) risk assessment:*
When identifying biomechanical risk factors associated with a task or job, a variety of biomechanical 'tools' can be applied (e.g. the NIOSH Lifting Equation, WATBAK, etc.). In a less structured sense, general information about MSD risk factors (i.e. force, posture, repetition) and data derived from biomechanics are often used during preliminary observations to identify potential problem jobs or tasks.

2. *Education:*
Prevention strategies aimed at reducing or preventing work-related MSDs often include an education component, targeted at different functional groups within an organization. For example, employees are educated about risk factors for MSDs and/or about 'proper' work methods. Managers need to understand the impact that their operational decisions can have towards MSD risk factor development. Biomechanical information forms the basis of much of this education.

3. *Prescriptive workplace design:*
Ergonomists can help designers and engineers to create safe, healthy and efficient tools, products, workspaces, work systems, etc. by providing data about human capabilities and limitations. For example, hand tool grip forces, or item weights to be lifted. In the physical sense, much of this data is derived from biomechanics research.

4. *Comparative evaluations:*
Given a choice between buying tool X or tool Y, for example, one may evaluate and compare the tools across a variety of features to help form a purchasing decision. These comparisons can address biomechanical requirements of use, to answer questions about associated levels of MSD injury risk.

5. *Staffing flexibility:*
By performing biomechanical analyses of work processes or jobs within an organization, input can be made regarding how 'accommodating' the work is to various segments of the working population. This is particularly relevant for today's aging workforce, and in terms of return-to-work programs.

QUESTIONS OF SUITABILITY

General biomechanical principles and generic information have been an invaluable aid to this author in accomplishing the types of tasks described above. However, the use of more numerically-oriented tools and data has sometimes caused this author to ask the questions, "Does this really apply here?", or "How confident am I that this tool's output is valid for my situation?". Specific concerns have centred on:

1. *Sample size:*
Analytical tools or data sets that have been developed using data from a relatively small number of subjects.

2. *Age of subjects:*
Tools and data sets developed through use of data collected from only young, healthy student subjects.

3. *Gender:*
Has data been derived from all males, a mixed subject pool, or separate groups of males and females? Has the data been treated separately or are data from both genders grouped? These issues are not always clear.

4. *Usability of output:*
Data sets or analytical tools with outputs expressed in units that are not intuitively or easily understood (without a series of unit conversions) in applied work settings by lay staff.

5. *Variability in reported MSD risk factor threshold limits:*
Studies that attempt to establish limits for these risk factors vary widely in their recommendations.

6. *Evaluation tools for non-expert users:*
Tools that are relatively simple to use and which produce a number as their output are often used by non-experts that know little about how to use the tool correctly, appropriately, nor about cautions associated with interpreting the results.

WISH LIST

From the perspective of an ergonomics practitioner, working in settings where workers (many aging, more women, with otherwise sedentary lives, etc.) are performing physical work , it would be reassuring to have some of the above issues addressed. In an 'ideal' world, the biomechanics field would provide *more* of the following:
1. validation studies for tools developed.
2. strength data using larger sample sizes.
3. industrially-based studies and data.
4. data specific to older workers and to female workers.
5. explicit statements to non-expert users about when, and to whom, a tool can be validly applied. Statements about how over-or under- estimates of parameters will influence results.
6. consensus data/output from the biomechanics community, for example for MSD risk factor threshold limits.

ACCURACY OF ERGONOMICS ASSESSMENT APPROACHES AND INJURY PREVENTION

Jack P. Callaghan
Department of Kinesiology, University of Waterloo, Waterloo, Canada, callagha@uwaterloo.ca

INTRODUCTION

The desired outcome for all occupational biomechanics assessments of workers is to prevent worker injury. This outcome is independent of whether the work evaluation is performed in the design phase (proactive or upstream) or on active jobs (reactive or downstream). The fundamental approach in job evaluations is to compare exposure magnitudes with known acceptable levels. These approaches include net joint moments and strength values, joint forces and tolerance data, and postural deviations from optimal positions. While most assessments examine an individual's exposure magnitudes, the available tolerance values represent population or sample averages. These averages have variances or confidence ranges, implying the threshold limits should be viewed as fuzzy or grey areas rather than absolute limits. The focus of this paper is twofold, the first is to highlight the importance of an examiner's expertise and judgment in risk evaluation and the second is to examine the accuracy of occupational biomechanics approaches.

RESULTS AND DISCUSSION

The importance of understanding these soft guideline values is crucial in classifying jobs and the expertise of the individual interpreting the results is an integral component of an assessment. Figure 1 highlights two scenarios that can cause difficulty in task risk classification, scenario 1 where values are very close to the tolerance limit and scenario 2 where the exposure equals the limit value. Due to the inherent error in the standards; is the upper star in scenario 1 really a risk and the lower safe? The risk must be interpreted in conjunction with other known risk factors for developing LBP such as prior injuries. Continuing to use the NIOSH lumbar compression limits as an example of inherent error, the proposed compression threshold limits are 3400N as an action limit (safe for *most*) and a maximum permissible limit of 6400N (hazardous for *most*) (Waters et al., 1993, NIOSH, 1981). The rationale for these being fuzzy guidelines rather than hard guidelines is obvious in the descriptor *most*. Additionally, the relationship between compression and risk of injury in the biomechanics studies used to help establish these guidelines reveal that even with compression values below 2500N there was a 5% incidence rate of workers developing low back pain (NIOSH, 1981). If cadaver compression studies are also examined, roughly 10% of the reported specimens had failures below the 3400N action limit (Jager et al., 1991). For shoulder strength data, even when the values are broken into gender and age categories there is a large variance in the means (i.e. 20% for female shoulder flexion)(Lannersten et al., 1993).

It is therefore clear that tolerance values include some magnitude of error. On the other side of the exposure – tolerance relationship, the occupational biomechanics assessment tools also have intrinsic error. This spans from the fundamental errors such as the anthropometric variables of segment masses used in rigid link models to the design or

simplification of an approach to make it usable in an industrial setting. The resulting increase in error or loss of accuracy and the importance of this error are crucial in determining a worker's risk. The design of a 3D cumulative analysis tool will be used as an example of accommodations that are made to allow ergonomists with limited time and access to advanced research equipment to assess workplace exposures. Workplace tasks are performed dynamically in 3D space, with varying external loads typically for an 8 hour shift. However, using 3D motion tracking at high data sample rates with a force measurement device inserted between the worker and external objects to quantify 8 hours of industrial exposure is impractical. Using static rather than dynamic measures reduces sample requirements but imposes approximately 10% error. The error in using representative tasks to extrapolate to a shift exposure is unknown but using a single task measure to extrapolate can introduce errors as large as 20% compared to only 5% when an average of 4 task repeats was used (Dunk et al., 2004).
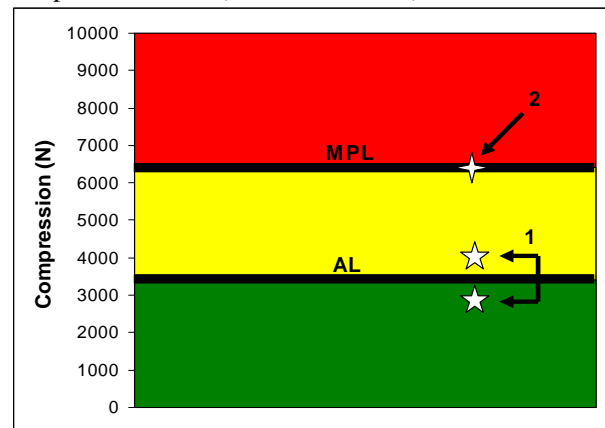

Figure 1: Low back compression exposure limits from NIOSH (Waters et al., 1993, NIOSH, 1981). Two scenarios illustrating difficulties in classifying worker risk occur when values are just below or above threshold values (scenario **1**) and values fall on threshold limits (scenario **2**).

SUMMARY

The errors in both assessment tools and tolerance limits highlight the need for assessments to be performed by individuals with a solid understanding of how these errors can effect the assignment of risk to a job and/or worker.

REFERENCES

Dunk et al. (2004) *Applied Ergonomics*; Submitted.
Jager et al. (1991) *Int J Ind Ergonomics*;8:261-277.
Lannersten et al. (1993) *Clinical Biomechanics*;8:235-242.
NIOSH (1981) NIOSH Technical Report No. 81-122.
Waters et al. (1993) *Ergonomics*;36:749-776.

ACKNOWLEDGMENTS

LINKING SEGMENTS: MODELS FOR SUCCESS

Joan M. Stevenson, Ergonomics Research Group, Queen's University, Kingston, Canada stevensj@post.queensu.ca

BACKGROUND

The relationship between basic, applied and service research is understood in the university environment but not as clearly delineated to the industrial world. We understand that tools must be validated before the scientific community will accept them for applied use or feel comfortable with these tools in the hands of practitioners. Yet in industry, where the survival is a year by year challenge, service is considered a necessity and applied research is a luxury during profitable times. In addition, developing trust between the researcher and company is paramount before any research can take place. From our experience, reversing the research model allows this trust to develop and researchers to learn the plant culture and develop common ground.

An example of a reversed model is with DuPont Canada (Kingston site). We began by providing an education and ergonomics program in a nylon plant. Our philosophy was to involve both management and workers in aspects where they had responsibility. Once this phase was completed, we are asked to give ergonomic feedback on a workstation and then conduct a follow-up study to see if it was effective. Satisfaction with these activities gave us a chance to introduce the company to a longitudinal study of low back pain. We believe the basic research would not have occurred without the progressive introduction of research into the workplace.

APPLIED TO BASIC RESEARCH

The model of service-applied-basic research is difficult because of the time spent and the distractions that can occur. It is easier to move from applied to basic research. I will give two examples of this type of program. We had experience with Defence Research and Development Canada in that we developed biomechanical assessment tools to aid with the design and evaluation of new load carriage systems for the Canadian Forces. We build objective simulators to measure pressure, forces, moments and relative motions. In order to validate this system, we needed to compare to soldiers' opinions. We had good success on this

front but the answers could only take us to discomfort scores. We are now working on relating these discomfort scores to models of tissue tolerance limit values for skin contact pressure. A similar story can be described vibration in mining vehicles. A research consortium has been working with the mining industry in Ontario to improve the vibration in large haul vehicles. The project has gone from line of sight challenges and strategies to reduce seat vibration to an examination of whether the tolerance limit values for rotated trunk postures increase spinal resonance and, therefore, whether the standards should be higher. Both of these situations demonstrate how applied research can uncover basic questions that need to be addressed.

DESIGN-BASED APPROACHES

Another approach to working with industry is to develop a design-based approach where industry and universities have separate roles but common goals. For example, in designing the new Canadian Forces load carriage system, a separate company designed the pack but we used the simulators to provide rapid answers to design-based questions. In this way the biomechanical tools saved design iterations and testing time. This type of approach has been expanded to children's backpacks were the design issues have not been studied. In this study, our partner was the Ontario Chiropractic Association, where they are concerned about children's back health. This has led to a program of study were education and optimal pack design are the key factors. Another applied question has been initiated at the university and an industrial partner found to assist with the development of the personal lift augmentation device (PLAD). Here, the company is contracted to design the device while we continue with the role of developing new design concepts and testing the device.

Regardless of which strategy was used, success hinges on finding and developing a good idea and building a good relationship with your industrial partner. Linking these segments is the start of a model for success.

LINKING OCCUPATIONAL BIOMECHANICS RESEARCH WITH THE REAL WORLD

Anne Moore
School of Kinesiology and Health Science, York University, Canada, amoore@yorku.ca

INTRODUCTION

A recent detailed breakdown of 2002 lost time injuries in the U.S. found work related musculoskeletal disorders (WRMD) accounted for 34% of all lost time injuries with a median of 9 days off from work. Of these 86.4% were considered to be the result of overexertion and repetitive motion, 50.4% were back and 25.9% were upper limb and shoulder (Bureau of Labor Statistics, 2004). A goal to reduce injury and costs constitute a starting point as to why it is important to perform occupational biomechanics research. How will this be achieved? Ideally, we would like to fully understand the etiology of each of the different WRMD, along with associated tissue tolerances. Practically, we will be asked "what works?" Intervention studies allow us to test the effectiveness of a specific ergonomic change in the workplace (e.g. Amick et al, 2003) and are an important step in providing evidence based best practices. Workplace intervention studies require multidisciplinary teams and face methodological issues associated with study design and implementation (Cole et al, 2003). However, the occupational biomechanist has a key role in such teams as a biomechanical analysis of loading changes associated with an intervention helps us to understand why an intervention is (or is not) effective. Also, understanding and quantifying the exposure that leads to change helps us to generalize the results and expand our knowledge of injury mechanisms (Wells et al, in press). The goal of this presentation will be to discuss issues associated with performing occupational biomechanics field research.

DISCUSSION

Full biomechanical analysis within an intervention study often involves a nested sample within the larger group due to time and costs. Table 1 highlights some considerations for field research. Issues to consider include participation rate/self selection, sample size, treatment versus control, comfort, participant burden and sustained participation. Measurement timing can pose a balance between long term use of an intervention and other changes in the workplace. Change is a factor you can count on in the workplace. Ideally the only change that occurs between testing pre-intervention and post-intervention is the intervention you planned for. Experience has shown, however, that you must plan for job changes among the participants, changes in technology, and changes in work level. The role of the control group to account for these changes can be compromised by the difficulty in limiting its exposure to the intervention. Detailed exposure measurements such as EMG, allow evaluation of the intervention in a framework of injury mechanisms (Wells et al, in press) and in a framework of change (Amick et al, 2004). The measures taken should be tied to the hypothesis of change and have various strengths and weaknesses (Van Eerd et al, 2004). The ability to breakdown exposure specific to the use of the intervention in the workplace is particularly useful (Moore et al, 2003).

SUMMARY

Measuring detailed exposure to biomechanical loads in the field is an important step in linking the "what works" with "why". This is a key role in an intervention study team.

REFERENCES

Amick, B. et al (2003). Spine, 9, 398-405.
Amick, B. et al (2004). ISOES proceedings.
B.L.S. (2004), http://www.bls.gov/iif/oshcdnew.htm,
Cole, D. et al (2003) Scand J Work Environ Health; 29(5): 396-405.
Moore et al (2003), ISB proceedings.
Wells, R. et al. (in press) Scan J of Work & Env Health.
Van Eerd et al (2004), PREMUS proceedings.

ACKNOWLEDGEMENTS

Table 1 Some considerations for measurement for workplace intervention studies.

Issues	Laboratory vs. Workplace
Subjects	Untrained/temporary vs trained
	Recruitment and Number (both)
Time Frame	Day(s) vs. months
Intervention	More variables controlled vs. Realistic use
	Isolate task of interest vs. multiple tasks
	Change of Interest vs. multiple changes (other than intervention)
Measures	Increased equipment complexity vs. equipment portability/electrical issues
	Increased subject burden (set-up, research related time off task) vs. Workplace support (time away from workplace, time off task, # repeat measures)
	Dedicated equipment vs. Instrumentation possible

HIP PASSIVE STIFFNESS MEASURES IN HEALTHY SUBJECTS: A RELIABILITY STUDY

Anabèle Brière, Sylvie Nadeau and Denis Gravel

Centre de recherche interdisciplinaire en réadaptation, Institut de réadaptation de Montréal
Ecole de réadaptation, Université de Montréal, (Québec), H3C 3J7, Canada.
Denis.Gravel@Umontreal.ca

INTRODUCTION

It has been shown that joint stiffness decreases an individual's ability to perform functional activities (Nadeau et al., 2001; Hof, 2001). At the hip, a reduced joint range of motion in extension modifies the kinematics, decreases the gait speed and reduces the controlateral stride length in individuals with hip diseases such as osteoarthritis (Murray et al., 1971). To improve the functional level in these patients, the first step is to measure joint stiffness adequately. The purpose of this study was to estimate, using an experimental method, the reliability of three stiffness parameters (moment, angle and rigidity) at three knee positions in healthy subjects.

METHODS

Twenty healthy subjects, aged between 20 and 63, were assessed on two days separated by a one-week interval. A Biodex dynamometer modified to assess the subject in a side-lying position was used to move the right lower limb passively at a slow velocity (15°/s) and to record the hip angle and passive moment during the movement (**Fig. 1**). EMG was used to control the hip muscle activity level. Three passive oscillations in flexion and extension with the knee positioned at 0° (K0°), 45° (K45°) and 90° (K90°) of flexion were performed each day. Passive stiffness of the hip flexion structures was quantified by three parameters: the moment (Nm) at a specific angle, the angle (°) at a specific moment and the rigidity (Nm/°). For each subject, the specific angle and moment were the same across trials and days. The parameters were derived from the moment-angle curve of each subject. The reliability of the stiffness measures was evaluated by the generalizability theory (Shavelson and Webb, 1991). First, the variances associated with the "subject", "day" and "trial" factors and their interactions were calculated. The reliability coefficients and standard errors of measurement (SEM) were then computed for a practical design comprising five trials in one day.

Fig. 1: Experimental setup.

RESULTS AND DISCUSSION

The reliability coefficients were moderate for the moment and angle parameters (0.61 to 0.78) and low for the rigidity at the three knee positions (0.26 to 0.35) (**Table 1**). Overall, the reliability coefficients were not affected by the knee position, except for the angle parameter at K45° which became highly reliable. The maximal SEM values were 6.65 Nm, 7.8° and 0.36 Nm/° for the moment, angle and rigidity parameters, respectively. The main source of error variance was the subject-day interaction factor, which accounted for 12.9% to 58.4% of the total variance, depending on the stiffness parameter and the knee position. A systematic increase in the stiffness values on the second day was also noted. The "trial" factor variance was low, revealing a high intra-trial reliability. In general, the reliability of the moment and angle parameters was good and the SEMs were acceptable. The poor reliability of the rigidity parameter could be explained by the fact that it was calculated using only two successive values at the end of the moment-angle curve instead of more scattered values. Regarding the systematic day factor error, this could be associated with a different alignment of the hip rotation axe between day 1 and day 2.

SUMMARY

This study used a free-gravity experimental method to assess the reliability of the hip joint stiffness parameters in healthy subjects. The results revealed that the reliability was good for two of the three parameters assessed (moments and angles). They also showed that the method needs improving to ensure a more similar positioning of the hip and limb from one day to the other.

REFERENCES

Hof, A. L. (2001). *Neural Plasticity,* **8** (1-2), 71-81.
Murray, M. et al. (1971). *Journal of Bone and Joint Surgery*, **53**, 259-274.
Nadeau, S. et al. (2001). *Critical Reviews in Physical and Rehabilitation Medicine,* **13** (1), 1-25.
Shavelson, R. J. and Webb, N. M. (1991). *Generalizability Theory* Newbury Park. Sage.

ACKNOWLEDGMENTS

Table 1: Reliability coefficients and SEMs of the three hip stiffness parameters at the three knee positions

	K0°			K45°			K90°		
	Moment	**Angle**	**Rigidity**	**Moment**	**Angle**	**Rigidity**	**Moment**	**Angle**	**Rigidity**
Reliability	0.71	0.61	0.35	0.70	0.78	0.26	0.73	0.61	0.26
SEM	6.65 Nm	6.18°	0.36 Nm/°	5.98 Nm	5.61°	0.25 Nm/°	5.58 Nm	7.8 °	0.29 Nm/°

WHEELCHAIR SKILLS TESTING AND TRAINING:
PROTOCOLS FOR CLINICAL AND RESEARCH PURPOSES

R.L. Kirby,[1] C. Smith,[2] K.L. Best,[2] C.G. Corkum[2] and D.A. MacLeod[3]

[1]Division of Physical Medicine and Rehabilitation and [2]School of Health and Human Performance, Dalhousie University, Halifax, Canada, kirby@dal.ca
[3]Clinical Locomotor Function Laboratory, Queen Elizabeth II Health Sciences Centre, Nova Scotia Rehabilitation Centre Site, Halifax, Canada

INTRODUCTION

The wheelchair is the most important therapeutic tool in rehabilitation. Much is now known about the biomechanics of wheelchair propulsion. Nevertheless, there is still much room for improvement in the wheelchair-provision process. The purpose of this report is to describe the current status of our ongoing development and evaluation of a set of testing and training protocols for manual wheelchair skills.

METHODS

We have been developing the Wheelchair Skills Program (WSP) since 1995. It consists of the Wheelchair Skills Test (WST) and the Wheelchair Skills Training Program (WSTP). Development has taken place in an iterative fashion, formally evaluating the measurement properties of the WST and carrying out controlled trials of WSTP efficacy.

RESULTS AND DISCUSSION

To date, we have studied >500 research participants, many of them on two or more occasions. There have been no serious adverse incidents during testing or training. The measurement properties of the WST have been very good to excellent. The WSTP has been efficacious in improving the wheelchair skills of wheelchair users, caregivers and occupational therapy students. A number of interesting problems (e.g., curb ascent and wheelie performance) have been identified that lend themselves to biomechanical solutions. On the basis of the studies to date, the WSP was upgraded to the 57-skill Version 3.1 in March 2004.

SUMMARY

The WSP is a valuable set of tools for clinicians and researchers.

REFERENCES

A list of our wheelchair-related publications and the WSP Manual can be downloaded from our website: www.wheelchairskillsprogram.ca.

ACKNOWLEDGEMENTS

GENERALIZED METHOD FOR SIZING TRANSTIBIAL PROSTHETIC SOCKETS IN HOMOGENEOUS POPULATIONS

Mary Beshai[1], Tim Bryant[2], Rob Gabourie[3],

[1]M.Sc, P.Eng, Queen's University, Department of Mechanical Engineering, Kingston, ON, beshai@me.queensu.ca
[2]PhD, P.Eng, Queen's University, Department of Mechanical Engineering, Kingston, ON
[3]CPO(c), Niagara Prosthetics and Orthotics, St. Catharines, ON

INTRODUCTION

In post conflict regions, there is often a need to fit a large number of amputees in a relatively short period of time with prosthetic limbs. However, the lack of experienced prosthetists and the necessary materials and tools to design and fabricate custom sockets creates an unsatisfactory environment where many are without the prosthetic limbs they need.

The objective of this study is to examine homogeneous amputee populations in Thailand and Vietnam and develop a statistical method by which appropriate socket shapes and sizes are specified to meet the needs of these groups. It is proposed that the use of a limited number of prefabricated sockets, within the framework of a three-tiered fitting regime, be considered to allow the local prosthetists to increase the number of patients assisted while maintaining appropriate levels of prosthetic care. This is based on the concept that a primary fit (Tier 1) is achieved with a prefabricated socket, a secondary fit (Tier 2) is achieved with slight modifications to the prefabricated socket, and a tertiary fit (Tier 3) requires a custom socket to be fabricated.

METHODS

The specific objectives of the study are:

- To apply statistical methods to describe the residual limb sizes and shapes of a sample of anthropometric data from amputees in Thailand and Vietnam,

- To develop a family of generalised prosthetic socket sizes and shapes for the sample populations, and

- To validate the proposed prosthetic socket sizing model on samples of the Thailand and Vietnam amputee population by indicating the likely distribution of patients who would require primary, secondary, and tertiary fits.

Research into the use of principal components analysis (PCA) for biomedical application has yielded successful results, including elbow prosthesis design (Wevers, 1985), gait waveform analysis (Deluzio, 1997), and post surgical joint alignment analysis (White, 2001), and prosthetic socket design (Beshai, 2003). PCA was performed on a set of key residual limb variables from data collected in Thailand and Vietnam. Partitioning the principal component distributions to different shapes and sizes, and the inclusion of a socket liner model formed the basis of the sizing model. Application of tolerance models, developed for otherwise healthy post-traumatic amputees, allows a reduction in the number of required sockets. Socket rectification models were applied based on current prosthetic practices and recommendations were made for specific socket dimensions for manufacturing.

RESULTS AND DISCUSSION

Anthropometric measurements were collected from transtibial residual limbs of 15 patients in Thailand and 25 patients in Vietnam. Despite the small sample sizes, it was possible to approximate the measurements with a normal distribution. A principal components analysis indicated that two components could describe the limbs: the first principal component (F_1) has the greatest impact on the model and describes a general shape while the second component (F_2) introduces slight modifications to that shape.

This approach allows the determination of a limited number of sizes, 83-92% of the variance within the Vietnam, Thailand, and Combined sample populations. In a post-hoc analysis of fit, the three size two shape model required a custom (Tier 3) fit 8% of the time, whereas a Tier 1 or Tier 2 fit was achieved 36% and 56% respectively within the Vietnam sample, as shown in Table 1. This indicated that relatively few sizes could be used to fit homogenous populations.

Residual Limb Model			Fitting Levels		
Shapes	Sizes/Shape	Method	Tier 1	Tier 2	Tier 3
3 shapes (A, B, C)	5 Sizes (a,b,c,d,e)	All sizes	44%	52%	4%
1 shape (B)	5 Sizes (a,b,c,d,e)	Universal Optimization 1	28%	56%	16%
3 shapes (A, B, C)	1 Size (c)	Universal Optimization 2	12%	48%	40%
3 Shapes	2 Sizes	Universal Optimization 3	36%	56%	8%
5 Sizes (Ad, Bd, Be, Cc, Ce)		Specific Optimization (minimal sizes)	28%	68%	4%
7 sizes (Ab, Ad,Bb, Be, Cb, Cd, Ce)		Specific Optimization (best coverage)	44%	52%	4%

Table 1: Residual limb model and anticipated patient fit.

SUMMARY

The study demonstrates that principal components analysis, accompanied by acceptable tolerance models, is a practical approach to sizing a transtibial amputee population and has shown that the methodology is transferable to other homogeneous amputee populations.

REFERENCES

Wevers, HW, *et al.*, (1985), J. *Biomed Engineering*, **7**, 241-6
Deluzio, KJ, (1997), *PhD Thesis*, Queen's University
White, DA (2001), *M.Sc Thesis*, Queen's University
Beshai, LM (2003), *M.Sc. Thesis*, Queen's University

ACKNOWLEDGMENTS

A PLANAR KINEMATIC MODEL OF SWING PHASE FOR TRANSFEMORAL PROSTHETIC SYSTEMS

C.B. Higgs[1,2], J.T. Bryant[1,2], R.Gabourie[3], C.K. Mechefske[1]

[1]Department of Mechanical Engineering, Queen's University, Kingston, Ontario, Canada, bryant@me.queensu.ca
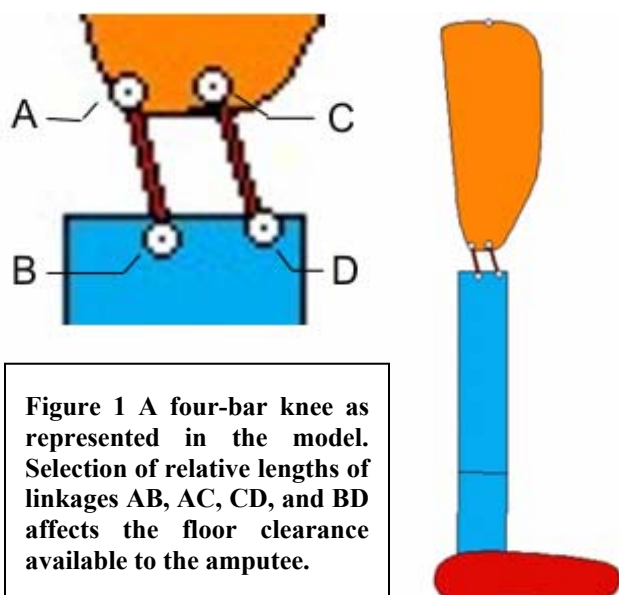[2]Human Mobility Research Council, Kingston General Hospital, Kingston, Ontario, Canada
[3]Niagara Prosthetics and Orthotics, St. Catharine's, Ontario, Canada

INTRODUCTION

Ground clearance is an important consideration for the transfemoral (TF) amputee. Upon flexing the knee the effective length between the hip and the toe of a single-axis knee increases. Amputees wearing such knee joints with a solid ankle must lift their prosthetic leg from the hip to avoid dragging their toes on the floor; this results in an inefficient and unnatural gait. A four-bar knee can enhance toe clearance if the linkages of the four-bar knee are positioned favourably.

Using a planar dynamic model of the stance phase of TF amputee gait (Dundass CK and Mechefske CK, 2000) as a basis, a kinematic model of the swing phase has been developed. In this model, the ground clearance associated with different four-bar knee designs can be compared quantitatively and visually (in the sagittal plane); thus knee component design can be better optimised.

Figure 1 A four-bar knee as represented in the model. Selection of relative lengths of linkages AB, AC, CD, and BD affects the floor clearance available to the amputee.

METHODS

An OPTOTRAK® camera system was used to collect kinematic data for the gait of a TF amputee walking on level ground. The subject was an excellent walker and wore a four-bar knee prosthesis by Century XXII®. From these data, thigh, pylon, and foot angles and trajectories were determined. The thigh angle and trajectory were inputs to the swing phase model.

The exact positions of the pin joint connections of the four-bar knee were located by a ShapeGrabber® laser scanner.

While the subject was seated, his shoe sole was traced by a digital probe. Two known points on the pylon were located by the probe to allow the shoe-sole trace to be located in the local pylon coordinate system. The shoe-sole trace was then plotted at each instant during the swing phase. The percentages of the gait cycle where minimum ground clearance occurred, and the corresponding thigh angle, were noted.

RESULTS AND DISCUSSION

As expected, quantifiable and significant changes in ground clearance were observed when the locations of the knee pin joints, i.e. A, B, C, D, were adjusted in the model. With a fixed thigh, comparisons were made between the effective thigh-to-toe length of a single axis knee and that of three commercially-available four-bar knees. The model and bench top results agreed to within one and a half millimetres.

Each amputee develops a unique gait strategy that is most efficient, comfortable, and least painful for them. Energy requirements, kinematics and kinetics of TF amputee gait change to adapt to different prosthetic knee alignments or knee controller designs (Schmalz T et al., 2002; Stein JL and Flowers WC, 1987). Any adjustment made to the four-bar linkage lengths or pivot locations then may result in adaptations to the amputee's gait strategy. This model thus serves as a consistent basis for comparison between prosthetic components by representing one consistent gait pattern.

This model allows a systematic comparison of different knee designs. For each thigh angle observed in the gait lab, the ground clearance associated with several possible knee angles can be recorded for multiple knee designs. Consultation with an experienced prosthetist throughout the modeling process confirmed the practicality of the model as a design tool.

SUMMARY

A sagittal-plane model of the kinematics of a TF prosthetic component has been developed. This model is sensitive to changes in knee component design and is a useful design tool to predict ground clearance in the swing phase.

REFERENCES

Dundass CK and Mechefske CK (2000). *International Society of Biomechanics XVIIIth Congress - Book of Abstracts*, Munchenstein, Switzerland.

Schmalz T et al. (2002). *Gait and Posture,* **16**, 255-263.

Stein JL and Flowers WC (1987). *Journal of Biomechanics,* **20**, 19-28.

REACH MOVEMENT IN PARKINSON'S DISEASE: EFFECTS OF DEMAND, MEDICATION, AND PLANNING

Jon Doan[1], Ian Q. Whishaw[2], Sergio M. Pellis[2], Oksana Suchowersky[3], Lesley A. Brown[1]
[1]Department of Kinesiology, University of Lethbridge, Lethbridge, AB, T1K 3M4, jon.doan@uleth.ca
[2]Department of Psychology and Neuroscience, University of Lethbridge, Lethbridge, AB, T1K 3M4
[3]Heritage Medical Research Clinic, University of Calgary, Calgary, AB, T2N 4N1

INTRODUCTION

Basic forms of learned motor plans persist for patients into the late stages of Parkinson's disease [Bennett et al., 1995; Rand et al., 2000; Whishaw et al., 2002]. However, expression of these movements can be disrupted by the perception of threatening environmental constraints, such as walking in crowded situations. It is possible that common cognitive resources are used both to interpret context and to produce movement for Parkinson's disease patients (PD) [Bond and Morris, 2000; Morris et al., 2000]. The purpose of this study was to quantify deficits in spatiotemporal kinematics among PD, in response to increased task accuracy demand, and to investigate the influences of PD drug treatment and directed pre-planning on these kinematics [Johnson et al., 2003]. The movement studied was an ethologically-valid reaching task.

METHODS

7 PD in on and off medication conditions (ON, OFF) and 6 controls (OAC) participated in this experiment. Subjects performed a seated drinking task, comprised of a targeted reach, grasp, transport to mouth, sip, and return to lap. Task demand was manipulated by changing liquid fill level (high task demand condition (FULL), fill volume$\geq$110 ml; low task demand condition (LOW), fill volume$\leq$20 ml) in a plastic glass target (diameter = 0.06 m, maximum fill volume = 150 ml). In both target conditions, the glass was placed on a self-standing pedestal at a horizontal reach distance normalized to subject arm length. Participants wore vision-occluding goggles (PLATO, Translucent Technologies, Toronto, ON) that served to initially conceal target condition. During pre-test instructions, subjects were informed that there would be two preparatory events: the opening of the goggles, and a subsequent audio 'GO' signal, which would follow at one of four latencies (0 ms, 200 ms, 500 ms, 800 ms). Instructions to subjects emphasized using the 'GO' signal latency period to pre-plan reach.

Joint displacement data were collected using a standard passive reflective marker set and a commercial motion analysis system (PEAK Products, Englewood, CO). Movement phase onset times were derived from the reach wrist velocity derivative using positive and negative versions of a velocity-based algorithm. EMG signals were collected from the anterior deltoid and the bicep of the reach arm, and participants were seated on a force plate for recording centre of pressure trajectory during preparation and reach.

RESULTS

Results showed that OFF had longer durations for all reach events. In addition, OFF used delayed movement sequences (absolute times to peak velocity, peak acceleration, and peak deceleration) and reduced peak velocity and acceleration magnitudes to complete the REACH. OFF showed further decreases in peak velocity and acceleration, as well as relative phase duration, for initiating and executing high accuracy reaches. While ON were still deficient in duration of REACH and peak REACH velocity and acceleration, compared to OAC, they showed no significant increase in deficits with higher task accuracy constraints. A most compelling finding was that both ON and OAC showed an ability to make use of 500 ms and 800 ms pre-planning periods to decrease motor response time to both the LOW and FULL targets (Figure 1), while OFF only showed benefit from pre-planning at the longest latency (800 ms) in minimal task demand (LOW).
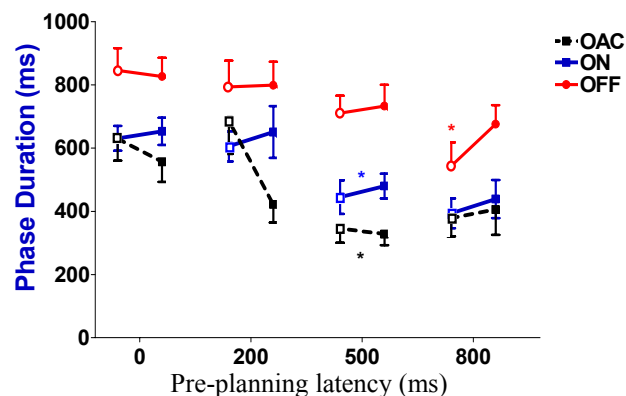

Figure 1: Mean phase duration times (with SEM) for pre-motor response phase (PRT), at all pre-planning levels. Mean PRTs to LOW targets are open symbol in each pair, while mean PRT for FULL reach is the closed symbol. (* p<0.05)

SUMMARY

These results show that interpreting and satisfying increased accuracy demands in a real-world task can alter the expression of movement among OFF, and suggest that a cognitive resource sharing conflict may be responsible for the negative effect. PD medication and directed pre-planning may help to reduce this conflict by enabling a more typical, unconscious expression of this well-learned motor plan.

REFERENCES

Bennett KMB, et al. (1995). *Brain*, **118**: 959-970.
Bond J, Morris, M.(2000). *Arc. Phys. Med. Rehb.* **81**,110-116.
Johnson AM. et al. (2003). *Mot. Control*, **7**, 71-81.
Morris M. et al. (2000). *Gait Posture*, **12**, 205-216.
Rand MK et al. (2000). *Neuropsychologia*, **38**, 203-212.
Whishaw IQ., et al. (2002). *Behav. Brain. Res.*, **133**, 165-176.

ACKNOWLEDGEMENTS

POSTURAL CONTROL IN TRANS-TIBIAL AMPUTEES

Hugo Centomo[1,2] and François Prince[1,2,3]
[1] Department of Kinesiology, University of Montreal, Canada
[2] Gait and Posture Laboratory, Marie Enfant Rehabilitation Center, Montreal, Canada
[3] Department of Surgery, Faculty of Medicine, University of Montreal, Canada
e-mail : hugo.centomo@umontreal.ca

INTRODUCTION

Many studies on postural control adult amputees have been performed. However, findings so far are non-consistent perhaps due to the wide variation in the use of balance measures, subject population (type and time of amputation) and health status conditions (e.g. diabetes)[1-3]. Little is known about the postural stability in child trans-tibial amputees. We investigated the postural steadiness by using the mechanism described by Winter et al.[4] where in normal adults, the displacement of the right and left center of pressure (COP) have been associated to an ankle strategy (COP_c) in A/P direction while a hip load/unload (COP_v) strategy was used in M/L. The purpose of this preliminary study is compared the postural steadiness of child trans-tibial amputees and a control group.

METHODS

Four unilateral trans-tibial amputee children (mean age = 12 years) and 5 healthy children (mean age = 10 years) were tested. Subjects were asked to stand in dual stance as still as possible during two 120-s trials on two adjacent AMTI force platforms. COP_{net} was estimated as follow:

$$COP_{net} = COP_l \frac{R_{vr}}{R_{vr} + R_{vl}} + COP_r \frac{R_{vl}}{R_{vr} + R_{vl}}$$

where COP_l and COP_r are the COP's under the left and right foot respectively; R_{vl} and R_{vr} are the vertical ground reaction forces under the right and left foot. The COP_c is estimated by:

$$COP_c = \overline{R_l} \times COP_l + \overline{R_r} \times COP_r$$

where $\overline{R_l}$ and $\overline{R_r}$ are the average vertical ground reaction force.
The COP_V was estimated as follow:

$$COP_v = COP_{net} - COP_c$$

Root mean square (RMS) amplitude was calculated for each parameter. A Mann and Whitney test was used to evaluate the difference between the control and the amputee groups.

RESULTS AND DISCUSSION

As shown on Figure 1, there is no significant difference in all postural parameters (COP_{net}, COP_c and COP_v) between the control group and the trans-tibial amputee group in both A/P and M/L directions. However, a significant correlation (r=0.7) between the amplitude of COP_{net} and age in A/P and M/L was observed.
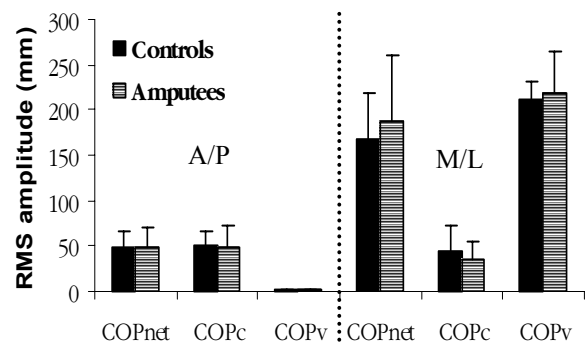

Figure 1. COP_{net}, COP_c and COP_v displacement (in mm) in A/P direction for trans-tibial amputees and controls subjects.

These preliminary results showed that trans-tibial amputee children used the same postural mechanisms than the control group. The variation of postural parameters seems to be more an effect of maturation than an effect of muscle, squeletal or proprioceptive lost. Trans-tibial amputees may used there proprioceptive information more efficiently to compensate their musculo-squeletal lost.

ACKNOWLEDGMENTS

REFERENCES

[1]Fernie, GR & Holliday, PJ, JBJS 60-A, 895-8. 1978
[2]Isakov, E, & al., Arch Phys Med Rehab 73, 174-8. 1992
[3]Vittas, D & al., Prosth Orth Inter 10, 139-41. 1986
[4]Winter, DA & al., Neuro Res Com 12, 141-8. 1993

THE MASSES OF RIGID AND WOBBLING LEG TISSUES CONTRIBUTE LITTLE TO TIBIAL RESPONSE PARAMETERS FOLLOWING HEEL IMPACT

Jeffrey D. Holmes[1], Janice M. Flynn[2], and David M. Andrews[3]

[1]Department of Rehabilitation Science , University of Western Ontario, London, Ontario, Canada, jdholmes@uwo.ca

[2]Department of Kinesiology, University of Waterloo, Waterloo, Ontario, Canada

[3]Department of Kinesiology, University of Windsor, Windsor, Ontario, Canada

INTRODUCTION

The effect that wobbling mass (Gruber et al., 1987) has on force transmission through the leg as a result of impulsive heal impacts can be influenced by the magnitude of the masses of the various segment tissues, the coupling between soft and rigid tissues, and level of leg muscle activation. The purpose of this study was to quantify the contribution of leg tissue masses and muscle activation levels to peak tibial acceleration (PTA), time to peak tibial acceleration (TTP), and maximum rate of peak tibial acceleration (RTAmax) following heel impact.

METHODS

A human pendulum similar to Lafortune & Lake (1995) delivered controlled impacts to the unshod dominant foot of 40 university-aged subjects (20 males, 20 females). External impact forces, tibial accelerations, and tibialis anterior (TA) and gastrocnemius (G) activation levels were measured simultaneously with a vertically erected force plate, uniaxial skin mounted accelerometer, and bipolar surface EMG electrodes, respectively. Individual tissue masses including bone mineral content (BMC), fat mass (FM), lean mass (LM), and wobbling mass (WM) [FM+LM], were determined through anthropometric prediction equations (Holmes et al., 2003). Simple linear regression was used to quantify the contribution of the tissue masses and muscle activation levels to the tibial response parameters (PTA, TTP, RTAmax).

RESULTS AND DISCUSSION

The soft and rigid tissue masses for both genders accounted for very little variance in PTA, TTP, and RTAmax in general (Table 1). Muscular activation did account for a significant amount of variance in TTP and RTAmax for the female sample. Coefficients of determination indicated G activation levels played a more predominant role in determining tibial response parameters than TA. These findings lend support to earlier evidence, that changes in muscle activity could be utilized as a strategy to alter the response of the leg during running (Nigg & Liu, 1999).

Considering that tissue mass magnitude, and muscular activation accounted for no more than approximately one third of the total variance in any of the tibial response parameters, it is likely that mechanical coupling between the wobbling and rigid masses is extremely important for determining the response of the leg to perturbation. Modeling efforts by Nigg & Liu (1999) support this. They showed that decreases in stiffness and damping coefficients between rigid and soft tissues resulted in alterations to tibial response parameters.

SUMMARY

Leg tissue mass magnitudes and muscle activation accounted for little variance in tibial response parameters following impact. The mechanical coupling between the rigid and soft tissue masses of the leg are therefore likely very important for explaining the response of the leg to impact.

ACKNOWLEDGEMENTS

REFERENCES

Gruber, K. et al. (1987). *Biomechanics XB*, 1095-1099.

Holmes, J.D. et al. (2003). Proc.of Int. Society of Biomechanics XIXth Congress, Dunedin, New Zealand.

Lafortune, M.A., & Lake, M.J. (1995). *Journal of Biomechanics,* **28(9)**. 1111-1114.

Nigg, B.M., & Liu, W. (1999). *Journal of Biomechanics*, **32**, 849-856.

Table 1. Coefficients of determination (r) from univariate analysis of PTA, TTP, and RTAmax (* = p≤ 0.05)

		Tissue Masses				Leg Muscle Activation Levels	
		BMC	FM	LM	WM	%MVC TA	%MVC G
Male	PTA	0.025	0.127	0.063	0.007	0.309	0.107
	TTP	0.182	0.157	0.384	0.346	0.148	0.099
	RTAmax	0.097	0.005	0.121	0.118	0.252	0.162
Female	PTA	0.255	0.102	0.259	0.139	0.153	0.409
	TTP	0.148	0.175	0.024	0.115	0.350	0.543*
	RTAmax	0.270	0.060	0.311	0.191	0.260	0.598*

INFLUENCE OF ANTHROPOMETRIC PREDICTION MODELS ON INVERSE DYNAMICS SOLUTIONS

Guillaume Rao, David Amarantini, Eric Berton, Daniel Favier

Laboratoire d'Aérodynamique et de Biomécanique du Mouvement, Université de la Méditerranée, Marseille, France,

amarantini@labm.univ-mrs.fr.

INTRODUCTION

The fundamental problem of inverse dynamics (Hatze, 2000) relates body segments displacements with net joint forces and torques. The inputs required for implementing this approach include kinematics, dynamics and inertial properties of body segments. The sensitivity of inverse dynamics solutions to anthropometric prediction models (APM) remains unclear: it is considered either insignificant (Pearsall and Costigan, 1999), or conversely significant (Silva and Ambrosio, 2004) because the influence of anthropometric parameters cannot be simply quantified. Indeed, masses, center of mass locations and moments of inertia cannot be considered as independent and changes in these parameters may differently influence joint kinetics depending on the conditions of movement.

Resorting to seven APM, the present study aims at providing further clarifications about the influence of anthropometric parameters on estimated kinetics. The 3D net forces and torques were computed at the ankle, knee and hip joints during gait performed at three different speeds. Statistic comparisons were applied to anthropometric parameters and to joint kinetics in order to discuss our results with those depicted in literature.

METHODS

Seven subjects (3 males and 4 females) participated in this study. 3D coordinates of fifteen markers, placed on subjects' anatomical landmarks according to the Helen Hayes Hospital markers set, were recorded at 120 Hz using a six cameras Vicon 624 motion analysis system. The ground reaction force was recorded at 600 Hz using an AMTI forceplate invisibly fixed into the floor. Seven APM (1 geometrical, 3 cadaver-based, 3 derived from living subjects) were applied to estimate mass, position of center of mass and moments of inertia at the foot, the shank and the thigh.

Subjects were asked to perform barefoot passings on the walkway with right foot forceplate contact at three different walking cadences: Preferred, Low and Fast.

3D net forces and moments at the ankle, knee and hip joints were estimated by solving inverse dynamics of a 4-link model of the lower limb using Vicon BodyBuilder. Anthropometric inputs were iteratively derived from each prediction model.

For comparisons, we focused our investigations on the net joint moments around the flexion/extension axis. Results were normalized by subjects' body weight and time was expressed as percentage of total gait cycle duration. One-way Anova (*Models* effect) were conducted to check the influence of APM either on BSP components, on peaks or on RMS deviations between kinetic profiles.

RESULTS AND DISCUSSION

The analysis of inertial properties of body segments showed considerable variations due to the use of different APM. The variations range from 15.02 % for the mean shank center of mass location to 96.15 % for the thigh mean moment of inertia (Table 1). ANOVA indicated a significant *Model* effect on all anthropometric parameters at the foot, the shank and the thigh.

However, each APM behaves differently, thus creating particular inter-dependency between inertial body parameters.

Table 1 Amplitude of variation between APM estimates (%)

	Relative amplitude of variation		
	Foot	Shank	Thigh
Mass	37.40 %	15.81 %	38.37 %
Moment of Inertia	60.56 %	53.43 %	96.15 %
CoM Position	31.99 %	15.02 %	17.96 %

Typical influence of APM on net joint moment estimates for fast cadence is shown at the hip joint on Figure 1. Although the characteristic features of kinetic profiles remain unchanged at all joints, the analysis of the influence of APM on each joint kinetics revealed major variations of the flexion/extension moment amplitudes, varying up to 43 %, 14 % and 18 % for RMS and up to 16 %, 18 % and 20 % for peaks at the ankle, knee and hip joints, respectively. Variations due to APM were either higher or similar during swing and stance because angular accelerations influence the values of the inertial component in the equations of motion. However, ANOVA and post-hoc comparisons showed a significant *Model* effect only when all inertial parameters are under- or over-estimated by using a given APM. On the contrary, kinetic estimates could remained unchanged despite large variations between APM due to possible compensations between inertial, centrifugal, Coriolis and gravitational terms of the equations. The influence of the conditions of movement was not obvious: the effect of APM is lower at Low than at Preferred and Fast walking cadences, meaning that APM effect interact with that of cadence.

The results of this study provide evidence that APM highly affect inverse dynamics solutions. Clarifications are given for the implementation of APM in order to produce accurate estimates of joint kinetics for applications in biomechanics.
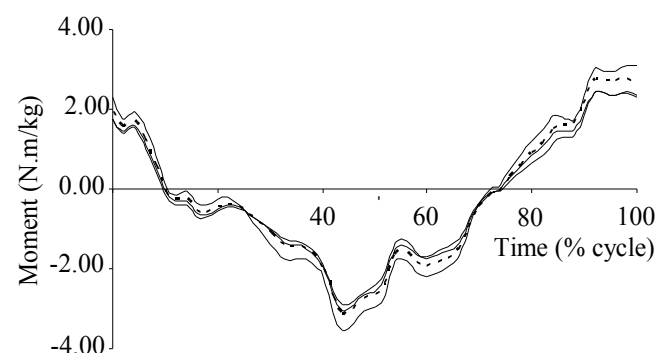

Figure 1: influence of APM on the flexion/extension net joint moment at the hip joint for fast cadence. Each pattern corresponds to the solutions from inverse dynamics with anthropometric data derived from one of the 7 used APM.

REFERENCES

Hatze, H. (2000). *Biol Cybern*, **82**, 133-41.

Pearsall, D.J., Costigan, P.A. (1999). *Gait Posture*, **9**, 173-83.

Silva, M.P., Ambrosio J.A. (2004). *Gait Posture*, **19**, 35-49.

MOVEMENT WITHIN THE SOFT TISSUE PACKAGE DURING IMPACT PHASE OF RUNNING.

Katherine A. Boyer[1] and Benno M. Nigg[2]

Human Performance Laboratory, [1]Department of Mechanical And Manufacturing Engineering and [2]Department of Kinesiology.
University of Calgary kath@kin.ucalgary.ca

INTRODUCTION

The concept of muscle tuning considers the body as a vibrating system and the impact force in locomotion as an input signal into the body with a magnitude and effective frequency. The impact force is transmitted through the body as a wave of acceleration; an increase in muscle activity to dampen the soft tissue vibrations is expected in response to inputs near the resonance frequency of the soft tissue package. Evidence supporting the concept of muscle tuning in one soft tissue package during running has recently been provided (Boyer and Nigg, in press). This support is based on point measurements of soft tissue frequency and acceleration amplitude measurement. Due to differences in natural muscle tension, the overlying tissue and the level of muscle activation from different muscles within a soft tissue package, the mechanical properties may not be uniform throughout the soft tissue package. The control of vibration can only occur in the muscles, therefore if active damping is occurring then vibration must be present within a muscle. However, evidence of vibration within a muscle due to impact has not yet been provided. Therefore, the purpose is to determine if there is a) movement between muscles within a soft tissue package b) movement within a muscle following impact in heel-toe running.

HYPOTHESES

It is expected that a) there will be movement between muscles within a soft tissue package and b) there will be length changes within one muscle.

METHODS

The subject ran at 4.5 m/s on a 16m long runway with a force platform (Kistler, Type Z4852/C) imbedded at its center. Tri-axial accelerometers were placed on the skin overlying the vastus medialis (VM), vastus lateralis (VL), distal rectus femoris (RF1) and proximal rectus femoris (RF2) muscles to quantify tissue movement as described earlier (Wakeling et al., 2002). EMG was measured with bipolar surface electrodes for the RF. Tissue displacement was obtained by double integration of the acceleration signals with $v_o = 0.8$ m/s. All data were sampled at 2,400Hz. Significance of soft tissue responses were tested with repeated measures ANOVA ($p < 0.05$).

RESULTS

- There was a ±10% difference in vibration frequencies for the VM, RF1, and RF2.
- There was a ±50% difference in the vibration frequencies between VL and VM, RF1, and RF2.
- There was a small (±14%) difference in vibration frequency within the muscle (RF).

- There was a change in distance between muscles from t_{TD} to $t_{impact\ peak}$, VM to RF1 10 mm, VM to RF2 20mm, VM to VL 8mm.

Table 1 Frequency and acceleration of quadriceps muscles.

Muscle	VM	RF1	RF2	VL
f [Hz]	51.0 (2.78)	54.8 (2.85)	62.6 (3.87)	77.7* (4.00)
a(peak)	44.9 (3.18)	43.1 (1.31)	43.2 (2.85)	16.5* (1.38)

Mean ± (SE) n=19, 4.5 * $p < 0.05$

- There was a change in length of the RF due to differences in a_{peak} time for RF1 and RF2 (Fig 1).
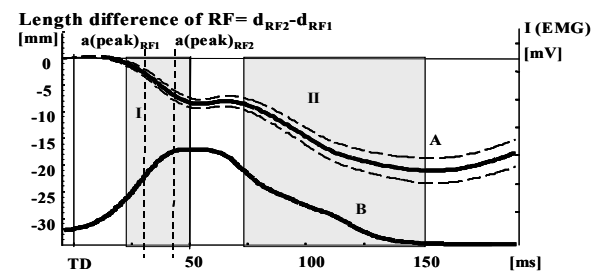

Fig 1 A) Length changes within the RF muscle for the stance phase of running. (I) due to impact wave transmission, (II) due to movement task.
Mean (SE), n=19.
B) Corresponding EMG activity rectus femoris

DISCUSSION

A wave of acceleration travels through the soft tissue package following impact in heel-toe running. This wave results in movement of the soft tissue package relative to the skeleton, movement between muscles within a soft tissue package and within a muscle. The differences in vibration frequency and amplitude are small (10%) between the medially located muscles and larger between the medially and laterally located muscles (50%). This may be due to differences in the passive tension between muscles and the influence of the illiotibial band. Within a muscle the amplitude of acceleration for proximal and distal location is the same, however there is a shift timing of the vibration and a small difference in the vibration frequency between locations. The result is a change in length of the muscle during the impact phase of running. As proposed by the muscle-tuning concept activating the muscle just before and after heel-strike may control this length change. What remains unclear is the correlation between surface measurement and the movement of underlying muscle. Thus, caution is advised when extrapolating measured length changes to the actual changes in the muscle

REFERENCES

Boyer K.A. and Nigg B.M. (in press) *J Biomech.*
Wakeling J.M et al (2002). *J Appl Physiol* 93: 1093-1100

ADAPTATION TO UNILATERAL CHANGES IN LOWER LIMB
MECHANICAL PROPERTIES DURING TREADMILL WALKING

Jeremy W. Noble and Stephen D. Prentice
Gait and Posture Laboratory, Department of Kinesiology, Faculty of Applied Health Sciences.
University of Waterloo, Waterloo, Canada, jwnoble@uwaterloo.ca

INTRODUCTION
In order for the Central Nervous System (CNS) to effectively control the movement of the lower limbs during locomotion it must have sufficient knowledge of the mechanical properties of the lower limb. Previous studies have manipulated limb mechanics by placing an additional mass on the lower limb and reported the changes in limb kinematics and kinetics (Martin et al 2000, Reid & Prentice 2001), however these experiments have not examined how the adaptation evolved immediately following the addition of the mass or its subsequent removal. The purpose of this study was to determine how the CNS adapts to a unilateral change in the lower limbs' mechanical properties. Specifically, bilateral changes in the limb kinematics and kinetics of treadmill gait will be examined in the steps immediately following the addition and subsequent removal of a mass attached to the leg segment.

METHODS
Five healthy young adults were instructed to walk on a treadmill moving at 1.56 m/s for 5 minutes (PRE). Bilateral limb and trunk kinematics were obtained from an OPTOTRAK system (Northern Digital Inc., Waterloo ON) and infrared emitting diodes placed on anatomical landmarks defining a seven segment representation of the limbs and trunk. Individuals were then fitted with a 2 kg mass placed at the centre of mass of the left leg before performing a second 5 minute walking trial (WEIGHT). This was then followed by a 5 minute trial where the participant had no additional mass (POST) placed on the leg.

Segment and joint kinematic time histories were determined using the conventions described by Winter (1991) and net joint moments and powers in the sagital plane were calculated at the ankle, knee and hip joints during the swing phase using standard inverse dynamics (Winter, 1991). Discrete variables including step length, step time and peak joint angles were also calculated for each step. These step measures were then divided into bins of 5 steps to determine any differences within the trials and when a stable walking pattern was attained. These variables were also compared between trials in order to establish condition effects.

RESULTS AND DISCUSSION
After the application of the additional mass, the most notable changes in joint kinematics were observed in the knee angle. Initially the peak knee flexion angle of the weighted limb was greatly reduced but was followed by a gradual increase in knee flexion in subsequent steps (Fig. 1). The peak knee flexion did not return to the amount seen in the PRE condition. Kinematic changes at the hip and ankle were less pronounced. There was an increased amount of dorsiflexion of the ankle during swing.

In the WEIGHT condition the knee exhibited an increase in the extensor moment at the beginning of swing, and an increased flexor moment at the end of the swing phase. These increased moments served to increase the braking action of the knee joint in the weighted limb at the beginning and end of swing to control the momentum of the mass placed on the leg. The hip served to assist in swinging the limb forward with an increased hip flexor moment to increase the amount of hip pull off power at the beginning of swing.
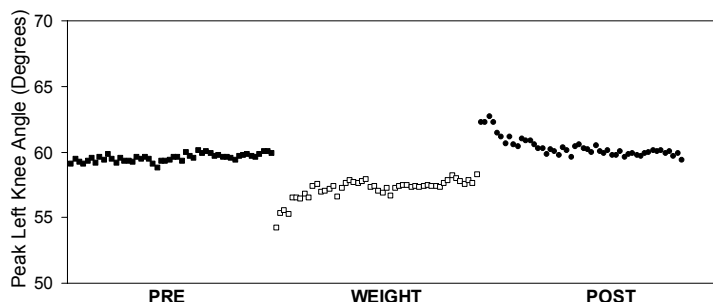

Figure 1: Peak knee angle of the weighted limb in PRE, WEIGHT and POST conditions. Each point represents an average of five consecutive steps.

Following the removal of the mass (POST), there was an increase in the peak knee angle above that observed in the PRE condition, which gradually returned to the peak knee angle that was observed in the PRE condition. This was accompanied by a decrease in the knee extensor moment at the onset of swing and a small decrease in the power absorption at the beginning of swing. There was also an increase in the peak hip angle for the first 35 steps after the removal of the additional mass, although there were no significant changes in hip joint kinetics. There were no significant differences in the weighted ankle kinematics or kinetics between the PRE and POST conditions.

SUMMARY
The results of this study showed that the CNS was able to adapt to changes in the mechanical properties of the lower limb within 40-45 steps, and that increased absorption was required at the knee of the weighted limb to control the heavier limb. Increased pull off power was also required at the hip.

REFERENCES
Martin PE et al (2000). IV WCB. Calgary AB.
Reid MJ & Prentice SD (2001). *Neurosci Res Com*, **29**, 79-87.
Winter DA (1991) The Biomechanics and Control of Human Gait. Waterloo, Waterloo Biomechanics.

ACKNOWLEDGEMENTS

THE EFFECT OF LOAD PLACEMENT AND FATIGUE ON SPINAL CURVATURE AND POSTURE IN PREPUBESCENT CHILDREN

Heather M. Brackley and Joan M. Stevenson
School of Physical and Health Education, Queen's University, Kingston, Canada

INTRODUCTION

Although a weight limit of 10-15% body weight has been well established in the literature for children carrying backpacks on a daily basis, little work has been completed on the design of children's backpacks (Brackley and Stevenson, 2004). Previous work with adults has shown that the design of a pack is important to the comfort and postural adaptations required by the user (Stevenson, 2005). The purpose of this study is to determine the load location (high, medium or low load) that has the least impact on both spinal curvature and body posture while standing or walking in both a rested and fatigued state.

METHODS

Data were collected using a repeated measures design on 15 grade five students at a local school. Each student carried 15% of their body weight with the centre of mass in three locations, high (+ 26.8 cm above L5), medium (+20.3 cm above L5) or low back (+10.3 cm above L5), on three separate days. Spinal curvature and postural measures were taken for unloaded standing, rested standing, rested walking, fatigued walking, and fatigued standing. All fatigued measurements were taken after the child had walked 1000m around the school. Ratings of perceived exertion (1-10) were collected every 250m to determine if the children felt fatigued and at the end of the trial, a body map diagram was used to rate their discomfort by region. Additional information regarding backpack use, physical activity, and anthropometrics were also collected from each student on the first day.

Spinal curvature was measured using a specially designed backpack with 16 rods, attached to high resolution linear potentiometers, protruding in a vertical line from the pack. Composite analysis of the 16 rods provides a non-invasive and portable estimation of spinal curvature. Postural changes were determined using 2-dimensional video. The ankle, hip, base of neck, C7, ear and head orientation were digitized using the PEAK Motus V.3 System. The posture measures evaluated were: total body lean (TBL), trunk forward lean (TFL), cranio-vertebral angle (CVA) and head angle (HA).

RESULTS AND DISCUSSION:

The average age of subjects was 10.43 ± 0.27 years with an average body mass index of 19.23 ± 3.36 kg/m^2. Fourteen of the fifteen subjects in the study used a backpack to transport their belongings to and from school, indicating the subjects have experience with this device.

Ratings of perceived exertion (RPEs) follow a linear pattern for all three load placement conditions with no significant difference between the three conditions. A significant difference ($p<0.05$) in RPEs between lap 1 (350m) and lap 4

(850m) is present indicating fatigue did occur in all three conditions.

Results indicate absolute postural changes (TFL+CVA+HA) were greater with high placement than mid and low placement. Spinal curvature changes were greater with the low placement, especially with fatigue. No trends were apparent in the TBL data. Postural changes from unloaded standing were greater with walking and increase with fatigue. The modifications made in both posture and curvature were quite variable between subjects and further study into the relationship between these factors is required.

Figure 1. Absolute postural changes from unloaded standing in 4 measurement conditions and 3 load placement positions
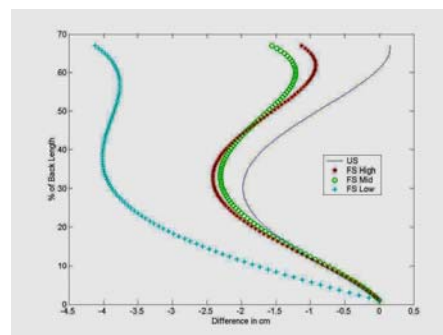

Figure 2. Changes in spinal curvature for 3 load placement positions at fatigued standing

SUMMARY

Although preliminary results demonstrate high inter-subject variability, which negated significance, the mid-placement appears to minimize the changes from unloaded standing posture and unloaded spinal curvature for children of this age. Further study is required to understand the relationship between postural changes and spinal curvature.

REFERENCES
Brackley, H.M. and Stevenson, J.M. (in press) *Spine*
Stevenson, J.M. *et al.* (in press) *Ergonomics*

ACKNOWLEDGEMENTS

THE EFFECTS OF STIFFNESS AND SPEED ON UPPER LIMB ELECTROMYOGRAPHY DURING JOYSTICK USE

Greg Northey[1], Michele Oliver[1], Alex Mclean[2], and Jim Sexsmith[3]
[1]School of Engineering, University of Guelph, Guelph, Ontario, Canada, gnorthey@uoguelph.ca
[2]Dalhousie Medical School, Halifax, Nova Scotia
[3]Faculty of Kinesiology, University of New Brunswick, Fredericton, New Brunswick

INTRODUCTION
The utilization of heavy machinery is a common practice for many industries all over the world. Heavy equipment operation now requires intense work with hand controls in repetitive short-cycle movement patterns and fixed sitting positions with the hands and arms being used 50 to 95% of the working time (Grevsten and Sjögren, 1996). The manipulation of joysticks requires almost constant upper limb muscle activation coupled with a wide range of repetitive wrist and upper limb positions and motions, all of which can increase the operator's susceptibility to repetitive strain injuries. However, no study has been undertaken to assess a comprehensive selection of primary upper limb muscles required for hydraulic actuation joystick manipulation in four primary directions and under variable speed and stiffness conditions. The purpose of this study was to analyse the joystick manipulation induced internal loads on the upper limb, allowing for a more complete assessment of which joystick motion(s) potentially pose the most risk in the development of repetitive strain injuries.

METHODS
After providing informed consent, eight healthy right handed male subjects aged 22 to 43 years (26.3 ± 7.3 yr) participated in the study. All subjects were unfamiliar with hydraulic actuation joystick operation. Eight muscles (pectoralis major, upper trapezius, anterior deltoid, posterior deltoid biceps brachii triceps brachii flexor carpi radialis and extensor carpi radialis) were selected for surface EMG analysis using bipolar Ag-AgCl surface electrodes (Multi Biosensors Inc, pre-gelled, 0.4 mm diameter). Three right handed hydraulic actuation joysticks from the most common type of North American excavator were studied, one with normal stiffness setting and the others with lighter and heavier springs respectively. Each joystick was instrumented with an array of four Hall effect sensors (Honeywell SS495A1 high performance miniature ratiometric linear solid state Hall effect sensors, sensitivity 3.125 mV± 0.156, excitation voltage ±10V) and rare earth magnets (Lee Valley Tools Ltd.) to allow for the accurate assessment of joystick displacement. All EMGs and Hall effect signals were recorded at a sampling frequency of 1024Hz using Noraxon Myoresearch™ software (version 2.02, Noraxon USA Inc) and a 12-bit A/D converter (Noraxon USA Inc). The subjects were asked to move the joystick from rest (neutral joystick position) straight to the endpoint of joystick motion (approximately 22° of rotation) in one of four directions (forwards, backwards, inwards and outwards) and back to neutral again. Each subject was asked to perform a 'fast' and 'slow' version of each motion for each joystick stiffness, giving six experimental conditions for each motion. Subjects performed each experimental condition twice. All EMG data (MVC, SMVC, windowed trial data) were full wave rectified and second order butterworth low pass filtered at 6Hz and normalized to isometric MVC and peak dynamic. Intra-subject ensemble averages were created for each experimental condition and integrated EMG (iEMG) and peak EMG were found and analysed using a general linear model (GLM) which assessed the effects of speed, stiffness and motion effects on EMG activation.

RESULTS AND DISCUSSION
This joystick is designed to keep the wrist in a more natural semi-pronated position, thereby reducing wrist flexion and extension. However, for both iEMG and peakEMG, motion comparisons indicate that the outwards direction causes the largest activation change (peakEMG of 21% MVC) for flexor carpii radialus, indicating that at the extreme points of joystick outwards motion the flexor tension can be quite high to maintain wrist and hand posture and minimum grip force on the joystick. In addition, this design appears to have transferred the strain of the motion onto the shoulder region. All shoulder muscles studied were activated to the greatest degree in the forward direction (peakEMG of 71% MVC for upper trapezius, 43% MVC anterior deltoid and 39% MVC posterior deltoid.) and the upper trapezius had the highest peakEMG values for all motions except backwards (only anterior deltoid displayed more). This indicates that all motions require a large amount of shoulder postural control to support the arm and hand in the posture preferred by the operator or required to complete the motions. Armrests may be responsible for much of the upper trapezius and deltoid muscle loading due to the forced posture demands they require and lack of support in the forward direction.

Of the three joystick stiffnesses, the heavy joystick was found to have the highest values for the muscle activation variables. Speed was found to be significant for all muscles in all variables except for the anterior deltoid iEMG. In all cases, the higher speed produced the higher activity level. While the GLM procedure revealed a number of significant interaction effects between combinations of speed, motion and stiffness, it is clear that joystick controls that require or allow high speeds will increase muscle activation.

Overall, every joystick motion was shown to require at least a constant low level (between 2-5% MVC) muscle activation for all muscles. When coupled with the motion and postural demands this suggests that hydraulic-actuation joystick use can contribute to the development of long term muscular pain and injury. The results of this study indicate that joystick range of motion may be an important contributor to the development of repetitive strain injuries.

REFERENCES
Grevsten,S. and Sjögren,B. (1996) Symptoms and sickleave among forestry machine operators working with pronated hands. *Applied Ergonomics* **27**, 277-280.

ACKNOWLEDGEMENTS

TOLERANCE LIMIT VALUES FOR MANUAL ELECTRICAL CONNECTOR TASKS

Jim R. Potvin, Joel A. Cort, I. Christina Calder, Michael J. Agnew

Faculty of Human Kinetics, University of Windsor, Windsor, ON, Canada, jpotvin@uwindsor.ca

INTRODUCTION

There are some tasks, within automobile assembly, that are repeated at many different workstations throughout the process of building the vehicle. One such task is the mating of electrical connectors. However, we know little about human capabilities for these tasks and, thus, it is difficult to design them safely. The purpose of the current study was to investigate the human limitations for electrical connector tasks in automotive manufacturing. It is anticipated that the results of this study will further our understanding of the demands of electrical connector tasks so that future tasks can be designed to reduce the risk of repetitive strain injuries to the upper limbs.

METHODS

The study employed a psychophysical methodology which included 24 female subjects from a wide range of working ages. Each subject was provided with a total exposure of 27 hours to simulated electrical connector tasks and at least 18 hours of training before each final testing session. The independent variables in this study were Grip Type (Oblique Grasp, Finger Press, Pulp Pinch), Insertion Frequency (2, 7 and 12/minute) and Wrist Posture (Extended, Neutral, Ulnar Deviated). Each subject performed all combinations of Frequency and Grip Type but were randomly assigned to only one of the Wrist Posture conditions (n=9).

Each task was performed with a device that allowed for the simulation of electrical connection tasks. This device traveled a distance of 1.3 cm with each insertion. With an unmarked dial, subjects could adjust the tension on a spring to control the required effort, and force-time histories were recorded with an in-line force transducer. Subjects were instructed to work at the highest efforts that they would find acceptable for an eight hour period. For each trial, the dependent variables were Peak Force and Force Impulse.

RESULTS/DISCUSION

Subjects were observed to provide very reliable estimates of their maximal acceptable forces and impulses for each of the nine conditions tested (3 Frequencies x 3 Grip Types) as each subject was randomly assigned to one of the three wrist postures. Within-subject coefficients of variation (CVs) were observed to be approximately 10% for both force and impulse measures. Statistical analyses indicated significant main effects of Grip Type and Frequency for Peak Force and Force

Impulse, with no significant effects of wrist posture and no interactions between variables. Oblique Grasps were observed to result in higher acceptable efforts than both the Finger Press and Pulp Pinch, and the acceptable efforts were observed to decrease with increasing insertion frequency. Tolerance Limit Values (TLVs) were calculated as those forces and impulses that would be acceptable to at least 75% of females. On average, subjects selected acceptable Peak Forces that were 62-63% of their absolute maximum for Pulp Pinch and Finger Press grips and 48% of maximum for the Oblique Grasps. The consistency of these relative efforts may indicate that psychophysical limits may be approximated as some percentage of maximal strength values.

The results of this study increase our understanding of human capacities for electrical connection tasks and provide limits that will allow for the design of safer manufacturing workplaces.
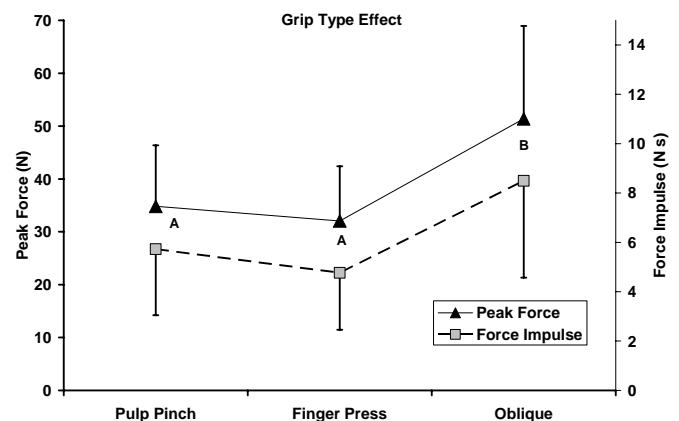

Figure 1: Main effect of Grip Type on Peak Force and Force Impulse. Means with the same letter are not significantly different. Standard deviation bars are shown.

Table 1: Summary of TLVs for Peak Force (PKF) and Impulse (IMP). The are demands predicted to be acceptable to 75% of females for the given frequencies

	Pinch Grip		Oblique Grasp		Finger Press	
	PKF (N)	IMP (Ns)	PKF (N)	IMP (Ns)	PKF (N)	IMP (Ns)
2/min	28.2	4.2	41.6	6.2	26.0	3.5
7/min	27.4	4.0	40.4	5.9	25.2	3.3
12/min	25.7	3.6	37.9	5.3	23.6	3.0

ACKNOWLEDGEMENTS

THE EFFECT OF WORK PAUSES AND TYPING RATE ON THE BIOMECHANICAL DUTY CYCLE

Gillian Del Monte and Anne Moore

School of Kinesiology and Health Science, York University, Canada, gdelmont@yorku.ca

INTRODUCTION

Work-related musculoskeletal disorders (WRMSDs) are a continuing problem in the workplace; including jobs involved with keyboard use. One of the risk factors associated with keying is static exertion (Gerard et al, 1996). The extensors of both the wrist and fingers are active not only to perform a keystroke, but also remain active between keystrokes against the force of gravity and passive muscle forces. One way to lessen the effects of static loading is to implement adequate muscular rest. Studies have investigated various work-rest schedules, however many of these studies have focused primarily on subjective measurement. Without measuring muscular activation, one does not know if the muscles are indeed resting. It is also unclear whether a job consisting of alternating periods of keying and listening, such as those found in call centers, would provide acceptable levels of static muscular activity. The purpose of this study is to analyze the electromyographic (EMG) signal to investigate the amount of rest taken throughout an alternating keying and listening task; and in turn, to determine how this is affected by keying speed.

METHODS

Surface EMG from the extensor indicis (EI), extensor carpi radialis brevis (ECRB), flexor digitorum superficialis (FDS), and trapezius (TRAP) was recorded from the dominant arm of four touch typists (2 male, 2 female). RMS EMG was collected at 10Hz using a commercially available system (ME3000P8, MEGA Electronics, Finland). Prior to collection, subjects performed a standard typing test to establish their maximum typing speed. On testing day, each subject performed two alternating tasks, each with a cycle time of one minute, over a 10-minute period. The first task was text entry controlled for speed. Participants were instructed to input scrolling text as it appeared to them the computer screen. The second was a listening task. Subjects were fitted with a headpiece similar to that of a call-centre employee, through which a short story was dictated to them. Subjects were instructed not to enter text during this alternate task. No further instructions were given. The protocol was repeated at two different keying speeds: natural (80% maximum) and fast (90% maximum). There was a five-minute break between trials.

Table 1. Percent rest taken during keying, listening, and over the 10-minute trial (total), (mean across subjects and cycles).

	Natural			Fast		
	Keying	Listening	Total	Keying	Listening	Total
EI	0.08	43.80	19.67	0.18	22.93	11.61
ECRB	0.12	19.61	9.83	0.02	14.59	7.45
FDS	7.88	59.79	38.01	5.02	48.61	36.65
TRAPS	16.08	35.46	29.67	5.79	34.09	20.51

EMG was analyzed using the static (10th %ile), median (50th %ile) and peak (90th %ile) levels of the APDF (Jonsson, 1982), as well as a gaps analysis (Veiersted et al, 1990). Both analyses were performed over the complete 10-minute trial and over each individual cycle of keying and of listening.

RESULTS AND DISCUSSION

Results suggest that 10% rest is not available for the forearm muscles, particularly the extensors, during keying (Table 1). The alternate task does provide some relief, predominantly for the flexors; however, static loading is still present within the extensors (Figure 1). Furthermore, with the two tasks combined, the ECRB did not achieve rest 10% of the time. This suggests that the participants did not tend to rest their hands/fingers when the task allowed for it. Increased speed was associated with increased error rate, increased Peak EMG levels (Figure 2) and decreased rest even during the listening task. These results have implications in both the design of tasks and in operator training.
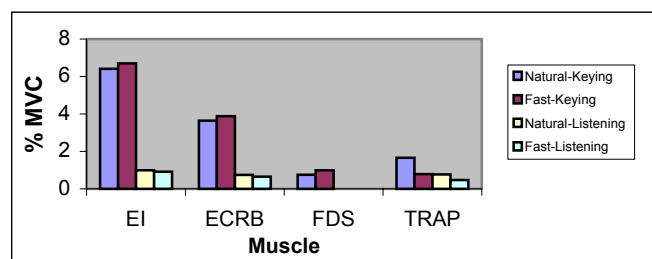

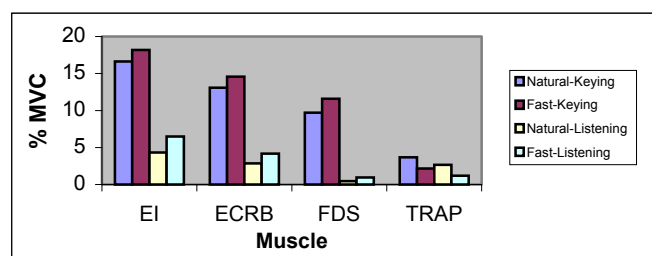**Figure 1:** Static APDF (mean across subjects and cycles).

Figure 2: Peak APDF (mean across subjects and cycles).

REFERENCES

Gerard, M.J. et al (1996). *Am Ind Hyg Assoc J,* **57**, 849-860.
Jonsson, B. (1982). *J. Human Erg*. **11**, 73-88.
Veiersted, K et al (1990). *Int Arch Occ Env Health* **62**, 31-41.

SHEAR INSTABILITY OF THE L4-L5 JOINT: EXAMINATION OF SPINAL MUSCULATURE REINFORCEMENT POTENTIAL

Samuel Howarth and Stuart McGill
Department of Kinesiology, University of Waterloo, Waterloo, Canada, sjhowart@ahsmail.uwaterloo.ca

INTRODUCTION

Overloading of supporting tissues in the back to the point of plastic deformation causes instability (Oxland et. al., 1991) such that reinforcing the instability is a primary objective of many therapeutic approaches. Instability in neutral postures is most effectively reinforced by muscle contraction that leads to increased muscle stiffness (Stokes & Gardner-Morse, 2003). Numerous models have been developed to quantify the rotational stability of the lumbar spine. The energy approach common with determining instability in Euler buckling was not applicable because the mode of buckling in shear is precisely the mode of external force application. Thus, a new method for determining instability in shear was developed. The objective of this work was to determine the ability of the muscles to counteract shear instability at the L4-L5 joint.

METHODS

An anatomically based computer model of the L4-L5 joint was created containing facets, ligaments, and muscles acting at the L4-L5 joint. Mechanical properties of the individual elements were incorporated into a displacement driven algorithm that computed the forces from the individual elements given an applied anterior shear displacement of 0.002 cm along the shear axis of the L4-L5 joint until the first failure of a mechanical structure.

Initially, the algorithm would determine the force-displacement relationship for an intact segment. Afterwards, systematic reductions in overall joint stiffness were performed by either eliminating ligaments, or reducing the stiffness of the disc and or facets to determine the force-displacement relationship for an incomplete motion segment, thus simulating joint injury. The stability index was determined as the displacement driven force difference between the intact and incomplete cases.

For each of the incomplete cases, the muscle force required to buttress the instability was determined by the magnitude of the stability index.

RESULTS & DISCUSSION

The primary result is that the muscle force vector, no matter which combination of activation patterns are created, cannot provide large forces to directly buttress large anterior shear instability (Figure 1).
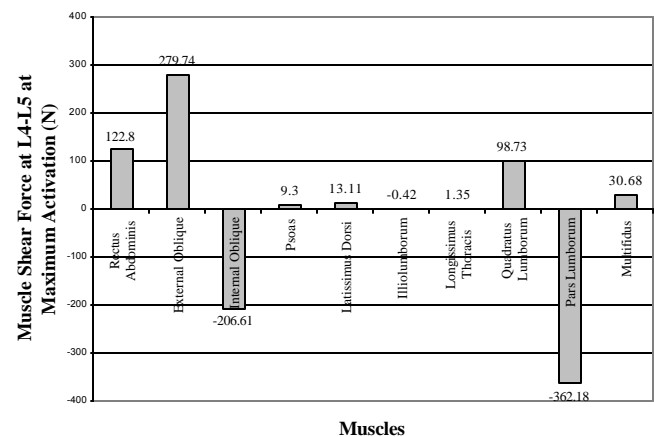

Figure 1 - Ability of individual muscles at L4-L5 in directly resisting applied anterior shear loads when iteratively set to 100% activation.

Moreover, scaling of a known motor pattern that buttresses anterior shear proved that *in vivo* muscle recruitment is insufficient to fully buttress anterior shear instability. This suggests that the muscles have a secondary mechanism that resists anterior shear loads. Muscle when not activated is compliant, and shears readily. However, activation of a muscle increases the stiffness within the muscle, making it more resistant to changes in configuration, and more specifically resists shear displacement. While this is a possible mechanism for muscles to buttress shear, another mechanism has already been established. It has been shown that increased compression increases the overall stiffness of the spine in all modes. Thus, the muscles act as a group to increase the stiffness of the spine through compression which also increases the spine's resistance to shear.

SUMMARY

Shear stability is obtained by muscle activation, but the muscle's mechanism of action is multipurpose.

REFERENCES

Oxland, TR et al (1991). *J. Orthop. Research*, **9**, 452-462.
Stokes, IAF & Gardner-Morse, M (2003). *J. Electromyogr. Kinesiol.*, **13**, 397-402

ANTAGONIST MUSCLE FORCES PREDICTED BY AN OPTIMIZATION MODEL OF THE SPINE USING STABILITY AS A CONSTRAINT FACTOR

Stephen H.M. Brown[1,2], Jim R. Potvin[1]

[1] Department of Kinesiology, University of Windsor, Windsor, Ontario, Canada
[2] Department of Kinesiology, University of Waterloo, Waterloo, Ontario, Canada,
shmbrown@uwaterloo.ca

INTRODUCTION

A major limitation of optimization models of the spine is that they do not predict activity in muscles functioning in a manner purely antagonistic to the external load. Co-activation of antagonist muscles is essential to maintaining stability about the spinal joints (Cholewicki et al., 2002). The purpose of this paper is to demonstrate that the inclusion of spine stability measures as constraints in an optimization model of the spine force the accurate prediction of antagonist muscle forces.

METHODS

A single-joint (L4L5) spine model was developed and tested based on the anatomical data of Cholewicki & McGill (1996).

Two different optimization cost functions were tested in this study: 1) minimization of the sum of the cubed muscle forces; 2) minimization of the intervertebral force at the L4L5 joint.

An experimentally-based level of spine stability about each anatomical axis was set as a constraint in the optimization scheme. These levels of stability were predicted from regression equations developed from a pool of in vivo EMG data for a variety of loading conditions. Stability was estimated, based on the minimum potential energy (PE) concept, as the second derivative of the PE of the spinal system.

A variety of pure flexion and pure right lateral bend external moment conditions were tested on 11 male subjects. Experimentally derived muscle and compression forces were compared to those predicted by the optimization schemes.

RESULTS

Without the inclusion of stability constraints in the optimization model, antagonist muscles were never predicted as being active. In contrast, when stability levels were constrained in the model to levels estimated by the regression equations, antagonist muscles were predicted to be active. Furthermore, these active antagonist predictions were shown to agree quite well with experimental findings.

Errors in the estimation of the compressive force acting at the L4L5 joint were significantly reduced (p<0.05) with, as compared to without, the inclusion of stability constraints in the optimization model (ie. Figure 1).

DISSCUSION

This study demonstrated that the inclusion of moderate levels of spine stability, as a constraint in an optimization model, allowed for the prediction of trunk muscle co-activity and improved predictions of spine compressive loading. This is believed to be the first instance of an optimization model predicting activity in muscles acting in a purely antagonistic manner to the external loading. When not constraining stability levels in the model, co-activation of the trunk muscles was never shown to occur, and consequently, levels of spine instability were predicted in a high number of trials.

From the results of this study it can be concluded that spine stability levels are an important factor to be considered in the modeling of trunk muscle function. Furthermore, it appears that stability levels play a role in dictating trunk muscle recruitment patterns, and that muscle co-activation serves as a means of maintaining an optimal level of stability for a given loading situation.

REFERENCES

Cholewicki, J., McGill, S.M. Clinical Biomechanics 11:1-15, 1996.
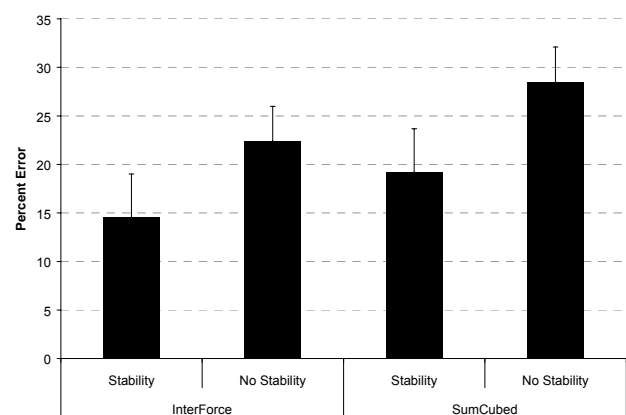Cholewicki, J., Van Vliet II, J.J. Clinical Biomechanics 17:99-105, 2002.

Figure 1: Percent error between experimentally derived and model predicted compressive forces. Predictions from each of the two cost functions, both with and without stability constraints, are shown for conditions with a pure flexor external moment.

DIFERENTIATING LIFTING TECHNIQUE BETWEEN THOSE WHO DEVELOP LOW BACK PAIN AND THOSE WHO DO NOT

Allan Wrigley[1], Wayne J. Albert[1], Kevin J. Deluzio[2], Joan M.Stevenson[3]

[1]Faculty of Kinesiology, Human Performance Lab, University of New Brunswick, Fredericton, Canada
[2]School of Biomedical Engineering, Dalhousie University, Halifax, Canada
[3]School of Physical & Health Education, Queen's University, Kingston, Canada

INTRODUCTION

The disadvantages of using summary statistics for describing waveforms are that the descriptive measures must be chosen a priori and the temporal characteristics of the trajectories may be lost, reducing the sensitivity of subsequent hypothesis testing (Khalaf et al., 1999). The purpose of this study was to demonstrate the ability of principal component analysis (PCA) to identify differences in lifting technique.

METHODS

Sixteen kinematic and kinetic waveforms describing the 2D motion of the trunk and box were extracted from the Queen's DuPont Low Back Pain Research Study database (Stevenson et al., 1997) of healthy male workers performing sagittal lifts of a 15kg box. Our objective was to determine if these biomechanical measures could discriminate those individuals who remained healthy over a two-year monitoring period (CON, n=50) and those who developed low back pain (LBP, n=58). PCA (Jackson, 1991) was applied to matrices consisting of each of the 16-waveform variables from both groups. All waveform data was transformed into principal components (PC)s using an eigenvector analysis of the covariance matrix. The number of PCs retained for comparison (k) was determined using parallel analysis (Jackson, 1991). PC scores were calculated by projecting the original data points into the new coordinate space defined by the k PCs. The k PC scores for each variable were used as the dependent measures in a one-way ANOVA in order to determine if there were any significant group differences.

RESULTS AND DISCUSSION

Significant group differences ($P < 0.05$) were found for four of the discrete measures and five of the PC scores. The number of PCs retained for each waveform variable ranged from two to six, and accounted for an average of 94.02% of the variance in the datasets. The retained PCs and PC scores adequately represented ($\alpha = 0.05$) the original dataset for an average of 94.44% of the participants, indicating that the PCs captured the key features within the waveforms. Kinematically, the groups differed in their placement and control of the load near the end of the lift. Kinetically, it appears that the pattern of change from a higher to lower sacral extension moment leads to a correspondingly earlier increase in thoracic extension moment for the LBP group (Figure 1). The trunk compression pattern was similar to that of sacral extension moment.

SUMMARY

The PCA technique was able to identify important biomechanical differences between the groups where traditional analyses failed. Furthermore, this research has been able to relate differences in lifting technique to the development of LBP.

REFERENCES

Jackson (1991) *A User's Guide to Principal Components*. New York, Wiley.
Khalaf et al. (1999) IEEE Trans. Rehab. Eng., **7(3):**278-288.
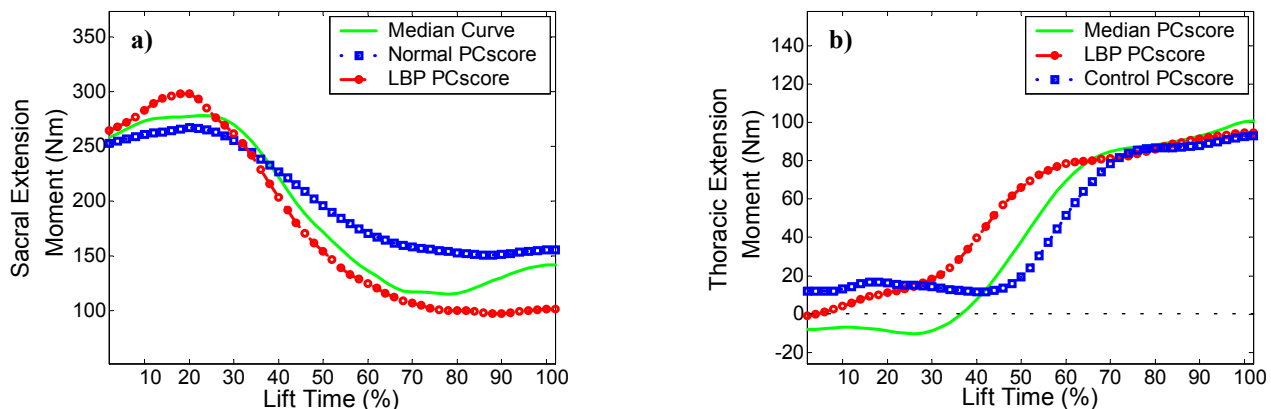Stevenson et al. (1997) IOS Press, Inc., Burke, 256-260.

Figure 1:
a) Representative curves based on PC scores for sacral extension moment PC2 that were extracted to illustrate the mode of variation captured. **b)** Curves that were extracted in the same way to illustrate thoracic extension moment PC3. Of particular interest is the region at approximately 35% of the lift time where the LBP sacral extension moment changes from higher than the median curve to lower, and the thoracic extension moment correspondingly begins to rise.

THE SCALING OF THE ANATOMY OF THE BONES OF THE HUMAN ARM

K.M.A. Weiss-Bundy[1] and A.B. Thornton-Trump[2]

[1] Human Performance Laboratory, University of Calgary, Calgary, Canada, karyn@kin.ucalgary.ca
[2] Department of Mechanical and Industrial Engineering, University of Manitoba, Winnipeg, Canada

INTRODUCTION

Dissections of the human arm have been done for many purposes; however, few of those dissection studies have reported the height and weight of the human specimens from which the arm was taken. For many purposes, the height and weight of the subject from which the arm was taken is not of particular significance. However, in any study of the moment arms of the flexor and extensor muscles of the arm, the moment arms are functions of specimen size. In order to determine the muscle forces required to create joint moments, the specific anatomy of the bones of the arm must be known. It is therefore desirable to be able to scale the anatomy of the bones to the size of the subject. Muscle leverage depends on the dimensions of the bones since the bone diameter contributes to muscle moment arm about the joint. A method to scale the bone diameters and the positions of points of origin and insertion of muscles is required. Such scaling must relate to the height and weight of the range of workers likely to use a workstation. This work was undertaken to determine the correlations of bone anatomy to the distribution of height and weight within the human population.

METHODS

A literature search was undertaken to find anatomical studies of bone and muscle anatomy in which the height and weight of the subject was given. Co-ordinate systems had to be defined and related to the rest of the body and the neutral carriage position of the arm. Data in Murray (1997) provided sufficient detail to relate the co-ordinate systems to the bone anatomy at the shoulder. The measurements of the bone anatomy were translated into a common co-ordinate system so correlations could be developed for the muscle points of origin and insertion. Once the bone and muscle anatomy was established, correlations between the bone and segment dimensions were developed and subsequently correlations with subject height and weight, using data from Diffrient et al. (1974).

RESULTS AND DISCUSSION

Most points of origin and insertion of the flexor and extensor muscles on the surface of the bone are related to the bone length in a linear fashion. Muscle moment arms are derived from a three-dimensional vector relationship based on vectors to points of origin and insertion of the muscle relative to the axis of rotation of the joint. The angle of joint excursion varies the muscle moment arms and thus the effectiveness of the muscles in creating moment about the joint. It is thus necessary to establish the vector relationships to model any joint over any angle. The bone diameter is a fundamental vector in establishing such a model. A sample of the correlations of bone anatomy with bone length and thus to subject height and weight are shown in Table 1. More anatomical dissection information is needed before better relationships can be established. Figure 1 shows the fit of the correlation curve to the raw data for the length of the humerus.
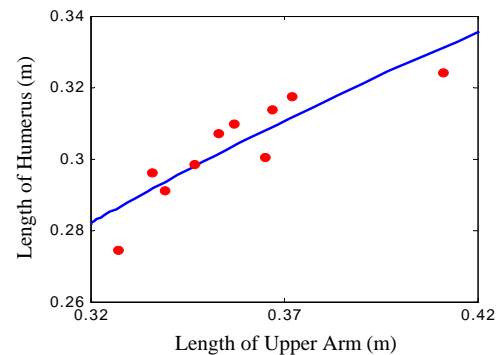

Figure 1. Correlation curve between humerus length and upper arm length to the raw data points

CONCLUSIONS

A set of correlations was developed to relate bone anatomy to height and weight of human subjects. Some of these correlations are strongly non-linear with bone length. Anatomical studies generally fail to give subject height and weight, thus making it impossible to correlate bone parameters required for modeling and scaling human muscle forces. Similar correlations for thoracic bone dimensions are required if modeling of the human arm is to be reliable.

REFERENCES

Diffrient, N. et al. (1974). *Humanscale 1/2/3*. Cambridge, MIT Press.
Murray, W.M. (1997). *Ph.D. Thesis*, Northwestern University.

Table 1. Sample Correlation Equations

y	*x*	Mathematical Relation	Correlation Coefficient
Upper Arm Length	Subject Height	$y = 1.9274 \times 10^3 + 0.1516 \cdot x$	$r = 0.9972$
Humerus Length	Upper Arm Length	$y = 0.520784 + 0.94734 \cdot \ln(x)$	$r = 0.8825$
Biceps Origin, *x*-coordinate	Humerus Length	$y = 0.645314 + 0.312888 \cdot \ln(x)$	$r = 0.9700$

MEASURING BIOMECHANICAL EXPOSURES DURING SNOW CRAB BUTCHERING

Angela J. Tate and John Molgaard
Faculty of Engineering and Applied Science, Memorial University of Newfoundland, St. John's, Canada,
angelat@engr.mun.ca

INTRODUCTION

Snow crab butchering is a unique occupational task that has never been studied biomechanically before. We report here on a study in one plant. Butchering is the process of removing the crab leg/shoulder sections from the carapace. Workers pick up the crab from a conveyor and strike the carapace against a blunt knife, separating the legs from the body. Workers then press the shoulder against brushes rotating at 250rpm to remove any gut or gills that remain attached. Sections are then struck against the edge of a chute to knock out any gut and/or to remove the mandible. The workstations were originally designed for an all male worker population. It is only in the past three seasons that females, of a typically shorter stature, have begun to work on the butchering line in this plant. The worker population has a high reported prevalence of upper limb discomfort. The goal of this study is to assess the exposure to biomechanical risk factors and make recommendations for improvements to reduce exposure.

Figure 1 The investigator working at a crab butchering workstation.

METHODS

A 3D link segment model of the upper limb has bee developed to determine the biomechanical exposure to the shoulder, elbow and wrist. The model will be used in the coming crab season in the plant with real workers under real working conditions to determine exposure to joint loads, impacts, repetitiveness, and awkward postures. Kinematic data collected using video, forces data from instrumented workstation elements, and two accelerometers will be used. The relative height of the workstation with respect to the worker will be varied to determine if there are better workstation configurations. Because of the seasonal nature of the crab industry, data collection is only possible between May and August. Preliminary data has been collected on one female (25years old, 172cm, 72kg) and one male (27 years old, 193cm, 84kg) performing a simulated crab butchering task in the lab, and have been processed using the kinematic model.

RESULTS AND DISCUSSION

The preliminary ergonomic assessment, using both video recordings and observation, established the task to be highly repetitive with a cycle time of 3 to 7 seconds. Laboratory measurements indicate that the force required to separate the carapace from the legs/shoulders is of the order of 250N, and acceleration of the hand during the impact phase to be of the order of 50g. Interviews with workers revealed that almost all the butchers had upper limb pain/discomfort at some time during the season and attributed it to the physical demands of the job. This task is performed for 8 to 12 hour shifts, 4-6 days/week, for 16 to 20 weeks depending on the availability of crab for processing.
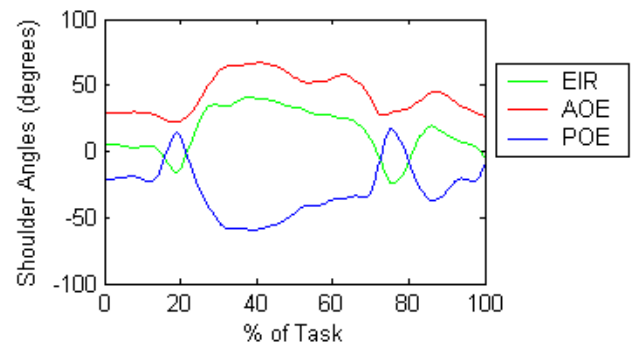

Figure 2 Shoulder joint angles from a preliminary simulated crab butchering task with a female subject. EIR-external/internal rotation, AOE- Angle of elevation, POE-Plane of elevation.

SUMMARY

The anecdotal high prevalence of upper limb cumulative trauma disorders in the crab processing industry has not been well investigated. The complex 3D exposure to biomechanical risk factors; including posture, force, vibration, and repetitivity, have not been before assessed. A model and protocols have been developed for use in the plant with real workers to measure the biomechanical exposures and to investigate the worker-workstation interaction.

ACKNOWLEDGEMENTS

INJURIES AMONG YOUNG GIRLS (5-14 YEARS) ENGAGED IN COMPETITIVE GYMNASTICS: DATA FROM THE CANADIAN HOSPITALS INJURY REPORTING AND PREVENTION PROGRAM (CHIRPP), 1998-2002

Steven R. McFaull

Research Analyst, Injury and Child Maltreatment Section, Health Surveillance and Epidemiology Division, Centre for Healthy Human Development, Population and Public Health Branch, Health Canada

INTRODUCTION

Gymnastics is a very repetitive activity and some elements can impart very large loads on the body. Panzer et al (1998) found lower extremity impact forces for the double backward somersault of up to 14.4 times body weight per foot. High levels of force can create acute injuries or, with the high exposure of repetitive practice, chronic conditions. At present, the vast majority of competitive participants are children (Daly et al, 2001), and most will suffer an injury by adolescence (Cahill and Pearl, 1993). There is concern that repetitive, high impact stress on the growing musculoskeletal system, which has a high cartilage content relative to adults, can result in permanent injury or deformity. Biomechanics studies provide an important contribution to the injury prevention process. To test and develop injury countermeasures, biomechanists need detailed epidemiological data to guide the process. The Canadian Hospitals Injury Reporting and Prevention Program (CHIRPP) is a rich source of injury data. The purpose of this study was to provide descriptive detail of competitive gymnastics-related injuries to young girls.

METHODS

CHIRPP is an injury surveillance system managed by Health Canada in which the emergency departments of 10 paediatric and 5 general hospitals participate. The database was searched for records of gymnastics-related injuries sustained by girls aged 60-179 months in organized competition or practice between 1998 and 2002.

RESULTS AND DISCUSSION

In total, 858 cases were identified. Girls 10-14 years were most frequently injured, with the peak occurring in 13 year-olds (1,172/100,000 CHIRPP cases of all types). The type of equipment or activity was known in 717 (83.6%) of the cases. Of these, the balance beam was the most frequent (29.8%), followed by floor routines (26.5%), uneven parallel bars (24.7%), the vault (11.2%), trampoline (5.6%) and other (2.3%). About one-third of all the injuries occurred during dismount or landing. Handsprings, cartwheels and tucks were common elements. About 80% of the injuries were to the extremities (41% upper, 39% lower) and upper extremity fractures were the single most frequent injury (27%). Fractures accounted for 66% of all upper extremity injuries compared to 23% for the lower extremities. About 85% of all lower extremity fractures were to the most distal structures (i.e. ankle, foot or toes) whereas the proximo-distal distribution of fractures for the upper extremities was less skewed. Overall, 7.2 % of the athletes were admitted to hospital compared to 2.4% for all cases of

organized sports among females, 5-14 years of age. Table 1 shows the proportion of fractures, sprains/strains, closed head injuries and admissions to hospital by type of equipment. Injuries occurring on the uneven bars result in more serious injuries (based on hospital admissions) compared to the other types of equipment.

Table 1. Type of equipment by main natures of injury/admissions. Percentage of all cases for the specific equipment type

Equip. Type	Fractures	Sprain/ strain	MCHI/ Concussion	Admitted
Balance Beam (n=214)	43.0	29.9	0.5	7.5
Uneven Bars (n=177)	45.8	24.9	2.8	15.3
Floor (n=189)	27.0	42.3	2.4	4.2
Vault (n=80)	47.5	23.8	3.8	7.5
Trampo- line (n=40)	35.0	27.5	2.5	10.0
Other (n=17)	29.4	47.1	0.0	0.0

MCHI: Minor closed head injury

SUMMARY

A large proportion of competitive gymnastics-related injuries in young (5-14 years) girls are fractures. The uneven bars have twice the admission rate of either the beam or the vault and over six times that of all organized sports (females, 5-14 years). Countermeasures may involve analysis of equipment design/components, difficulty of a routine, landing surfaces and strength training (particularly for the upper extremities).

REFERENCES

Panzer et al (1988). *Biomechanics XI-B*, Amsterdam, Free University Press.
Daly R.M. et al (2001). *Br J Sports Med*, **35**, 8-20.
Cahill BR and Pearl AJ (1993). *Intensive Participation in Children's Sports*, Champaign, Ill., Human Kinetics.

THORACO-LUMBAR KINEMATICS DURING SINGLE LIMB PULLING EXERTIONS

Scott N. MacKinnon[1] and Christopher L. Vaughan[2]

[1]School of Human Kinetics and Recreation, Memorial University of Newfoundland, St. John's, Canada, smackinn@mun.ca
[2]Department of Human Biology, University of Cape Town, Cape Town, South Africa

INTRODUCTION

Pulling exertions are a common form of manual materials handling yet little is known about the manner in which an operator exerts a submaximal force in a horizontal direction. Benchmark data documenting trunk kinematics should help occupational biomechanists identify aspects of isoinertial pull exertions that might predispose an operator to increased risk of acute and chronic low back injuries. The purpose of this study was to examine whether variations in workstation parameters and load magnitudes would affect lumbar spine and load kinematics of subjects exerting single-handed pulls originating from diverse locations in the frontal plane. It is hypothesized that as the pull location moves away from the sagittal and frontal planes, and as the pull load increases the magnitudes of the thoracolumbar kinematics, as measured by a lumbar motion monitor, will increase.

METHODS

This study examined one-handed pull exertions originating from four locations about the frontal plane performed by 20 healthy male subjects. These pull origins were described within a standard planar system and were relative to the morphology of each subject. Two pull heights were tested - orbital height and elbow height - through two parasagittal planes. The sagittal planes occurred through the gleno-humeral joint centre when the arm was held relaxed at the subject's side and another plane lateral to this, at a distance defined by the length of the centre of the subject's gleno-humeral joint to the centre of the elbow joint. Each subject was required to exert these pulling actions against loads of 6, 12 and 18% of lean body mass. The magnitudes of these loads and prescribed postures were based on previous work (MacKinnon, 2001; 2002).

An isoinertial pulley system was employed to provide a horizontal resistance against which the subject exerted a pull and load-return action. This device also monitored load kinematics and kinetics. A Lumbar Motion Monitor (LMM) was employed to assess the displacement, velocity and acceleration time-series data for side bending, flexion/extension and rotation of the spine (Marras *et al.*, 1992) during the pulling exertions.

RESULTS AND DISCUSSION

There were no significant differences in the load displacements, pull times and peak and mean pull velocities between loads and pull locations. The mean pull time and peak velocity for all cycles were 1.21 (+/- 0.01) seconds and 1.28 (+/- 0.05) m.s^{-1} respectively.

As to be expected, there were significant differences for peak and mean pull forces ($p < 0.0001$ and $p < 0.0001$ respectively) and peak and mean pull powers ($p < 0.0001$ and $p < 0.0001$ respectively) between all load conditions but not between the four pull locations within a load condition. The mean peak forces for the 6, 12 and 18% loads were 67 (+/- 1) N, 123 (+/- 1) N and 183 (+/- 1) N respectively. The mean peak powers for the 6, 12 and 18% loads were 70 (+/- 1) W, 120 (+/- 1) W and 186 (+/- 1) W respectively.

These findings suggest that a subject will tend to increase the magnitude of the angular velocity and acceleration for both back extension (33 to 141 deg.s^{-1} and 129 to 539 deg.s^{-2} respectively) and axial rotation (42 to 76 deg.s^{-1} and 139 to 276 deg.s^{-2} respectively) in order to accommodate the demands of increased pull loads. However, only back extension kinematics were altered with changes in pull origin, although some exertions were attempted at a location considerably lateral to the anatomical sagittal plane. Magnitudes of angular velocities and accelerations were found to be comparable to those observed for lifting tasks considered to place an operator at high risk for low back disorders during lifting tasks (Marras et al., 1995).

SUMMARY

The null hypothesis was rejected as LMM measurements increased as pull origin were moved nearer the boundaries of a frontal plane reach envelope. It is concluded that repetitive, submaximal pull exertions such as those examined in this study may predispose an operator to risk of overuse injuries because of the considerable dynamic motions required of the trunk, and such handle locations should be avoided in workstation design particularly if coupled with heavy pull loads.

REFERENCES

MacKinnon, S.N. (2001). Ergonomics SA, 13(1),25-32.
MacKinnon, S.N. (2002). Ergonomics, 45(4), 253-266.
Marras, W. et al. (1995). Ergonomics, 38(2), 377-410.

ACKNOWLEDGEMENTS

EFFECTS OF FUNCTIONAL ANKLE INSTABILITY ON LANDING KINETICS
DURING A LATERAL HOP MOVEMENT

B. J. Monteleone[1], J. L. Ronsky[2,3], W. H. Meeuwisse[1,2], and R. F. Zernicke[1,2,3]
Faculties of Medicine[1], Kinesiology[2], and Engineering[3], University of Calgary, Calgary, Canada,
bmontele@ucalgary.ca

INTRODUCTION

Ankle joint complex (AJC) injuries are common during sports and activities (Garrick, 1977). Following an AJC injury, many patients are classified with functional ankle instability (FAI), with increased predisposition to re-injury (Ekstrand & Gillquist, 1983; Freeman et al., 1965). A possible mechanism of FAI is that patients may experience different AJC forces during tasks that are commonly associated with injuries. The purpose of this study was to assess ground reaction forces in subjects with FAI versus normals during a lateral hop movement.

METHODS

Subjects: Two groups: 1) Normal—No prior AJC injuries (n=6) and 2) previously injured subjects (n=6) with *functional ankle instability*. FAI was defined as two or more AJC sprains or one AJC sprain with continued chronic symptoms such as pain and/or instability, with no AJC fracture or surgery.
Instruments: Two force platforms (Kistler, 9286, Winterthur, Switzerland and AMTI, OR6-5, Watertown, MA) recorded kinetics at 1200 Hz during the lateral hop movement. In addition, kinematics and muscle activity were recorded with eight cameras and electromyography, respectively. Only ground reaction force data are presented here.
Design: Cross-sectional, observational, data collection during the task.
Task: The lateral hop movement consisted of multiple lateral-medial hops over an obstacle onto adjacent force platforms.
Procedure: Each subject was instructed to perform as many lateral hops as possible during the 6-s trial. At least 15 trials were recorded for each test leg. The middle 5 trials were used for analysis in an attempt to minimize a learning effect and/or fatigue.
Outcome Measures: Vertical impact force peak (VIF) and medial-lateral horizontal impact force peak (HIF). The impact force was the first peak that occurred within 5 ms and 50 ms of ground contact.
Data and Statistical Analysis: Raw force plate data were processed for the lateral hop movement (EVA—V5.00 and Kintrak—V6.2.2, Motion Analysis Corp., Santa Rosa, CA). Means and standard deviations were calculated for each outcome measure in the medial and lateral directions.

RESULTS AND DISCUSSION

The patterns of the vertical impact forces were consistent during the lateral hop movement. In contrast, the medial-lateral impact forces were not as consistent with the subjects using a medial or lateral landing strategy moving in each of the directions.

The following are means (SD) of the different impact forces. Moving *laterally*, the VIF was 11.5 N·kg^{-1} (8.0) for the FAI group and 9.6 N·kg^{-1} (2.2) for the normal group; HIF was 0.3 N·kg^{-1} (0.3) laterally for the FAI group and 0.8 N·kg^{-1} (0.6) laterally for the normal group. While moving *medially*, the VIF was 9.7 N·kg^{-1} (3.8) for the FAI group and 10.2 N·kg^{-1} (2.7) for the normal group; HIF was 0.2 N·kg^{-1} (0.7) medially for the FAI group and 0.0 N·kg^{-1} (0.2) for the normal group.

Potentially, disrupted AJC control mechanisms may affect FAI. The increased predisposition of AJC injuries associated with FAI raised the possibility of having altered impact forces during tasks that have increased risk for injury. The ability to minimize the contact forces during these activities may be inhibited with FAI. It was hypothesized that greater impact forces may be responsible for the chronic AJC symptoms and increased injuries associated with FAI. There were trends in the results that while moving laterally during the lateral hop movement, differences existed in the vertical and medial-lateral impact forces between the FAI and normal groups. Moving laterally during sports is a common mechanism of AJC injury. The results of this study suggested that altered vertical and medial-lateral ground reaction forces may be related the increased risk of injury, but more data will be needed to confirm that.

SUMMARY

The impact forces tended to be different in the lateral direction during the lateral hop movement. Further analysis, with more subjects, may help determine if the observed differences are statistically and/or clinically relevant. In the future, combining the impact force data with other outcome measures, including joint moments, kinematics, and EMG during the lateral hop movement may further elucidate altered control mechanisms of FAI.

REFERENCES

Ekstrand, J. & Gillquist, J. (1983). *Med. Sci. Sports Exerc.,* **15,** 267-270.
Freeman, M.A.R. et al., (1965). *J. Bone Joint Surg. (Br.),* **47,** 678-685.
Garrick, J.G. (1977). *Am. J. Sports Med.,* **5,** 241-242.

ACKNOWLEDGEMENTS

Computer-aided design to investigate line-of-sight and postural demands on mining equipment

Alison Godwin[1] Tammy Eger[1] Al Salmoni [2]
[1]Occupational Performance Research Lab – Laurentian University
[2] Faculty of Kinesiology – University of Western Ontario

INTRODUCTION

Line-of-sight testing on underground mining equipment has previously been performed using tedious, manual methods. The advent of computer-aided design programs has made line-of-sight testing both faster and more versatile. These programs allow accurate, 3-D models of machinery to be loaded and assessed with simple, user-friendly commands. Previous research findings have shown that testing prototype modifications within this environment is useful from a manufacturer and ergonomic perspective.

Advanced anthropometric and human motion characteristics have also been incorporated into these programs to allow realistic analysis of the human body within the modeled machine (Das and Sengupta, 1995). Apart from assessing simple line-of-sight issues, researches have been able to evaluate the potential consequences of awkward postures adopted by the human operator while attempting to view hazards around the machine.

Operators of load-haul-dump (LHD) machines use postures that include twisting, lateral and forward bending of the trunk and twisting of the neck to spot hazards (Boocock and Weyman, 1994). These postures may be held statically, at extreme ranges of motion for long shift periods while the operator is exposed to vibration. Seat rotation and seat height interventions have been successfully implemented to reduce awkward postures in other industries where extreme trunk and neck postures are prevalent (Toren and Oberg, 1999).

METHOD

Seat rotation intervention was analyzed in the Classic JACK v4.0 virtual environment. Three different operator sizes (1st, 50th and 99th percentile) were positioned in the cabin with appropriate hand and foot constraints. The dependent variables included postural variables (trunk rotation, trunk lateral bend, trunk flexion/extension, neck rotation), low-back load variables (compression, shear, moments, muscular activity) and visibility measures (number of visual attention locations and percent of visible area). Fifteen virtual movement strategies were developed to represent typical workers and each worker was tested with the seat in neutral and rotated to 20 degrees and 45 degrees.

RESULTS AND DISCUSSION

The general relationship observed was that as seat rotation increased, VAL and visible line-of-sight area increased while postural load variables decreased. For the most part, twenty degrees of seat rotation was beneficial but 45 degrees produced significantly greater changes to postural load and visible VALs. Figure 1 demonstrates that external oblique and internal oblique muscles show the greatest reduction in muscle asymmetry as seat rotation increases. Preliminary results revealed that reductions in joint force, muscular tension and joint angles could be seen in the ergonomic feedback provided by the computer-aided program.

SUMMARY

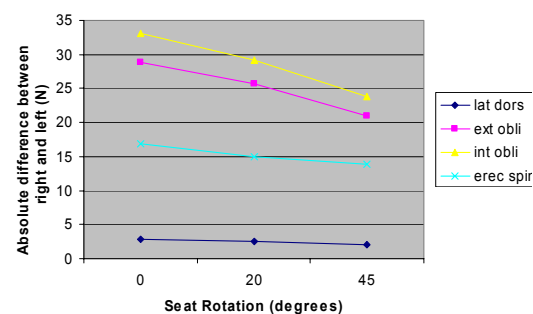Using human factor assessment tools in a virtual

Figure 1: The absolute difference between right and left trunk muscles (muscle asymmetry) decreases with increasing amounts of seat rotation.

environment was a safe way to test design prototypes and revealed which situations cause undue postural stress on the operator.

REFERENCES

Boocock, M.G., & Weyman, A.K. (1994). Task analysis applied to computer-aided design for evaluating driver visibility. In *Proceedings of the 12th IEA Triennial Congress* (vol. 4,pp.261-263). Toronto, Ontario, Canada.

Das, B., Sengupta, A.K. (1995). Computer-aided human modelling programs for workstation design. Ergonomics, 38(9):1958-1972

Toren, A., Oberg, K. (1999). Maximum isometric trunk muscle strength and activity at trunk axial rotation during sitting. Applied Ergonomics, 30:515-525.

DEVELOPMENT OF A CLINICAL MEASURE OF CENTER OF PRESSURE IN SITTING

Julie Côté[1,4], Marc Therrien[1,2], Michèle Lacoste[1] and François Prince[1,2,3]

[1] Research Center of the Marie Enfant Rehabilitation Center, Sainte-Justine Hospital, Montreal, Quebec, Canada
[2]Department of Kinesiology, [3]Department of Surgery, University of Montreal, Montreal, Quebec, Canada
[4]Department of Kinesiology and Physical Education, McGill University, Montreal, Quebec, Canada, julie.cote2@mcgill.ca

INTRODUCTION
In quiet standing, the position of the center of pressure (COP), calculated from a force platform, has often been used to infer the stability of upright posture (Winter, 1995). This concept has seldom been used to assess sitting posture or to measure the influence of pathologies. Some studies have measured the COP displacement of spinal cord injured adults in quiet sitting using a force platform (Seelen et al., 1997; Chen et al., 2003; Aissaoui et al., 2001). However, when evaluating children in their own wheelchairs, the use of a force platform would not be appropriate since it does not fit into their wheelchairs. Soft pressure mapping systems can be inserted at the wheelchair seat interface and can serve to evaluate the pressure distribution and COP location. Nevertheless, the validity of this tool in measuring the COP location during sitting remains to be established. This study compares COP measurements from the pressure mapping system and a force platform in healthy children during quiet sitting and reaching tasks.

METHODS
Recordings of quiet sitting (static) and reaching tasks (reach) were made from thirteen able-bodied children (6b, 7g, age range: 7 to 15 yrs). Reaching was performed at 130% of arm length towards a target placed at 30° from the sagittal plane and at shoulder height. An AMTI force platform was installed on a seating simulator. A one-inch thick polyurethane foam cushion was fixed on the force platform. A pressure-sensing mat (FSA, Vista Medical Ltd) was then attached on the seat cushion. The seat depth and the height of the footrest were standardized. The seat tilt angle was fixed at 0° and the seat-to-back angle between 95° and 100°, in order to accommodate the subject's geometry and comfort. COP data were extracted in both A/P and M/L directions. Range and Root Mean Square (RMS) amplitudes (cm) of COP displacement were then calculated over trials. Correlation coefficients were calculated between COP displacement data from FSA and force platform.
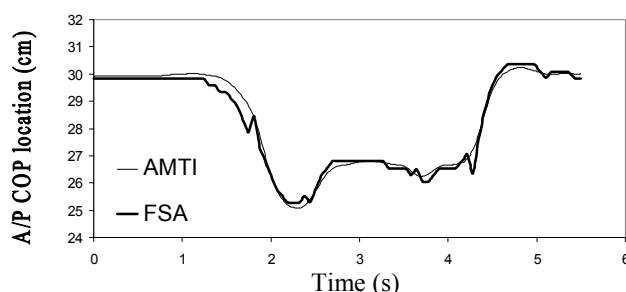
RESULTS AND DISCUSSION

Figure 1: COP displacement (A/P) of a typical subject during a reaching task.

Results suggest that there is a close correspondence between COP displacement measured from the FSA and AMTI systems (Figure 1, Table 1) during both tasks.

Table 1 Average and (SD) of COP range and RMS amplitudes, in cm, measured from FSA and AMTI.

	AMTI		FSA	
	Range	RMS	Range	RMS
M/L				
Static	0.31 (0.23)	0.05 (0.04)	0.40 (0.17)	0.07 (0.03)
Reach	5.85 (1.49)	1.82 (0.53)	5.00 (1.17)	1.56 (0.42)
A/P				
Static	0.28 (0.22)	0.04 (0.04)	0.42 (0.24)	0.08 (0.04)
Reach	6.74 (1.32)	2.13 (0.64)	7.02 (1.43)	2.34 (0.69)

Correlation coefficients between COP parameters of both systems ranged from 0.37 to 0.98, with most being above 0.8 (Table 2). The lowest exist between COP time series during the static task. This can be explained by the lower spatial resolution of the FSA system (approximately one sensor every inch), whereas the AMTI system measures COP data to the nearest 0.002 cm. Another factor could be the saturation of some FSA captors (under the buttocks) during acquisitions, which was minimized by the use of the polyurethane foam.

Table 2 Average correlation coefficients between AMTI and FSA COP parameters during quiet sitting and reaching tasks.

Static	M/L	A/P	Reach	M/L	A/P
Time	0.43	0.37	Time	0.98	0.97
Range	0.96	0.91	Range	0.80	0.82
RMS	0.92	0.75	RMS	0.97	0.92

SUMMARY
The FSA system can be used to quantify postural stability using COP displacement data. Caution should be exercised when analysing time series of tasks of small COP amplitudes (approximately less than 1 cm).

REFERENCES
Winter DA (1995) *A.B.C. of Balance during Standing and Walking*. Waterloo, Waterloo Biomechanics.
Seelen, HAM et al (1997). *J.Electromyogr Kinesiol*, **7**, 149-60.
Chen CL et al (2003). *Arch Phys Med Rehab*, **84**, 1276-81.
Aissaoui R et al (2001). *Arch Phys Med Rehab*, **82**, 274-81.

ACKNOWLEDGMENTS

INFLUENCE OF Q-ANGLE ON LOWER EXTREMITY MOMENTS DURING RUNNING

Sang Kyoon Park and Darren J. Stefanyshyn
Human Performance Laboratory, Faculty of Kinesiology,
University of Calgary, Calgary, Canada, spark@kin.ucalgary.ca

INTRODUCTION

The Q-angle in the frontal plane has been suggested as an important factor in the development of overuse knee injuries (Heiderscheit et al., 2000). An excessive Q-angle produces increased rearfoot eversion that in turn causes an increased tibial internal rotation. This excessive tibial internal rotation, coupled with the femoral external rotation could contribute to altered loading at the knee. The increased internal joint loading, as indicated by the increased joint moments, may cause local stress at the knee, and therefore, pain after repetitive submaximal loading cycles (Stefanyshyn et al., 1999). However, there are conflicting data in the literature concerning the influence of lower limb alignment on the dynamic internal loading about the knee (Harrington, 1983). Thus, the purpose of this investigation was to study the influence of Q-angle on the knee joint moments during running.

METHODS

Ten recreational male runners (mean age = 27.8 ± 6.7 years; mean mass = 79.6 ± 8.9 kg; mean height =177.9 ± 4.0 cm) with no history of lower extremity symptoms or injuries were recruited for this experiment. Q-angle was measured 2-dimensionally with a digital camera and goniometer and used to divide subjects into two groups (low Q-angle and high Q-angle). Subjects then performed 15 running trials with reflective markers on their right leg. Standard control running shoes and six high-speed cameras (240 Hz, Motion Analysis Corp.) were used to record kinematic data. Ground reaction forces were collected by a force plate (2400 Hz, Kistler). The speed of running during each trial was fixed at 4.0 ± 0.2 m/sec. Data were analyzed with Kintrak software (Motion Analysis Corp.). The joint moments were calculated using inverse dynamics and by modeling the leg as three rigid segments representing the thigh, shank, and foot. Joint moments were normalized by body mass (Nm/kg) for statistical analysis. Student t-test for group comparison was performed with Stata 7.0 program.

RESULTS AND DISCUSSION

It was anticipated that the magnitude of joint moments at the knee depends on the Q-angle created by the femur and tibia in the frontal plane. The measured Q-angle was significantly different between groups (P=0.000; Table1). However, the results in this study did not show an influence of Q-angle on knee joint moments (Table1). Q-angle did not increase knee internal rotation, abduction, or extension moments during running. A possible explanation is that the Q-angle was measured statically but used as a predictor of dynamic movement (Heiderscheit et al., 2000). Perhaps, a dynamic measurement of the Q-angle would provide more information than one measured in a static situation. Also, compensatory mechanisms that reduce the loading at the knee may exist when the frontal axis is changed during gait. The Q-angles of most subjects in this experiment were within the normal range (10°-17°). It may be difficult to find the possible influence of the Q-angle on lower extremity dynamics from the normal population. Furthermore, the accuracy of the methods used to measure the Q-angle is questionable because small errors in anatomical markers could affect the value of the Q-angle. For future studies, more subjects including individuals with excessive or low Q-angles may help understand the influence of lower limb alignment on knee joint moments.

SUMMARY

The results did not support the assumption that an increased Q-angle would increase lower extremity moments during running.

REFERENCES

Harrington I. J. (1983) *J. Bone & Joint Surg.,* **65**: 247-259.
Heiderscheit et al. (2000) *J. Orthop. Sports Phys. Ther.,* **30(5)** 271-278.
Stefanyshyn, D. et al. (1999) *Proc. 4th Foot Biomech. Symp. ,* Canmore, Canada 86-87.

Table 1 Q-angles and knee joint moments of the low Q-angle and high Q-angle Groups.

Knee joint moments (Nm/kg)	Group		*P*
	Low Q-angle (n=5); $8.1° \pm 0.4°$	High Q-angle (n=5); $15.4° \pm 1.7°$	P=0.000*
External rotation	0.184 ± 0.057	0.164 ± 0.052	0.581
Abduction	-1.330 ± 0.300	-0.936 ± 0.460	0.147
Extension	2.310 ± 0.659	2.902 ± 0.627	0.183

THE EFFECT OF ACCELEROMETER PLACEMENT ON ENERGY COST ESTIMATES FOR TREADMILL WALKING AT DIFFERENT SPEEDS AND INCLINES

E.L. Morin, J.M. Stevenson, S.A. Reid, C. Hare and J.T. Bryant
Ergonomics Research Group
Queen's University, Kingston, Ont. morine@post.queensu.ca

INTRODUCTION

It has been found that energy expenditure can be estimated from whole body accelerations for specific activities. Whole body acceleration is generally recorded using accelerometers mounted at the lumbar spine, waist or hips (e.g. Bouten et al., 1997a; Hendelman et al., 2000) Bouten et al., (1997a) estimated energy cost for a range of activities using a triaxial accelerometer mounted at the second lumbar vertebra. The outputs were rectified and summed over 1 minute intervals to give a single parameter, IMA_{tot}. A pooled correlation coefficient of $r = 0.89$ was found between IMA_{tot} and energy expenditure measured using indirect calorimetry.

The objective of this study is to assess the correlation of body accelerations recorded at two locations – over the sternum and the lumbar spine – with energy expenditure, during treadmill walking at different speeds and inclines. This was done to assess the suitability of the sternum recording location with respect to accepted practice.

METHODS

Eight physically fit male subjects (mean ht=1.77 m; wt= 78.3 kg; age=23.6) completed two 18-minute treadmill walks. In one case, the treadmill speed varied from 3.22 to 4.83 to 6.44 km/h in 6 minute intervals; in the other case the treadmill incline varied from 0° to 5° to 10° in 6 minute intervals. Each subject's $V\dot{O}_2$ was continuously monitored using a TEEM 100 oxygen analyzer and Aerosport122 software. One triaxial accelerometer (Crossbow model CXL10LP3) was mounted over the sternum and a second was mounted over the lumbar spine. The accelerometers were fixed to the skin using a skin adhesive (SkinBond®). The accelerometer data were sampled at 100 Hz and stored using a Embla™ data logger.

Full data sets for 3 speeds were obtained from six subjects, giving $n = 18$; full data sets for 3 inclines were obtained from four subjects and results for 0° and 5° were obtained from two subjects, giving $n = 16$. Averaged rms values for the acceleration data were computed over 2 minute steady state periods at each speed and incline for the mediolateral (x-); vertical (y-) and anteroposterior (z-) axes. The rms magnitude of the acceleration was computed as:

$$magnitude = \sqrt{x_{rms}^2 + y_{rms}^2 + z_{rms}^2} \qquad (1)$$

All offsets were removed from the data, prior to computing the rms values, to minimize the effect of the gravity vector on the processed results.

RESULTS AND DISCUSSION

The mean values and standard deviations for the $V\dot{O}_2$ and the magnitude of the rms accelerations for each condition are summarized in Table 1.

Table 1: Average $V\dot{O}_2$ and rms magnitudes

Speed	3.22 km/h	4.83 km/h	6.44 km/h
VO2	8.24±1.14	10.28±1.61	15.65±1.93
A1 – mag	2.15±0.14	3.30±0.46	5.18±0.76
A2 – mag	2.67±0.24	4.12±0.60	6.35±1.09
Incline	**0°**	**5°**	**10°**
VO2	9.89±1.94	13.44±1.64	19.32±1.14
A1 – mag	3.24±0.25	3.45±0.30	3.97±0.5
A2 – mag	3.77±0.36	3.58±0.35	3.85±0.41

A1 – sternum accelerometer; A2 – lumbar accelerometer

A correlation analysis betweeen the average rms values on each axis as well as the rms magnitude and the average $V\dot{O}_2$ values was performed. In all but one case the highest r value was obtained for correlation between the rms magnitude and $V\dot{O}_2$. These results are summarized in Table 2.

Table 2: Correlation coefficients for 2 accelerometer locations

Location	Changing speed	Changing incline
Sternum	$r = 0.955$	$r = 0.794$
Lumbar	$r = 0.956$	$r = 0.274$

The results show that $V\dot{O}_2$ increases as both speed and incline increase. The rms magnitude of accelerations measured at both recording locations increases as speed increases and this parameter is well correlated with $V\dot{O}_2$. The accelerations are less well correlated with $V\dot{O}_2$ for increasing incline, but the sternum location is better correlated than the lumbar location.

Bouten et al. (1997b) studied the effect of accelerometer location on the prediction of energy cost and concluded that, for various locations, accelerations were still well correlated with energy cost for level walking. The results of this study support that conclusion for changing speed, but not for changing incline and indicate that energy cost might be better predicted for walking with changing incline using an accelerometer mounted at the sternum.

REFERENCES

Bouten, C et al. (1997a). *IEEE Trans. Biomed. Eng.*, **44**, 136-147.
Bouten, C et al. (1997b) *Med. Biol. Eng. Comput.*, **35**, 50-56.
Hendelman, D et al. (2000) *Med. Sci. Sports Exerc.*, **32** (Suppl 9), S442-S449.

ACKNOWLEDGMENTS

ASSESSMENT OF RELATIVE MOTION BETWEEN A BACKPACK AND TORSO FOR DIFFERENT LOADS

Anita Lee[1], Derrick E. Bouchard[1] and Evelyn L. Morin[2]

[1]Department of Electrical and Computer Engineering, Royal Military College of Canada, Kingston, Ontario, Canada, anita.lee@rmc.ca
[2]Department of Electrical and Computer Engineering, Queen's University, Kingston, Ontario, Canada

INTRODUCTION

This research is part of a larger study at Queen's University to establish load-bearing guidelines for the Canadian Forces with respect to metabolic energy cost, as well as to examine biomechanical effects of carrying heavy loads for long durations.

Using the load carriage simulator (LCS) developed by the Ergonomics Research Group at Queen's University (Bossi et al, 2001), the relative motion between a mannikin and the newly designed Clothe the Soldier rucksack (Reid et al, 1999) was assessed using tri-axial electronic accelerometers.

The purpose of this research is: (1) to assess the changes in forward lean angle of the torso required to balance the moments at the hip for different loads, (2) to quantify the relative movement of the backpack with the body for different loads.

METHODS

The LC simulator consists of an anthropometrically weighted mannikin (50th percentile male), which is covered with a skin-like surface. It is driven by computer controlled pneumatic activators that are programmed to create a vertical displacement pattern of +/- 2.54 cm amplitude and 1.8 Hz frequency, where the motion is defined by a sine wave.

The simulator mannikin was outfitted with a military combat shirt, helmet and backpack. Two triaxial accelerometers (Crossbow model CXL10LP3) were used in the study. The accelerometers are small (1.9x4.76x2.54cm) and light-weight (46-gm). One was mounted inside the pack and one was mounted on the mannikin's sternum. In both cases, the positive y-axis of the accelerometer was oriented vertically.

Four sets of data were collected with loads of 16.6 kg, 25.9 kg, 38.7 kg and 50 kg placed in the backpack. The mannikin was set to move at a pace of 5.6 km/hr (1.6 m/s). Ten independent trials were done for each of the four loads. Prior to each trial, the backpack was removed and placed back on the mannikin and the tensions in the shoulder straps and waist belt were adjusted to be the same as in the previous trial.

At the start of each session (for the four different loads), the tilt of the mannikin was adjusted such that medial-lateral moment at the hips was zero. This moment is measured using a load cell located at the level of the mannikin's hips.

RESULTS AND DISCUSSION

The mean tilt angle for both the mannikin and pack from the ten trials at each load was calculated and the results are shown in Figure 1. The mannikin's tilt angle varied between 11.4^{o} to 16.2^{o} for the four loads with no apparent trend. There was a linear trend apparent for the pack tilt angle, where the mean tilt angle decreased from 18.1^{o} for the 16.6 kg load to 8.2^{o} for the 50 kg load with an R^2 of 0.993.
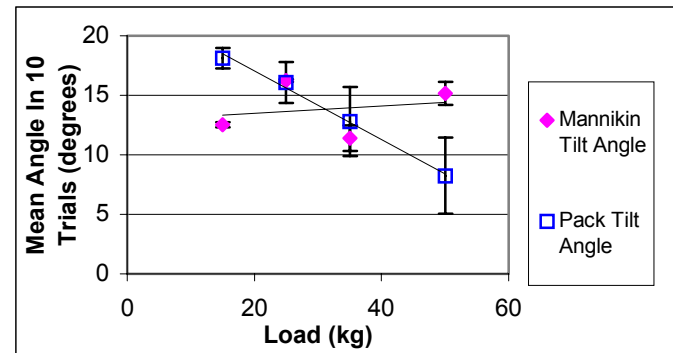

Figure 1: Comparison of Mannikin and Pack Tilt Angles At 16.6 kg, 25.9 kg, 38.7 kg and 50 kg Loads

Using the mannikin and pack tilt angles, the data were aligned and the mean absolute relative differences in vertical accelerations were calculated for the ten trials of the four loads. These differences were: 1.1653 m/s^2, 1.6023 m/s^2, 0.899 m/s^2 and 1.1574 m/s^2 for the 16.6 kg, 25.9 kg, 38.7 kg and 50 kg loads respectively. In all cases the mannikin's accelerations were greater than the pack's accelerations.

SUMMARY

In this study, no clear tilt angle in the mannikin was found. The decreasing tilt angle for the backpack indicates that the pack is oriented more vertically as load increases. This may be due to greater rotation of the pack itself about its centre of gravity with higher load.

In addition, no clear trend in the absolute differences in the vertical accelerations between the mannikin and the pack was found. Thus, it will be necessary to examine other parameters, such as relative side-to-side accelerations, to describe the interaction between the backpack and the body.

REFERENCES

Bossi, L.L. et al (2001). Proceedings, NATO-RTO Workshop on Soldier Mobility, 14.1-14.7.

Reid, S. A. et. al (1999). *Clothe the Soldier Integrated Load Carriage System Phase IIID.* PWGSC Contract No. W7711-8-7461/991/SRV

ACKNOWLEDGEMENTS

A QUANTITATIVE CLASSIFICATION TO DETERMINE EXTENT OF SPINAL ARTHRODESIS FOR ADOLESCENT IDIOPATHIC SCOLIOSIS

H. Wu[1], P.Poncet[1], J. Harder[2], F. Chariet[3], H. Labelle[4], R. F. Zernicke [1,2], J. L. Ronsky [1]

[1] Department of Mechanical and Manufacturing Engineering and [2]Department of Surgery, University of Calgary; [3]Département de génie informatique, École Polytechnique de Montréal; [4] Service d'Orthopédie, Hôpital Sainte-Justine, Montréal, Canada.
hongfawu@enme.ucalgary.ca

INTRODUCTION

Adolescent idiopathic scoliosis (AIS) is a complex three-dimensional deformity of spine and rib cage. The complicated relationship between torso image and spinal deformity has been investigated using an artificial neural network (ANN).[1] While partially successful, the trained ANN did not efficiently approximate this relationship using the existing extracted intrinsic and extrinsic indices. Features of 3D curvature of spine and rib cage, such as vertebral displacement, rotation, lateral tilt and sagittal curvature could be good candidates for intrinsic indices[2]. Although some AIS classification methods have been suggested,[3,4] a quantitative classification for AIS based on feature extraction has not been reported. The purpose of this research was to develop a quantitative classification to determine the extent of spinal arthrodesis for AIS based on feature extraction methods.

METHODS

Standard stereoradiographs (T1-12 and L1-5) of 141 adolescent patients with idiopathic scoliosis were obtained in the Alberta Children's Hospital (Calgary, AB) and Ste.-Justine Hospital (Montreal, PQ), and used to generate three-dimensional reconstructions (Fig.1). For comparison purposes, the 3D spinal curvatures were first translated, with L5 as the coordinate system origin, and subsequently normalized. A continuous parametric form of the smooth curve that best fit the vertebrae was created by least square curve fitting of Fourier-series functions (3rd order)[5]. The subtractive clustering method[6] was adopted to estimate the number of patterns and to select the rough center of each pattern, based on the density of surrounding data clouds. These data were used to initialize the Fuzzy c-Means clustering[7], from which the final classification was obtained.
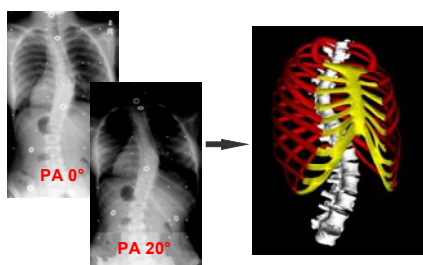

Fig. 1 Three-dimensional reconstruction of spine and rib cage with PA0° and PA20°

RESULTS

Fifteen patterns were recognized and the estimated cluster center for each pattern was selected by the subtractive clustering algorithm. After applying Fuzzy c-Means clustering technique, 141 spinal curves were classified into fifteen patterns with 6 to 13 members each. Fifteen clustering centers were generated by adjusting the membership functions of each

data vector (Fig. 2). The new quantitative classification system correctly identified five thoracic curve types of King-classification (considering the spinal curvature on the coronal plane only), but also recognized thoraco-lumbar, lumbar, double, and triple major curves. This new classification could be more effective for identifying sagittal plane spinal deformities than other classification[3] approaches with three components: curve type, a lumbar spine modifier, and a sagittal thoracic modifier.
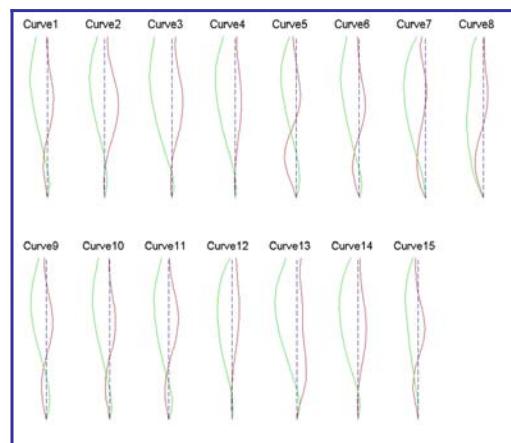

Fig. 2 Fifteen patterns are quantitatively recognized with Fuzzy c-means clustering. Red and green lines represent the spinal curvatures on the coronal and sagittal planes, respectively. The blue line is the vertical line going through the central vertebra L5.

SUMMARY

Scoliotic spinal curvatures can be quantitatively classified into different patterns using seven coefficients of a Fourier-series function (3rd order) to represent a translated and normalized 3D spinal curvature. Fifteen AIS patterns were identified with the new classification by applying techniques of subtractive clustering and Fuzzy c-Means clustering. The dimension of the original spinal curvature data has been decreased from 17x2 to 7x2, which is useful for the definition of an ANN to functionally approximate the relationship between torso image and spine (and rib cage). The clinical implications of this new quantitative classification will be investigated further.

REFERENCES

[1] Jaremko et al., *J.Biomech.Eng*.,124(5),2002. [2] Carlson. *J. Pros.&Orth*., 2003. [3] King et al., *J. Bone&Jnt Surg.*, 64A (9),1983. [4] Lenke et al.,*J. Bone&Jnt Surg.*, 83A(8), 2001.[5] Poncet et al., *Spine*, 26(20), 2001. [6] Chiu, S. *J. Intell.&Fuzzy Sys.*, 2(3), 1994. [7] Bezdek et al., *Fuzzy Models for Pattern Recognition*. IEEE Press, 1992.

ACKNOWLEDGEMENTS

IN VIVO ASSESSMENT OF CONGRUENCE IN THE PATELLOFEMORAL JOINT OF HEALTHY SUBJECTS

Kim McLaughlin, Parag Dhar, Nicole Baker, Janet Ronsky
Department of Mechanical and Manufacturing Engineering, University of Calgary, Calgary, Canada

INTRODUCTION

Joint incongruity has been suggested to be a potential risk factor in the initiation and progression of degenerative joint diseases such as osteoarthritis (OA)[1]. An anatomical abnormality in the joint may create a mismatch between contacting surfaces leading to abnormal joint forces and stresses. Radiography is the most widely used imaging modality for the clinical assessment of joints. However, this technique is limited for measures of joint congruence as it provides only subchondral bone shape to infer the profile of the articular cartilage which does not necessarily match the contour of the underlying bone[2]. In addition, the joint is typically examined in only one position and loading condition. The complex 3D geometry of the joint may not be adequately characterized by planar measurements. A method for quantifying patellofemoral (PF) joint geometry under various loading and joint alignment conditions using magnetic resonance (MR) imaging[3] overcomes the limitations of current x-ray approaches for assessing joint congruence. Previous work has examined the congruency of the knee joint but not during physiological loading[1]. The purpose of this work was to quantify PF joint congruence and examine the changes during flexion and in a loaded/unloaded condition.

METHODS

MR imaging (1.5T GE unit, FSPGR, 2 mm slice thickness, 3.5 min. data acquisition) was used to quantify the left and right PF joint geometry of 4 healthy adults (mean age = 25.4 years, height = 164.4 cm, weight = 56.6 kg). Ethics approval for all procedures was provided. The knee was imaged during two conditions (unloaded (UL), loaded (L) at 10% maximal voluntary force) and two joint alignments (15°, 30° flexion) using a custom designed loading apparatus. A mathematical joint model was developed through image segmentation and feature extraction, 3D reconstruction of each surface using a thin plate spline and contact determined with a proximity algorithm[3]. A congruence index (CI) was determined using a point contact method, where the curvatures of two contacting surfaces were transformed into an equivalent surface. The principal curvatures of the equivalent surface were determined and compared to a flat plane. A CI (equal to zero for two perfectly congruent surfaces) for all contact points was determined based on the principal curvatures[3]. An overall CI for the joint was found using three methods: CI at the centroid of the contact area, mean of the CI for all points, and RMS of the CI at all points. These methods were compared to determine which CI measure best represented the overall joint congruence. Also, changes during flexion and in a loaded and unloaded condition were examined. Differences were compared using a two-sample t-test with a p-value less than 0.05 indicating significance.

RESULTS

For overall CI, no statistically significant differences (*) were observed between the mean and RMS techniques throughout all angles and in the unloaded and loaded condition. The centroid method provided varied results (Table 1).

Table 1: Comparison of methods to calculate total CI

Condition	Two sample t-test p-value		
	Centroid vs. Mean	Centroid vs. RMS	Mean vs. RMS
15 UL	* 0.0002	* 0.0001	0.21
15 L	0.33	0.09	0.08
30 UL	0.09	0.08	0.53
30 L	* 0.02	* 0.0009	0.12

Using the approach which took the mean CI over the contact area, the mean CI was found for the 7 healthy knees at the two flexion angles for loaded and unloaded conditions (Table 2).

Table 2: Mean CI for 7 knees imaged

Subject	Congruence Index (mm^{-1})			
	15 UL	**15 L**	**30 UL**	**30 L**
S4 (left)	0.144	0.166	0.144	0.160
S4 (right)	0.229	0.142	0.153	0.205
S7 (left)	0.113	0.148	0.129	0.135
S7 (right)	0.123	0.152	0.319	0.157
T1 (right)	0.152	0.199	0.134	0.143
U1 (left)	0.126	0.151	0.142	0.128
U1 (right)	0.101	0.138	0.124	0.135
Mean	0.141	0.157	0.164	0.152
Std. Dev.	0.042	0.021	0.069	0.026

There were no statistically significant differences in the mean CI between the loaded and unloaded condition at each knee flexion angle (p-value = 0.41 and 0.67 for 15° and 30°, respectively). Also, the difference in mean CI at 15º and 30º in the unloaded condition was not statistically significant; the same was true for the loaded condition at these two angles (p-value = 0.50 and 0.75 respectively).

DISCUSSION AND CONCLUSIONS

Overall, the CI determined at the centroid is a poor measure to represent the congruence of the joint. When comparing the CI of the knee in various conditions, it is suggested to take the mean CI of all contact points. While it was speculated that the joint would become more congruent (lower CI) with loading and increasing flexion angle, no significant trends were observed. However, large variability within and between subjects was observed in the data, making determination of trends difficult. This suggests that increased sample size is required before these results can be generalized. Overall, the method used to determine the CI is capable of detecting differences when loading and position vary and could provide a basis for evaluation of joint disorders and treatment effects.

References: 1: Hohe, J. et al (2002). Magn. Reson. Imaging, 47, 554-561 **2**: Adam, C. et al (1998). J Anat., 193, 203-14 **3**: Baker (2001): MSc Thesis – U of Calgary.

TWO NOVEL TECHNIQUES FOR ERROR REDUCTION IN RSA

Bryan Donnelly[1], Janet Ronsky[1] and Richie Gill[2]

[1] Department of Mechanical Engineering, University of Calgary, Calgary, Alberta, Canada, bddonnel@ucalgary.ca
[2] Nuffield Department of Orthopaedic Surgery/OOEC, University of Oxford, Nuffield Orthopaedic Centre, Oxford, England

INTRODUCTION

Roentgen Stereophotogrammetric Analysis (RSA) has been used to predict early failure of prosthetic joints within 2 years of surgery. The improved accuracy and precision of RSA could potentially lead to a reduction in the time needed to predict implant failure [5,6]. The accuracy and precision of RSA are affected by several factors including the calibration frame and the algorithm used to reconstruct the radiographs from two dimensional images into three dimensional coordinates.

The purpose of this study was to
1) Investigate whether the accuracy and precision of the current reconstruction algorithm (DLT) can be improved by implementing a non-linear Bundle Adjustment Method (BAM) [2] with various correction factors [4]:
   i. BAM with both affine and radial distortion correction (SBAM).
   ii. BAM with Radial Distortion correction (BAM_RD).
   iii. BAM with Affine Distortion correction (BAM_AD).
2) Examine the effects of the algorithms upon the accuracy and precision in both analog and digital format x-rays.
3) Compare the performance of a novel new calibration frame to the older uniplanar frame design.

METHODS

The study consisted of 4 groups of stereopair x-rays taken of a plastic gauge object with embedded fiducial markers of known dimensions:
1) Ten analogue type x-rays with a traditional uniplanar frame design.
2) Ten analogue type x-rays with a new RSA frame design.
3) Ten digital type x-rays with a traditional uniplanar frame design.
4) Ten digital type x-rays with a new RSA frame design.

The images from all 4 groups were evaluated by all 5 reconstruction algorithms (DLT, BAM, BAM_RD, BAM_AD, SBAM).

The 3D reconstruction of the gauge object was compared to a gold standard achieved through a Coordinate Measurement-Machine (CMM). To compare the reconstruction algorithm to the gold standard, a technique known as Procrustes Analysis was implemented [3]. Typically used in morphology applications, it is a 3D rigid body transformation using a least squares minimization scheme to superimpose data sets. The outcome is a 3D vector describing the error between the reference and trial data for each individual point on the calibration frame.

RESULTS AND DISCUSSION

The SBAM algorithm was the superior method as it either equaled or outperformed all other algorithms including the DLT for both analogue and digital x-rays. Statistical significance was found.

Although the resolution of the digital x-rays was only 152 pixels/inch versus the analogue resolution of 256 pixels/inch, the accuracy and precision for both formats was very similar. This would further support the findings of Bragdon et al [1] and would indicate that the digital format is a suitable modality for RSA research.

The new calibration frame was the superior frame for digital format x-rays however for analogue type x-rays the accuracy and precision were inferior to the older uniplanar frame design. This inferior performance was attributed to error propagation due to physical characteristics of the apparatus. The results from the new calibration frame in the digital format are an improvement over any accuracy and precision values currently published [1].

SUMMARY

The iterative non-linear solution provides an important step in improving the accuracy and precision of the 3D reconstruction process of RSA.

Implementing the modified bundle adjustment method could assist in decreasing trial study numbers when testing new prosthetic components, will allow earlier detection of micromotion and loosening of prosthetic joints and may assist in earlier failure prediction of implants.

REFERENCES

[1] Bragdon CR. et al., (2004). *J. Orthop Rsch*, **22**, 659-664.
[2] Brown, DC. (1976). *Intl. Arch. Of Photog*, **21**(3). Paper3.
[3] Gower, J. C.,(1975). *Psychometrika*, **40**, 33-50
[4] Habib, A. et al., (2002). *Photog Rec. J*, **17**(100):635-650.
[5] Kärrholm, J. et al.,(1994). *J Bone Jt Surg (Br)*, **76**, 912-917.
[6] Önsten, I. et al. (2001). *J. Orthop Rsch*, **19**, 1162-1167.

ACKNOWLEDGEMENTS

NARMAX AND ARMAX REPRESENTATION OF DYNAMICS OF ROBOT FOR SHOE TESTING

Gye-Rae Tack[1,2] ; Gerald Cole[1] ; Benno Nigg[1]
[1] Human Performance Laboratory, University of Calgary, AB, Canada, cole@kin.ucalgary.ca
[2] Biomedical Engineering, Konkuk University, Chungju, Chungbuk, Korea

INTRODUCTION

A robotic shoe testing system that mechanically simulates human motion was proposed to overcome the problems associated with human subject tests [1]. The Stewart platform robot includes a parallel linkage that permits movement of the platform with 6 degrees of freedom relative to a fixed foot/shoe system. Functional testing of footwear with this system can be performed in two ways: i) changes in kinetics between shoes can be compared for the same motion input, or ii) changes in movement pattern that produce the same kinetic response can be compared between shoes. In pursuit of ii), above, the objective of this project is to develop a method to predict the robot motion trajectory that produces a specified force and moment acting on the foot for a particular human motion. In order to solve this problem, it is imperative to understand the dynamics of robot for shoe testing.

METHODS

The dynamics of the robotic system includes many variables (robot itself, shoe, surface, etc.), making it difficult to find the structure of the system. Thus, it is appropriate to instead use a functional identification to determine the relationship between the kinematic input and the kinetic output. There are several methods for function identification approach such as functional series (Wiener and Volterra series), and parameter estimation [2, 3]. For this study, parameter estimation approach was selected due to the multi-input and multi-output nature of the problem and then tested for human motion [4]. Leontaritis et al. showed that by expanding the system output in terms of past inputs and outputs using a nonlinear autoregressive moving average model with exogenous inputs (NARMAX) model, a concise representation of a wide class of nonlinear systems can be obtained [5].

$$y(n) = F[x(n), x(n-1), \ldots, x(n-n_x), y(n-1), \ldots, y(n-n_y),$$
$$e(n-1), \ldots, e(n-n_e)] + e(n)$$

where F: any nonlinear function; y: output; x: input; e: prediction error; and n_x, n_y, n_e: delay terms for each signal.

For this study, inputs consist of a time series of a 3D translation vector and three rotation angles (roll, pitch and yaw) of the ground relative to the foot. Outputs consist of a time series of 3D force and moment vectors acting on the foot. A second order polynomial function is used as F for NARMAX case, and a linear function is used as F for ARMAX case.

There exist several methods to solve the above problem. In this study the method proposed by Korenberg et al. [6] was used together with a Gram-Schmidt orthogonalization, making it easy to handle various input signals and to select a proper set of system variables.

RESULTS AND DISCUSSION

Figure 1 shows preliminary results for the forces measured on the foot when an experimentally measured movement path of the foot relative to the ground for a v-cut motion was used as input to the robot. The kinetics measured by the robot clearly differs from the experimentally measured kinetics for the particular trial. The dynamics of the robot system is different from that of the human. Therefore, it is necessary to adapt/modify the robot's trajectory using the proposed method, this work is currently under investigation.
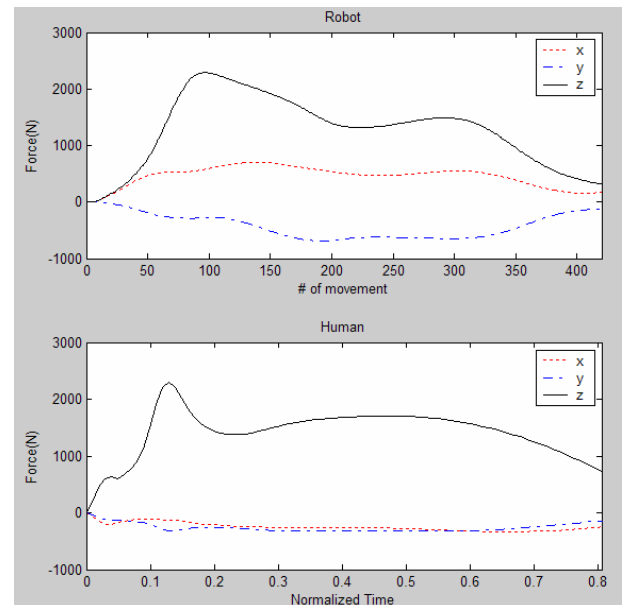

Fig. 1 Ground reaction force of robot and human subject for a lateral v-cut movement

SUMMARY

The methodology to predict the new motion trajectory for a robotic footwear testing system that will produce similar force and moment to human motion was proposed in this study using ARMAX and NARMAX.

REFERENCES

1. Goldsmith, P. (1998), *Annual Conference on Control, Automation, Robotics, and Vision*, Singapore, 6-13
2. Kearney, R.E. et al. (1990) *CRC, Critical Reviews in Biomedical Engineering*, Boca Raton, FL, 55-87
3. Kukreja, S.L. et al. (2003) *IEEE Trans. Biomedical Engineering*, **50**, 70-81
4. Billings, S.A. et al. (1989) *Int. J. Control*, **49**, 2157-2189
5. Leontaritis, I.J. et al. (1985) Int. J. Control, **41**, 303-344
6. Korenberg, M.J. et al. (1988) *Int. J. Control*, **48**, 193-210

ACKNOWLEDGMENT

DEVELOPMENT OF A NEW METHOD TO DETERMINE KNEE VARUS/VALGUS

Jonathan Singer and D. Gordon E. Robertson
School of Human Kinetics, University of Ottawa, Ottawa, ON, Canada, jsing042@uottawa.ca

INTRODUCTION

Excessive knee varus/valgus is known to alter joint loading patterns, placing unusual stresses on the articular surfaces, joint capsule and ligaments. Such stresses can be the result of either a chronic condition, such as genu varum or valgum (Kerrigan et al., 2002), or an acute injury, which may occur during physical activity (Besier et al., 2001).

Three-dimensional videography and inverse dynamics have been extensively used to quantify the varus/valgus moment at the knee. Such analyses can often be time consuming for the clinician, who must assess many patients, and difficult for the researcher, who may wish to set up equipment to collect data in remote locations. As such, the purpose of this investigation was to develop a new method to determine the external knee varus/valgus moment. The proposed method employs strain gauges, configured to measure the bending moment applied to the lateral support of a knee brace. It is hoped that this approach will have application in orthotic evaluation and sport biomechanics.

METHODS

Four strain gauges–two active and two Poisson–were wired in a Wheatstone bridge and applied to the distal aspect of the lateral support of a functional knee brace, such that the bending moment applied to the support could be measured. To determine the sensitivity of the lateral support, the most distal aspect was securely clamped in a vice and a range of known forces were applied to the support at a point just below the hinge. Applied moment of force values were correlated with the lateral support gauge output voltages. The sensitivity of the lateral support gauges was determined by the slope of the least squares regression line. Sensitivity values were obtained for both varus and valgus directions.

Sample data from two subjects, performing a number of simple walking and crossover cutting trials, were collected with the participant wearing the instrumented brace. To ensure consistency among the cutting trials, the angle of cut was monitored, effectively falling between 30 and 60 degrees from the original direction of motion. Force platform data, using one Kistler force platform, were collected simultaneously with lateral support strain gauge data for the stance phase of the left leg during one stride. All data were sampled at 240 Hz for the duration of stance and swing phases. Force platform data were reported according to the ISB reactionary coordinate system.

RESULTS AND DISCUSSION

Figure 1 illustrates the typical moment of force pattern that was applied to the brace during one stride, beginning and ending at heel-strike. It is interesting to note that in the walking condition, the moment applied to the brace lacks the initial peak that has been reported to occur within the initial 15-30% of the stance phase (Allard et al., 1997). This may be due to the fact that the internal valgus moment of force effectively controls the varus motion of the leg during weight acceptance, resulting in a smaller applied moment to the brace. The second varus peak, occurring just prior to toe-off, corresponds with the internal valgus moment that typically occurs during 60-85% of stance (Allard et al., 1997). The moment applied to the brace in the crossover cut appears to be representative of that condition, whereby a greater moment is applied over the duration of stance.

Peak varus moment of force values for the walking and crossover cut condition were 0.59 N·m and 0.67 N·m, respectively. Although the peak varus moment applied to the brace was larger in the crossover cut condition, it was not substantially so. This may be due to the relatively low coefficient of static friction ($\mu=0.52$) between the shoe sole and the force platform, barring the participant from sufficiently planting the foot and performing a vigorous cut. As the participants were aware of the need to perform a crossover cut, the small difference between the two applied moments may also be caused by postural adjustments made in preparation for the cut, in attempt to protect the knee structures (Besier et al., 2001).

From this, future work entails comparing applied moments to internal knee moments and collecting data in vivo to account for concerns due to friction and anticipatory mechanisms.
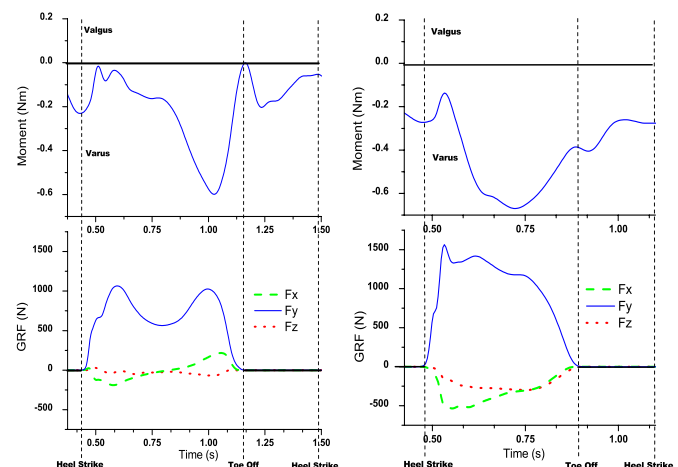

Figure 1: External bending moment of force applied to the lateral support (top) and corresponding ground reaction forces (bottom) during walking (left) and lateral cutting (right).

REFERENCES

Allard, P. et al. (1997). *Three-dimensional Analysis of Human Locomotion*. Toronto, Wiley.
Besier, T.R. et al. (2001). *Med Sci Sports Exerc*, **33**, 1176-1181.
Kerrigan, D.C. et al. (2002). *Arch Phys Med Rehabil*, **83,** 889-893.

OPTICAL IMAGING TECHNIQUES AND STEREO-RADIOGRAPHY APPLIED IN 3D RECONSTRUCTION OF SCOLIOTIC HUMAN TORSO

D. Robu[1], P.Poncet[1], F.Cheriet[3], R.F.Zernicke [2,1], J.L. Ronsky [1,2]

[1] Department of Mechanical and Manufacturing Engineering, Faculty of Engineering, University of Calgary,
[2] Faculty of Kinesiology, University of Calgary, [3]Ecole Politechnique, Montreal, drobu@ucalgary.ca

INTRODUCTION

A non-invasive innovative technique has been developed to detect spinal curve deformities associated with scoliosis from precise 3D computerized torso surface reconstruction and torso surface asymmetry measurements. The complex relations between torso surface and spine deformity were quantified with a laser optical scanning system (Poncet et al., 2000) and a 3D stereo radiographic reconstruction technique (Dansereau et al., 1990) using Artificial Neural Networks (Jaremko et al., 2002). To enable the integration of more accurate data (<1mm) with faster data acquisition, we implemented a new torso scan system (Fig.1) (InSpeck, Montreal). The purpose of this research is to evaluate the factors that influence the 3D torso reconstruction accuracy with the new optical imaging technology.

METHODS

The InSpeck imaging system uses Moire fringe patterns of white halogen light to capture torso surface data from rapid exposures (0.7s).
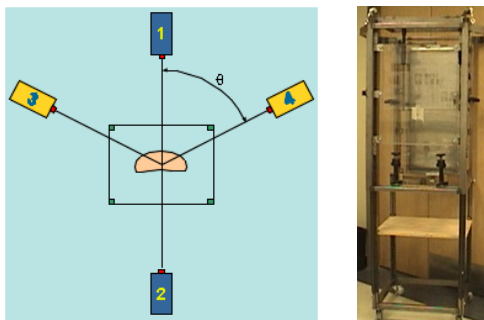

Figure 1: Inspeck System set up (θ=60°,75°,90°) and Patient Positioning Aparatus

Concurrently, two radiographs (postero-anterior with 0° and 20° inclination) are obtained while the patient stands still in a positioning and calibration apparatus. Unobstructed torso imaging (4 cameras) of the subject within the positioning apparatus is required.
Two key factors that may influence accuracy of the 3D torso reconstructions will be evaluated: camera orientations (60°, 75°, 90°) relative to the calibration object and object of interest, and ambient lighting levels that can affect the quality of calibration.
System evaluation was completed through repeat measurements (n = 5) and comparison of two custom designed and fabricated test objects: a regular trapezoidal shape and a scoliotic mannequin based on 3D reconstruction surface models created from optical imaging with custom software (Fig.2).
Radiopaque markers at known locations measured using a CMM provided landmarks for evaluation of the 3D surface registrations.
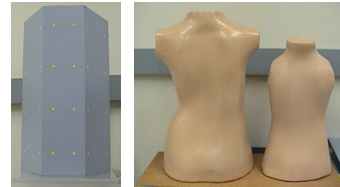

Figure 2: Trapezoidal and Scoliotic Test Objects

A comparison for the CMM and optical measurements was completed on the regular trapezoidal shape calculating the distances between all the possible combinations of 2 points from all the 16 points (representing the centers of the markers) located on each side. To enable the vizualization of the spatial superimposition for the center of the markers, their 3D coordinates were transformed in the same coordinate system and represented in a 3D graph (Fig.3).

RESULTS

Based on image registration and assessment of resultant surfaces, mean results for camera orientation at 60° are within 1.36 (3.24) mm (Fig.3).
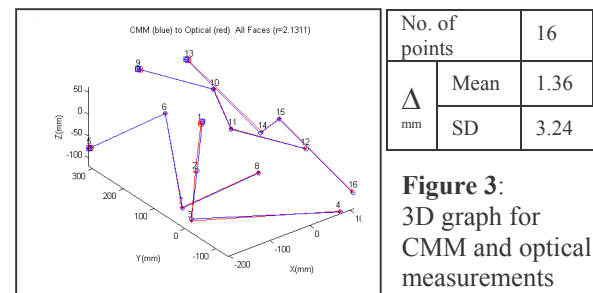

No. of points		16
Δ mm	Mean	1.36
	SD	3.24

Figure 3: 3D graph for CMM and optical measurements

The optimal setup will be based on comparison with data obtained for the 75° and 90° camera orientations, and different lighting levels. Results to date indicate substantial improvements with increased camera angle orientations, yielding results in the <1mm range. Additionally, minimal lighting levels are required for adequate 3D reconstructions, with projector level lighting proving insufficient.

SUMMARY

High quality and repeatable torso surface imaging using the InSpeck system requires careful and consistent equipment setup. The custom test objects designed enable a reliable approach to evaluate system performance at multiple centers. Once optimized, this research will provide an accurate, cost effective, clinically useful portable torso surface imaging and modeling system suitable for clinical studies of scoliosis diagnoses, and treatments.

REFERENCES

Poncet et al., *CMBBE, Vol.4, 2000*; Dansereau et al.., *Societe Canadienne de Genie Mechanique,* **2**:61-4, 1990; Jaremko et al., *J.Biomech.Eng.* **124**(5), 2002

HABITUATION OF 10-YEAR-OLD HOCKEY PLAYERS TO TREADMILL SKATING

Kelly Lockwood, Gail Frost and Amy Brown
Department of Physical Education & Kinesiology, Brock University, Ontario, Canada, kelly.lockwood@brocku.ca

INTRODUCTION
Dry land training modalities and methodologies have been criticized for lack of sport specificity and translation to performance. Skating movements are not precisely replicated by either running or cycling and these modalities may not adequately train the musculature and sport-specific movement patterns required by the hockey player. A skating treadmill, with a surface composed of a series of parallel polyethylene slats secured to a motor-driven belt system, has been introduced to address this issue. To date, studies conducted using these treadmills have focused primarily on physiological assessment (Nobes et al, 2003; Dreger & Quinney, 1999). For the skating treadmill to be accepted as training tool, the adaptability and specificity of the movement patterns should be assessed. The purpose of the study was to assess changes in the kinematic variable during a six week habituation period on a skating treadmill (Acceleration Inc.[TM] Fargo, ND).

METHODS
Seven male, Atom A hockey players who were injury-free and had no previous treadmill skating experience volunteered for the study. Parental and subject informed consents were obtained and the research was approved by the research ethics board of the university. Physical characteristics of the subjects are shown in Table 1.

Table 1 Subject Characteristics. (Mean ±SD)

Age (yrs)	10.59 ± 0.30
Height (cm)	135.64 ± 6.01
Weight (kg)	34.56 ± 7.81
Skating Experience (yrs)	5.71 ± 0.76

Ten reflective markers were placed on anatomical landmarks on the lateral surface of the left side of the body and the medial surface of the right side of the body to facilitate a 2D kinematic analysis. Players were fitted with a harness that secured them to an overhead track to ensure safety while skating. Polar[TM] heart rate (HR) monitors were used to evaluate work intensity. Skaters wore their own skates, sharpened to their own specifications.

Subjects completed one training session per week for six weeks. Each session included a warm up and four, 1-minute skating intervals at progressively increasing speeds. The range of speeds used over six weeks was 10.5 – 22 km·hr^{-1}. Selected speeds were repeated weekly for comparison purposes. Treadmill incline remained constant at 0% grade for all sessions. Verbal encouragement was provided, however technical coaching was limited to *"skate as you would on the ice"*. After each bout, HR was recorded and skaters indicated their perceived level of exertion using the Children's Effort Rating Table (CERT) (Eston & Lamb, 2000).

The sagittal plane of motion was videotaped at 30 fps using a Panasonic 300X digital camcorder. Data were imported into Hu-M-An™ motion analysis software and ten consecutive strides were selected from each bout for each participant for analysis. Stride rate (SR), stride length (SL) and trunk angle (TA) with respect to the horizontal were determined.

Descriptive statistics for one speed (10.46 km·h^{-1}) are shown in Table 2. A within-subject repeated measures analysis of variance was used to detect differences among these variables over six weeks of training. Significance was set at $p<0.05$.

RESULTS AND DISCUSSION
Over six weeks of training, significant differences in both SR and SL were evident at 10.46 km·h^{-1}. Tests of within-subject contrasts revealed a significant linear trend, such that SR decreased and similarly SL increased over time. No significant differences were seen in trunk angle or heart rate for this speed of skating.

SUMMARY
In conclusion, within 24 minutes of exposure to treadmill skating, significant changes were seen in SR and SL contributing to a visibly more efficient skating style. Further analysis will include a continuum of skating speeds as well as an on ice comparison of the same kinematic variables.

REFERENCES
Dreger, R. & Quinney, HA (1999). *Can J. Appl. Physio*. **24**(6), 559-569.
Eston, R. & Lamb, K. (2000). *Paediatric Exercise Science and Medicine* (ed. N. Armstrong & W. van Mechalen) Oxford University Press, Oxford, UK.
Nobes et al (2003). *Can J. Appl. Physio*. **28**(1), 1-11.

ACKNOWLEDGEMENTS

Table 2 Stride rate, stride length, trunk angle and heart rate at 10.46 km·h^{-1} (Mean (±SD)

Week	Stride Rate (strides·s^{-1})	Stride Length (m)	Trunk Angle (degrees)	Heart Rate (beats·min^{-1})
1	1.09 ± 0.19	2.74 ± 0.44	63.38 ± 2.45	165.71 ± 16.18
2	0.96 ± 0.11	3.08 ± 0.37	63.21 ± 3.35	164.00 ± 12.30
3	0.98 ± 0.09	2.99 ± 0.28	67.23 ± 4.97	153.71 ± 14.05
4	0.88 ± 0.07	3.33 ± 0.28	64.51 ± 3.44	150.14 ± 13.67
5	0.85 ± 0.12	3.49 ± 0.50	64.70 ± 5.52	158.14 ± 8.97
6	0.86 ± 0.05	3.41 ± 0.22	67.76 ± 3.36	155.14 ± 10.51

A KINEMATIC ANALYSIS OF AN ULTRA-MARATHON RUN

Megan Moreau and Pierre Gervais

Sports Biomechanics Laboratory, Faculty of Physical Education and Recreation
University of Alberta, Edmonton, Alberta, Canada, pierre.gervais@ualberta.ca

INTRODUCTION

In this new millennium athletes are pushing their bodies to new limits in the pursuit of glory in extreme sporting events. This study took one of these events, a 100 km ultra-marathon run and analyzed the running kinematics of elite runners during the race. Williams and Cavanaugh (1987) both related a greater maximum hip extension angle and a smaller knee angle at toe-off to more efficient gaits. Interestingly, individuals running in a fatigued state have been noted to run in an almost seated position, compensating for lower body stiffness by stretching their leg extensors (Candau et al., 1998). It has also been noted that elite distance runners display more efficient kinematics in the latter stages of a race. The possible application of this study may include modification of training and race strategy, and if teamed with the breadth of knowledge in the physiological aspect of such events, faster and more efficient racers.

METHODS

The subjects were all finishers of the International Association of Ultrarunners (IAU) 100 km World Challenge, under the patronage of the International Amateur Athletic Federation (IAAF). Each runner was between the age of 20-39 years, had completed at least one 100 km race in a time 6:45:00 (hrs:min:sec) or better, and were members of their respective national teams. The sagittal view of the top ten and final three elite male finishers were videotaped from the end of the 10 km loop which was run ten times. A field of view 2.4 m in length was captured at the 10, 50, 70, 90, and 100 km marks. Data was gathered using a JVC Cybercam 9800 digital video camera, recording at 60 Hz with a shutter speed of 1/250, and analyzed using the Ariel Performance Analysis System (APAS).

Data was smoothed using a fourth order, zero-lag Butterworth digital filter with cut-off frequencies ranging between 6 to 8 Hz. Smoothed data was then used to acquire the vertical oscillations, trunk lean, hip flexion and extension, knee flexion and extension, shank angles, and joint ranges of motion. A repeated one-way analysis of variance was performed on the data for statistical analysis.

RESULTS AND DISCUSSION

For each of the variables measured: trunk and shank angles with respect to vertical; thigh angle with respect to horizontal; hip and knee joint angles; hip and knee joint flexion and extension ranges of motion; and the vertical displacement of the hip. There were no statistically significant changes observed, therefore no significant deterioration of the running gait.

There were two interesting trends to be noted. Knee joint flexion decreased notably, though not to a degree of statistical significance, from the 10 km point to 100 km point. The means knee joint flexion angle for all 13 subjects at 10 km was 69.2 degrees, as compared to 74.0 degrees at the 100 km mark. This trend can be seen clearly in Figure 1.
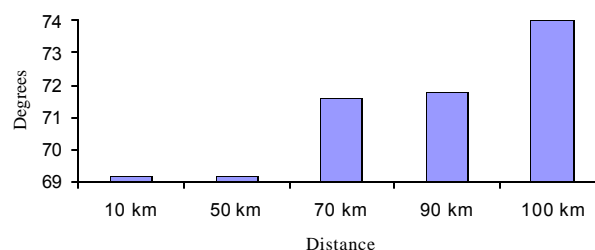

Figure 1: Mean knee joint angle for all thirteen subjects at each of the five captured distances during the 100 km run.

A second trend noted was one toward less thigh segment extension as the race progressed. At 10 km, the mean for all subjects was 119.1 degrees compared to 113.0 degrees at 100 km. This display of less thigh segment extension should be expected when the extreme, 100 km, distance of the ultra-marathon is considered. The lack of a statistically significant finding can be related to the study by Williams and Cavanaugh (1987), where it was noted that better economy runners displayed greater leg extension throughout a fatiguing run than lower economy runners. Both groups of finishers, the top ten and bottom three are considered high economy, elite runners. If the leg isn't extended maximally, specifically at toe-off and immediately following toe-off, the result will be a less powerful push-off, shorter stride length, slower hip flexion velocity, and ultimately a slower run velocity.

SUMMARY

Though no kinematic measure was found to be statistically significant there were two trends noted, primarily less knee joint flexion and thigh segment extension, as the run progressed. The gait mechanics measured were not easily perturbed in these highly efficient runners.

REFERENCES

Williams, KR & Cavanaugh, PR (1987) *Eur J App Physiol,* **63**, 1236-1245.
Candau, R. et al (1998) *Eur J App Physiol*, **77**, 479-485.

A COMPARISON OF THREE BACK HANDSPRING PROGRESSIONS

Pierre Gervais, Tom Wu and J. Steven LeBlanc

Sports Biomechanics Laboratory, Faculty of Physical Education and Recreation
University of Alberta, Edmonton, Alberta, Canada, pierre.gervais@ualberta.ca

INTRODUCTION

The back handspring is a fundamental tumbling skill taught to children early in their gymnastics training. Koh *et. al.* (1992) and Hall (1982) have suggested that risk of overuse injuries may result from poorly executed back handsprings. Learning of skills is often associated with less than ideal technical execution. Gymnastics Canada has promoted the use of progressions and alternative equipment configurations to enhance a fruitful learning environment that is effective and safe (Kinsman, *et. al.*, 1986). The purpose of this study was to address the question as to which of 3 popular learning progressions maybe most favourable to acquiring the back handspring.

METHODS

Two girls and 3 boys, between the ages of 10 and 12 years, were recruited for the study. The children were all familiar with the 3 back handspring progressions. The children were fitted with reflective markers over the joint centres on the side of the body closest to the camera. Data was collected using standard 2D video techniques using a JVC GR-DVL9800 camera operating at 60Hz. Video data reduction and analysis was performed using the APAS system by Ariel Dynamics Inc.

The three back handspring progressions (conditions) consisted of 1) a spotted standing back handspring, 2) a snap down back handspring in which the child started in a handstand position on a 30 cm hard foam block and snapped down to their feet proceeding immediately into a back handspring and 3) a standing back handspring performed down an inclined mat. The incline mat is a common learning tool used in gymnast instruction. The mat used for this study had a 2m base and height of 46cm providing a slope of 13 degrees. For the 3rd condition the gymnasts started with their feet on the inclined mat near the top and executed the back handspring down the incline. One of the gym centre's coaches assisted in the spotting of the back handsprings. Temporal kinematics, angular momentum, and joint reaction forces and moments during hand contact were derived from the video data. A one-way ANOVA with repeated measured was used for statistical analysis. The p-level was set at 0.05.

RESULTS AND DISCUSSION

No significant differences were found between conditions on joint reaction force and net joint moments. These findings are in agreement with an earlier study, which compared similar back handsprings, by force plate and video analysis (Gervais et al, 2003).

Gluck (1982) described a good back handspring as one that increases the linear velocity of the CM, raises the CM and increases the angular momentum in the direction of progression. Gluck maintained that these desirable traits were the result of a leg snap, which was initiated with hip hyperextension and shoulder hyperflexion during hand contact. No significant differences were observed in the flight time from initial foot contact to hand contact or during hand contact for the three back handspring conditions. There were no significant increases in angular momentum during the hand contact phase yet there was a significant increase seen in the horizontal velocity of the body's CM at foot contact following the snap down from hand contact (Table 1). The subjects made initial hand contact in a significantly more vertical body position using the inclined mat (condition 3) as illustrated by the angle of incidence (the angle formed between a negative horizontal, the wrist and the body's CM).

CONCLUSION

Based on Gluck's descriptors of an effective back handspring, the results of this study support the usefulness of performing the back handspring down an incline for learning and practice.

REFERENCES

Gluck, M. (1982) *Mechanics for Gymnastics Coaching*, Charles C. Thomas Pub, Springfield Il.
Gervais, P. et al (2004) Proc XIXth ISB, 120.
Hall, S. (1986). *Med Sci Sports and Ex.* **18**(6), 599-602.
Kinsman, T. *et al* (1986). *Coaching Certification Manual Level 3 Men*, Gymnastics Canada.
Koh, T.J. *et al* (1992). *Am J Sports Med.* **20**(1), 61-66.

Table 1 Measured variables of the three back handspring conditions. Data are means (SD)

Condition	Flight Time (ms)	Hand contact time (ms)	Angle of incidence	CM hor. vel. (m/s)	Δ Ang. Mom (sec^{-1})
1) Spotted	230 (71)	263 (34)	79.05^o (4.54)	1.81 (0.48)	-0.070 (0.301)
2) Block	213 (61)	273 (48)	76.99^o (5.87)	1.76 (0.21)	-0.099 (0.713)
3) Inclined	183 (22)	267 (87)	86.64^o (5.54)*	2.26 (0.45)*	-0.496 (0.454)

   * significant at p<0.05

CHILDREN'S WORKSTATIONS: POSTURAL CHANGES DURING COMPUTER GAMES

Carol Murphy, Heather Brackley, Mohammad Abdoli, Joan Stevenson.
Biomechanics/Ergonomics Laboratory, 148PEC, Queen's University, Kingston, Canada, dcmurph@cogeco.ca

INTRODUCTION

The increasing incidence and disability associated with RSI and MSD and their frequency among computer users has led to concern. This concern has been extended to young children who are potentially also at risk for these injuries. This risk is increased by the fact that children are often required to play and work on computer workstations which are designed for adult anthropometrics. The effect of the adult workstation on a child's postures and their joint and segmental angles was examined.

The purpose of this research study was to examine the quality and quantity of postural movements exhibited by five year olds when using an adult workstation to play a computer game.

METHODS

Six physically active 5 year old boys and girls were asked to participate in the study. After ethics approval by parents, children were asked to give verbal assent. Each child was asked to wear a dark shirt which was tucked in at the waist. Joint markers were placed on the shoulder, elbow, wrist, and third knuckle for upper limb joint angles.   For head orientation, the earlobe and two sweat-band markers were used. For back orientation, bilateral extended markers were placed at the level of C7, T7, T12 and L5. Although not always visible at all times, the hip, knee and ankle were marked for lower limb kinematics. The chair served as a calibration factor.

Once outfitted, each child was asked to play a pre-selected computer game for 30 minutes. The game set-up involved use of the keyboard initially, but thereafter it was primarily mousing. Digital images were taken perpendicular and posterior to the subject for the total time. After 30 minutes, each child was asked to complete a series of shoulder shrugs and head flexion, extension, lateral bending and rotation to determine their full range of motion.

Using Pinnacle Studio DV software, the time that subjects spent in static postures and the frequency and nature of their postural changes were recorded from the time counter. Then, individual images were extracted from each segment in order to evaluate the posture that the child was assuming. The specific postures of interest from the side camera were 1) angles of the a) upper thoracic, b) lower thoracic, c) thoracolumbar, d) pelvic tilt, 2) head flexion angle, 3) hip angle, 4) knee angle, 5) elbow angle, 6) wrist angle and 7) ear-eye angle From the rear camera, the points of interest were angles from the horizontal of the a) C7, b) T7, c) T12, d) L5, e) head tilt and 2) shoulder abduction angle, 3) elbow angle and 4) radio-ulnar deviation.   Positional factors that were evaluated were: 1) eye to screen distance, and 2) percent height of eyes from the top of the screen. Data were analyzed using descriptive statistics and comparing their postures to recommended postures for office ergonomics.

RESULTS AND DISCUSSION:

Preliminary analysis of the data appears to indicate that five year old children make a number of postural changes and adaptations in order to work at an adult size workstation. Data also shows that their postures do not fall within recommended guidelines for workstation ergonomics. Further, the joint and segmental angles examined appear to exceed recommended safety limits. Therefore, the postural adaptations and compensations that children are required to perform would appear to put them at risk for musculoskeletal injury.

SUMMARY

Based on these preliminary results it would be advisable to devise recommendations and guidelines for children's workstation design. This need is deemed to be imperative based on the increasing use of computers both in school and at play and the increasing amount of time spent at the computer on a daily basis. (Jacobs, 2002)

REFERENCES

Gillespie, R.M. *Work*. 2002;18(3):249-59
Jacobs, K. Baker, NA. *Work*. 2002;18(3):221-6
Straker, L, Briggs A, Greig A. *Work*. 2002; 18(3):239-48

ACKNOWLEDGEMENTS

ANGULAR KINEMATICS IN ASSISTED AND RESISTED SPRINTING AS COMPARED TO FREE SPRINTING

J Steve LeBlanc and Pierre L Gervais

Sports Biomechanics Lab, Faculty of Phys. Ed. and Rec., University of Alberta, Edmonton AB, Canada, steve.leblanc@ualberta.ca

INTRODUCTION
Sprinting is a component of many sports, and consequently many athletes and coaches employ various training modalities to develop running speed, particularly assisted (or "over-speed") and resisted sprinting. Only limited research has been published on the effectiveness of these training modalities (e.g., Corn & Knudson, 2003; Majdell & Alexander, 1991) despite their popularity among sport practitioners. Assisted sprinting is thought to lead to increases in stride rate and/or stride length by inducing changes in neuromuscular function. The use of resisted sprinting is thought to be an effective method to induce movement-specific strength gains leading to increased stride length. The scientific literature has been inconclusive as to the effectiveness of these sprint training modalities. The purpose of the present study was to compare angular kinematics during sprinting under assisted and resisted conditions as compared to normal free sprinting in the top-speed and acceleration phases of a sprint.

METHODS
Six subjects (age 21.8 ±1.7 years, height 1.78 ±0.08m, mass 77.0 ±8.6kg) were recruited from the University of Alberta varsity track and field team. Subjects completed 3 trials of each of 4 conditions: assisted sprinting (AS); free sprinting (FS); resisted sprinting (RS); and, a sprint start (SS). The AS condition was achieved using a pulley-based manual towing system, and the RS condition was achieved using a resistance chute (approximately 1 m^2). One trial per subject per condition was randomly selected for kinematic analysis.

Two cameras (60 Hz) were positioned with overlapping fields giving a sagittal view of the subject for approximately two full running strides. Subjects were fitted with retro-reflective hemispherical markers 1cm in diameter over the joint centres on the right side of the body. Video was analysed with APAS™ software using an 8-point, 6-segment model representing the right side of the body. Data was digitally filtered within APAS™ (filter cut-offs of 6 Hz in x, 8 Hz in y). The angular kinematic parameters of interest were: total range of motion in the thigh segment, knee joint, and upper arm segment; and, peak angular velocities of flexion and extension of the thigh segment, knee joint, and upper arm segment.

Thigh and upper arm segment angles were defined relative to the right horizontal at the proximal end. Knee angle was defined as the included joint angle between the thigh and shank segments. Repeated measures ANOVA (α=0.05) was used for statistical analysis to identify trends in the angular kinematics across the four conditions.

RESULTS
The average running speed of each condition as compared to FS (9.40 m/s) was: 6.8% faster for AS (10.04 m/s); 7.1% slower for RS (8.74 m/s); and 6.8% slower for SS (8.76 m/s). Mean values for each of the angular kinematic parameters of interest are presented in Table 1. The repeated measures ANOVA showed no significant differences for any of the kinematic parameters between any conditions.

DISCUSSION
From the present analysis, it appears that the AS condition did not result in greater amplitude or speed of movement than FS with regards to the angular kinematic parameters. This seems to run counter to the commonly held belief among sport practitioners that assisted sprinting will induce greater speeds of movement, and perhaps altering neuromuscular function. Similarly, the RS condition did not seem to result in any noticeable changes in angular kinematics. These results may have impilcations for sport practitioners designing training programs to develop maximum running speed. More research is necessary to clarify what, if any, short- and long-term effects on sprinting performance may result from the use of assisted and resisted sprint training modalities.

REFERENCES
Corn, RJ & Knudson, D (2003). Effect of elastic-cord towing on the kinematics of the acceleration phase of sprinting. J. Str. and Cond. Research, 17(1), pp.72-75.
Majdell, R & Alexander, MJL (1991). The effect of overspeed training on kinematic variables in sprinting. J. Human Mvt. Studies, 21, pp.19-39.

ACKNOWLEDGEMENTS

Table 1: Means (and standard deviations) of angular kinematic parameters for the four conditions.

		AS	FS	RS	SS
Thigh	ROM	96.1 (5.7)	94.7 (7.1)	97.1 (7.5)	92.6 (7.7)
	Peak Flex. Vel.	719.8 (16.3)	721.8 (56.0)	704.9 (29.4)	692.1 (40.8)
	Peak Ext. Vel.	-605.9 (29.1)	-606.1 (37.3)	-585.5 (49.2)	-575.6 (43.0)
Knee	ROM	114.9 (4.8)	114.7 (6.9)	115.0 (9.7)	111.5 (4.0)
	Peak Flex. Vel.	-1099.0 (33.1)	-1137.4 (83.4)	-1137.6 (110.6)	-1108.9 (80.2)
	Peak Ext. Vel.	1084.0 (50.8)	1066.0 (54.9)	1014.5 (81.3)	1036.3 (56.7)
Upper Arm	ROM	117.7 (9.9)	113.2 (11.4)	121.7 (12.6)	114.4 (12.2)
	Peak Flex. Vel.	839.5 (98.2)	825.7 (73.0)	857.8 (68.5)	905.4 (75.7)
	Peak Ext. Vel.	-754.2 (139.2)	-692.5 (81.3)	-699.3 (80.6)	-785.3 (149.7)

COMPARISON OF CHANGES IN TORSO SHAPE ASYMMETRY AND SPINAL DEFORMITY OF SCOLIOTIC SUBJECTS BEFORE AND AFTER SURGERY

P. Poncet[1], D. Robu[1], J. Jaremko[1], J. Harder[2], F. Cheriet[3], R. F. Zernicke [1,2], J. L. Ronsky [1]

[1] Dept. of Mechanical and Manufacturing Eng., University of Calgary, 2500 University Drive NW, poncet@ucalgary.ca and
[2] Department of Surgery, University of Calgary, Alberta, Canada, [3] Ecole Polytechnique of Montreal, Montreal, Quebec, Canada

INTRODUCTION

The adolescent idiopathic scoliosis (AIS) is a complex three-dimensional (3-D) deformation of the musculo-skeletal system of the trunk, with prevalence of about 1-3% in the general population. Among patient with AIS, about 1/1000 will need surgical treatment to correct the deformity with spinal instrumentation. About 15000 such surgeries are performed every year in North America (SRS, 1997). Surface deformity is often the primary patient complaint in scoliosis, and scoliosis treatment such as surgery may not correct the surface deformity (Pratt et al., 2002). Here we propose to use our 3D imaging system (Poncet et al., 2000) to produce a more complete description of the torso deformity before and after treatment. The purpose of this study is to compare changes in all measured surface (extrinsic) and spinal deformity (intrinsic) indices before and after surgery occurs and to extract indices that will best characterize the cosmetic asymmetry. This will help better assess an individual's torso surface changes due to spinal surgery in scoliosis and could contribute to an improved understanding of the 3D effects of surgery that may ultimately aid in design of more effective surgical treatment.

METHODS & RESULTS

Three-dimensional torso models (Figure 1) of five scoliotic patients were generated before and after spinal surgery from surface data acquired by laser cameras and X-rays taken concurrently as the patient stood in the same position (Poncet et al. 2000).
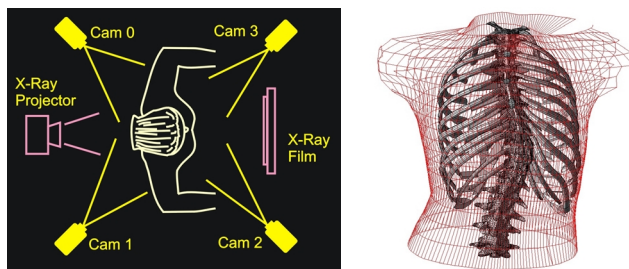

Figure 1: a) Laser cameras and X-ray layout for concurrent torso surface and spine imaging b) Superimposed 3D torso surface mesh and spine/rib cage

The Cobb angles of the instrumented primary curves were reduced from 51.4º (37-65º) to 34.6º (20-55º). Clinical indices of spinal deformity and torso surface asymmetry indices (Jaremko et al., 2002)(Figure 2) were compared for each patient pre- and postoperatively. Significant correction changes of the torso shape were detected in indices including the lateral deviation of the torso centroid line, the orientation of cross-sectional principal axes of inertia (PAX), the rib hump and the left-right asymmetry of half-centroid locations. However, indices such as the lateral deviation of the line of spinous processes, the back surface rotation (BSR), the difference between PAX and BSR, the moments of inertia and

the section aspect ratios showed relatively subtle asymmetry correction compared to spinal deformity. Because of some discrepancy between spine and torso deformity correction, trunk asymmetry should be assessed for an objective evaluation of the effect produced by a specific treatment.
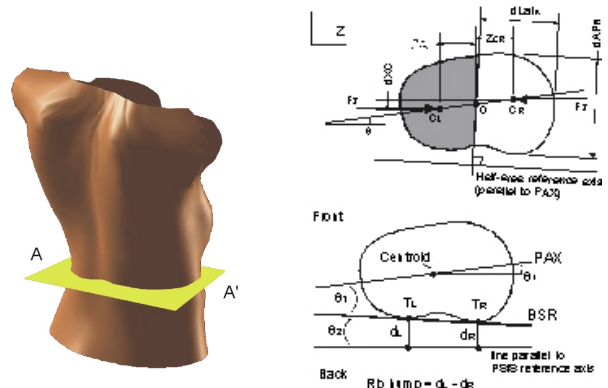

Figure 2: Calculation of selected torso asymmetry indices

SUMMARY

Torso deformity is often the most concern of a patient with scoliosis. Here we have shown that we can acquire 3D torso surface and reliably measured a set of indices of transverse torso asymmetry. Three-dimensional torso surface model of patients were generated from surface data acquired by laser cameras. Clinical indices of spinal deformity and torso surface asymmetry indices were compared before and after surgery for five patients. Although significant correction changes of the torso shape were detected in some indices, others showed relatively subtle asymmetry correction compared to spinal deformity.

We are currently processing data from more patients to identify those patterns of changes that may be clinically significant and/or worthy of further quantification. This will allow selection of the set of indices that best characterizes torso deformity. We also propose to compare, with surface and radiographic measurements, changes in patient subjective assessment of deformity and other symptoms such as back pain, before and after surgery occurs. In future stages of the project we could use our results to guide improved techniques of scoliosis surgery and quantify the outcomes.

REFERENCES

[1] Pratt, R., Burwell, R., Cole, A., and Webb, J., *Spine,* **27**(14): 1543-1550, 2002. [2] Poncet et al., *CMBBE,* **4**:59-75, 2000. [3] Jaremko, JL. et al., *Clin Biomech,* **17**(8): 559-568, 2002.

ACKNOWLEDGEMENTS

THE EFFECTS DIFFERENT POSTURES AND ADIPOSE CONTENT ON THE BIODYNAMIC RESPONSE OF THE HUMAN SPINE TO WHOLE-BODY VIBRATION

Robert Jack[1], Tammy Eger[2], Lloyd Reed[3] and Cynthia Whissell[4]
[1]Center for Research in Human Development, Laurentian University, Sudbury, Canada
[2]School of Human Kinetics, Laurentian University, Sudbury, Canada
[3]Department of Physics and Astronomy, Laurentian University, Sudbury, Canada
[4]Department of Psychology, Laurentian University, Sudbury, Canada

INTRODUCTION

Many studies have found that having a bent or twisted trunk while exposed to WBV increased the risk of low back and neck pain. Postures like the seated bent posture should transmit vibration up the spine more readily because of increased rigidity or stability of the spine as a result of differences in the angle of the pelvis, the spinal curvature, intervertebral disc pressure, and muscle tension (Anderson, Murphy, Ortengren, and Nachemson, 1979). The angle of flexion of the knee joints may also influence the shape of the lumbar spine and muscle activity, thereby influencing the transmission of vibration up the spine (Chaffin, Anderson and Martin, 1999). The intention of this study was to assess the effects of different seated postures and adipose content on the transmission of vibration up the spine.

METHODS

Male university students aged 19 to 25, with less than 5 years of expose to vibration were recruited for the study. All subjects were verbally screened for a history of neck or back problems.

Subjects were exposed to WBV while adopting 5 unsupported trunk positions (15, 10, 0, -10 and -15, +/- 2.5 degrees from vertical), and 4 hip positions position (-10, 0, 10, and 20 degrees from the horizontal). WBV measurements were taken for each posture combination so that vibration transmission from the seat exposure to the head could be calculated. Subjects sat on a vibrating seat for 30 seconds. Vibration exposure measurements were taken with a triaxial accelerometer placed on the seat pan between the ischial tuberosities and a tri-axial accelerometer mounted on the head (via a harness) following basicentric guidelines. All vibration measurements followed the guidelines set out in the 1997 ISO 5349 standard.

Hydrostatic weighing was conducted to determine the subject's adipose content. All hydrostatic weighing followed the protocol laid out by Adams (1998).

RESULTS AND DISCUSSION

Results indicate that adipose content of the individual had no significant effect on the transmission of vibration up the spine. Vibration exposures at 4Hz had significantly more transmission up the spine than vibration exposures at 6.3Hz. Vibration exposures in the Z-axis had significantly more transmission up the spine than vibration exposures in the X- and Y-axes. Also, a significant interaction was found between trunk position, frequency and axis of exposure.

Based on the results of this study and the findings of others a 10 degree forward lean posture with low vibration exposure levels where the dominant frequency of exposure occurs at 6.3 Hz appears to place the worker at minimal health risks from exposure. Adopting this posture may decrease problems associated with vibration transmission up the spine. This posture and exposure combination would also ensure minimal postural deviation and fatigue, which allows the operator to maintain this optimal posture but might also improve productivity.

SUMMARY

The results of this study will hopefully help to identify strategies to reduce WBV exposure and aid in designing seats with characteristics that could optimise vibration transmission through the operator. Future studies should look at various patterns of muscle activity to gain a clearer picture of how postures are affecting vibration transmission up the spine.

REFERENCES

Adams GM (1998) Exercise Physiology: Laboratory Manual 3rd ed. Boston, McGraw-Hill.
Anderson, G.B.J. et al (1979). The Influence of Backrest Inclination and Lumbar Support on Lumbar Lordosis. Spine, 4, 52-58.
Chaffin, D.B. et al (1999) Occupational Biomechanics. Toronto, John Wiley and Sons.

CHANGES IN PELVIC AND LUMBAR ANGLES WHILE PERFORMING THE POSTERIOR PELVIC TILT AND ABDOMINAL HOLLOWING MANEUVER DURING NORMAL AND MAXIMUM REACH LIFTS

Heather L. Butler[1], John W. Kozey[1,2] Cheryl L. Hubley-Kozey[3] and Jorge Acquirre[2]

[1]Department of Industrial Engineering, Dalhousie University, Halifax, Canada, hbutler@dal.ca

[2]School of Health and Human Performance and [3]School of Physiotherapy, Dalhousie University, Halifax, Canada

INTRODUCTION

Tissue strain and low-back injury have been associated with non-neutral lumbar-pelvic (LP) postures (Scannell, and McGill, 2003). As a result various clinical approaches have emerged to reduce the risk of low-back injury. These approaches include the Abdominal Hollowing (AH) maneuver and incorporating the Posterior Pelvic Tilt (PPT) during functional activities (Richardson et al, 1992). However, little evidence exists regarding whether the LP position during the AH changes from neutral or if either approach can even be maintained during a lifting task. Therefore, the objective of this investigation was to evaluate the pelvic and lumbar angles for healthy subjects while performing lifts using three techniques; their Preferred Lifting Style (PLS), and incorporating a PPT as well as the AH maneuver. These results will help determine the LP motion during a lifting task while performing common prescribed therapeutic techniques.

METHODS

Healthy college-aged females (4) and males (16) performed a 2-hand lift of a 3.8-kg load 5cm off a surface (elbow height adjusted) using 2-horizontal reach conditions (normal and maximum). For each condition subjects were instructed first to perform the lift in their PLS and then perform the randomly assigned PT or AH techniques. Training for correct PPT and AH positioning was provided after the PLS condition. Three trials were randomly performed within each technique. During each condition the movement was recorded 2-dimensionally in the saggittal plane. The 4-sec protocol was divided into 4-phases: normal standing (1), reach (2), lift-up(3) and lift-down(4). The movement included phases 2-4. Coordinates from fin-markers placed at L1 and S1 were digitized using Human™ motion analysis system. The pelvic angle ($PA=\theta_1$) and lumbar angle ($LA=180-(\theta_1+\theta_2)$) were the dependent measures and calculated as shown in Figure 1. Two 5-factor (subjects, trial, reach, technique, phase) repeated measures analysis of variance (ANOVA) models tested the main effects and interactions for pelvic and lumbar angle separately. Alpha was set at 0.05 for all tests and a Bonferroni correction was used for the post-hoc analyses of significant results.
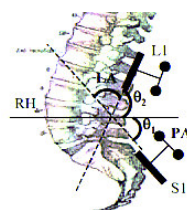

Figure 1: Schematic diagram of the lumbar spine and fin markers at L1 and S1 with pelvic (PA) and lumbar angle (LA).

RESULTS AND DISCUSSION

The ANOVA revealed a statistically significant ($p<0.05$) technique*phase interaction in both reach conditions for PA and LA. There was no trial effect indicating measurement consistency. Average PA and LA for each experimental condition are shown in Table 1.

During the PLS technique the LP position was determined to be neutral since the LA measured in our study were similar to the observed angles that resulted in minimal passive tissue strain in the work of Scannell and McGill (2003). Compared to the PLS the PA showed significant posterior rotation during the AH maneuver in the lifting phases in normal reach and reach and lift-up phases in maximum reach conditions.

It was observed that the PA was maintained throughout the movement for both PLS and AH. However during the AH technique in both the normal and maximum conditions the LA was significantly lower in phase 4 than phase 1 indicating a shift toward hypolordosis. It was also observed that the PA was significantly different between phase 2 and 4 during the PPT maneuver indicating an inability to maintain PA once the PPT maneuver was accomplished.

SUMMARY

The LA and PA were both maintained during the lift and did not differ from normal standing for the PLS only. LP position was not maintained during the movement for PPT or the AH maneuvers.

REFERENCES

Levine, D. and Whittle, M.W. (1996). *JOSPT*, **24**, 130-35.
Richardson, C. et al (1992). *Austr J Physio*, **38**, 105-12.
Scannell,J. and McGill,S. (2003).P*hysical Therapy*, **83** 907-17.

Table 1: Average PA and LA for normal and maximum reaches in three pelvic positions across the four phases of the lift.

| Phase | | Pelvic Angle (deg) | | | | | | Lumbar Angle (deg) | | | | | |
| | | Normal | | | Maximum | | | Normal | | | Maximum | | |
		PLS	PPT	AH	PLS	PPT	AH	PLS	PPT	AH	PLS	PPT	AH
1.	Stand	-71.3	-72.5	-72.5	-71.3	-72.3	-72.1	30.4	29.0	29.7	30.4	29.7	29.6
2.	Arm off	-71.6	-81.9*+	-73.2	-71.4	-81.2*+	-73.2+	30.1	14.2*+	28.1	30.3	15.2*+	28.1
3.	Lift-up	-71.3	-80.6*+	-73.0+	-70.9	-80.2*+	-72.6+	29.2	16.0*+	27.5	28.1	15.3*+	26.6
4.	Lift-down	-71.3	-79.6*^+	-73.1+	-70.6	-78.9*^+	-72.2	28.9	16.9*+	26.8*	28.1	17.0*+	26.3*

Significantly different (within each pelvic position) *from phase 1, ^ from phase 2
+Significantly different from PLS (within each phase)

EVALUATING THE PENALTY FUNCTION IN A ROBOTIC STEP ADJUSTMENT ALGORITHM

Claire Kenny-Scherber, Mike Greig, and Aftab Patla
Gait and Posture Lab, University of Waterloo, Waterloo, Canada

INTRODUCTION
Current research on biomorphic robots attempts to identify a human based algorithm for step length adjustment. Models for step length regulation are based on distance from a goal object (Lewis & Simó, 1999). The robotics industry has implemented an algorithm for adjusting step length called the penalty function based on perception-action coupling during the approach to a goal object (Lewis & Simó, 2001). The purpose of this algorithm is to allow the robot to adjust foot placement and smoothly reach the goal object without breaking stride velocity or losing stable posture. This work investigates the biological relevance of this algorithm and the validity of using distance based models for step length adjustment.

METHODS
Six healthy participants were recruited for the study. Participants randomly started at one of 5 starting points at distances of 5.00 m, 4.85 m, 4.70 m, 4.55 m, and 4.40 m from a flat paper goal object (15 x 45 cm) taped to the floor. The foot placement pattern was monitored by infrared markers (placed on the toe, fifth metatarsal, and heel of each foot). The experiment consisted of 100 trials. In trials 1-50 the participant walked comfortably on the walkway and landed with their toe on the goal object and kept walking to the end of the walkway. In trials 51-100 the participant wore a thick belt around their lower thigh that restricted their normal step length by approximately 22.1%. While wearing the belt they performed the same task as in trials 1-50.

RESULTS AND DISCUSSION
Intertrial analysis. Foot placement variability profiles showed a systematic decrease in variability starting 4 or 5 footfalls from the goal object in the restricted and unrestricted conditions. There was no statistical difference between the conditions ($F(1, 5)=5.41$, $P=.0675$), however step number had a significant effect on variability ($F(5, 25)=290.33$, $P<.0001$). These results support existing unrestricted gait literature (Montagne et al., 2000) and showed that control of foot placement is the same in both conditions. Results of distance of a given step from the goal object show that the systematic decrease in variability is not a function of distance to the goal object. Step number has an effect on distance from the goal object ($F(5, 25)= 16.43$, $P<.0001$). Therefore the robot algorithm for step length adjustment should not be based on a distance model.

Trial-by-trial analysis. An average of 2.25% and 0.36% of trials were unregulated (i.e. all adjustments were within 4% of the average step pattern) in the unrestricted and restricted conditions respectively. On average 45.5% and 68.4% of trials were mixed (i.e. when both lengthening and shortening adjustments occur in the same step sequence) in the unrestricted and restricted conditions respectively. The percent mixed trials was significantly higher in the restricted condition ($F(1, 5)=51.44$, $P=.0008$). Regulation is most often initiated at step N-5 in both conditions and decreases with each step ($F(5, 25)=18.58$, $P<.0001$). In the restricted condition regulation was always initiated before step N and was initiated at step N-5 more than in the unrestricted condition ($F(5, 25)=9.73$, $P<.0001$). This indicates that when motion is restricted there is a tendency to initiate regulation earlier in the approach phase and it is not possible to make a large one-time adjustment at step N. This result provides some support for the penalty function algorithm since regulation is shown throughout the approach phase. Regardless of condition continuity of regulation is a function of step number. The later regulation is initiated the more likely it is to be continuous ($F(5, 20)=20.93$, $P<.0001$). The relation between adjustment needed and adjustment produced becomes statistically linear ($P<.05$) at step N-3 for both conditions. This confirms that although regulation is initiated at step N-5, adjustments become effective at N-3.

SUMMARY
To employ perception-action coupling in an adaptable biped robot and prevent large one-time adjustments Lewis et al. (1999) implemented a penalty function based on energy cost. In this study, the restricted condition prevented participants from making large changes in step length. If the penalty function was an effective perception-action control algorithm, adjustments made early in the approach phase would have been more accurate than the results showed for the restricted condition. Since this was not seen a factor other than the penalty function governs foot placement adjustment in humans. Examination of average velocity and its variability for a given step shows that acceleration regulation may be a dictating factor in foot placement control. Participants made adjustments based on accurately reaching a goal object and maintaining constant velocity.

REFERENCES
Lewis, M.A. et al. (2001). *Autonomous Robots,* 11-3, 221-226.
Lewis, M.A. et al. (1999). *Connection Science, Special Issue of Adaptive Robotics,* 3-4, 331-344.
Montagne, G. et al. (2000). *Journal of Motor Behavior,* 32, 37-43.

AKNOWLEDGEMENTS

DOES FORCE DEPRESSION IN SKELETAL MUSCLE DEPEND ON THE SPEED OF SHORTENING?

Tim R. Leonard and Walter Herzog

Faculty of Kinesiology, University of Calgary, Calgary, T2N 1N4, leonard@kin.ucalgary.ca

INTRODUCTION

When a muscle is shortened while activated, its steady-state isometric force following shortening will be smaller than the corresponding isometric force obtained at the same length during a purely isometric contraction. This loss of force following active shortening has been termed force depression (Herzog, 1998).

Force depression was first described more than fifty years ago and along with other findings, it was observed that force depression increased with decreasing speeds of shortening (Abbott and Aubert, 1952). This result has been observed universally (Maréchal and Plaghki, 1979; Herzog and Leonard, 1997; Lee and Herzog, 2003), and has become a generally accepted result.

However, when a muscle is shortened at different speeds, its force will change in accordance with the force-velocity property (Hill, 1938). Therefore, there exists the possibility that force depression is NOT associated with the speed but the force during shortening. However, there are no data that would allow distinguishing between the two possibilities. Therefore, the purpose of this study was to test if force depression was related to the speed or the force of shortening.

METHODS

All procedures were performed on cat soleus (n=8), and the set up of all testing was identical to that described previously (Herzog and Leonard, 1997). Briefly, cats were anesthetized, fixed in a stereotaxic frame, and the soleus was isolated and its distal end attached to a muscle puller. Soleus length and force were measured by the muscle puller, and activation was given through a tibial nerve cuff electrode.

Active shortening at a given magnitude (9 or 12 mm or about 9-12% of muscle length) and activation (30Hz) were performed at 3, 9, and 27 mm/s. Force depression obtained at the final length was compared to the corresponding force obtained from isometric reference contractions. Then, the same shortening contractions for the 9mm/s shortening speed were performed at reduced activation levels (about 15Hz) so that the force during shortening was as close as possible to that obtained for the 27mm/s shortening speed at 30 Hz. Similarly, shortening contractions at 3mm/s were performed at reduced activation levels to match the shortening forces of the 9 and 27mm/s shortening speeds.

RESULTS AND DISCUSSION

When shortening was performed at different speeds but constant activation, force during shortening was consistently lower for fast compared to slow speeds of shortening (Fig 1,

trace 3a vs 27). For these cases, force depression was greater at the slow compared to the fast speed of shortening (Fig. 1, $\Delta FD_2 > \Delta FD_1$). When shortening at the same speed but different activation levels, force depression was increased for greater forces of shortening (Fig. 1, trace 3a vs. 3b), thereby suggesting that it is the force of shortening, and not the speed, that affects force depression. Finally, when the speed of shortening was different but the forces during shortening were about the same, force depression was also similar (Fig. 1, trace 3b vs. 27), providing direct evidence that it is not the speed but the force of shortening that affects force depression.

We conclude that the generally accepted idea that force depression is associated with the speed of muscle shortening is not correct. Rather, we provide direct evidence that force depression is constant for different speeds of shortening, if force is kept constant during shortening, and that force depression varies for constant speeds of shortening, if force is changed during the shortening phase. Therefore, the mechanisms underlying force depression are associated with the force but not the speed of shortening.
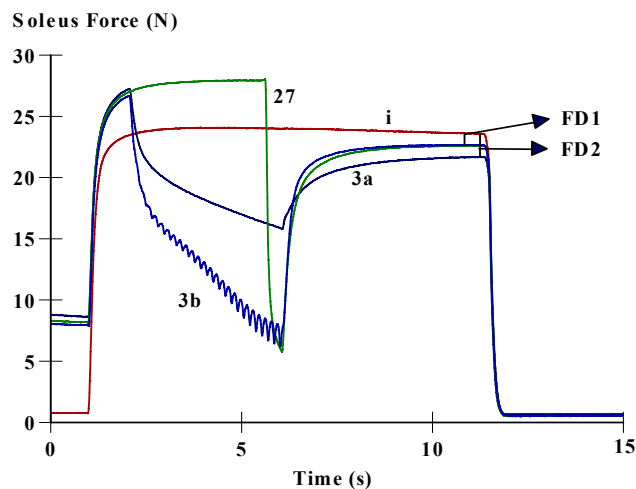

Soleus Force (N)

FIGURE 1: Force-time histories of an isometric reference contraction (red, i), and shortening contractions performed at 3mm/s (3a – 30Hz, 3b – 8Hz) and 27 mm/s (27-30Hz). Note that force depression for 3b and 27 is virtually identical ($\Delta FD1$), and that $\Delta FD1$ is smaller than force depression for 3a ($\Delta FD2$).

REFERENCES

Herzog W. *J Electromyogr Kinesiol* **8:**111-7, 1998
Abbott BC, Aubert XM. *J Physiol* **117**:77-86, 1952
Maréchal G, Plaghki L. *J Gen Physiol* **73**:453-67, 1979
Herzog W, Leonard TR. *J Biomech* **30(9)**:865-72, 1997
Lee HD, Herzog W. *J Physiol* **551**:993-1003, 2003
Hill AV. *Proc Royal Soc London* **126**:136-95, 1938

LOAD INDUCED FLUID FLOW SIMULATION IN CORTICAL BONE

Nicolas Hamilton[1], Dennis Coombe[2], David Tran[2] and Ronald F. Zernicke[1,3]
[1]Department of Mechanical and Manufacturing Engineering, University of Calgary, Calgary, Canada
[2]Computer Modeling Group, Calgary, Canada
[3]Faculty of Kinesiology, University of Calgary, Calgary, Canada

INTRODUCTION

It is generally accepted that loading induced fluid flow is one of the key factors in the triggering of the bone remodeling process through which bones maintain adequate bone mass and architecture (Knothe Tate, 2003). To develop a model that will provide a more complete picture of fluid flow in bone, STARS, a CMG (Computer Modeling Group) porous media fluid flow and geomechanics simulator designed for oil recovery applications, was used. A model was constructed to run on STARS to study the effect of cyclical loading on fluid flow and nutrient transport in cortical bone.

METHODS

A 3D model of a long bone was constructed based on μCT images obtained from mouse tibia cross sections. A representative cross-section from the mid-diaphysis was chosen for the model. Haversian canals were modeled as high porosity vertical channels situated throughout the sample. Five cycles of compressive axial loading and unloading were applied to one side of the model, thus simulating bending in the bone.

The simulation was run to study the different local fluid flow patterns within the bone using actual bone geometry, as well as the effect of Haversian canals on local fluid flow. The simulation was used to study the effect of cyclic loading on nutrient transport within the bone.

RESULTS AND DISCUSSION

The simulation showed that within the cross-section, the greatest fluid flow velocities occurred near the neutral axis (Fig. 1). Since the neutral axis is the area where the greatest circumferential strain gradients are found, fluid flow velocities were anticipated to be greatest near that site. The spatial variation in fluid velocities underlined the importance of using μCT images to acquire the proper geometry in such a models.

The simulation also revealed that fluid velocities were greater in areas surrounding Haversian canals (Fig. 1). This suggested that the inclusion of Haversian canals in a bone fluid flow model was crucial to gain a proper understanding of the fluid flow patterns.

Fig. 1 Simulated fluid flow magnitude in a loaded mouse tibia simulation. Load is applied on right side of model.

Lastly the model showed that nutrient transport from the Haversian canal to the bone matrix was enhanced by cyclical loading (Fig. 2). The output from the model reinforced that dynamic loading plays an important role in the delivery of nutrients to bone cells that are situated within the bone cortex. Similar results were previously found experimentally in sheep bone (Knothe Tate, Knothe, 2000).
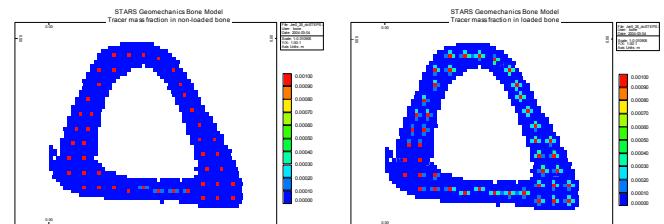

Fig. 2 Simulated tracer mass fraction in a mouse tibia. The model to which the load is applied is on the right while the left side shows a non-loaded section of bone. The simulated tracer was initially placed in the Haversian canals.

The results of using STARS in the simulation of bone fluid flow was successful in the current model both in terms of providing results consistent with experimental findings and offering a relatively wide view of fluid flow patterns in loaded bone. Our simulation confirmed that μCT images can readily be incorporated into such a model. One limitation of the current model was that only a cross-section of a tibia was used to model the bone. A second limitation was that Haversian canals were idealized as vertical channels whereas in reality these canals form a complex structure of interconnected channels. These limitations will be addressed in future modeling.

SUMMARY

A 3D computer model based on μCT images created to simulate fluid flow in cyclically loaded bone showed that fluid flow was greatest near the neutral axis of the bone and that Haversian canals had an important positive influence on local fluid velocities. The model showed that tracer transport was increased in the loaded bone after only five cycles. The STARS simulator was successful in providing realistic modeling results of fluid flow in cortical bone.

REFERENCES

Knothe Tate ML (2003) *J Biomech* 36, 1409-1424
Knothe Tate ML, Knothe U (2000) *J Biomech 33*, 247-254

ACKNOWLEDGEMENTS
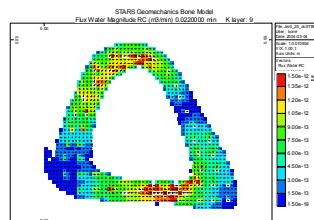
PASSIVE LUMBAR FLEXION STIFFNESS IS ALTERED WITH EXPOSURE TO PROLONGED SITTING

Tyson A.C. Beach[1] (tbeach@ahsmail.uwaterloo.ca), Robert J. Parkinson[1], J. Peter Stothart[2], Jack P. Callaghan[1]
[1]Department of Kinesiology, Faculty of Applied Health Sciences, University of Waterloo, Waterloo, ON, Canada
[2]School of Human Kinetics, Faculty of Health Sciences, University of Ottawa, Ottawa, ON, Canada

INTRODUCTION

As a strategy to prevent or manage low back pain in the workplace, it is often recommended that prolonged periods of sitting be interrupted with other activities to promote postural variations. However, changes in passive lumbar flexion stiffness (PFS) while sitting may increase the risk of low back injury if certain movements are performed following sitting. The objective of this study was to determine whether exposure to prolonged sitting would lead to changes in PFS.

METHODS

Passive lumbar flexion moment-angle (M-A) curves were obtained before (*Session 1*), during (*Session 2*), and after (*Session 3*) student volunteers (6 ♂, 6 ♀) performed 2 hours of seated deskwork. M-A data were collected by pulling the participants through their full voluntary range of lumbar flexion on a customized frictionless jig (Parkinson et al. 2004). Surface EMG signals from the trunk extensor muscles (T9 and L3 spinal levels) were monitored throughout pulling trials to ensure that activation did not exceed 5% of that documented in maximal voluntary isometric contractions.

M-A curves were fit with 6th-order polynomials (Dickey and Gillespie 2003) and then numerically differentiated to identify *low* and *high breakpoints* (greatest % changes in instantaneous slopes). These breakpoints formed the boundaries of 3 regions (*low*, *transition*, and *high stiffness zones*) (Figure 1).

The slopes of linear trend-lines, fit to each of the stiffness zones, were used as a measure of PFS. Changes in breakpoints were also documented, as was the range of lumbar flexion between these breakpoints (*transition range*). A left- or right-shift in the breakpoints was considered to represent increased or decreased PFS, respectively. The maximum lumbar flexion angles to which participants could be pulled on the frictionless jig was also documented, as range of motion was considered to be inversely related to PFS.
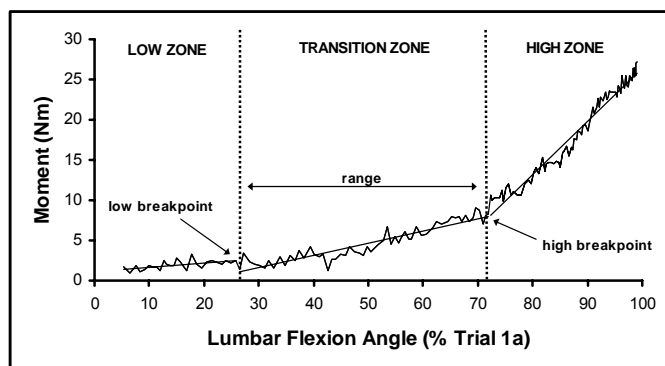

Figure 1: A typical M-A curve marked with the measures of PFS.

RESULTS AND DISCUSSION

Time-varying changes in PFS were observed with exposure to prolonged sitting. Males and females did not exhibit the same response to this exposure; PFS increased in males after 1 hour of sitting (Figure 2), while no systematic changes in PFS were observed in females.
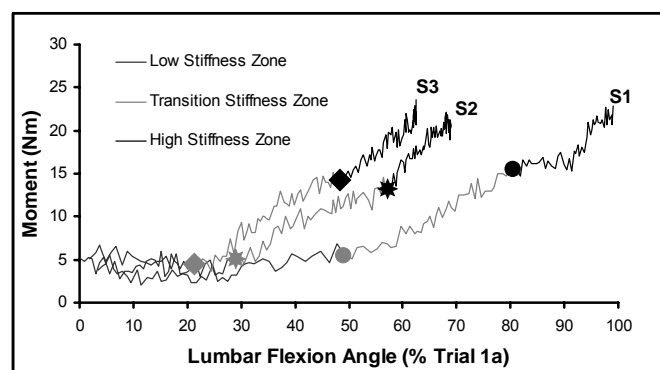

Figure 2: The male PFS response. M-A curves after the 1st and 2nd hours of sitting were left-shifted with respect to those obtained before sitting. This response was indicated by changes in low and high breakpoints in Sessions 1 (●,●), 2 (✳,✳), and 3 (◆,◆) and also by observed decreases in the range of lumbar flexion across Sessions.

To our knowledge there is no clear explanation for the gender-specific responses observed in this study. Nevertheless, these results were consistent with those of Callaghan and McGill (2001), as they also reported decreases in the maximum voluntary range of active lumbar flexion in males following prolonged sitting.

These findings suggest that structures providing passive resistance to lumbar flexion (e.g., spinal ligaments and intervertebral discs) may be recruited at lower lumbar flexion angles in males, and therefore may be subjected to greater stresses at a given lumbar angle following prolonged sitting. While a systematic response was not observed in the females studied, time-varying *changes* were observed in several measures of PFS. With regards to injury prevention, the results indicate that full lumbar flexion movements (e.g., stooped lifting) should be avoided following prolonged sitting.

REFERENCES

- Callaghan, J.P., McGill, S.M. (2001). *Ergonomics* **44**:280-94.
- Dickey, J.P., Gillespie K.A. (2003). *J Biomech* **36**:883-8.
- Parkinson, R.J. et al. (2004). *Clin Biomech*, In press.

ACKNOWLEDGMENTS

BIOMECHANICAL PROPERTIES WHICH INFLUENCE JUMPING PERFORMANCE IN THE FROG, *RANA PIPIENS*

Danny Peterson, Motoshi Kaya, Walter Herzog
Human Performance Laboratory, University of Calgary, Canada
peterson@kin.ucalgary.ca

INTRODUCTION

Many significant advances have been made in the field of muscle biomechanics over the past 50 years (e.g., Huxley and Niedergerke, 1954). However, knowledge in this field is far from complete. For example, our understanding of *in vivo* muscle function is sparse and incomplete. Frogs provide an ideal system for investigating *in vivo* muscle characteristics because a great amount of our knowledge of muscle contraction in based on frog muscle (e.g., Gordon *et al*., 1966; Huxley and Simmons, 1971; Lutz and Rome, 1994).

Frogs are versatile jumpers in that they can jump very well in different directions, with different take-off angles, and over a range of distances. The purpose of the current study was to analyze a wide variety of jumps in terms of the distance jumped and the take-off angles to elucidate the mechanism by which frogs control jumping performance. Analysis was performed on the whole frog, and on a single muscle (the plantaris longus – PL), considered a major contributor to frog jumping performance. To date, direct measures of *in vivo* force production by a major jumping muscle in frogs has been unsuccessful. We hypothesize that the PL force will correlate to the jumping distance and serve as an important point of control in jumping performance.

METHODS

The *in vivo* PL muscle force was measured using a custom-built buckle force transducer (Walmsley *et al*., 1978). Instantaneous fibre lengths were measured using the ultrasound transit time technique, sonomicrometry (Sonometrics), and the corresponding fibre velocities were obtained by the time derivative of fibre length. Muscle activation patterns were measured using bipolar, fine wire, indwelling electrodes (Cooner Wire) inserted into the midbelly of the PL. Ground reaction forces were measured via a custom-built force plate, and the jumps were recorded with a high-speed digital video camera (MotionScope, Redlake Imaging) at a sampling frequency of 1000 Hz.

RESULTS AND DISCUSSION

Data were collected from 10 frogs and 59 jumps. For illustration, we discuss here the shortest and longest jumps from one frog. The two jumps will be referred to as large and small. The peak PL forces for the large and small jumps were 3.9 N and 1.7 N, respectively (Figure 1). This relationship between PL force and jump distance was consistent across all jumps (R^2=0.67).

Jumping performance in frogs is often correlated with the power the muscles are able to produce during the propulsive phase. The shortening velocities for the two jumps (Table 1) are more similar in magnitude than the force values. This suggests that force production of the muscles may be a more important factor than shortening velocity in controlling jumping performance.
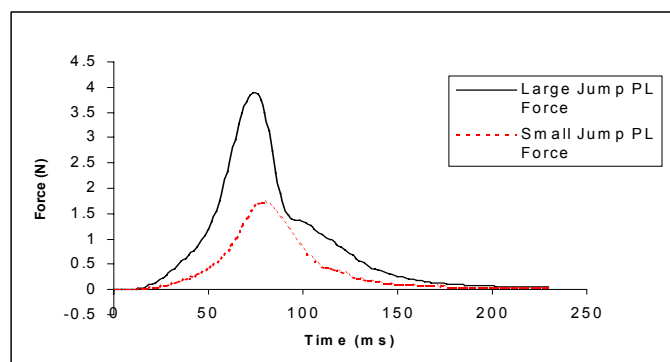

Figure 1: PL forces for large and small jumps.

SUMMARY

Here we show for the first time direct *in vivo* forces recorded from a muscle considered a major contributor to frog jumping. The frog appears to control its jumping performance by altering both the force it produces, as well as the rate of shortening. The current data seem to suggest that force modulation is the more important of the two in controlling jumping performance *in vivo*.

REFERENCES

Gordon, A.M., *et al*. (1966) *J.Physiol.* **181**, 170-192.
Huxley, A.F., Niedergerke, R. (1954) *Nature* **173**, 971-973.
Huxley, A.F., Simmons, R.M. (1971) *Nature* **233**, 533-538.
Lutz, G. J., and Rome, L. C. (1994) *Science* **263**, 370-372.
Walmsley, B., *et al*. (1978) *J. Neurophysiol.* **41**, 1203-1215.

ACKNOWLEDGEMENTS

Table 1 Various biomechanical factors are compared for the smallest and largest jumps obtained from one frog

Jump	Distance (cm)	Angle (°)	Peak Grd Rxn Force (x,z;N)	PL 'Power' (W/kg)	PL Peak Force (N)	PL Short. Vel. (m/s)
Large	67	57	(0.54, 1.12)	199	3.9	0.027
Small	40	43	(0.43, 0.68)	66	1.7	0.020

EFFECT OF WALKING SPEED ON KNEE BIOMECHANICS IN A MODERATE KNEE OSTEOARTHRITIC AND ASYMPTOMATIC POPULATION

Scott Landry[1], Kelly McKean[1], Cheryl Hubley-Kozey[2], William Stanish[3] and Kevin Deluzio[1]

[1]School of Biomedical Engineering, Dalhousie University, Halifax, Canada, landrys@dal.ca
[2]School of Physiotherapy, Dalhousie University, Halifax, Canada
[3]Department of Surgery (Orthopaedics), Dalhousie University, Halifax, Canada

INTRODUCTION

Osteoarthritis (OA) is a debilitating disease commonly affecting the knee (Felson et al., 1987). Understanding the mechanics of OA early in the disease process, using gait analysis, will help in the design and application of non-invasive interventions aimed at helping individuals cope with the pain and disability of the disease. The purpose of this gait study was to identify biomechanical features that are different in a moderate knee OA and asymptomatic subject group and determine the effect of walking speed on these features.

METHODS

A three-dimensional gait analysis of the lower limb was used to compare a moderate knee OA (N=40) and an asymptomatic population (N=43) with no history of lower limb pain or injury. The OA subjects were recruited from a knee arthroscopy waiting list at the local orthopaedic clinic. The OA subjects underwent the gait analysis prior to arthroscopy or at least one year after exploratory arthroscopy. The degree of OA was quantified clinically and radiographically using the Kellgren-Lawrence grading scheme. The gait analysis had subjects walk at a self-selected speed and a faster speed ($\approx$ 30% faster than self-selected). Stride characteristics, knee joint angles and net external knee joint moments were analyzed using t-tests, principal component analysis (PCA) (Deluzio et al. 1997) and a 2-factor repeated measures model.

RESULTS

No significant differences in stride characteristics (i.e. stride length, stride time and speed) were found between the control and OA group, at both the self-selected and fast walking speed. Radiographic assessment of the OA subjects showed that 90% of the subjects had KL scores of 3 or less. These KL scores combined with no differences in stride characteristics is evidence that the OA population being studied is indeed in the mild to moderate disease state. The only differences in group demographics were due to OA subjects having a greater mass and thereby larger BMI (Table 1).

Table 1 OA and Control Demographics. Data are mean (SD)

	Ht. (m)	Wt. (kg)	Age (yr)	BMI
Controls	1.71 (0.1)	72.6 (16.4)	50.2 (10.1)	24.7 (4.4)
OA	1.74 (0.1)	93.5 (17.6)	54.9 (14.4)	31.0 (5.3)
P-value	Not Sign.	<0.001	Not Sign.	<0.001

PCA and the repeated measures model found several significant differences between groups (OA and control) and between speeds (self-selected and fast) in net external knee joint moments and knee joint angles. The knee flexion angle was found to be approximately 3° smaller (P<0.05) throughout the gait cycle in the OA population, at both the self-selected and fast walks. The faster walking speed also resulted in an

overall increase in knee flexion angle (P<0.001), which was most evident at peak flexion during stance.

The magnitude of knee adduction moment (Figure 1A) during stance was approximately 30% larger for the OA group at both walking speeds. The faster speed affected the shape of the adduction moment curve during stance by increasing the ratio of the peak moment during early stance and the peak moment during late stance (p<0.001). The peak flexion moment (Figure 1B) during the first 20% of the gait cycle was found to be 20% smaller (p<0.05) in the OA group at both speeds. Increasing speed also tended to increase this peak flexion moment (p<0.001). The overall amplitudes of the flexion moment were significantly different for both group (p<0.05) and speed (p<0.001), with the largest magnitude being the control group (1.33±0.3 Nm/kg) during the fast walk and smallest being the OA group (0.84±0.3 Nm/kg) during the self-selected speed. The faster walk resulted in an increase in peak knee external rotation moment during early stance. An overall shift towards an internal rotation moment for the OA subjects was also evident and this was correlated with the knee flexion moment (R^2=0.42).
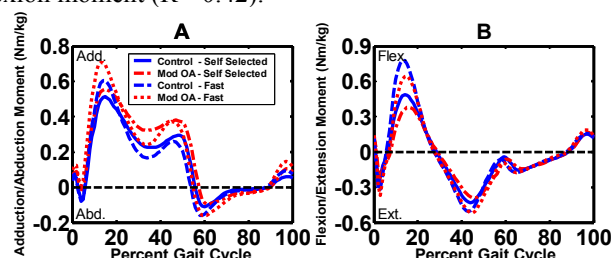

Figure 1 A) Net external adduction / abduction and B) flexion / extension moment of OA and control groups at both speeds.

SUMMARY

The faster speed tended to increase the overall magnitude and/or amplitude of knee moments and angles, which was different from the effect of OA. Knee OA resulted in a reduced knee flexion angle, reduced knee flexion/extension moment amplitude, reduced external rotation moment and an increase in knee adduction moment magnitude. It is believed that the reduced knee flexion angle and knee flexion/extension moment amplitude in OA subjects requires a smaller activation or strength in the quadriceps. This reduction in quadriceps could result in a less stable knee joint and thereby an increase in knee adduction moment magnitude, which may lead to accelerated damage to the knee joint (Sharma et al. 1998).

REFERENCES

Deluzio et al. (1997). *J. Hum. Mov. Sci.*, 16, 201-217.
Felson et al. (1987). *Arthritis and Rheum.*, 30, 914-918.
Sharma et al. (1998). *Arthritis and Rheum.*, 41, 1233-1240.

A COMPUTER-GENERATED MODEL OF CARPAL TUNNEL MECHANICS

Jeremy P.M. Mogk, MSc and Peter J Keir, PhD

School of Kinesiology & Health Science, York University, Toronto, Ontario, Canada, jpmogk@yorku.ca

INTRODUCTION

The etiology of work-related carpal tunnel syndrome (CTS) remains elusive. Median nerve compression may be due to impingement or increased hydrostatic pressure. Deviation of the wrist from a neutral posture is known to increase carpal tunnel (CT) pressure, and is likely due to a change in CT volume and/or the volume of its contents. CT volume has typically been determined by integration of the cross-sectional area (CSA) of contiguous magnetic resonance (MR) images. Until recently (Bower & Keir, 2003), CT volumes have only been reconstructed in a neutral wrist posture, and assuming specific CT boundaries (Richman et al., 1987). Issues arising with reconstructing images of non-neutral wrists include errors due to off-axis viewing angle (parallax error) and maintaining consistent boundary definitions between postures. While non-neutral volume reconstruction is essential to understanding mechanisms of CTS, the error associated with volume rendering using MRI must be evaluated. This study represents a progression in the development of a 3D model of the carpal tunnel, examining whether a modified cylinder can predict changes in carpal tunnel shape which occur with deviated postures.

Model development
The initial model (Mogk & Keir, 2003) consisted of a simple cylinder whose orientation and dimensions varied with the manipulation of wrist posture. The wrist was modeled as a series of beams linked by ball joints, restricted to movement in the flexion-extension plane. This model allowed for only a general comparison of changes in CT shape with wrist deviation, and the effects of parallax error on CSA and volume estimation. Thus, to improve the anatomic fidelity, individual carpal bones were reconstructed from MR images of a neutral wrist (Bower & Keir, 2003) and carpal kinematics applied from the literature (Moojen et al., 2002). The carpal tunnel remained a simple cylinder, with uniform dimensions throughout its length based on the distal end parameters. Volume and CSA predictions could now be directly compared to MRI, but only for the distal portion of the tunnel. Further model refinements are explained below.

METHODS

Axial MR images of a neutral wrist (Bower & Keir, 2003) were used to reconstruct CT surfaces and carpal bones using Maya™ software (v5.0, Alias®, Toronto, Canada). This surface reconstruction represented the shape the carpal arch and transverse carpal ligament (TCL) in a neutral wrist posture. Changes in carpal kinematics were determined from the same MR images with the wrist in 30° flexion and 30° extension. These translations and rotations were applied to the modified cylinder to predict changes in tunnel shape with wrist deviation. CSA was calculated using vertical slices taken along the CT length in each posture to simulate MRI measurements, and, similar to MRI, was measurable only when both tunnel surfaces were transected. CSA values were compared to those determined from MRI, while tunnel volumes predicted by the model were compared to the integration of CSAs measured from MRI.

RESULTS AND DISCUSSION

The changes in CT shape predicted by the model were in general agreement with those determined directly from MRI. Model predicted CSAs were similar to those measured from MRI through the proximal half of the flexed tunnel, but a consistent 5-10% underestimation existed through the distal half. In extension, predicted CSAs were upwards of 25% larger than MRI through the proximal tunnel, and 10% greater for the distal portion. This appeared to be mainly due to the model not predicting the tunnel flattening seen with MRI. Tunnel volume was predicted to decrease 11% from neutral to 30° flexion, which was consistent with the 15% reduction calculated from MRI. However, an 8% increase was predicted from neutral to 30° extension, while MR calculations revealed a 30% reduction. This appears to be largely due to changes in the orientation of the tunnel boundaries for which MRI cannot account. The power of this modeling technique provides a tool by which the limitations associated with MRI may be evaluated. This method shows promise of more refined modeling of the tunnel to examine contributions of various parameters to median nerve loading, including potential sites of impingement. Inclusion of the tunnel contents (tendons and median nerve) and TCL material properties are expected to improve parameter prediction in non-neutral postures. This will also improve the potential to help define tunnel boundaries and changes in their orientation with wrist deviation. Future uses of the model will include determining the relationship between CT volume and pressure in deviated postures, and the effects of flexor tendon loading.
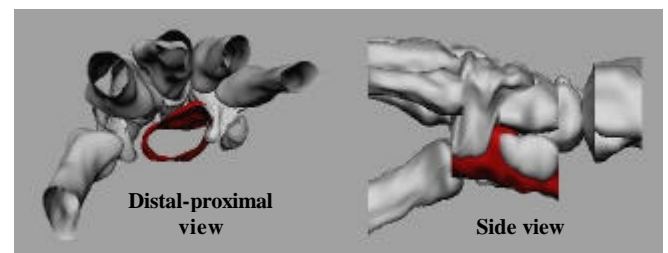

Figure 1: Illustration of the model, showing constructed bone geometry and the cylinder representing the CT (in red).

REFERENCES

Bower, J.A. & Keir, P.J. (2003). *Proc 27th ASB Conf.*
Mogk, J.P.M. & Keir, P.J. (2003). *Proc 27th ASB Conf.*
Moojen, T.M. et al. (2002). *Clin Biomech*, **17**, 506-514.
Richman, J.A. et al. (1987). *J Hand Surg*, **12A**, 712-717.

ACKNOWLEDGEMENTS

A BIOMECHANICAL EVAUATION OF CHILD SAFETY SEAT INSTALLATION: REAR AND FORWARD FACING

Mandy Fox, Sabrina Sarno, and Jim Potvin.
Faculty of Human Kinetics, the University of Windsor, Windsor, Ontario
child_safety@hotmail.com

INTRODUCTION

Motor vehicle accidents are the leading cause of death in children over one year of age (Johnston, Rivara, & Soderberg, 1994). Surprisingly, most parents realize that child safety seats (CSS) are important, yet more than 80% are improperly installed (Biagioli, 2002). When used properly, child safety seats can reduce death by 71% for infants and 54% for toddlers. The reason for this high frequency of errors is unknown. Possible explanations include engineering/design problems, physical difficulty, and/or cognitive complexity (Wegner & Girasek, 2003).

PURPOSE

The purpose of the current study was to examine the physical demands, specifically the postures and forces, which are necessary to correctly install a child safety seat. Given the excessive prevalence of installation errors, it is critical to determine whether these errors are related to the physical demands of installing the seat. This study will focus on rear and forward facing child safety seats and attempt to identify the future direction of child safety seat redesigns.

METHODS

Flyers were posted at various locations around the city to recruit volunteers who have children in child safety seats. A total of 31 subjects, with a mean age of 31 years, volunteered to participate. The subjects were videotaped re-installing their seat and securing their child in the seat. If the seat was improperly installed, the errors were recorded and the subject was required to re-do the task. A force gauge was used to measure three forces: the magnitude of force needed to tighten the tether, the harness, and the seatbelt. A subjective questionnaire was completed to determine the perceived physical exertion and task complexity associated with each task. Still photos of seatbelt, harness, and tether tightening postures were captured from the videotape. The snap shots were then modeled in 3D Static Strength Prediction Program (3DSSPP) to determine the moments, percentage of population who can complete the task, and total spine compression force.

RESULTS

Sixty-two errors were observed in total. Harness errors accounted for 60% of all rear facing errors and 47% of all forward facing errors. In conclusion, 84% of the forward facing group made errors and 67% of the rear facing group made errors, which could lead to serious injury of the child in the case of an accident.

On average, compression at L4/L5, which fluctuated with posture requirements, did not exceed the NIOSH action limit (AL) of 3400 N for any of the tasks (Waters et al, 1993). *Figure 1* illustrates a modest variability between tasks, though there was an obvious seat facing affect. Fifty-four percent and 20% of individuals, based on a 75th percentile female population, would be unable to completely install the forward and rear facing seat, respectively. Child safety seat installation, both forward and rear facing combined, is too physically demanding for 37% of the population. Biagioli (2002) stated that 80% of child safety seats are improperly installed, and the current study states that 37% of individuals do not posses the physical strength necessary to install them, thus the task's physical demands may account for 46% of installation errors. The results of this study emphasize the need for car seat redesign, making installation easier and improving child safety seat-vehicle compatibility.
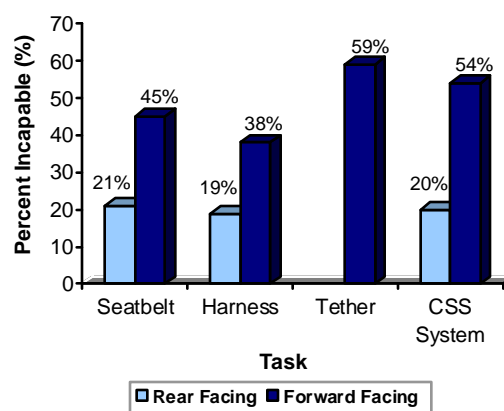

Figure 1: Percentage of population incapable of installing rear and forward facing child safety seats.

REFERENCES

Biagioli, F. (2002). Proper use of child safety seats. *American Family Physician*. May 15, **65(10)**: 2085-2090.

Johnston, C., Rivara, F.P., & Soderberg, R. (1994). Children in car crashes: Analysis of data for injury and use of restraints. *Pediatrics*. **93(6)**: 960-965.

Waters, G. et al. (1993). *Revised NIOSH equations for the design and evaluation of manual lifting tasks*. Ergonomics, **36(7)**: 749-776.

Wegner, M.V., & Girasek, D.C. (2003). How readable are child safety seat installation instructions? *Pediatrics*. **111(3)**: 588-591.

ACKNOWLEDGEMENTS

3D DYNAMIC MODEL OF BIOMECHANICAL FACTORS IN LOAD CARRIAGE

J.T. Bryant, S.A. Reid, J.M. Stevenson, M. Abdoli

Ergonomics Research Group[1] Queen's University, Kingston, Ontario, Canada   bryant@me.queensu.ca

INTRODUCTION

A 3D dynamic biomechanical model (DBM) of a human trunk carrying a backpack, capable of estimating biomechanical factors when provided with 3D accelerations and material property inputs is described. This model is being developed in VisualNastran 4D® (VN4D) to integrate current understanding of human biomechanical limits with the demands of backpack load carriage. Research has shown that biomechanical factors such as shoulder and lumbar reaction force as well as skin contact pressures are strongly correlated to physical discomfort when wearing a backpack (Stevenson et al., (1996, 1998). Additionally, a significant body of research exists on injury modes such as lower back and spinal injury, cumulative effects of lifting and repetitive activity McGill, (2002). The DBM is being developed to relate the effects of trunk born loads to these injury modes.

MODEL DESCRIPTION

A 50 percentile male body shape was split at L5/S1 and a rigid joint created there. The mass, location of the centre of mass and inertial properties of the upper torso were defined based on 50 percentile male anthropometric values. Rucksack dimensions, mass (25kg) and 3D moments of inertia were taken from previous studies, Stevenson et al. (2002). The model uses a coefficient of friction value of 0.9, consistent with damp skin, Sanders et al. (1998), Naylor P.F.D.(1955).

Straps were modeled as a Voigt-Kelvin visco-elastic material with a linear spring in series with a linear damper to reproduce the effect of a compliant shoulder pad and stiff webbing material. Positions of strap ends are monitored and no strap forces are applied when the strap is slack.

Accelerations from human testing were recorded using a Crossbow® triaxial accelerometer (CXL10LP3, +/- 10 g) affixed to each subjects' sternum, Stevenson et al. (2002). This DC coupled device records a signal having two components; one due to the orientation of the accelerometer in the gravitational field, and a second due to muscle induced accelerations of the torso. DC offset was calculated by taking the average signal value over the entire circuit. This value was subtracted from each data point leaving the instantaneous component of acceleration corresponding to muscle induced accelerations.VN4D cannot directly input 3D acceleration but can use velocities. Acceleration data was numerically integrated using the trapezoid rule to provide a torso forcing function.

RESULTS - Model Outputs

Torso accelerations during walking with a 25 Kg backpack were analysed. The program outputs upper and lower torso

forces including forces at L5/S1 and an example of these appears as Figure 1. Shear force is +Y and vertical force is+Z. In his book on low back disorders, McGill (2002) summarized a list of risk factors. This composite list includes "static posture … specifically prolonged trunk flexion and a twisted or laterally bent trunk" and "peak and cumulative low back shear force, compression force and extensor moment." Static posture, trunk flexion and exposure to low back shear are typical in most backpack situations.
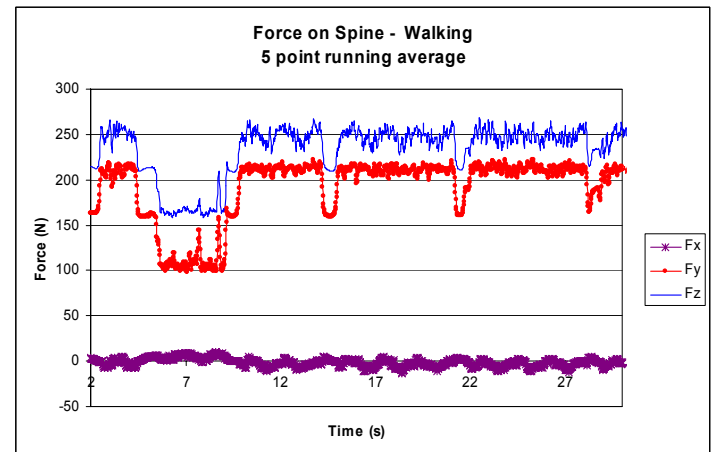

Figure 1: Estimated Forces at L5/S1, Fx: Medial/lateral Shear, Fy: Anterior/Posterior Shear, Fz: Compressive Load.

DISCUSSION

Work continues on modelling and validating all major pack components and refining suspension system parameters. User control over centre of mass location and inertial properties has been added allowing parametric studies of the effects of these variables on the load distribution to the torso. Overall objectives include estimating contact pressure distributions on specific body regions given a set of suspension system compliance parameters.

REFERENCES

Cholewicki, J., McGill, S.M. (1996) *Clin. Biomech*. 11(1):1-15
McGill, S.M., Human Kinetics Eur. Ltd. 2002.
Naylor, P.F.D., Br. J. of Derm, 1955; V67: 238-239.
Sanders, J.E., Greve, J.M., J. of Rehab R & D, Jn 1998, V35, No.2: 161-176.
Stevenson, J.M, Good, J.A. Devenney, I.A. DRDC No. W7711-0-7632-06, June 2002.

ACKNOWLEDGEMENTS

EFFECTS OF BACKREST DESIGN ON COMFORT AND BIOMECHANICS OF SEATING

Steven M. Carcone and Peter J. Keir, PhD

School of Kinesiology & Health Science, York University, Toronto, Canada, steven.carcone@sympatico.ca

INTRODUCTION

The role of the chair backrest is generally considered to be to maintain normal lumbar lordosis and improve comfort. Backrests have been evaluated using EMG (Andersson et al. 1975), spinal angles (Andersson et al. 1979), and subjective measures, such as discomfort questionnaires (Coleman et al. 1998). In an attempt to improve user comfort, the use of supplementary backrests has become common, while support for their use has been largely anecdotal. While comfort is important, there has been very little research to relate comfort and biomechanical variables, nor is there a link between ergonomic seating guidelines and comfort. In a pilot study examining EMG and pressure distribution, we found that the use of a lumbar pad altered both peak and average pressure. EMG was unable to differentiate between conditions with any consistency, as it was quite low and highly variable (Keir, 2003). There is a need to establish backrest design criteria as well as relationships between comfort and 'ergonomically sound' postures. The purpose of this study was to examine the effect of backrest configuration (lumbar pad depth) on pressure distribution, spine posture, and comfort.

METHODS

Thirty volunteers (15 males: mean age 25 ± 3 years and 15 females: mean age 21 ± 2 years; mean height: men = 1.77 ± 0.08 m; women = 1.65 ± 0.05 m; body mass: men = 78 ± 15 kg; women = 61 ± 9 kg) and no history of low back pain were recruited from the university population. Additional anthropometric data was collected including waist girth, hip girth, leg length, torso length, and shoulder breadth. Participants typed a standardized text passage at a computer workstation, which was individually adjusted according to CSA guidelines. Five backrest configurations were used: 1. Chair only; 2. Chair and supplementary backrest; 3. Chair and supplementary backrest with *small* lumbar pad; 4. Chair and supplementary backrest with *medium* lumbar pad; 5. Chair and supplementary backrest with *large* lumbar pad. Two capacitive-based pressure mats (X236, Xsensor Technology Corporation, Calgary, AB) were used to measure the interface pressure on the backrest and the seatpan. Cervical and lumbar angles were measured using two flexible resistors [11.4 cm x 0.03 cm x 0.05 cm (Flex Sensor, Images SI Inc., Staten Island, NY)], which were centred over the spinous process and the middle of the cervical (C4) and lumbar (L3) regions. Trials were 15 minutes in duration with a 5-minute break between conditions. Pressure distribution (average pressure, average peak pressure, average contact area, and centre of pressure) and spinal posture data were collected over a 5-minute period at 0 and 10 minutes of each condition, consisting of three samples of 1-minute in duration. At the end of each collection period, a body part discomfort questionnaire was administered. In addition, a backrest condition rating was completed at the end of each trial, as well as a rank-order questionnaire, which was completed at the conclusion of the entire protocol.

RESULTS AND DISCUSSION

This was the first study to examine the relationships between comfort, anthropometrics, and biomechanical variables (posture and pressure distribution). Based on preliminary analysis, there appears to be a relationship between anthropometrics and comfort, as well as spinal posture. Lowest average pressure on the chair back appears to be associated with use of the supplementary backrest without a lumbar pad (Fig. 1). In addition, the average peak pressure and average contact area also appear to be lowest when using the supplementary backrest only. Further, the size of the lumbar pad altered the centre of pressure position on the seatpan. By combining these data with comfort questionnaires and individual anthropometrics, our understanding of the possible relationships between comfort and pressure analysis will be enhanced. This will ultimately lead to improved backrest design and selection criteria.
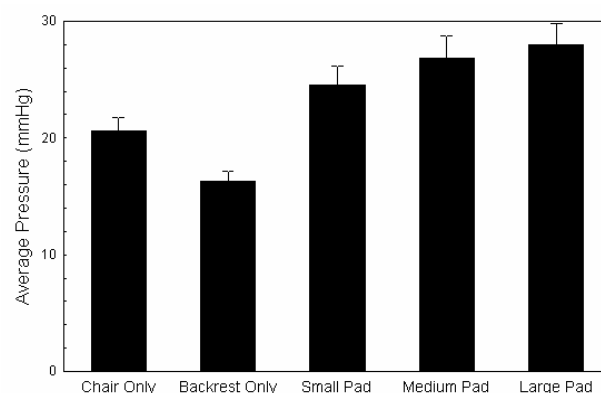

Figure 1. Average pressure (backrest) as a function of backrest condition (bars are SEMs).

REFERENCES
Andersson et al. (1975) *Orthop Clin North Am*, **6**, 105-120.
Andersson et al. (1979) *Spine*, **4**, 52-58.
Coleman et al. (1998) *Ergonomics*, **41**, 401-419.
Keir (2003) *Proc. 19th ISB Conf.*

ACKNOWLEDGEMENTS

DESIGN SPECIFICATIONS FOR AN ACTIVE COMPLIANT SURFACE FOR USE AS AN ABDOMINAL SIGN SIMULATOR

D. L. Russell[1]   O. Kendler[1]   J. Bass[2]

[1] Department of Mechanical and Aerospace Engineering, Carleton University, Ottawa, Canada, *drussell@mae.carleton.ca*
[2] Department of Surgery, Childrens Hospital of Eastern Ontario, Ottawa, Canada

INTRODUCTION A device, called a Basic Abdominal Sign Simulator has been proposed. The device is a surface that reacts to tactile stimulation in a way that mimics the response of the abdomen during palpation. Abdominal palpation is a commonly practiced method of diagnosis. Students can have little exposure to patients with abdominal pathologies and can finish their surgical and emergency rotations before palpating a single patient with such conditions. Improved skills should result in an earlier diagnosis, fewer complications and improved outcomes. The abdominal simulator is designed to provide an alternative practical approach for palpation training. The simulator is an active surface that has a distributed and controlled response to applied forces. The mechanical challenges in developing this surface center on achieving appropriate local mechanical responses and in smoothly varying the response over the surface. The surface must mimic a patient in a normal state or where abdominal pathologies are present. This paper will focus on the design specifications for the mechanical response.

DISCUSSION During palpation of the abdomen there are two broad categories of signs – guarding and tenderness. Guarding is an increase in abdominal wall tension due to muscle spasms in response to the palpation and represents the body protecting an affected organ or area. Guarding may be either involuntary or voluntary depending on whether the patient can suppress the response. Tenderness is an increase in pain as a result of the palpation. The maximum force that a human finger can apply has been reported [Burdea, 1996] as 50 N with the maximum continuous force level of 15 N. Studies of abdominal tenderness [Postuma, 1987] yield corresponding levels of forces. Culver [Culver, 1999] states that *superficial* or light palpation should reach a depth of 1cm while deep palpation should reach 4 cm depth. Based on these studies and discussions with teaching physicians we have created a mechanical description of palpation for use in the device design, see Figure 1.

SUMMARY The figure shows nonlinear force deflection curves for four cases. For superficial palpation the depth is limited to 1cm and the force levels remain low. The specific relationship between force and displacement is not known but should be smooth. In a healthy case further force will generate penetrations of up to 4 cm. The simulator is aimed at generating two distinct local responses allowing it to present a range of pathologies. At a specified depth
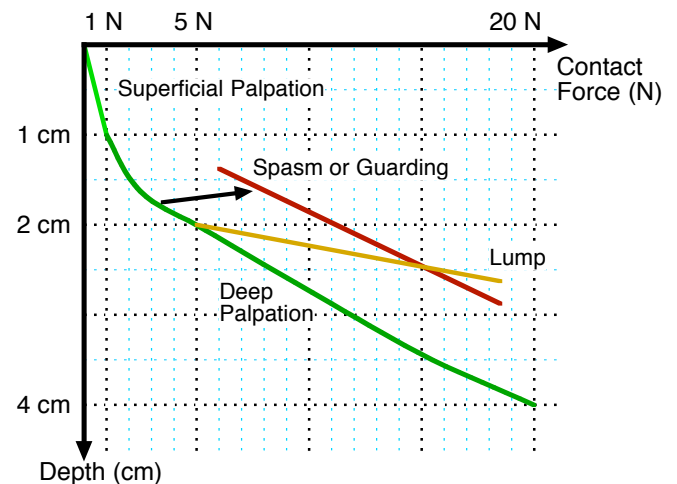

Figure 1: Forces encountered during palpation.

the stiffness of the surface will change to a higher level to simulate the presence of guarding or a lump. The stiffening should be controlled in amount and in its distribution over the surface. The second response to be designed into the surface is a "*twitch*" where at a predetermined depth or force level a sudden change change in stiffness will result in a movement or twitch to a new position with a different level of stiffness. Current design approaches under consideration for the creation of the surface include the possible use of smart materials including eletro-active polymers.

REFERENCES - INCOMPLETE

Burdea, G. (1996) Force and Touch Feedback for Virtual Reality, John Wiley & Sons, New York, USA

Postuma, R. (1987) *Abdominal Tenderness Threshold in Suspected Childhood Appendicitis.*, presented at the Canadian Association of Peadiatric Surgeons, Winnipeg

J. Culver (1999) *Exam Techniques and Equipment.*, www.ttuhsc.edu/SOM/FamMed/lectures/examtech.html

THE EFFECT OF LOAD, SPEED AND INCLINE ON OXYGEN CONSUMPTION DURING LOAD CARRIAGE

Joan M. Stevenson, Evelyn L. Morin, Carrie L. Johnston, Ian M. Janssen, J. Tim Bryant, Susan A. Reid
Ergonomics Research Group, Queen's University, Kingston, Canada stevensj@post.queensu.ca

INTRODUCTION

Our research goal is to determine if a triaxial accelerometer can be used to assess performance of both physiological and biomechanical factors during load carriage. Ultimately we wish to develop an equation that will contain a physiological factor and a biomechanical factor. Our first objective was to examine the relationships between energy expenditure and load, incline and speed during load carriage. These data will be compared to other predictive equations for load carriage from the scientific literature (Holewijn and Meeuwsen; Pandolf et al. 1977; Quesada et al., 2000).

Uniaxial and triaxial accelerometers have been used to assess energy expenditure with strong predictive power (r^2=0.76 to 0.81) for walking, running and tasks of daily living (Bouten et al., 1994; 1997). Morin et al. (2002) first used a triaxial accelerometer to determine the movement responses under load carriage conditions during a circuit that contained marching and obstacles. Results revealed that a triaxial accelerometer could be used to determine changes in gait patterns in response to load as well as movement signatures in response to obstacles (e.g., balance beams, branch duck and fence climb, etc). Thus, a second goal was to determine if tri-axial accelerometers could capture additional information about both physiological and biomechanical measures. This paper is devoted primarily to the physiological measures.

METHODS

Eight physically fit male subjects (ht=1.77 m; wt= 78.3 kg; age=23.6) were tested on a treadmill for maximal oxygen consumption (with Aerosport TEEM 100 metabolic cart and software) using a modified Balke protocol. Their mean VO_2max was 55.7 ml/kg/min. Prior to testing with a Canadian military backpack, Cross-Bow® triaxial accelerometers were attached to the sternum using Skin-Bond® (also placed in the pack and on the pelvis but not used for this study). A baseline was taken as a gravity reference for the accelerometer prior to data acquisition. These data were stored in an Embla® datalogger and processed as mean and RMS values for x, y, z and r values. The subjects were also outfitted for direct oxygen consumption (VO_2) measures using the TEEM 100 metabolic cart. On four separate days with adequate rest between trials, subjects completed either 0 kg and 38.7 kg loads or 25.9 kg and 16.6 kg loads under either: 0º, 5º and 10º inclines at 4.83 km/hr or speeds of 3.22 km/hr, 4.83 km/hr and 6.44 km/hr. The protocol involved walking on the treadmill for six minutes under each specific condition with accelerometer and oxygen consumption data extracted from 4 ½ to 5 ½ minutes as the steady state condition. Repeated measures ANOVAs and stepwise regression analyses were used to examine significant relationships and prediction of VO_2 for various speeds, inclines and loads.

RESULTS AND DISCUSSION:

ANOVA results revealed a significant increase in VO_2 with increasing load, incline and speed ($p<0.05$). Using regression analyses, 83% of the variance in VO_2 was explained by the following equation.

$$VO_2 = 2.56 + .107*(incline)^2 + .335*(speed)^2 + 0.182*(load)$$

Although these results were slightly curvilinear for incline and speed, the linear effect explained 80% of the data variance. These responses are similar to the scientific literature.

Using data from the sternum accelerometer only (except for load mass), 65% of the data variance could be explained by load mass, side/side mean acceleration and resultant RMS values. If accelerometer data were combined with the previous analyses, 84.4 % of the variance in VO_2 was explained.

$$VO_2= 3.33 + 1.08*Incline + 0.42*Speed^2 + 0.21*Mass + 0.28*R\text{-}RMS^2 + 0.06*RMean$$

The added variables from the accelerometer can be explained by changes in the gait patterns with load. Interestingly, it is possible to extend the accelerometer data to gather both speed and incline data. The speed variable could be calculated from the frequency of the signal. Knowing the accelerometer's orientation with respect to gravity, it is possible to determine its tilt and consequently the tilt of the body. With further accelerometer data processing, all variables needed to predict performance could be calculated from the accelerometer.

SUMMARY

The energy demands of load carriage have been predicted previously based on knowing a number of load carriage conditions. However, no one has studied 3D accelerometer data to determine its ability to predict physiological measures. A sternum accelerometer alone can explain 65% of energy demands and up to 84% with added knowledge about the speed and incline conditions.

REFERENCES
Boutin, C. et al. (1997). IEEE Biomed. Eng. 44:136-147.
Holewijn, M. & Meeuwsen T. (2001) RTO MP056, 1:1-12.
Morin , E. et al., (2003) IEEE Biomed Eng Conference, 1-8.
Pandolf C.E. et al., J. Appl. Physiol. 43(4) 577-581, 1977.
Polcyn A.F.et al., (2001) RTO(NATO) MP056, 7:1-11.
Quesada P.M. et al. (2000) Ergonomics 43(3): 293-309.

KNEE KINEMATICS, KNEE KINETICS AND HIP KINETICS IN MEDIAL COMPARTMENT KNEE OA.

Monica Maly[1], Patrick Costigan[2] and Sandra Olney[1]
[1]School of Rehabilitation Therapy, Queen's University, Kingston Canada
[2]School of Physical and Health Education, Queen's University, Kingston Canada

INTRODUCTION

Knee osteoarthritis (OA) is the leading cause of chronic disability amongst community dwelling adults. Recent studies of gait have combined data on subjects with medial and lateral compartment OA[1], failed to compare the knee OA population to older adults[1] or had small sample sizes[2]. Our objective was to compare the knee kinematics, knee kinetics and hip kinetics during walking in people with OA predominantly in the medial compartment to healthy older adults.

METHODS

Knee OA Group (OA, n=54): subjects over age 50 with medial compartment knee OA. Healthy Older Adult Group (CON, n=52): subjects over age 50 without knee pain or OA changes on radiographs. Data were collected using the QUESTOR Gait Analysis in Three Dimensions (QGAIT) system. The QGAIT system incorporates joint geometry data from standardized radiographs to more accurately transform the surface marker location into the subject-specific joint centre. Data was collected with an Optotrack optoelectric system (Northern Digital, Waterloo, Canada), a force plate (AMTI, Massachusettes, USA) and QUESTOR precision radiographs. Radiographs were obtained with the subjects barefoot on a calibrated turntable, inside a frame fixed relative to the x-ray source. Surface landmarks to be used for gait trials were marked with a lead bead. Anterior-posterior (knee, hip) and lateral radiographs (knee) were obtained. Radiographs were calibrated. Correction vectors were measured from the surface landmarks into the hip and knee joint centre. Six infrared emitting diodes (IREDs) were used during the walking trials. Four IREDs were placed over anatomical landmarks (greater trochanter, lateral femoral condyle, fibular head, lateral malleolus) and two IREDs on anteriorly projecting probes attached to thigh and shank. Five walking trials were sampled at 100 Hz. Independent t-tests were performed on the mean spatio-temporal characteristics. Independent t-tests were performed on mean peak values for knee kinematics, knee kinetics and hip kinetics.

RESULTS AND DISCUSSION

The OA group (n=54), had a mean age of 68.3 ± 8.7 years, of which, 32 were female. The CON group (n=52), had a mean age of 63.6 ± 6.4 years, of which, 27 were female.

Table 1: Spatio-temporal Characteristics

	Stride Length (m)	Cadence (steps/min)	Velocity (m/s)	% Stance Time
OA	1.2 ± 0.19	50.2 ± 6.6	1.02 ± 0.24	68 ± 3.2
CON	1.3 ± 0.15	51.7 ± 5.0	1.12 ± 0.18	65 ± 2.7
p	0.005	0.156	0.009	0.001

Table 2: Peak Knee Angles, Forces and Moments

Parameter (+ve/-ve)	OA	CON
Add/Abd Angle (°)	9.4 ± 5.2	3.9 ± 6.6**
Flex/Ext Angle (°)	64 ± 9	63 ± 6.3
Int Rot/Ext Rot Angle (°)	3.6 ± 5.1	3.0 ± 10
Ant/Post Force (N/kg)	3.2 ± 0.6	3.4 ± 0.5
Med/Lat Force (N/kg)	0.19 ± 0.1	0.28 ± 0.2*
Prox/Dis Force (N/kg)	0.88 ± 0.1	0.97 ± 0.1*
Add/Abd Moment (Nm/kg•m)	0.46 ± 0.2	0.41 ± 0.1*
Flex/Ext Moment (Nm/kg•m)	0.27 ± 0.2	0.38 ± 0.2*
Int Rot/Ext Rot Moment (Nm/kg•m)	0.13 ± 0.1	0.11 ± 0.0*

*p value < 0.05, **p value < 0.001

Table 3: Peak Hip Forces and Moments

Parameter (+ve/-ve)	OA	CON
Ant/Post Force (N/kg)	1.4 ± 0.6	2.0 ± 0.7**
Med/Lat Force (N/kg)	0.40 ± 0.3	0.27 ± 0.2*
Prox/Dis Force (N/kg)	1.5 ± 1.2	2.1 ± 0.3**
Add/Abd Moment (Nm/kg•m)	0.66 ± 0.2	0.80 ± 0.1**
Flex/Ext Moment (Nm/kg•m)	0.60 ± 0.3	0.78 ± 0.3**
Int Rot/Ext Rot Moment (Nm/kg•m)	0.06 ± 0.03	0.08 ± 0.04*

*p value < 0.05, **p value < 0.001

The OA group walked more slowly than the CON group. Concurrently, the OA group had a decreased stride length and increased stance time. The peak knee adduction angle was greater in the OA group while the peak medio-lateral shear and axial force at the knee was reduced in comparison to CON. A greater peak knee adduction moment was noted in the OA group compared to healthy older adults as has been reported in other studies. The peak knee flexion and internal rotation moments were lower compared to CON. It is noteworthy that all hip kinetics were different between the OA and CON groups.

SUMMARY

Several knee kinematic, knee kinetic and hip kinetic variables are different between healthy adults and those with medial knee OA. Many of these differences appear disproportionately large compared to the relatively small difference in gait speed between the groups. Although the subjects in this study were not instrumented to investigate hip joint angles, these data indicate that the hip joint may play a significant role in the altered mechanics of the knee in people with knee OA.

REFERENCES

[1]Kaufman, K.R. et al (2001). *J Biomechanics* **34**, 907-915.
[2]Gok, H. et al (2002). *Acta Orthop Scand* **73**, 647-652.

ACKNOWLEDGEMENTS

MEDIAL AND LATERAL MUSCLE ACTIVATION DIFFERENCES BETWEEN HEALTHY CONTROLS AND MODERATE KNEE OSTEOARTHRITIC GAIT

Cheryl Hubley-Kozey[1,2], Kevin Deluzio[2], Scott Landry[2], Jennifer McNutt[2], Mina Agarabi[2] and William Stanish[3]
1. Schools of Physiotherapy and 2.Biomedical Engineering and 3. Department of Surgery, Dalhousie University, Halifax, Canada clk@dal.ca

INTRODUCTION

Differences in responses of the knee musculature of Osteoarthritic (OA) subjects have been reported during walking. Most reports are for severe OA (Childs et. al., 2004) with little known about differences in neuromuscular control strategies of those with mild to moderate OA. It is unclear whether neuromuscular impairments are a result of, or cause of, disease progression. Thus it is important to study neuromuscular strategies early in the disease progression to ascertain their impact on the pathogenesis of the disease. The purpose of this study was to compare neuromuscular responses during walking between the medial and lateral sites of the quadriceps, hamstring and gastrocnemius muscles between healthy controls and those with moderate knee OA.

METHODS

Forty two subjects with healthy knees (CON) and 39 moderate knee OA subjects were studied. All subjects signed a written consent in accordance with institution policy. Knee OA subjects had to be able to walk a city block, jog 5 meters and climb stairs in a reciprocal fashion, and have symptomatic unilateral moderate OA. After skin preparation, Ag/agCl Meditrace (10mm) surface electrodes were placed over the rectus femoris, vastus lateralis and medialis, lateral and medial hamstring and lateral and medial gastrocnemius muscles based on standard placements. Motion (Optotrak[TM]), force plate (AMTI [TM]), and electromyographic (AMT-Bortec[TM]) data were recorded during level walking for five trials at i) a self-selected (C1) and ii) a fast (C2) walking speed (150% of self-selected speed). Following the walking trials a series of eight maximal voluntary isometric contractions (MVIC) were elicited for EMG nomalization. The EMG signals were digitized at 1000 Hz using the analogue data capture feature of the Optotrak[TM] motion capture system. The EMG signals were full-wave rectified, then low passed filtered at 6 Hz. to yield a linear enveloped signal. The EMG waveforms for the walking trials were amplitude normalized to the MVIC, and then time normalized to 100 percent for one gait cycle. An ensemble-average profile was calculated for the five trials for each subject, muscle and condition. A pattern recognition procedure (Hubley-Kozey and Vezina, 2003) was applied to the matrices of profiles for the three quadriceps (X=101X486), the two hamstrings (X=101X324) and the two gastrocnemius (X=101X324) separately. The *scores* for the principal pattern were calculated and a three-factor (group, muscle and condition) analysis of variance model was used to test main effects and interactions. All significant effects (p<0.05) were tested using a Bonferonni post hoc test.

RESULTS AND DISCUSSION

Subject information is in Table. The WOMAC scores and *radiographic data* (50% were grade I or II) supports that we have a sample of subjects with *moderate* knee OA. Mass and WOMAC were significantly (p<.05) different between groups. Five principal patterns explained 96, 97 and 98 % of the variance in the waveforms for the quadriceps, hamstrings and gastrocnemius muscles, respectively. Figure 1 illustrates principal pattern one for each muscle group which will be the focus of the results presented. This feature captures the general shape and the overall amplitude of the EMG profiles of the respective muscle groups. The results from the ANOVA of the *scores* for principal pattern one showed muscle by group interactions for the quadriceps (p=.063), hamstrings (p=.002) and gastrocnemius (p=.016). No differences were found between the groups for the vastus medialis, however, vastus lateralis and rectus femoris were lower for the CON, and the rectus femoris was significantly lower than vastus medialis for the CON group. There were no difference between the lateral and medial hamstrings for the CON, but the lateral hamstring was significantly higher than the medial hamstring for the OA. Finally, the medial gastrocnemius was significantly higher for the CON than the OA. The OA subjects recruited their lateral sites to higher percentages of MVIC than the CON, and the medial sites were recruited to similar or lower for the OA group compared to the CON group. These strategies suggest that the OA subjects preferentially recruit lateral sites to counterbalance the high adductor moment and reduce medial joint loading during early stance, and preferentially reduce medial gastrocnemius activity during late stance (around 40%), a phase in the gait cycle when a high knee adductor moment typically occurs.

Table Demographic and speed information for C1 and C2

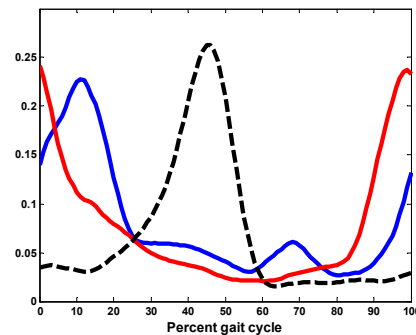|	Age	Height	Mass	WOMAC	C1	C2
CON	50 y	1.71 m	73 kg*	1.2*	1.37m/s	1.87m/s
OA	54 y	1.73	91 kg	34.3	1.34m/s	1.85m/s

Figure 1 Principal pattern 1 for the quadriceps (83%) in blue, hamstrings (85%) in red and gastrocnemius (88%) black dotted. Percent trace for principal pattern in parenthesis ().

SUMMARY

The CON and moderate OA subjects had similar shaped profiles with subtle differences, but did not illustrate the high co-activation patterns reported for severe OA. The results support a medial versus lateral site difference, consistent with the OA subjects attempting to increase activity of the lateral sites and reduce activity in the medial sites.

REFERENCES

Childs et.al. (2004) *Clinl Biomech,* **19**, 44-49.
Hubley-Kozey and Vezina (2003) *Clinl Biomech,* **17** ,621-629.

ACKNOWLEDGEMENT

KNEE BIOMECHANICS OF MODERATE AND SEVERE KNEE OSTEOARTHRITIS PATIENTS

K.J. Deluzio[1], C.S.N Landry[1], J.A. Astephen, C.L. Hubley-Kozey[1], M.J. Dunbar[1,2], and W.D. Stanish[2]

[1]School of Biomedical Engineering, Dalhousie University, Halifax, Canada, kevin.deluzio@dal.ca
[2]Dept. of Surgery, Dalhousie University, Halifax, Canada

INTRODUCTION
The pathomechanics of knee osteoarthritis (OA) are not well understood, nor are the causes for it to progress more rapidly in some individuals than others. Modern gait analysis offers a unique means to measure the biomechanical response to diseases of the musculoskeletal system during activities of daily living. Identifying the mechanical factors of gait associated with knee OA is important in understanding the initiation and progression of OA as well as in planning therapeutic interventions. The objective of this study was to quantify differences in knee biomechanics associated with differences in the severity of knee osteoarthritis.

METHODS
We measured 3-D knee joint kinematics and kinetics from 43 subjects with healthy, asymptomatic knees, 40 subjects with moderate knee OA and 21 patients with severe, end-stage knee OA. The moderate OA group was selected from the waiting list for arthroscopies at a local sports medicine clinic, and the severe OA group were evaluated prior (< 1 week) to receiving a total knee replacement. The normal subjects were recruited from the general population and were asymptomatic, without evidence or history of arthritic disease or record of surgery to the lower limbs. All subjects gave their informed consent to our protocol that passed our internal ethics review board. The waveform data was analysed using principal component analysis (Deluzio et al.1997). In this approach each kinematic and kinetic time series for each subject was transformed into a set of principal component (PC) scores that correspond to the major features of the waveform. Analysis of variance and post-hoc tests were then performed on these scores.

RESULTS
The severe OA group was older than the other two groups, and both the moderate and severe OA groups were heavier than the normal group. There was no difference in stride characteristics between the moderate OA and normal groups. The severe OA group walked slower (Table 1).

We found differences in the knee joint kinematics between the three groups. The overall level of knee flexion throughout the gait cycle (flexion angle PC1) for the moderate OA group was 3º less than the normals (p<0.05), and the severe OA group was 6º less flexed than the moderate OA group (p<0.05). The amount of knee flexion in swing relative to stance (flexion angle PC2) was 11º less for the severe group than either of the moderate OA or normal group (p<0.05).

The moderate OA group had a larger overall magnitude of the adduction moment during stance (adduction moment PC1) than the normal group, while the severe OA group was not different from either group. The size of the adduction moment between late stance relative to early stance (adduction moment PC2) was larger for the severe group than either group (p<0.05), and the moderate OA group was larger than the normal group (p<0.05).

The first peak of the net external flexion moment (flexion moment PC1) was smaller for the moderate OA compared to the normals (p<0.05), and the severe OA group was smaller than the moderate OA group (p<0.05). The magnitude of the second peak in the flexion moment was reduced in the severe OA group relative to either of the other groups (p<0.05).
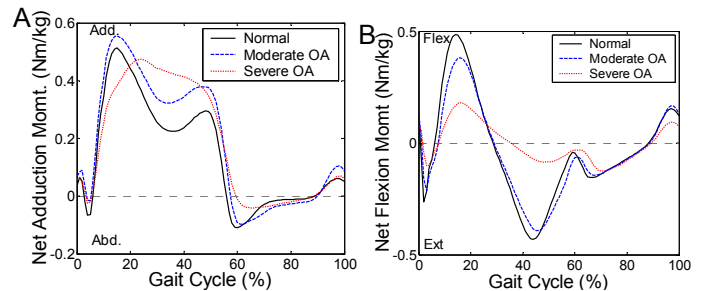

Figure 1. A: The net external adduction moment at the knee. flexion moment data, and B: the net external flexion moment.

DISCUSSION AND CONCLUSION
This study examined the gait patterns of patients with different severity of osteoarthritis. Severe OA gait was characterized by changes in stride characteristics, knee joint angles, moments. Moderate OA gait was not associated with changes in stride characteristics, but did reveal some similar changes in knee joint angles and moments, but to a lesser degree. Examining the knee joint biomechanics across the disease spectrum, may contribute to understanding the pathomechanics of the osteoarthritis.

REFERENCES
Deluzio,K.J.; et al. (1997) *J. of Hum. Mov. Sc.* 16: 201-217.

Table 1 Subject Characteristics. Significant differences are indicated in the last row of the table. These are the results of multiple comparison post-hoc tests (Tukey) performed after one-way ANOVA (p<0.05).

	Age (yr)	Height (m)	Weight (kg)	BMI	Walking Speed (m/s)
N: Normal (n=43)	50.2 (10.1)	1.71 (0.1)	72.6 (16.4)	24.7 (4.4)	1.37 (0.19)
M: Moderate OA (n=40)	54.9 (14.4)	1.74 (0.1)	93.5 (17.6)	31.0 (5.3)	1.31 (0.24)
S: Severe OA (n=21)	60.0 (16.8)	1.73 (0.1)	97.4 (16.4)	32.7 (5.1)	0.90 (0.23)
Significant differences	S > (M = N)	p = 0.4	(S = M) > N	(S = M) > N	S < (M = N)

ELECTROMECHANICAL RESPONSE OF ARTICULAR CARTILAGE IN CONTACT WITH AN ARTHROSCOPIC PROBE

LePing Li and Walter Herzog

Human Performance Laboratory, Faculty of Kinesiology, University of Calgary, Canada **leping@kin.ucalgary.ca**

INTRODUCTION
The streaming potentials in articular cartilage have been found to be a sensitive index of tissue degradation (Garon et al., 2002). Changes in streaming potentials might partially be responsible for modulating chondrocyte metabolism (Kim et al., 1995). Recent efforts are being made to explore the possibility of diagnosing arthritis by measuring the potentials using an arthroscopic probe. This study was aimed to address specific issues of such attempts using a theoretical approach based on finite element modeling.

METHODS
Articular cartilage was modeled as a fibril-reinforced fluid-saturated material (Li and Herzog, 2004) with streaming potentials. The probe-cartilage interaction was approximated as a rigid sphere (radius: 5.25mm) in contact with a tissue disk (radius: 6mm; thickness: 1.13mm) adhered to a rigid surface. The actual disks used in the experiments had much larger radii, and were attached to bone of 5mm thickness. However, previous calculations indicated that the deformation was confined to the vicinity of the contact region in cartilage only. In the experiments, a displacement of 200μm was applied in 1s, and then released in 0.2s. In the theoretical analyses, we also considered stress relaxations at various strain rates.

RESULTS AND DISCUSSION
The patterns of the streaming potentials were similar to those of fluid pressure. The potential at cartilage surface decreased with distance (r) from the contact centre, to zero for the open (not contacted) surface (Fig.1). The tissue shape was not recovered upon withdrawing the probe (contact was lost before 1.2s, Fig.1); it took about 300s for the deformation to mostly disappear (not shown). This extended recovery period may produce errors if repeat measurements are performed at one site in clinical application.

The strain-rate dependent transient load was mainly produced by collagen network (Fig.2), which agrees with our previous results for unconfined compression. When fibril-reinforcement was not considered, the strain-rate dependence was essentially lost for the compression rates calculated, and the predicted load became very low (Fig. 2). The latter case corresponds to the biphasic model according to Wu et al (1998). Therefore, a conventional biphasic model can not be used to determine collagen degradation, and can only be used to analyze the response to low-speed compression (< 0.2μm/s). The fibril-reinforcement only produced a load difference of (0.291-0.250)N at equilibrium. However, the corresponding peak load difference was 21.5N (75.4×0.291-1.90×0.250) at 200μm/s. The large difference in load in the transient phase was partially caused by an under-estimation of the contact area by the biphasic model (not shown).

Unlike the mechanical response, streaming potentials were sensitive to the fluid properties, such as conductivity (not shown). The stress and load response, in addition to the electrical response, provide important information to characterize cartilage properties. However, controlling the compression rate in clinical application is of utmost importance if accurate and reliable results are to be obtained.
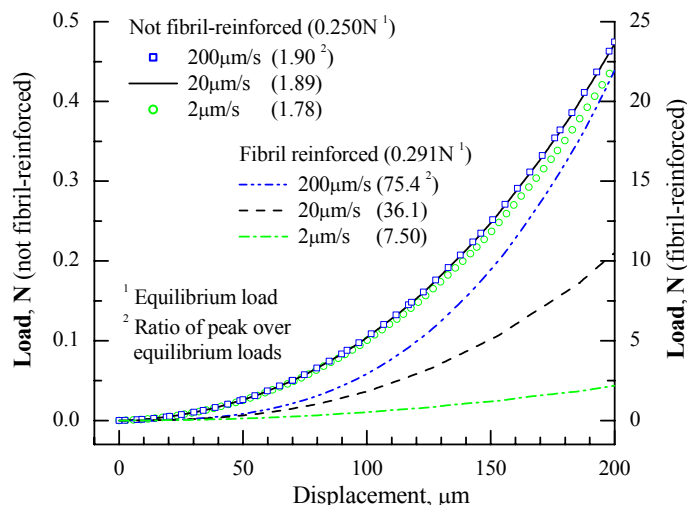
REFERENCES
Garon, M et al (2002). *J Biomechanics* **35**, 207-216.
Kim, YJ et al (1995). *J Biomechanics* **28**, 1055-1066.
Li, LP & Herzog, W (2004). *J Biomechanics* **37**, 375-382.
Wu, JZ et al (1998). *J Biomechanics* **31**, 165-169.

ACKNOWLEDEMENTS

Fig. 1 Potential at the Probe-Cartilage Contact Surface

Fig. 2 Effect of Fibril-Reinforcement on the Compressive Load

THE EFFECT OF MUSCLE ACTIVATION TIMING ON FIBER STRAIN DURING ECCENTRIC CONTRACTIONS

Timothy A Butterfield, Walter Herzog
Faculty of Kinesiology, Human Performance laboratory
University of Calgary, Calgary, Alberta, Canada

INTRODUCTION

Muscle strain injuries have been long associated with eccentric contractions (Garrett, 1996), with the magnitude of injury being related to the magnitude of strain (Lieber and Fridén, 1993). Thus fiber strains have been estimated from known MTU strains (Lieber and Fridén, 1994) in an effort to understand their role in contraction induced injury. However, it is well known that for many contractile conditions the fiber dynamics, and thus the fiber strain, may differ significantly from the muscle-tendon unit (MTU) strain (Griffiths, 1991). In addition, there is anecdotal evidence that alteration of activation during an eccentric contraction may precipitate MTU injury (Agre, 1985), perhaps by magnifying the dissociation between fiber strain and MTU strain. However, there are no studies in which the effects of small changes in the timing of activation on fiber and MTU dynamics have been assessed. The purpose of this study was to determine the effects of small changes in the timing of activation for a given eccentric contraction of the MTU on fiber dynamics, so as to possibly gain novel insight into eccentric contraction-induced muscle injury.

METHODS

Eight NZW rabbits were anesthetized and secured supine in a custom designed sling, and the foot was attached rigidly to the footplate of a servo motor. Stimulation of the tibialis anterior (TA) was performed through a surgically implanted cuff-type electrode placed on the peroneal nerve and attached to a Grass (S8800) stimulator. Activation of the TA was supramaximal ($3x$ α-motoneuron threshold) for 500 ms during each MTU stretch-shortening cycle. Fiber length and muscle length were determined by implanting two sonomicrometry crystals on a central fascicle (Griffiths, 1991) and using a tendon travel approach (An, 1984), respectively. Fiber strain was determined from the shortest fiber length during the stretch-shortening cycle (1, Fig. 1). *Protocol 1* consisted of plantar flexion (eccentric TA action) beginning at the onset of activation, through a range of motion of 35° from 70°-105° at 70°·sec^{-1}. Afterwards, the foot was returned (concentric TA action) to the start angle passively. The entire eccentric protocol consisted of five sets of ten repetitions with a two minute rest between sets. *Protocol 2* was identical to the first, however the timing of activation was changed, with activation preceding plantar flexion by 100 ms. This resulted in a 100ms isometric contraction prior to stretch, with the TA being deactivated for the last 100 ms of plantar flexion.

RESULTS AND DISCUSSION

Despite a constant MTU strain and activation duration between the two protocols, alteration of activation timing resulted in greater fiber shortening preceding active fiber stretch (Black arrow to 1, Fig. 1), and an increased (50%) peak
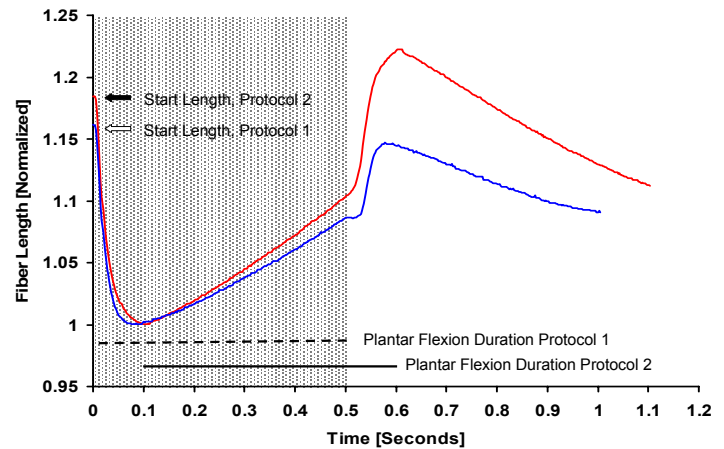

Figure 1. Effect of altering activation timing on fiber length changes during one complete eccentric-concentric cycle. Mean fiber lengths of protocol 1 (—) n=6, and protocol 2 (—), n=10, are shown. Shaded area represents 500 ms activation timing for protocols 1 and 2.

fiber strain for protocol 2 compared to protocol 1. Also, peak fiber strain occurred during MTU shortening in protocol 1, but MTU lengthening in protocol 2 (Fig. 1). These results illustrate that a small change in activation timing for a given stretch-shortening cycle of the MTU, can cause dramatic changes in fiber strain.

SUMMARY

Here, we show that a shift in activation by 100 ms resulted in an increase in peak fiber strain from ~15% (protocol 1) to ~23% (protocol 2), for an increase of almost 50%. It seems quite possible that such a dramatic change in fiber strain may affect the risk for muscle injury. We conclude, therefore, that activation timing may be a potent factor for muscle injury, because of the changes associated with fiber strain.

REFERENCES

Agre, J.C. (1985). *Sports med.* **2**, 21-33.
An, K.N. (1984). *Biomech Eng,* **106**, 280-282
Garrett, W.E. (1996). *Am J Sports Med*, **24**, S2-S8.
Griffiths, R.I. (1991). *J Physiol*, **436**, 219-236.
Lieber, R.L., and Fridén,J. (1993). *J Appl Phys,* **74**, 520-526
Lieber, R.L., and Fridén J. (1994). *J Appl Phys*, **77**, 1926-1934

ACKNOWLEDGEMENTS

History Dependent Force Production in Sub-Maximal Human Voluntary Contractions

Mir Ali Eteraf Oskouei, Elissavet N. Rousanoglou, and Walter Herzog
Human Performance Laboratory, University of Calgary, Calgary, Alberta, T2N 1N4, Canada
E-mail: oskouei@kin.ucalgary.ca

INTRODUCTION

Force depression (FD) can be defined as the loss of steady-state isometric force after active muscle shortening, and force enhancement (FE) as the increase in steady-state isometric force following muscle stretch [1,3]. FD and FE have been observed on all structural levels: single fibers and myofibrils, isolated muscles, and intact muscles [1,2,4], and have been reported for maximal and sub-maximal artificial stimulation of muscles [1,2] as well as for maximal voluntary contraction in humans [5]. However, FD and FE have not been studied for sub-maximal voluntary contractions. Therefore, it is not known if FD and FE occur during normal everyday movements. The purpose of this study was to test whether FD after shortening and FE after lengthening exist for sub-maximal voluntary muscle contraction.

METHODS

Force depression and force enhancement were determined by comparing the steady-state isometric force at a given thumb adduction angle with the corresponding steady-state isometric forces obtained following shortening and stretching of the adductor pollicis group. All procedures were identical to those described by Lee and Herzog [4,5] with two exceptions:
i) All contractions were performed at sub-maximal levels; that is, at either 30% of the maximal isometric force, or at an activation level (integrated EMG) corresponding to the values obtained at 30% of MVC, and ii) Visual feedback was provided to the subjects so they could match either 30% of MVC, or the integrated EMG corresponding to 30% of MVC.
The force depression experiments were performed with 16 volunteers and the force enhancement experiments with 14 volunteers.

RESULTS

The steady-state force following adductor pollicis shortening at 30% of MVC was decreased for all 16 subjects by a mean value of 21% (± 9%) from the corresponding isometric reference force when activation was kept constant (Figure 1, FD). The steady-state integrated EMG following muscle shortening was increased for all subjects by a mean value of 18% (± 11%) as compared to the corresponding isometric reference EMG when force was kept constant (Figure 2, FD).
No consistent results were observed for the force enhancement test, as subjects fell into two groups showing distinctly different results. Eight of the 14 subjects had statistically significant FE (10% ± 6%) and activation depression (16% ± 6%) following adductor pollicis stretching compared to the isometric reference contractions when activation and force were kept constant, respectively (Figure 1 and 2, FE-8 subjects). The remaining six subjects showed no changes in force or activation following muscle stretching when compared to the corresponding reference contractions (Figure 1 and 2, FE-6 subjects).
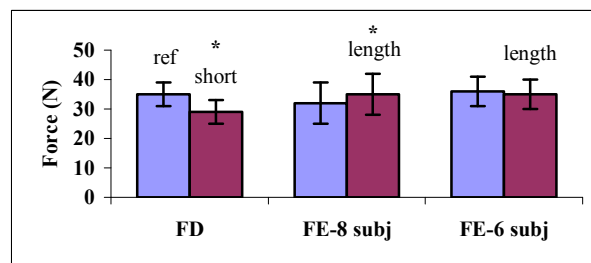

Figure 1. Mean (±1SD) isometric reference force (ref), isometric after shortening (short), and after lengthening (length) during FD and FE tests (*p<0.05).

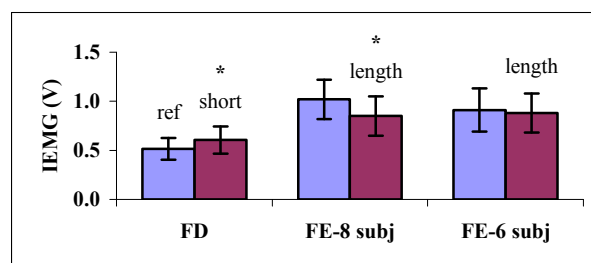**Figure 2.** Mean (±1SD) integrated EMG in FD and FE tests (*p<0.05).

DISCUSSION

Here, we demonstrate for the first time that force depression occurs in a systematic manner for sub-maximal voluntary contractions. FD manifested itself as a decrease in force when activation was kept constant at 30% of MVC, or as an increase in activation when force was kept constant at 30% of MVC.
Force enhancement was observed in 8 out of the 14 subjects, but was not observed in the remaining 6 subjects. We subsequently repeated the entire FE test protocol with all subjects and found that those who had consistent FE in the first testing session, also had it in the second session, and analogous for the six subjects who showed no FE.

CONCLUSION

Force depression is a property that is maintained in sub-maximal voluntary contractions, and thus, must be considered in the analysis of normal everyday movements. Force enhancement occurs in some subjects but not in others for sub-maximal voluntary contractions. It is not clear at this point why force enhancement is not observed consistently in all people.

REFERENCES

1. Abbott BC and Aubert XM (1952). *J Physiol*, **117**, 77-86.
2. Edman KAP et al (1978). *J Physiol*, **281**, 139-155.
3. Herzog W and Leonard T(1997). *J Biomech,* **30(9)** 865-872.
4. Lee HD and Herzog W (2002). *J Physiol,* **545**, 321-330.
5. Lee HD and Herzog W (2003). *J Physiol,* **551(3)** 993-1003.

EFFECTS OF OVERSAMPLING AND SIGNAL RECONSTRUCTION ON SURFACE ELECTROMYOGRAPHIC SIGNALS

Jennifer L. Durkin and Jack P. Callaghan

Department of Kinesiology, University of Waterloo, Waterloo, ON, Canada, durkinjl@healthy.uwaterloo.ca

INTRODUCTION

The Nyquist theorem states that an analog signal must be digitally sampled at at least twice the highest frequency present (f_c) to avoid aliasing. While data collected at rates slightly above f_c retain the frequency content of signal, time-series representations often result in decreased amplitude measurements and phase-shifting (Hamill et al., 1997). Sampling at rates 4-10 times higher than f_c circumvents this problem, however Hamill et al. (1997) successfully used Shannon's reconstruction theorem to return time-series signal representation to normal for kinematic and impact data sampled at $2f_c$. The purpose of this study was to determine whether signal amplitude and timing information is compromised in electromyographic (EMG) data by sampling at rates just above f_c and whether the application of Shannon's reconstruction theorem can correct these deficiencies, if present.

METHODS

Surface EMG data was collected from the biceps brachii of 4 males and 4 females. All signals were differentially amplified, prefiltered (bandwidth=0.01-1KHz) and simultaneously sampled at 20KHz and 2KHz. Brief standing elbow isometric flexion contractions were performed at 100, 80, 50, 25, 10, 5 and 2.5% MVC. The 2KHz signal was then downsampled to 1KH and the 2KHz and 1KHz signals were reconstructed to a sampling rate of 20KHz using Shannon's reconstruction theorem (RC) as in Hamill et al. (1997). One 10s trial of cyclic isometric contractions and relaxations was also recorded, downsampled and reconstructed as for the previous contractions. All data were full wave rectified (FWR) and filtered (LE) using a 2nd order Butterworth filter with a cutoff frequency of 2.5Hz. All EMG data except the varying trials were normalized to peak 20KHz MVC amplitude and peak amplitude of the raw, FWR and LE signals, average EMG (AEMG) of FWR and LE signals, mean power frequency (MPF) of raw signal were measured. Varying EMG trials were normalized to the peak MVC amplitude of the respective sampling rate and gaps analyses were performed with a gap period constituting an amplitude of less than 0.5% MVC for >= 0.2s. Number of gaps and average gap times were recorded. Repeated measures analyses of variance (ANOVA) followed by Tukey HSD post hoc analyses determined where significant differences existed between the five sets of signals.

RESULTS AND DISCUSSION

No significant differences were found between the three sampling rates for the AEMG, LE peak amplitude, MPF, or the gaps measurements. The RC signals were significantly different from the 2KHz and 20KHz signals for raw and FWR peak EMG amplitudes. Significant RC raw overestimations were seen at the 100 and 80%MVC contraction levels (Fig. 1) and 1KHz RC FWR overestimations were seen at the 80%

level (Fig. 2). The minimal differences seen in this study between the oversampled and reconstructed signals are supported by Ives and Wigglesworth (2003) who showed that sampling at rates greater than $2f_c$ provided no improvement on surface EMG timing and amplitude measurements.

SUMMARY

The few differences seen between the five signals, coupled with the processing time required for signal reconstruction (approx. 1.75 hours for a 10s signal on a 2.2GHz processor), suggest that oversampling and signal reconstruction is unnecessary for surface EMG measurements.
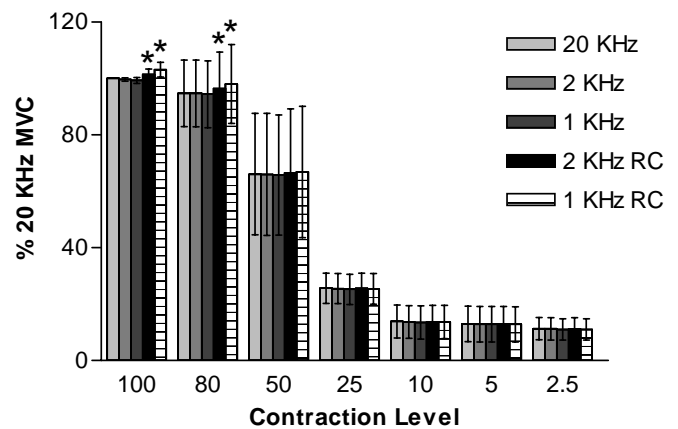

Figure 1. Comparison of mean (± SD) raw peak EMG amplitudes between three signal frequencies. * indicates significant difference
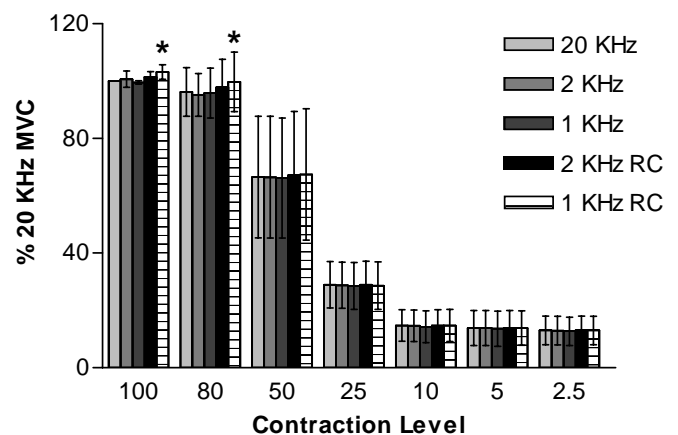

Figure 2. Comparison of mean (± SD) full wave rectified peak EMG amplitudes between three signal frequencies. * indicates significant difference.

REFERENCES

Hamill, J et al. (1997). J Appl Biomech, **13**,226-238.
Ives, J.C. & Wigglesworth, J.K. (2003). Clin Biomech, **18**,543-552.

OPTIMIZATION-BASED PROCEDURES FOR THE PREDICTION OF JOINT MUSCULAR EFFORTS

David Amarantini [1], Luc Martin [2], Violaine Cahouët [2]

[1] Laboratoire d'Aérodynamique et de Biomécanique du Mouvement Humain, Université de la Méditerranée, Marseille, France,
amarantini@morille.univ-mrs.fr

[2] Laboratoire Sport et Performance Motrice, Université Joseph Fourier, Grenoble, France

INTRODUCTION

Estimation of muscular efforts is a critical point in movement analysis, especially for biomechanical applications. At a given joint, estimating the net moment deals with solving the problem of inverse dynamics, while predicting the efforts of opposing muscles requires to solve an under-determined system of equations associated to muscle redundancy. Combining optimization with information redundancy can be a solution in order to provide accurate estimates of muscles' efforts in accordance with all available experimental data.

Our purpose is to describe two distinct optimization-based models, one using static optimization of accelerations to solve inverse dynamics (SOA, Cahouët et al., 2002) and one combining numerical optimization and EMG data to estimate agonist and antagonist muscle moments (OPT, Amarantini and Martin, in press). These approaches could be used either independently or jointly to improve the accuracy and reliability of joint moments estimates.

METHODS

To improve inverse dynamics solutions, SOA is proposed. First, optimal accelerations were calculated by implementing least-squares minimization with weight coefficients, in order to account for the influence of both dynamics and kinematics measurements accuracy. Next, inverse dynamics were solved using a Lagrangian formulation of the equations of motion. The application to rapid symmetrical arm raising was conducted with a 4-link model of human body. The ground reaction and 2D positions of 4 markers placed on subject's left side were provided as inputs. Net joint moments, accelerations and ground reaction signals estimated using SOA were compared with those obtained using classical 'top-down' and 'bottom-up' methods by using RMS error.

To estimate agonist and antagonist muscle moments, OPT is developed. Muscle redundancy at the knee was solved in two steps: first, EMG from Gastrocnemius, Biceps Femoris, Rectus Femoris and Vastus Medialis sampled from 9 subjects during isometric contractions were optimally processed with non-linear least-squares curve-fitting to match the net moment (M_K). Next, the subjects were instructed to walk-in-place at their natural cadence. The ground reaction and the trajectories of 4 markers fixed onto subjects' right leg were recorded to estimate M_K. The EMG signals recorded during stepping were processed with the coefficients obtained from isometric calibration and then used as inputs to an optimization process that provided both flexor and extensor moments estimates. Statistical tests were conducted to compare OPT solutions with those from Olney and Winter (1985).

RESULTS AND DISCUSSION

Angular accelerations calculated by numerical differentiation showed relative RMS errors of 10.7 %, 12.6 % and 6.3 % with

those given by SOA at the ankle, hip and shoulder joints, respectively. The deviations between force-plate signals and the estimations of horizontal and vertical forces and transverse moment are lower using SOA than 'top-down' (respectively 2.8 *vs.* 38.6 %, 0.2 *vs.* 4.6 % and 0.7 *vs.* 9.5 %). For the net joint moments at ankle, hip and shoulder joints, the absolute RMS values are respectively 35.7 Nm, 21.0 Nm, 14.4 Nm between SOA and 'top-down' and 2.6 Nm, 8.0 Nm, 16.0 Nm between SOA and 'bottom-up'. SOA predicts optimal angular accelerations in best accordance with kinematic and dynamic measurements and produces best estimations of ground reaction components as well as more realistic estimations of net joint torques than 'top-down' and 'bottom-up' methods.

For isometric conditions, the performances of OPT were similar to those from Olney and Winter (1985), providing estimates of M_K with RMS error less than 4 % and satisfactory predictions of flexor and extensor moments. As improvement, OPT method avoids possible inconsistencies because of the constraints enforced on the sign convention. In dynamic conditions (Figure 1), the ability to predict M_K is dramatically improved with OPT, which produces estimates of M_K with RMS error less that 1 %. Also, muscular moments were physiologically realistic and all muscles were predicted to be active with OPT because of the account of muscle dynamics and biarticularity.
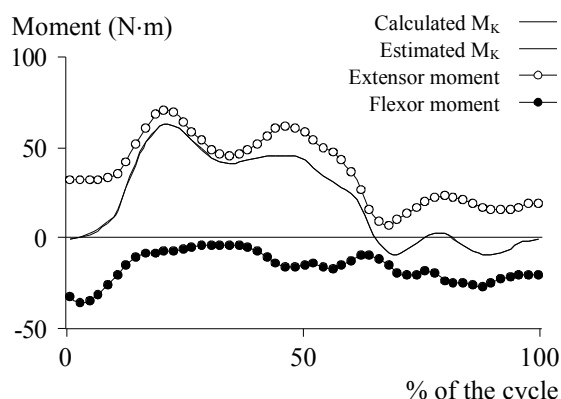

Figure 1: Net, extensor and flexor moments estimated at the knee with OPT for a typical stepping in place cycle. M_K estimated using OPT is similar (overlaid) to that calculated using inverse dynamics.

The formulation of optimization problems with the use of information redundancy produces more reliable estimates of net as well as agonist and antagonist joint moments. Further use of SOA and OPT methods may be used in diverse rehabilitation, motor control and human motion analysis.

REFERENCES

Olney, S.J., Winter, D.A. (1985). *J Biomech*, **18**, 9-20.
Amarantini, D., Martin, L. (in press). *J Biomech*.
Cahouët, V. (2002). *J Biomech*., **35**, 1507-1513.

ARTHRITIS - A Social and Economic Epidemic

W.D. Stanish, MD, FRCS(C), FACS
Professor of Surgery, Dalhousie University
Director, Orthopaedic and Sport Medicine Clinic of Nova Scotia

In 2000, arthritis and rheumatism affected nearly 4 million Canadians, age 15 years and older, representing 16% of this population.

Residents of Nova Scotia reported arthritis and rheumatism most frequently, as 23% of the population over the age of 15, arthritis was the second and third most common chronic condition reported by women and men respectively.

Prevalence of arthritis amongst Canadian 15 years of age and older is projected to increase by almost 1% every five years. The projected prevalence of more than 20% by the year 2026. It is estimated that within 25 years, 6.4 million Canadians, 15 years of age and old, will have the disease.

The proportion of people with arthritis reporting disability days was more than twice that of people with other chronic conditions.

An individuals perception and evaluation of her health often yields information about the impact of illness and disease. The proportion of individuals who reported fair and poor health increased with increasing age and was greatest amongst people living with arthritis.

Arthritis also influences an individuals participation in the labor force. Over 1 in 10 individuals of working age reported having arthritis. The proportion of people not working was highest amongst those with arthritis in comparison to those with other or no chronic conditions.

Approximately 80% of individuals with arthritis in all age groups reported taking pain relievers such as Acetaminophen and anti-inflammatory medications. In all age groups the proportion who took pain relievers, narcotic pain medications and/or anti-depressants are highest in individuals suffering with arthritis than those with chronic conditions.

Arthritis is a major cause of morbidity, disability in health care utilization in Canada. Since 1994 the number of hip and knee replacements performed on individuals with arthritis related conditions has shown a marked increase. The rate of knee replacement has increased by 36%. Hip replacements by 10%. Patients are becoming younger and the hospital stays are becoming briefer.

A large number of Canadians, 163 in every 1000 people over the age of 15 years, visited a physician in 1998/1999 for arthritis and related conditions. On average, each person made about two visits for an estimated total of 8.8 million visits for all of Canada per year.

In 1986 the economic burden of musculoskeletal diseases in Canada was estimated to be 11.4 billion. By 1998, this number had swollen to 16.4 billion, with arthritis chewing up 4.4 billion. Arthritis accounts for nearly one third of hospital care expenditures for musculoskeletal disease; over 40% of drug expenditures; and more than 1/4 of both musculoskeletal mortality costs and morbidity due to long term disability.

Women accounted for approximately 60% hospital care expenditures, prescription drug expenditures and mortality costs, and one half of morbidity costs due to long term disability.

Excerpt: Arthritis in Canada: An ongoing challenge
Published by Health Canada   2003

PATHOMECHANICS OF KNEE OSTEOARTHRITIS - CAN GAIT EXPLAIN IT?

H.S. Gill and J.J. O'Connor
OOEC/NDOS, University of Oxford, Oxford, UK
richie.gill@orthopaedic-surgery.oxford.ac.uk

INTRODUCTION

Involvement of mechanical factors in osteoarthrosis (OA) has been well documented (Radin et al 1991). For OA of the human lower limb, the impulse imparted at heelstrike has been suggested as a pathogenic factor. It has also been reported that there is a large amount of variation in the level of impulse experienced by different individuals, and it is suggested that those who experience large impulses are at a greater risk of developing OA. The current study investigated gait patterns of twelve normal subjects to establish the gait determinants responsible for producing large impulses at heelstrike and also used a simulation model to investigate how control effort would need to be modified to reduce heelstrike impulse.

METHODS

Gait analysis was performed on 12 asymptomatic normal subjects, average age 30.4 years (22.2-43.3 years). Six sets of gait data were collected for each subject, using a standardised protocol (Kabada 1990). Prior to the measurements, the subjects were acclimatised to the laboratory and were instructed to walk with their normal gait pattern. All data were collected with the subjects barefoot.

An accelerometer ankle cuff was then attached to the right leg of the subject, just above the malleoli. The subject was then asked to walk normally, the gait pattern was observed to ensure no changes had occurred due to the addition of the cuff. If no changes were observed, video and analogue data were collected for three further trials. For all trials, video data was collected at 50Hz and analogue data at 1000Hz. The peak a_z (vertical) accelerometer readings (termed azp) were used to distinguish between subjects with large heelstrike loading and those with small heelstrike loading.

RESULTS

On the basis of azp the subject group was divided into two groups, those with peak deceleration greater than 4.7g were termed the loader group and those with peak deceleration less than 4.7g were termed the non-loader group. The loader group consisted of seven members with mean azp of -5.9±0.3g. The non-loader group had five members and mean azp of -3.6±0.5g. Typical accelerometer traces for both a loader and non-loader subject show the differences in these peak decelerations (Figure 1).

Of the kinematic variables, ankle trajectory during swing was markedly different between groups, the non-loader group raised the ankle significantly higher during swing than the loader group (p < 0.001). The maximum value of occurred

at approximately 70% of the gait cycle for both groups, the loader group appear to reach the maximum sooner in the gait cycle than the non-loader group. This difference in the late swing was shown more clearly by the vertical ankle velocity, for the loader group at heelstrike was -0.25±0.16m/s compared to -0.01±0.07m/s for the non-loader group (p < 0.04).
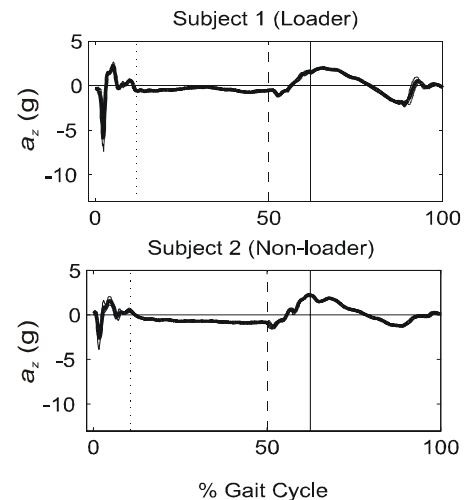

Figure 1. Vertical accelerometer traces

DISCUSSION and CONCLUSION

This study has shown that the test population was divided into two groups that displayed markedly different loading during the heelstrike phase of the gait cycle, which could be attributed to differences in the vertical velocity of the ankle at heelstrike. We hypothesis that those individuals with large impulsive loading may be at higher risk of developing OA. The differences in loading were most apparent in the sagittal plane. Subtle differences in the trajectories of the thigh appear to be responsible for producing the large differences in ankle velocity at heelstrike. The standard methods of representing gait pattern may mask important gait pattern characteristics.

REFERENCES
Kadaba, M. P., H. K. Ramakrishnan, et al. (1990). "Measurement of lower extremity kinematics during level walking." J Orthop Res 8(3): 383-92.
Radin, E. L., D. B. Burr, et al. (1991). "Mechanical determinants of osteoarthrosis." Semin Arthritis Rheum 21(3 Suppl 2): 12-21.

MECHANICAL FACTORS OF KNEE OSTEOARTHRITIS DETECTED THROUGH GAIT ANALYSIS

K.J. Deluzio

School of Biomedical Engineering, Dalhousie University, Halifax, Canada, kevin.deluzio@dal.ca
[2]Dept. of Surgery, Dalhousie University, Halifax, Canada

INTRODUCTION

The pathomechanics of knee osteoarthritis (OA) are not well understood, nor are the causes for it to progress more rapidly in some individuals than others. Modern gait analysis offers a unique means to measure the biomechanical response to diseases of the musculoskeletal system during activities of daily living. Gait analysis offers the potential to: (i) gain insight into the pathogenesis of knee OA, and (ii) evaluate and design treatment interventions. We have found that this potential can be realized through the use of pattern recognition techniques applied to gait data. I will review some of our work in using these techniques for the analysis of gait data of patients with knee osteoarthritis.

GAIT ANALYSIS AND KNEE OA

Standard gait analysis involves the measurement 3-D body segment kinematics, ground reaction forces, and perhaps electromyography. These data are combined with biomechanical modeling to provide estimates of dynamic joint kinematics (joint angles), and kinetics (joint loads) throughout the gait cycle.

This great volume of data overparameterises the biological system, pointing to the need for data reduction for meaningful interpretation of gait data. Researchers have investigated new analysis techniques including fuzzy systems, multivariate statistics, fractal dynamics, artificial neural networks, and wavelet transforms (2;3). We have focused our attention on the multivariate statistical techniques of principal component analysis and discriminant analysis(5). This work, emphasized *evaluating individual gait waveforms* (i.e. patient gait data) according to a known standard that described normal gait. *Normal* gait was defined by the gait pattern of 30 asymptomatic elderly subjects with no history of knee injury or disease. Unicondylar arthroplasty patient gait data were introduced to the model to quantify the change in the gait pattern(4).

Subsequent work has focused on discriminating between subject groups. We have used principal component analysis as part of a pattern recognition scheme to successfully discriminate between *normal and severe OA gait*. The principal component analysis of the flexion angle data for 60 asymptomatic age matched subjects, and 60 patients with end-stage knee OA are shown in Figure 1. While the waveform data from the two groups overlap, the second principal component (PC2) is able to separate the two groups. This PC corresponds to the overall range of knee motion. Similar analysis revealed that OA patients have a larger magnitude of the adduction moment during stance and reduced amplitude of the net flexion/extension moment.

More recently, we have been exploring ways to perform the *simultaneous* analysis of *multiple* gait waveform measures, as well as to incorporate discrete parameters such as radiographic alignment measures and anthropometric measures (i.e. body mass index) (1). The rationale is that gait measures are related to each other and to discrete measures, and these relationships may be important to OA. Frontal plane static alignment and dynamic loading have received much attention in the literature. Our pattern recognition-based analysis found that the two most discriminatory features were: (i) a frontal plane loading and alignment factor, and (ii) loading response factor.

Interventions to slow the progression of knee osteoarthritis are aimed at patients with *early to moderate OA*. We are now investigating gait data of patients with moderate knee OA compared to a group of 40 healthy age matched controls. Our preliminary findings suggest that patients at this early stage of the disease maintain the *visual* aspects of gait including joint kinematics, and gait velocity. However, differences are apparent in joint moments, and neuromuscular function. It is our aim to associate these differences with non-surgical interventions.
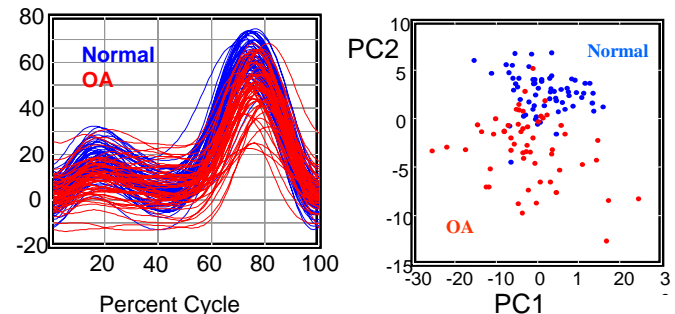

Figure 1. (left) The knee joint flexion angle during one gait cycle. (right) Scatter plot of the first two PCs for these subjects.

DISCUSSION

The analysis and clinical interpretation of gait data is difficult, and multivariate statistical techniques offer promise in identifying underlying biomechanical factors of pathology such as knee OA. This problem is further challenged by the lack of valid, reliable means for measuring the presence and severity of knee OA. This is mainly a symptom-driven disease, and the objective of early intervention is pain management rather than addressing underlying biomechanical factors. It is hoped that longitudinal studies that address these factors may demonstrate that it is possible to slow or stop the progression of the disease by augmenting the biomechanical environment of the knee.

References
1. Astephen,JA. & Deluzio,KJ (In Press) J Eng in Med. 2. Chau,T (2001) Gait Posture. 13:49-66. 3.Chau,T (2001) Gait Posture. 13:102-120. 4.Deluzio,KJ et al. (1999) Hum Mov Sci 18:701-711. 5. Deluzio KJ et al. (1997) Hum Mov Sci 16:201-217.

NEW INSIGHTS INTO OSTEOARTHRITIS USING NOVEL IMAGING MODALTIES, JOINT DYNAMICS, BIOLOGY AND ROBOTICS

J. Ronsky[1], J. Tapper[1], Y. Funakoshi[2], M. Hariu[2], R. Howard[3], L. Marchuk[2], N. Shrive[2, 3], C. Frank[2]

Departments of [1]Mechanical and Manufacturing Engineering, [2] Surgery and [3]Civil Engineering, University of Calgary;

jlronsky@ ucalgary.ca

INTRODUCTION

Dynamic knee instability due to ligament deficiency is a significant clinical problem that has been associated with a high incidence of development of secondary osteoarthritis [1]. The combined role of biological and mechanical factors in the pathogenesis of joint degeneration are not well understood, thus hindering our ability to optimize joint reconstructive surgery aimed at restoring joint integrity. Altered joint kinematics following ligament deficiency have been associated with cartilage degradation. While early degenerative changes have been observed in the superficial cartilage layer[2], the role of surface mechanics in the development of these changes is unknown. Altered surface velocity, an important determinant of the coefficient of friction at the joint and thus joint lubrication, may be a critical factor linking joint instability and joint degeneration. Precise quantification of forces in ligaments and soft tissue structures for intact and ligament deficient joints has been challenging to date. Accurate repeatable representation of in-vivo physiologic loading conditions has remained a major challenge.

The ovine stifle joint is a promising in-vivo model for the investigation of the interactions of mechanical and biological factors in joint injuries, joint degeneration and reconstructive surgery. An integrated approach to investigate these relations was developed incorporating in-vivo kinematics, biological assessment and robotics. This paper describes the key components including: detailed accurate description of joint kinematics in intact and ligament deficient joints, novel segment imaging, assessment of cartilage degeneration, and accurate reproduction of in-vivo kinematics using robotics for evaluation of force distribution in joint tissue structures.

In-vivo kinematics of the ovine stifle joint over 20 weeks following ligament transaction were quantified, and compared to those measured in the intact joint. Corresponding measures of joint degeneration were evaluated. Resulting joint loads and forces in tissue structures were evaluated in-vitro by precisely reproducing in-vivo joint motion using a parallel robot. We hypothesized that ligament transection would alter in vivo joint kinematics, and that gross cartilage degenerative changes would be evident at 20wks after ligament transection. Further, we hypothesized that changes in joint surface velocity after ligament transection may play a role in joint degeneration.

METHODS

Ovine stifle joint model: 8 skeletally mature trained Suffolk sheep were studied while walking at 2mph on a standard treadmill. The in vivo kinematics were measured for 30 strides with the joint intact, and at 2, 4, 8, 12, 16 and 20 weeks following either transection of the anterior cruciate and medial collateral ligaments (n=5) or sham surgery (n=3) [3].

In vivo kinematic measurement: A 4-camera motion analysis system (120Hz) and bone markers in the tibia and femur were used to measure the tibiofemoral joint kinematics. Following euthanization, the marker positions and bone surface geometry were measured within anatomical coordinate systems using a spatial digitizer, and registered with the motion analysis data. The 3D bone surface geometry was reconstructed using surface modeling software.

Analysis of kinematic data: The 3D marker coordinates were tracked and smoothed (quintic spline; cutoff 6Hz). Transformation matrices between global and anatomical coordinate systems were calculated from marker position data. Global position data were differentiated to obtain global marker,and relative bone velocities. For each specimen, the in vivo kinematics (intact, 2, 20 wk) were compared.

Analysis of joint degeneration: At 20 weeks after intervention, the joints were examined and graded for cartilage degeneration and osteophyte formation (modified Drez Score). Osteochondral plugs were taken and histological changes were graded using a modified Little Score. Changes in the transected joints were compared with the contralateral joints (n=5), sham joints (n=3), and age-matched normal joints (n=3) using a Wilcoxin Rank Sum Test (p<0.05).

Joint Force Determination: The bones were repositioned based on in-vivo kinematic data in a parallel robot setup. Resultant joint forces throughout complete stride cycles were measured with a universal force moment sensor. Serial sectioning of ligaments and the meniscus enabled determination of loads in individual structures using the superposition principle.

RESULTS

Altered in-vivo kinematics were consistently observed with ligament transection, particularly in anterior/posterior translations. Degenerative cartilage changes were significantly greater in the ligament transected joints relative to the both the contralateral and sham transected joints. Both the magnitude and direction of the relative surface velocities in the transverse plane of the tibial plateau were significantly changed after ligament transection in all five experimental subjects (p<0.05). The robotic system demonstrates the ability to accurately reproduce in-vivo joint kinematics in-vitro, and measure the resulting joint and specific structure loads.

SUMMARY

Direct relations between altered joint kinematics, loading mechanics and degenerative cartilage changes have been identified with this promising integrated approach. The controlled reproduction of in-vivo kinematics with the parallel robot and force/moment sensor configuration offers promising potential for new insights into underlying mechanisms in OA.

REFERENCES

[1] Marshall JL & Olsson SE: *JBJS* 53(8): 1561-70, 1971. [2] Muir,H. and Carney,S.L. (1986). [3] Tapper JE et al., *J. Biomech. Eng.* 126:301-5, 2004.

ACKNOWLEDGEMENTS

ASSESSMENT AND MANAGEMENT OF OSTEOARTHRITIS OF THE KNEE

W.D. Stanish, MD, FRCS(C), FACS
Professor of Surgery, Dalhousie University
Director, Orthopaedic and Sport Medicine Clinic of Nova Scotia

THE PHILOSOPHY

The Disease

Osteoarthritis is described as a generally progressive loss of articular cartilage, accompanied by attempted repair and remodeling. Notwithstanding the process of aging, hyaline cartilage becomes degenerative basically under two conditions.
(Ref: Felson DT. Epidemiology of Hip and Knee Osteoarthritis. Epidemiology Review, 1988, 10:1-28)

#1 **Hyaline cartilage overload.** In situations of disturbed joint mechanics; e.g., genu varus, hyaline cartilage degeneration can occur depending on the degree of external demand. Articular cartilage possesses a very high tolerance for mechanical loading and can tolerate stresses up to but below 25 N/m^2. Most athletic physical activities, such as running, trigger articular surface stresses in the range of 4-9 N/m^2. With severe single impact loads, insult to the chondrocyte and/or matrix will prompt initial blistering of the joint surface. If the mechanical disturbance is not rectified, then progressive joint surface fissuring, followed by erosion, can occur.
(Ref: Buckwalter JA, Mankin HJ. Articular Cartilage II: Degeneration and osteoarthrosis, repair, regeneration, and transplantation. JBJS 79A: 612-632, 1997)

#2 **Hyaline cartilage underload.** In the clinical situation of forced immobilization and/or underload, an unfavorable circumstance exists for hyaline cartilage. This clinical situation occurs far less frequently than overload but does require the same attention to therapeutic intervention. In the face of a significant injury to the hyaline cartilage, a period of immobilization after such injury may prevent degeneration. Forced motion and loading may be counterproductive in attempting to achieve hyaline cartilage restoration.
(Ref: Williams JM, Brandt KD. Immobilization Ameliorates Chemically Induced Articular Cartilage Damage. Arthritis and Rheumatism, 27: 208-216, 1984. Buckwalter JA. Activity Versus Rest in the Treatment of Bones, Soft Tissue and Joint Injuries. Iowa Orthopaedic Journal, 15: 29-42, 1995.)

The Treatment
A successful treatment program must address and deal effectively with:
#1 Controlling the **PAIN COMPONENT**
(Ref: Brooks PM, Day RO. Non-steroidal Anti-inflammatory Drugs - Differences and Similarities. New England Journal of Medicine, 1991; 324: 1716-1725.)
In most cases of early degenerative joint disease (Grade I/Grade II) it is usually necessary to address the intermittent exacerbations of joint pain. Invariably there is an inflammatory component that when treated successfully, enters into remission. The treatment for the pain can be effective with such simple techniques as activity modification, analgesia and/or physical modalities.

(Ref: Panush RS. Is Running Associated with Degenerative Joint Disease? JAMA 255: 1152-1157, 1986)

#2 Controlling the **MECHANICAL COMPONENT**
Invariably degenerative joint disease within the knee is associated with a disturbed mechanical component. If, in fact, the pain component is not rectified with a simple medication and/or modality, then the introduction of strategies to alter the disturbed mechanics are essential.
(Ref: Articular Cartilage: Composition Structure Response to Injury and Methods of Facilitating Repair. Buckwalter JA, Rosenburg IC, Hunziker EB: Chapter in - Articular Cartilage in Knee Joint Function; Basic Science and Arthroscopy, (ed) J.W. Ewing, Raven Press, New York, 1990, pp 19-56. Fundamentals of Articular Cartilage and Meniscus Biomechanics, Now VC, et al. Articular Cartilage in Knee Joint Function; Basic Science and Arthroscopy; (ed) J.W. Ewing, Raven Press, New York, pp 1-18. Brand RA; Joint Lubrication, (ed) Albright and Brand; The Scientific Basis of Orthopaedics, 2nd ed., Appleton & Lang, 1987, pp 373-386. Biomechanical Gait Analysis of Morbidly Obese Women. El Hawary R, Stanish WD, Kozey J, Kirby RL, McLeod DA, Perey BJ. (unpublished)

INTERVENTIONS TO CONTROL PAIN IN THE DEGENERATIVE KNEE

#1 Local Pain Control

1. Cryotherapy

The intermittent use of ice, particularly on the knee joint, has proven most successful in controlling the exacerbation (inflammatory phase) within the degenerative athletic knee. The simple process of applying a packet of frozen vegetables for a 20/30 minute period can be as effective as the commercially available products that are more refined.
R(Ref: Melzack R, Wall PD. Pain Mechanisms: A New Theory. Science 150, pp 971-979, 1965. Waylonis GW. The Physiological Effects of Ice Massage. Archives Physical Medicine Rehabilitation, 48: 47-52, 1967)

2. Intra and Periarticular Use of Cortisone Injections in the Knee

Although an extremely useful technique, the intermittent use of intra-articular cortisone should be deployed with caution. The potential risks of provoking hyaline cartilage degeneration, the hazards as they relate to joint infections, and the limitations of cortisone should be fully discussed and disclosed with the patient.
(Ref: Postuma P, Stanish WD. The Intra-articular and Periarticular Use of Corticosteroid in Knee and Shoulder. The Clinical Journal of Sport Medicine, Vol. 4, No. 3, pp 155-159, July 1994.)

Recent Concepts

#1 There are few clinical indications for the use of intra-articular steroids in chronicosteoarthritis.

ASSESSMENT AND MANAGEMENT OF OSTEOARTHRITIS OF THE KNEE

W.D. Stanish, MD, FRCS(C), FACS
Professor of Surgery, Dalhousie University
Director, Orthopaedic and Sport Medicine Clinic of Nova Scotia

#2 Theoretically corticosteroids might inhibit cartilage formation and repair: this has been found in animal studies when injected in very high doses.

#3 Osteoarthritis has been recognized to have an inflammatory component since the turn of the 19th century; more recent studies continue to corroborate this fact. As such, intra-articular steroids could in theory slow or halt the disease process. In the dog model of osteoarthritis, intra-articular steroids reduced the severity of cartilage lesions as well as the size and number of osteophytes.

#4 A few blinded controlled trials have demonstrated a statistically significant decrease in subjective pain perception with steroids at one week after injection of Triamcinolone. However, at 4 or more weeks follow-up, differences between control and treatment cases had resolved.

#5 Intra-articular steroids have a role in managing the acute exacerbation of osteoarthritis. They may offer significant short term relief and any concerns regarding detrimental effects in the articular cartilage are academic, particularly in the patient that is nearing total knee arthroplasty.

(Ref: The Intra-articular and Periarticular Use of Corticosteroids in the Knee and Shoulder. Clinical J. of Sports Medicine, 4:155-159, 1994. Dieppe PA, Sathapatayavongs B, Jones HE, et al. Intra-articular steroids in osteoarthritis. Rhomboidal Rehabil 1980; 19(4): 212-7. Doyle DV. Tissue calcification and inflammation in osteoarthritis. J. Pathol 1982: 136(3): 199-216. Friedman DM, Moore ME. The effect of intra-articular steroids in osteoarthritis: a double-blind study. J. Rhomboidal 1980; 7(6): 850-6. Jones AK, al-Janabi MA, Solanki K, et al. In vivo leukocyte migration in arthritis. Arthritis Rheum 1991; 34(3): 270-5. Pelletier JP, Martel-Pelletier J. In vivo protective effects of prophylactic treatment with tiaprofenic acid or intra-articular corticosteroids on osteoarthritic lesions in the experimental dog model. J. Rhomboidal 1991; 18(suppl 27): 127-30)

2.   Electrical Stimulation

The intermittent use of transcutaneous electrical stimulation (TENS) has proven to be a popular modality for the reduction of pain. Acupuncture, acupressure and similar type interventions could be explored. They are uniformly non invasive and thus extremely safe and patient friendly.
(Ref: Stanish WD, Curwin S. Special Techniques in Rehabilitation. In: The Crucial Ligaments. (Ed) JA Feagin, Jr. Churchill Livingstone, New York, Edinburgh, London, Melbourne, pp 773-781, 1988.)

3.   Systemic Pain Control

   i)   Analgesics
   ii)   Non-steroidal Anti-inflammatories

Very frequently the deployment of a simple pain medication can allow the athlete to continue to participate in the face of a degenerative knee. The patients are usually very compliant when it comes to the intermittent use of a medication rather than accepting drugs that must be used over a long period of time; i.e., non-steroidal anti-inflammatories. Currently there is some compelling evidence that suggests that anti-inflammatory medications used over a prolonged period of time function as an anti-metabolite and may, in fact, disturb the normal reparative process.

Non-Steroidal Anti-Inflammatory

#1 The tissue response to injury initiates a cascade consisting of inflammation and hyperalgesia. After a nauseous stimulus, peripheral nerves release prostaglandins, substance P and related peptides.

#2. The resultant prostaglandin mediated inflammatory process is characterized by vaso dilation, in creased vascular permeability, followed by hyperalgesia.

#3. Traditionally the analgesic properties of NSAIDs have been attributed to their effects on the peripheral synthesis of prostaglandins. This would cause a decrease in the inflammatory response to injury, reducing pain perception.

#4. Recent in vivo animal studies suggest that the central response to painful stimuli may be modulated by NSAID inhibition of prostaglandin synthesis.

#5. Therefore it has been suggested that NSAIDs can reduce both acute pain and the subsequent hyperalgesia response via central mechanisms.

(Ref: Non-steroidal Anti-inflammatory Drugs in Sports Medicine; Weiler JM, Albright JP, Buckwalter JA. In: Non-Steroidal Anti-inflammatory Drugs. (Ed) Lewis AJ, Furst DR, New York, Publisher - Marcel Dekker, 1987, pp 71-88. Management of Inflammation of the Knee; Stone J, Zarins B. In:Articular Cartilage in Knee Joint Function; Basic Science in Arthroscopy, (ed) JW Ewing, Raven Press, pp 167-189. Simon LS. Actions in Toxicity of Non-Steroidal Anti-inflammatory Drugs. Curr. Opin. In Rheumatology, 1995, 7: 159-166. Brooks PM, Day RO. Non-Steroidal Anti-inflammatory Drugs - Differences and Similarities. New England Journal of Medicine, 99: 324, pp 1716-1725.) Controversies in the Perioperative Use of Non steroidal Anti-inflammatory Drugs. Souter AJ, Fredman B, White PF. Anesth. Analg, 1994; 79:1178-90.)

VISCOSUPPLEMENTATION IN THE TREATMENT OF OSTEOARTHRITIS
Recent Concepts

#1 Hyaluronan in both articular tissues and synovial fluid plays a critical role in contributing to joint homeostasis and

ASSESSMENT AND MANAGEMENT OF OSTEOARTHRITIS OF THE KNEE

W.D. Stanish, MD, FRCS(C), FACS
Professor of Surgery, Dalhousie University
Director, Orthopaedic and Sport Medicine Clinic of Nova Scotia

maintaining normal function. It has been recognized for many years that in osteoarthritis the molecular weight and concentration of hyaluronan is diminished.

#2 Recognition that there is altered synthesis of hyaluronan by synovial sites in osteoarthritis, led to the concept of viscosupplementation.

#3 Viscosupplementation was first used to treat post traumatic osteoarthritis in race horses in the early 1970's. It has been used to treat human osteoarthritis in some countries since 1987.

#4 Most studies of viscosupplementation with hyaluronan have shown them to be better than placebo and as affective as non-steroidal anti-inflammatories in the treatment of osteoarthritis.

#5 There are two classes of hyaluronan based products currently available for clinical use. Low molecular weight hyaluronan (0.5 - 1.2 MW) and hylan molecular weight. In general, the higher the molecular weight of hyaluronan product, the longer it resides in the joint.

#6 Recent controlled randomized clinical trials confirm that five weekly intra-articular injections of hyaluronan in patients with osteoarthritis are generally well tolerated, provide sustained relief of pain and improved patient function, and were as at least as effective with fewer adverse reactions as continuous treatment with Naproxen for 26 weeks.

#7 There is accumulating evidence from animal models of osteoarthritis that hyaluronan based therapy may be chondro protective.

(Ref: Marshall, KW. Viscosupplementation for Osteoarthritis: "Current Status, Unresolved issues and Future Directions". Viscosupplementation: A new concept in the treatment of arthritis; J. of Rheumatology 1993; Supp. 39, pgs. 3-9. Marshall, KW. The Current Status of Hyalan Therapy for the Treatment of Osteoarthritis; Today's Therapeutic Trends, 1997; 15: 99-108. Lussier, A, et al. Viscosupplementation with Hyalan for the Treatment of Osteoarthritis: Findings from clinical practice in Canada; J. of Rheumatology, 1996; 23: 1579-1585. Altman, RD et al. Intra-articular Sodium Hyaluronate in the Treatment of Patients with Osteoarthritis of the Knee: A randomized clinical trial. J. of Rheumatology, 1998; 25: 11, pgs. 2203-2212. Smith, MM; Ghosh, P. The Synthesis of Hyaluronic Acid by Human Synovial Fibroblasts is Influenced by the Nature of Hyaluronate in the Extra Cellular Environment. Rheumatological J. International, 1987; 7:pg. 113-122. Ghosh, P. The Role of Hyaluronic Acid in Health and Disease: Interactions with cells, cartilage and components of the synovial fluid. Clinics in Experimental Rheumatology; 1994; 12: pg. 75-82.)

INTERVENTIONS TO CONTROL MECHANICAL OVERLOAD IN THE DEGENERATIVE KNEE

#1 Reduction in Body Weight

Ongoing research suggests a significant reduction in joint reaction force with the reduction in body weight. This is particularly true if, in fact, the athlete suffers with disturbed joint mechanics; i.e., genu varus.

(Ref: Biomechanical Gait Analysis of Morbidly Obese Women, El Hawary R, Stanish WD, Kozey J, Kirby RL, McLeod DA, Perey BJ. Proceedings of the Canadian Academy of Sports Medicine, Vancouver, 1997. Newton PM et al. The Effect of Life Long Exercise on Canine Articular Cartilage. Am. J. Sports Medicine, 25: 282-287, 1997. Felson DT, et al. Weight Loss Reduces the Risk for Symptomatic Knee Osteoarthrosis in Women. The Framingham Study; Annals of Internal Medicine; 116(7), pp 535-539, 1992.)

#2 Activity and Footwear Modification

(Ref: Cooper C et al. Mechanical and Constitutional Risk Factors for Symptomatic Knee Osteoarthritis: Differences Between Medial, Tibial, Femoral and Patello-Femoral Disease. J. of Rheumatology, 21: 307-313, 1994. Buckwalter JA, Lane NE. Athletics and Osteoarthritis. AJSM 25(6), 1997, pp 873-881.)

#3 Knee Bracing

The unloader brace has proven to be most popular and readily accepted by patients. The science may be soft, however ongoing research provides convincing evidence of the ability to normalize joint mechanics with the use of knee and foot orthoses.

(Ref: Application of a Lateral Heel Wedge as a Non Surgical Treatment for Varus Gonarthrosis; Giffin JR, Stanish WD, MacKinnon S, MacLeod DA, J. of Prosthetics and Orthotics, Vol. 7, No. 1, Winter/1995. Effective Axial Alignment of the Lower Extremity on Articular Cartilage of the Knee; Coventry M. In: Articular Cartilage and Knee Joint Function, Basic Science in Arthroscopy; (ed) JW and Raven Press, pp 311-317. Valgus Knee Bracing for Medial Conarthrosis; Horlick SJ, Loomar RL. Clinical Journal of Sports Medicine, 1993, pp 251-255. Use of Lateral Heel Wedges in the Treatment of Medical Osteoarthritis of the Knee; Keating EM, et al. Orthopaedic Review, 1993, 12: 921-924. Functional Knee Braces and Dynamic Performance: A Review. Kramer JF, et al. Clinical Journal of Sports Medicine; 7: 32-39, 1997.)

CONCLUSIONS

Osteoarthritis of any joint is a degenerative disorder with disturbance of the joint surface. It can ordinarily be controlled with a program designed to mediate the issue of pain, followed by mechanical unloading.

Surgical intervention is reserved as a very last resort.

PREDICTION OF BACK STRENGTH USING ANTHROPOMETRIC AND STRENGTH MEASUREMENTS IN HEALTHY FEMALES

Mei Wang[1], A. Leger[2], G.A. Dumas[3]

[1]Department of Mechanical Engineering, Queen's University, Kingston, Ontario, Canada, mwang55@uwo.ca
[2]School of Rehabilitation Therapy, Queen's University, Kingston, Ontario, Canada, al7@post.queensu.ca
[3]Department of Mechanical Engineering, Queen's University, Kingston, Ontario, Canada, dumas@me.queensu.ca

INTRODUCTION

Back extension strength is an important parameter for low back pain studies. However, the measurement of back muscle strength is problematic in certain populations like low back pain patients and pregnant women. The purpose of the current study is to develop a regression equation to predict back extensor muscle maximal voluntary contraction (MVC) based on several anthropometric measurements using the multiple regression technique. As this study is part of a larger project on pregnancy, one of the criteria for choosing the independent variables was that they should not change much due to pregnancy. As such, the equations developed in this study can be applied both to general female low back pain and pregnancy populations.

METHODS

One hundred and six non-pregnant female subjects, age 18 to 42 and with no history of back pain in the past year, were recruited. Height, Fat Free Mass, Chest Depth, Trunk Length, Shoulder Circumference, Arm Circumference, Mass, Age, Quadriceps Strength (QMVC) and Grip Strength (MaxGrip) were the factors chosen to develop the prediction equation. The testing protocol included four parts: anthropometric measurements, back extensor muscle strength, quadriceps muscle strength and grip strength measurements.

The back muscle strength was measured in the ITEC (Isometric Trunk Ergonomic Chair) (Frigault, 2003). The force signals were measured with two parallel force transducers. The back MVC was measured as both force (N) and moment at L4/L5 (Nm).

The Pearson product-moment correlation coefficients (r) between each factors were calculated. The backwards stepwise analysis was performed to choose the best fit variables for both moment and force models. Further backwards stepwise analyses were performed to develop simplified models for application convenience purpose. The predictive ability of the models was checked using the cross-validation technique on 20 subjects not used for the models. The back strength was predicted for the validation group using the developed models and the predicted values were then compared with the actual ones using correlations and paired-samples t-test. All the statistical analyses were performed using SPSS statistical package.

RESULTS AND DISCUSSION

Four models were developed:

Moment at L4/L5 (Nm)=-5.914-89.07*Height(m) + 489.7 * TrunkL(m)+0.136*MaxGrip (N)+0.07958*QMCV(N); R^2=46.9

Back Strength (N)=895.49-522.36 * Height (m) + 3.212 * Mass(kg)+0.556*MaxGrip (N)+0.585*QMVC (N);R^2=48.2

Simplified Models:

Moment at L4/L5 (Nm)=-111.758+0.105*QMVC (N) + 452.2 * TrunkL (m); R^2=40.4

Back Strength (N)=292.539+0.78*QMVC (N); R^2=39.1

The models developed in our study explained more variance of the back strength than the models in the literature. No multicollinearity problem was found in our models. The validation study showed that the observed MVC was highly correlated with the predicted one, r=0.706-0.826. Paired-samples t-test showed that the mean differences between them were not significantly different from zero.

SUMMARY

In conclusion, mass, height, trunk length, grip strength and quadriceps strength are the best predictors for back extensor strength in this study. Both R^2 and the validation study show that the models developed in this study can give us a good prediction of back extensor MVC. The models can be used for a general female population in the age range of 18 to 42 years old including low back pain patients and the pregnancy population.

REFERENCE

Frigault R., Dumas G.A., Leger A., "Development Of Testing Equipment And Protocol For Trunk Extensor Fatigability" *Proceedings of 2003 ISB* , NZ, p. 113.

Table 1: Validation results: Correlation between predicted and measured variables and paired t-test of difference

Model	Correlation (r)	p(Correlation)	95% Confidence Interval of the difference		p (2-tailed t-test on difference))
			Lower	Upper	
Moment	.711	.000	-7.2726	16.9912	.412
Force	.765	.000	-48.5722	53.4832	.921
Simplified model for moment	.706	.001	-8.85	15.94	.556
Simplified model for force	.826	.000	-57.348	42.8099	.765

THE EFFECT OF ROD HEIGHTS AND FEET POSITIONS WHEN LIFTING ITH RODS

André Plamondon[1], Alain Delisle[1], Karin Trimble[2] and Pierre Desjardins[1,3]
[1] Institut de recherche Robert Sauvé en santé et en sécurité du travail (IRSST), Québec, Canada
[2] School of Human Kinetics, Laurentian University, Sudbury, Ontario, Canada
[3] Centre de recherche interdisciplinaire en réadaptation du Montréal métropolitain,
site Institut de réadaptation de Montréal, Montréal, Québec, Canada
Email : plamondon.andre@irsst.qc.ca

INTRODUCTION

It is well recognized that manual material handling accounts for a large proportion of back injuries. To date, the majority of studies have focussed on the lifting of rectangular shaped objects. However, there is a paucity of studies focusing on the lifting of rods or long awkward heavy objects. In-The-Hole (ITH) drilling is a heavy repetitive mining task, which has been identified as having a relatively high incidence and severity rate of low back injuries.

PURPOSE

The purpose of the study was to examine how the low back load experienced by ITH operators changed when lifting a vertical drilling rod (1.61 m, 35 kg) using four different feet positions and two rod heights. In addition, a symmetrical lift with a lifting index (LI) of 1 also served as a comparison to determine possible risk of low back injury.

METHOD

Eleven experienced ITH operators participated in the study but 2 were excluded for technical problems. All subjects had no history of serious back injury or any recent discomfort. Each subject was required to lift a vertical drilling rod until the upper body was in an erect posture using four different feet positions (0° = subject facing the rod, 45° = subject oblique to the rod, 90° = subject right side to the rod; and freestyle). In addition two rod height conditions were studied where the base of the vertical rod was supported either (1) at the ground level (height of rod CG = 0.83 m) or (2) on a rack of 20 cm (height of rod CG = 1.03 m). All lifts were performed toward the right side of the subject and in a randomized order. Finally, each subject lifted a box of 21.5 kg in the sagittal plane which corresponded to a LI of 1 in the NIOSH lifting equation (Waters et al., 1993). A LI of 1 indicates that the weight of the load lifted corresponds to the recommended weight limit that will be acceptable for 75% of female workers and 90% of male workers. Reflective markers were placed on the subjects and three video cameras were used to record their displacement. Ground reaction forces at the feet were measured with a force plate (Kistler, type 9281B, Winterthur, Switzerland). At last, two surface electrodes were applied on the right and the left erector spinae (ES) at the level of L3

A dynamic 3-D lower body model was used to estimate the net reaction moment at L5/S1. Detail of the model is described in Plamondon et al. (1996). This model included seven segments (feet, shanks, thighs and pelvis). The L5/S1 moments were expressed relative to an anatomical coordinate system axes of the trunk..

RESULTS

Lifting from a rack reduced the resultant moment (resultant of the 3 moments about L5/S1) from 268 Nm at the ground level to 223 Nm. This result is consistent with the EMG results for the left (ES_L) and right (ES_R) erector spinae where the EMG_{PEAK} was always smaller with the use of a rack compared to the ground level (Trimble et al.,2003).

Most of the subjects adopted either the 0° feet position or a position where the right foot was at 0° and the left foot at 45° as the freestyle. Figure 1 shows the resultant peak moment found for the different conditions. There were no significant difference on the resultant moment at L5/S1 between the different feet positions The magnitude ranged between 211 Nm (0° face-rack) and 278 Nm (90° side- no rack). However, the EMG of ES_L revealed that the 90° feet position resulted in higher EMG_{PEAK} than the freestyle and 0° position from the ground (Trimble et al., 2003). Surprisingly, the resultant peak moment for the NIOSH lift was equivalent to those experienced during the rod lifting from the rack (NIOSH = 232 Nm; rod lifting = 223 Nm). However, the asymmetrical moment (resultant of longitudinal and sagittal moments) was very low in the NIOSH compared to the ITH lifting.
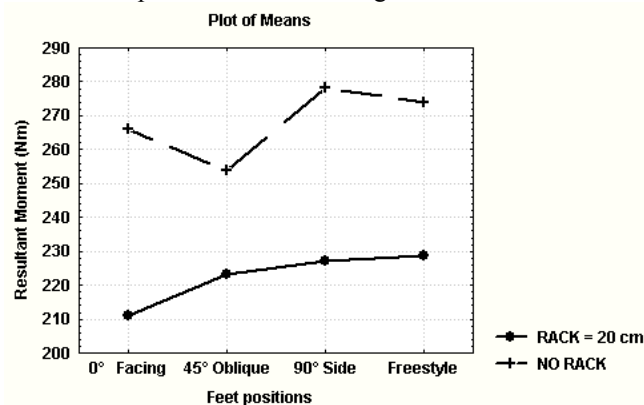

Figure 1. Resultant moment when lifting rod from the ground or the rack and from four feet positions.

DISCUSSION AND CONCLUSION

Vertical height had a significant effect on the resultant moment and EMG_{PEAK}. Lower was the vertical position of the rod at the start of the lifting, higher was the load on the back. This is in agreement with Lavender et al (2003) who found that the peak moments were significantly greater when lifting from lower height. The resultant peak moment did not change significantly with the different feet positions although 90° feet position (without the rack) was higher for both the resultant moment and EMG_{PEAK}. Moreover, the peak moment for the NIOSH lifting was equivalent to the rod lifting with the rack. These results suggest that the use of a rack is an important element to reduce the load of the back during ITH operations. However, these preliminary results need to be confirmed. Research in this area will help to better understand the load on the back during complex 3D tasks leading to better workplace lifting recommendations

REFERENCES

Lavender et al (2003). *Int.J.Ind.Ergo*. **31,** 51-59.
Plamondon et al (1996). *Clin. Biomec*. **11**,101-110.
Trimble,K et al (2003). ISB 2003, New-Zealand.
Waters, T. R. et al (1993). *Ergonomics* **36**, 749-976.

THE LUMBAR RESPONSES OF SITING ON A STABILITY BALL AND IN AN OFFICE CHAIR

Diane Gregory, Natasa Kavcic, Nadine Dunk, Stuart McGill, Jack Callaghan
University of Waterloo, Waterloo, Ontario. dgregory@uwaterloo.ca

INTRODUCTION

Low back pain (LBP) is a predominate disorder in the office workplace. This has lead to interest in seeking alternatives to the traditional office chair, one of these being the stability ball. Sitting on a stability ball has been claimed by various fitness supply companies to increase trunk muscular activity and thus reduce low back pain. The lack of quantitative support for the use of stability balls as office chairs, led us to examine the biological response to sitting on a stability ball for a prolonged period of time compared to in an office chair.

METHODS

Several layers of investigation were conducted: muscle activation and lumbar spine/pelvis kinematics; lumbar kinetics while sitting; and seat pressure distribution analysis. Individuals from a university population were involved in all investigations.   In the muscular and lumbar kinematic investigation, muscle activation of eight trunk muscles was measured using surface electromyography, and lumbar spine posture was measured using an ISOTRAK 3-Space system. Both musculature and postural responses were measured while individuals performed various computer workstations based tasks while sitting on a stability ball for one hour, and an office chair for one hour. Ratings of perceived discomfort were also recorded throughout the collection period using a 100mm visual analog scale.   The kinetic investigation examined the stability index as well as compression at L4/L5 using an EMG driven model while individuals sat on a stability ball for 30 min. and a wooden stool for 30 min. Lastly, a pressure distribution analysis was conducted while individuals sat on a stability ball and an office chair for short durations (5 sec).

RESULTS AND DISCUSSION

The average muscle activation for the trunk muscles examined did not differ between sitting on a stability ball and sitting in an office chair, except for the left thoracic erector spinae which was significantly higher while on the ball (2.06 %MVC) compared to the chair (1.36 %MVC). In addition, co-contraction of the trunk flexor and extensor muscles did not differ between the sitting conditions.   The only postural difference observed between sitting conditions was increased posterior pelvic tilt relative to upright standing while on the chair (23.3°) versus on the ball (18.3°). Given that lumbar spinal posture did not differ between sitting conditions (neither average lumbar flexion nor range of lumbar flexion), increased hip flexion while sitting on the ball may have been responsible for the decreased pelvic tilt observed.   Perceived discomfort was found to be significantly greater after the one-hour sitting period on the stability ball versus the chair (figure 1).

The kinetic investigation revealed no significant differences in stability or compression at L4/L5 between the stability ball and the stool. Although the total contact force measured while seated on a stability ball and on an office chair did not differ, the pressure distribution analysis revealed a greater contact area of the seat-user interface while on the stability ball compared to on the office chair (figure 1). Increased contact area may be a potential cause of discomfort due to increased soft tissue compression while on the stability ball. This notion corresponds to the finding of higher perceived discomfort after prolonged sitting on the stability ball.
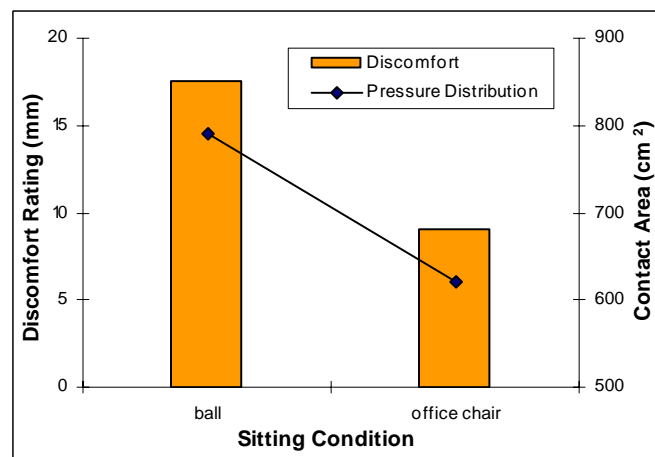

Figure 1. Comparison of rating of perceived discomfort and pressure distribution on stability ball and office chair.

SUMMARY

Based on the findings of this study, sitting on a stability ball does not greatly alter trunk muscle activation or lumbar spinal posture compared to sitting in an office chair. In addition, the stability index and the magnitude of compression at L4/L5 while sitting on a stability ball do not differ from that on a wooden stool.   However, it appears that the increased discomfort observed while on the stability ball may be due to the increased contact area observed during the pressure distribution analysis and potentially alteration in pelvic.

In conclusion, there do not seem to be any advantages to sitting on a stability ball for prolonged periods of time. However, the increased discomfort while sitting on the ball as well as possible safety issues question its use as an alternative to the traditional office chair.

ACKNOWLEDGMENTS

EFFECTS OF TRUNK MUSCLE FATIGUE AND LOAD TIMING ON SPINE MECHANICS DURING SUDDEN HAND LOADING

Diane E. Grondin, Jim R. Potvin

Department of Kinesiology, University of Windsor, Windsor, Ontario   jpotvin@uwindsor.ca

INTRODUCTION

To understand the control of spine mechanics during fatigue and sudden loading, it is important to consider the spine from a stability perspective by testing the agonist and antagonist muscles.   However, previous research looking at fatigue during sudden loading has mainly focused on back extensor fatigue (Allison & Henry, 2002; Granata et al., 2001; Parcero, 2000).   Consequently, this research has been unable to determine how the system responds when the abdominal muscles are also fatigued. The purpose of this study was to investigate the control of spine mechanics in the presence of back and abdominal muscle fatigue during sudden hand loading, with a primary focus on spinal stability.

METHODS

Fifteen females received a sudden load into a box held in the hands, at either a time that was known (T_K) and at a random time within a 10 second window (T_R). Participants received these loading trials while rested (F_0), with back extensor muscle fatigue (F_E), and with a combination of trunk extensor and flexor muscle fatigue (F_{EF}). Measures were taken of trunk angle, center of pressure (CoP) and the average surface EMG amplitudes for the thoracic and lumbar erector spinae (TES and LES), the external oblique (EO) and internal oblique (IO). trunk muscles (TES, LES, EO and IO), and on the Trunk Angle and CoP. Each dependent measure was made during the Baseline period (250-300 ms before loading), Pre loading period (0-15 ms before loading) as well as the peak response to loading (Figure 1). A 3 X 2 (3 fatigue levels, 2 timing conditions) ANOVA was performed with repeated measures.
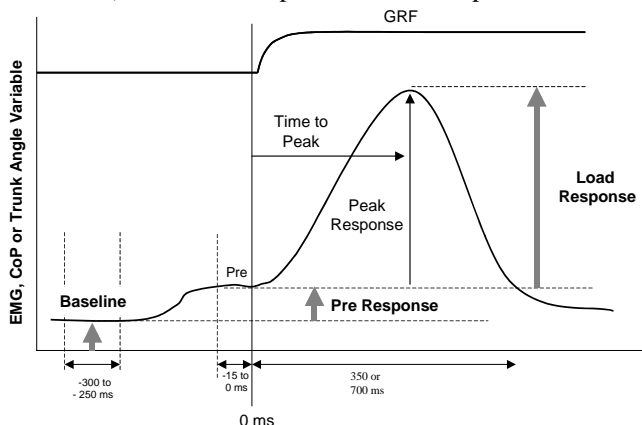

Figure 1: Hypothetical graph indicating the different stages of the loading trials and the determination of the dependent variables.

RESULTS AND DISCUSSION

Baseline: There was a significant effect fatigue on the baseline measures of all four EMG channels. For the TES, there was a progressive increase in amplitude from F_0 to F_E to F_{EF}. For the LES, EO and IO, this trend existed but only the F_O and F_{EF} were significantly different. (Figure 2)

Pre Loading: There were no statistically significant effects that would be deemed to be functionally relevant

Peak Response: There was a significant increase in EMG amplitude for the two trunk extensor muscles monitored (TES and LES) as the load timing became more uncertain ($T_R > T_K$).
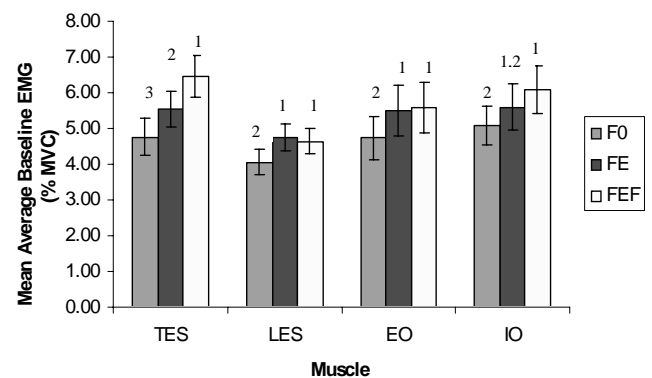

Figure 2: Main effects of fatigue for each muscle during the Baseline phase (n=15 for each). Standard error bars are presented. Bars with the same number are not significantly different.

Because the Peak Responses following the perturbation were enhanced in the random timing condition, preparations must have taken place prior to the anticipated perturbations, perhaps in other segments of the body that were not measured. Also, the load impact may not have been great enough to elicit large preparations. The heightened Baseline activity with fatigue suggests that there may have been a perceived need for higher spinal stiffness whenever the spine was fatigued, and not just in preparation for an impending perturbation. The increased activation of opposing muscle groups is evidence of cocontraction during fatigue and supports the concept of heightened spinal stability.

REFERENCES

Allison, G. & Henry, S. (2002) *Clin Biomech*, 17, 414-417
Granata, K., et al. (2001) *JEK*, 11, 247-254
Parcero, B., Potivn, J. (2001) *Proc Int. Soc. Biomech.*, Zurich, Switzerland

PROOF OF PRINICPLE FOR A PERSONAL LIFTING ASSIST DEVICE

Mohammad Abdoli E[1]*, Amin Kamalzadeh[2], Joan Stevenson[1], Michael Agnew[1]
[1]Biomechanics and Ergonomics Lab, 148 PEC, Queen's University, Kingston, Canada *0ema@qlink.queensu.ca
[2]Robotics Lab, Mechanical Engineering Dept, Queen's University, Kingston, Canada

INTRODUCTION

A new personal lift augment device (PLAD) was developed that can be worn by workers, thus allowing them to gain additional elastic energy for lifts that fall within their perceived capacity. Unlike back belts, this device acts parallel to the back muscles and can be thought of as an external force generator that provides additional elastic energy for lifting tasks, thus allowing the user to accomplish a lift using less of his/her own muscle force. These internal forces are transferred by the PLAD to the shoulders, pelvis and lower legs. The purpose of this paper is to describe the mechanical effect of the on-body PLAD in 3D lifting and evaluate how much of the back moments and forces are transferred to the PLAD during different types of lifts.

METHODS

Acquisition Systems. Three systems of data acquisitions were needed for this project. Three Fastraks® were synchronized into one computer in order to provide 12 electromagnetic sensors with 6 dof. Each Fastrak® was calibrated for signal distortion using a custom calibration jig throughout a 1.5*1.5*2m working envelope. Using Labview 6.1 program, simultaneous data acquisition at 30 Hz was collected using a single record transmission approach in a continuous loop with only a single event marker running in parallel. A 10 sec. sample was used to collect the down and up phases of the lifts. On a slave computer, sampling at 1000 Hz, six custom strain gauges were recorded using an A-Tech amplifier with all data synchronized with hand switch.

Data Collection. For validation, 10 male subjects with no history of back pain wee recruited. Then, Fastrak® sensors were positioned at the centre of gravity of the hands, forearms, arms, thighs, as well as the head, C7, T9 and L5. For both the PLAD and no PLAD conditions, subjects executed various lifts from floor to waist height under a variety of conditions (symmetric/ asymmetric; light/medium/heavy; freestyle/stoop/squat). Feedback questionnaires were also given.

Data Processing. The Fastrak® data were filtered at 6 Hz with a double pass Butterworth filter at 6 Hz and used to compute angular orientations of the body segments using the projection angle method. A 5 point numerical differentiation method that uses the best fit fourth order polynomial was used to obtain angular velocities and accelerations. These were combined with segmental inertial properties (Winter, 1990) to calculate joint angles, velocities and accelerations. A link segment model was constructed in Visual Nastran 4D (Abdoli et al 2004) whereby the L4/L5 moments, compressive and shear forces were calculated and represented. For PLAD conditions, the force contributions of the elastic elements were subtracted from the total L4/L5 moments so that the reduced contribution required due to the PLAD could be calculated.

RESULTS AND DISCUSSION

Preliminary evidence shows that the on-body PLAD does reduce the L4/L5 moments, shear and compressive forces in 3D (Figure 1). It is hypothesized that injured workers could be returned to their jobs more quickly if a safe, effective and user-accepted ergonomic aid was developed for manual materials handling tasks such as lifting, holding or carrying tasks.
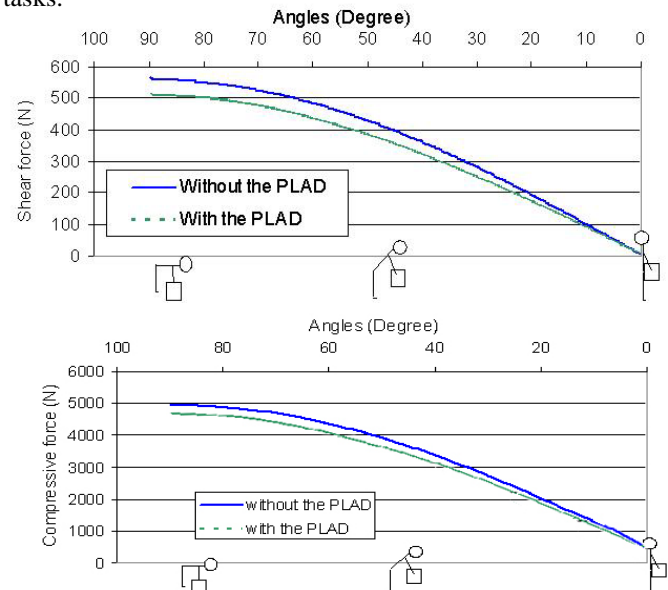

Figure 1 Shear and Compressive forces exerted on the L4/L5 disc of a subject lifting a 10 kg object with and without PLAD

SUMMARY

The development of a safe, effective and user-accepted personal lift augmentation device (PLAD) has the potential for very high impact on the way in which LBDs are controlled and treated. PLAD can reduce the Shear and compressive forces about 5-20%.

REFERENCES

Abdoli ME, Agnew MJ, Stevenson JM (2004) Integration Of Electromagnetic Tracking Systems And Virtual Reality Simulation For 3-D Dynamic Analyses Of Spinal Loading. CD Proceedings of the Eighth International Symposium on the 3-D Analysis of Human Movement, Tampa, Florida. pgs 1-2.

Winter DA. (1990). Biomechanics and Motor Control of Human Movement. Second Edition, John Wiley & Sons Inc

EFFECTS OF PLATFORM MOTION ON THORACO-LUMBAR KINEMATICS DURING LIFTING EXERTIONS

Scott N. MacKinnon, Michael Holmes and David Behm

School of Human Kinetics and Recreation, Memorial University of Newfoundland, St. John's, Canada, smackinn@mun.ca

INTRODUCTION

The harsh climatic conditions of the North Atlantic pose critical problems in day-to-day operations. These add to the challenges operators face when attempting to derive best work practices that improve productivity and reduce risk of accident and operator injury. It can be argued that there is a direct relationship between working in unstable environments and the incidence of injury. Li (2002) reported that between the years 1989-98, 46.2% and 19.8% of the accidents or deaths of seafarers worldwide were caused by slips/ falls and manual materials handling (MMH) respectively. Acknowledging the economic importance of maritime industries, it becomes paramount that the risks be identified and mediated.

Traditionally, MMH activities are studied under stable platform conditions. However, vessels in maritime environments are far from stable and furthermore, often expose the operator to awkward, unexpected perturbations. While there has been limited biomechanical investigations of low back stresses in seagoing occupations (Kingma et al, 2003; Törner et al, 1994), these studies support the notion that motion environments increase the risk of injury or accident but fail to elucidate what platform motion or subject-related characteristics are responsible for these increased risks.

METHODS

Nine healthy male subjects provided informed consent to participate in the study. A Lumbar Motion Monitor (LMM) was employed to assess the displacement, velocity and acceleration time-series data for side bending, flexion/extension and rotation of the spine (Marras *et al.*, 1992) while the subject performed two-handed lifting tasks. The experimental conditions include lifting two loads, each with a mass of 11.4Kg, except one load was solid and the other was liquid in a ½ full container. These were lifted through a vertical displacement of 750mm commencing at a height of 230mm from the floor. The horizontal displacement was standardized to 330mm from the front edge of the feet.

A motion base was employed to simulate a motion in 4 metre seas, with random wave period of 5-10 seconds. Data were collected while the subject was orientated at 0 (i.e. pure pitch motion), 45 and 90 (i.e. pure roll motion) degrees to the long axis of the simulator. A no motion condition was collected to provide a baseline comparison. In total there were eight conditions (2 loads X 4 motions).

RESULTS AND DISCUSSION

A repeated measures ANOVA was employed to assess trunk motions across the experimental conditions. Each plane of motion was considered separately. No significant differences in sagittal plane motions were observed. With respect to maximum side bending velocities, the no motion conditions were significantly different to the motion conditions for both loads ($p < 0.05$). Maximum twisting velocities showed similar trends as the side bending motions, except for the no motion/stable load and the 0° orientation, where no differences were noted ($p < 0.05$). Figure 1 reports the maximum angular velocities for these conditions.
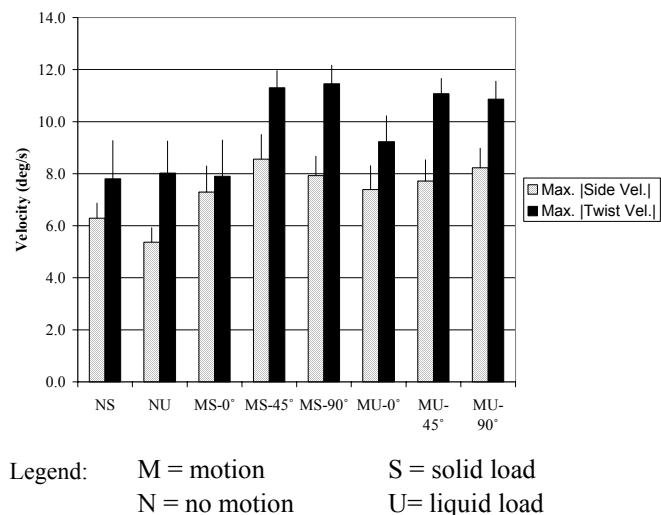

Legend: M = motion S = solid load
         N = no motion U= liquid load

Figure 1: Maximum (+s.e.m.) side and twisting velocities across conditions.

While the magnitudes of the motions were not large, there were consistent trends due to the motion state and orientation of the subjects. These data are critical for developing seakeeping criteria. While these trunk motions do not seem to put the subject at risk for over-exertion injuries (Marras et al. 1995), future studies must consider electromyographic recordings of muscles involved in trunk core stability.

REFERENCES

Kingma, I. et al. (2003). Int. J. Ind. Erg., 32,51-63.
Li, K.X. (2002). Proc. of AME Conference, Nov. 13-15th.
Marras, W. S. et al. (1992). Int. J. Ind. Erg., 9(1), 75-87.
Marras, W. et al. (1995). Ergonomics, 38(2), 377-410.
Törner, M. et al. (1994). Ergonomics, 37(2),345-362.

ACKNOWLEDGEMENTS

COMPARISON OF MOMENT POWERS PRODUCED DURING FORWARD AND BACKWARD STAIR DESCENT

François D. Beaulieu,[1,3] Pelland, L.[1,2,4] and D. Gordon E. Robertson[1,5]

[1]School of Human Kinetics, [2]School of Rehabilitation Sciences, University of Ottawa, Ottawa, Canada
[3]fdbeauli@uottawa.ca, [4]lpelland@uottawa.ca, [5]dger@uottawa.ca

INTRODUCTION

The purpose of this project was to investigate the mechanics of descending stairs in the forwards and backwards directions. The idea behind this project was to determine whether descending stairs backwards was safer and easier than descending in the usual forwards direction. With backwards descent a fall tends to be less injurious because the fall is towards the stairs rather than down the stairs but does it require greater effort?

METHODS

Ten subjects (4 females, 6 males) participated in the study. They first descended stairs five times facing backwards and then five times facing forwards but at the same pace as backwards. The stairs (20 cm rise, 30 cm tread) were equipped with Kistler force platforms on the second last step and on the landing. A digital camera filmed one side of the subject at 60 fps while stair forces were collected at 200 Hz. Sagittal planar, inverse dynamics was applied to obtain the forces and moments of force at the ankle, knee and hip joints (Winter 1991). Moment powers were computed from the products of the joint angular velocities and the moments of force: $P_j = M_j . \omega_j$. Each subject's moments and powers were body mass normalized and ensemble averaged to create a grand ensemble (GE). Only the data from the second last step will be presented.

RESULTS AND DISCUSSION

The moments and powers for forward stair descent were similar to those reported by McFadyen and Winter (1988). Figure 1 shows the grand ensemble averages (n =10 subj. × 5 trials) for the ankle moments and powers of backwards stair descent. Label TO indicates toe-off and the start of swing phase. There was no initial dorsiflexor power phase as occurs with level walking, instead a large plantar flexor eccentric phase (A0) occurred for both forwards and backwards descent. Backwards descent had a statistically higher peak power (A0) than did forward descent. Second, immediately after A0 a concentric plantar flexor burst occurred that was not present for forward descent but there was reduced eccentric work (A1) by the plantar flexors as compared to forwards descent or level walking. Thirdly, A2 was considerably reduced compared to level walking and forwards descent. In particular, less concentric work (A2) was necessary for backward stair descent presumably because of the reduced demand to clear the edge of the step.

Figure 2 shows similar curves for the knee moments and powers. The knee concentric extensor burst, K2, was larger compared to forward descent. But, the major significant difference (P<0.003), compared with forward descent, was the reduction of the eccentric power of the extensors prior to toe-off (K3). This difference could be significant for people with disabilities because of the heavy loading that must occur to the patellar tendon. Another important difference between the two descents was the location of the centers of pressure of the ground reaction forces. For forward descent, they tended to be close to the edge of the step but for backwards descent they were consistently farther from the edge (P<0.001). Thus, the chance of slipping over the step edge was reduced when backing down the steps.
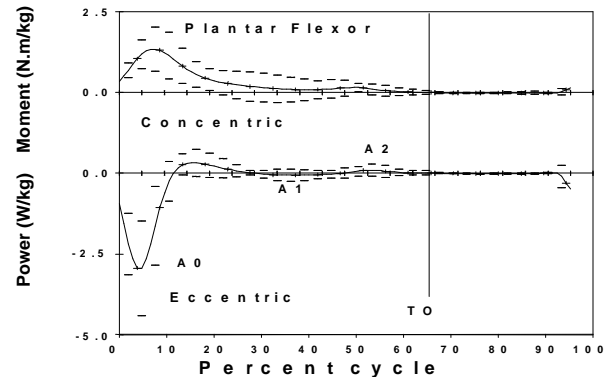

Figure 1. Ensemble averages ±95th% confidence intervals of the ankle moment and powers of backward stair descent.

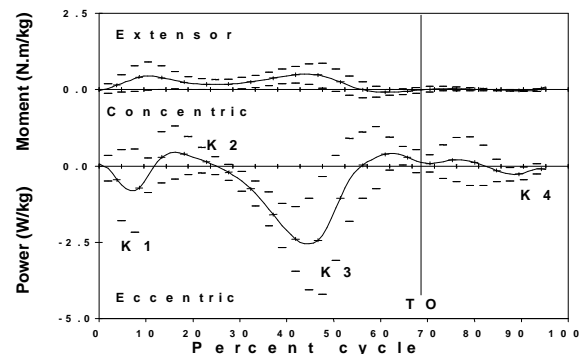**Figure 2.** Ensemble averages ±95th% confidence intervals of the knee moment and powers of backward stair descent

SUMMARY

Forwards and backwards stair descent require higher levels of joint kinetics than walking but backward descent demanded less peak knee moment and eccentric power than forward descent. In the backwards descent the foot positioning was more posterior to the edge of the step reducing the chance of slipping.

REFERENCES

McFadyen BJ & Winter DA (1988) An integrated biomechanical analysis of normal stair ascent and descent, *J Biomech*, 21:733-41.
Winter DA (1991) *The Biomechanics & Motor Control of Human Gait.* 2nd ed. Waterloo: Waterloo Biomechanics

ACKNOWLEDGEMENTS

THREE-DIMENSIONAL KINEMATIC AND KINETIC ANALYSIS OF ACTIVITIES OF DAILY LIVING IN INDIA

Andrea Hemmerich[1], Heather Brown[1], Amanda Knutson[1], SSK Marthandam[2], Urs Wyss[1]
[1]Department of Mechanical and Materials Engineering, Queen's University, Kingston, ON, Canada, hemmerich@me.queensu.ca
[2]Sri Ramachandra Medical College and Hospital, Chennai, India

INTRODUCTION

Orthopaedic devices, such as hip and knee replacements, have generally been designed to accommodate the range of motion (ROM) required for activities common in Western cultures, including walking, stair climbing, and rising from a chair (Mulholland and Wyss, 2001). Accepted treatment of severe bone afflictions, such as OA, is often rejected by people in non-Western cultures upon discovery that the range of flexion following treatment would not accommodate activities such as squatting, kneeling, and sitting cross-legged (Villar et al., 1988). Furthermore, little is known about the forces and moments that a device would be required to withstand at these extreme ranges of motion. The purpose of this study is to collect kinematic and kinetic data at the hip, knee, and ankle joints during squatting, kneeling, and cross-legged sitting activities from subjects in India.

METHODS

Thirteen elderly subjects (9 male, 4 female) were recruited for this study in Chennai, India. The average subject age was 56.2 years (SD 8.6), average height was 156.0 cm (SD 9.0), and average weight was 54.5 kg (SD 7.3). Each subject was asked to perform 6 trials of each of the following activities that they carried out on a regular basis: squatting with heels up (i.e. balanced on flexed toes), squatting with heels on the ground (i.e. foot flat), kneeling with ankles dorsi-flexed, kneeling with ankles plantar-flexed, and sitting cross-legged. Kinematic data was collected using the Fastrak[TM] by Polhemus with four sensors placed at the foot, shank, thigh, and sacrum. A non-magnetic force plate (AMTI) was used to simultaneously collect ground reaction forces during each trial. From the synchronized data, an inverse dynamics approach using a link-segment model was used to calculate the floating axis angles, joint reaction forces and moments at the ankle, knee, and hip. Each trial was split into two phases: getting into activity position and returning to a standing position. Each phase was normalized to a 100% cycle.

RESULTS AND DISCUSSION

From Table 1, it is apparent that knee range of motion can easily exceed 150º of flexion during the activities studied. Maximum hip flexion values reached 120º for several subjects in various activities; however, the overall mean ROM angles are lower due to the high variability between subjects. Interestingly, only 2 of 13 subjects were comfortably able to kneel with ankles plantar-flexed; this may be attributable to religious customs in this region of India. Sources of error associated with the application of the rigid body model used to calculate the kinematics include soft tissue movement and shifting of the sensors.

A typical plot of one phase of an individual activity in a single plane is shown in Figure 1. The plot illustrates the knee flexion and corresponding extension moment required to rise to a standing posture from the squatting with heels flat position. When the flexion angle begins to decrease, a characteristic peak moment appears. This demonstrates the dynamic forces required to accelerate the body upwards.

Table 1 Maximum Joint Range of Flexion (SD) for Several Activities of Daily Living in India.

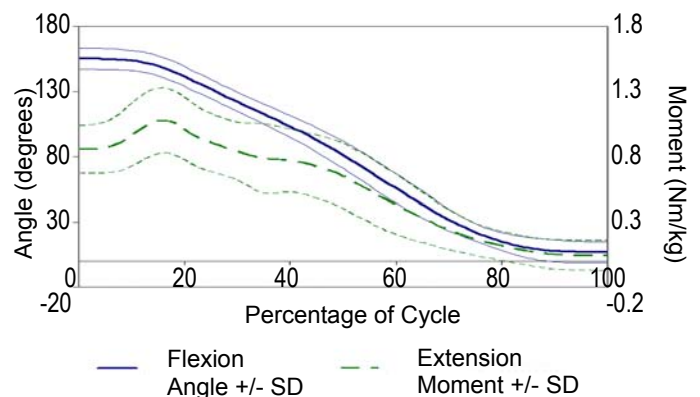| Activity [Number of Subjects]	Ankle [degrees]	Knee [degrees]	Hip [degrees]
Squatting Heels Up [13]	34 (6)	155 (11)	94 (23)
Squatting Heels Flat [12]	34 (7)	151 (12)	100 (24)
Kneeling with ankles dorsi-flexed [10]	40 (7)	160 (10)	85 (19)
Kneeling with ankles plantar-flexed [2]	67 (-)	163 (-)	96 (-)
Sitting Cross-legged [13]	48 (12)	149 (32)	91 (23)

Figure 1 Knee Flexion Angle and Extension Moment during rise to stand from Squatting Heels Flat position [n=12].

SUMMARY

For the 5 prescribed activities, mean hip and knee flexion ranges commonly exceeded the ranges of motion typically allowed by most currently available joint replacements. It is essential to know the forces and moments that occur at the joint under high range of motion conditions in order to design prosthetic joints that will accommodate these extreme angles.

REFERENCES

Mulholland,S.J. and Wyss,U.P. (2001). *Int.J.Rehabil.Res.* **24,** 191-198.
Villar,R.N., Solomon,V.K., and Rangam,J. (1988). *Tropical Doctor* **18,** 21-24.

ACKNOWLEDGEMENTS

OBSTACLE AVOIDANCE STRATEGIES USING A SONIC PATHFINDER

T. Claire Davies and Aftab E. Patla

Gait and Posture Laboratory, University of Waterloo, Waterloo, Ontario, Canada, cdavies@ahsmail.uwaterloo.ca

INTRODUCTION

Individuals with visual impairments must rely on haptic information to provide them with obstacle preview. Although the long cane has become the most common primary device for detecting obstacles on the ground, sonar systems have gained widespread acceptance as secondary mobility devices to detect obstacles that are not ground based (wall-mounted bookcases, tree branches). Preview allows an individual sufficient time to change the travel path to avoid the obstacle (Patla, 2001). The goal of this study was to examine accuracy and precision of control of adaptive locomotion using haptic preview information obtained by sonar signals. Subjects were required to detect obstacles above chest height using a Sonic Pathfinder and to walk underneath them (Heyes, 1984).

METHODS

Six healthy, young university students with normal vision participated in this study: four females and two males.

Obstacle avoidance during locomotion was studied under two sensory conditions: (a) *full vision* (FV); (b) *Sonic Pathfinder* (SP). In the SP condition, participants underwent three hours of training using a sonar obstacle detection system from the Ross McDonald School for the Blind. Within each sensory condition, five different obstacle heights were used (height 1 at chest level, heights 2 - 5 were each 10 cm higher than the previous). Five trials for each obstacle height were collected as well as 10 control trials for FV and 25 for SP. All the trials for each sensory condition were completely randomised.

Optotrak was used to track the position of 24 body-mounted markers. Head clearance (HC), vertical velocity (HVy), horizontal velocity (HVx) at the obstacle, the minimum head position or maximum clearance (MHP), the distance from the minimum head position relative to the obstacle position (HDMx), and the position of the greater trochanter relative to the minimum head position were calculated (GTminHD).

RESULTS AND DISCUSSION

A two way ANOVA with sensory condition and height were conducted for each of the aforementioned measures. There was a significant interaction effect between condition and height for the MHP ($p<0.001$) (Figure 1). MHP was similar regardless of obstacle height with FV. With the SP the maximum head clearance increased with obstacle height, but this did not correspond to a constant minimum head position. The subjects detected the obstacle and modified their trajectory but were not as accurate as with FV.

Clearance of the obstacle occurred on the upward trajectory with the SP and the downward trajectory with FV ($p<0.0004$).

The HVx was significantly higher for FV ($p<0.0010$). Although clearance was attained using the SP in all but 8 trials, the decreased velocity while passing under the obstacle indicates lack of confidence about the ability to extract sensory information accurately and precisely as compared to FV. Spatial updating with SP depends on the frequency of the system requiring the subject to approach more slowly. The time required to detect an obstacle with sonar, then convert the information into auditory signals is much longer than for visual processing of light. Online adjustment with FV allows greater precision as the trajectory can be more frequently modified while approaching the obstacle.
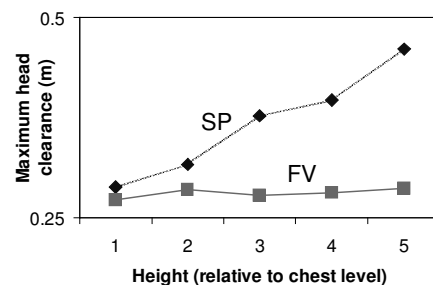

Figure 1: Maximum vertical distance from the obstacle.

There were no significant differences of GTminHD, thus subjects compensated to a greater degree with their lower body than upper body. By flexing the knees while maintaining the upper body stance, the centre of gravity can stay within the base of support and greater stability can be achieved.

In the past, research has shown that the variability of obstacle clearance is higher for the haptic condition than with vision (Patla *et al.*, 2004). A two-way ANOVA was conducted on the variability of the measures. SP variability was greater than FV in HC ($p<0.0040$), HDMx ($p<0.0001$), and MHP ($p<0.0416$). Increased variability in the SP condition indicates the lack of precision with sensory information from the SP.

SUMMARY

Adaptation occurred earlier in the SP condition than FV to ensure adequate clearance. The increased variability when using the SP relative to FV indicates that the accuracy of the head clearance using the SP suffered relative to vision. The frequency of spatial updating with SP does not occur as quickly as with vision, thus haptic updating reduces accuracy.

REFERENCES

Heyes, AD (1984) *Elec. &Wireless World,* **90**, 26-29.
Patla AE *et al.* (1991) *J Exp Psychol Hum Percept Perform.* **17**(3): 603-34.
Patla AE *et al.* (2004) *Exp Br Res* DOI: 10.1007/s00221-003-1714-z

LOCOMOTOR ADAPTATIONS TO TRUNK LOADING DURING VOLUNTARY GAIT MODIFICATIONS

Erika N. Hasler, Brendan F.D. Carney-Kilian and Stephen D. Prentice
Gait and Posture Laboratory, Department of Kinesiology, University of Waterloo, Waterloo, Canada
enhasler@uwaterloo.ca

INTRODUCTION

The production of safe limb trajectories while walking is essential to avoid injuries caused by trips or falls. This seemingly simple task becomes difficult when segment or body parameters are altered with the addition of external loads as is evident in various industrial and recreational settings (e.g. tool belts, backpacks with hip belts) which has been shown to result in greater knee flexion upon heel contact (Knapik et al, 1996). The presence of a cluttered environment further challenges the control of locomotor movements. To safely walk over obstacles requires the ability to actively flex and transport the lower limb over such barriers. It has been demonstrated that although the ankle, knee and hip actively contribute to this withdrawal, much of the flexion is mediated by knee flexor action (McFadyen & Winter 1991, Patla & Prentice 1995). The inability to actively provide gait modifications to compensate for the additional external loads may jeopardize the production of safe limb trajectories. As a result, the modification of the locomotor strategies in response to changes in trunk loading was examined during unobstructed and obstructed walking.

METHODS

Eight participants (mean age: 22.9yrs, ht: 1.73m & mass: 69.9kg) were instructed to perform three walking tasks: level unobstructed walking and walking over 10cm and 30cm obstacles. The tasks were performed under three trunk loading conditions: non-weighted (NW), weighted (W) and weight removed (WR). A total of 90 trials (10 trials per walking/ loading condition) were completed. For obstructed trials, the obstacle was placed at a mid-swing position halfway along the walkway, such that the right foot always led over the obstacle. For weighted trials, additional mass approximating 10% of the participants' body mass was equally distributed around their waist.

Three-dimensional kinematic data for the trunk and limbs, recorded using the OPTOTRAK system (NDI, Waterloo, ON) and ground reaction force data, recorded using two force plates (AMTI, Waterdown, MA) were used to determine net joint moments and powers at the ankle, knee and hip using inverse dynamics techniques (Winter, 1991). Limb trajectory and angular joint kinematics were also determined across all conditions and tasks and evaluated at toe-off, over the obstacle and at heel contact.

RESULTS AND DISCUSSION

The addition of the weight and subsequent removal did not significantly alter the amount of toe clearance in the three walking conditions despite a decreased elevation observed at the proximal end of the limb (ie greater trochanter; $p<0.05$) during the W condition. Adaptations were observed through increased hip and knee flexion over the obstacle ($p<0.05$).
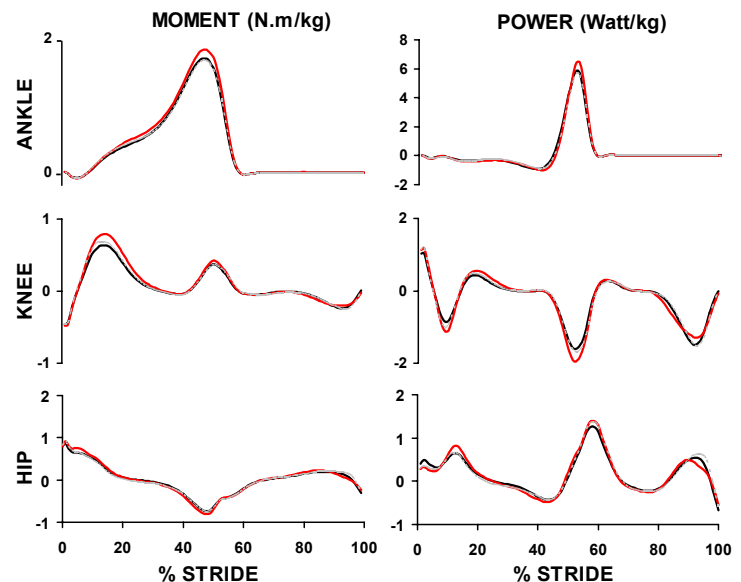

Figure 1: Ankle, knee and hip moments & powers during 10cm obstacle condition. Average profile (N=8) displayed from HC to HC. Black = NW, Red = W, Grey = WR.

Increased knee flexion was also observed at heel contact in the W condition. Added support, though early and late stance phases, was provided by increased knee extensor and plantarflexor moments, respectively (Fig. 1). During W conditions, increased peak ankle push-off power was accompanied by increased hip pull-off power. It appears that much of the increased limb flexion during W conditions can be attributed to the added push-off action during late stance.

SUMMARY

With increased trunk loading, individuals were still able to successfully produce safe limb trajectories over obstructions during voluntary gait modifications. The added weight required increased limb support during stance but did result in a lower elevation of the trunk. Push-off actions appeared to serve both the added support demands and the increased flexion of the limb.

REFERENCES

Knapik, J. et al (1996). *Applied Ergonomics*, **27**, 3, 207-216.
McFadyen BJ & Winter DA(1991) *Neurosci Res Comm,* **9** 37-44.
Patla AE & Prentice SD (1995). *Exp Brain Res*, **114**, 500-506.
Winter DA (1991). *The Biomechanics and Motor Control of Human Gait*, Waterloo, Waterloo Biomechanics.

ACKNOWLEDGEMENTS

UNEVEN TERRAIN AS A PERTURBATION TO THE CENTRE OF MASS MOTION DURING LOCOMOTION.

Stephen D. Perry (sperry@wlu.ca), Alison Radtke and Chris Goodwin.
Department of Kinesiology & Physical Education, Wilfrid Laurier University, Waterloo, ON, Canada

INTRODUCTION

Evidence that precise postural control is required for gait over uneven terrain lends this task to be an excellent potential diagnostic tool with which to evaluate the postural control system[1, 2]. It provides a unique window into a portion of the postural system that is important in everyday activities. Gait over uneven terrain allows us to investigate how well an individual is able to adapt to the changing orientation of the support surface. This work is a validation of a simulated uneven terrain setup that will allow for investigation into the multi-dimensional nature of the postural control system. This setup will be a critical evaluation tool for future investigations of postural control during gait.

METHODS

Each subject (n=19, mean age 23.8 yrs old) was asked to walk along an 8-metre walkway. Prior to using the simulated uneven terrain each subject's step length was recorded and the platforms were placed at each foot contact position. During gait over the uneven terrain the subjects were instructed to look straight ahead, not down at the inclined platforms (thus eliminating visual input and forcing primary control initiated from the sensory information from the lower limbs). During each trial the orientation of the two inclined platforms located on the force plates were randomly changed, so as to present an unpredictable uneven terrain. Participants walked over each configuration of inclined platforms five times. The platforms were placed upon force plates in the walkway so as to capture two successive foot contacts during walking. Each subject was also instrumented with electromyographical electrodes (for recording muscular activity) and OptoTrak Ired markers (for tracking segmental and centre of mass (COM) movement (13-segment model)). For this abstract, only the results from two conditions will be reported. The two conditions are when the two platforms on the force plates were slanted to participant's left when walking forward and then when the two platforms were slanted to the right of the participant.
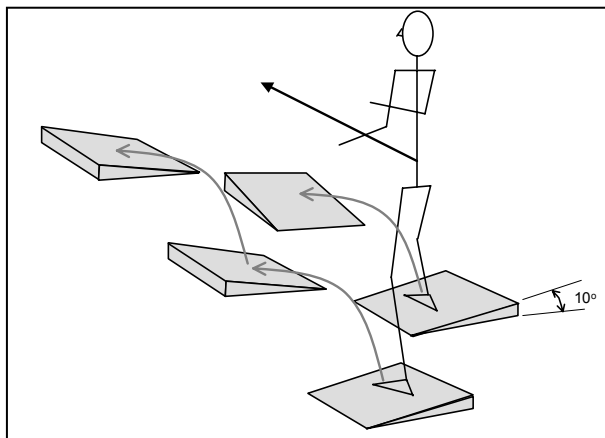

Figure 1: Uneven terrain experimental setup.

RESULTS

These results are preliminary, full presentation of results will be displayed at the conference. Initial findings, when corrected for foot position, show that the COM was 1.8 cm's (SD 2.0; p = 0.002) closer to the left stance foot during gait over inclined platforms that were slanted towards that stance foot as compared to level walking. Additionally the COM was on average 0.7 cm's (SD 1.8; NS) further away from the left stance foot, as compared to level walking, when walking over inclined platforms slanted away from that stance foot.
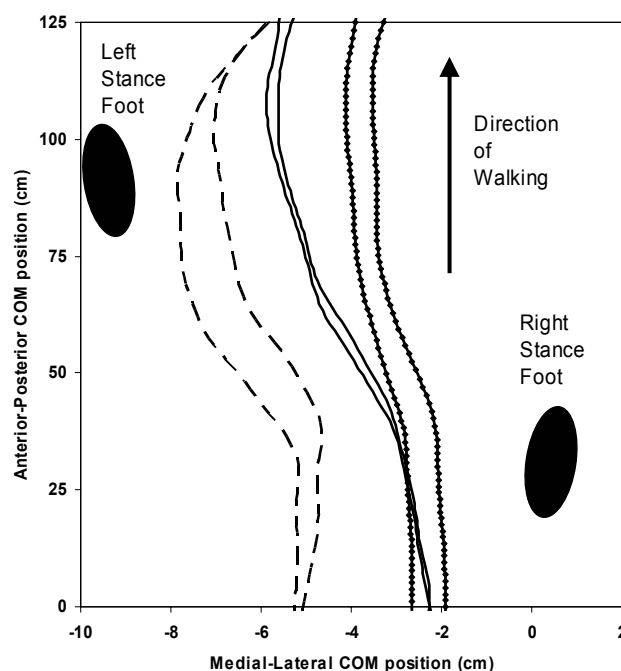

Figure 2: Transverse plane motion of the COM during level walking (solid lines) vs. terrain slanted to the subject's left (dashed line) and slanted to the subject's right (dotted line).

DISCUSSION

The substantial shift of the COM during gait over this uneven terrain does not seem to cause any immediate imbalance to the young adults tested here. However, older adults with postural control or sensory deficits may experience a larger affect; hence this presents a simple balance perturbation test to evaluate their level of balance control.

REFERENCES

1. Black, S.E., Maki, B.E. and Fernie, G.R., In H. Barber and J. Sharpe (Eds.), Vestibulo-ocular Reflex, Nystagmus and Vertigo, Raven Press, New York, 1993, pp. 317-335.
2. Maki, B.E., JAGS, 45 (1997) 313-320.

ACKNOWLEDGEMENTS

THE IDENTIFICATION OF CLINICALLY RELEVANT GAIT VARIABLES IN CHILDREN WITH HYPOTONIA

Victoria Chester[1], Edmund Biden[2], and Maureen Tingley[3]

[1]Faculty of Kinesiology, University of New Brunswick, Fredericton, Canada, vchester@unb.ca
[2]Department of Mechanical Engineering, University of New Brunswick, Fredericton, Canada
[3]Department of Mathematics and Statistics, University of New Brunswick, Fredericton, Canada

INTRODUCTION

Hypotonia, or decreased muscle tone, is a common diagnosis in infants and children. The presence of hypotonia is generally indicative of an underlying neuromuscular or genetic disorder (i.e. Down's syndrome). Hypotonic children typically exhibit ligament laxity, instability of the lower limb joints, limb deformities, abnormal walking patterns, and delayed acquisition of independent walking (Caselli et al., 1991). Despite these serious orthopaedic problems, there are few studies that provide a comprehensive analysis of the walking patterns of hypotonic children. The purpose of this study was to: 1) objectively assess and analyze the walking patterns of hypotonic children and 2) determine the gait variables which differentiate hypotonic gait patterns from age-matched normative data using statistical classifiers.

METHODS

Data were collected from 60 normal children aged 1-13 years and 15 hypotonic children, aged 1- 11 years. A six-camera Vicon 512 motion analysis system and two force plates were used to obtain temporal-spatial, kinematic, and kinetic parameters during walking. Segment inertial parameters were estimated using a mathematical model of the human body (Jensen, 1978). Joint rotations were expressed using Euler angles and an inverse dynamics approach was used to estimate the joint moments and powers. Using the normative data, methods of data reduction were developed based on primary directions of variation from mean behaviour. Joint angles were characterized by their first and second derivatives (Tingley et al., 2002), and kinetic parameters were characterized by the time integral and scaled root-mean-square values of the moment and power curves (Chester, 2003). Quantifying the variation of an individual's gait data from the mean normative values led to a set of seven one-dimensional scores that classified gait patterns as normal, unusual or extreme based on population percentiles. The seven scores were: sagittal angle score, trunk kinematic score, pelvic score, stance moment and power scores, and swing moment and power scores. These seven scores could be combined into a single one-dimensional score of normality. Classification results were examined to determine the number of hypotonic individuals classified as unusual or extreme based on the various scores. We then examined which subcomponents of each score system were differentiating between hypotonic and normative data.

RESULTS AND DISCUSSION

Statistical tests of the differences between the hypotonic and normative data used the eight scores as input data. The results of nonparametric Mann-Whitney tests of median scores showed significant differences ($p<0.05$) for all scores between the two groups of children. That is, the hypotonic children, as a group, were detected from normal movement patterns. Classification results revealed that 11 out of 15 hypotonic children were classified as extreme or unusual by the overall one-dimensional score. Four children were classified as normal walkers. An examination of their gait data revealed that these children were indeed within the bounds of normal kinematic and kinetic values. This was due to a history of successful physiotherapy and orthotic prescriptions. The overall one-dimensional score was then decomposed into its subcomponents to identify the strongest discriminators of hypotonic gait for the remaining 11 children. Standardized mean differences in the normative and hypotonic data revealed that the kinematic scores were the most successful discriminators of hypotonic gait. Standardized mean differences in the normative and hypotonic coefficients showed that hypotonic abnormalities were most readily identified by examining sagittal angles, angular velocity and acceleration patterns of the pelvis (tilt and rotation), knee varus, foot rotation, trunk rotation, trunk obliquity (lateral trunk flexion), and trunk angular acceleration.

In contrast, kinetic measures were poor discriminators of hypotonic gait. This was likely due to the similar variability between the two groups and the skewed distribution of scores which formed the normative training set for the kinetic score system. The best kinetic scores were the stance phase sagittal ankle moment and power, and swing phase frontal hip moment and power.

SUMMARY

This study has found several key gait measures that differentiate between hypotonic and normative gait patterns. Hypotonic children have received little attention in terms of the possible benefits of gait analysis. A greater awareness of the variables that deviate from normative values for this population will increase our understanding of the disorder and aid in treatment planning and evaluation.

REFERENCES

Caselli, M. A., Cohen-Sobel, E., Thompson, J., Adler, J., & Gonzalez, L. (1991). Biomechanical management of children and adolescents with Down syndrome. *Journal of the American Podiatric Medical Association, 81(3)*, 119-127.

Chester, V. (2003). The identification of clinically relvant gait variables. Ph.D Thesis. University of New Brunswick.

Jensen, R. K. (1978). Estimation of the biomechanical properties of three body types using a photogrammetric method. *Journal of Biomechanics, 11*, 349-358.

Tingley, M., Wilson, A., Biden, E., & Knight, W. R. (2002). An index to quantify normality of gait in young children. Gait and Posture, 16, 149-158.

GENETIC-RELATED OBESITY DOES NOT ADVERSELY AFFECT BONE MECHANICAL AND MORPHOMETRICAL PROPERTIES

Jeremy LaMothe[1,2], Raylene Reimer[1,2], and Ronald Zernicke[1,2,3]
Faculties of Kinesiology[1], Medicine[2], and Engineering[3]
University of Calgary, Calgary, Alberta, Canada, jlamothe@kin.ucalgary.ca

INTRODUCTION

Obesity is at epidemic proportions throughout the developed world and its prevalence is rapidly rising. The prevalence of obesity in Canadian children nearly tripled from 1981-1996 (Tremblay and Willms, 2000). High-fat high-sucrose (HFS) diets—pervasive in North America—are linked to obesity and have been shown to deleteriously affect bone health (Zernicke et al., 1995). Male JCR:La-corpulent rats lack the leptin receptor, are severely obese, hyperphagic, hypertriglyceri-demic, hyperinsulinemic, and patently insulin resistant (Russell et al., 1994) . These rats exhibit several attributes typical of the obese-diabetic-hypertensive-dyslipidemic syndrome observed in humans (Defronzo and Ferrannini, 1994). Given that dietary (HFS) induced obesity can deleteriously affect bone health, *we hypothesized that genetically-induced obesity (JCR:La-corpulent rats) would deleteriously affect bone biomechanical properties, relative to lean control rats.*

.

METHODS

We assessed axial (L_6) and appendicular (tibial) morphometrical and mechanical properties of skeletally mature male JCR:La-corpulent rats (n=8) and age-sex-matched lean control rats (n=7). Morphometrical properties (e.g. cross sectional area, I_{xx}) were determined by micro-computed tomography scanning (Skyscan 1072). After scanning, tibiae were broken in three point-bending, and vertebrae were broken in axial compression (LaMothe et al., 2003). Biomechanical testing outputs were used to determine structural properties (e.g., maximal load). Structural properties were used in conjunction with morphometical properties to determine material properties (e.g., maximal stress). A muffle furnace was used to determine mineral ash fractions (LaMothe et al., 2003). Mann-Whitney-U tests were used with a significance level of $p \leq 0.05$ to determine if significant differences existed between the two groups.

RESULTS AND DISCUSSION

Obese rats were significantly heavier (>107%) than lean rats. Despite this arrant disparity in body mass, there were no significant differences in L_6 and tibial morphometrical properties between obese and lean rats (**Figure 1a**). Similarly, there were no significant differences in L_6 or tibial mineral ash fractions, and structural and material properties between genetically obese and lean rats (**Figure 1b**). Therefore, our hypothesis was rejected. Conversely, HFS-induced obesity can provoke significant decrements in bone material properties (Zernicke et al., 1995). **Figure 1b** highlights key differences that we revealed regarding the impacts of diet-related vs. genetic-related obesity on bone. L_6 maximal stress and ash fraction were significantly less in the diet-related obese rats (HFS diet; from Zernicke et al., 1995), but those material properties were not different for the genetic-related JCR:La-corpulent rats. Thus, we concluded that diet-related obesity affects bone health via a different mechanism than genetic-related obesity.
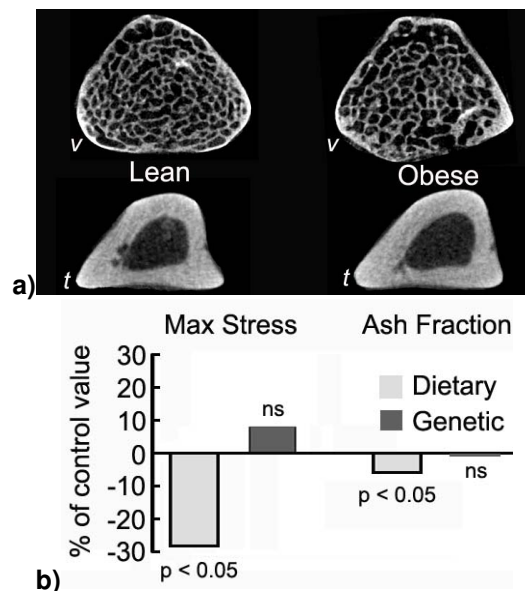

Figure 1. L_6 (*v*) and tibial (*t*) transverse cross sectional μCT images for lean and genetically obese rats (**a**). Maximal stress and mineral ash fraction for diet-related obesity (HFS diet), and genetic-related obesity (JCR:la-corpulent rats presented) represented as a percentage of control values (**b**). Dietary values from Zernicke et al., 1995.

SUMMARY

These unique findings may have implications in assessing the impact of obesity on bone health as there may be disparate effects between dietary factors that promote obesity and the array of adipokines and other factors (e.g., leptin) released from adipose tissue mass. Elucidating key dietary factors that promote bone health in an obesigenic environment will be critical in the future.

REFERENCES

Tremblay MS and Willms JD (2000). *CMAJ*, **163**, 1429-1433.
Zernicke RF et al. (1995). *Bone*, **16**, 25-31.
Russell et al. (1994). *Metabolism*, **43**, 538-543.
Defronzo RA and Ferrannini E (1994). *Diabetes Care*, **14**, 173-194.
LaMothe JM et al. (2003). *J Appl Physiol*, **95**. 1739-1745.

ACKNOWLEDGEMENTS

LINKING VENTILATION MECHANICS WITH SPINE STABILITY: NORMAL AND PATIENTS

Simon Wang[1], Eric Hentschel[2], and Stuart McGill[1]
[1]Department of Kinesiology, University of Waterloo, Waterloo, Canada, s9wang@uwaterloo.ca
[2]Department of Respirology, Grand River Hospital, Kitchener, Canada

INTRODUCTION

For the normal person, abdominal muscles are recruited to create moments to move the torso, assist in active expiration, and support and stabilize the lumbar spine through continuous isometric contraction. Our recent evidence suggests there is an entrainment cycle of these muscles to ventilation during challenged breathing, which affects the stability of the lumbar spine. Obstructive Pulmonary Disease patients are unique in that they use their abdominal muscles continually, to assist with breathing. The question that arises from these observations is: will respiratory patient's breathing patterns compromise their spine stability?

METHODS

Recordings were made from Chronic Obstructive Pulmonary Disease (COPD) patients and a healthy control group. Bilateral electromyographic recordings were collected from the rectus abdominis, external obliques, internal obliques, latissimus dorsi, thoracic erector spinae, and lumbar erector spinae. Recordings of lumbar spine kinematics, full body kinematics, and ventilatory flow were also taken, all of which formed the input for a model to quantify spine stability. Challenged breathing tasks of maximal voluntary ventilation (MVV), slow breathing (6 bpm), breathing through a small rubber straw, and a cycle ergometer bout were attempted by each subject. A spine load challenge of holding a weight in front of the pelvis was also incorporated with the breathing challenges.

RESULTS AND DISCUSSION

In the healthy population, abdominal muscle mechanics were seen to follow a relaxation-contraction cycle which matched the inspiration-expiration cycle during all challenged breathing tasks. Primarily the internal oblique and to a lesser extent the external oblique were recruited to assist with expiration. To compensate for the moment created by the abdominals the thoracic and lumbar erector spinae were also active in the same cyclic pattern. When input into the stability model, these muscle patterns produced an oscillation in spine stability that increased with inspiration, just as expiration started, and decreases with full expiration (Figure 1).
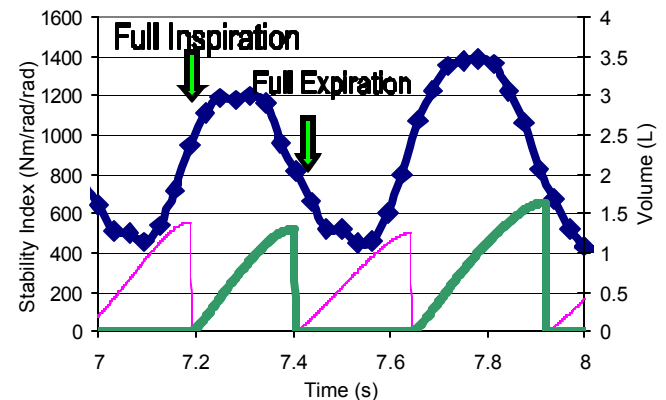

Figure 1: Maximal Voluntary Ventilation over one second. Two respiration cycles from a normal subject. Stability Index (Diamond line), Inspiration (thin line), Expiration (thick line).

These results give us the first part of understanding the links between ventilation mechanics and spine stability. The second step to this understanding is currently underway with the collection of COPD patients through a similar protocol. Interestingly, these patients have shown a different cyclic pattern of entrainment to breathing where they use their back muscles to assist with inspiration, even at rest. Repeated use of their back muscles may cause fatigue and could lead into motor patterns that put their backs at risk.

SUMMARY

Ventilation during challenged breathing has a direct affect on lumbar spine stability, in that the greatest stability is at full inspiration and the lowest level at full expiration. Previous research has shown that bad backs compromise stability (McGill et al, 2003 and McGill et al, 1995). This study suggests that compromised lungs could also do the same. Findings from this study may provide insight to athletic enhancement for sprinters and weightlifters, and could assist in improving the backs of those enrolled in pulmonary rehabilitation programs.

REFERENCES
McGill, S.M. et al (2003). *Ergonomics*, **46**(7), 731-746.
McGill, S.M., et al (1995). *Ergonomics*, **38**, 1772-1792.

ACKNOWLEDGEMENTS

DISTRIBUTION OF TISSUE LOADS SUPPORTING THE LOW BACK DURING THE FLEXION RELAXATION PHENOMENON IN SITTING AND STANDING POSTURES

Nadine M. Dunk[1], Stephen H.M. Brown, Jack P. Callaghan

Faculty of Applied Health Sciences, Department of Kinesiology, University of Waterloo, Waterloo, ON, Canada

[1]Corresponding author e-mail: nmdunk@uwaterloo.ca

INTRODUCTION

Prolonged sitting has been identified as being associated with low back pain, however there has been little progress in identifying the source of the pain. A recent study (Callaghan and Dunk, 2002) observed that a slumped sitting posture elicited the flexion relaxation (FR) phenomenon in the thoracic erector spinae muscles. It is possible that the passive tissues of the vertebral column were loaded to support the increased moment at L4/L5 in the slumped sitting posture. However, the range of lumbar motion assumed during seated postures may not recruit the passive tissues whose contributions have been shown to remain low until 75% of the full flexion RoM (Adams et al, 1994). Thus we were driven to examine the distribution of loads on the different lumbar spine tissues during flexion relaxation in a slumped sitting posture using an anatomically detailed model of the spine that was sensitive to muscle activity and lumbar curvature. Additionally, the load distribution during standing FR was examined to determine any differences in tissue load transfer from seated FR.

METHODS

The testing protocol consisted of five trials each of standing full forward flexion and seated forward flexion (rounding of the lumbar spine to a "slouched" seated posture). The flexion-extension cycle was comprised of three phases: Phase 1 and 3 corresponded to upright standing/sitting, while phase 2 represented the flexion relaxation (FR) phase where a flexed posture was maintained. Myoelectrical activity from 7 trunk muscles was collected bilaterally, while body segment displacements were recorded with video. Lumbar flexion was determined from fin markers attached at T12/L1 and L4/L5. A 58 muscle, EMG driven dynamic biomechanical model of the spine was used to partition the moments acting about the L4/L5 joint amongst active (muscle) and passive (muscle, disc, ligament, fascia) tissues.

RESULTS AND DISCUSSION

During standing full flexion, 7 out of 8 subjects exhibited FR in both thoracic and lumbar erector spinae (ES) muscles. Six out of eight subjects exhibited FR in their thoracic (ES) during slumped sitting; FR was not observed in any other monitored muscles in seated flexion.
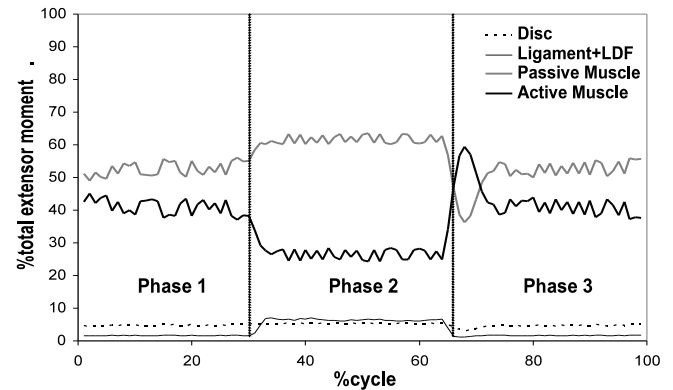

Figure 1: Typical tissue moment distribution time histories expressed as a percentage of total extensor moment during the slumped seated flexion task.

During standing FR, the active extensor muscles only supported 23.84% of the total extensor moment while the ligaments accounted for most of the decreased active extensor muscle moment support (Table 1). In the slumped sitting FR phase, the ligaments only supported 5.42% of the extensor moment, while the passive muscle moment accounted for the largest portion of the moment (52.27%). Figure 1 shows the transfer of the moment from active muscle to the passive tissues during slumped sitting. Our subjects' seated spine postures ranged, on average, from 49 to 81% of maximum flexion. Ligament tension has been shown to remain low for much of the range of flexion (Adams et al, 1994). Further, the intact torso is stiffer than the osteoligamentous spine over moderate ranges of motion, suggesting that passive tissue, other than ligaments and discs, contribute to stiffness (McGill et al, 1994).

SUMMARY

According to this model, the extensor moment in slumped sitting is largely supported by passive force generated by stretching the musculature. It appears as though the ligaments are only loaded a small amount in this posture and may not be the source of low back pain during sitting.

REFERENCES

Adams, MA et al (1994). *Clin Biomech*, **9**, 5-14.
Callaghan, JP, Dunk, NM (2002). *Clin Biomech*, **17**, 353-360
McGill, SM et al (1994). *Spine*, **19**, 696-704

Table 1: Percentage of the total extensor moment about L4/L5 distributed amongst the different lumbar tissues during standing and seated flexion.

	Standing			Sitting		
	Phase 1	Phase 2	Phase 3	Phase 1	Phase 2	Phase 3
Disc	-0.095 (0.17)	3.90 (0.29)	-0.037 (0.42)	4.23 (0.65)	5.17 (0.66)	3.52 (0.59)
Ligament+LDF	3.02 (0.41)	25.05 (4.26)	2.85 (0.47)	1.57 (0.13)	5.42 (1.05)	1.49 (0.13)
Passive Muscle	41.50 (2.67)	47.21 (2.68)	39.14 (2.76)	43.56 (2.63)	52.27 (2.53)	39.02 (2.89)
Active Muscle	55.57 (2.92)	23.84 (4.45)	58.04 (2.83)	50.64 (3.00)	37.14 (3.52)	55.98 (3.19)

OBJECTIVE MEASUREMENT OF TRUNK MOTION PATTERNS
IN HEALTHY INDIVIDUALS AND PATIENTS WITH MECHANICAL LOW BACK PAIN

Einas Al-Eisa[1], David Egan[1], Kevin Deluzio[2], and Richard Wassersug[1]
[1]Department of Anatomy & Neurobiology, Dalhousie University, Halifax, Canada
[2]School of Biomedical Engineering, Dalhousie University, Halifax, Canada

INTRODUCTION

In chronic low back pain (LBP), pain avoidance and the adaptation to pain that takes place in the musculoskeletal system long after the initial injury, can lead to functional pathologies. Therefore, when pain relief is the primary goal of treatment, functional pathologies associated with LBP may remain and cause future recurrence.   Such functional pathologies include abnormal movement patterns.

There is much variability, however, in trunk motion among both asymptomatic and patient populations (Gomez et al., 1991), and consequently no consensus on what constitutes normal trunk movement. Pathology in the back might affect both the pattern of the movement as well as the range. Asymmetry of movement could give some insight on the underlying pathology. The objective of our study was to examine differences in range and asymmetry of trunk lateral flexion (LF), axial rotation (AR), and the coupled movements between LF and AR among asymptomatic individuals and patients with LBP.

METHODS

A total of 113 subjects were classified into two groups: control group with no history of LBP (n=59; 25 males and 34 females, mean age ± SD = 31.1 ± 6.9), and LBP group with predominantly unilateral symptoms that persisted in the 6 months prior to the study (n=54; 27 males and 27 females, mean age ± SD = 33.4 ± 7.2). To measure trunk kinematics, we used the Qualisys™ Motion Analysis System. Reflective skin markers were attached to the person's back to model the spine as four rigid body segments: sacral, lumbar, lower and upper thoracic (figure 1). In this study we report on the movement of the lumbar and lower thoracic segments relative to the sacrum.

Each subject was instructed to laterally flex (or rotate) from the neutral position as far as possible (to his/her endpoint) to one side, then sweep uninterrupted to the other side, then return to the erect stance. The original starting neutral position was used as the baseline around which we measured asymmetry. All movements were measured three times and averaged. To quantify movement asymmetry we divided the absolute difference between the right and left end range by the total range of motion.

Figure 1: A participant with markers attached and the four rigid bodies used to model the spine**.**

RESULTS AND DISCUSSION

Table 1: Results of the multivariate ANOVA for differences between the groups in the <u>main</u> motion. Data are p-values.

Movement	Range of motion	Movement asymmetry
Lumbar LF	0.401	0.023*
Lumbar AR	0.858	0.001*
Thoracic LF	0.020*	0.823
Thoracic AR	0.024*	0.143

This study demonstrates objective differences in patterns of <u>lumbar</u> movement between normal subjects and those with LBP. The LBP group had significantly higher <u>lumbar</u> motion asymmetry than the normal group, but the groups did not differ significantly in asymmetry of <u>thoracic</u> motion.

Previous studies that failed to discriminate between normal subjects and LBP patients did not quantify motion of the lumbar and lower thoracic spine separately (Masset et al., 1993). In our study, the control group displayed a pattern of greater <u>thoracic</u> ROM in the main motion than the LBP group, but there was no difference between the groups in the <u>lumbar</u> range of motion. The reduced range of thoracic motion in the LBP group could be due to guarding behavior to avoid pain.

The LBP group had higher range (p=0.024) and asymmetry (p=0.009) in <u>coupled</u> lumbar rotation than the control group. Clearly, this indicates that LBP can affect coupling behavior.

Asymmetry of lumbar movement may be a better indicator of functional deficit than range of lumbar movement in LBP.

REFERENCES

Gomez T, et al. (1991). *Spine,* **16**, 15-21.
Masset D, et al. (1993). *Int J Industrial Ergonomics*, **11**, 279-290.

THE ROLE OF TORSION IN INTERVERTEBRAL JOINT FAILURE MECHANICS

Janessa D. M. Drake, Crystal D. Aultman, Stuart M. McGill, Jack P. Callaghan

Faculty of Applied Health Sciences, Department of Kinesiology, University of Waterloo, Canada, jdrake@ahsmail.uwaterloo.ca

INTRODUCTION

The lumbar spine is routinely exposed to axial torque during the performance of industrial and daily activities. However a lack of understanding of the modulating influences of torsion on the compressive strength and behaviour of the intervertebral joint (IVJ) under repetitive loading exists. The objectives of this work were to determine the effects of torsion on the one-time (acute) compressive strength and repetitive failure mechanics of the intervertebral disc and vertebrae.

METHODS

Porcine cervical spine motion segments were subjected to two loading conditions: acute and repetitive. In the acute condition, cervical spine (C5/6) segments were compressed to failure at a rate of 3000N/s combined with 0N·m, 5N·m, 10N·m, 20N·m, and 30N·m of static axial torque. The repetitive study applied repetitive flexion/extension motions and 1472N of compression with 0N·m and 5N·m of static axial torque to cervical spine (C3/4) segments. A full description of the loading apparatus has been published elsewhere (Callaghan & McGill, 2001, Aultman et. al., 2004). Resultant structural failure to the intervertebral disc and vertebrae were documented using planar radiography and visual inspection.

RESULTS AND DISCUSSION

Increasing axial torque significantly reduced the ultimate strength of motion segments during one-time compressive loading (Figure 1). Damage was confined to the endplate and trabecular network of the vertebral body. In the repetitive
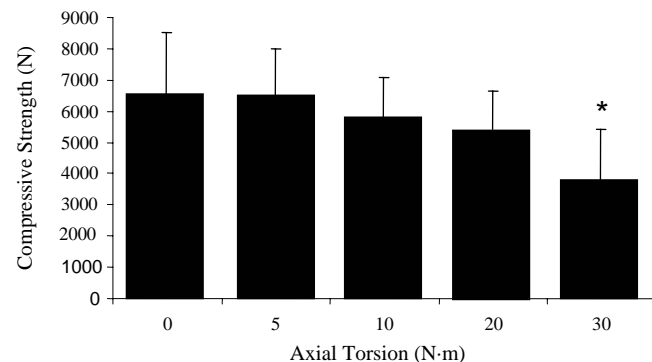

Figure 1: Ultimate compressive strength for the one-time loading to failure condition.

condition, a higher incidence of facet fractures (Figure 2) and earlier onset trends of initial disc injury (Figure 3) and herniation were found in the torsion group. The earlier failure of the IVJ with torsion in repetitive loading mirrors the failure at lower magnitudes of compression (with increasing magnitudes of torsion) observed in the acute condition. While the two studies differed with respect to the mechanism of failure, both studies support that the addition of torsion can alter both the occurrence and mechanism of injury.
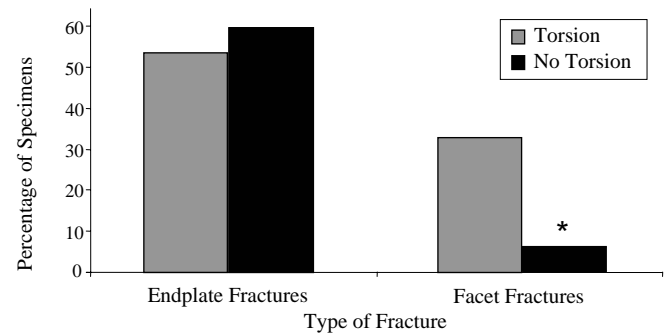

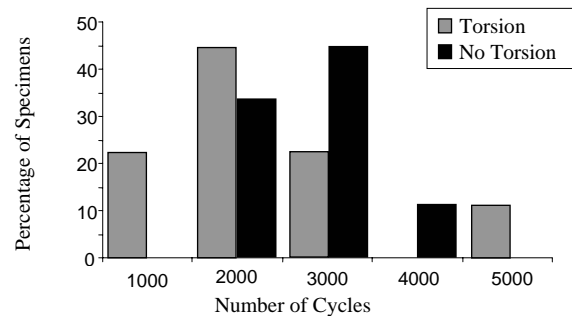**Figure 2:** Vertebral fractures produced during the repetitive loading condition.

Figure 3: The number of cycles to disc injury onset (radiographically determined).

CONCLUSIONS

Static torsion increased the vulnerability of the spinal motion segments in both acute and repetitive combined loading schemes. These studies support the speculation that torsion constitutes a verifiable risk for the development of injury (Pope and Novotny, 1993). While failure appears to occur in the endplate with no facet damage in the acute condition, the repetitive condition with torsion resulted in destruction of the annulus and facet fractures. Small magnitudes of static torsion alter the failure mechanics of the intervertebral disc and vertebrae in combined loading, with increased static torsion reducing the acute compressive strength of the spine.

SUMMARY

These unique studies indicate that combined torsional loading, whether acute or repetitive in nature, alter the failure mechanics of the spine segments indicating that even small magnitudes of joint torsion has deleterious consequences.

REFERENCES

1. Callaghan & McGill (2001). *Clin Biomech*, **16**, 28-37.
2. Aultman, Drake, Callaghan, & McGill (2004). *Spine*, **In Press**.
3. Pope & Novotny (1993). *J Biomech Eng*, **115B**, 569-74.

ACKNOWLEDGEMENTS

3D TRUNK POSTURES AND CUMULATIVE LOW BACK LOADS DURING NON-OCCUPATIONAL TASKS

Christina Godin[1], David Andrews[2], and Jack P. Callaghan[3]

[1,2]Department of Kinesiology, University of Windsor, Windsor, Ontario, Canada, [2]dandrews@uwindsor.ca,
[3]Department of Kinesiology, University of Waterloo, Waterloo, Ontario, Canada

INTRODUCTION

Punnett et al. (1991) have shown that trunk posture is an independent risk factor for the reporting of low back pain. Cumulative loads have also been linked to low back pain in occupational settings (Norman et al., 1998). Despite this, little has been reported about the physical characteristics of non-occupational tasks including trunk postures and hand loads. Therefore, the purpose of this study was to examine the distribution of trunk postures and hand loads that occur in typical non-occupational tasks and to offer insight into the relationship between these variables and cumulative low back loads.

METHODS

Ten participants (5 females, 5 males) were videotaped for two hours each during typical home activities. Postures of the trunk, neck, and upper limbs together with hand load information and each subject's anthropometric data were input into a computerized posture sampling prediction tool, 3DMatch (Callaghan et al., 2003), which calculates reaction and joint forces at L4/L5 as well as moments in 3D. Time spent in each trunk posture category (neutral, mild, moderate and severe flexion/extension, lateral bend, and axial twist) was determined as a percentage of the entire two-hour session. Cumulative loads were determined by rectangular integration of the load-time histories. Peak loads were the maximum loads obtained over the session.

RESULTS

Subjects maintained neutral trunk postures for 85.3% of the time (Figure 1). Of the ten participants only a single subject exceeded a trunk flexion angle of 90°. Only 2 participants extended the trunk, with the maximum extension angle being 22.5°. Maximum trunk lateral bend and axial twist angles did not exceed 35° for any subject. Participants deviated from neutral most often for trunk flexion (11.4% time outside neutral) than in the other two axes. Very little time was spent in severe postures. Hand loads ranged from 0.23 kg to 31 kg. Maximum hand loads for all subjects ranged from 5 kg (pull fridge door open) to 31 kg (pull off swimming pool cover). The mean peak compression force was 3913 N ($\pm$ 1266 N), with half the subjects reaching values above the 3400 N NIOSH AL (NIOSH, 1981). Cumulative compression values for the 2-hour period averaged 7.8 MN*s ($\pm$ 3.1 MN*s).

DISCUSSION AND CONCLUSIONS

High postural demands and cumulative loading are associated with low back pain (Punnett et al., 1991; Norman et al., 1998) in industry. Our results show that cumulative loads in non-occupational tasks were quite high even though trunk postures were primarily neutral and maximum hand loads were on average, relatively low. This emphasizes the contribution of exposure time to the accumulation of low back loads, irrespective of the setting.

REFERENCES

Callaghan et al. (2003). *Proceedings of ACE*, London.
NIOSH (1981). Technical Report No. 81-122
Norman et al. (1998). *Clin. Biomech.*, **13**, 561-573.
Punnett et al. (1991). *Scand J. Work Env. & Health,* **17**, 337-346.

ACKNOWLEDGEMENTS
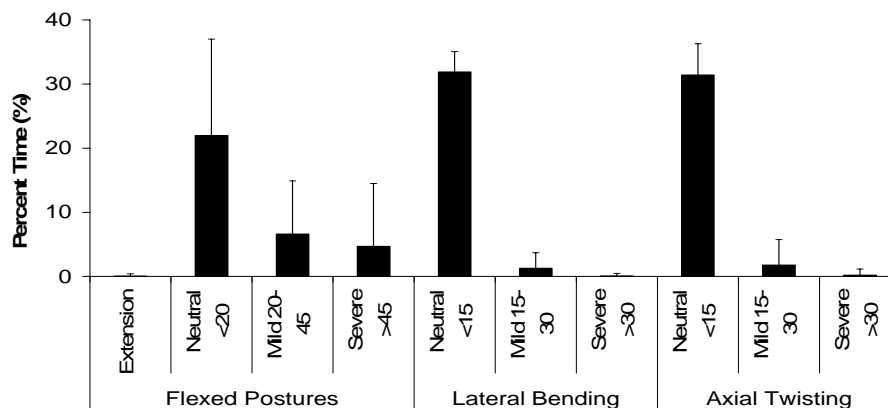
Figure 1: Mean percent time spent in the various trunk postures.

FOOT MAPPING OF VIBRATION SENSITIVITY THRESHOLDS

Thorsten Sterzing, Michael Uttendorfer and Ewald M. Hennig

Biomechanics Laboratory, University of Duisburg – Essen, Germany, thorsten.sterzing@uni-essen.de

Introduction

The human foot nowadays is fully accepted to function not only as a supportive or propulsive structure but also to be of considerable importance as a source of sensory input [1]. Clinically, sensory malfunction of the foot may cause substantial problems, e.g. in diabetes patients. However, external sensory input at the foot also affects the healthy population. Plantar sensory input has been shown to be capable of altering plantar pressure patterns during walking and running [2]. Sensory input by ankle taping improves foot position awareness [3]. So far, the vast majority of research focused on sensory input with regard to the plantar foot region. Jeng et al. (2000) also referred to sensory thresholds of five sites of the dorsal foot [4]. The present study aimed for creating a complete and detailed mapping of the sensory thresholds of the healthy human foot with regard to vibration stimuli.

Methods

Vibration sensitivity thresholds were determined by usage of a modified Horwell Neurothesiometer (Scientific Laboratory Supplies Ltd., Nottingham, UK) at a frequency of 100 Hz. 48 subjects (24 females, 24 males) between 20 and 35 years old took part in the testing. Sensitivity thresholds of the right foot were tested at 30 selected different anatomical locations at the plantar (P), dorsal (D), medial (M) and lateral (L) foot regions as there were:

P1	heel	D6	metatarsal head III
P2	arch medial	D7	metatarsal head V
P3	arch intermedius	D8	phalanx distal I
P4	arch lateral	D9	phalanx media III
P5	mh I	D10	phalanx media V
P6	mh III	M1	medial malleolus
P7	mh V	M2	medial calcaneus
P8	phalanx distal I	M3	os naviculare
P9	phalanx distal III	M4	metatarsal basis I
P10	phalanx distal V	M5	metatarsal head I
D1	ankle joint	L1	lateral malleolus
D2	metatarsal basis I	L2	lateral calcaneus
D3	metatarsal basis III	L3	metatarsal basis V
D4	metatarsal basis V	L4	metatarsal head V
D5	metatarsal head I	A1	achilles tendon

Results and Implications

The human foot shows anatomical sites and regions with significantly different vibration sensitivity thresholds. The mean detectable vibration amplitude across all subjects for the selected anatomical sites varied between 1 and 6 µm but deviated considerably for single anatomical sites and for individual subjects. Both gender groups revealed the same threshold pattern across the whole foot surface (Figure 1). However, females in general show significantly lower sensitivity thresholds than males when regarding the mean values across all 30 anatomical sites ($p<0.05$). When splitting the foot up in anatomical regions, for both gender groups the plantar region is the most sensitive, followed by the lateral and the medial foot region whereas the dorsal foot region is the most insensitive region ($p<0.01$). Gender differences exist for the dorsal ($p<0.01$) and medial ($p<0.05$) foot regions (Figure 2).

Figure 2: Vibration thresholds mean values [µm]
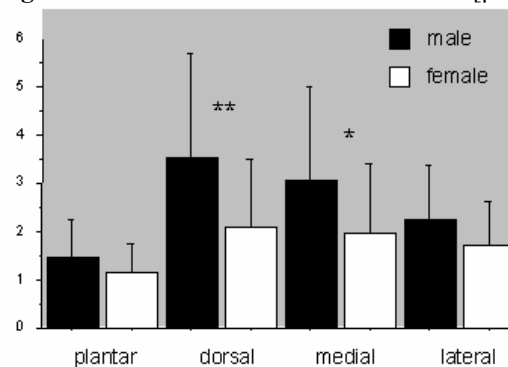
These findings are suited to better understand the foot as a receptor of external stimuli and thus as a provider of sensory information for the central nervous system.
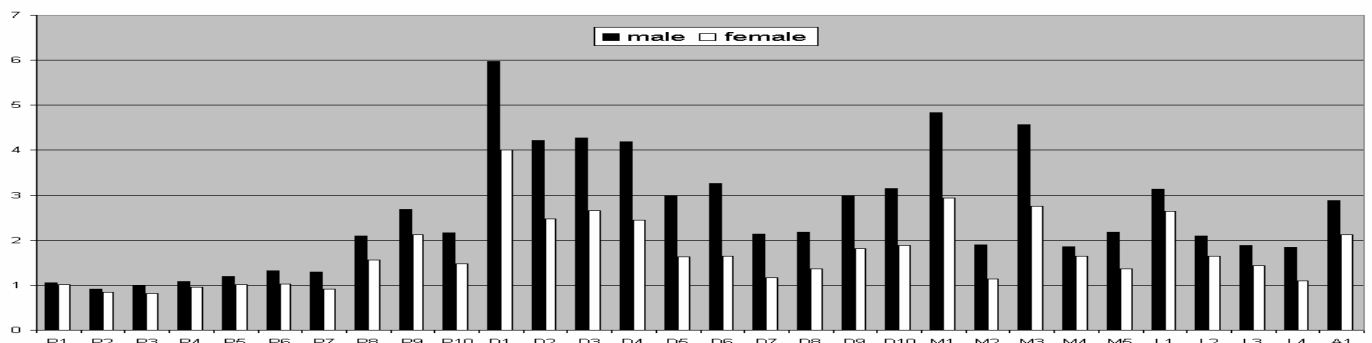
References

[1] Cavanagh, P.R. (1999). XVIIth ISB Congress, Calgary, Canada.
[2] Chen, H. et al (1995). Clin. Biomechanics 5, 271-274.
[3] Robbins, S. (1995). Br. J. Sports Med., 4, 242-247.
[4] Jeng, C. et al (2000). Foot & Ankle Int., 6, 501-504.

Acknowledgements

Figure 1: Vibration thresholds, mean values [µm]; SD not displayed for visual clarity (see text)

A CROSS-BRIDGE-BASED MODEL OF FORCE DEPRESSION: INSIGHTS INTO THE UNDERLYING MECHANISMS

David T. Corr* and Walter Herzog
Human Performance Laboratory, University of Calgary, Calgary, AB, Canada
*email: dcorr@kin.ucalgary.ca

INTRODUCTION

Force depression (FD), a well-accepted characteristic of skeletal muscle in which the force produced following active shortening is smaller than that produced isometrically at the same final length, has been demonstrated in both whole tissue and single fiber preparations (*e.g.* Maréchal and Plaghki, 1979; Sugi and Tsuchiya 1988), yet its mechanisms remain unknown. While typically analysed at steady-state, we believe that the transient response of the force contains valuable information that, in conjunction with modelling, can improve our understanding of the underlying mechanisms of FD. In this study, we created a cross-bridge based FD model of skeletal muscle based on the hypothesis that the depression of force is due to a reduction in the cross-bridge bonding rate. Model simulations addressed the dependence of both the transient and steady state aspects of FD on shortening velocity, shortening amplitude, and mechanical work of the muscle-tendon unit. These simulations, when compared with recent experimental data, may help elucidate the underlying mechanisms of FD.

METHODS

The muscle model contains a contractile element (CE) in series with a compliant tendon. The CE was represented by a two-state Distribution-Moment (DM) model, in which the solution to the cross-bridge model, originally proposed by Huxley (1957), was approximated using a Gaussian cross-bridge attachment distribution, where the first three moments of the bond distribution represent CE stiffness, force, and elastic energy, respectively (Zahalak and Ma, 1990). The force-length relation of the muscle-tendon unit was assumed hyperbolic (Woittiez et al., 1984). To account for FD, the cross-bridge bonding rate function (*f*) was assumed to decrease with the mechanical work produced by the muscle (f_1-const*work). This approach is consistent with experimental studies in which the work produced by muscle shortening was found to relate to steady-state FD (Herzog et al., 2000), and is based on the idea that FD is caused by a stress-induced inhibition of cross-bridge attachments (Maréchal and Plaghki, 1979). Modelling parameters for cat soleus muscle and tendon were taken from the literature (Cole et al., 1996), and simulations were run in MATLAB for a tetanically-stimulated muscle-tendon unit subjected to three shortening amplitudes (3, 6, 9mm) at three shortening speeds (3, 9, 27mm/s). To analyse the transient behaviour, the force following active shortening, $F(t)$, with the fully-activated muscle held at the final length, was fit ($R^2 > 0.99$) using an exponential function,

$$F(t) = F_{inf} - Ae^{-kt},$$

where F_{inf} represents the depressed force at steady state, A the recoverable force, and k the exponential growth rate. Simulations were compared to experimental results obtained previously on cat soleus muscle (n=8) undergoing identical shortening contractions to those modelled here.

RESULTS AND DISCUSSION

Model simulations showed that a work-based reduction of the cross-bridge binding rate produced results consistent with both transient and steady-state FD experimental data. In our model, steady-state FD increased with work, decreased with shortening speed (constant shortening amplitude), and increased with shortening amplitude (constant speed), as observed experimentally by Herzog et al. (2000). Likewise, the exponential growth rate (*k*) decreased with work, and at a given speed, the recoverable force (*A*) increased with work: matching transient trends observed in recent FD experiments (Lee and Herzog, 2003). Furthermore, the increased steady-state FD was accompanied by a reduction in CE stiffness (Fig. 1). This
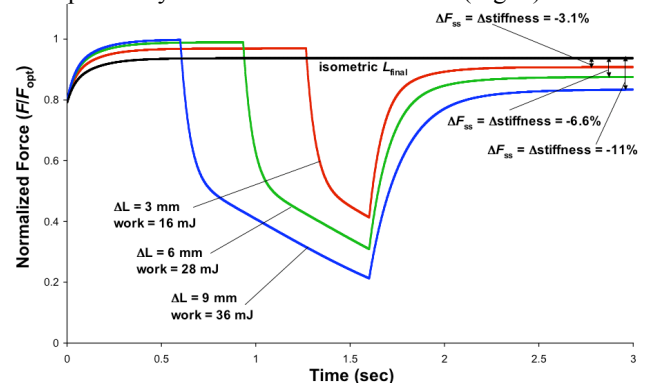

Figure 1: Simulation of three length changes (3, 6, 9 mm) at a constant shortening speed (9mm/s), ending at the same final length, illustrating the effect of shortening amplitude and mechanical work on steady-state FD and stiffness.

supports the findings of Sugi and Tsuchiya (1988), and strengthens the idea that FD is caused by a reduction in the number of attached cross-bridges (Ford et al., 1981). Our cross-bridge based model provides the relationship between work and steady-state FD, and gives the correct transient force behaviour and the correct force recovery as a by product. These theoretical results, coupled with recent experimental evidence, strongly suggest that FD may be caused by a single mechanism: a stress-related decrease in the cross-bridge attachment rate.

REFERENCES

Cole GK et al., (1996) *J Biomech* **29(8)**, 1091-1104.
Ford LE et al., (1981) *J Physiol (London)* **311**, 219-249.
Herzog W et al., (2000) *J Biomech* **33**, 659-668.
Huxley AF (1957) *Prog Biophys Biophys Chem* **7**, 255-318.
Lee HD and Herzog W, (2003) *J Physiol* **551.3**, 993-1003.
Maréchal G, Plaghki L (1979) *J Gen Physiol* **73**, 453-467.
Sugi H, Tsuchiya T (1988) *J Physiol (London)* **407**, 215-229.
Woittiez RD et al., (1984) *J Morphol* **182**, 95-113.
Zahalak GI and Ma SP (1990) *J Biomech Eng* **112**, 52-6.

ACKNOWLEDGEMENTS

BIOMECHANICAL BEHAVIOR OF MUSCLES IN THE ABDOMINAL WALL REINFORCED BY A POLYMER MESH

Uwe Schomburg and Michael Gregor
Helmut-Schmidt-Universität (UniBw H), Hamburg, Germany
e_schomb@unibw-hamburg.de, gregor@unibw-hamburg.de

INTRODUCTION

The abdominal wall is build up of different load carrying layers, particularly fascias and muscles. Due to an overstraining especially of a post-operative scar in the abdominal wall an incisional hernia might happen (Schumpelick 1999). Experience has shown that normal sutures have a high rate of recurrence. To reduce this rate reinforcing artificial meshes have been implanted successfully either onlay, inlay or sublay. For the meshes different polymers are in use, e. g. polypropylene, polyester, polyethylene terephthalate and expanded polytetra-fluorethylene. They are all chemically inert, non-immunogenic, non-toxic but biologically they can generate inflammation, fibrosis, infections and other undesired reactions (Klosterhalfen 1999). In addition chronic pain and a stiff scar plate around the mesh can appear. Definitely the pore size and the filamentous structure (monofil or multifil) of the mesh have a strong influence on the reactions mentioned (Klinge 2002). But some effects can be explained by mechanics. So the paper focuses in particular on the mechanical aspects. For the mechanical analysis the properties of the biological tissues in the abdominal wall and of the meshes have to be measured first.

METHODS

As really no appropriate stress strain curves of passive muscles and fascias were available, tests were carried out.

As testing material hybrid pigs were chosen, because the properties of their abdominal walls are similar to those of humans.

One of the most complicated problems in testing soft tissues is the development of a suitable clamping in order to avoid slipping and to achieve fracture outside the clamping. Therefore an appropriate clamping was developed.

Tests were carried out directly post mortem but before rigor mortis occurred. The fascia was carefully separated from the muscle. All experiments were performed at room temperature. The applied strainrate was 25%/min, which corresponds to the respiration velocity.

The experiments were conducted on the passive components of the abdominal wall. Due to the fibre orientation, the properties of the muscles are transversely isotropic. For that reason tensile tests parallel and perpendicular to the fibre direction were performed to characterize the tensile properties of the different layers of the abdominal wall. In the case of transversely isotropic materials, the shear stiffness perpendicular to the fibre direction is independent of the tensile stiffness. Therefore simple shear tests with the components of the abdominal wall were also performed, so that the properties of the abdominal wall are fully characterized. We also measured the in vivo "prestrain" of the muscles by marking a patch on the intact muscle, cutting it out and measuring the patch again. The results explain the differences between earlier published results of tests in vivo and in vitro.

The mesh tests were conducted with specimen 10cm long and 5cm wide. Before clamping the meshes were folded to 1/3 of their width to reduce necking.

RESULTS AND DISCUSSION

The measured stress strain curves of the biological tissues show the expected scatter and highly non-linear behavior, which could be assumed without much loss of accuracy as elastic. In addition a considerable anisotropy can be recognized.

The stress strain relations of the meshes reveal that the different meshes have quite different stiffnesses but in comparison with the biological tissues they are all much stiffer. The meshes also show an anisotropic, non-linear and nearly elastic behavior under the circumstances which are here to be assumed. Finite element simulations of the moving abdominal wall (e. g. by breathing) get somewhat complicated due to the situation that the mesh is attached to the prestrained biological tissues. First simplified finite element calculations reveal the highest stresses at the edges of the mesh.

These high stresses lead to the inflammation which was observed by pathologists in particular at the edges of meshes with a high ability to attach to biological tissues, like PP-, PES- and PET-meshes. The finite element solution also gives some indications about scar formation.

SUMMARY

The mechanical properties of the abdominal wall and of reinforcing polymer meshes were measured and used for finite element simulations of the movement of the reinforced abdominal wall.

REFERENCES

Schumpelick, V., Kingsnorth, A. N. (Eds.) (1999). Incisional Hemia. Springer, Berlin Heidelberg New York.
Klosterhalfen, B., Klinge, U. (1999) in: Schumpelick, V., Kingsnorth, A. N. (Eds.). Incisional Hemia. Springer, Berlin Heidelberg New York.
Klinge, U. et al (2002). J. Surg. Res. 103: 208-214.

FOOT TYPE CLASSIFICATION USING DISCRIMINANT FUNCTION ANALYSIS

M. Anbarian[1, 3], P. Allard[1], S. Hinse[2], N. Farahpour[3], A. Fall Diagne[4] and C. Tanaka[1,5]
[1] Kinesiology Department, University of Montreal, Quebec, Canada
[2] Cryos Technology Inc. Joliette, Canada, [3] Ph. Ed. Department, Bu-Ali Sina University, Hamadan, Iran
[4] Génie informatique, École Polytechnique de Montréal, Canada, [5] Universidade Sao Paulo, SP-BR, mehrdad.anbarian@umontreal.ca

INTRODUCTION
Foot form and function has been the core of many studies; however successful foot ailments classification remains limited. The difficulty lies in part on the means of assessing foot disorders such as visual inspection, foot morphology, radiography, etc. and on a few measurements to characterize foot morphology (Razeghi and Batt, 2002). There is a need to classify foot types based on several foot measurements taken from different perspectives to better describe foot morphology in a clinical environment. The objectives of this study are to: a) determine the geometric parameters that best characterize the differences between pes cavus (PC), pes planus (PP), pronation (PRO) supination (SUP) and a normal (NO) foot type and b) classify these feet into their appropriate group using the determined geometric parameters.

METHODS
321 feet were sorted into 4 pathological groups, pes cavus (n=115), pes planus (n=52), pronation (n=80) and supination (n=48) and a normal group (n=26) by an experienced podiatrist.

A digital camera was used to capture black and white images taken from the antero-posterior, postero-anterior and medio-lateral views of weight-bearing feet as well as from the posterior view of the foot in plantar flexion with weight bearing. Camera-subject distance was fixed at approximately 1.7 m though subjects were asked to assume a free standing foot position to avoid imposing a fixed stance position. The pictures were then processed by a numerical filter where the grey levels were transformed into a color-coded image highlighting muscle and bone prominences. This process facilitated the measurement of 15 foot angles (Fig. 1).

A stepwise discriminant function analysis (DFA) was performed to determine the relevant geometric characteristics the groups. Then, the sample previously sorted in 5 groups was classified according to 15 foot angles.
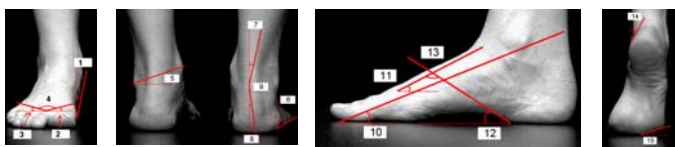

Figure 1: Foot angles description.

RESULTS AND DISCUSSION
DFA revealed 4 significant functions explaining 68.2%, 24.0%, 5.8% and 2.1% of the variance respectively. The model identified 9 angles (3, 4, 5, 6, 9, 10, 12, 13 and 15) in stepwise analysis to discriminate between groups. The first function differentiated the PRO group from the others and mostly correlated with angles 9 (0.73) and 12 (0.46) (Table 1). These parameters were previously used to recognized abnormal foot structure. Second function distinguished the NO group from the others using angles 4, 3, 15 and 10.

Five foot types were classified using the above 9 parameters. With the DFA approach, 81.4% of the feet were successfully classified. Only, the PP group was poorly identified (50%) as compared to a mean success rate of 89% for the other four groups (Fig, 2). To our knowledge no one has yet reported a classification in which both able-bodied and pathological feet were presented. Furthermore, previous studies were limited to three foot pathologies or less (McPoil and Hunt, 1995).

SUMMARY
321 feet were divided into a group of able-bodied feet and four types of pathological feet. 15 angle measurements taken from color-coded images from four views were taken to describe the feet. From these, DFA identified 9 angles to characterize all feet. Still using DFA, the feet correctly classified 81% of the cases.

Table 1: Structure matrix and functions at group centroids

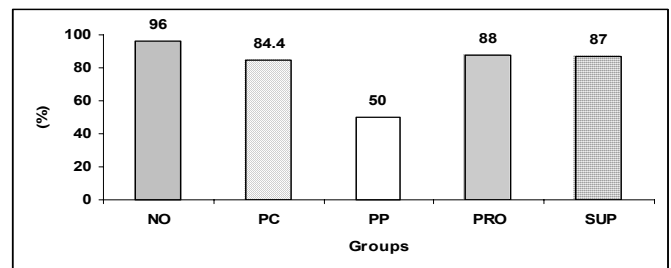| Angle | Structure matrix | | | | Group | Group centroids | | | |
| | Function | | | | | Function | | | |
	1	2	3	4		1	2	3	4
3	.13	.57	.11	.54	NO	-.9	3.4	-.59	-.24
4	-.20	.62	.41	-.09		-1.5	-.07	.47	-.07
5	-.09	-.02	.34	-.27	PC				
6	-.11	.26	-.22	.04		1.8	.41	.07	.7
9	.73	.1	.45	-.35	PP				
10	-.17	.43	.11	-.11		2.4	-.53	-.11	-.31
12	-.5	-.1	.12	-.12	PRO				
13	.48	.14	-.02	.58		-2.4	-1.2	-.85	.1
15	.07	.51	-.07	.29	SUP				

Figure 2: Classification results.

REFERENCES
Razeghi M and Batt ME (2002)*Gait and posture*, **15**, 282-291.
McPoil TG and Hunt GC (1995*) JOSPT*, **21**: 6, 381-388.

FORCE-LENGTH RELATIONSHIP OF MOUSE SOLEUS AND OPTIMAL STIMULATION PARAMETERS FOR FORCE ENHANCEMENT PROTOCOLS

Andrew Betik and Walter Herzog

Human Performance Laboratory, Faculty of Kinesiology, University of Calgary, Calgary, Canada

INTRODUCTION

Over the last decade or so, our laboratory has contributed significantly to the history-dependence of muscle force literature (Herzog and Rassier 2004). The mechanisms of force depression and force enhancement still remain elusive. Engagement of a passive elastic element upon active stretching has been hypothesized as a contributing factor in force enhancement (Edman et al. 1978, Herzog and Leonard 2002, Labeit et al. 2003). In order to further investigate this mechanism, we will be performing experiments on the soleus muscle of normal and knock-out mice. To do this, it is necessary to understand the force-length properties of this muscle, along with the involvement of passive force as the muscle is stretched. It is also necessary to understand optimal stimulation parameters that will allow for, 1) fused tetanus; 2) maintenance of a stable force for prolonged contractions (6-8 s); and 3) appropriate relaxation times between contractions. This data represents preliminary work to force enhancement experiments on the mouse soleus.

METHODS

Adult male, C57 mice (age ~ 5 months), were anesthetized with an isofluorane/oxygen mixture. The hindlimb was dissected, and all muscles except the soleus were separated from the Achilles tendon. A part of the calcaneous that was connected to the tendon was cut and clamped to a load cell (LCFA-150, Omega, Laval, Canada), which was attached to a muscle puller (404 LXR, Compumotor, Calif). Bipolar electrode hooks were brought in contact with the tibial nerve for soleus stimulation. The muscle preparation was kept at ~35°C using a warm saline drip (0.9%) and an adjustable infrared heat lamp. During initial testing, stimulation frequency (30Hz – 200Hz), duration (0.5 s – 8 s) and rest time (15 s – 180 s) were altered between contractions to determine optimal conditions for future experiments. Stimulation pulses were 0.1 ms duration and the voltage was three times greater than the αlpha-motoneuron threshold (~2V) to ensure complete activation.

Force-length relationships were determined by increasing the length of the muscle by at least 0.4mm increments and stimulating the muscle at 40Hz for 1 s with 60 s rest between contractions. Muscle position is arbitrary, with 0mm being the shortest muscle length in which muscle force is zero (or near zero). Passive forces were subtracted from the total force in order to achieve an active force-length relationship, as well as a passive force-length relationship.

RESULTS AND DISCUSSION

Figure 1 represents a typical force-length relationship of the mouse soleus muscle. The plateau region is in the range of 4.0-4.4mm. Peak forces were in the range of 180mN – 300mN (at 40Hz), in good agreement with the literature (Askew and Marsh 1998, Lynch et al. 2001). The passive force at this muscle length was ~12% of the active force.
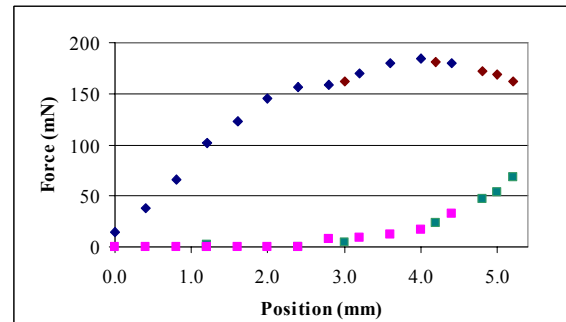

Figure 1: Typical force-length relationship of the mouse soleus stimulated at 40Hz. 0mm is an arbitrary position in which muscle force was closest to zero.

Passive force was negligible until ~2.0mm. For prolonged contractions (8 s), muscle force was unchanged using a 50Hz stimulation frequency. Using higher frequencies, the force would decrease as a result of fatigue. For lower stimulation frequencies (30 and 40Hz), we observed a slight increase in force over the 8 s contraction. Our lab often uses 30Hz for the cat soleus, however, unlike the cat soleus which is near 100% slow twitch fibre, the soleus of the mouse is only ~60% slow twitch (Warmington et al. 2000). During repeated contractions under the same parameters and same muscle length, we found forces to be consistent and repeatable with 60 s rest. 45 s and less did not provide enough recovery after long contractions, whereas longer rest did not improve the consistency of force measurements compared to 60 s rest.

SUMMARY

Optimal stimulation parameters of 50Hz stimulation frequency and 60 s rest between contractions have been determined for future force enhancement experiments on the mouse soleus. Understanding the typical force-length relationship allows us to perform experiments on different parts of the force-length curve, and to compare normal to knock-out models of the mouse soleus.

REFERENCES

Askew, G.N. and Marsh, R.L. (1998). *J Exp Biology*, **201**: 1527-1540.

Edman, K.A.P. et al. (1978). *J Physiol*, **281**, 139-155.

Herzog, W. and Leonard, T.R. (2002). *J Exp Biology*, **205**:1275-1283.

Labeit et al. (2003). *PNAS*, **100**(23): 13716-13721.

Lynch et al. (2001). *J Physiol*, **535** : 591-600.

Rassier, D.E. and Herzog, W. (2004). *J Appl Physiol*, **96** : 419-427.

Warmington et al. (2000) *Int J Obes Relat Metab Disord*, **24**, 1040-1050.

DETERMINATION OF CRITICAL TRANSITORY PERIODS
IN POSTURAL CONTROL OVER LIFE SPAN

Nicolas Termoz[1,2] and François Prince[1]

[1]L.P.L., Centre de réadaptation Marie Enfant, Hôpital Sainte Justine, Montréal, Québec, Canada
[2]Laboratoire S.P.M., U.F.R.A.P.S., Université Joseph Fourier, Grenoble, France, nicolas.termoz@ujf-grenoble.fr

INTRODUCTION

Postural control is a complex process that implies neural integration from multiple cues such as proprioception, vision, vestibular and audition. In the first part of life, the development of this ability is non linear and mainly depends on the maturation of these sensory cues [1] whereas in its late part, neurosensorial degeneration interferes to increase instability [2]. Several studies analyzed the developmental aspects of postural control over a wide span of life [3] but none has tried to determine critical transition periods in the maturation and degeneration processes. Therefore, the aim of the present study is to determine these transitory postural phases based on a relevant postural variable.

METHODS

Postural sway behaviour was assessed using an AMTI platform (20Hz) during 120 s of quiet standing in three groups: 18 children (12.6 yrs ± 1.9), 20 adults (31.7 yrs ± 8.9) and 16 elderly (69.4 yrs ± 6.5). The sway parameter investigated was the mean velocity of the centre of pressure (Vel_{COP}) along the anterior-posterior (A/P) and medial-lateral directions (M/L). This parameter was recognized as the most sensitive to postural developmental variable [1] and the most reliable one for postural study [4]. We have calculated a linear fit for each group and the critical transition periods between children and adults (Pt1) and between adults and elderly (Pt2) were determined by calculating the intersection point of the two consecutive linear fits. A one-way ANOVA was performed to assess differences ($p<0.05$) between groups along the A/P and M/L directions.

RESULTS AND DISCUSSION

Figure 1 reports the overall distribution of the Vel_{COP} along the A/P and M/L directions. As expected, there was a rapid improvement of postural control from the children to the adults followed by a slow decline to older ages. The statistical analysis (Table1) revealed group effects along both the A/P ($F_{2,51}=13.68$; $p<0.001$) and M/L axes ($F_{2,51}=27.71$; $p<0.001$).

	A/P	M/L
Children	8.7 mm.s^{-1} (± 2.9)*	6.8 mm.s^{-1} (± 3.1)*
Adults	5.3 mm.s^{-1} (± 1.4)*	2.7 mm.s^{-1} (± 1.0)
Elderly	6.8 mm.s^{-1} (± 1.3)*	2.6 mm.s^{-1} (± 0.7)

Table 1: Vel_{COP} for the three groups along the A/P and M/L axes. * Significantly different from the other groups.
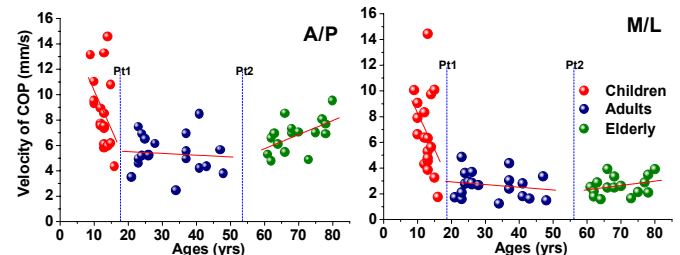

Figure 1: Distribution of Vel_{COP} for the three groups and corresponding linear fit.

The intersection points between the linear fits revealed a mean age of $Pt1_{A/P}=17.9$yrs and $Pt1_{M/L}=19.5$yrs between the children and the adults group, and $Pt2_{A/P}=54.0$yrs and $Pt2_{M/L}=55.2$yrs between the adults and the elderly group.

These points were almost similar in the A/P and M/L directions suggesting that the postural maturity is achieved at around 18 years old and that the impact of slow degeneration processes on postural control occurs at around 55 years old. The improvement of postural control is related to the maturity of neurophysiological factors as well as the internal knowledge of inertial and dynamical parameters of the body. Therefore, it is not surprising that adult-like postural control appears when growth processes are completed. In contrast, older people could increase the Vel_{COP} in order to stimulate plantar mechanoreceptors such as Meissner's Corpuscle and to make up for their decrease in sensory information processing. Finally, the U-shape distribution observed in the present study only concerns ages from 9 to 80 because, for younger children, Kirshenbaum et al., (2001) recently reported a non-monotonic evolution in postural control strategy with a transition around 8 years old. Nevertheless, the method proposed in the present study allows to determine the actual periods of postural maturity and of the first impact of sensory degenerative processes in balance regulation.

SUMMARY

In the present study, we developed a method to determine the periods when the postural control is adult-like and when it first undergoes the effects of natural sensory degeneration. Our results revealed that postural maturity is achieved close to 18 and that neurosensorial degeneration actually acts on postural control around 55.

REFERENCES

[1] Kirshenbaum, N. et al (2001) *Exp Brain Res*, **140,** 420-431.
[2] Alexander, N.B. (1994) *J Am Geriatr Soc*, **42**, 93-108.
[3] Berger, W. (1992) *Exp Brain Res*, **90**, 610-619.
[4] Lafond, D. (2004) *Arch Phys Med Rehab*, in press.

CHANGES IN MONO- AND BIARTICULAR MUSCLE ACTIVATION PATTERNS WHILE LEARNING TO DIRECT PEDAL FORCES

Christopher J. Hasson, Rachel E. Merrell, Richard E.A. van Emmerik, and Graham E. Caldwell

Biomechanics and Motor Control Laboratories, University of Massachusetts, Amherst, MA, USA, cjhasson@excsci.umass.edu

INTRODUCTION

Research has suggested that mono- and biarticular muscles have unique roles in producing movement (van Ingen Schenau 1989). It has been posited that monoarticular muscles act primarily as force generators, while biarticular muscles assist in 1) transferring energy between joints, and 2) directing external forces by distributing joint moments. The present study is a preliminary investigation of possible changes in the activation patterns of mono- and biarticular muscles during the learning of a novel one-legged cycling task. It was anticipated that the activation of the biarticular muscles, but not the monoarticular muscles, would transition from a general to a more specific pattern once the task is learned.

METHODS

Three male recreational cyclists participated in the study. Participants were required to practice one-legged cycling on a bicycle mounted on a computerized ergometer. Prior to the experiment, participants were instructed on the correct way to direct their applied pedal forces. At any given position in the crank cycle, the ideal direction of force application is perpendicular to the crank arm. The goal of the pedaling task was to minimize errors between the applied and ideal force directions. For reference, 0º (360º) represents the crank with the pedal at the highest position, 180º at the lowest position.

Each participant attended a single test session lasting about 90 min. A total of 15 training trials were performed, with an additional post-training trial completed 20 min after the 15th trial. Each trial consisted of a warm-up, followed by 1 min of one-legged cycling using the left leg. Data were collected for 5 s at the beginning, middle, and end of each training trial. A 5 min rest was provided between the trials. During each rest interval, participants were given visual and verbal feedback about their performance on the force-directing task.

Kinematic, kinetic, and electromyographic (EMG) data were collected. The kinematic data were sampled at 200 Hz; the kinetic and EMG data were sampled at 1000 Hz. Five digital cameras were used to collect three-dimensional kinematic data, with markers placed on the bicycle to yield the crank and pedal angles. Kinetic data were measured using a clip-in pedal instrumented with two load washers, mounted on the left crank arm of the bicycle (Caldwell et al. 1998). EMG data were collected via bipolar surface electrodes from 4 monoarticular [tibialis anterior (TA), soleus (SO), vastus lateralis (VL), and gluteus maximus (GM)], and 3 biarticular [rectus femoris (RF), semitendinosus (ST), and gastrocnemius (GA)] muscles of the left leg.

To quantify the performance of the task, the root-mean-squared error (RMSE) between the direction of the applied force vector and the ideal force vector was calculated. EMG data were rectified, low-pass filtered at 10 Hz, and normalized to the crank cycle. Muscle activation times were then determined relative to crank position (0º – 360º).

RESULTS AND DISCUSSION

Following the practice trials, all participants showed an improvement in their force directing ability (Table 1). Muscle activation patterns changed in both mono- and biarticular muscles (Table 1), although it appears each participant used a unique strategy throughout the learning process (Figure 1).
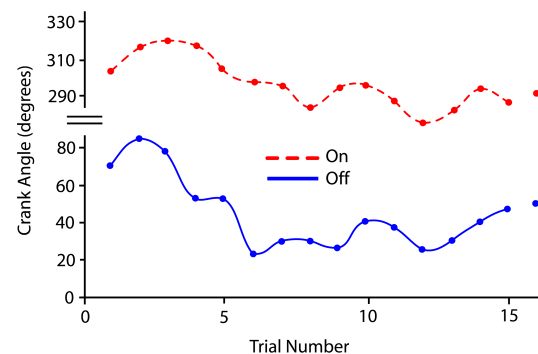

Figure 1. Exemplar data from a single participant showing changes in RF activation (onset & offset).

SUMMARY

The present study provides evidence that participants were able to learn a novel one-legged cycling task, and that the timing of their muscular activations was altered. At this stage of learning, it seems that both mono- and biarticular muscles are involved in the learning process.

REFERENCES

Caldwell, G.E. et al (1998) *J. Appl. Biomech.,* **14,** 245-59.
van Ingen Schenau, G.J. (1989) *Hum. Mov. Sci.,* **8,** 301-37.

Table 1. Changes in RMSE and muscle activation timing in mono- and biarticular muscles for all participants pre – post training.

Participant	RMSE (%)[A]	Monoarticular Muscles [Δ in timing (degrees)][B]				Biarticular Muscles [Δ in timing (degrees)][B]			
		VL On	VL Off	TA On	TA Off	RF On	RF Off	ST On	ST Off
1	24.13	1	13	41	10	26	29	30	4
2	30.41	95	23	†	†	38	33	28	26
3	20.87	18	21	127	1	12	25	64	2

[A]Percent improvement in RMSE (between the applied and ideal force directions).
[B]Absolute change in muscle activation timing, based on the angular position of the crank arm; †corrupt data.

SENSITIVITY OF THE PLANTAR FOOT IN DIFFERENT AGE GROUPS

Beate Prätorius, Thomas L. Milani

Department of Human Locomotion, University of Duisburg-Essen, Germany, beate.praetorius@uni-essen.de

Introduction

It is well documented that human balance control is determined by the integration of the somatosensory, the visual and the vestibular system [2]. The abilities of balance control decrease with ageing [3]. Moreover, the essential role of the somatosensory system with regard to balance control has been proven [2, 4].

It has been shown that tactile thresholds increase significantly with age [7]. Moreover, e.g. in Parkinsons Disease – that is associated with impaired balance control [6] – the sensitivity of the plantar foot is dramatically reduced in comparison to healthy, age matched subjects [5]. These findings underline the importance of sensory input of the foot sole for balance control in daily tasks and consequently for sportive activity.

Therefore, the purpose of this study was to determine sensitivity thresholds in children, young adults, senior adults and PD-Patients.

Methods

412 Participants of three different age groups and one group of PD-Patients (Parkinsons Disease) were examined. The age of the groups was: 8 ± 2.5 Yrs. (Children), 25 ± 2.5 Yrs. (Students), 64 ± 4.3 Yrs. (Seniors) and 67 ± 7.5 Yrs. (PD-Patients). Tactile thresholds were determined by usage of Semmes-Weinstein Monofilaments (North Coast Medical, Inc., San Jose, CA) with a modified 4, 2 and 1 Stepping Algorithm [1]. Vibration thresholds were detected due to amplitude increase of a Vibration-Exciter at a frequency of 30 Hz. For both of the skills thresholds of five locations of the plantar foot (heel (1), arch (2), 1st (3) and 5th (4) metatarsal head and hallux (5)) were determined. Sensitivity thresholds were averaged and analyzed with inferential statistics (t-test). A sensitivity parameter for each subject was determined by averaging tactile and vibration thresholds for the five foot locations.

Results and Discussion

In general, the results show an increase of tactile as well as vibration thresholds with ageing. However, the characteristics of increase are different:

Regarding the tactile sensitivity, the increase of the different thresholds under the five locations is fairly constant with ageing. Furthermore, the differences between the foot locations within the age groups increase with ageing as well. Comparing the single locations a sensitivity pattern could be determined: Arch, Hallux, 1st metatarsal head, 5th metatarsal head and heel (from most sensitive to least sensitive). This pattern persists in all tested groups. Under the five foot locations, significant differences ($p < .01$) between all age groups could be revealed (Fig. 1) when comparing the tactile sensitivity values.

The vibration threshold values also increase with ageing: Comparing the averaged sensitivity parameters there are significant differences between all age groups for vibration ($p < .01$) thresholds (Fig. 2). Surprisingly, vibration thresholds of children and students show no statistically different values, whereas considerable differences between young and older subjects, respectively patients could be found. In seniors and patients the vibration thresholds are significantly higher. Regarding the single locations under the foot there is no constant sensitivity pattern between the groups.

Summary

Results out of this study confirm a significant increase of tactile and vibration thresholds with ageing.

The loss of tactile and even more vibration sensitivity in ageing could be an explanation for reduced balance control. Therefore, therapy treatments with respect to foot sensation should be considered in training programs to maintain balance control in elderly and patients.

References

[1] Dyck, P.J. (1998). Neurology, 43, 1508-1512
[2] Maurer, C. et al. (2000). Neurosci. Lett., 281, 99-102.
[3] Neil, B.A. (1994). JAGS, 42, 93-108.
[4] Perry S. D. et al. (2000). Brain Research 877, 401-406.
[5] Prätorius, B. et al. (2003). Neurosci. Lett., 346, 173-176.
[6] Rogers, M.W. (1996). CGM, 12, 825-845.
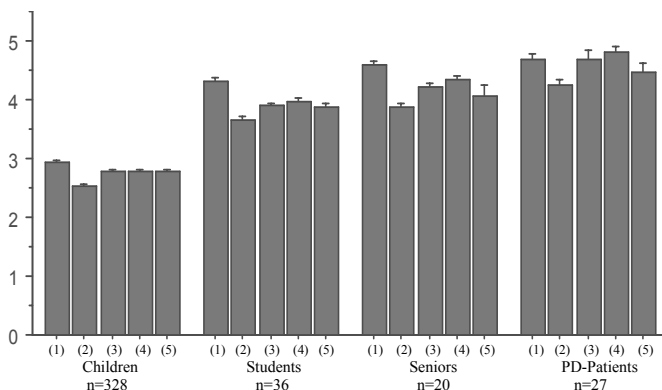[7]Thornbury, J.M. et al. (1981), J Gerontol., 36, 34-39, 115-122.

Fig. 1: Thresholds of tactile sensitivity for five locations (1)-(5) (in SWM)
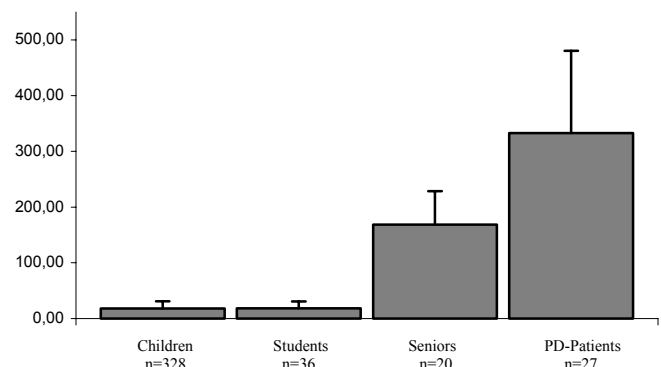

Fig. 2: Thresholds of vibration sensitivity for five locations (1)-(5) (in SWM-units)

POSTURAL RESPONSES IN FRONTAL PLANE TO STEPWISE MONOPOLAR ANODAL GVS

N Deshpande and A E Patla

Department of Kinesiology, University of Waterloo, Waterloo, Ontario

INTRODUCTION: Transmastoidal binaural bipolar galvanic vestibular stimulation (GVS) causes an imbalance in firing rate of two vestibular nerves. This induces postural responses in frontal plane (mediolaterally) when facing forward and in sagital plane (anteroposteriorly) when head is turned to one side (Lund & Broberg, 1983, Cauquil et al., 2000). Since the firing rate of the vestibular nerve on the anodal side reduces significantly (Goldberg et al., 1984), this pilot study investigated postural responses to binaural monopolar anodal GVS that were possibly mediated by a bilateral decrease in vestibular information thus reducing overall vestibular bias.

METHODS: 5 healthy subjects stood facing forward for one minute with their eyes closed on a hard surface (EC) and on foam (EC+F). The subjects selected their natural stance width on the hard surface that was maintained throughout the experiment. On randomly selected trials in these two conditions, transmastoidal GVS (1mAmp) was started between 10 to 15 seconds after initiation of the data collection and was maintained for 10 seconds (EC+GVS and EC+F+GVS). The net center of pressure (CoP) was recorded. The peak to peak (p-p) CoP excursion, CoP velocity (Vel), variability of CoP excursion (RMS) and mean power frequency (MPF) were analysed in EC+GVS and EC+F+GVS condition for 3 bins: 10 seconds prior to GVS (pre-stim), 10 seconds during stimulation (stim) and 10 seconds after stimulation (post-stim) to isolate the effects of GVS under different sensory conditions. To this effect, a separate repeated measure ANOVA was used for anteroposterior (A-P) and mediolateral (M-L) directions.

RESULTS: Fig. 1 presents the M-L CoP excursion in pre-stim, stim and post-stim 10 second bins of a representative subject for one trial standing on foam.

When subjects stood on foam, p-p and Vel significantly increased in M-L direction during GVS application (in stim bin) compared to prior the GVS (pre-stim). The RMS values in

M-L direction increased in stim bin irrespective of the support surface. The decrease in p-p, Vel and the RMS values in post-stim bin, however, did not reach pre-stim level, possibly due to a mild postural response when GVS was switched off (see Fig.1) None of the sway parameters in sagital plane were significantly altered in stim bin on either support surfaces. The MPF was not affected by the GVS in either direction (Table1).

Table 1: Peak to peak (P-P) CoP excursion, CoP velocity (Vel), RMS of CoP excursion and mean power frequency (MPF) for pre-stim, stim and post-stim bins of EC+F+GVS condition in anteroposterior (A-P) and mediolateral (M-L) direction. * shows a significant difference during GVS, at p=0.05

		P-P (cm)	Vel (cm/sec)	RMS (cm)	MPF (Hz)
	Pre-stim	2.46±0.19	1.15±0.09	0.58±0.04	0.43±0.03
A-P	stim	2.71±0.20	1.55±0.12	0.63±0.05	0.40±0.03
	Post-stim	2.49±0.19	1.32±0.10	0.65±0.05	0.43±0.03
	Pre-stim	1.41±0.11	0.63±0.05	0.34±0.02	0.49±0.04
M-L	stim	2.40±0.18*	1.27±0.09*	0.51±0.04*	0.47±0.03
	Post-stim	1.76±0.13	0.77±0.06	0.39±0.03	0.48±0.03

DISCUSSION: The transmastoidal monopolar anodal stimulation clearly elicited postural responses in frontal plane, primarily when standing on foam. Reduced postural stability in frontal plane observed in this study can be attributed to overall decrease in vestibular system bias leading to reduced vestibulospinal drive on postural muscles; that manifested more prominently when the information from the remaining two sensory systems namely, vision and lower leg somatosensoty system, were unreliable. The A-P CoP displacement did not increase with monopolar anodal GVS while standing on a hard surface as reported by Cauquil et al. (1998). This inconsistency may have resulted from differences in the electrode configuration and a smaller base of support used in their study. However, a lack of monopolar GVS effect on postural parameters in sagital plane on the foam surface in this study should be interpreted with caution due to a low statistical power in that direction. Ongoing research will investigate the utility of transmastoidal monopolar anodal GVS as an experimental tool to suppress vestibular information during various dynamic tasks such as perturbed standing and locomotion.
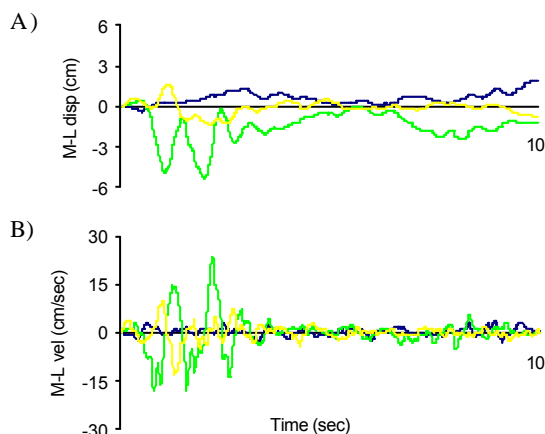

Fig 1: Mediolateral CoP displacement (A) and velocity (B) profiles in pre-stim (blue), stim (green) and post-stim (yellow) bins in EC+F+GVS condition. Both, displacement and velocity increased significantly when stepwise monopolar GVS was applied while standing on foam. The increase in magnitude during initial response to GVS is apparent.

REFERENCES :

Lund S and Broberg C. 1983 Acta Physiol Scan. 117 (307-9),
Goldberg JM et al. 1984 J Neurophysiol 51 (1236-56)
Severac Cauquil A et al. 1998 Neurosci Lett 245 (37-40)
Severac Cauquil A et al. 2000 Exp Brain Res 133 (501-5)

EXPERIMENTAL ANALYSIS OF TRIBOLOGICAL PROPERTIES OF BIOMATERIALS USED FOR ORTHOPEDIC IMPLANTS

Radek Sedlacek, Jana Rosenkrancova

Czech Technical University, Faculty of Mechanical Engineering, Department of Mechanics,
Technicka 4, 166 07 Prague, Czech Republic, radek.sedlacek@fs.cvut.cz

INTRODUCTION

No known surgical implant material has ever been shown to be completely free of adverse reactions in the human body. However, long-time clinical experience of use of the biomaterials has shown that an acceptable level of biological response can be expected, when the material is used in appropriate applications.

This article deals with very specific wear resistance testing of the bio-compatible and bio-stable materials used for surgical implants. The abrasion is indispensable parameter for evaluation of the mechanical properties. This type of testing is very important for appreciation of new directions at the joint replacement design (for example in total knee replacement). The special experiments were carried out in collaboration with company Walter Corporation - developing and producing bone-substitute biomaterials and implants.

METHODS

The special wear resistance tests, called "Ring On Disc", were carried out with pairs of different biomaterials (100 hours of testing per each tested pair). The experiment was executed according to ISO 6474:1994(E). International Standard deals with evaluation of properties of biomaterials used for production of bone spacers, bone replacement and components of orthopedic joint prostheses. The standard requires a long-time mechanical testing at which a complete volume of worn material is evaluated. The test conditions, requirements on the testing system and specimens' preparation are closely determined. The testing objectivity is ensured by the procedure for the specimens' treatment and their evaluation.

The method is based on loading and rotating two pieces from biomaterials (Fig. 1). A ring is loaded onto a flat plate from different material. The axial load that is applied on the ring is all the time constant. The ring is rotated through an arc of $\pm 25°$ at a frequency of (1 ± 0.1) Hz for a given period of time (100 ± 1) hours. There is distilled water using as the surrounding medium.
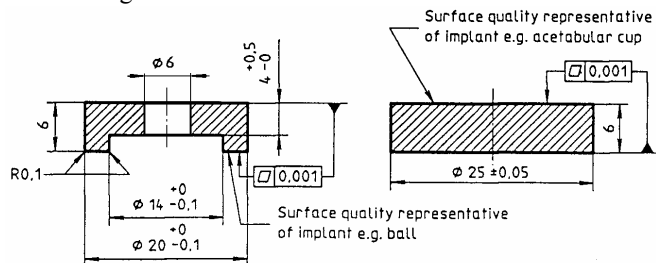

Figure 1: Geometry of ring and disc test pieces with dimensions.

The special jigs for fixing both specimens during testing were developed and produced. The disc-holding device is equipped with the especial joint to ensure the plane of the disc surface coincides with the plane of the ring surface at all times during the test.

As a measure of wear resistance is determined and used volume of the wear track on the disc. The wear track cross-sectional area is analyzed from measured profile and the volume is calculated for each disc alone. After that the average volume is calculated for group of specimens.

The experiment was carried out on the top quality testing system MTS 858 MINI BIONIX placed in "Laboratory of Human Biomechanics" at the Czech Technical University in Prague (Czech Republic, Europe Union).

RESULTS AND DISCUSSION

The tests were executed with 5 groups of specimens from different materials. There were 5 tested pairs in each group. That means 5x5x100 hours of testing. The finished parameters obtained in this test - the wear volume - were calculated (see Tab. 1)

Table 1 – Final parameters of mechanical testing.

Material of RING	Material of DISC	Wear volume [mm^3]
Zirconia ceramics (Y-TZP)	Alumina ceramics	0,16
Zirconia ceramics (Y-TZP)	Pressed UHMWPE	2,95
Zirconia ceramics (Y-TZP)	UHMWPE	4,64
Titanium alloy (Ti$_6$Al$_4$V) with DLC	UHMWPE	6,61
Zirconia ceramics (Y-TZP)	PEEK (PolyEtherEtherKetone)	7,59

SUMMARY

We obtained the objective information about wear resistance for these combinations of materials. The resulting wear volume indicates the amount of elements that are loosening during loading of the bone substitute implant in human body and describes one from the mechanical properties.

REFERENCES

Sedlacek, R. – Rosenkrancova, J. (2003). *Bioceramics*, **16**, 703 – 706, Porto, Portugal

Sedlacek, R. – Konvickova, S. – Sochor, M. (2002). *International Journal of Applied Mechanics and Engineering*, **7**, 47 – 50, Zielona Gora, Poland

Sedlacek, R. – Rosenkrancova, J. (2001). *Workshop CTU*, **8**, 788 – 789, Prague, Czech Republic

ACKNOWLEDGEMENTS

ADAPTABILITY OF THE POSTURAL CONTROL MECHANISMS TO DELAYED TEMPORAL RELATIONSHIP BETWEEN THE MOTOR ACTION AND ITS CONSEQUENCES

Félix Berrigan and Martin Simoneau

Faculté de Médecine, Division de Kinésiologie, Université Laval, Québec, Québec, Canada,
E-mail: Martin.Simoneau@kin.msp.ulaval.ca

INTRODUCTION

It is well known that human can adapt its motor commands to novel dynamic consequences during object manipulation or reaching movement[1,2,3]. Less is known, however, about the ability of the CNS to learn new temporal relationship between the predicted and actual consequences of a descending motor command. For example, when a delay is introduced between the moment that the person self-initiates a perturbation and the moment that the perturbation occurs, the temporal relationship between the predicted and actual consequences of the motor action is necessary changed. Hence, the neural internal model has to be modified in order to capture the new causal relationship between the motor action and its consequences[4]. In the present study, we sought to examine the capability of the human brain to learn a delayed temporal relationship between the motor actions and its consequences during balance control.

METHODS

Ten healthy young adults participated in this study (8 men, 2 women; age 24.0 ± 4.8 years; height 1.75 ± 0.09 m; weight 73.3 ± 9.7 kg). Participants were standing upright barefoot on a force platform. Participants were told to stand still at all times keeping their feet flat on the ground, and to minimize joint movements. A steel cable was attached to a belt located at the third lumbar vertebrae that ran through a pulley and was attached to an electromagnet. The electromagnet held a preload, which was connected to a time delay generator device that allowed us to add a constant delay between the instant that the subjects switch off the electromagnet and the release of the preload. Participants were submitted to three experimental conditions. In the first condition (Pre), the participants' self-triggered the release of the preload which dropped instantly. In the second condition (Delay), a 540 ms delay (delay of 500 ms plus manufacture delay) was added between the moment the participants initiate the unloading and the instant the preload actually dropped. In the last condition (Post) the delay was withdraw. For the Pre, Delay and Post condition, thirty, sixty and thirty trials were performed. Participants had to stop the forward momentum generated by the unloading by reversing their joint torques which previously counteracted the backward force (preload).

RESULTS AND DISCUSSION

The results indicated that the participants chose a predictive torque strategy when the unloading was not delayed. During the first five trials of the Delay condition (Delay 1-5), the participants still used predictive torque strategy to counteract the expected unloading (see Fig. 1). They, however, modified rapidly their postural control strategy. After thirty trials (Delay 26-30) participants reacted to the unloading (*reactive torque strategy*). Interestingly, we also observed a modification of the postural control strategy within the Post condition. For the first five trials, the onset of the forward CP velocity followed the unloading (*reactive torque strategy*). At he end of the Post condition, the onset of the CP forward velocity preceded the unloading (*predictive torque strategy*). Altogether, these results demonstrated that the CNS, within thirty trials with a delay, could not shift forward in time a predictive torque strategy. On the other hand, it could easily switch from a reactive to a predictive torque strategy within thirty trials in the Post-delay condition when the temporal relationship between the motor action and its consequences is instantaneous.
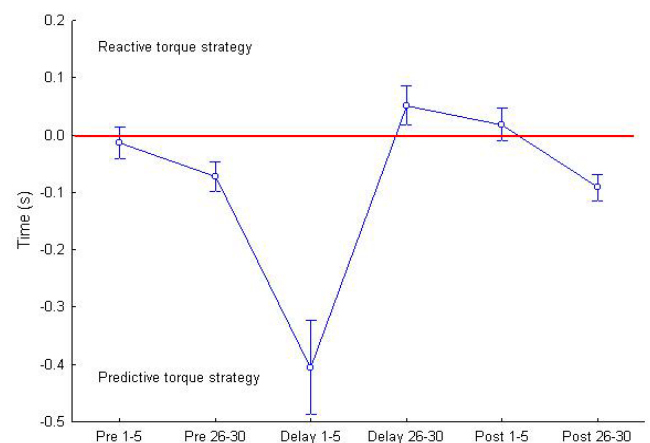

Figure 1: Onset of the CP forward velocity, before (predictive) or after (reactive) the unloading for the trials 1 to 5 and 26 to 30 of each condition.

In a study that assessed the affect of temporal delay (250 ms) in predictive grip force control, participants after being exposed to 250 trials succeeded in shifting forward in time their predictive grip force[4]. Hence, it is possible that the CNS could have returned to a predictive torque strategy with more trials in the Delay condition. It is also possible that the capacity of the brain to capture a new temporal relationship between the motor actions and its consequences is constrained by the duration of the delay.

SUMMARRY

The results of the present study suggest that during balance control the CNS could not shift forward in time a predictive torque strategy that would counteract a self-triggered delayed perturbation. Finally, the results demonstrated that the CNS could across trials, when the delay was withdraw, goes from a reactive to a predictive torque strategy within 30 trials.

REFERENCES

1. Johansson R.S. & Westling G. (1988). *Exp Brain Res*, **71**, 1-15.
2. Wing, A.M. et al (1997). *Exp Brain Res*, **116**, 122-130.
3. Toussaint, H.M. et al (1998). *Exp Brain Res*, **120**, 85-94.
4. Witney, A.G. et al (1999). *J. Neurophysiol*, **82**, 2039-2048.

COMPARISON OF LOADED AND UNLOADED RAMP DESCENT

Jordan Thornley[1] and D.G.E. Robertson[2]
Department of Human Kinetics, University of Ottawa, Ottawa, Canada
[1]j_thornley5@hotmail.com   [2]dger@uottawa.ca

INTRODUCTION

Little research exists examining the kinetics and kinematics of sloped walking. Upon unloaded ramp descent, significant changes in hip, knee and ankle powers have been recorded at a grade of 19% (Kuster *et al.*, 1995). However, no study has examined the compensatory effects of loaded ramp descent. It is believed that high loads placed on the lower extremity during downhill walking play a critical role in the development of joint and muscle soreness (Schwameder *et al.*, 1999). The implications of loaded slope walking may play on degenerative joint disease and other lower limb pathologies. As well, the revision of building codes to require ramps at public facilities allow an alternate way of transporting loads from one level to another. This research will help evaluate the means by which we transport loads down ramps.

METHODS

A sample population of five male volunteers participated in the study. Subjects were required to walk down a ramp with a 10-degree decline. Five trials were completed carrying no load and five trials were completed carrying 18.0 kg. Subjects were instructed to walk at a comfortable cadence.

A Kistler force plate recorded the ground reaction forces while a VHS camera collected the sagittal view trajectories of markers placed on the left side of the body. The video data were digitized and then kinematics of the three segments of the lower extremity computed. The force platform data were rotated to compensate for the 10-degree incline and then combined with the kinematic data, using inverse dynamics, to obtain the net moments of force and their associated powers at the ankle, knee and hip (Winter & Robertson, 1978). For comparative purposes the moments and powers were normalized to body mass. The data were ensemble averaged and normalized to body mass. All data were processed using Biomech Motion analysis system and Bioproc2.

RESULTS AND DISCUSSION

There appeared to be no significant difference between the net moments and peak powers of the ankle, knee and hip joints in comparison to unloaded ramp descent. As seen in Figure 1, A1 has depressed relative to level walking but remains unchanged in relation to unloaded ramp descent. Peak power of the ankle (A2) during loaded descent remained similar to that of unloaded ramp descent. No increase in concentric power at A2 indicates there was no additional requirement for propulsive force during load carriage.

A similar relationship existed amongst the moments and powers of the knee during unloaded and loaded descent. Both methods of descent possessed a clearly defined K1 and K3, while K2 assumed a negative value (Figure 2). Initial knee absorption following IFS (K1), failed to significantly increase during loaded descent. Load absorption may have been

achieved by the upper extremity or possibly a greater mass is required to exact a change in absorption requirements.

Hip moments and powers remained relatively inactive during both loaded and unloaded descent.
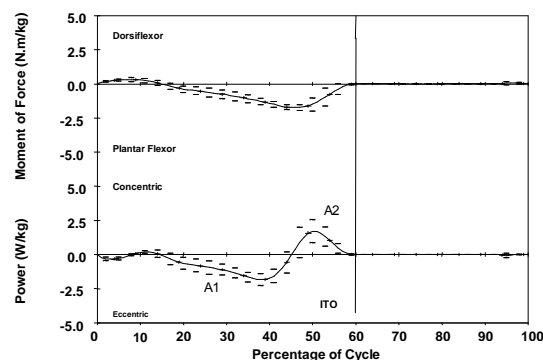

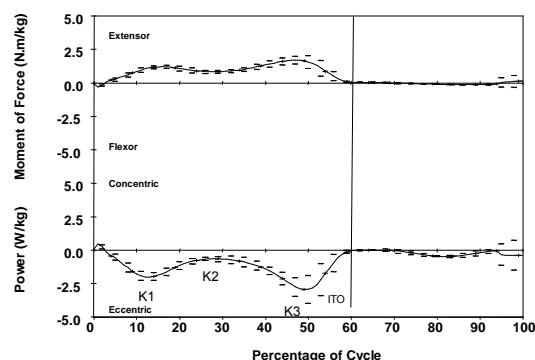**Figure 1.** Typical ankle net moments and powers (+/– 1 SD) for loaded ramp descent in a male subject.

Figure 2. Typical knee net moments and powers (+/– 1 SD) for loaded ramp descent in a male subject.

SUMMARY

The ankle was not required to generate additional propulsive force to carry a load down a ramp (see A2 of Figure 1). Likewise, the knee was not required to absorb additional force immediately following IFS (see K1 of Figure 2). A lack of significant results indicate that loaded ramp descent places no additional work load on the ankle, knee or hip, in comparison to unloaded ramp descent.

REFERENCES

Kuster *et al.* (1995). Kinematic and kinetic comparison of downhill walking. *Clinical Biomechanics*. **10**, 79-84.

Schwameder *et al.* (1999). Knee joint forces during downhill walking with hiking poles. *Journal of Sport Sciences*. **17**, 969-978

Winter, D.A. & Robertson, D.G.E. (1978). *Biological Cybernetics,* **29**, 137-142.

DIGASTRIC MUSCLE ACTIVITY: EVIDENCE FOR A ROLE IN NECK FLEXION?

Gray, J.R.[1], Skaggs, C.D.[2], & McGill, S.M.[1]
[1] Department of Kinesiology, University of Waterloo, Waterloo, Ontario, Canada. jrgray@uwaterloo.ca
[2] College of Chiropractic, Logan University, Chesterfield, Missouri, USA.

INTRODUCTION

To date, the relevance of the suprahyoid muscles (which includes the digastric muscle) in controlling head movement has remained largely unrecognized. Anatomical texts describe that neck flexion is governed by both the deep neck flexors and sternocleidomastoid (SCM) muscles. Research on muscle activity during neck flexion has concentrated on the deep neck flexors, such as Longus Colli (e.g., Jull et al., 2003). In the treatment of temporomandibular disorders (TMD), clinical insights have pointed to the potential importance of the suprahyoid muscles in producing and controlling neck flexion movements (e.g. Rocabado, 1983).

The supra- and infrahyoid muscles are traditionally described in terms of their contributions to mandible depression or hyoid elevation or depression (Moore & Dalley, 1999). However, their location superficially on the anterior wall of the neck, inferosuperior orientation, and attachment to the sternum, mandible, and cranium, suggests a potential role as a neck flexor. Although there are few human investigations that have studied the role of the hyoid muscles, Bérzin (1995) suggested that they did not take part in the movement of the head in upright posture.

Interestingly, no studies have evaluated the hyoid muscles while the body is supine despite their obvious relevance to neck flexion in this position. The current study was conducted to evaluate the activity of the digastric and SCM muscles as a result of orofacial muscle contraction and isometric head support in supine.

METHODS

Five women and five men (age = 29(6) yr; height = 1.72(0.11) m, mass = 69.1(17.3) kg) were recruited from the university population. All subjects were healthy with no history of TMD. SEMG of the suprahyoid (digastric) and sternocleidomastoid (SCM) muscles was measured during isometric MVCs in a neutral head position. The digastric MVC was conducted by self-resisted jaw opening, and the sternocleidomastoid MVC was conducted by forceful head flexion against the subject's own resistance.

SEMG was then recorded while subjects sat in an upright position and performed three different randomly-assigned orofacial muscle contraction conditions: no orofacial activity (NO); light orofacial activity (LO) which involved placing the tongue on the roof of the mouth, keeping teeth apart, and lips together, and; forceful orofacial activity (FO) which involved pressing the tongue into the roof of the mouth, keeping teeth apart, and pursing the lips.

Subjects then laid supine and held their heads isometrically in anatomic neutral slightly off of the support surface. Each of the three conditions were again performed in random order. Three trials, each of 15s, were collected for each condition. EMG was A/D converted at 12 bit resolution at 1024Hz. Signals were full wave rectified and low pass filtered (single pass Butterworth) at 2.5 Hz, and then normalized to maximum activity recorded from isometric MVC trials taken in the test position. Differences in average normalized activity (nEMG) between conditions for each muscle were assessed using a one-way ANOVA with Bonferroni correction ($\alpha = 0.01$).

RESULTS AND DISCUSSION

When tested in the seated position, activity of the digastrics increased consecutively between the NO, LO, and FO conditions, suggesting that this technique is capable of increasing the activity of the digastric, but not SCM, muscles.

When tested in the supine position with the head supported off of the surface, digastrics was relatively higher than SCM in all conditions ($p<0.01$), yet the type of orofacial activity did not have any additional effect on average digastric or SCM muscle activity in the supine test position.

We found that forceful contraction of the orofacial muscles selectively alters digastric muscle activity in upright posture, but does not further increase digastric activity in supine. This may be caused by the already high activity required of the neck flexors which must support the weight of the head.

The SCM muscle is considered the major superficial neck flexor. The higher relative involvement of digastrics than SCM during isometric supine head support suggests that the digastric muscle plays a potentially important role in neck flexion. This function has largely gone unconsidered among clinical practitioners and scientists alike. Additional research on the force contributions of the suprahyoid muscles to neck movement, as well as the efficacy of specific training for the orofacial muscles, should be investigated.

Table 1. Summary of muscle activity in each condition.

%nEMG	Upright			Supine		
	NO	LO	FO	NO	LO	FO
Digastrics	3.5	8.6	38.1	75	70.2	70.6
	(2.4)	(9.0)	(24.1)	(18.3)	(14.9)	(17.1)
SCM	0.9	1.6	8.6	23.1	23.2	23.5
	(0.3)	(1.9)	(11.5)	(9.9)	(10.3)	(9.4)

REFERENCES

Bérzin, F. (1995). *J. Oral Rehab.*, **22**, 825-829.
Jull, G., et al. (2003). *Physical Therapy*, **83**, 899-906.
Moore, K & Dalley, A.F. (1999). *Clinically oriented anatomy, 4th ed.* Baltimore, Lippincott, Williams & Wilkins.
Rocabado, M. (1983). *Dent Clin North Am*, **27**, 573-594.

EFFECTS OF HAND PLACEMENT STRATEGIES ON MOVEMENT PATTERNS AND MUSCULAR DEMANDS DURING A POSTERIOR TRANSFER IN INDIVIDUALS WITH SPINAL CORD INJURY

Dany Gagnon, MSc[1], Sylvie Nadeau, PhD[1], Denis Gravel, PhD[1] & Luc Noreau, PhD[2]

[1] Université de Montréal, Centre de recherche interdisciplinaire en réadaptation du Montréal métropolitain, Canada

E-mail : sylvie.nadeau@umontreal.ca

[2] Université Laval, Centre interdisciplinaire de recherche en réadaptation et intégration social, Québec City, Canada

INTRODUCTION

Since the upper-body musculature acts as primary motor components during transfer activities in individuals with spinal cord injury (SCI), better understanding of movement patterns and muscular demands at the trunk and upper extremities would contribute to increase existing knowledge for transfer training. The ability to transfer in individuals with SCI has not been studied extensively (1-3). The objective of the study was to examine kinematic patterns and electromyographic (EMG) activity in individuals with SCI during a posterior transfer toward an elevated surface using different hand placement strategies.

METHODS

Ten males (age=39,2±9,3 years; time post-injury=15,1±11,7 years) with complete motor SCI (C7 to L2), able to perform a posterior transfer independently on a level surface participated. Subjects were asked to move their body posteriorly toward a 10-cm elevated surface using three different hand placement strategies (Fig.1).
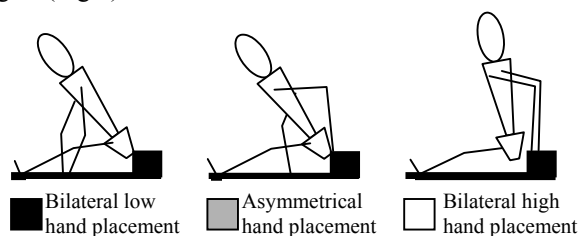

Figure 1: Hand placement strategies suggested to complete the posterior transfer toward a 10-cm elevated surface

Three-dimensional kinematic variables describing positions and angular displacements of the head, trunk, shoulder and elbow were obtained with a Peak Performance System. EMG data were recorded using surface electrodes placed over the biceps, triceps, anterior deltoid, pectoralis major, latissimus dorsi and trapezius muscles on the dominant side. To quantify the muscular demand, EMG data recorded during transfers were normalized to values obtained during maximal static contractions (% EMG max) performed on a Biodex dynamometer. Signals from pressure sensitive contacts placed under buttocks and hands were used to determine pre-lift, lift and post-lift phases of the transfers. Descriptive statistics are presented and trends are identified.

RESULTS AND DISCUSSION

Nine subjects completed the experimental task using various hand placement strategies: seven with bilateral hand placement, five with asymmetrical hand placement and only three with bilateral high hand placement strategies. Hand placement strategies influence angular displacements in the sagittal plane (Fig. 2). Bilateral high hand placement was characterised by additional extension at the shoulder and limited flexion at the trunk. Subjects might rely on a "lift" pattern to transfer when hands were placed on the elevated surface. Oppositely, data suggest utilisation of a "forward trunk flexion" pattern when

bilateral high hand or asymmetrical hand placement strategies were used. Levels of effort were high (>50% of the EMG max) in the anterior deltoid, pectoralis major and trapezius muscles (Fig.3). Bilateral hand placement strategy generated highest muscular demands at the anterior deltoid, triceps and latissimus dorsi. Additional efforts might be needed by these muscles to execute the "lift" toward the elevated surface. Low demands were observed at the triceps and latissimus dorsi when bilateral low hand placement strategy was used.
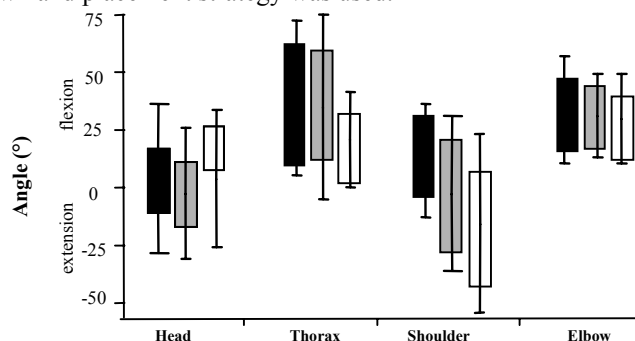

Figure 2: Mean minimum and maximum angles (SD) in the sagittal plane during all phases of transfers.
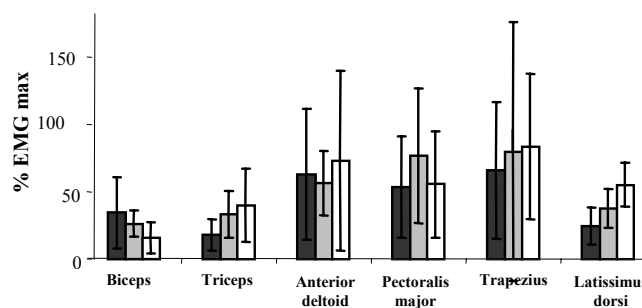

Figure 3: Mean % EMG max (SD) during the lift phase

SUMMARY

Data suggest that initial hand placement influences movement patterns and muscular demands during transfers. The "forward trunk flexion" pattern was used more often than the "lift" pattern since it possibly optimize the angular momentum generated by the axial skeleton prior to lifting the body. Biomechanical research is required to better understand relative contributions of muscle strength and trunk control during transfer activities in individuals with SCI.

REFERENCES

1. Allison, G. Crit Rev Phys Rehab Med 1997;9(2):131-150.
2. Nyland J et al. Spinal Cord 2000;38:649-657.
3. Gagnon, D (2002) Master thesis, University of Montreal.

ACKNOWLEDGEMENTS

A BIOMECHANICAL MEASURE TO ASSESS GAIT ECONOMY
AND TREATMENT OUTCOME IN RHEUMATOID ARTHRITIS PATIENTS

Christopher R. Goodwin and Michael R. Pierrynowski

School of Rehabilitation Science, McMaster University, Hamilton, Canada, goodwic@mcmaster.ca

INTRODUCTION

In the clinical literature there is a noticeable absence of objective biomechanical outcome measures to assess gait economy/efficiency. The biomechanical economy quotient (BEQ) has been proposed as an objective measure of gait economy (Kerrigan et al, 1996). The quotient is calculated as the measured versus predicted sacral height during gait, based on the classic Determinants of Gait (Saunders, Inman & Eberhart, 1953). Despite promising results in earlier studies, the measurement properties of the outcome are unknown. Therefore, a series of parameter estimation studies examined the measurement properties (validity, reliability, and sensitivity to change) of the BEQ within a rheumatoid arthritis and healthy cohort sample in order to substantiate the utility of the BEQ in future biomechanical research.

METHODS

Rheumatoid arthritis patients with foot involvement (N=18) and age-matched controls (N=18) underwent gait analysis in the Human Movement Laboratory, McMaster University. Kinematic data analysis from the sacrum and heels provided BEQ values. Construct validity was determined in both groups by comparing BEQ values at various gait speeds to traditional non-biomechanical measures of gait economy (VO_2 and heart rate). The reliability of the BEQ was determined through analysis of the between-trial standard error of measure (SEM) and intra-class correlation coefficient (ICC). The sensitivity to change of the BEQ is currently under investigation. We hypothesize that the sensitivity of the BEQ to subtle variation in shoe insole hardness will allow researchers to confidently detect small changes in gait economy.

RESULTS AND DISCUSSION

Preliminary results indicate construct validity of the BEQ for rheumatoid arthritis patients and age-matched controls. There is a strong relationship between observed BEQ values at varying gait speeds compared to results in the energy cost literature under similar conditions. Reliability calculations for the BEQ currently indicate a between-trial SEM of 0.0965. Thus, the expected variability of the outcome measure appears to be approximately ten percent from trial to trial. This degree of error is reduced significantly when multiple gait cycles comprise each trial. Preliminary results indicate that the biomechanical economy quotient (BEQ) is a valid and reliable measure of gait economy in clinical and control groups. Final data analysis is underway to verify these measurement properties and to determine the sensitivity of the outcome.

REFERENCES

Kerrigan DC et al (1996). *Am J Phys Med Rehabil,* **75**, 3-8.
Saunders JB, Inman VT, Eberhart HD (1953). *J Bone Joint Surg,* **35**, 543-558.

ACKOWLEDGEMENTS

SYMMETRY IN BETWEEN LIMB COORDINATION DURING GAIT TRANSITIONS

Jeffrey M Haddad, Joseph Seay, Richard E. A. van Emmerik & Joseph Hamill

Department of Exercise Science, University of Massachusetts-Amherst, Amherst, Massachusetts, USA
E-mail: jhaddad@excsci.umass.edu

INTRODUCTION

Bipedal locomotion requires spatio-temporal coordination both between and within the limb segments. This coordination is typically modified in response to changes in either external (e.g. surface characteristics) or internal task constraints (e.g. fatigue). Coordinative changes during a gait transition have primarily been observed within the limb (Diedrich & Warren, 1995). Little research has examined coordinative changes that occur between the limbs. Interestingly, within a gait mode (such as walking) research has suggested that coordinative changes may occur at the between limb level to a greater degree than the within limb level, where the changes in between limb coordination may actually be an adaptation to the altered constraints of the task (Haddad et al., 2004). Thus, the purpose of this study was to investigate the dynamics of between limb coordination in the gait transition region (from a walk to a run).

METHODS

Bilateral kinematic data were collected while subjects either walked or ran on a treadmill as speed was systematically increased. Subjects were told that as the treadmill speed increased they should either walk or run, as they felt comfortable. The treadmill was started at 1.3 m/s and was systematically increased to 3.3 m/s in increments of 0.1 m/s every 30s. Treadmill speed was adjusted via custom written software; thus the subjects were not privy to any feedback regarding the current treadmill velocity or adjustments in belt velocity. During each 30-second speed plateau, kinematic data were recorded over the last 20 seconds.

Continuous relative phase (CRP) was used to assess between limb coordination. CRP was calculated as the difference in the phase angles specific to each coupling. The three interlimb couplings examined were the thigh-thigh, leg-leg, and foot-foot. Prior to calculating CRP, the phase angles of the right segments were time shifted such that the heel strikes of the right and left homologous segments matched in time. This time shifting procedure allowed the final CRP measure to be a spatio-temporal measure of symmetry, where a CRP time series about zero-degrees would be indicative of perfect spatio-temporal interlimb symmetry.

RESULTS AND DISCUSSION

Preliminary analysis showed that changes in interlimb coordination occurred in all three couplings examined. Thus, it appears that coordinative adaptations occur over both proximal and distal limb segments. In all three couplings, increases in spatio-temporal asymmetries between right and left homologous segments were observed near the transition region (Figure 1). The symmetry values showed a third order polynomial trend within both the walking and running speeds.
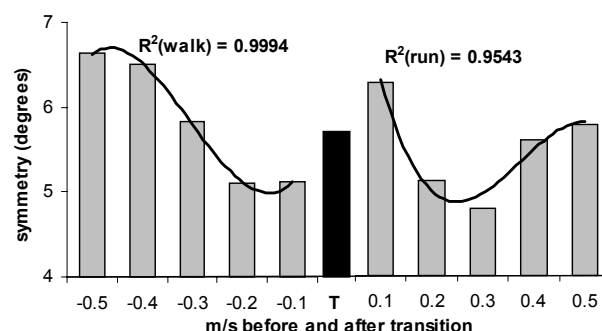

Figure 1: Average symmetry (across strides) in the thigh-thigh coupling (collapsed across each stride) at each of the speeds. The black bar indicates the transition speed. This trend was observed in the other couplings examined.

Previous research has shown changes in within limb coordinative patterns during the walk to run transition (Diedrich & Warren, 1995). In the present study changes in symmetry (between limb coordination) were found to occur both within a gait mode and in the transition between gait modes. It appears that adaptations in coordination during a walk to run transition are more complex than previously thought. Asymmetry may be a functional mechanism over which gait adaptation occur (Sadeghi, 2000). A better understanding of the etiology of dynamic gait asymmetry may lead to understanding adaptations that occur not only in gait transitions, but also in response to various motor pathologies.

CONCLUSIONS

It appears that alterations in spatio-temporal gait symmetry are a mechanism that is utilized to adapt to the new coordination modes required as one transitions between a walk and a run. Further, the locomotory system may actively alter its between limb symmetry as a mechanism to adapt to the altering constraints of the task.

REFERENCES

Diedrich, F.J. & Warren, W.H. (1995). *J Exp Psychol Hum Percept Perform,* **21**, 183-202.
Haddad, J. et al., (2004). Submitted to *Gait & Posture*.
Sadeghi, H. (2000). *Gait and Posture,* **12**, 34-45.

COORDINATION VARIABILITY IN THE GAIT TRANSITION REGION WITH VARYING SPEED INTERVALS

Joseph Seay, Jeffrey M Haddad, Richard E. A. van Emmerik & Joseph Hamill

Department of Exercise Science, University of Massachusetts-Amherst, Amherst, Massachusetts, USA
E-mail: joeseay@excsci.umass.edu

INTRODUCTION

An increase in variability has been found to be a characteristic feature of transitions between coordination patterns. This increase has been found in many empirical paradigms, including transitions in bimanual coordination (Kelso, 1995) as well as transitions from a walk to a run (Diedrich & Warren, 1995). Recently, however, it has been suggested that changes in variability are not characteristic of transitions from a walk to a run (Kao et al., 2003). Differences in results may stem from methodological differences between studies. More specifically, differences in how treadmill belt velocity is scaled (both step length and magnitude) as well as the specific coordinative couplings examined could change experimental outcomes.

The purpose of this study was to investigate coordination variability in the gait transition region at different velocity step intervals over multiple segmental coordinative couplings.

METHODS

Bilateral kinematic data were collected while young adult subjects either walked or ran on a treadmill as speed was systematically increased. Subjects were told that as the treadmill speed increased they should either walk or run, as they felt comfortable. The treadmill velocity started at 1.3 m/s and was systematically increased in increments of 0.1 m/s to 3.3 m/s during two protocols that differed by the length of the time at a particular velocity. For the first protocol speed was increased every 10 seconds. For the second protocol, treadmill speed was increased every 30 seconds. Treadmill speed was adjusted via custom written software, thus the subjects were not privy to any feedback regarding the current treadmill velocity or adjustments in belt velocity.

Continuous relative phase (CRP) was used to assess variability in both interlimb and intralimb segmental coordination. CRP was calculated as the difference in the phase angles specific to each coupling. The intralimb couplings examined were the thigh-leg and leg-foot on the right side. The interlimb couplings examined were the thigh-thigh, leg-leg, and foot-foot. CRP variability was defined as the average standard deviation of CRP across each of the stride cycles.

RESULTS AND DISCUSSION

Preliminary analysis showed that the nature of CRP variability during a gait transition is dependent on the couplings examined as well as the dynamics of the velocity increase. In the present study CRP variability in the intralimb couplings tended not to increase in the transition region.

These findings are similar to those observed by Kao et al. (2003). CRP variability did; however, tend to increase in or near the gait transition region in the interlimb couplings examined. Interestingly, this trend was only observed during the 10-second time step (Figure 1a), but not in the 30-second time step (Figure 1b). This finding indicates that the nature of variability changes could be dependent on either the specific time step dynamics or the specific couplings examined.
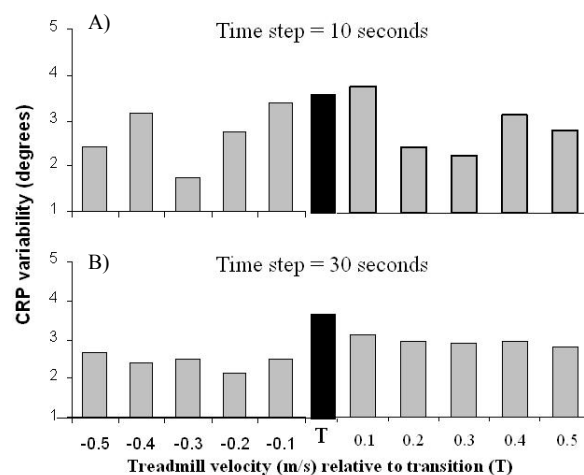

Figure 1: Average CRP variability (across strides) in the leg-leg coupling (collapsed across each stride) at each of the speeds. The black bar indicates the transition speed. This trend was also observed in the other couplings.

CONCLUSIONS

Previous research has yielded conflicting results regarding CRP variability during a gait transition. Our findings indicate the nature of CRP variability is dependent on both the dynamics of the velocity increase and the specific couplings examined.

Further dissection of time step and coupling differences in transitional variability may lead to a more comprehensive understanding of gait transitions and lower limb coordination.

REFERENCES

Diedrich, F.J. & Warren, W.H. (1995). *J Exp Psychol Hum Percept Perform,* **21**, 183-202.
Kao, J.C., et al., (2003). *J. Motor Behavior*, **35**, 3, 211-214
Kelso, J.A.S. (1995). *Dynamic Patterns: The self-organization of brain and behavior.* Cambridge, MA, MIT Press.

EFFECTS OF MUSCLE MODEL Po VALUES ON SIMULATED JUMPING PERFORMANCE

Graham E. Caldwell[1], Katherine A. Eck[1], Mark A. King[2] and M.R. 'Fred' Yeadon[2]
[1]Department of Exercise Science, University of Massachusetts, Amherst, MA, USA, gc@excsci.umass.edu
[2]School of Sport and Exercise Sciences, Loughborough University, Loughborough, UK

INTRODUCTION

Pandy (1990) reported that forward dynamics simulation jump heights are sensitive to parameters chosen for muscle actuators that drive the musculoskeletal model. This sensitivity suggests that subject-specific parameters should be used in simulations, yet most models use general parameter values (e.g. from cadaver studies) that exhibit great variability. The present study investigated the effect of variations in muscle model maximal isometric strength (Po) values on vertical countermovement jump (CMJ) simulations. To that end, sets of Po values were drawn from existing studies, while one set was generated from magnetic resonance imaging (MRI) of one specific subject. Simulation results from identical models with the different Po sets were compared to each other and to experimental jumping data to assess the effect of Po variation.

METHODS

Six healthy adult males (27 ± 3yrs, 1.84 ± .05m, 77.8 ± 7kg) performed maximal vertical CMJs from an AMTI™ force plate. Sagittal plane motion of reflective markers was recorded with 5 Qualisys™ digital cameras at 200 Hz, while force plate and electromyographic (EMG) data were sampled simultaneously at 1000 Hz. EMG data were recorded from a Noraxon™ telemetry unit and bipolar surface electrodes for 7 muscles [gluteus maximus (GM), rectus femoris (RF), hamstrings (HA), vastus lateralis (VL), gastrocnemius (GA), soleus (SO), and tibialis anterior (TA)] of the right leg. EMG data were rectified and smoothed (10 Hz) to determine activity onset and offset times. All data were output as a percentage of the jumping stance period prior to takeoff.

The planar simulation model had 4 rigid segments [feet (Q1), legs (Q2), thighs (Q3) and HAT (Q4)] with anthropometrics based on one experimental subject (S_{MRI}). The equations of motion were generated by Autolev™ in the form:

$$A(\theta) \propto = B(\theta, \omega) + gC(\theta) + Fm + Fc$$

where A, B and gC are inertia, Coriolis and gravity matrices, and θ, ω and ∝ are segment angular positions, velocities and accelerations, respectively. Fm represents net extensor joint torques and Fc is a ground/heel constraint. Fm resulted from the activation of 8 Hill muscle actuators representing GM, RF, HA, VL, GA, SO, TA and iliopsoas (IL). After activity onset a muscle actuator remained "on", with the exception of IL and TA which could turn off. Simulated jump performance was dictated by the actuator onset (8) and offset (2) times. Simulated annealing (Goffe et al., 1994) was used to find the 10 actuator times that produced the highest jump height.

One set of muscle actuator Po values (for model M_{MRI}) was computed from transverse MRI data for subject S_{MRI}, assuming a maximal muscle stress value of 40 N/cm^2. The other sets of Po values were drawn from research studies, scaled to the mass of S_{MRI} (Table 1). CMJ simulations were performed for each Po set.

Table 1: Po values (N) used in 3 simulation models.

	GM	IL	HA	RF	VL	GA	SO	TA
M_{MRI}	3900	3000	3700	3300	17900	5400	7000	1900
M_N	2831	3200	5874	2206	14436	5039	8037	3114
M_S	5258	7649	4207	3346	10039	2868	5736	2295

RESULTS AND DISCUSSION

Model M_{MRI} jumped 2.5 cm higher than subject S_{MRI}, with kinematics similar to the subjects (Fig. 1), but with altered segment range of motion. Varying the muscle actuator Po values altered the kinematic patterning (Fig. 2), the optimal jump height, and the timing of muscle activation onsets and offsets (Table 2). Therefore, the Po set chosen not only altered the optimal jump height, but also dictated the coordination pattern chosen for the optimal height simulation.
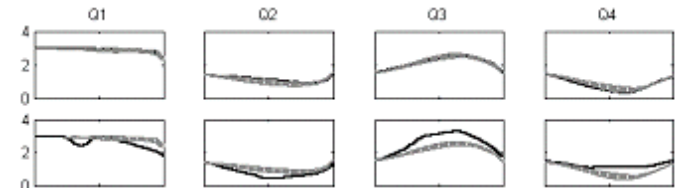

Fig 1. Mean ± SD angular displacements for 6 subjects (gray), subject S_{MRI} (black, top) and model M_{MRI} (black, bottom).
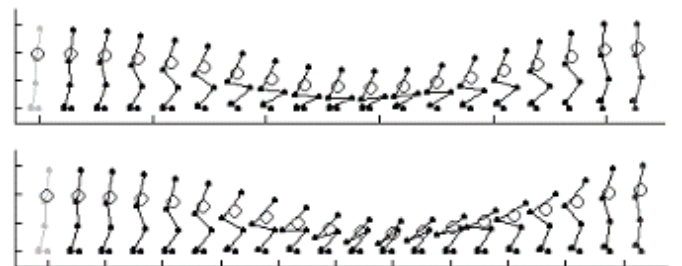

Fig 2. Optimal jump kinematics: top: M_{MRI}; bottom: M_N.

Table 2: S_{MRI} and model jump heights (in cm; JH) and onset times (in % stance time).

	JH	GM	HA	RF	VL	GA	SO	TA on	TA off
S_{MRI}	30.0	52	45	28	28	66	59	24	87
M_{MRI}	32.5	34	15	6	37	14	43	26	93
M_N	39.4	30	34	6	45	70	22	33	95
M_S	36.9	14	54	3	60	82	13	27	100

SUMMARY

These simulations confirm that model CMJ performance is very sensitive to muscle actuator Po values, and illustrate the importance of obtaining subject-specific muscle parameters.

REFERENCES

Goffe, W.L. et al. (1994). *Journal of Econometrics* **60,** 65-99.
Pandy, M.G.(1990). *Multiple Muscle Systems,* pp 653-662.

POSTURAL ASYMMETRIES DURING QUIET AND UNCONSTRAINED STANDING

Molly B. Johnson, Jebb G. Remelius, Richard E.A. van Emmerik, and Joseph Hamill
Neuroscience & Behavior Program and Department of Exercise Science,
University of Massachusetts, Amherst, Massachusetts, USA, mjohnson@nsm.umass.edu

INTRODUCTION

Postural stability in movement and quiet standing have been major topics in motor control research. Studies have shown that asymmetries are prevalent in gait (Sadeghi, 2000), and in quiet standing (Winter, 1993). However, the mechanisms for these asymmetries are poorly understood. It is proposed that asymmetries in quiet standing are related to patterns found in habitual standing postures. The use of unconstrained standing in this study was intended to reflect standing posture in normal daily settings. It is hypothesized that asymmetrical patterns of the Center of Pressure (COP) variability and body weight distribution found in quiet standing will be magnified in unconstrained standing.

METHODS

Seven healthy, young participants volunteered for this study, four female and three male. Data were collected using two AMTI force plates, mounted side by side. The force plate output was sampled at 100 Hz.

Each participant was recorded barefoot for four 30 sec trials, two in the quiet and two in the unconstrained condition. During quiet standing, participants were instructed to stand balanced on two feet with arms at their sides. During unconstrained standing, participants were instructed to stand how they would most typically stand if waiting in line. They were allowed to do whatever they chose with their upper body. During all conditions, participants were to keep their feet within paper tracing marks made of each foot on the force plates.

Force plate output was recorded and passed through a fourth order, zero-lag, 20 Hz low-pass Butterworth filter. COP data were analyzed for each foot, and used to calculate COPnet (Winter, 1993). The body weight distribution was taken from the vertical force component in each force plate, and represented as a percentage of total body weight. For each trial, the weighted limb (COPw) was determined by which leg carried greater than 50% of the body weight, and the non-weighted limb (COPnw) was determined by which leg carried less than 50% of the body weight. Variability of the COP in the anterior-posterior (A/P) and medial-lateral (M/L) directions for COPw, COPnw, and COPnet were determined by the standard deviations in each COP. Paired t-tests were run between the unconstrained and quiet conditions for the two components of each COP variability measure, and for the body weight distribution.

RESULTS AND DISCUSSION

Asymmetries were seen in the body weight distribution in all trials. The mean body weight distribution between weighted and non-weighted legs was 57.5% to 43.5% in quiet standing and 70.0% to 30.0% in unconstrained standing. The weighted and non-weighted legs remained the same across all trials for all but one participant. A paired t-test showed significantly greater differences in weight distribution between the two legs in the unconstrained conditions (p<.05).

Paired t-tests showed significantly greater variability of the M/L COPnet, A/P COPnw, and the M/L COPw in the unconstrained condition (p<.05). Though greater variability was observed in the A/P COPnet, M/L COPnw, and the A/P COPw in the unconstrained condition, they were not significant (p>.05) (Figure 1).
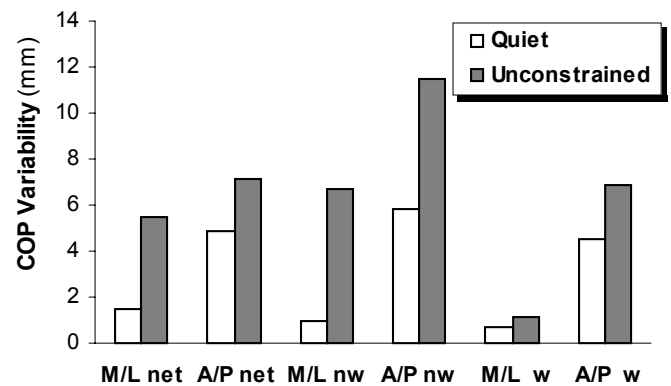

Figure 1: Mean COP variability in quiet and unconstrained standing conditions for medial-lateral and anterior-posterior components of the COPnet, COPnw and COPw.

The reasons for the greater asymmetries found in unconstrained standing are not clear. It may be that each leg functionally plays a different role in standing, as has been proposed in gait (Sadeghi, 2000), so that one is used for weight-bearing, and the other for stabilization. It is also possible that the asymmetries in unconstrained standing are dysfunctional. The habitual use of asymmetrical, unconstrained postures in daily life may actually skew our ability to be balanced between our two feet.

SUMMARY

The present study provides evidence that asymmetries exist in both quiet and unconstrained standing. Asymmetries in body weight distribution and COP variability were generally greater in unconstrained standing. These data support the prediction that greater postural asymmetries exist in unconstrained standing.

REFERENCES

Sadeghi, H, et al (2000), *Gait and Posture*, **12,** 34-45.
Winter, DA, et al (1993), *Neuroscience Research Communications*, **12**, 141-148.

CHARACTERIZING STEP WIDTH AND STEP LENGTH ADJUSTMENTS FOR THE IMPLEMENTATION IN ROBOTIC LOCOMOTION CONTROL

Michael A. Greig[1], Aftab E. Patla[1] and M. Anthony Lewis[2]

[1]Department of Kinesiology, University of Waterloo, Waterloo, Canada, magreig@ahsmail.uwaterloo.ca
[2]Iguana Robitics Inc. Urbana, IL, USA

INTRODUCTION

Legged locomotion and the ability to choose foot placement allows substantial flexibility in the terrain that can be traveled. Foot placement has been shown to not be random, but instead is a calculated choice based on information from visual input, and a priori knowledge and experience (Patla et al., 1999). Understanding where the location of the zone area with respect to a normal foot placement results in a transition from stepping short to long or medial to lateral exists is an important factor in the development of adaptable robotic locomotion (Lewis and Simó, 1999). With the primary criteria for step decision being minimizing the vector distance between normal foot placement and the alternate position (Patla et al., 1999), a simple metric adjusting a robot's foot placement should be possible. This work aims to better understand and characterize the zone of transition from stepping short to long or, separately, medial to lateral in step length and step width adjustments.

METHODS

Twelve healthy young adults free of neurological disorders and any lower limb problems completed one of two protocols examining either constrained step length or step width adjustments. Participants stepped on the centre of an embedded black screened LCD monitor, but avoided stepping on any white area. A total of 80 normal walking and 80 experimental (16 X 5 repetitions) conditions were completed. Step adjustment type and success were monitored qualitatively. Foot position was tracked by infra-red markers (Northern Digital Inc.) placed on the big toe, base of the 5th metatarsal and the lateral heel to determine the resultant magnitude difference and angle of the foot placement adjustment relative to the average normal foot placement.
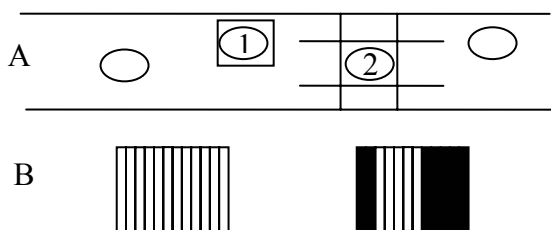

Figure 1: A - Schematic of walkway setup. Screen change triggered at 1, step adjustment made at 2. Vertical lines at 2 depict foot placement constraint for step width (SW) adjustment; horizontal lines show constraint for step length (SL) adjustment. B – Depiction of screen sectioning for SW setup (left = medial). Combinations of twelve 3.0 X 29.5 cm sections activated (white) for experimental conditions (eg. shown on right). Screen rotated 90º for SL setup.

RESULTS AND DISCUSSION

Participants made the transition from a short to long step when the area to avoid reached approximately 7 cm forward from the normal foot placement. The rate of change of the transition was not significantly influenced by the penalty type. Equally penalizing stepping short or long did not significantly influence the step choice as participants preferred to step long. Early analysis (n = 3) has shown that in only one of the sixteen conditions was the foot placement adjustment significantly correlated with the placement of the preceding step. Therefore earlier foot placement did not bias towards a given adjustment.

Participants showed an equal probability of stepping medial or lateral at approximately 10 cm lateral to the normal foot placement. The rate of change from medial to lateral is significantly affected by the type of medial/lateral (M/L) penalty. Participants also preferred stepping laterally when there was an equal M/L penalty. Patla et al. (1999) identified that preference is given to stepping long and medial however these findings are in contradiction and may be a factor of the task constraints. Analysis showed that constraining the foot placement in the frontal plane significantly influences foot placement choice. This is further supported by the observation that 82% of the medial-lateral adjustment errors were due to stepping long. Case analysis of M/L foot placement with respect to the normal average did not support a prior step bias to a given adjustment. Foot placement position of the adjusted step and its preceding step were not significantly correlated.

SUMMARY

Program control of a robot in step adjustment should not utilize an abrupt change point for foot placement adjustments. The changes seen within this study are gradual, especially in the plane of progression. Control must also consider the effect of foot placement constraints on the direction of progression as these results have shown a bias laterally compared to an unconstrained environment (Patla et al., 1999).

REFERENCES

Lewis, MA and Simó, S (1999). *Connection Science,* **11(3/4)**, 331-344.
Patla AE et al. (1999). *Experimental Brain Research,* **128(4)**, 441-450.

ACKNOWLEDGEMENTS

HOW ACCURATE ARE SOLIDS MODELS MADE FROM CT SCAN DATA?

Heidi-Lynn Ploeg[1], Leone Ploeg[2], Nick Byrne[1], Sylvana Garcia[1], Mariana Kersh[1], Deepthi Nair[1]
[1]Departments of Mechanical and Biomedical Engineering, University of Wisconsin, Madison, WI, USA,
http://www.engr.wisc.edu/me/faculty/ploeg_heidi-lynn.html
[2]Human Mobility Research Centre, Queen's University, Kingston, ON, Canada

INTRODUCTION

Computer models of bones are essential tools for research in orthopaedics, preclinical analysis of orthopaedic implant designs, and in computer aided surgery. In these applications, solid models of bones are routinely created from computed tomography (CT) scan data; however, there are few studies (Viceconti 99 & 96, Zannoni 98) that have quantified the effects of the process parameters, on the error of the resulting geometry. The purpose of this study was to determine the magnitude of the error in solid models generated from CT-scan data and to which factors the error was most sensitive.

METHODS

Part 1. Point cloud data from segmented CT-scan data (0.625 mm spacing and thickness, 120 kV, 30 mA) and laser scans of 3 composite bones (items 3103, 3301, 3301) from Pacific Research Laboratories, Vashon, Washington, USA were compared.

Part 2. Reconstructed volumes of simple shapes were compared to solid models created using measured dimensions. The effect of process parameters was investigated using a one quarter fractional factorial design with the following factors:

1. CT-scan axis orientation: parallel and perpendicular to sample axis;
2. CT-scan slice thickness: high (1.25 mm) and low (0.625 mm);
3. CT-scan slice spacing: high (1.25 mm) and low (1.625 mm);
4. material density: high (aluminium 6063 2700 kg/m^3) and low (solid rigid polyurethane foam 320 kg/m^3);
5. specimen fill: full and hollow (wall thickness 3.18 mm);
6. specimen feature: without and with a 6.35 mm wide centered slot; and,
7. specimen shape: cylinder (25.4 mm diameter x 25.4 mm height) and cube (25.4 mm^3).

Hardware: The CT-scanning was performed using an GE Litespeed[16] CT scanner from GE Medical Systems, Waukesha, WI. Laser scanning was performed using a laser scanner from Applied Precision, Mississauga, ON with a SG - 100 ShapeGrabber Scanning Head.
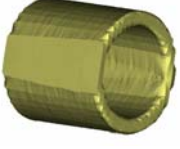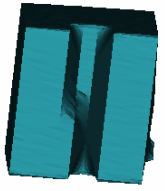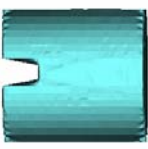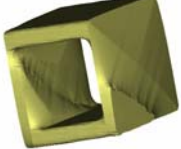
Software: The CT-scan data was segmented with Mimics and MedCad from Materialise, Ann Arbor, MI. The point cloud comparison was performed with Polyworks Inspector by InnovMetric, Sainte Foye, Qc. Solid modeling was performed with Unigraphics from EDS, Plano, TX.
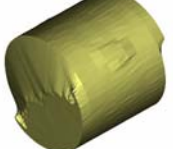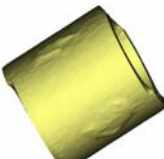
RESULTS

Part 1. The mean error of the point cloud data (28,520 points) from the segmented CT-scan data compared to the laser scan data was 0.75 mm, with a standard deviation of 0.31 mm. The range of error was 1.5 to -2.1 mm (composite bone 3103).

Table 1. Segmented CT-Scan Data

a) Scan Axis Perpendicular to the Sample Axis.

	Fine Spacing	**Coarse Spacing**
Fine Thickness		
Coarse Thickness		

b) Scan Axis Parallel to the Sample Axis.

Fine Thickness		
Coarse Thickness		

SUMMARY

The accuracy of volumes reconstructed from CT-scan data is affected by scan spacing, thickness and orientation. The volume of the segmented CT scan point cloud data of the composite bone was underestimated (maximum -2.1 mm) on the proximal and distal ends of the bone and overestimated in the metaphyseal regions (maximum 1.5 mm).

REFERENCES

Viceconti, M. et al (1999). *J. Medical Engineering and Technology*, **23**(2), 77-81.
Zannoni, C. et al (1998). *Medical Engineering & Physics*, **20**(9), 653-659.
Viceconti, M. et al (1996). *Annual International Conference of the IEEE Engineering in Medicine and Biology - Proceedings*, **2**, 674-675.

COMPARISON OF RAMP AND STAIR DESCENT

Andrew Post[1] and D.G.E. Robertson[2]
Department of Human Kinetics, University of Ottawa, Ottawa, Canada
[1]apost033@uottawa.ca   [2]dger@uottawa.ca

INTRODUCTION

Recent research regarding stairs has focused on muscle action and reaction forces while moving down stairs. For example, it is known that higher loads on the knee exist while descending the stairs (Yu *et al*., 1997) as compared with level walking.

These higher joint reaction forces have been suggested as being one reason why many people who ascend or descend stairs frequently have developed joint injuries. A need exists to find a method of vertical movement that eases the reaction forces to a point where fewer joint injuries occur. A solution may lie in the use of ramps. Unfortunately, few studies comparing the benefits and faults of ramps and stairs exist.

This project investigated the differences in the moments and powers of the joints of the lower extremity during stair and ramp descent. This knowledge may be used to determine the differences between these two styles of gait and be applied to rehabilitative interventions such as hip, knee and ankle replacements. This information may also be used to develop more efficient prosthetic devices.

METHODS

A sample population of five male and five female volunteers were used for this study. Subjects were asked to walk five times down a ramp set at a 10-degree decline at a normal gait speed, followed by five stair descent trials (30 cm tread, 20 cm riser). Kistler 9286AA and 9281B force plates were used to collect the force data on the second and fourth step. A Panasonic VHS camera collected the sagittal view trajectories of markers placed on the left side of the body. The force and motion data were processed using the Biomech Motion Analysis System and Bioproc2 to determine the ankle, knee and hip moments and moment powers. The data normalized to body mass and were ensemble averaged and all statistics were calculated at +/–1.96 standard deviations.

RESULTS AND DISCUSSION

The kinetics of ramp and stair descent differ from each other in the ankle and hip joints while the knee joint had similar power and moment requirements for both methods of descent. During stair descent, the higher peaks seen during eccentric plantar flexor activity in the ankle at foot-strike (FS) demonstrated that the ankle acted as a shock absorber and functioned to help control the body's descent to the next step. During ramp descent, however, a higher ankle plantar flexor peak occurred during the push-off phase.

With respect to the hip, few similarities existed between the kinetics of ramp and stair descent; stair descent had minimal hip activity while ramp descent had a profile similar to that of walking (Winter, 1991). Unlike the ankle and the hip, the knee showed similar phases of activity for ramp and

stair descent; the same peaks were present at FS and at toe-off (TO). These peaks occurred as result of the use of the knee as a shock absorber of the leg. The knee first dissipated energy at FS and then at TO, and since the body was being lowered, the knee dissipated more energy as the contralateral foot contacted the lower surface.
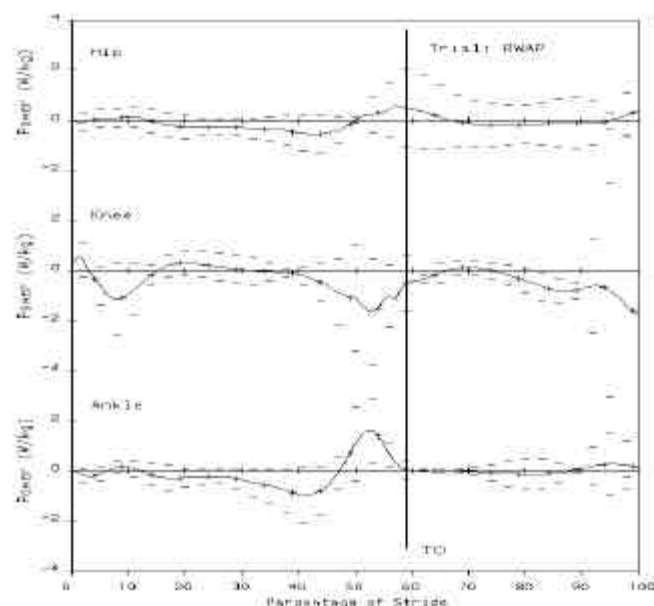

Figure 1: Typical hip, knee and ankle moment powers for ramp descent (TO=toe-off). Errors bars represent 95th% confidence intervals.

SUMMARY

Each style of gait affected the joints differently. Ramp descent required more hip activity than stair descent, as well as a more forceful push at toe-off (60% of cycle in Figure 1). The ankle had a more stressful eccentric plantar flexor activity at foot-strike during stair descent (10% of cycle in Figure 1). The knee did not show any significant difference in stress between ramp and stair descent. The support moment was noticeably higher for stair descent than for ramp descent.

The lack of significant results suggests that neither mode of descent is better for knee problems; however, the results do suggest that persons with ankle pathologies or having recently undergone ankle replacement surgery should consider avoiding stairs and use ramps instead.

REFERENCES

Winter, D.A. (1991) *Biomechanics and Motor Control of Human Gait.* 2nd ed. Waterloo: Waterloo Biomechanics
Yu et al. (1997) *Clin Biomech*, **12**, 286-293.

ROLE OF VISION AND VISUAL ATTENTION IN THE CONTROL OF RAPID STEPPING REACTIONS TRIGGERED BY POSTURAL PERTURBATION

John L. Zettel , Amy Peters, Andrea Holbeche, Yin-Yin Chung, William E. McIlroy, and Brian E. Maki

Centre for Studies in Aging, Sunnybrook & Women's Health Sciences Centre, University of Toronto, Toronto, Canada

john.zettel@sw.ca

INTRODUCTION

Numerous studies have demonstrated that vision contributes to the control of postural stability, predominantly affecting slow or low-frequency balance corrections[1]. However, no studies have directly addressed the role that vision must play in acquiring information about environmental constraints that may influence the selection or execution of triggered balancing reactions. Rapid, triggered compensatory stepping reactions must be directed and scaled appropriately in order to arrest the center-of-mass motion suddenly evoked by an unexpected perturbation, but the control of these reactions must also take into account the location of obstacles and other environmental constraints on foot trajectory and step placement[2, 3]. It is not known whether the CNS is able to acquire the requisite visual information in "real time", after onset of postural perturbation, or whether this information is acquired prior to perturbation onset, remembered, then applied after the perturbation.

In the present study, we examined the timing of changes in visual attention and gaze direction occurring during the execution of forward-directed compensatory stepping reactions evoked by unpredictable postural perturbation. We sought to determine whether: 1) the CNS can acquire the necessary visual information about environmental constraints prior to perturbation onset, or must instead redirect gaze at the floor surface during the execution of the reaction; 2) any such need to redirect gaze during the reaction is influenced by increasing demands for accurate control of the foot trajectory; and 3) the switching of visual attention that typically precedes foot-lift can be attributed to changes in gaze direction.

METHODS

Step reactions were evoked in healthy young adults (20-35) via sudden platform translation. Perturbation magnitude and direction were varied unpredictably; analyses focussed on forward steps evoked by large (0.9m/s) perturbation. Frontal obstacles and/or targets for foot placement were used, in some trials, to increase demands for accurate foot movement. Attention switching was monitored using a dual-task paradigm involving visuomotor pursuit tracking: subjects used thumb motion to track pseudorandom movement of a target displayed on a computer screen; switching of attention was inferred to occur at onset of significant deviation (sudden error) in tracking[2]. Changes in gaze (due to head or eye movement) were recorded with an eye-tracker system. Forceplates were used to determine step timing and a video system was used to characterize the limb trajectories. Preliminary observations from seven subjects are presented here; statistical analysis of the full cohort (n=12) will be presented at the meeting, along with an older adult cohort.

RESULTS & DISCUSSION

Gaze redirection toward the floor tended to occur more frequently as the demands for accurate control of the foot movement increased (p=0.04). In the task involving the *obstacle-plus-target*, there was a gaze shift toward the floor, prior to foot-contact, in 40% of trials. In contrast, there was never any gaze redirection when the foot motion had *no-constraint*, and less than 15% of trials exhibited gaze redirection with the *obstacle-only* or *target-only*. The timing of the downward gaze shift varied widely (140-625ms), but most commonly occurred prior to foot-off (67% of trials).

Switching of visual attention from tracking task to balance-recovery task (as inferred from sudden onset of significant tracking error) followed perturbation onset in 86% of trials. Constraint condition did not have a statistically significant effect on the frequency of tracking deviation (p=0.20); however, tracking deviation was most consistent in the most demanding task; 100% of *obstacle-plus-target* trials. In comparison, significant tracking deviation occurred in 78% of *no-constraint* trials, 85% of *obstacle-only* trials and 77% of *target-only* trials. The average onset time of tracking deviation was 231+117ms, and did not differ significantly between constraint conditions (p=0.14). The tracking deviation began prior to foot-off in 94% of cases, with an average interval of 162+102ms between onset of tracking deviation and foot-off.

Amongst the trials where tracking deviation and gaze shift could both be determined reliably, visual-attention switching occurred in 91% of these trials, but gaze shift was detected in only 20% of the tracking-deviation trials. While aversion of gaze from the computer screen would obviously be a cause of tracking error, this was the case in only four trials. In the remaining 16 trials, the tracking deviation preceded gaze deviation (204+94ms vs. 378+155ms); however, the time interval between the two events was not consistent and varied widely between trials (s.d. 124ms, range 7 to 442ms).

SUMMARY

The switching of visual attention associated with the initiation of rapid, perturbation-evoked stepping reactions was not linked to overt changes in visual fixation. Spatial features of the support surface were apparently "remembered" prior to perturbation onset and used to help plan or guide the foot trajectory and step placement, thereby allowing both vision and attention to be directed to other demands during the execution of the balance reaction.

REFERENCES

1. Diener HC, Dichgans J, Guschlbauer B, Bacher M. Hum Neurobiol 1986; 5: 105-113.
2. Maki BE, McIlroy WE. Phys Ther 1997; 77: 488-507
3. Maki BE, McIlroy WE, Fernie GR. IEEE Eng Med Biol Mag 2003; 22:20-26.

ACKNOWLEDGEMENTS

STRATEGIES TO AVOID COLLISION WITH MOVING DOORS

Sandra Prentice, Michael Cinelli and Aftab Patla
Gait and Posture Lab, Department of Kinesiology, University of Waterloo
Waterloo, Canada, sandrap@healthy.uwaterloo.ca

INTRODUCTION

Navigating through a cluttered environment requires one to use perception-action coupling to safely avoid obstructions. In the case of automatic doors, one must judge the distance between the doors as well as the person's distance from the doors in order to safely pass through them. The purpose of this study was to determine if subjects alter their walking velocity or posture in order to safely traverse a set of moving doors.

METHODS

Six healthy participants walked at their normal cadence towards motor-driven sliding doors which were triggered two steps ahead by forceplate contact. Three conditions (close, open and no movement of the doors) and three aperture settings (90, 110, 130cm) were randomly presented. Movement of the doors occurred on half the trials (60) and the velocity of door movement varied for each trial within a condition.

The participants were instrumented with 6 infrared light emitting diodes (IREDs) along the torso and head and 2 IREDs were placed on the doors. The Optotrak system was used to collect kinematic data. Participants wore headphones to mask the noise of the motor to eliminate the use of auditory cues.

RESULTS AND DISCUSSION

All trials in which the participant did not attempt to pass through the doors (44) and those trials where the participant collided with the doors (4) were eliminated from statistical analysis.
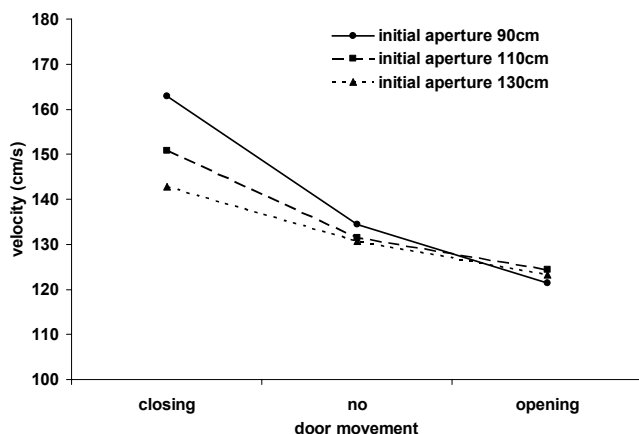

Figure 1: Subject's velocity 10 sec prior to door crossing

Door width at the time of door crossing indicated that during the Open condition, subjects consistently passed through the doors at a set width. In the Close condition, door width at the time of door crossing was directly proportional to the initial door aperture used.

Postural adjustments were made in the Close 90 and Close 110 conditions such that participants rotated their trunk to decrease the distance of their shoulders as they passed through the doors (modified shoulder width)(Fig. 2). This was supported in the transverse shoulder angle calculations as well. Regression analysis indicated that shoulder angle adjustments were timed with the onset of door movement rather than time of door crossing.
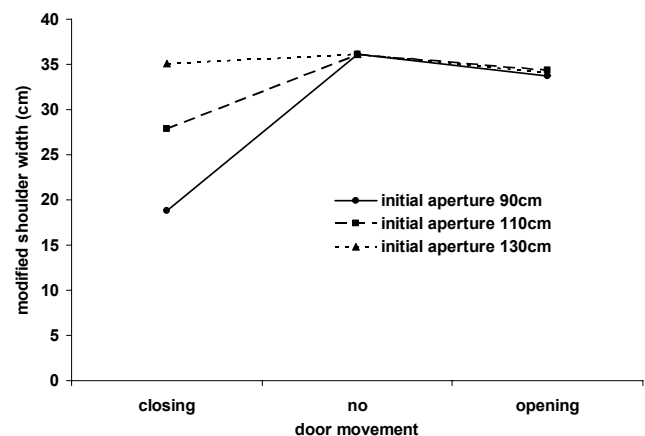
Figure 2: Modified shoulder width at time of door crossing

SUMMARY

Adjustments made were based on perception-action coupling. The initial door aperture and the onset of door movement drive a response that allows for safe passage through the doors. In less threatening conditions (Close 130, Open) only velocity adjustments were made. In more threatening conditions (Close 90, 110) subjects made adjustments in both velocity and posture to minimize the risk of collision.

REFERENCES

Lee, D.N. (1998). *Ecological Psychology,* **10(3-4),** 221-250.
Montagne, G. et al. (2003). *Q. J. Exp. Psych*. *A*, **56(3),** 51-67.
Stoffregen, T.A. (2000). *Ecological Psychology*, **12(1),** 1-28.

ACKNOWLEDGEMENTS

INTERACTION BETWEEN GASTROCNEMIUS AND SOLEUS DURING STEADY-RATE CYCLING

David J. Sanderson[1], Phil Martin[2], and Dave Kenyon[3]
[1]School of Human Kinetics, University of British Columbia, Vancouver, B.C. Canada, david.sanderson@ubc.ca
[2]Department of Kinesiology, Penn State, University Park, PA. USA, [3]BCIT, Burnaby B.C.

INTRODUCTION

This paper presents an extended analysis of data presented by Sanderson et al. (1999). They reported that the two members of Triceps Surae reflected different EMG responses to increased cadence at a given power output and suggested the Soleus was more sensitive to changing force demands whereas the Gastrocnemius was more sensitive to changing speed needs. A second peak in the EMG profile was reported but not commented on. With increased cadence (50-110 rpm) this peak appeared in Soleus but disappeared in Gastrocnemius. The purpose was to examine this hypothesis in light of the length and velocity characteristics of these muscles during cycling at a constant power output.

METHODS

Participants (n=12 expert cyclists (10M, 2F), with a mean (SD) age of 25.7 (3.7) years, mass 73.1 (6.3) kg, and height 179.4 (5.7) cm.) rode for a minimum of five minutes at each of six randomly presented cadences (50, 65, 80, 95, and 110 rpm) at a constant nominal power output of 200 W while EMG from Soleus and Gastrocnemius muscles and lower-limb sagittal-plane video were recorded. Data collection occurred in the final minute of the test protocol and lasted for three revolutions of the crank per collection period. Marker kinematics were used first to compute the angle of the knee and ankle joints and then the muscle lengths of the Soleus and Gastrocnemius muscles using equations developed by Grieve et al. (1978) over the complete pedalling cycle. These data were then differentiated using a finite central differences method to reveal velocity of shortening used to identify periods of concentric and eccentric activity.

RESULTS AND DISCUSSION

These data, presented in Figure 1, show two global changes in the excitation pattern of these muscles in response to cadence manipulation. First, during the propulsion phase Gastrocnemius excitation increased with increased cadence whereas Soleus excitation remained relatively constant. Second, during the recovery phase, a second peak in excitation became evident in Soleus with increased cadence whereas in Gastrocnemius an albeit small, second peak decayed and was not evident at the 110-rpm condition. Gastrocnemius lengthened until about 90 degrees of crank rotation whereas the Soleus muscle had begun to shorten by about 45 degrees of crank rotation. The velocity data indicated that the shortening phase for Soleus was much shorter in duration than for Gastrocnemius. These data suggested a potential difference in function between Soleus and Gastrocnemius such that the Soleus was primarily involved in generating initial propulsive force and the Gastrocnemius maintained output later in the

cycle. Perhaps this prolonged force resulted from the stretch in Gastrocnemius that occurred in the initial portion of the pedalling cycle. During the 180°-270° sector of crank rotation Soleus was acting concentrically while Gastrocnemius acted eccentrically. The changes in Gastrocnemius and Soleus excitation profiles may, in part, be related to the high and increasing shortening velocity of the Gastrocnemius at higher cadences. The simultaneous flexion of the knee and dorsi-flexion at the ankle may have put the Gastrocnemius at a disadvantage for effective contraction. This might suggest that both length and velocity characteristics for Gastrocnemius and Soleus favour the Soleus for force production. However, these recovery phase peaks are small and it is not clear how they impact overall cycling mechanics. Nonetheless. This provides an interesting opportunity to examine influence of the mechanical environment on excitation.

REFERENCES

Grieve, D.et al. (1978). *Biomechanics VI.* pp. 405-412.
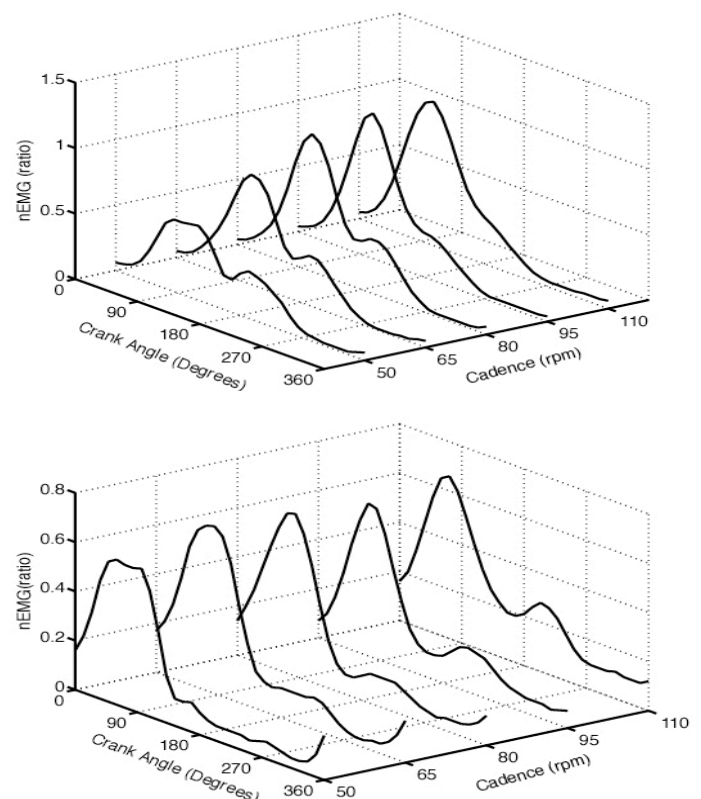Sanderson, D. et al. (1999). *MSSE* 31(5), Suppl. 357.

Figure 1. Mean Gastrocnemius (top) and Soleus (bottom) excitation patterns normalized to the 50-rpm condition as a function of cadence and crank angle.

COMPARISON OF LOADED AND UNLOADED STAIR DESCENT

Joe Lynch[1] and D.G.E. Robertson[2]
Department of Human Kinetics, University of Ottawa, Ottawa, Canada
[1]jlync022@uottawa.ca   [2]dger@uottawa.ca

INTRODUCTION

Recent research regarding stairs has focused on muscle action and reaction forces while moving down stairs. For example, it is known that higher loads on the knee exist while descending the stairs (Yu *et al.*, 1997) as compared with level walking. McFayden & Winter (1988) have shown high peak powers at the knee when walking down stairs, while the hip is used for forward continuance. Unfortunately, few studies compare the mechanical differences in normal stair descent and loaded stair descent. The implications of loaded stairs descent may play on degenerative joint disease and other lower limb pathologies is of value. Knowing the stresses on the lower extremity joints can help with carrying limits in workplaces or daily activities.

METHODS

A sample population of three male and two female volunteers were used for this study. Subjects were asked to walk five times down stairs normally (30x20 cm steps), followed by five stair descent trials with the subject carrying a 16 kg load in the frontal plane. A Kistler 9281B force plate recorded the force data while digital camera collected the sagittal view trajectories of markers placed on the left side of the body. The kinematic data were combined with force platform data by inverse dynamics to determine the net moments and powers at the ankle, knee and hip (Robertson & Winter, 1980). The data were ensemble averaged and normalized to body mass. All data were processed using the Biomech Motion Analysis System.

RESULTS AND DISCUSSION

Figures 1 and 2 show the body mass normalized powers produced by the hip, knee and ankle moments of force during loaded and unloaded stair descent, respectively. The stride cycle for these figures begins and ends at toe-off. Foot-strike is indicated with a vertical line. There were no significant differences in the patterns of the net moments and powers at ankle, knee and hip joints between the loaded and unloaded conditions. In both the loaded and unloaded conditions large eccentric knee powers occurred just before toe-off but even though the peak power was smaller for the unloaded condition shown in Figure 2 the differences across subjects were not significant.

Notice the low powers at the hip for both conditions. This is typical for stair descent since the hip moments of force are not needed as much as during level gait since the horizontal distance to swing the leg is small–only 30 centimetres.

The ankle, like the other two joints, does not differ when a load is added. Its main function was to absorb energy after foot-strike (IFS) to cushion the toe landing during stair descent. It was not a significant contributor to push-off as occurs during level locomotion.
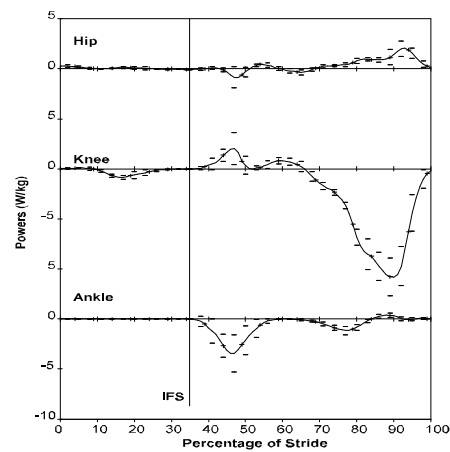
Figure 1: Typical moment powers (W/kg) of the hip (top), knee and ankle during loaded (16 kg) stair descent
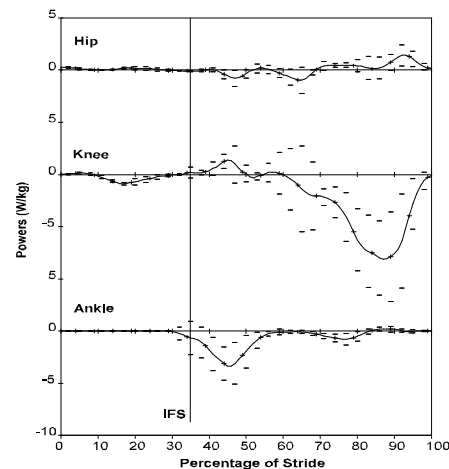
Figure 2: Typical moment powers (W/kg) of the hip (top), knee and ankle during unloaded stair descent

SUMMARY

The moment powers of the ankle, knee and hip failed to show any significant differences with the addition of a 16 kg frontal load. There was slightly greater knee eccentric extensor power but this was not significantly different across subjects due to the higher variability during the loaded condition.

REFERENCES

McFayden B, Winter, DA (1988). *J Biomech*, **21**, 733-44.
Robertson DGE, Winter DA (1980). *J Biomech*, **13**, 845-54.
Yu et al. (1997). *Clin Biomech*, **12**, 286-93.

ON THE MEASUREMENT OF RESIDUAL STRESSES DUE TO CEMENT
POLYMERIZATION PERTINENT TO CEMENTED HIP IMPLANTS

Natalia Nuño and Dominic Plamondon
Département de génie de la production automatisée, ETS,
Laboratoire de recherche en imagerie et orthopédie
Université du Québec, Montréal, Canada
natalia.nuno@etsmtl.ca

INTRODUCTION

One of the main concerns in the success of long-term survivorship of Total Hip Arthroplasty (THA) is the attachment of the prosthesis to the bone. Implant loosening of cemented hip implants is a major cause of late failure of THA. It is believed that separation of the stem-cement interface and fractures in the cement may initiate the initial loss of fixation of the implant.

The bone cement (PMMA) serves as grouting material to fix the implant to the bone in cemented hip implants. During the operation, the bone cement is inserted in a liquid state between the femoral component of the implant and the bone and polymerization occurs. During polymerisation of the cement, residual stresses are generated in the bulk cement. The process of cement curing is a complex solidification phenomenon where transient stresses are generated and the residual stresses vary with different boundary conditions during curing (Ahmed et al., 1982). The cement does not have a chemical bond with the stem nor the bone, however it fills completely the space between the two and serves to distribute the load being transferred from the stem to the bone. A recent experimental and numerical study, Nuño and Amabili (2002), has shown the importance of including the residual stresses due to cement curing in predicting the load transfer of cemented hip prostheses. However, the precise magnitude of these stresses is still not well documented. The main objective of this study is to devise an experiment to measure directly the residual stresses due to cement curing at the stem-cement interface.
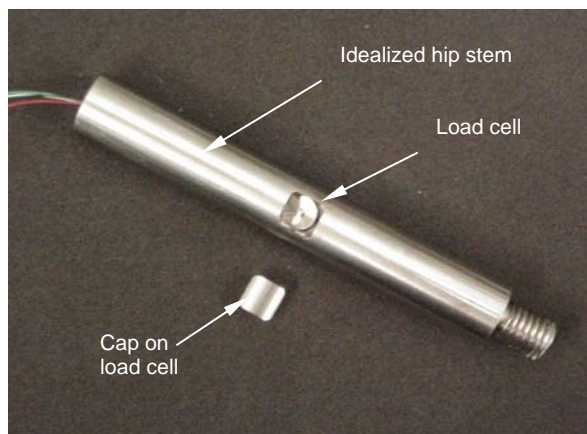

Figure 1. Load cell inserted into the idealized hip stem

MATERIALS AND METHODS

A sub-miniature load cell, 9.5-mm diameter, (ELFM-B1-50L, Entran) is inserted inside an idealized prosthesis (19-mm diameter) to measure directly the radial residual stresses of the bone cement on the stem. The bone cement polymerizes between the stem and the synthetic bone, 30-mm inside diameter and 40-mm outside diameter, made of E-glass-filled epoxy (Sawbones Inc.), used to simulate the cortical bone constraint surrounding the bone cement. The load cell was inserted inside an opening of similar dimensions of the load cell. A cap was machined to cover perfectly the load cell and to close the opening. The wires of the load cell are passed through a small opening in the center of the stem along the axial direction to protect tem (Figure 1). The load cell measures the load exerted from the bone cement on the stem at the stem-cement interface. The tests are conducted at body temperature of 37°C to simulate the *in-vivo* conditions.

Before starting the experiment, different preliminary tests were performed to validate the accuracy of the load cells under different conditions: I) offset of the load cell; ii) stability of the reading measurement with and without a load placed on it; iii) effect of a variation of temperature on the reading.

DISCUSSION

The experiments are being conducted for five idealized cemented hip implants. The residual stresses are being investigated for an early post-operative situation and as a function of time to determine cement creep. A control load cell is used to verify that the eventual relaxation of the radial stresses is due to cement creep and not to variations of the load cell with time. These experimental results of the residual stresses generated in the bulk cement will be included in numerical models of cemented hip prostheses to better predict the load transfer at the stem-cement interface of the implant.

REFERENCES

Nuño, N., and Amabili, M. (2002). *Clin. Biomech, 17*, 41-48.
Ahmed A.M. et al. (1982). *ASME J. Biomech. Eng*, 104, 28-37.

ACKNOWLEDGEMENTS

RECOVERY FROM AN UNEXPECTED RIGHTWAY PUSH DURING WALKING ON A LATERALLY CONSTRAINED WALKWAY

Fariba Bahrami[1, 2], Stephen Hill[2], and Aftab Patla[2]

[1]Control & Intelligent Processing Center of Excellency (CIPCE), University of Tehran, Tehran, Iran, fbahrami@healthy.uwaterloo.ca
[2]Gait and Posture Laboratory, Department of Kinesiology, University of Waterloo, Waterloo, Canada

INTRODUCTION

The underlying challenge of locomotion is to control the centre of mass (COM) and the base of support (BOS), which are both moving and changing over time. The COM is within the BOS only during the two brief double support phases of the gait cycle. Stability during gait is managed by applying anticipatory, predictive, and reactive modifications to the gait pattern (Patla, 2003). Reactive strategies are, by definition, produced in response to unexpected sensory information, such as the sensations associated with being pushed. Townsend (1985) demonstrated that swing foot placement control could be used to stabilise balance in gait. Oddsson et al (2004) showed that the lateral positioning of the foot with respect to the COM is the most important factor in controlling the ML (medio-lateral) acceleration of the COM.

It has been demonstrated that the principles established about stability of standing can not be applied directly to the situation of walking (e.g., Sinkjaer et al, 1996). The recovery from an unexpected gait perturbation is a reactive one that continues for at least two steps following the perturbation onset (Hill et al, 1999). In this study we investigated the recovery responses to rightward pushes to the trunk during walking on a walkway of restricted width. The reactive recovery from these perturbations was examined in terms of the relationship between the perturbation direction and the single support side at the perturbation onset.

METHODS AND MATERIALS

Six healthy female adults (16-24 years) participated in this study. Rightward ML trunk push perturbations were delivered to the left shoulder with a custom-built computer-controlled mechanical perturbation device. Participants walked on the level floor at their natural speed. The lateral boundaries of the walkway were restricted either by a blue floor covering (B) or by wooden kick-plates (W). Perturbation onset occurred either during the left single support (LSS) or the right single support (RSS) phases of the gait cycle. From collected kinematics, the ML velocity of the body COM (VZcom), trunk rotational velocities in the frontal and transverse planes (VRoll, VYaw, respectively) were obtained. The instants in time when these variables attained their maximum values (TmaxVZ, TmaxVR, TmaxRoll, TmaxVY, TmaxYaw) were determined. Step width (Z_{step}) and length (X_{step}), and times of heel-contact (HC) and foot-flat (FF) for the perturbed step (1stHC, 1stFF) and FF of the second step (2ndFF) after perturbation were also detected.

RESULTS AND DISCUSSION

The results indicate that for the LSS trials, in response to the perturbation, the step was widened (Z_{step}(LSS)=25.5±5.6 cm versus Z_{step}(no-perturbation)= 10.18±2.73 cm). Whereas, for RSS trials, the left swing foot in response to the perturbation crossed over medio-laterally in front of the right stance foot ($Zstep$(RSS)=-4.3±3.4 cm). Therefore, based on the single support side at the perturbation onset, different strategies were applied to stabilize the movement. Our results also show that TmaxVZ did not change based on the single support side (TmaxVZ(LSS)= 0.375±0.084 s, TmaxVZ(RSS)= 0.377±0.15 s). However, the boundary conditions of the walkway were considered in the process of controlling the ML velocity of the COM (TmaxVZ(B)= 0.41±0.12 s, TmaxVZ(W)= 0.34±0.11 s). The percentage of the decrease in the ML and rotational trunk velocities (Table 1) indicate that following perturbation, recovery of the rotational movement of the trunk was accomplished more quickly than in the ML direction.

Table 1: Percentages of the decrease in the linear and rotational velocities, calculated relative to the corresponding peak-to-peak values.

	LSS	RSS
MaxVZ-VZ(2ndFF)	38.3%	49%
MaxVR-VR(2ndFF)	80.2%	66.8%
MaxVY-VY(2ndFF)	71%	83.4%

CONCLUSIONS

The results of this study indicate that boundary conditions of the walkway affected the control of movement in the ML direction. While, single support side at perturbation onset effected the rotational movement of the trunk. On the other hand, step length of the first step after perturbation was modified based on the single support side at perturbation onset and the walkway boundary conditions, whereas the ML component of that step was affected only by the single support side at the perturbation onset. In addition, stabilization of the rotational movement of the trunk in the frontal and transverse planes has been accomplished more quickly than stabilization of the ML movement of the body. These trunk rotations were an answer to the mechanical perturbation of the trunk itself, and most probably were stabilized through stiffness control. All of these findings indicate that balance recovery after perturbation was mainly based on a foot placement strategy (change in the base of support).

REFERENCES

Patla, A.E. (2003). *Eng in Med Biolog IEEE*, **22** (2), 48-52.
Townsend, M.A. (1985). *J Biomech*, **27**, 1339-1346.
Oddsson, L.I.E. et al (2004). *Gait & Posture*, **19**, 24-34.
Sinkjaer, T. et al (1996). *J Neurophy*, **76** (2), 1112-1120.
Hill, S.W. et al (1999). *In Proc of 29th Annual Meeting of the Society for Neuroscience,* **25**: 912 #366.12.

STABILITY ANALYSIS OF MEDIO-LATERALLY PERTURBED GAIT

Fariba Bahrami[1,2], Stephen Hill[2], and Aftab Patla[2]

[1]Control & Intelligent Processing Center of Excellency (CIPCE), University of Tehran, Tehran, Iran, fbahrami@healthy.uwaterloo.ca
[2]Gait and Posture Laboratory, Department of Kinesiology, University of Waterloo, Waterloo, Canada

INTRODUCTION

Traditionally, stability in legged locomotion is taken to refer to *static stability* (Full et al, 2002). However, the static stability criterion is satisfied only during the two double support phases (20% of a gait cycle). Thus, it is necessary to define a *dynamic stability* criterion for gait. Full at al (2002) defined dynamic stability during locomotion as the ability of characteristic measures (e.g., velocities) to return to their steady state, periodic gait values after a perturbation. Stability during gait is managed by applying anticipatory, predictive, and reactive modifications to the gait pattern (Patla, 2003). This study focuses on reactive responses to unexpected perturbations during gait. Tang et al (1998) observed that in perturbed gait, postural activity from the leg and thigh muscles was the key to balance control. Accordingly, MacKinnon et al, (1993) demonstrated that the whole body medio-lateral (ML) balance is achieved predominantly by the placement of the supporting foot relative to the horizontal location of the COM. Bauby and Kuo (2000) suggested that during walking, in the sagittal plane the body may exploit passive dynamic properties of the limbs; but that in order to maintain ML stability, the body must apply active control. Oddsson et al (2004) mentioned that the ML trunk motion during walking behaves like a periodic stable system, which after a platform perturbation will go out of its nominal path. They used the trajectory of the trunk response to the perturbation as it returned to its nominal path to investigate the gait stability. Most of the previous gait perturbation studies employed slip perturbations, which disrupted the base of support (BOS). In the present study, we have analyzed the recovery response time to an ML trunk perturbation during gait along a walkway of restricted width. The settling/recovery time of the step width and length, and that of the ML velocity of the COM after the onset of the perturbation at heel-contacts (HC) were used to quantitatively study the stability of gait. The effect of the relationship between perturbation direction and the single support side at the perturbation onset was also considered.

METHODS AND MATERIALS

Six healthy female adults (16-24 years) participated in this study. Rightward ML trunk push perturbations were delivered to the trunk with a custom-built computer-controlled mechanical perturbation device. The participants walked on the level floor at their natural speed. The lateral boundaries of the walkway were restricted. Perturbation onset occurred either during left single support (LSS) or right single support (RSS) phase of the gait cycle. Each participant also performed 10 non-perturbed gait control trials. From collected kinematics, the ML velocity of the body COM, step width and length at HCs before and after perturbation were detected.
Step width and length are two important characteristics of foot placement. This study employs the notion of **settling time** to quantify the speed of the recovery from a perturbation. The **settling times** for step width (SETZ) and length (SETX), and the absolute changes in the ML velocity of the COM (ΔVZ_{com}) between two successive heel-contacts (SETΔVZ) were determined. For each of the mentioned variables, the settling time has been defined to be the number of the steps needed to be taken until that variable returns to its average nominal values plus or minus one (for ΔVZ_{com}) or two (for step length and width) standard deviations. The average value was calculated from control trials.

RESULTS AND DISCUSSION

The results indicate that the settling time of the step length for LSS trials (SETX(LSS)=2.35±0.76 steps) was significantly longer than that of the RSS trials (SETX(RSS)=1.97±0.75 steps). While, there were no significant differences between settling times of ΔVZ_{com} and the step widths when the two groups of the LSS and RSS trials were compared. On the other hand, settling time of the step lengths (SETX=2.22±0.75 steps) was significantly shorter than the settling times of the step widths (SETZ=3.43±0.82 steps) and ΔVZ_{com} (SETΔVZ= 3.05±0.91 steps). While, the difference between SETZ and SETΔVZ was not significant.

CONCLUSIONS

Our results indicate that the settling time of step width was not significantly different from the recovery time of the HC-to-HC changes in the ML velocity of the COM. On the other hand, balance recovery in the anterio-posterior (AP) direction was accomplished more quickly than in the ML direction. In LSS trials, since the rightward push caused the COM to move away laterally from the stance foot, the recovery time of step length was longer than in the RSS trials, where the COM was pushed towards the BOS. Thus, in order to stabilize the movement after the rightward perturbation of the trunk, the foot placement was modified both in the AP and ML directions. However, the ML stability measures (step width and ML velocity of the COM) exhibited longer time to return to their steady-state values than the AP measure (step length) did. The longer ML settling times are consistent with the application of an active ML stability control (Bauby and Kuo, 2000).

REFERENCES

Full, R.J. (2002) *Integ and Comp Biol*, **42**, 149-157.
Patla, A.E. (2003) *Eng in Med Biolog IEEE*, **22** (2), 48-52.
Tang, P.F. et al (1998) *Exp Brain Res*, **119**: 141-152
MacKinnon, C.D. and Winter, D.A. (1993) *J Biomech*, **26,** 633-644.
Bauby, C.E. and Kuo, A.D. (2000). *J Biomech*, **33**, 1433-1440
Oddsson, L.I.E. et al (2004) *Gait & Posture*, **19**, 24-34.

THE QUANTIZATION OF THE THREE QUADRICEPS MUSCLES BETWEEN TWO WALKING CONDITIONS

Mina Agarabi[1], Cheryl Kozey[1,2], Kevin Deluzio[1], Scott Landry[1], Jennifer McNutt[1] and Dr. Stanish[3]
[1]School of Biomedical Engineering, Dalhousie University, Halifax, Canada, magarabi@dal.ca
[2]School of Physiotherapy, Dalhousie University, Halifax, Canada
[3]Department of Surgery, Dalhousie University, Halifax.Canada

INTRODUCTION

Recruitment of the lower extremity muscles during gait can be characterized by temporal patterns of muscle activity. Key principal patterns of the measured muscle activity are hypothesized to originate from a common pattern generator in the central part of the brain (Ivaneko, in press). Previous studies have reported differences in relative amplitudes and phases for rectus femoris and vastus lateralis activity with speed changes (Shiavi et.al., 1987, Yang and Winter, 1985). In this study, we expanded the analysis to a larger sample, measured from three quadriceps sites and utilized principal component analysis of ensemble averaged muscles patterns to determine the individual muscle's unique role as well as synchronicity among the quadriceps. The objective of this study was to determine the interaction of the measured surface electromyographic (EMG) patterns of the quadriceps between two walking conditions.

METHOD

Forty-two healthy subjects with no prior history of knee pain, injury, surgery or osteoarthritis participated in the study. Participants were asked to walk along a 5 meter walkway at a normal speed and at 150% of their normal speed-five trials each. Surface electrodes (Ag/ag cl Meditrace [TM]) were placed over the vastus lateralis, vastus medialis and rectus femoris to record muscle activity during walking. Subjects were asked to produce maximal voluntary isometric contractions (MVIC) for knee extension and flexion against a Cybex isokinetic dynamometer at 15 and 45 degrees in supine and knee flexion while prone. EMG signals were amplified (AMTI-8, Bortec, Canada), sampled at 1000Hz, full wave rectified and low pass filtered at 6Hz. The linear enveloped EMG from the walking trials was amplitude normalized to the MVIC and time normalized to one gait cycle. Ensemble averages of five walking trials for each muscle, for each subject and each condition were calculated and a matrix (101X252) of the average waveforms was factored (Hubley-Kozey and Vezina, 2003). The *scores* for the principal patterns were derived and a two way ANOVA (muscle,condition) was used to test main effects and interactions for the *scores* representing the principal patterns.

RESULTS AND DISCUSSION

Descriptive Statistics: Condition 1: 1.37m/s +/- 0.19; Condition 2: 1.88m/s +/- 0.24; Age: 51 +/- 10.04; Five principal patterns account for 96.3% of the variance in the total waveform across the three muscles. Three of the five principal patterns (1,3,5) had muscle by condition interaction ($p<0.05$) and two (2 and 4) had significant muscle main effects ($p<0.05$). The first principal pattern, accounted for 84% of the variance, capturing a burst of activity at foot flat (10-15%) and a second burst of smaller amplitude at swing (60-65%). This pattern is common to all three muscles suggesting temporally synchronized co-activity among the quadriceps and supports

previous work illustrating common patterns and common drives to these muscles (Ivaneko, in press). There were significant differences for all pairwise comparisons illustrating that the contribution of pattern one to the total waveform for each muscle differed and they differed between conditions as well. The highest *score* was for the vastus medialis (condition 2) and lowest *score* for the rectus femoris (condition 1).
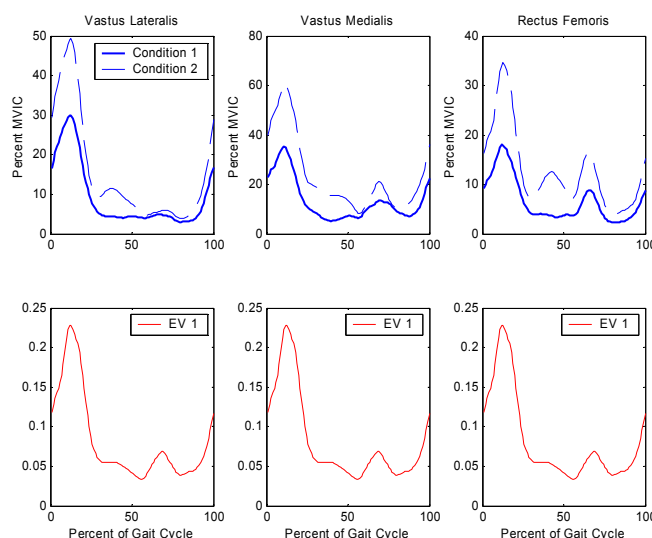

Figure 1: Top row-MVIC of quadriceps for two conditions as a function of the gait cycle and bottom row-principal pattern 1

The significant differences among muscles and group by condition interactions for the other four principal patterns suggest that there are differences in the temporal waveforms that are muscle dependent and are also altered by speed.

SUMMARY

While the principal pattern explained a large percentage of the variance in waveforms among muscles, the significant difference between the muscles suggests selective recruitment and varying roles of the individual quadriceps during gait, some of which were altered with speed. In addition, the significant difference among muscles across conditions does not support the theory that an increase in walking speed causes a consistent increase in the activity across all three muscles. Understanding the role of the quadriceps and the variance present in the waveform during gait provides a standard to assess abnormal EMG patterns associated with gait.

REFERENCE

Hubley-Kozey and Vezina (2002) *Clin Biomech,* 17, 621-629.
Ivaneko,Y.P. et al. (2004) J. Appl *Phys in Press*
Shiavi, R. et al. (1987) *Rehab Res and Develo*, 24, 13-23.
Yang, J.F. Winter, D.A. (1985) *Electroencephalography and clinical Neurophysiology*, 60, 485-491.

ACKNOWLEDGEMENT

FE modelling of dynamically induced micromotion for a polished tapered THR stem

K Polgár, DW Murray, JJ O'Connor, HS Gill
NDOS, University of Oxford, Botnar Research Centre, Nuffield Orthopaedic Centre, Oxford, OX3 7LD

Introduction: The design philosophy of polished tapered total hip replacements (THR), such as the Exeter, intends for them to migrate distally within the cement mantle. As well as migration, dynamically induced micromotion (DIMM) occurs as a result of functional activity between the implant and the cement. The aim of the current study was to develop and validate a finite element (FE) model of the Exeter/cement/bone system which can be used to predict DIMM and investigate the stresses induced in the cement mantle during functional activity.

Methods: In the context of the current study, DIMM is defined as the displacement of the implant component relative to the bone when moving from double leg stance to single leg stance on the operated limb. Using Roentgen Stereophotogrammetric Analysis (RSA), DIMM was measured in 21 patients implanted with Exeter stems 3 months post-operatively.

A previous study, using a reduced FE model of the Exeter stem and the surrounding cement mantle focused on the solution of the contact problem at the stem-cement interface. It was demonstrated that sliding contact combined with Coulomb friction and an appropriate parameter setting could be used to predict DIMM of a polished tapered stem. For the purposes of the current study, the previous simple model was incorporated into the FE model of the Muscle Standardised Femur and validated against the RSA measurements for DIMM. For the current extended model, loading included muscle forces representing all active muscles acting on the femur. The effect of initial cement stresses and interdigitation was also considered.

Results: The Exeter stem demonstrated significant DIMM (p< 0.017). The FE model, accounting for sliding contact at the cement–implant interface was able to predict similar distal migration of the head and the tip. The results of both the calculations and the measurements showed that the femoral head moves medially, distally and posteriorly relative to the bone. In the cement mantle, maximum principal stresses were oriented circumferentially (Fig.1), minimum principal stresses were oriented radially. When the taper got engaged, submicroscopic movements which did not recover following unloading still took place and accumulated.

Discussion: The results of the present study showed that it is possible to measure DIMM in the Exeter stem and combine this with FE modelling of the contact mechanism. Future studies will include various activities, such as walking or stair climbing. Based on accumulated submicroscopic movements, short-, mid- or long-term migration patterns will be predicted.
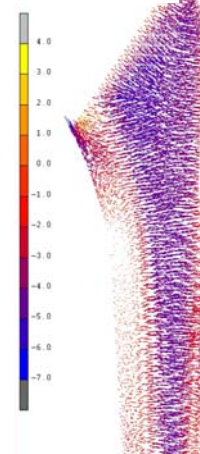
σ_{11} (MPa)

Fig. 1 Tensor plot of the maximum principal stresses in the cement mantle

3D CHARACTERIZATION AND LOCALIZATION OF ANATOMICAL LANDMARKS OF THE FOOT

Xiang Liu[1], Wangdo Kim[1] and Burkhard Drerup[2]

[1] School of Mechanical & Production Engineering, Nanyang Technological University, Singapore, mwdkim@ntu.edu.sg
[2] Klinik und Poliklinik für Technische Orthopädie und Rehabilitation, Universtätsklinikum, Münster, Germany

INTRODUCTION

The anatomical landmarks on the body surface are important to shape and motion analysis. This paper presents a method for extracting anatomical landmarks on the foot from scattered 3D surface points collected by FastSCAN (Polhemus, Colchester, Vermont, USA). By least squares surface fitting, the surface is reconstructed from the scattered points and the Gaussian curvature and mean curvature are calculated. The landmarks formed by underlying muscles and skeletal structures distinguish themselves clearly on the Koenderink shape index maps (Koenderink, 1999). The loci of landmarks avail possible medical application such as the determination of tibial torsion and tibial nail length.

METHODS

A plaster cast was taken from the right foot of a 40-year-old healthy man. Measurement was done by the FastSCAN laser scanner (Polhemus, Colchester, Vermont, USA). In our application several views from different directions were taken. The density of measurement points was about 40 points/cm².

It is easy to calculate the Gaussian curvature and mean curvature once the analytical equation of the surface has been given. But from the experiment, we can only get discrete data, for example the (x, y, z) coordinates of isolated points. A second order polynomial with six degrees of freedom is fitted to the scattered points:

$$z = c_1 + c_2 p + c_3 q + c_4 p^2 + c_5 pq + c_6 q^2 \qquad (1)$$

where p and q are the local coordinates with respect to the respective grid point (x_{ik}, y_{ik}) centring the fitted patch:

$$p = x - x_{ik}, \; q = y - y_{ik} \qquad (2)$$

By minimizing the difference between the scattered points and the surface represented by (1) with weighted least square method and normal equations, we can fit the second order polynomial surface patch in a small area around the centre point and calculate the six coefficients, from which the Gaussian curvature and mean curvature could be derived (Frobin, 1982&1985).

RESULTS AND DISCUSSION

The Koenderink shape index maps of the ankle regions and the underside of the foot (Fig. 1) clearly separate the convexity from the concavity and characterize the foot surface. For simplicity, we categorize the shapes into three surface types instead of nine provided by Koenderink shape index. Each type of shape's color changes its deepness according to the surface types. For example, when the surface changes from ridge via dome to spherical cap, the color on the colorbar changes from light red to deep red concomitantly. The white is taken as transition between different colors for clear differentiation of different surface types (concave, convex or saddle-shaped). As a result, the outer malleolus and inner malleolus emerge from their neighbourhood. Besides these two expectable regions, on the underside of the foot, there are at least 4 possible landmarks: the convex region formed by the distal ends of first and second metatarsal, the distal end of fifth metatarsal, the concave region under the arch and the heel. Due to the instability of the toes, they are obliterated from the consideration of landmarks.

Figure 1. The 3D display of map of Koenderink shape index of the ankle area (from 3 different viewpoints) and the underside of the foot. Red: convex, green: saddle-shaped, blue: concave, white: transitions between these three different shapes.

SUMMARY

The method has provided an objective way of determining anatomical landmarks. The found medial and lateral malleoli could be used to determine the tibial torsion and the tibial nail length if the anatomical landmarks (tibial tubercle and tibial condyles) below the knee are extracted too.

REFERENCES

Koenderink, J and Doorn, A. van (1999). *Image and Vision Computing*, **10** (8), 557-565.
Frobin, W and Hierholzer, E. (1985). *Proceedings of SPIE Biostereometrics '85*, **602**; 109-115.
Frobin, W and Hierholzer, E. (1982). *Journal of Biomechanics*, **15**, 379-390.

GAZE STABILIZATION OF BALANCE
WITH AND WITHOUT AN ANKLE FOOT ORTHOSIS: A PILOT STUDY

Vickers J. N., [1] Ronsky J.L., [2,3] Ramage B.,[3] Morton T.B. [1] & Park S. [4]
[1] Faculty of Kinesiology & [2] Faculty of Engineering, University of Calgary
[3] McCaig Centre for Joint Injury and Arthritis Research, Heritage Medical Centre, Calgary
[4] Ewha University, Korea

INTRODUCTION

Despite extensive research "it is still not known what serves as the cue for visual stabilization of posture" (Strupp et al, 2003, 352). When a target is viewed in frontal space, sway is minimized by the vestibular ocular reflex thereby nullifying retinal slip. When saccades or pursuit tracking occur sway increases. Suppression of eye movements is known to reduce sway and improve balance when fixating near targets (Jahn et al, 2002). Fixations hold the gaze on one location in space and provide on-going sensory feedback of target location. When an external cue is present, fixation is typically maintained within 1 degree of visual angle of the target (Strupp et al, 2003). The purpose of this study was to determine the effects of wearing an ankle-foot orthosis while fixating a plain surface devoid of external cues. Orthoses are designed to improve posture and decrease sway, but little research has been carried out to determine the effects of wearing an orthesis when external cues are absent. Fixation frequency, fixation duration, and inter-fixation visual angle were assessed while normal participants maintained balance and fixated a vertical plain surface, with and without an orthosis.

METHODS

Four adults, (age 20-24) maintained balance for 3 trials of 30 s while fixating a surface 2 meters in front. Two served as controls and fixated an *x* at eye height. Fixation data were collected using a mobile eye tracker (ASL 501H) and a magnetic head tracker (Flock of Birds). Eye-head software at 60 Hz generated line of gaze relative to the surface. Eyenal software determined fixation onset when the gaze (standard deviation) was within 0.5 degrees of visual angle for 100 ms; fixation duration was a minimum of 100 ms; inter-fix angle was measured in degrees of visual angle between the first fixation recorded and each subsequent fixation. Separate repeated measures ANOVA's were used to determine fixation differences due to condition (No orthosis, Orthosis) x Trials (3).

Email: vickers@ucalgary.ca

RESULTS AND DISCUSSION

The results in the control condition (*x*) were similar to those found in past studies for fixation frequency (M = .33/s; SD = .31/s), fixation duration (M = 4.05 s; SD = 2.04), and inter-fix visual angle (M = .24 degrees; SD = .34). Analysis of fixation relative to the plain surface found a significant difference for inter-fix angle $\underline{F}_{(2, 10)}$ = 6.58, $\underline{p} < 0.05$, indicating fixation was maintained closer to the initial fixation location with the orthosis than without (see Fig 1). Wearing the orthosis had no effect on fixation frequency or duration, indicating a similar level of focus was maintained irrespective of the ankle-foot orthosis. Significant trials effects showed that fixation frequency increased, fixation duration decreased, and inter-fixation angle increased across trials, suggesting holding fixation was difficult for the full 90 s. Since fixation duration and fixation frequency were not affected by wearing the orthosis, then it was unlikely that the difference in inter-fixation angle was due to loss of focus; instead the results suggest that wearing the orthosis improved fixation stability relative to the plain surface.
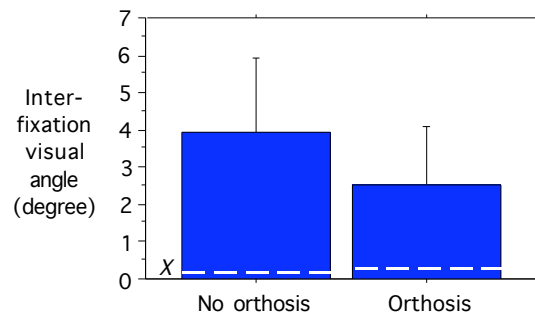

Figure 1. Mean inter-fixation angle with and without an ankle-foot orthosis (white line show mean angle to the *x*).

REFERENCES

Jahn et al, T. (2002). Suppression of eye movements improves balance. *Brain,* 125; 2005-2011.

Strupp et al (2003). Eye movements and balance. *Annals New York Academy of Sciences*, 1004, 352-358.

ACKNOWLEDGEMENTS

CONTRACTILE HISTORY INFLUENCES THE FORCE-VELOCITY RELATIONSHIP OF SKELETAL MUSCLE

Sharon R. Bullimore, Jong Sun Park, Tim R. Leonard, and Walter Herzog
Human Performance Laboratory, Faculty of Kinesiology,
The University of Calgary, Calgary, Canada, walter@kin.ucalgary.ca

INTRODUCTION

It has been known for a long time that the steady state isometric forces following muscle shortening are depressed, and following stretch are enhanced compared to the corresponding purely isometric reference contractions (e.g. Abbott and Aubert, 1952). However, it is not known whether force depression and enhancement also occur during dynamic rather than just static contractions.

The purpose of this study was to investigate the effect of shortening and stretching of skeletal muscle on dynamic force production. Specifically, we preceded standard force-velocity testing (Hill, 1938) by shortening or stretch of the activated muscle, and compared the force-velocity properties obtained in this way with those obtained without prior shortening or stretch. We hypothesized that active shortening would decrease the forces at equivalent speeds, and active stretch would increase the forces compared to those obtained for the standard force-velocity relationship.

METHODS

Experiments were performed on cat soleus muscles (n=8). Muscles were isolated in situ and were activated through electrical stimulation of the tibial nerve. A standard force-velocity relationship was obtained for speeds of shortening and stretch of 5, 10, 20, 40, and 60mm/s. These speeds were selected as it is known that the maximal speed of soleus shortening is about 180mm/s (Spector et al., 1980), and that 60mm/s produces approximately 20% of the maximal isometric force. Once the reference force-velocity relationship was obtained, eight additional force-velocity relationships were obtained by preceding the standard force-velocity test by shortening and stretch of 3, 6, 9, and 12mm magnitude at a speed of 6mm/s. Force-velocity properties were then normalized relative to the isometric force of the standard force-velocity relationship and plotted for comparison.

RESULT AND DISCUSSION

Force-velocity relationships preceded by shortening of the activated muscle had smaller forces at all speeds, and force-velocity relationships preceded by stretch had greater forces at all speeds compared to the force-velocity relationship obtained without prior shortening or stretch of the muscle (Figure 1). These results are strong evidence that force depression and force enhancement occur during dynamic contractions and do not only occur in isometric steady-state situations. As for the static situations, in these dynamic situations, force depression increases with increasing amounts of shortening, and force enhancement increases with increasing amounts of stretch. Force depression effects appear to be greater in general than force enhancement effects. Finally, the relative effects of force depression and force enhancement are greatest at the fastest speeds of shortening (Figure 2). We conclude from these results that the history-dependent effects of force production observed for static situations for over half a century also occur in dynamic situations.
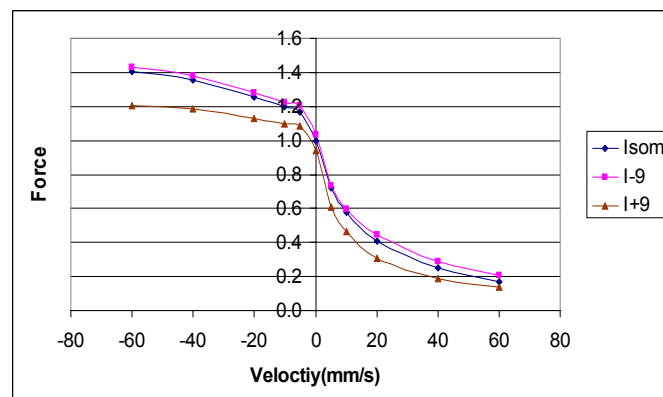
Figure 1: Normalized Force-Velocity relationships, Isom = standard curve. I-9 and I+9 = force-velocity curves preceded by 9mm of stretch or shortening, respectively.
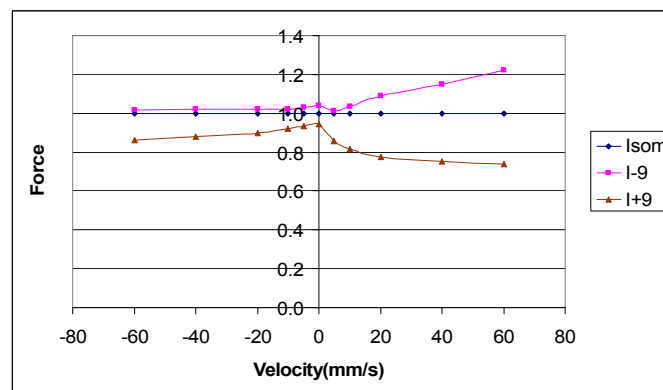
Figure 2: Percentage of force depression (brown) and force enhancement (pink) from the standard reference curve (1.0) for force-velocity curves preceded by 9mm of shortening and stretch, respectively.

REFERENCES

Abbott and Aubert (1952), *J Physiol.(London),* **117,** 77-86.
Hill, A.V.(1938), *Proc. Royal Soc. London,* **126**, 136-195.
Spector, S.A. et. al. (1980), *J Neurophysiol,* **44(5)**, 951-60

SIT-TO-STAND ANALYSIS IN SUBJECTS WITH KNEE OSTEOARTHRITIS.

Mohammad Alkhazim Alghamdi[1], Sandra Olney[2], Patrick Costigan[2]

[1] College of Applied Medical Sciences, King Faisal University, Dammam, Saudi Arabia

[2] School of Physical and Health Education, Queen's University, Kingston, Canada.

malkhazim@hotmail.com

INTRODUCTION

Standing up from a sitting position (STS) is an essential task of normal daily life (1). STS is rarely investigated in subjects with knee osteoarthritis (OA). The purpose of this study was to describe the biomechanics of STS movement in subjects with mild to moderate knee OA and subjects without knee OA.

METHODS

28 patients (7 men and 7 women) with mild to moderate knee OA and 14 subjects (10 men and 18 women) without knee OA participated in the study. The study was approved by Queen's University Human Research Ethics Committee.

An Optotrack optoelectronics motion analysis system integrated with a forceplate was used to collect STS biomechanical data. Using two-sided adhesive tape, infra-red emitting diodes (IREDs) were placed laterally over the anatomical landmarks of the head of 5th metatarsal, lateral aspect of heel, lateral malleolus, fibular head, femoral epicondyle and greater trochanter. Two projecting probes with an IRED attached to their endpoints were attached to the subject's thigh and shank. In addition, one anchor probe with one IRED was placed on the 7th cervical spinous process and one anchor probe with three IRED markers arranged in a triangle shape was placed at the back of the spine at the L5-S1 vertebra. All extremity markers were placed on the side of the body that faced the cameras. A wooden stool (armless and backless chair) with a height of 44.5 cm was used. Prior to standing, subjects were asked to sit in a normal way with about 75% of the thigh on the stool, arms folded across the chest and the foot of the tested leg resting on the force plate.

Queen's Gait Analysis in Three Dimensions (QGAIT) software was used to compute the outcome data. Based on the inverse dynamic algorithm model, QGAIT utilized marker data, force plate data, anthropometric data and joint center correction vector data to execute the necessary normalized angles, forces, and moments for knee and hip joints in three dimensions.

Calculated parameters were averaged among different trials for each subject and used later on for statistical analysis. Non-paired t-tests were used to compare outcome variables between OA and non-OA subjects.

RESULTS AND CONCLUSION

Table 1: Mean (st. deviation) for STS events shown to be significantly different (p<0.05) in subjects with OA from subjects without OA.

	Subjects without OA	Subjects with OA
STS time (s)	1.5 (0.17)	1.8 (0.3)
Initiating buttock lift (% of STS)	27.2 (3.6)	28.6 (4.7)
Maximum ankle dorsiflex (% STS)	48.5 (3.8)	50.4 (6.5)
Trunk flex/ext,deg	12.8 (6.5)	15.1 (7.2)
Hip ab/adduction	12.8 (4.2)	14.7 (7.2)
Knee ab/adduction	9.6 (3.6)	12.5 (7.1)

The OA group had significant differences in STS time, trunk flexion/extension, hip adduction/abduction, and knee adduction/abduction from the non OA group (Table 1). There were no significant differences between the two studied groups in peak forces of the knee or peak moments of either knee or hip. Table 2 shows peak hip lateral-medial (LM) and hip distal-proximal (DP) forces, which were significantly different in the OA group from the non OA group. The P-value was <0.05.

Table 2: Mean (st. deviation) of peak hip LM and DP forces. Forces measured in N/kg

	Subjects without OA	Subjects with OA
Hip LM forces	0.18 (0.15)	0.42 (0.37)
Hip DP forces	-3.25 (0.66)	-2.76 (0.70)

The study concluded that STS analysis could be a valuable tool in evaluating knee OA and intervention outcome for subjects with knee OA.

REFERENCE

1. Ikeda ER et al (1991). *Phys. Ther.,* 71, 743-81.

THE EFFECT OF GAIT LOADS ON THE PROGRESSION OF RADIOGRAPHIC KNEE OSTEOARTHRITIS: A 5-11 YEAR FOLLOW-UP

Scott K. Lynn and Patrick A. Costigan

School of Physical and Health Education, Queen's University, Kingston, Canada,

6SKL1@qlink.queensu.ca

INTRODUCTION

Knee osteoarthritis (OA) has been found to be the most common cause of chronic disability amongst the elderly (Felson, 1998). There is evidence that joint load is a factor in the progression of osteoarthritis (Hurwitz *et al.*, 1998; Miyazaki *et al.*, 2002) and, while altered gait profiles have been linked with osteoarthritis, it is not known if abnormal gait is a cause or effect of the disease. This is due to the compensations that those with symptomatic OA make in their gait patterns in an effort to decrease pain (Schnitzer *et al.*, 1993). No longitudinal studies have tracked gait profiles of asymptomatic subjects looking for the development of OA.

METHODS

Data was collected on 28 originally healthy, elderly subjects during an initial visit and again 5 to 11 years later. Knee gait forces and moments were calculated in all 3 planes using information from an optoelectronic motion tracking system, force plate and scaled radiographs (Li *et al*, 1993). Gait curves were reduced by taking the average magnitude during the stance phase and kinematic data was used to calculate gait time-distance parameters. Also, standardized radiographs from both visits were scored for signs of OA (Scott *et al*, 1993) and a clinical questionnaire (WOMAC®) assessed the degree of OA symptoms (Bellamy *et al*, 1988).

RESULTS AND DISCUSSION

The radiographic scores increased (became more osteoarthritic) over time while the gait time-distance measures and knee gait loads were constant in those subjects who remained without clinical symptoms of OA after the follow-up period. Although other studies have found differences in gait between elderly and young populations (Murray *et al*, 1969; Winter *et al*, 1990), the current work suggests that with increasing age, elderly gait can remain stable as long as there is an absence of injury/disease. The fact that radiographs became more osteoarthritic suggests that, even in the absence of clinical symptoms, a certain amount of wear and tear on the joint over many years is normal.

Some of our returning subjects had gone on to develop clinical symptoms of OA during the follow-up period. Two of these subjects were especially interesting as the subject with the highest adduction moment went of to develop OA in the medial compartment of the knee while the subject with the lowest adduction moment developed OA in the lateral compartment. The adduction moment curves for these two subjects during both visits are shown in Figure 1.
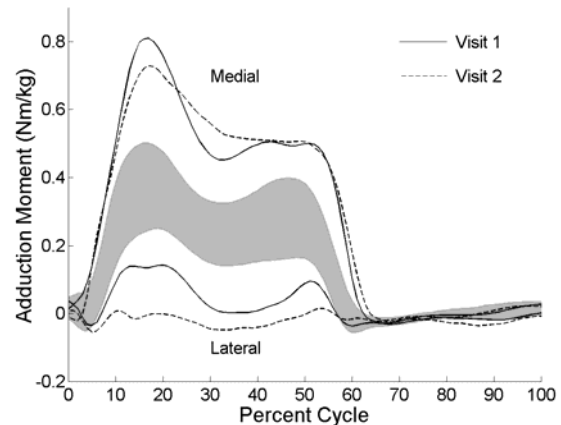

Figure 1. The knee adduction moment for the medial and lateral OA case study subjects – visit 1 and 2. The elderly normal group's initial visit mean +/- 1 SD (n=23) is represented by the shaded region.

This longitudinal result supports previous work that has linked the adduction moment to the progression of OA (Hurwitz *et al.*, 1998; Miyazaki *et al.*, 2002) but a larger sample size is needed.

There was also a significant correlation discovered between the adduction moment and the lateral-medial (LM) shear force in all subjects. It has been suggested that shearing forces are detrimental to cartilage (Lee *et al*, 2002; Tomatsu *et al*, 1992) and therefore this relationship needs to be examined further.

SUMMARY

Results suggest that elderly knee gait kinetics can remain stable over time. Also, the medial and lateral OA subjects suggest that their extreme gait profiles may be important in explaining cartilage break down and the development of OA.

REFERENCES

Bellamy, N. et al (1988). *J Rheum*, **15**, 1833-1840.
Felson, D.T. et al (1987). *Arth Rheum*, **30**, 914-918.
Hurwitz, D.E. et al (1998). *J Biom*, **31**,423-430.
Lee, M.S. et al (2002). *J Orthop Res*, **20**, 556-561.
Li, J. et al (1993). *J Biomech Eng*, **15**, 392-400.
Miyazaki, T. et al (2002). *Ann Rheum Dis*, **61**, 617-622.
Murray, M.P. et al (1969). *J Gerontol*, **24**, 169-178.
Schnitzer, T.J. et al (1993). *Arth Rheum*, **16**, 1207-1213.
Scott, W.W. et al (1993). *Invest Radiol*, **28**, 497-501.
Tomatsu, T. et al (1992). *J Bone Joint Surg (Br)*, **74B**, 457-462.
Winter, D.A. et al (1990). *Physical Therapy*, **70**, 340-347.

GENDER DIFFERENCES EXIST IN OSTEOARTHRITIC GAIT

Kelly McKean[1], Scott Landry[1], Cheryl Hubley-Kozey[2], Michael Dunbar[3], William Stanish[3] and Kevin Deluzio[1]

[1]School of Biomedical Engineering, Dalhousie University, Halifax, NS, kmckean@dal.ca
[2]School of Physiotherapy, Dalhousie University, Halifax, NS
[1]Division of Orthopaedic Surgery, Dalhousie University, Halifax, NS

INTRODUCTION

Osteoarthritis (OA) is a dynamic, progressive disease causing significant disability and loss of function. Knee OA is 2-3 times more prevalent in females than males[1]. A larger knee adduction moment, which is an indication of the dynamic load on the medial compartment of the knee has been associated with radiographic disease severity, progression and surgical outcome of knee OA[2]. These relationships have been established without differentiating between genders. The purpose of this study is to determine differences in gait patterns between healthy and OA males and females and the relationship to clinical measures of disease severity.

METHODS

A 3D gait analysis of the lower limb was used to compare knee OA subjects (M=28, F=15) with asymptomatic subjects (M=18, F=24). The knee OA group was diagnosed clinically and radiographically with moderate knee OA. The asymptomatic group had no history of lower limb pain or injury. All subjects completed WOMAC knee osteoarthritis questionnaire. A 2-way anova was used to determine differences between disease and gender for kinematic and kinetic waveforms of the hip, knee and ankle and WOMAC scores.

RESULTS AND DISCUSSION

An interaction was found between gender and disease in both kinetics and kinematics at the knee and ankle joints (Fig 1). OA females exhibited a smaller amplitude i) knee flexion angle (p=0.02) and ii) knee internal rotation angle (p=0.01) compared to male OAs and asymptomatic subjects. OA females also produced a smaller amplitude i) ankle internal rotation moment (about the long axis of distal tibia) (p=0.05) and ii) knee adduction moment (p=0.09) than the other three groups.
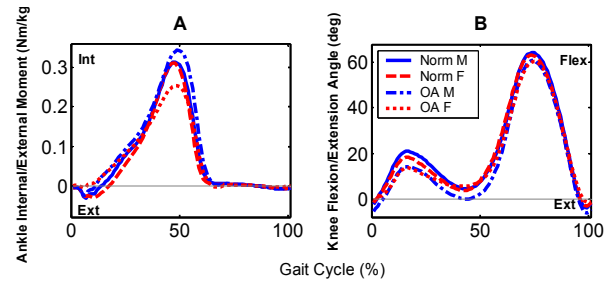

Figure 1: Principal component analysis[3] was performed on the gait waveforms. An interaction effect between gender and disease was found in ankle int/ext moment (p=0.05) and knee flexion angle (p=0.02).

Clinical measures of pain, function and BMI did not reveal a significant interaction between gender and disease (Table 1), however females reported higher values for all measures. Stiffness was borderline significant, with females reporting more than the other three groups (p=0.06).

It is clear that female patients with knee OA exhibit different biomechanics than their male counterparts. Decreased moments of force and range of motion at the joints generated by females may be driven by clinical symptoms of disease severity including pain, stiffness and function. In addition, compensatory strategies at one joint may be used to alleviate pain and dysfunction in the affected joint. Multivariate analysis is required to determine the complex interaction between biomechanics and clinical symptoms including pain, stiffness, function and radiographic severity.

REFERENCES

1. Buckwalter JA et al. (2000). Clin Orthop. 372,159-68.
2. Wang, JW et al. (1990). J Bone Joint Surg Am. 72(6) 905-9.
3. Deluzio, KJ et al. (1997). J Hum Mov Sci. 16, 201-217

Table 1: Clinical descriptors for normal and osteoarthritic (OA) males and females. Data are mean (SD). Two-way anova was used to test for group effect, sex effect and group/sex interaction.

Group		BMI (m^2/kg)	WOMAC Pain	WOMAC Stiffness	WOMAC Function	WOMAC AGGREGATE
Normal	Male	24.65 (3.16)	0.22 (0.55)	0.11 (0.32)	1.33 (1.67)	1.67 (3.91)
	Female	24.38 (3.63	0.13 (0.45)	0.17 (0.82)	0.67 (2.46)	0.96 (3.69)
OA	Male	30.75 (4.41)	6.79 (3.18)	3.18 (1.54)	20.75 (13.45)	30.71 (18.19)
	Female	31.40 (5.40)	8.40 (4.27)	4.27 (1.62)	25.33 (11.96)	38.00 (15.31)
Sex Effect (p-value)		0.85	0.22	0.37	0.36	0.24
Group Effect (p-value)		0	0	0	0	0
Interaction (p-value)		0.61	0.16	0.06	0.22	0.16

BIOMECHANICS OF THE BONE-LIGAMENT-COMPLEX IN LATE STAGE OSTEOARTHRITIS FOLLOWING ANTIRESORPTIVE DRUG THERAPY.

C.J. MacKay, M.R. Doschak, G.R. Wohl, R.F. Zernicke
McCaig Centre for Joint Injury & Arthritis Research, University of Calgary, cjmackay@ucalgary.ca

INTRODUCTION

Anterior cruciate ligament disruption (ACLX) can lead to chronic joint instability and mechanical deterioration of the femur-medial collateral ligament (MCL)-tibia complex (Bray *et al.*, 1997, Doschak *et al.*, 2001). Antiresorptive bone drug therapy (bisphosphonate–BP) has been shown to preserve bone at the MCL insert and normalize MCL complex laxity up to 6 wk post ACLX (Doschak *et al.*, 2001). However, the relationship between changes in the material and structural properties of the MCL (including the bone-ligament interface) and the progression of osteoarthritis (OA) is still unclear. The purpose of this study was to evaluate the effects of BP drug therapy on MCL-complex laxity and MCL material properties in the rabbit ACLX model of OA.

METHODS

Thirty-eight skeletally mature New Zealand White rabbits were divided into 3 groups. Two groups received unilateral ACLX of the right knee. One group of 14 ACLX rabbits were dosed (0.01mg/ml) daily with the BP Risedronate for 24 wk. The second group of 12 ACLX animals remained untreated for 24 wk, and served as age-matched OA controls. The third group of 12 age-matched, unoperated rabbits was evaluated as normal controls. The structural and material properties of the bone-MCL complex were evaluated by measuring MCL-complex laxity, and the change in elastic modulus of the MCL during low-load static and cyclic relaxation. All measures were compared with cartilage/joint gross morphology and histology for evidence of OA progression.

RESULTS AND DISCUSSION

Mechanical testing of the MCL-complex showed a significant increase in joint laxity for all ACL deficient animals (2.3 times that of normal controls; p<0.05[Fig.1A]). There were no significant differences in laxity between the untreated and the BP-dosed ACLX cohorts. Cyclic low-load relaxation data indicated a dramatic reduction in stiffness of load-relaxation of the MCL following surgery that was not inhibited with BP dosing [Fig. 1B].
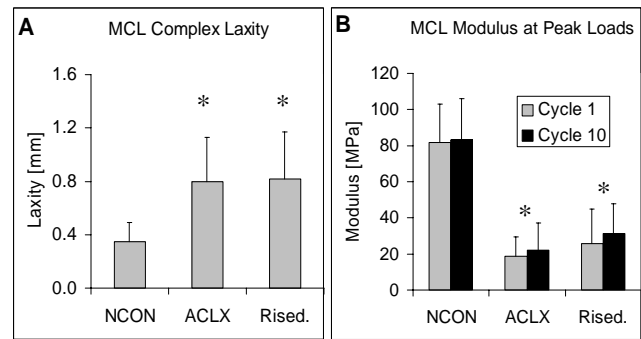
∗ Significantly different from NCON ($p < 0.05$)

Figure 1: A; MCL complex laxity **B;** MCL modulus at peak loads.

The elastic modulus calculated for both the ACLX and dosed cohorts were significantly less (p<0.05) than that of normal controls. Normal control MCL modulus increased (2%) between the first and tenth loading cycles. For the ACLX and dosed groups, the MCL modulus increased by 18% and 20% respectively. The percent relaxation of the MCL over a 20 min period of static loading was significantly reduced in both ACLX (-41%) and dosed groups (-45%) compared to normal controls.

CONCLUSIONS

While daily Risedronate dosing may inhibit bone remodeling at the bone-ligament insertion in an OA model, this was insufficient to conserve normal joint-complex function beyond an early stage. Thus, both structural and material behaviours of the MCL-complex deteriorated as OA progressed. Our findings suggest that bone remodeling at the ligament insertion influences joint-complex behaviour *early* after loss of the ACL, whereas changing ligament properties influence joint-complex behaviour in the later stages.

REFERENCES

1. Bray, R. et al. (1997). *J. Orthop Research,* **15**, 830-836
2. Doschak et al. (2001). *J. BMin Res,* **17**, S491.

THE EFFECTS OF CUSTOM-ORTHOSES FOR RUNNERS DIAGNOSED WITH PATELLOFEMORAL PAIN SYNDROME

Yukiko Toyoda[1], Benno Nigg[1], Preston Wiley[1] and Neil Humble[2]
[1]Faculty of Kinesiology, University of Calgary, Calgary, Canada, yukiko@kin.ucalgary.ca
[2]Department Surgery, University of Calgary, Canada

INTRODUCTION
Running injuries most frequently occur at the knee joint and patellofemoral pain syndrome (PFPS) has been the most common diagnosis (James et al., 1978, Taunton et al., 2002). Foot orthoses have been successfully used to reduce overuse pain including PFPS. Despite the number of studies, the role of foot orthoses in reducing overuse pain is not yet well understood. Possible reasons are: 1) most studies tested only rearfoot kinematics, 2) some studies were 2-D and/or used shoe markers, thus introducing errors, 3) many types of orthoses, which may have different effects, were tested, 4) few studies have investigated orthoses with injured populations. Furthermore, no studies have investigated the biomechanical effects of foot orthoses in relation with pain. Therefore, the purpose of this study was to investigate the effects of custom-made foot orthoses on 3-D kinematics and kinetics in the ankle and knee joints in runners diagnosed with PFPS.

METHODS
Five runners (171.5±4.4cm, 67.4±5.6kg) have been initially recruited for this study. All subjects were diagnosed with PFPS by a physician and a podiatrist confirmed that they had pronated feet which contributed to their symptoms. They were otherwise healthy with no history of traumatic lower limb injuries or surgeries, and had never used orthoses before.
Custom-made foot orthoses were prescribed for each subject. Foot orthoses consisted of a semirigid polypropylene shell (custom molding at non-weight bearing subtalar neutral position) with thickness adjusted for patients' weight and a Spenco cover. Subject specific postings were added to both rear- and forefoot as needed.
The study followed a prospective design. Baseline data were collected without using foot orthoses. The subjects performed twenty running trials at their natural running speed (2-3.2 m/s). Kinematic data was collected using 3D motion capture system with 6 cameras (240Hz). Reflective markers (3/segment) were placed on the foot, shank and thigh. Running sandals were used to allow the reflective markers to be placed directly on the foot. Kinetic data was collected using a force plate (2400 Hz). The subjects received their orthoses after the baseline data collection and underwent a gradual two-week adjustment followed by a two-week treatment period. After these four weeks, treatment data were collected in the same manner but with custom-made foot orthoses.

3-D ankle and knee joint kinematics and kinetics were calculated using inverse dynamics approach. Baseline (without orthoses) and treatment (with orthoses) data were compared subjectively for these five initial subjects.

RESULTS
Table 1 summarizes the individual results for both with and without custom-made foot orthoses. For kinematic variables, excursion values (difference from value at heel strike to maximum) rather than maximum values were used to minimize day-to-day variability in comparing data. Changes in foot eversion were subject specific. However, greater than 10% reduction in foot abduction was shown in 4 of 5 subjects, and knee internal rotation was reduced in all subjects when using custom-made orthoses. There were no systematic changes in knee abduction or external rotation moments.

DISCUSSION
All subjects reported that their pain was reduced after using custom-made orthoses. It was shown that runners with PFPS had larger maximum knee abduction and external rotation moments than normal runners (Stefanyshyn et al., 1999). The results of this study, however, did not show systematic reduction in knee joint moments by orthotic intervention. However, we found systematic reduction in tibial internal rotation both with respect to the foot (foot abduction) and the femur (knee internal rotation) when custom-made orthoses were used. Tibial rotation influences patella tracking, and therefore may be related to the onset of PFPS. Hence, it is speculated that the reduction of pain in PFPS runners in this study was attained by reducing tibial rotation angle with orthotic intervention.

REFERENCES
James, S.L. et al (1978). *Am J Sport Med,* 6**,** 40-49.
Taunton, J.E. et al (2002). *Brit J Sport Med,* 36**,** 95-101.
Stefanyshyn, D.J. et al (1999). *4th Symposium on Footwear Biomechanics,* Canmore, Canada.

ACKNOWLEDGEMENTS

Table1. Individual results for kinematic and kinetic variables. Values are mean (standard error).

subject	1		2		3		4		5	
orthotic condition	without	with	without	with	without	with	without	with	without	with
eversion excursion [°]	15.0 (0.3)	13.7 (0.3)	15.1 (0.2)	11.3 (0.3)	13.8 (0.2)	14.2 (1.1)	12.2 (0.3)	12.7 (0.4)	14.9 (0.3)	12.7 (0.4)
foot abduction excursion [°]	5.5 (0.4)	1.7 (0.3)	8.7 (0.3)	6.0 (0.4)	2.6 (0.3)	6.9 (0.3)	7.0 (0.3)	3.3 (0.3)	4.8 (0.4)	0.8 (0.2)
knee int. rotation excursion [°]	16.7 (0.5)	12.1 (0.4)	20.1 (0.8)	18.3 (0.7)	11.6 (0.3)	7.3 (0.3)	8.8 (0.4)	7.5 (0.6)	7.0 (1.0)	5.5 (0.8)
max knee abduction moment [Nm]	70.4 (1.5)	66.0 (1.0)	63.1 (1.3)	62.9 (0.8)	85.6 (1.2)	57.2 (0.9)	43.2 (0.7)	53.8 (0.7)	91.6 (1.8)	99.3 (1.7)
max knee ext. rotation moment [Nm]	14.1 (0.7)	16.4 (0.7)	11.9 (0.6)	18.0 (0.4)	28.2 (0.7)	6.4 (0.6)	3.1 (0.2)	6.3 (0.3)	38.0 (0.6)	33.9 (0.7)

SEGMENAL CONTRIBUTIONS TO THE FINAL CLUB HEAD SPEED IN A GOLF SWING

Koon Kiat Teu[1], Wangdo Kim[1], Franz Konstantin Fuss[1] and John Tan[2]

[1] School of Mechanical & Production Engineering, Nanyang Technological University, Singapore, mwdkim@ntu.edu.sg
[2] Physical Education & Sports Science, National Institute of Education, Singapore

INTRODUCTION

Most golfers tend to associate the improvement of their games with the improvement of their golf swing. The knowledge of how one uses the different segmental motion to strike the ball may provide valuable information. The objective of this study is to ascertain the contribution of the segmental rotations to the club head speed of a golf swing.

METHODS

The method involved utilizing electrogoniometer (biometrics, UK) to obtain the joint angles of the left arm throughout the motion. The time history of shoulder, elbow, forearm and wrist movement can be recorded. With the use of Dual Euler velocity analysis (Fisher, 1999), the velocity of the measured segment as well as the end-effectors can be calculated. The analysis could then ascertain the contribution of the different segmental rotations to the club-head speed.

The golf swing in this study was depicted as a five segment model (L1 - L5) as shown in Figure 1. Orthogonal Cartesian frame was attached to each segment. The directions of the three axes of each frame were constructed so as to approximate the different axes of rotation for each segment and the origin was located at the center of each relevant joint. The constructed orthogonal axes for the three arm segments were assumed to represent their anatomical axes. The valgus/varus rotation at the elbow joint was assumed as zero. The longitudinal rotation of the hand at the wrist joint was also assumed to be zero. The shaft and clubhead of the golf club were assumed to be rigid bodies.

The Dual Euler angles method (Ying and Kim, 2002) was used. The screw motion sequence Zy'x'' was observed in this study. Each of the joints was simulated to be driven by a motor that produce the angular rotations equivalent to contractions of spanning muscles. The dual velocity of the end point (i.e. the point on the center of the club head) is given by the contribution of each motor such that:

$$^{5}\hat{V}_{30}^{5} = {}_{3}^{5}\hat{M}(^{3}\hat{V}_{10}^{3} + {}^{3}\hat{V}_{21}^{3} + {}^{3}\hat{V}_{32}^{3})$$

$$= {}_{3}^{5}\hat{M} \, {}_{2}^{3}\hat{M} \, {}_{1}^{2}\hat{M} \, {}^{1}\hat{V}_{10}^{1} + {}_{3}^{5}\hat{M} \, {}_{2}^{3}\hat{M} \, {}^{2}\hat{V}_{21}^{2} + {}_{3}^{5}\hat{M} \, {}^{3}\hat{V}_{32}^{3}$$

where ${}^{R}\hat{V}_{ij}^{p}$ = dual velocity at a point P of body i relative to body j in terms of the unit vectors of frame {R}. The forward velocity of the club head can be defined as the y-component of ${}^{5}\hat{V}_{30}^{5}$ whose direction is always normal to the club head (Fig 1).
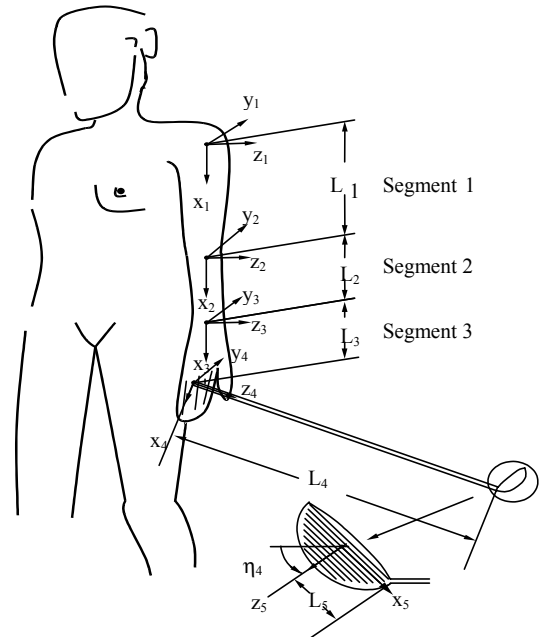

Figure1: The anatomical position and positions of frames on the subject and the club head

RESULTS AND DISCUSSION

From this study, the external rotation of the upper arm, the forearm supination, and hand flexion were noted to have contributed the highest to the final velocity of the club head. Although the wrist "uncocking" (hand flexion) did play a part in achieving a high club head speed, the contribution of the external rotation of upper arm and supination of the forearm were also significant. These two joint actions are not detectable if two-dimensional approaches were used. Details of such joint actions can only be uncovered with the present three-dimensional segmental analysis.

SUMMARY

The method provides an efficient approach of assessing the effectiveness of the arm segment rotations in producing club head speed. This method can be easily applied to other sports to describe and assess the contribution of segmental rotations to performance. In general, the method provides convenient access to movement recording and analyses. This method of analysis provides detailed information which may be omitted with other approaches

REFERENCES

Fischer,IS.(1999). *Dual-number methods in kinematics, statics, and dynamics*. Boca Raton, CRC Press.
Ying, N. and Kim. W. (2002), *J.Biomechanics* **35,** 1647-1657

REALISTIC TESTING OF RIOT HELMET PROTECTION AGAINST PROJECTILES

Cathie L. Kessler, Jean-Philippe Dionne, Doug Bueley, Aris Makris, Ismail El Maach

Med-Eng Systems Inc., Ottawa, Ontario, Canada
E-mail: ielmaach@med-eng.com   Web: www.med-eng.com

INTRODUCTION

The NIJ and CSA standards for testing of riot helmets [NIJ, 1984; CSA, 2002] require drop tower testing, in which helmeted headforms are dropped on anvils and stationary helmets are impacted by falling objects. The CSA standard also provides information regarding weights and impact energies of typical human-propelled projectiles from crowd management situations. In the current testing, inertia effects introduced by artificial supports are removed by impacting a free-falling mannequin with objects representative of these projectiles.

METHODS

All testing was performed on a Hybrid II mannequin representing the 50th percentile. Spherical objects representing a billiard ball (210 g, 98 km/h), full beverage can (360 g, 87 km/h), and half-brick (954 g, 67 km/h) were propelled at the mannequin using a standard baseball pitching machine. A tri-axial cluster of accelerometers (PCB Piezotronic 350A03) was located in the head of the mannequin, with the origin of the coordinate at the nasal root. High-speed digital video was taken at 500 fps, and data was collected through a computerized data acquisition system at a rate of 10 kHz and filtered at 1650 Hz with a 4-pole, low-pass, Butterworth filter [SAE, 1995].

The mannequin was hung from a quick-release mechanism, allowing it to be in a state of free-fall (i.e. unsupported) at the time of impact. As the 'ball' exited the pitching machine, it passed through an optical sensor, triggering the release mechanism, the camera, and the data acquisition. Impacts were aimed at the forehead (unprotected), or the centre/top of the visor (protected). Because of the difficulty in accurately aiming the impacts, a minimum of ten data points was taken in each case. A single helmet was used throughout the testing.

RESULTS AND DISCUSSION

The Head Injury Criterion (HIC) was used to assess the probable level of injury due to head acceleration [Versace, 1971]. This value was then used to calculate the scores for the Abbreviated Injury Scale (AIS), which gives the probability of the injury falling into various levels of severity [Prasad et. al, 1985]. A weighted average of the AIS values obtained for the given HIC was also calculated.

Values of the peak acceleration, HIC, and average AIS are shown in Table 1. As can be seen, the impacts on an unprotected head consistently produce a very high probability of a lethal injury (AIS 6 represents a fatal injury; AIS 5 represents an injury causing unconsciousness for more than 24 hours), while the impacts against a helmeted head produce a 100% probability of no injury at all.

SUMMARY

An unconstrained mannequin was subjected to projectile impacts in the head, both with and without a helmet. Estimates of the severity of the head injury were made using the Head Injury Criterion (HIC) and the Abbreviated Injury Scale (AIS), allowing for comparison between the protected and unprotected cases. For all three objects tested, the results show that wearing a helmet makes the difference between sustaining a lethal injury and remaining virtually unharmed. These tests differ from those required by most helmet standards, in that an unconstrained mannequin was used, thereby accounting for imparted inertia. Further, a realistic impact was generated. These, together, make the testing much more representative of actual use, and also make comparisons with the unprotected case possible. These results are similar to those of previous 'realistic' riot helmet testing performed with baseball bat impacts [Kessler et al., 2003].

REFERENCES

1. National Institute of Justice (1984), Standard-0104.02
2. Canadian Standards Association (2002), Standard Z611-02
3. Society of Automotive Engineers (1995). *SAE-J211/1*.
4. Versace, J. (1971). *Proceedings of 15th Stapp Car Crash Conference*, 771-796
5. Prasad P, Mertz HJ (1985), *Society of Automobile Engineers*, SAE Paper Number 85-1246
6. Kessler, C. et al. (2003). *Proceedings of the 27th Annual Meeting of the American Society of Biomechanics*

Table 1: Results for Impacts of Protected and Unprotected Mannequin Heads – Average of 10 (± SD)

Mass (kg)	Unprotected Impacts				Protected Impacts			
	Impact Energy (J)	Peak Acc. (g's)	HIC	AIS	Impact Energy (J)	Peak Acc. (g's)	HIC	AIS
0.210	80.2 (1.6)	440 (113)	3121 (619)	5.85 (0.36)	77.4 (2.6)	23 (3)	6.2 (1.7)	0 (0)
0.360	94.6 (27.2)	660 (81)	7226 (1882)	6 (0)	103.4 (2.0)	41 (7)	22.6 (5.4)	0 (0)
0.954	144.6 (12.2)	635 (197)	9630 (5612)	5.80 (0.62)	146.4 (11.8)	64 (10)	69.9 (26.5)	0.04 (0.04)

GOLF SWING MECHANICS AND MUSCLE FUNCTION IN TWO DIFFERENT GOLF SWINGS

Uwe G. Kersting[1] and René Ferdinands[2]

[1]Department of Sport and Exercise Science, University of Auckland, Auckland, New Zealand
[2]Department of Physics and Electronic Engineering, University of Waikato, Hamilton, New Zealand

INTRODUCTION

Golf as one of the most popular recreational sports in New Zealand is gaining increasing popularity in numerous countries. The repetitive nature of the sport in combination with asymmetrical postures occurring during the swing have been associated with a large number of injuries reported in golfers. Main areas for injury are the lower back and upper extremities (McCarrol, 1996). Electromyography (EMG) has been used in this context to estimate differences in muscular activation between athletes with and without lower back pain (Horton et al., 2000). No effect of fatigue on muscular activations was demonstrated in previous work (Horton et al., 2000). Indications for a modified timing of muscle activations, which might help stabilising the lumbar spine, have been discussed (Horton et al., 2000; Hermens et al., 2000). A review of the literature indicates that muscle function during the golf swing is not comprehensively understood. Recently, an optimised golf swing has been presented to enable an increased power production as well as placing less stress on the locomotor system, particularly the lumbar spine.

The purpose of this study was twofold. A cautious evaluation of limitations for surface EMG (sEMG) from various muscle groups during the golf swing was performed. Based on this evaluation recommendations for sEMG were derived. Using these recommendations two different golfing techniques were investigated regarding their muscular activation patterns.

METHOD

Six high level golfers using one out of two different swing techniques were tested in this study. Athletes were filmed with a 3D video capture system (Eva, Motion Analysis, USA; 8 cameras, 240 Hz). Forty-eight retroreflective markers were used to give a full body representation of the golfer with club and ball. Each subject performed five maximum speed trials while two force platforms simultaneously measured the ground reaction forces. EMG signals were recorded synchronously using a 16 channel EMG system (biovision, Germany) from several combinations of the following muscles: erector spinae, rectus abdominis, obliqe abdominals, biceps and triceps humeris, pectoralis major, deltoid, wrist flexors and extensors.

FINDINGS

The collection of surface EMG from trunk muscles did not demonstrate serious problems with regard to movement artifacts. For the shoulder and upper arm muscles considerable movement of the respective muscle bellies against the skin were demonstrated. Therefore, a set of recommendations for electrode application was established with reference to SENIAM guidelines (Hermens et al., 2000).
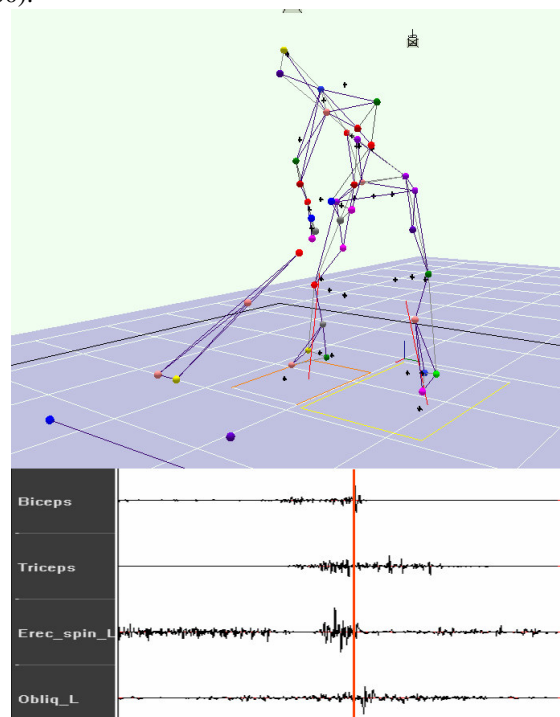

Figure 1: Example of the new golf swing showing four EMG channels.

For the two golf swings compared in this study marked differences in timing and magnitude of muscular activations were demonstrated for all trunk muscles and the biceps and triceps. Results indicate an overall lower activation level of the trunk muscles for the new golf swing. Regarding the timing of muscle actions greatest differences were shown for the muscles of the upper arm. Further, a more pronounced feed forward activation was demonstrated for subjects using the new technique (Hodges & Richardson, 1999). Implications for the loading of the lumbar spine have to be discussed with reference to kinematic and kinetic results.

REFERENCES

McCarrol, JR (1996). Clin Sports Med 15:1-7
Horton, JF, Lindsay, DM, MacIntosh, BR (2000). Med Sci Sports Exerc 33(10): 1647-1654
Hermens, HJ, Freriks, B, Disselhorst-Klug, C, Rau, G (2000) J Electrom Kinesiol 10: 361-374
Hodges, PW, Richardson, CA (1999). Arch Phys Med Rehabil 80: 1005-1012

ADDITIONAL VISUAL CUE ATTENUATES POSTURAL SWAY: IMPLICATIONS FOR PREVENTING FALLS

Michal Kuczynski and Adam Paluszak

Academy of Physical Education, Wroclaw, Poland, michkucz@awf.wroc.pl

INTRODUCTION

Recently, some authors have reported that slight additional tactile information from stable support can significantly decrease postural sway (Lackner et al, 1999; Krishnamoorthy et al, 2002). Although the physiological mechanisms of this phenomenon remain unknown, it has been suggested that such enhanced afferent may be used in rehabilitation of persons with deteriorated posture and help in preventing falls. While the former conclusion seems plausible, the latter appears rather unworkable. The purpose of this research was to investigate an alternative: the additional visual cue derived from comparing the relative position of two vertical lines placed at different distances in front of a standing subject. We hypothesized that such information may be effectively used by subjects and lead to attenuating their sway. Moreover, it can be easily implemented in the patients' population.

METHODS

Twelve healthy students (age 22 ± 1 ys., body mass 62 ± 9 kg, height 170 ± 8 cm) participated. They were asked to perform two 60 s. trials on a force plate in quiet stance with their feet together. In both trials they were instructed to use a visual cue to reduce their postural sway as much as they could. In trial 1 it was fixing the gaze on a 10 mm round black dot placed on the wall at the distance of 2.5 m and at the eyes' height. In trial 2 it was visual recording of the relative distance between a vertical stripe on the same wall and an edge of a vertical rod placed between the stripe and the subject 30 cm away from his/her eyes. The trial sequence was randomized. Statistics were computed using repeated Anova (2x2) and Scheffe post-hoc test.

During all trials the center of pressure (COP) was measured in both: sagittal (A/P) and frontal (M/L) directions with the sampling rate of 20 Hz. The COP signals were used to assess postural sway variability (COP standard deviation) as well as to reproduce the corrective signals (COP-COM). Based on those signals, the viscoelastic parameters (VE) of posture were evaluated: postural stiffness, viscosity, frequency, and damping (Kuczynski, 1999; 2003).

RESULTS AND DISCUSSION

Variability of the COP was less in trial 2 as compared to trial 1 (Figure 1). On average, postural sway decreased by 58% in the M/L plane (p<0.0009) and by 33% in the A/P plane (p<0.04). Analysis of the VE parameters disclosed changes caused by different visual cues in the M/L plane only. Specifically, the frequency of the corrective signal increased from 0.71 ± 0.08 in trial 1 to 0.85 ± 0.10 Hz in trial 2 (p<0.0002). As expected it was accompanied by similar changes in postural stiffness: 1163 ± 352 in trial 1 vs. 1610 ± 459 Nm/rad in trial 2 (p<0.0002). Variations in the remaining VE parameters were insignificant.

As opposed to the results regarding the role of light touch in attenuation of postural sway, our results can plausibly account for decreased variability of the COP in trail 2. By providing the subjects with the information about the relative position of the stripe-rod set, they were able to quite accurately record their sway in the M/L plane and use this error signal to consciously correct the M/L excursions of their bodies during quiet standing. These corrections required increased attention of the central nervous system and performing incessant interventions, hence the increased postural stiffness and frequency.
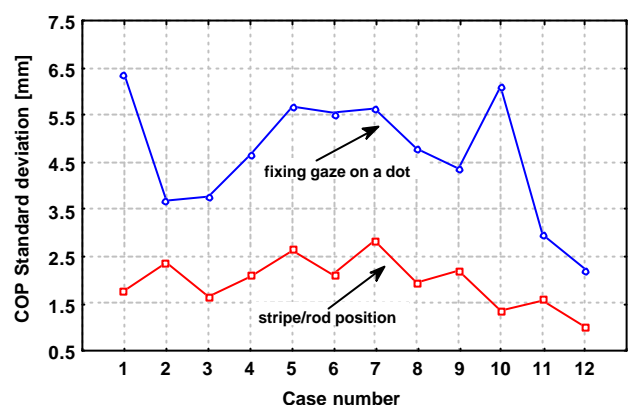

Figure 1. Variability of the M/L center of pressure across all twelve subjects in two trials with different visual cues.

Our experiment did not provide the subjects with any clue regarding their A/P sway, so the accompanying decrease of the COP variability in sagittal plane may appear rather surprising. However, it seems justifiable that any aid in posture maintenance in one plane may release some means involved in this particular task and apply them as additional support to control posture in the other plane. These results corroborate the notion about coordination between the two planes during standing. They are usually considered separately which, we believe, in an erroneous approach.

Our results further validate the VE model of quiet stance and elucidate the mechanisms of postural stability that are thought to be based on stiffness control (Winter et al, 1998). This experimental setting can be easily implemented for persons with deteriorated posture or at risk of falling, e.g. by wearing a cap with vertical elements attached to the visor.

REFERENCES

Lackner, J.R. et al (1999) *Exp Brain Res*, **126**, 459–466.
Krishnamoorthy, V. et al (2002) *Exp Brain Res*, **147**, 71–79.
Kuczynski, M. (1999) *Gait Posture*, **9**, 50–56.
Kuczynski, M. (2003) The Viscoelastic Model of Quiet Standing. Wroclaw, Academy Physical Education.
Winter, D.A. et al (1998) *J Neurophysiol*, **80**, 1211–1221.